



Durham E-Theses

Palaeoceanography of the holocene and late-glacial N.E. Atlantic: development and application of biomarker proxies of environmental change

Bendle, James Alexander Paul

How to cite:

Bendle, James Alexander Paul (2003) *Palaeoceanography of the holocene and late-glacial N.E. Atlantic: development and application of biomarker proxies of environmental change*, Durham theses, Durham University. Available at Durham E-Theses Online: <http://etheses.dur.ac.uk/4019/>

Use policy

The full-text may be used and/or reproduced, and given to third parties in any format or medium, without prior permission or charge, for personal research or study, educational, or not-for-profit purposes provided that:

- a full bibliographic reference is made to the original source
- a [link](#) is made to the metadata record in Durham E-Theses
- the full-text is not changed in any way

The full-text must not be sold in any format or medium without the formal permission of the copyright holders.

Please consult the [full Durham E-Theses policy](#) for further details.

Palaeoceanography of the Holocene and Late-Glacial N.E. Atlantic: Development and application of biomarker proxies of environmental change

Volume I: Text and Tables
Volume II: Figures and Appendices



University
of Durham

James Alexander Paul Bendle

A thesis submitted to the University of Durham in accordance with the requirements of the degree of Doctor of Philosophy in the Faculty of Science

Department of Geography

August 2003

A copyright of this thesis rests with the author. No quotation from it should be published without his prior written consent and information derived from it should be acknowledged.

57000 words



7 NOV 2003

Contents

Table of contents	I
Acknowledgements	IV
Abstract	V
Preface	VI
Abbreviations	VIII

Chapter 1: Introduction **1**

1.1. Quaternary palaeo-environmental indicators	4
1.2. Biomarkers as Quaternary palaeo-environmental indicators	5
1.2.1. Alkenones	6
1.2.1.1. Alkenones in Marginal Environments	10
1.2.2. <i>n</i> -Alkanes	16
1.2.3. Chlorophyll pigments	19
1.3. Bulk organic matter properties as Quaternary palaeo- environmental indicators	21
1.3.1. %TOC	21
1.3.2. C_{org}/N ratios	23

Chapter 2: Experimental Methodology **34**

2.1. Introduction	37
2.2. Wet Chemistry	38
2.2.1. Chemicals and preparative equipment	38
2.2.1.1. Glassware	38
2.2.1.2. Reagents and Solvents	38
2.2.1.3. Standards	38
2.2.2. Special Laboratory Equipment	39
2.2.3. Sample Work-Up	40
2.2.3.1. Lipid Extraction of Sediment Samples	40
2.2.3.2. Clean-Up of Sediment Samples – Compound Class Fractionation.	41
2.2.3.3. Lipid Extraction of Filter Samples	42
2.2.3.4. Clean-up of filter samples – saponification	43
2.2.3.5. Derivatisation (all samples)	43
2.3. Instrumental Analysis	43
2.3.1. Elemental analysis (Carbon and Nitrogen)	43
2.3.1.1. Appraisal of elemental analysis (Carbon and Nitrogen)	44
2.3.2. Total chlorins	44
2.3.2.1. Appraisal of total chlorins	45
2.3.3. Gas Chromatography with FID (GC-FID)	45
2.3.4. Gas Chromatography Coupled to Mass Spectrometry	46
2.3.5. Gas Chromatography Coupled to Mass Spectrometry with Ammonia Chemical Ionisation (GC-CI-MS)	46
2.3.6. Identification and Quantification of Analytes	47
2.3.6.1. GC- FID	47
2.3.6.2. Appraisal of GC-FID	48
2.3.6.3. GC-CI-MS	49
2.3.6.4. Appraisal of GC-CI-MS	50
2.3.7. GC-CI-MS compared to GC-FID.	51

Chapter 3: Distribution of long-chain alkenones in the Nordic Seas 53

3.1.	Introduction	56
3.2.	Aim and Objectives	58
3.3.	Background	59
3.3.1.	The contemporary physical and ecological oceanography of the Nordic Seas	59
3.3.1.1.	Physical Oceanography	59
3.3.1.2.	Ecological Oceanography	62
3.4.	Study Specific Experimental	64
3.4.1.	Filter samples, retrieval and storage	64
3.4.2.	Cores	66
3.5.	Results & Discussion	70
3.5.1.	Summary of <i>in situ</i> oceanographic conditions	70
3.5.2.	Alkenone Distributions in the Nordic Seas	72
3.5.2.1.	Absolute abundance	72
3.5.2.2.	%C _{37:4}	73
3.5.2.3.	U ^K ₃₇ and U ^K _{37'}	84
3.5.2.4.	C38 alkenones	88
3.5.3.	Alkenone distributions in core PL-96-126 – further appraisal of %C _{37:4} as a palaeo-SSS indicator.	89
3.6.	Conclusions	91

Chapter 4: Post-Glacial and Holocene palaeoceanography of the Icelandic shelf

100

4.1.	Introduction	103
4.1.1.	Background, aims and objectives	103
4.1.2.	Context – the Icelandic continental shelf	106
4.2.	Study specific experimental	109
4.2.1.	Biomarker analysis	109
4.2.2.	Chronology	110
4.2.2.1.	Radiocarbon dates	110
4.2.2.2.	Tephra markers	111
4.2.2.3.	Age models and stratigraphy	115
4.3.	Results and discussion	117
4.3.1.	Biomarker stratigraphy & correlations	117
4.3.1.1.	Post-Glacial 11.5 – 15kyr BP	117
4.3.1.2.	Holocene 0 – 11.6 kyr BP	120
4.4.	Conclusions	129

Chapter 5: Biomarkers and organic matter in coastal environments of N.W

Scotland: assessment of potential application to sea-level studies 138

5.1.	Introduction	142
5.2.	Aims and objectives	143
5.3.	Background	143
5.3.1.	Isolation basins and their application to sea-level studies	143
5.3.1.1.	Contemporary processes in modern isolation basins	143
5.3.1.2.	Relative Sea-Level	144
5.3.1.3.	Fossil isolation basins and the interpretation of former sea-levels	145
5.3.1.4.	Established sea-level indicators	148
5.3.1.5.	Sea-level index points	149
5.3.1.6.	Indicative Meaning	150
5.3.1.7.	Application of Data from Sea-Level Reconstructions	150
5.3.1.8.	Level of Accuracy	151
5.4.	Approach	152
5.4.1.	Sampling rationale	152
5.4.2.	Study specific experimental	153

5.4.2.1.	Modern basins	153
5.4.2.2.	Fossil basins	153
5.4.2.3.	Analysis for lipid biomarkers and bulk organic properties.	154
5.5.	Site descriptions and results of hydrographic measurements	155
5.5.1.	North-west Scotland	155
5.5.2.	Modern Basins	156
5.5.2.1.	Arisaig	156
5.5.2.2.	Knapdale	158
5.5.2.3.	Kintail	161
5.5.3.	Fossil Basins	162
5.5.3.1.	Arisaig	162
5.5.3.2.	Coigach	163
5.6.	Results and Discussion	166
5.6.1.	Modern Basins	166
5.6.1.1.	Particle size distributions	166
5.6.1.2.	Bulk organic geochemistry	166
5.6.1.3.	Lipid Biomarkers	167
5.6.1.4.	Within Basin Variability – Rumach Tidal Pond.	174
5.6.2.	Fossil Basins	175
5.6.2.1.	Arisaig	175
5.6.2.2.	Dubh Lochan (Coigach)	180
5.7.	Logit Regression Analysis	182
5.8.	Synthesis and Conclusion	186

Chapter 6: Overview and future work **198**

6.1.	Overview	201
6.1.1.	General	201
6.1.2.	Chapter 3: Distribution of long-chain alkenones in the Nordic Seas	202
6.1.3.	Chapter 4: Post-Glacial palaeoceanography of the Icelandic shelf.	204
6.1.4.	Chapter 5: Biomarkers and organic matter in coastal environments of N.W. Scotland: Assessment of potential application to sea level studies.	205
6.2.	Future work	206
6.2.1.	Chapter 3: Distribution of long-chain alkenones in the Nordic Seas.	206
6.2.2.	Chapter 4: Post-Glacial palaeoceanography of the Icelandic shelf.	207
6.2.3.	Chapter 5: Biomarkers and organic matter in coastal environments of N.W. Scotland: Assessment of potential application to sea-level studies.	208

Acknowledgements

I would like to thank my supervisors Prof. Ian Shennan and Prof. Antoni Rosell-Melé for devising my PhD project and providing support and guidance over the four years leading up to the submission of this thesis. Special thanks to:

- Toni for a great deal of support and scientific guidance, a true supervisor and friend.
- To Ian for his willingness to come late to the game and provide keen input.

I am also deeply indebted to my “surrogate supervisor” Dr Marie Russell (now at FRS Marine Laboratory). During her period at Durham, Marie spent a great deal of time insuring the “Dawson lab” (and the PhD students therein) met her high standards. Special thanks to Oksana Kornilova and Erin McClymont (my fellow “Dawson labbers”) for sharing many, many laboratory hours, ideas and occasional frustrations. Various aspects of this thesis were made possible by working visits to the laboratories of Prof. John Andrews (INSTAAR), Prof Richard Evershed (Bristol, OGU) and Dr Peter Hill (NERC tephra analytical unit). Many thanks to Dr Ian Bull and Dr Jim Carter who supervised me at Bristol and to Dr Mikie Smith for accommodating me whilst visiting INSTAAR. Many thanks to Prof. John Andrews and Dr Anne de Vernal (GEOTOP) for donating marine sediment cores for analysis. Thanks to Dr Patrizia Ziveri for identifying coccolithophores. Thanks to Dr Mark Maslin, who was involved in the initial conception of chapter 4 and whose infectious enthusiasm spurred my interest in palaeoceanography as a Quaternary Science MSc student at the University of London (UCL & Royal Holloway). Thanks to Harry A. ten Hove and Dr Rob Moolenbeek for identifying the mollusca picked for AMS ^{14}C dates (Zoological Museum, UVA, Netherlands). Thanks to Elizabeth Mackie for sharing her hydrological data-set.

Thanks to the scientific party and crew of the RRS *James Clark Ross* (cruise JR51). Especially, the Master (C. Elliot) and PSO (Prof. J. Dowdeswell) for leading the campaign, the Deck Engineer Simon Wright for tying the lab down, Neil Campbell (BGS) for fishing up the cores and Cólín Ó Cofaigh for advice with lithostratigraphical logs. Also Toni for “fighting our corner”, and, in no particular order, Martin, Neil, Cólín, Julian, Manon, Pete, Justin, Ros, Roy and Franny for good company.

I also wish to acknowledge the technical support of members of the Department of Geography, Durham. Particular thanks to Frank, Brian, Derek, Eddie and Neil for assistance in the lab and to Freda for decoding my lab orders.

The UK Natural Environmental Research Council (NERC) is thanked for providing the studentship that made this PhD possible. Further thanks are due to NERC for additional financial awards for AMS ^{14}C dates (NERC radiocarbon laboratory, East Kilbride) and for me to use the facilities at BOSCOR (Southampton Oceanography Centre), the Tephra Analytical Unit (Geology Department, University of Edinburgh) and the Organic Geochemistry Unit (School of Chemistry, University of Bristol). The Department of Geography is thanked for financial support to attend and present at the 7th International Conference of Palaeoceanography, Sapporo, Japan, September 2001. The European Geochemical Society is thanked for a young scientists travel award to attend and present at the EGS-AGU-EUG Joint Assembly, Nice, France, April 2003.

Finally, I would like to express my eternal gratitude to my wife Caroline, my family and friends for their continuous support, affection and encouragement. It was this factor above all others that enabled me to keep soldiering on.

Abstract

The aim of this thesis is to develop and apply novel climate proxies to understand the palaeoceanographic evolution of the N.E. Atlantic during the late-Glacial and Holocene. The proxies investigated are based on organic molecular compounds called lipid biomarkers and bulk organic matter properties. The primary focus is on long-chain alkenones, molecules which have been extensively used in mid and low latitude open oceans to reconstruct sea surface temperatures (SSTs) during the Quaternary. Thus, the relative abundance of some alkenones is related to the growth temperature of the algae at the time of the biosynthesis of these molecules (expressed in the $U^{K_{37}}$ and $U^{K_{37}'}$ indices). In high latitudes and coastal environments, the temperature dependence of alkenones is controversial, and the potential environmental information from alkenones is not yet well understood. In such locations there is increasing abundance of the $C_{37:4}$ alkenone (quantified as $\%C_{37:4}$). The presence of this component has been related to changes in the relative budget of freshwater in the surface ocean. A central aim of this thesis is to carry out an empirical investigation to find out the key environmental factors that control $\%C_{37:4}$ to assess its potential as a palaeoceanographic proxy. Research was conducted in the Nordic Seas and N.W. Scotland using samples from the water column, surficial sediment and sediment cores. The research undertaken can be broken down in three main sections:

Alkenone distributions in the Nordic Seas. The aim was to clarify and extend the application of alkenones as palaeoceanographic proxies in subpolar to polar environments. Samples of filtered sea surface POM were analysed and extremely high $\%C_{37:4}$ values (up to 77%) were measured in polar waters (up to 80% sea-ice cover). Values of $\%C_{37:4}$ across the Nordic Seas showed a strong association with water mass type. A combined data-set revealed a stronger correlation of $\%C_{37:4}$ to sea surface salinity (SSS, $R^2 = 0.72$) than to SST ($R^2 = 0.5$). However, scatter was observed in the relationship of $\%C_{37:4}$ to SSS, preventing confirmation of $\%C_{37:4}$ as a palaeo-SSS proxy. Values of $\%C_{37:4}$ in sea surface POM were high compared to surficial sediments. We discount preferential degradation of the $C_{37:4}$ alkenone and invoke dilution of the $\%C_{37:4}$ signal in sea surface sediments by advected allochthonous matter to explain this. The POM filter data suggest that, overall, $U^{K_{37}}$ is a more appropriate SST index for the Nordic Seas than $U^{K_{37}'}$. Examination of the scatter in the $U^{K_{37}'}$ versus SST relationship, shows that regions in the south of the Nordic Seas (including the Icelandic shelf) may yield reliable, alkenone based, palaeoceanographic reconstructions. Comparison of $\%C_{37:4}$ distributions with dinocyst proxies in a late Holocene core from the Barents Sea suggests $\%C_{37:4}$ may be a general marker for the influence of arctic/polar water in palaeoceanographic reconstructions.

The palaeoceanography of the Icelandic shelf for the post-Glacial period (0-15 kyr BP) was reconstructed from alkenone indices measured in three cores collected N and W of Iceland. One of the cores, JR51-GC35, contained a continuous record of Holocene sedimentation spanning 0 – 10.1 kyr BP. Superimposed on a general Holocene cooling trend in core JR51-GC35 were millennial scale oscillations of $\sim 2^\circ\text{C}$. The timing of the oscillations was in close agreement with the variability in IRD records from the East Greenland shelf and the timing of glacier advances in northern Iceland. A comparison of the $U^{K_{37}}$ -SST records from JR51-GC35 and a published core from the eastern Nordic Seas (MD952011) showed significant differences (superimposed on the general trend) in the timing of millennial scale climate events. This illustrates that Holocene climate evolution in the Nordic Seas was more complex than previously suggested, with significant climatic differences between the eastern and western Nordic Seas caused by the differential variability of the Irminger and Norwegian Currents with time.

The potential application for reconstructing past sea-level changes in N.W. Scotland of lipid biomarkers (alkenones, *n*-alkanes and chlorophyll derivatives), and bulk organic parameters ($\%TOC$, C_{org}/N) was assessed by a survey of modern basins (at different stages of isolation from the sea) and fossil basins (with known sea-level histories). A logit regression analysis of all the sediment samples was employed to find which of the biomarkers or bulk organic measurements could reliably characterise the sediment samples in terms of a marine/brackish or isolated/lacustrine origin. The results suggested an excellent efficiency for the alkenone index $\%C_{37:4}$ at predicting the depositional origin of the sediments. This study suggests alkenones could be used as an indicator of sea-level change in fossil isolation basins.

Preface

This thesis is the product of a NERC funded PhD project supervised by Prof. Antoni Rosell-Melé and Prof. Ian Shennan. This is the first PhD thesis from the Department of Geography, University of Durham, to be largely based on the analysis of organic matter in environmental samples (i.e. alkenones and other lipid extractable biomarkers). It is a product of the department's organic geochemistry laboratory, started by Prof. Rosell-Melé (now at UAB, Barcelona) and greatly influenced (in a practical sense) by Dr Marie Russell (now at FRS Marine Laboratory, Aberdeen). As such, this thesis benefits from organic geochemical expertise gained by Prof. Rosell-Melé at the Organic Geochemical Unit, University of Bristol (School of Chemistry) and the Fossil Fuels & Environmental Geochemistry Institute (University of Newcastle upon Tyne) and by Dr Russell at the University of Aberdeen, Department of Geology, the Oceanography Laboratory (University of Liverpool) and at the Department of Environmental Chemistry (ICER-CSIC), Barcelona. In Chapter 5 this thesis also benefits from the expertise of Prof. Ian Shennan and co-workers in the study of past sea-level changes. By encompassing a chapter concerned with past sea-level changes this thesis continues a tradition of sea-level research— within the Department of Geography - that goes back many decades.

The overall aim of this thesis is to extend and develop the application of biomarker and organic matter proxies of environmental change to specific, palaeoclimatically sensitive, marginal areas in the North East Atlantic. Chapter 1 introduces the theory and use of the biomarkers and bulk organic properties that are applied as palaeoenvironmental tools in this thesis: long-chain alkenones and associated alkyl alkenoates, *n*-alkanes, chlorin pigments, %TOC and C_{org}/N ratios. Chapter 2 outlines the general methodology used to generate the biomarker and bulk organic data and gives details of the benefits, limits and reproducibility of the analytical systems. Chapter 3 presents results from a study aimed at clarifying and extending the use of alkenone proxies for palaeoceanographic studies in the sub-polar to polar water regions of the Nordic Seas. Chapter 4 presents results of biomarker reconstructions of post-Glacial and Holocene palaeoceanography in high-resolution sediment cores from the Icelandic shelf. The aim of Chapter 5 is to assess the potential application of certain biomarkers and bulk organic properties for reconstructing relative sea level (RSL) change in N.W. Scottish isolation basins. The work collected here is a small contribution towards the goal of understanding the Earth's ocean-climate system.

Four papers - based on the data generated by this thesis - are in preparation for imminent submission to journals:

Bendle, J.A., Rosell-Melé, A., deVernal, A. Ziveri, P., The distribution of long-chain alkenones in the surface waters and sediments of the Nordic seas: Palaeoceanographic implications (in preparation for submission to: *Geochemistry, Geophysics, Geosystems*).

Bendle, J.A.; Rosell-Melé, Jennings, A.E, Andrews, J.T., A., High resolution $U^{K_{37}}$ -SST records from the Icelandic shelf during the post-Glacial and Holocene (in preparation for submission to: *Palaeoceanography*).

Bendle, J.A., Rosell-Melé, A., Cox, N.J.; & Shennan, I., Biomarkers in coastal environments of NW Scotland: assessment of potential for application to sea-level studies (in preparation for submission to: *Earth and Planetary Science Letters*).

Bendle, J.A., Rosell-Melé, Further evaluation of a biomarker proxy for surface salinity changes in the North Atlantic (in preparation for submission to: *Paleoceanography*)

Sections of this thesis have also been presented at several UK and international conferences over the past three years.

Abbreviations

- A&A - Long Chain alkenones and alkyl alkenoates
AF - Arctic front
AMS - Accelerator mass spectrometry
ARCICE - "Arctic ice and environmental variability" NERC thematic program
AW - Arctic water
BOSCOR - British ocean sediment core repository
BP - Before present
BSPF - Barents sea polar front
CHN – Carbon, hydrogen & nitrogen elemental analyser
 C_{org}/N - Molecular ratio of organic carbon to nitrogen
CSC - Continental slope current
CTD – Conductivity, temperature, depth probe
CV - Coefficient of variation
D-O Dansgaard-Oeschger
DOM - Dissolved organic matter
EGC - East Greenland current
EIC - East Iceland current
Et – Ethyl
eV - Electron volt
FC - Faroe current
GC - Gas chromatography
GC-CI-MS - Gas chromatography coupled to mass spectrometry with chemical ionization
GC-FID - Gas chromatography with flame ionization detector
GC-MS - Gas chromatography coupled to mass spectrometry
HMW - High molecular weight
HPLC - High pressure liquid chromatography
IC - Irminger current
IFF - Iceland-Faroe front
INSTAAR – Institute of Arctic, Antarctic and Alpine Research, University of Colorado
IRD - Ice-rafted debris
IS - Isolation stage
kyr - Thousands of years

LCK - Long chain ketones
LIA - Little Ice Age
LM - Light microscope
LMW - Low molecular weight
Ma - Millions of years
Me - Methyl
MNAW - Modified north Atlantic water
MS - Magnetic susceptibility
NAC - North Atlantic current
NAW - North Atlantic water
NCC - Norwegian coastal current
NCF - Norwegian coastal front
NCW - Norwegian coastal water
NIIC - North Icelandic Irminger current
NWAC - Norwegian Atlantic current
ODV - Ocean Data View and computer program for displaying oceanographic data
OM - Organic matter
PDA - Photodiode array detector
PDB - Peedee Belemnite
PF - Polar front
POM - Particulate organic matter
PSU - Practical salinity units
PW - Polar water
Refractory - Materials resistant to decomposition
RFC - Recirculated Faroe current
SC - Shetland current
SEM - Scanning electron microscope
SOC – Southampton Oceanography Centre
SSS - Sea surface salinity
SST - Sea surface temperature
TC - Total carbon
TOC - Total organic carbon
UV - Ultraviolet radiation
Vis. - Visible radiation
WOD 98 - World Ocean Database (1998)

WSC - West Spitsbergen current

XBT - Expendable bathythermograph probe

YD - Younger Dryas

σ_t - Sigma-t, the density of water as a function of *in situ* temperature, *in situ* salinity and atmospheric pressure.

1. Introduction



Cover image: "Galaxies of microscopic life" – SeaWiFS satellite image of Emiliana huxleyi blooms on the continental shelf south of Cornwall (UK) and west of Brittany (France).

Contents

1.1.	Quaternary palaeo-environmental indicators	4
1.2.	Biomarkers as Quaternary palaeo-environmental indicators	5
1.2.1.	Alkenones	6
1.2.1.1.	Alkenones in Marginal Environments	10
1.2.2.	<i>n</i> -Alkanes	16
1.2.3.	Chlorophyll pigments	19
1.3.	Bulk organic matter properties as Quaternary palaeo- environmental indicators	21
1.3.1.	%TOC	21
1.3.2.	C _{org} /N ratios	23

Tables

Table 1.1:	Long chain alkenones and alkyl alkenoates in marine sediments found and monitored (✓) in this thesis.	8
Table 1.2:	Alkenone/Alkenoate measurements and indices used in this thesis	9
Table 1.3:	Reported values of %C _{37:4} in the literature (<i>table continued over leaf</i>)	14
Table 1.4:	Characteristic autochthonous inputs of <i>n</i> -alkanes of biological origin.	17
Table 1.5:	Recognition of <i>n</i> -alkane inputs to recent sediments	18
Table 1.6:	Some major controls on TOC content of marginal basins (adapted from (Tyson, 1995))	22
Table 1.7:	A compilation of atomic C _{org} /N ratios of assorted biota and lacustrine samples (<i>table continued over leaf</i>).	24

(see volume II for figures).

1.1. Quaternary palaeo-environmental indicators

The Quaternary is the most recent geological period, beginning ~2.6 Ma BP and extending up to, and including the present. It consists of two epochs, the Pleistocene and the Holocene, the latter beginning at the termination of the Younger Dryas event 11.6 kyr BP (Grootes et al., 1993, from the GISP 2 ice core). The Holocene represents the most recent warm period in a Quaternary climatic range that extends from cold periods (glacials) - during which ice sheets reached maximal extent - to warm periods (inter-glacials) - during which ice sheets waned - and climate was similar to, or slightly warmer than, the present day. The high frequency and amplitude of climatic oscillations during the Quaternary makes the period geologically distinct. Quaternary environmental responses to large (i.e. glacial – inter-glacial changes of up to 15°C) and more subtle (e.g. intra-Holocene changes of ~2°C) changes in climate have left a legacy, from which may be reconstructed the associated environmental conditions at the time of formation or deposition.

There is a huge variety of techniques for reconstructing past climate change. Proxy methods¹ differ in longevity, sensitivity, resolution and completeness. It does not fall within the scope of this chapter to describe or even outline this diverse field. However, an example of the breadth of proxy evidence (by major category) is given below (recent reviews can be found in Lowe & Walker (Lowe and Walker, 1997) and Williams *et al.* (Williams et al., 1998):

- Geomorphological evidence:
 - e.g. Relict moraines, trimlines, striations, fossil dunes, cirque altitudes, periglacial landforms, raised shorelines, river terraces.
- Lithological evidence (from marine, lake, terrestrial sediments & ice):
 - e.g. Particle size distribution, till classification, organic carbon content, stable isotope measurements, wind blown dust content, biomarkers.
- Biological evidence:
 - e.g. Species assemblages of: pollen, diatoms, plant macrofossils, insects, mollusca, ostracods, foraminifera, radiolaria, coccolithophores, corals, vertebrates.

¹ The terms **proxy**, **proxy record** or **proxy method** are used in this thesis to refer to any line of evidence that provides an *indirect* measure of former climates or environments.

1.2. Biomarkers as Quaternary palaeo-environmental indicators

Organic carbon compounds are ubiquitous, abundant and sometimes overlooked components of oceans, lakes and sedimentary rocks (Summons, 1993). Directly, or indirectly, they fuel all biogeochemical processes. Many types of organic material have been recognised in sediments, the range of geolipids being considerable (for example see the reviews by: Brassell, 1993; Cranwell et al., 1987; Hedges and Oades, 1997; Meyers, 1997; Meyers and Ishiwatari, 1993b; Rosell-Melé, in press; Simoneit, 2002; Volkman et al., 1998). The distributions of lipid compounds has received special attention because they are easily extracted from sedimentary rocks and are amenable to analysis by a range of common chromatographic and spectrometric methods (Hedges and Oades, 1997). Many lipids have source specific origins; all reflect enzymatic control on their molecular structures. Many organisms have been found to possess the ability to regulate the biosynthetic production of their constituent lipids and thereby retain their viability under changing environmental conditions, such as fluctuations in temperature, light or salinity (e.g. Harwood and Russell, 1984).

This thesis is primarily concerned with biological marker compounds, or biomarkers. These are organic molecules found in the environment that can be unambiguously linked with biological precursor compounds. After biosynthesis, they can be incorporated into sedimentary rocks and preserved for geological periods in an unaltered or altered form. In this thesis we shall consider only those biomarkers soluble in organic solvents (“lipids”). An ideal biomarker palaeo-indicator would meet the following requirements (Brassell, 1993; Marlowe, 1984; Poynter and Eglinton, 1991; Rosell-Melé, in press):

- a) Biomarker data can be interpreted to relate to a palaeoenvironmental variable (e.g. SST).
- b) Target compounds should be biologically specific, preferably originating from organisms with a well constrained ecological niche.
- c) Known biological function in the source organism.
- d) Preservation: ideally compounds should survive quantitatively during deposition and subsequent burial.
- e) Established diagenetic pathway.
- f) Established transport mechanisms from production to burial (preferably quickly) in the sediments.

- g) Compounds should occur widely in space and time to provide information that is generally applicable to a variety of sedimentary regimes, preferably over an extended period of geological time.
- h) Factors controlling the generation of the signal must be known and preferably quantifiable by observation.
- i) The signal recorded should be amenable to quantitative analysis and calibration (preferably through routine techniques).

Additionally, in order to study the relationship between climatic variables and the biomarkers, it should be possible to carry out experimentation, both in the laboratory and by field observation (Rosell-Melé, 1994). Several compound types have potential or have been proved to be applicable as environmental indicators, for example: *n*-alkanes, carboxylic acids, *n*-alkanols, alkenones (and related alkyl alkenoates), alkenes, sterols, hopanoids and tetraethers. Their abundance and distribution may provide different sorts of information which can be used to attempt and/or contribute to the reconstruction of a climatic regime. In this thesis alkenones are the only biomarker group applied to all study areas, and *n*-alkanes in Scottish isolation basins. However, we take a multi-proxy approach, utilising – when feasible - additional methodologies that will provide supplementary or alternative environmental data.

1.2.1. Alkenones

The long-chain ethyl alkenones (alkenones) are long carbon chain (C_{37} , C_{38} , C_{39} & C_{41}) ketones with 2-4 double bonds or unsaturations. Together with the structurally related alkyl alkenoates, they form a suite of compounds that is almost ubiquitous in the sediments of the world's oceans. Alkenone and alkyl alkenoate structures are illustrated in Figure 1.1, while IUPAC nomenclature and shorthand notations are given in Table 1.1 (page 8). A summary of alkenone and alkenoate measurements used in this thesis is given in Table 1.2 (page 9). They are known to be synthesized by a limited number of haptophyte microalgae (the order Isochrysidales) and hence, in organic geochemical terms, can be considered biomarkers (Conte et al., 1995; Conte et al., 1994b; de Leeuw et al., 1980; Marlowe et al., 1984; Volkman et al., 1995; Volkman et al., 1980a). The most common biological source in world's oceans and contemporary sediments is the abundant and cosmopolitan coccolithophorid *Emiliania huxleyi* (Volkman et al., 1980a; Volkman et al., 1980b). In low latitudes, the coccolithophorid *Gephyrocapsa oceanica* may

also be a significant contributor (Volkman et al., 1995). In the fossil record, *E. huxleyi* becomes the dominant marine haptophyte in the last 50 – 70 kyr and first appears ~270 kyr BP (Flores et al., 1997; Thierstein et al., 1977). However, the occurrence of alkenones in the geological record precedes the appearance of *E. huxleyi*, as demonstrated by their identification in Eocene sediments (~45 Ma BP) (de Leeuw et al., 1980; Marlowe, 1984; Volkman et al., 1980b) and in two Cretaceous black shales dated at 100 Ma BP (Farrimond et al., 1986). The producer of alkenones in pre 260 kyr BP sediments is not known. However, based on co-occurrence of coccoliths and alkenones, Marlowe (1990) speculated that species of *Reticulofenestra* may be the source organism.

Since it was first demonstrated that alkenone abundance ratios in sediments changed in a systematic way with inferred temperature (Brassell et al., 1986a; Brassell et al., 1986b; Marlowe, 1984), a great deal of research has been conducted with the aim of confirming and calibrating this relationship. The temperature dependent nature of the distribution of the $C_{37:2}$ and $C_{37:3}$ alkenones has been confirmed by culture, surficial sediment and water column POM studies (e.g. Brassell, 1993; Muller et al., 1998; Prah et al., 2000; Prah et al., 1988; Prah and Wakeham, 1987; Rosell-Melé et al., 1995a; Sikes and Volkman, 1993; Sikes et al., 1997; Sonzogni et al., 1997; Ternois et al., 1997) (also see review by Herbert, 2001).

The U_{37}^K index was initially devised to quantify the degree of unsaturation of C_{37} alkenones (Brassell et al., 1986b) (see Table 1.2 page 9). However, subsequent culture experiments with a N.E. Pacific strain of *E. huxleyi* found that $C_{37:4}$ added non-linearity to the equation below 15°C (Prah and Wakeham, 1987). A better regression was achieved using $U_{37}'^K$, a simplified index that did not incorporate the $C_{37:4}$ component (Prah and Wakeham, 1987) (see Table 1.2 page 9). Moreover, this is practical as $C_{37:4}$ is hardly measurable in most middle to low latitude ocean sediments. Thus only the simplified $U_{37}'^K$ index is usually reported, except in a few cases (e.g. Bard et al., 2000; Madureira et al., 1997; Rosell-Melé, 1998; Rosell-Melé et al., 1997).

Values of $U_{37}'^K$ – once set biogeochemically by the algae – are not significantly altered by degradation in sedimentary processes

Table 1.1: Long chain alkenones and alkyl alkenoates in marine sediments found and monitored (✓) in this thesis.

<i>Designation</i>	<i>IUPAC nomenclature</i>	<i>Shorthand notation</i>	<i>Ammonia-Cl-MS</i>	
			<i>pseudo-molecular ions</i> m/ξ	<i>monitored</i>
alkenones				
A	heptatriaconta-8E,15E,22E,29E-tetraen-2-one	C _{37:4} Me	544	✓
B	heptatriaconta-8E,15E,22E-trien-2-one	C _{37:3} Me	546	✓
C	heptatriaconta-15E,22E-dien-2-one	C _{37:2} Me	548	✓
D	octatriaconta-9E,16E,23E,30E-tetraen-3-one	C _{38:4} Et	558	✓
E	octatriaconta-9E,16E,23E,30E-tetraen-2-one	C _{38:4} Me	558	✓
F	octatriaconta-9E,16E,23E-trien-3-one	C _{38:3} Et	560	✓
G	octatriaconta-9E,16E,23E-trien-2-one	C _{38:3} Me	560	✓
H	octatriaconta-16E,23E-dien-3-one	C _{38:2} Et	562	✓
I	octatriaconta-16E,23E-dien-2-one	C _{38:2} Me	562	✓
J	nonatriaconta-10E,17E,24E,31E-tetraen-one	C _{39:4}	572	
K	nonatriaconta-10E,17E,24E-trien-one	C _{39:3}	574	
L	nonatriaconta-17E,24E-trien-one	C _{39:2}	576	
alkyl alkenoates				
M	methyl heptatriaconta-7E,14E,21E-trienoate	C _{36:3} OMe	562	✓
N	methyl heptatriaconta-14E,21E-dienoate	C _{36:2} OMe	564	✓
O	ethyl heptatriaconta-14E,21E-dienoate	C _{36:2} OEt	578	✓

Table 1.2: Alkenone/Alkenoate measurements and indices used in this thesis.

<i>Measure</i>	<i>Equation</i>	<i>Reference</i>
ΣLCK	ΣC_{37} and ΣC_{38} alkenones	
U_{37}^{K}	$\text{C}_{37:2}\text{Me} - \text{C}_{37:4}\text{Me} / (\text{C}_{37:2}\text{Me} + \text{C}_{37:3}\text{Me} + \text{C}_{37:4}\text{Me})$	(Brassell et al., 1986b)
U_{37}'	$\text{C}_{37:2}\text{Me} / (\text{C}_{37:2}\text{Me} + \text{C}_{37:3}\text{Me})$	(Prahl and Wakeham, 1987)
$\% \text{C}_{37:4}$	$(\text{C}_{37:4}\text{Me} / \text{C}_{37:2}\text{Me} + \text{C}_{37:3}\text{Me} + \text{C}_{37:4}\text{Me}) \cdot 100$	(Rosell-Melé et al., 1998)
$\text{C}_{38}\text{Et} / \text{Me}$	$(\text{C}_{38:2}\text{Et} + \text{C}_{38:3}\text{Et} + \text{C}_{38:4}\text{Et}) / (\text{C}_{38:2}\text{Me} + \text{C}_{38:3}\text{Me} + \text{C}_{38:4}\text{Me})$	Adapted for this thesis to include $\text{C}_{38:4}\text{Me}$ from Conte <i>et al.</i> (1998)
$\Sigma\text{C}_{37} / \Sigma\text{C}_{38}$	$(\Sigma\text{C}_{37} \text{ LCK}) / (\Sigma\text{C}_{38} \text{ LCK})$	(Rosell-Melé et al., 1993)
$\% \Sigma\text{AA}$	$(\Sigma\text{AA} / \Sigma\text{LCK}) \cdot 100$	(Sawada et al., 1996)
$\text{U}_{38}\text{Me} =$	$\text{C}_{38:2}\text{Me} / (\text{C}_{38:2}\text{Me} + \text{C}_{38:3}\text{Me})$	(Conte and Eglinton, 1993)
$\text{U}_{38}\text{Et} =$	$\text{C}_{38:2}\text{Et} / (\text{C}_{38:2}\text{Et} + \text{C}_{38:3}\text{Et})$	(Conte et al., 1998)
$\text{U}_{38}\text{Me}^* =$	$\text{C}_{38:2}\text{Me} / (\text{C}_{38:2}\text{Me} + \text{C}_{38:3}\text{Me} + \text{C}_{38:4}\text{Me})$	Adapted for this thesis to include $\text{C}_{38:4}\text{Me}$ from Conte & Eglinton (1998)
$\text{U}_{38}\text{Et}^* =$	$\text{C}_{38:2}\text{Et} / (\text{C}_{38:2}\text{Et} + \text{C}_{38:3}\text{Et} + \text{C}_{38:4}\text{Et})$	Adapted for this thesis to include $\text{C}_{38:4}\text{Et}$ from Conte <i>et al.</i> (1998)

(e.g. Conte et al., 1992; Freeman and Wakeham, 1991; Madureira et al., 1995; Prahl and Muehlhausen, 1989; Teece et al., 1998) (also see recent review by Grimalt et al., 2000).

Generally, the alkenone signal incorporated into sediments, reflects in a direct way the integrated temperature record for growth of alkenone producers in surface waters (Prahl et al., 2000). Recent work by Rosell-Melé (2001) has also demonstrated that analysis of U_{37}' in standard samples by 24 leading laboratories produce data that are intercomparable within the considered confidence limits. This suggests that U_{37}' data produced by different scientific groups is comparable.

Despite the positive results outlined above, alkenone indices are not devoid of uncertainties. The initial U_{37}' - SST calibration derived from a culture of *E. huxleyi* (N.E. Pacific strain) by Prahl and Wakeham (1987) shows a clear linear relationship between U_{37}' and temperature in the range of 8 – 25°C. Interestingly, this linear regression equation is statistically the same as a regression between U_{37}' measured in global (60°N - 60°S) sediment core-tops and ocean-atlas mean annual SSTs (Muller et

al., 1998). However, a number of culture studies – on *E. huxleyi* and *G. oceanica* strains from various oceanographic locations - have produced different slopes for the relationship of $U_{37}^{K'}$ - SST (see Herbert, 2001, for review). Also, there is a systematic difference in the slope of the $U_{37}^{K'}$ – SST relationship, between global water column POM samples (Conte and Eglinton, 1993; Harada et al., 2003; Sicre et al., 2002; Sikes and Sicre, 2002; Sikes and Volkman, 1993; Ternois et al., 1998; Ternois et al., 1997) and the data from the culture by Prahl & Wakeham (1987) and from core-tops by Muller (1998). Whereby, the water column POM data generally lie in a field that gives warmer-than-predicted growth temperatures at a given $U_{37}^{K'}$, particularly in the range $\sim 5\text{-}15^{\circ}\text{C}$.

A number of recent studies highlight a degree of nonlinearity in the relationship of alkenones to SST at high ($> 25^{\circ}\text{C}$) and low ($< 8^{\circ}\text{C}$) temperature extremes (Conte et al., 2001; Pelejero and Calvo, 2003; Rosell-Melé, 1998; Sikes and Volkman, 1993; Sonzogni et al., 1997). It is apparent that in certain regions absolute temperatures derived from the “recommended” Prahl & Wakeham (1987) or Muller *et al.* (1998) equations are unrealistic. It has been suggested by Rosell-Melé (1995b) that this may apply to the Nordic Seas region, where - based on an extensive core-top data set - considerable scatter is seen in the $U_{37}^{K'}$ – SST relationship. In this region it is suggested that a calibration based on the original U_{37}^{K} index gives more accurate results. Other aquatic settings where the general oceanic $U_{37}^{K'}$ – SST relationship is not clearly applicable are marginal seas e.g. Schulz *et al.* (2000), coastal areas (e.g. Conte et al., 1994a) and lakes (e.g. Li et al., 1996; Thiel et al., 1997). High sedimentation rate, or low productivity sites, may also present a challenge to the use of alkenone indices as the alkenone signal has the potential to be diluted to levels below reliable detection ($< 10\text{ng}$ peak area) (Grimalt et al., 2001). In the following sections further background is given; relevant to the application of alkenones to the marginal environments investigated in this thesis.

1.2.1.1. Alkenones in Marginal Environments

1.2.1.1.1. The Nordic Seas (low end of the temperature spectrum)

In high northern latitude sediments the $U_{37}^{K'}$ index is subject to increasing error in cold waters below $\sim 10^{\circ}\text{C}$ (Rosell-Melé et al., 1993). This contrasts with the cold waters of the southern ocean, where $U_{37}^{K'}$ is well correlated to SST down to $\sim 3^{\circ}\text{C}$, or in the South Atlantic where the correlation reaches 0°C (Sikes et al., 1997). In the Nordic Seas,

increasing occurrence of the $C_{37:4}$ compound (which is rare in mid to low latitudes) is coincident with the increase in scatter in the $U_{37}^K - SST$ relationship. In the Nordic Seas surficial sediments the U_{37}^K index – which incorporates the $C_{37:4}$ compound – may be preferable to U_{37}^K , as it maintains a linear relationship to SST down to 6°C (Rosell-Melé, 1998). However, below 6°C neither index is correlated to SST. This is frustrating for palaeoceanographic investigations, as the cold water regions of the Nordic Seas plays a key role in the production of deep water masses, which drive the global thermohaline circulation. It has been shown that in such sediments the abundance of the $C_{37:4}$ compound (relative to the other C_{37} alkenones = $\%C_{37:4}$) seems to have a stronger relationship to SSS than SST (Rosell-Melé, 1998). Given this relationship, $\%C_{37:4}$ has been proposed as a tentative proxy to reconstruct Quaternary SSS changes in the northern Atlantic (Bard et al., 2000; Rosell-Melé, 1998; Rosell-Melé et al., 2002). It has been shown that there is no globally applicable relationship of $\%C_{37:4}$ to SSS or SST (Sikes and Sicre, 2001). However, recent regional studies have supported a stronger relationship of $\%C_{37:4}$ to SSS than to SST, in a number of water column POM samples from the Nordic and Bering Seas (Harada et al., 2003; Sicre et al., 2002).

1.2.1.1.2. Alkenones in lacustrine, coastal and brackish environments

As described above alkenones have been studied extensively in the mid-low latitude open ocean, where the sedimentary relationship between the alkenone U_{37}^K index and SST has been well established. Much less attention has been given to alkenone distributions and their precursor organisms in lacustrine (Cranwell, 1985; Li et al., 1996; Sheng et al., 1999; Thiel et al., 1997; Volkman et al., 1988; Zink et al., 2001) and coastal or brackish environments (Conte et al., 1994a; Ficken and Farrimond, 1995; Freeman and Wakeham, 1991; Schöner et al., 1998; Schulz et al., 2000). The lacustrine environments from which alkenones have been reported vary widely in their geographical location and environment and include fresh water lakes in the English Lake District, Russia and Germany (Cranwell, 1985; Zink et al., 2001) and saline lakes in China, Antarctica and Turkey (Li et al., 1996; Sheng et al., 1999; Thiel et al., 1997; Volkman et al., 1988) (the lakes in China and Turkey have never had a connection to the sea). The precursor organisms of alkenones from these environments have not been conclusively identified, and therefore culture experiments have not been carried out

with alkenone lacustrine producers to establish a relationship between alkenone unsaturation ratios and water temperature or other parameters.

Only a few previous studies have highlighted the potential of alkenones for investigating environmental change in coastal or brackish environments. Ficken and Farrimond (1995) looked into the lipid geochemistry of Framvaren fjord (Norway). Previously isolated from marine waters by isostatic uplift following the retreat of the Scandinavian ice sheet in the early Holocene, Framvaren was reconnected to marine waters through human engineering, in the year 1850 A.D. (Ficken and Farrimond, 1995). Two sediment cores retrieved from the fjord were shown to record a large increase in the abundance of alkenones coincident with the intrusion of marine waters. Alkenones were also deposited in the sediments during the earlier lacustrine phase, but at a much lower abundance relative to %TOC (Ficken, 1994). Re-examination of the data reveals that the alkenone distributions were characterised by prominent changes in values of %C_{37:4}, with mean values of 8% and 26% for the recent marine/brackish sediments and pre-1850 A.D. fresh water sediments respectively.

Recently Schulz *et al* (2000) described alkenone distributions from the surface sediments of the marginal Baltic Sea. The distribution was characterised by increasing values of %C_{37:4} and generally decreasing abundances of total C₃₇ alkenones along a salinity gradient from the Belt Sea (19.2 mean annual psu) to the Gulf of Finland (6.3 mean annual psu) (Schulz et al., 2000). The authors classify the alkenone data into two different groups, based upon within-class-distributions of the C₃₇ and C₃₈ alkenones; “pattern I” is for samples that resemble a “typical” *E. huxleyi* alkenone suite and “pattern II” for samples that are characterised by having no detectable C₃₈Me alkenones and elevated values of %C_{37:4}. Pattern I occurs in the surficial sediments of the western Baltic Sea where surface-water salinity is in excess of 7.7 psu, while pattern II occurs in the eastern Baltic Sea sediments beneath waters of <7.7 psu. These patterns have been shown to alternate in a Holocene sediment core from the Gotland deep and have been ascribed to the episodic occurrence of marine incursions (Schulz et al., 1997).

The elevated values of %C_{37:4} associated with the fresher Baltic Sea surficial sediments and the lacustrine phase of the Framvaren core contrasts with values from the global mid-low latitude oceans which typically have values of %C_{37:4} of less than 5%.

Observations of “unusually” high values of $\%C_{37.4}$ have also been reported for modern lacustrine sediments (Cranwell, 1985; Li et al., 1996; Thiel et al., 1997; Volkman et al., 1988), the Black Sea (Freeman and Wakeham, 1991) and from high latitudes regions of the north Atlantic (Rosell-Melé, 1998; Sicre et al., 2002, chapter 3 this thesis), southern ocean (Sikes and Volkman, 1997), the Sea of Japan (Ishiwatari et al., 2001) and the North Pacific (Harada et al., 2003).

A number of studies have addressed the possibility that alkenone unsaturation patterns in areas of variable salinity (e.g. fjords, or open ocean settings with marine ice meltwater), may reflect a salinity dependent shift in the biochemical synthesis of alkenones, or may originate from different source organisms or genetic strains that are adapted to lower salinity (Bendle and Rosell-Mele, 2001; Conte et al., 1994a; Ficken and Farrimond, 1995; Harada et al., 2003; Rosell-Melé, 1998; Rosell-Melé et al., 1998; Schöner et al., 1998; Schulz et al., 2000; Schulz et al., 1997; Sikes and Sicre, 2001). Local and regional studies have highlighted correlations between higher values of $\%C_{37.4}$ and lowered salinities (Harada et al., 2003; Rosell-Melé, 1998; Rosell-Melé et al., 1998; Schulz et al., 2000; Sicre et al., 2002). However there is great diversity in the slope of the $\%C_{37.4}$ - salinity correlation, between geographical locations and even between sample types from the same region (i.e. core top or water column) (Harada et al., 2003; Rosell-Melé et al., 2002; Schulz et al., 2000; Sicre et al., 2002; Sikes and Sicre, 2001). The balance of evidence suggests that there is no global linear relationship between $\%C_{37.4}$ and salinity as there is between U_{37}^K and SST (Sikes and Sicre, 2001). In Table 1.3 (page 14) there is a summary of reported $\%C_{37.4}$ values in the literature. This illustrates the observations of elevated $\%C_{37.4}$ values from a range of environments outside the mid-low latitude open oceans and in some cultures of haptophyte species that are not *E. huxleyi*. The work outlined above and summarised in Table 1.3 suggests that in coastal environments where sediments have been isolated or connected to the sea, the values of $\%C_{37.4}$ may be used to discriminate between relative inputs of C_{37} alkenones of an *E. huxleyi* marine source and those of a lacustrine or brackish source.

Schulz *et al* (2000) suggested that changes in the ratio of the $C_{38}Et$ to $C_{38}Me$ alkenones could help to distinguish marine *E. Huxleyi* source alkenones from alkenones produced either by an unknown source or from a physiological stressed *E. huxleyi* assemblage in <7.7 PSU waters. It has been suggested that alkenone inputs from the species *E. huxleyi*

Table 1.3: Reported values of %C_{37:4} in the literature. (table continued over leaf)

Location (or culture) Type	%C _{37:4}	Surface Salinity Range ¹	Surface Temp (°C) ¹	Sample Type ²	Source ³	Reference
Ocean						
Global mid- low latitude oceans	0 - 5	34 - 37 a.m.	5 - 27	SS	<i>E. huxleyi</i> & <i>G. oceanica</i>	various e.g. (Muller et al., 1998)
Southern Ocean	0 - 45	nr	-2 - 18	SS, F	Presumed <i>E. huxleyi</i>	(Sikes et al., 1997)
Nordic Seas	5 - 20	31 - 35	2 - 11	SS	Presumed <i>E. huxleyi</i>	(Rosell-Melé, 1998)
Nordic Seas	0 - 35	34 - 6 i.s.	4 - 20.1 i.s.	F	Presumed <i>E. huxleyi</i>	(Sicre et al., 2002)
Nordic Seas (AW) ⁴	0 - 12	> 35 i.s.	3 - 12 i.s.	F	<i>E. huxleyi</i> + unknown?	this thesis
Nordic Seas (ARW)	4 - 40	33.5 - 35 i.s.	5 - 12 i.s.	F	<i>E. huxleyi</i> + unknown?	this thesis
Nordic Seas (PW)	51 - 77	< 34.4 i.s.	< 5 i.s.	F	<i>E. huxleyi</i> + unknown?	this thesis
Bering Sea	18 - 41	< 32 i.s.	7 - 9 i.s.	F	Presumed <i>E. huxleyi</i>	(Harada et al., 2003)
Epicontinental Seas						
Baltic Sea (≥ 7.7 PSU)	8 - 29	7.7 - 19.2 a.m.	7.5 - 8.1	SS	<i>E. huxleyi</i>	(Schulz et al., 2000)
Baltic Sea (< 7.7 PSU)	11 - 35	6.3 - 7.5 a.m.	a.m.	SS	unknown	(Schulz et al., 2000)
Black Sea	3	nr ⁵	5 - 7.8 a.m.	SS	unknown	(Freeman and Wakeham, 1991)
Black Sea	3 - 12	nr	nr	F	unknown	(Freeman and Wakeham, 1991)
Near shore & coastal environments						
Framvaren fjord (Norway) marine phase	~ 8	nr	nr	SC	Presumed <i>E. huxleyi</i>	(Ficken, 1994)
Framvaren fjord (Norway) lake phase	~ 26	nr	nr		unknown	(Ficken, 1994)
Bjornafjorden & Samnangerfjorden (Norway)	10 - 17	15 - 33 i.s.	6.5 - 7.9 i.s.	F	<i>E. huxleyi</i> (including uncalcified strain)	(Conte et al., 1994a)
N.W. Scotti.s.h coastal basins (contemporary)	3 - 15	unknown	12 - 25 i.s.	SS	Presumed <i>E. huxleyi</i> + unknown?	this thesis
N.W. Scotti.s.h coastal basins (fossil)	2 - 40	unknown	unknown	SC	Presumed <i>E. huxleyi</i> + unknown?	this thesis
Lacustrine						
Lake Steiölingen (Germany)a. Holocene	21-33	fresh	nr	SS	Unknown - but many excluded	(Zink et al., 2001)
b. YD	44-66	fresh	nr	SS	including Haptophytes equivalents	(Cranwell, 1985)
Coniston Water (U.K.)	32	fresh	nr	SS	Unknown - possibly C _{37:4} M	(Cranwell, 1985)
Croose Mere (U.K.)	53.3	fresh	nr	SS		(Cranwell, 1985)

Upton Broad (U.K.)	60	fresh	nr	SS	Unknown - possibly C,Ch,M,P	(Cranwell, 1985)
Windermere (U.K.)	36.8	fresh	nr	SS	Unknown	(Cranwell, 1985)
Van (Turkey)	71	21.6 i.s.	5-18 i.s.	SS	Unknown - possibly C,D,M,S	(Thiel et al., 1997)
Gahai (China)	13	33 i.s.	- 31-28 a.r.	SS	Unknown	(Li et al., 1996)
Quinghai (China)	12	12 i.s.	- 31-28 a.r.	SS	Unknown - possibly Chromulina sp	(Li et al., 1996)
Erhai (China)	14	fresh i.s.	- 31-28 a.r.	SS	Unknown - possibly Chromulina sp	(Li et al., 1996)
Acc (Antarctica)	60	30-80 i.s.	-50- 6 a.r.	SS	Unknown - possibly Chromulina sp	(Volkman et al., 1988)
Unknown					Unknown	
<i>Cultures</i>						
CCMP1742	0-9.4	~35	8-25	LC	<i>E. huxleyi</i>	(Prah et al., 1993)
Various	0-1	~ 35	15	LC	<i>E. huxleyi</i> & <i>C. oceanica</i> (open ocean)	(Conte et al., 1995 and refs. therein)
Various	0.5-7	~ 35	15	LC	<i>E. huxleyi</i> (epicontinental and coastal)	(Conte et al., 1995 and refs. therein)
PML#92	6	nr	15	LC	<i>E. huxleyi</i> (English Channel, 1950)	(Marlowe et al., 1984)
PML#92d	7	nr	15	LC	<i>E. huxleyi</i> (English Channel, 1975)	(Marlowe et al., 1984)
PML#353	34	nr	15	LC	<i>Chrysothila lamellosa</i>	(Marlowe et al., 1984)
PML#528	42	nr	15	LC	<i>Chrysothila lamellosa</i>	(Marlowe et al., 1984)
PML#1	30	nr	15	LC	<i>Isochrysis galbana</i>	(Marlowe et al., 1984)
PML#507	11	nr	15	LC	<i>Isochrysis</i> sp.	(Marlowe et al., 1984)

1) a.m. = annual mean, a.r. = annual range, i.s. = *in situ*

2) S = surface sediments, F = filters, SC = sediment cores, LC = laboratory culture

3) Phylum Chrysophyta (fresh water):

- order Ochromonadales: D = *Dinobryon* sp., M = *Mallomonas* sp.
- order Prymensiales: C = *Chysochromulina* sp.
- order Chromulinales: Ch = *Chrysoococcus* sp., P = *Pseudopedinella* sp.

Phylum Haptophyta, class Haptophyceae (marine):

- *E. huxleyi* and *C. oceanica* are coccolithophorids. The *Chrysothila* genus and *Isochrysis* genus are from the order Isochrysidales

4) AW = Atlantic water mass, ARW = Arctic water mass, PW = Polar water mass

5) nr = not reported

and *G. oceanica* can be distinguished by their C_{37}/C_{38} alkenone or alkenoate/alkenone ratios (Prahl et al., 1993; Rosell-Melé et al., 1993; Sawada et al., 1996; Volkman, 2000) or by a plot of the U_{38Et}^K vs U_{38Me}^K unsaturation ratios (Conte et al., 1998). Therefore in a study of marginal environments where the alkenone patterns may be a function of changes in biological precursor assemblages or a product of salinity induced physiological stress, it is important to monitor changes in the full suite of alkenones and alkyl alkenoates.

1.2.2. *n*-Alkanes

These are organic compounds composed of straight-chains of carbon and hydrogen which are saturated, i.e. contain no carbon-carbon double or triple bonds. They are found in almost all sediments that contain organic matter, where they are usually the dominant compound class in the saturate fraction (Miles, 1994). *n*-Alkanes are derived from algae, bacteria and land plants (Tissot and Welte, 1978). Table 1.4 (page 17) is a summary of typical *n*-alkanes distributions from different biological sources. Table 1.5 (page 18) gives examples of how *n*-alkane distributions may be interpreted in recent sediments.

The characteristic distributions from algae and terrestrial higher plants differ significantly. The *n*-alkanes of algal origin show a predominance of odd-carbon chain lengths of low molecular weight (LMW) (typified by a maximum at C_{17} in the C_{15} - C_{21} range) and a slight even-carbon or no predominance in the high molecular weight (HMW) C_{27} - C_{35} range (Brassell, 1993; Brassell et al., 1978; Clark and Blumer, 1967; Goutx and Saliot, 1980; Kennicutt II and Comet, 1992). In contrast, *n*-alkanes of terrestrial higher plant origin show a strong predominance of odd-carbon chain lengths in the HMW C_{23} - C_{35} range and have essentially no predominance in the LMW C_{15} - C_{21} range. The relative predominance of odd-over-even carbon atoms number in *n*-alkanes is expressed numerically by the following index:

$$CPI_{n-m} = \frac{1}{2} \times \left(\frac{\sum C_{m+1} - C_{n+1}}{\sum C_m - C_n} + \frac{\sum C_{m+1} - C_{n+1}}{\sum C_{m+2} - C_{n+2}} \right)$$

(within the range from C_n to C_m of number of carbon atoms in the molecule (n and m are even numbers).

The reason for this difference is that all plants synthesize predominantly odd-carbon chain lengths, but vascular land plants synthesize long-chain cuticular waxes (C_{25} - C_{35}) to

preserve their leaf water content, whereas the aquatic algae synthesize short chain *n*-alkanes (C₁₅-C₂₁) (Hunt, 1979). Bacteria synthesize *n*-alkanes in the C₁₀ to C₂₉ range in relatively low abundances, compared to the synthesis of other compound classes such as hopanes and acyclic isoprenoids (Comet and Eglinton, 1987). Therefore, the bacterial *n*-alkane signal in sediments will often be insignificant compared to algal or higher plant inputs. Terrestrial vs algal sources of *n*-alkanes can also be estimated by the ratio of HMW (mostly higher plant) to LMW (mostly algal) *n*-alkanes (see Table 1.5, page 18). However, LMW *n*-alkanes are more labile than HMW homologues and therefore the measure may be biased by their greater relative degradation (Cranwell, 1976; Kawamura et al., 1987).

Table 1.4: Characteristic autochthonous inputs of n-alkanes of biological origin.

<i>Organism</i>	<i>Environment</i>	<i>Dominant Carbon No. (s)</i>	<i>CPI</i>	<i>Carbon No. Range</i>	<i>Modality</i>	<i>Example References</i>
Photosynthetic bacteria	Aquatic (pelagic)	C ₁₇ , C ₂₆	Low	14 – 29	Bimodal	(Cranwell et al., 1987)
Non-photosynthetic bacteria	Aquatic (benthic)	C ₁₇ – C ₂₀ C ₁₇ & C ₂₅	Low Low	15 – 28 15 – 29	Unimodal	(Han and Calvin, 1970)
Fungi	?	C ₂₉	--	25-29	Bimodal	(Yen, 1975)
Blue-green algae	Aquatic (pelagic)	C ₁₇	High	14 – 19	Unimodal	(Blumer et al., 1971)
Algae	Aquatic (pelagic)	C ₁₇	High	15-21	Unimodal	(Gelpi et al., 1970)
Brown algae	Aquatic (benthic)	C ₁₅	Low	15 – 26	Unimodal	(Youngblood and Blumer, 1973)
Red algae	Aquatic (benthic)	C ₁₇	Low	15 – 24	Unimodal	(Youngblood et al., 1971)
Zooplankton	Aquatic (pelagic)	C ₁₇ , C ₁₈ & C ₂₄	Low	18 – 54 or 20 – 28	Bimodal	(Cranwell et al., 1987; Giger and Schaffner, 1977)
Higher plants	Terrestrial	C ₂₇ , C ₂₉ or C ₃₁	High	15 – 57	Unimodal	(Caldicott and Eglinton, 1973)
Rotifer worms	Aquatic (mostly fresh)	C ₂₄	Low	20 – 52	unimodal	(Cranwell et al., 1987)
Insects	Terrestrial	?	High	21 – 55	?	(Jackson and Blomquist, 1976)

n-Alkanes have been used extensively as indicators of inputs of terrestrial or land derived organic matter to the marine environment (e.g. Huang et al., 2000; Ikehara et al., 2000; Kawamura, 1995; Ohkouchi et al., 1997; Philp, 1985; Zhao et al., 2003).

Moreover, they have been used in lacustrine environments to infer changes in the relative inputs of organic carbon from aquatic algal sources (including eutrophication) and watershed terrestrial biota (Cranwell, 1973; Cranwell et al., 1987; Kawamura and Ishiwatari, 1985; Kawamura et al., 1987; Meyers and Benson, 1988; Meyers and Ishiwatari, 1993b).

Therefore, these compounds give an insight on the relative contributions of organic carbon to a basin (lacustrine, coastal etc) from algal versus terrestrial plant sources. This may be useful in determining whether the increase in bulk %TOC observed in many fossil isolation basins - and associated in the literature with the early stages of isolation (Kjemperud, 1986) - is a product primarily of increased algal primary productivity/preservation within the basin, or rather of the enhanced accumulation, "trapping", of terrestrial plant carbon from the basin catchment area. However, it is important to note that marine and lacustrine algae have not been reported as producing *n*-alkane distributions that are characteristically different (Brassell et al., 1978; Cranwell, 1973; Gelpi et al., 1970; Youngblood and Blumer, 1973; Youngblood et al., 1971). Therefore, *n*-alkanes may not be used as absolute indicators of relative inputs of marine vs freshwater algal carbon.

Table 1.5: Recognition of *n*-alkane inputs to recent sediments.

<i>n</i> -Alkane parameter	Characterisation of parameter	Likely inference
Σ <i>n</i> -alkane (ng/g) C _{org}	High relative abundance	High inputs from <i>n</i> -alkane producers/ preferential degradation of more labile (than <i>n</i> -alkane) material
	Low relative abundance	Low inputs from <i>n</i> -alkane producers/ preferential degradation of <i>n</i> -alkanes (unlikely)
CPI ₂₅₋₃₃	High	Dominant higher plant inputs
	Low	Lower higher plant inputs, and/or dominant algal inputs
Long/Short (C ₂₇ + C ₂₉ + C ₃₁)/ (C ₁₇ + C ₁₉ + C ₂₁)	High	Greater relative higher plant inputs and/or degradation of LMW algal inputs
	Low	Greater relative algal inputs
Highest abundance of C _n	C ₁₅ and/or C ₁₇	Algal inputs dominant
	C ₂₇ , C ₂₉ , C ₃₁	Higher plants dominant

1.2.3. Chlorophyll pigments

Higher plants and algae synthesize a variety of pigmented organic compounds, principally for use in photosynthesis. The principal photosynthetic pigments used by plants and all the major algae classes are the chlorophylls, of which chlorophyll *a* (Chl *a*) is the most common (Jeffrey and Vesk, 1995) (see Figure 1.2). Chlorophyll pigments contain chromophore groups, typically conjugated C=C bonds, which absorb portions of the visible colour spectrum and give the molecules their characteristic colours. In addition they have oxygen containing functional groups. The double bonds and functional groups provide sites for microbial attack (Meyers, 1997). Incubation experiments with naturally-occurring sediments have shown that Chl *a* concentrations usually exhibit an exponential degradation, to a low background level (Sun et al., 1993). Various studies have shown that a series of transformation processes, including demetallation of the magnesium chelate, decarbomethoxylation ('pyro'-formation) and ester hydrolysis occur either within the water column or at the sediment/water interface, forming sedimentary phaeopigments, collectively termed "chlorins" (e.g. Baker and Palmer, 1979; Baker et al., 1978; Keely and Maxwell, 1991; Louda et al., 1980; Louda et al., 2002; Spooner et al., 1995; Spooner et al., 1994) (see Figure 1.2). Therefore, although chlorophyll compounds are quickly degraded in the water column and surface sediments, a small but significant fraction can be preserved as chlorins. UV/vis spectrophotometric measurement of absorption at a wavelength of 410nm, in recent sediments, primarily records the abundance of such chlorins (Higginson, 1999).

The feasibility of determining absolute marine primary export palaeoproductivity from chlorin pigments has been addressed by several authors (e.g. Higginson, 1999; Repeta et al., 1992). In the Atlantic Ocean, stratigraphic variations of chlorins in marine sediments have been related to palaeoproductivity in highly productive marine locations such as the upwelling areas of northwest, equatorial and southwest Africa (Brassell et al., 1986b; Harris et al., 1996; Summerhayes et al., 1995) but also in the North Atlantic and Nordic Seas (Rosell-Melé and Koç, 1997; Rosell-Melé et al., 1997).

The downcore trends in total abundance of chlorins depends - in common with all organic matter - on changes in export primary productivity and diagenesis. The latter being influenced by factors such as O₂ content of the water column and bottom water, residence time in the water column and at sediment/water interface before deposition,

molecular reactivity, formation of pigment complexes, adsorption and bioturbation (Higginson, 1999). Hence, due to the likely combined effect of the above factors, it can be complicated to isolate the palaeoproductivity signal from other variables at the time of deposition (Rosell-Melé, in press).

A further use of pigment analysis, is the classification of pigments by use of the ratio of absorbance between certain wavelength bands. Rosell-Melé *et al.* (1997) employed UV/vis spectrometry to detect and distinguish between chlorins and porphyrins in core BOFS 5K in the North Atlantic. Porphyrins (red fully aromatic tetrapyrroles) are late stage diagenetic products of chlorins, and were unexpectedly found in association with ice rafted debris (IRD). Since they have never been observed as indigenous components of sediments younger than the Late Pliocene (Keely *et al.*, 1994), these pigments were assigned an origin in ice-rafted, ancient organic rich sediments. The relative abundance of the chlorins and porphyrins can be estimated by measuring the absorbance in the Soret band (S; 360-420nm) and the satellite I region (I; 665nm) (Baker and Louda, 1986). The changing ratio of absorbance maxima in these two regions (S/I), can be used to recognise chlorin (1-5) and porphyrin (>10) pigments (Rosell-Melé *et al.*, 1997). Accumulation records of chlorin pigments were used to shed further light on the origin and effect of abrupt Heinrich Events (HE) in the North Atlantic. Marked and abrupt changes in Chl-derived pigments across sedimentary Heinrich layers (HL) were ascribed to oceanic conditions produced by ice-rafting. In particular, chlorins were found in association with IRD, but were apparently absent when IRD levels decreased to background levels. The authors concluded that abundant meltwater enhanced preservation of chlorins during HL deposition due to a reduction in deep-water formation and a concomitant reduction in bottom water oxygenation (Rosell-Melé *et al.*, 1997). However, the concentration of chlorins dropped as IRD (and porphyrin) values maximised, presumably due to the dilution of these products of autochthonous marine production by the input of allochthonous IRD material.

Tetrapyrrole pigments in four cores from the Nordic Seas were again utilised by Rosell-Melé and Koç (1997) to propose rapid and abrupt changes in the oceanic and climatic circulation system. The discovery of chlorins and porphyrins (by the S/I method described above) during the Younger Dryas and the end of the last glacial were interpreted as evidence for photosynthetic activity at these times. This, the authors

concluded, suggested the existence of open ocean conditions during (at least seasonally) ice free episodes in these cold periods.

1.3. Bulk organic matter properties as Quaternary palaeo-environmental indicators

1.3.1. %TOC

The natural imprint of organic matter in marginal basin environments includes both autochthonous and allochthonous contributions. The autochthonous input is comprised of the material generated within the basin (e.g. products of microalgae and macrophytes). Whereas the allochthonous input is transported into the sedimentary environment by water, wind, ice, human agency etc (e.g. refractory products of higher plants) (Brassell et al., 1978). Furthermore, organic inputs will be of either direct or indirect biological origin, since the organic matter may be incorporated directly into the sediment after biosynthesis by a precursor organism, or indirectly following modification either by biota, or by biological or chemical alteration during diagenesis (Summons, 1993).

Due to the ease of analysis, the abundance of organic matter in sediments is usually expressed as the relative dry weight percentage of organic carbon (%TOC). However, it should be noted that the relationship of %TOC to actual proportion of organic matter will vary according to the characteristics of the organic matter i.e. kerogen includes significant amounts of other elements especially hydrogen (3-10 wt%), oxygen (3-20 wt%), nitrogen (0-4 wt%) and sulphur (0-4 wt%) (Tyson, 1995). Therefore, a %TOC to “total organic matter” conversion factor of 1.7-1.9 has been suggested for modern marine sediments (Tyson, 1995 and refs therein).

The general trend of %TOC in modern, marginal sedimentary environments is illustrated by the composite transect in Figure 1.3. This relationship is characterised by decreasing %TOC from continental shelf to the abyssal depths. However, superimposed on this large scale trend are regional and local %TOC trends. For example, %TOC values generally increase toward localised depressions (sediment focusing) (Huc, 1988a; Huc, 1988b; Rashid, 1985). This is thought to be related to the correlations that exist between %TOC and particle granulometry and is regardless of

oxygen regime (Tyson, 1995). However, such patterns may be accentuated if the localised depressions are prone to oxygen deficiency (Tyson, 1995).

The environmental factors that control %TOC values in marginal sediments are numerous. Some commonly considered to be important are export primary productivity, allochthonous OC inputs, the O₂ content of the water column and bottom water, residence time in the water column and at sediment/water interface before deposition, sediment accumulation rate and particle size/texture, particle carbon loading and formation of monolayers (e.g. Emerson et al., 1987; Henrichs, 1992; Henrichs, 1993; Keil et al., 1994; Meyers and Ishiwatari, 1993a; Meyers and Ishiwatari, 1993b; Thompson and Eglinton, 1978; Tromp et al., 1995; Wakeham and Lee, 1993). A summary of the major controls on %TOC values in marginal environments is given in Table 1.6.

Table 1.6: Some major controls on TOC content of marginal basins (adapted from (Tyson, 1995)).

<i>Variables</i>	<i>Correlation with TOC</i>		
1. Primary productivity: a. Mean productivity	(+)		
b. New productivity	(+)		
c. Production half-time	(-)		
2. Water depth	(-)		
3. Plankton type a. Mineralized (siliceous or calcareous)	(-)		
b. Organic-walled	(+)		
4. Allochthonous organic matter inputs: a. Terrestrial	(+)		
b. Marine	(+)		
5. Sediment grain size: a. Mean	(-)		
b. % silt + clay	(+)		
6. Sediment accumulation rate a. Biogenic component	(+, <i>pars</i>)		
b. Siliciclastic component	(-)		
7. Mean dissolved oxygen of bottom water: a. > 1.0ml l ⁻¹	(+O ₂ -TOC)		
b. < 0.2-1.0 ml l ⁻¹	(-O ₂ +TOC)		
<i>Correlations between the above controls</i>			
1 and 2 (-)	2 and 4 (-)	3a and 5b (+)	4a and 5a (+)
1 and 3 (+)	2 and 5 (-)	3a and 6a (+)	4a and 6b (+)
1 and 6a (+)	2 and 6 (-)		
1 and 7 (-)	2 and 7 (±)		
<i>Other variables interacting with the above</i>			
A. Climate	(1,2,3,4,5,6,7)		
B. Watermass circulation	(1,3,4,5,6,7)		
C. Basin Topography	(1a, 2,4,5,6,7)		
D. Distance from fluvial inputs	(1a,3,4a,5,6,7)		
E. Tectonic regime	(2, 4a, 5 6b)		

All “other variables” are strongly interrelated. Variables B, C and D, in conjunction with factor 2 (above) are the consequences of ‘sea-level’.

1.3.2. C_{org}/N ratios

The presence or absence of cellulose in the plant sources of organic matter deposited in sediments of coastal basins influences the C_{org}/N ratio of the sediments. As shown by the examples in Table 1.7 (page 24), nonvascular aquatic plants have low C_{org}/N ratios, typically between 4 and 10, whereas vascular land plants, which contain cellulose, have C_{org}/N ratios of 20 or more (Meyers and Ishiwatari, 1993b; Muller and Mathesius, 1999). In theory in coastal basins where the contribution of organic matter from vascular land plants is small relative to water-column production, the sediments will show lower C_{org}/N ratios than those with higher relative inputs of vascular plant detritus. Therefore, C_{org}/N ratios can complement *n*-alkane distributions in elucidating changes in the relative inputs of terrestrial and algal organic matter during the isolation process.

Table 1.7: A compilation of atomic C_{org}/N ratios of assorted biota and lacustrine samples. (table continued over leaf)

Type of sample	C_{org}/N	Reference
Land Plants		
White oak, modern	276	(Hedges et al., 1985)
White oak, 25 Kyr-old	111	(Hedges et al., 1985)
Red alder, modern	264	(Hedges et al., 1985)
Red alder, 2.5 kyr-old	106	(Hedges et al., 1985)
Spruce, modern	546	(Hedges et al., 1985)
Spruce, 2.5 Kyr-old	541	(Hedges et al., 1985)
White spruce, modern	46	(Bourbonniere, 1979)
White spruce, 10 Kyr old	20	(Bourbonniere, 1979)
Willow, modern	58	(Meyers, 1990)
Cottonwood, modern	22	(Meyers, 1990)
Pinyon pine, modern	42	(Meyers, 1990)
Algae		
Average zooplankton and phytoplankton		
Benthic organisms and bacteria	5-6	(Bordovskiy, 1965; PrahI et al., 1980)
Walker Lake plankton	4.1-4.2	(Bordovskiy, 1965)
Diatom, <i>Asterionella Formosa</i>	8	(Meyers, 1990)
Green alga, <i>Chlamydomonas</i>	9	(Bourbonniere, 1979)
Lake Biwa mixed plankton	7	(Bourbonniere, 1979)
	6-7	(Nakai and Koyama, 1991)
Aquatic Macrophytes		
Greifswalder Bodden saline lagoon	6-44 (mean 17.5)	(Muller and Mathesius, 1999)
Lacustrine Surface Sediments		
Lake Biwa	6	(Meyers and Ishiwatari, 1993a; Meyers et al., 1984)
Lake Michigan	9	(Meyers et al., 1984)
Lake Michigan*	8	(Meyers and Benson, 1988)
Walker Lake	8	(Meyers and Ishiwatari, 1993b)
Pyramid Lake	9	(Qiu et al., 1993)
Lake Baikal	11	(Ho and Meyers, 1994)
Coburn Pond	12	(Hatcher et al., 1982)
Mangrove Lake	15	(Falbot and Johannessen, 1992)
Bosumtwi	14	This thesis
Loch nan Core	12	This thesis
Loch nan Eala	18	
Marine Near Shore/Shelf		
Loch nan Ceall (5 sites)	7-9	This thesis
Loch Sween	15	This thesis
Saline Lagoons		
Rumach tidal pond, (5 sites)	7-8	This thesis
Craiglin Lagoon (2 sites)	11	This thesis

References

- Baker, E. W., and Louda, J. W. (1986). Porphyrins in the geological record. *In* "Biological markers in the sedimentary record." (R. B. Johns, Ed.), pp. 125-226. Elsevier, Amsterdam.
- Baker, E. W., and Palmer, S. E. (1979). Chlorophyll diagenesis in IPOD Leg 47A, Site 397 core samples. *In* "Init. Rep. Deep-Sea Drill. Proj., 47 Pt.1." (U. von Rad, W. B. F. Ryan, and e. al., Eds.), pp. 547-551. U.S. Government Printing Office, Washington.
- Baker, E. W., Palmer, S. E., and Huang, W. Y. (1978). Early and intermediate chlorophyll diagenesis of Black Sea sediments: Sites 379, 380 and 381. *In* "Init. Repts. DSDP, 42, Pt. 2." (D. A. Ross, Y. P. Neprochnov, and e. al., Eds.), pp. 707-715. U.S. Government Printing Office, Washington.
- Bard, E., Rostek, F., Turon, J.-L., and Gendreau, S. (2000). Hydrological impact of Heinrich events in the subtropical Northeast Atlantic. *Science* **289**, 1321-1324.
- Bendle, J. A., and Rosell-Mele, A. (2001). Appraisal of alkenone indices as temperature and salinity proxies in the GIN seas and Holocene millennial-scale sea surface variability on the Icelandic shelf. *In* "In the 7th International Conference on Paleoceanography, Sep 16-22, 2001." Sapporo, Japan.
- Blumer, M., Guillard, R. R. L., and Chase, T. (1971). Hydrocarbons of marine phytoplankton. *Marine Biology* **8**, 183.
- Bordovskiy, O. K. (1965). Accumulation and transformation of organic substances in marine sediments. *Marine Geology* **3**.
- Bourbonniere, R. A. (1979). "Geochemistry of organic matter in Holocene Great Lake sediments." Univ. of Michigan.
- Brassell, S. C. (1993). Application of Biomarkers for delineating marine paleoclimatic fluctuations during the pleistocene. *In* "Organic Geochemistry: Principles and Applications." (M. H. Engel, and S. A. Macko, Eds.), pp. 699-738. Plenum Press, New York.
- Brassell, S. C., Brereton, R. G., Eglinton, G., Grimalt, J., Liebezeit, G., Marlowe, I. T., Pflaumann, U., and Sarnthein, M. (1986a). Palaeoclimatic signals recognized by chemometric treatment of molecular stratigraphic data. *Organic Geochemistry* **10**, 649-660.
- Brassell, S. C., Eglinton, G., Marlowe, I. T., Pflaumann, U., and Sarnthein, M. (1986b). Molecular Stratigraphy: a New Tool for Climatic Assessment. *Nature* **320**, 129-133.
- Brassell, S. C., Eglinton, G., Maxwell, J. R., and Philip, R. P. (1978). Natural background of alkanes in the aquatic environment. *In* "Aquatic Pollutants, Transformations and Biological Effects." (O. Huntzinger, L. H. Lelyveld, and B. C. J. Zoetman, Eds.), pp. 69-86. Pergamon Press, Oxford.
- Caldicott, A. B., and Eglinton, G. (1973). Surface waxes. *In* "Phytochemistry 3, Inorganic Elements and Special Groups of Chemicals." (L. P. Miller, Ed.), pp. 163. Van Nostrand Reinhold, New York.
- Clark, J. R., and Blumer, M. (1967). Distribution of *n*-paraffins in marine organisms and sediments. *Limnology and Oceanography* **12**, 79-87.
- Comet, P. A., and Eglinton, G. (1987). The use of lipids as facies indicators. *Geological Society Special Publication*. *In* "Marine Petroleum Source Rocks." (J. Brooks, and A. J. Fleet, Eds.). Blackwell, Oxford.
- Conte, M. H., and Eglinton, G. (1993). Alkenone and alkenoate distributions within the euphotic zone of the eastern North Atlantic: correlation and production temperature. *Deep-Sea Research I* **40**, 1935-1961.

Chapter 1: Introduction

- Conte, M. H., Eglinton, G., and Madureira, L. A. S. (1992). Long-chain alkenones and alkyl alkenoates as palaeotemperature indicators: their production, flux and early sedimentary diagenesis in the Eastern North Atlantic. *Organic Geochemistry* **19**, 287-298.
- Conte, M. H., Thompson, A., and Eglinton, G. (1994a). Primary production of lipid biomarker compounds by *Emiliania huxleyi*. Results from an experimental mesocosm study in fjords of southwestern Norway. *Sarsia* **79**, 319-331.
- Conte, M. H., Thompson, A., Eglinton, G., and Green, J. C. (1995). Lipid biomarker diversity in the coccolithophorid *Emiliania-huxleyi* (prymnesiophyceae) and the related species *Gephyrocapsa-oceanica*. *Journal of Phycology* **31**, 272-282.
- Conte, M. H., Thompson, A., Lesley, D., and Harris, P. G. (1998). Genetic and physiological influences on the alkenone/alkenoate versus growth temperature relationship in *Emiliania huxleyi* and *Gephyrocapsa oceanica*. *Geochimica et Cosmochimica Acta* **62**, 51-68.
- Conte, M. H., Volkman, J. K., and Eglinton, G. (1994b). Lipid Biomarkers of the Haptophyta. *The Systematics Association Special Volume. In "The Haptophyte Algae."* (J. C. Green, and B. S. C. Leadbeater, Eds.), pp. 351-377. Clarendon Press, Oxford.
- Conte, M. H., Weber, J. C., King, L. L., and Wakeham, S. G. (2001). The alkenone temperature signal in western North Atlantic surface waters. *Geochimica et Cosmochimica Acta* **65**, 4275-4287.
- Cranwell, P. A. (1973). Chain-length distribution of *n*-alkanes from lake sediments in relation to post-glacial environmental change. *Freshwater Biology* **3**, 259-265.
- Cranwell, P. A. (1976). Decomposition of aquatic biota and sediment formation: organic compounds in detritus resulting from microbial attack on the alga *Ceratium hirundinella*. *Freshwater Biology* **6**.
- Cranwell, P. A. (1985). Long-chain unsaturated ketones in recent lacustrine sediments. *Geochimica et Cosmochimica Acta* **49**, 1545-1551.
- Cranwell, P. A., Eglinton, G., and Robinson, N. (1987). Lipids of aquatic organisms as potential contributors to lacustrine sediments-II. *Organic Geochemistry* **11**, 513-527.
- de Leeuw, J. W., van de Meer, F. W., Rijpstra, W. I. C., and Schenck, P. A. (1980). On the occurrence and structural identification of long chain unsaturated ketones and hydrocarbons in sediments. In "Advances in Organic Geochemistry 1979." (A. G. Douglas, and J. R. Maxwell, Eds.), pp. 211-217. Pergamon, Oxford.
- Emerson, S., Stump, C., Grootes, P. M., Stuiver, M., Farwell, G. W., and Schmidt, F. H. (1987). Estimates of degradable organic carbon in deep-sea sediments from ¹⁴C concentrations. *Nature* **329**, 51-53.
- Farrimond, P., Eglinton, G., and Brassell, S. C. (1986). Alkenones in Cretaceous black shales, Blake-Bahama Basin, western North Atlantic. *Organic Geochemistry* **10**, 897-903.
- Ficken, K. J. (1994). "Lipid and sulphur geochemistry of recent sediments from oxic and anoxic environments." University of Newcastle upon Tyne.
- Ficken, K. J., and Farrimond, P. (1995). Sedimentary lipid geochemistry of Framvaren: impacts of a changing environment. *Marine Chemistry* **51**, 31-43.
- Flores, J. A., Sierro, F. J., G., F., Vázquez, A., and Zamarreno, I. (1997). The last 100,000 years in the western Mediterranean: Sea surface water and frontal dynamics as revealed by coccolithophores. *Marine Micropaleontology* **29**, 351-366.
- Freeman, K. H., and Wakeham, S. G. (1991). Variations in the distributions and isotopic compositions of alkenones in Black Sea particles and sediments. *Advances in Organic Geochemistry* **19**, 277-285.

- Gelpi, E., Schneider, J., Mann, J., and Oró, J. (1970). Hydrocarbons of geochemical significance in microscopic algae. *Phytochemistry* **9**, 603-612.
- Giger, W., and Schaffner, C. (1977). Aliphatic, olefinic and aromatic hydrocarbons in recent sediments of a highly eutrophic lake. In "Advances in Organic Geochemistry." (R. Campos, and J. Goni, Eds.), pp. 375.
- Goutx, M., and Saliot, A. (1980). Relationship between dissolved and particulate fatty acids and hydrocarbons, chlorophyll *a* and zooplankton biomass in Villefranche Bay, Mediterranean Sea. *Marine Chemistry* **8**, 299-318.
- Grimalt, J. O., Calvo, E., and Pelejero, C. (2001). Sea surface paleotemperature errors in U-37(K') estimation due to alkenone measurements near the limit of detection. *Paleoceanography* **16**, 226-232.
- Grimalt, J. O., Rullkötter, J., Sicre, M.-A., Summons, R., Farrington, J., Harvey, H. R., Goñi, M., and Sawada, K. (2000). Modifications of the C37 alkenone and alkenoate composition in the water column and sediment: Possible implications for sea surface temperature estimates in paleoceanography. *GEOCHEMISTRY, GEOPHYSICS, GEOSYSTEMS* **1**, Paper number 2000GC000053.
- Grootes, P. M., Stuiver, M., White, J. W. C., Johnsen, S. J., and Jouzel, J. (1993). Comparison of oxygen isotope records from the GISP2 and GRIP Greenland ice cores. *Nature* **366**, 552-554.
- Han, J., and Calvin, M. (1970). Branched alkanes from blue-green algae. *Journal of the Chemical Society Chemical communications*, 1490.
- Harada, N., Shin, K. H., Murata, A., Uchida, M., and Nakatani, T. (2003). Characteristics of alkenones synthesized by a bloom of *Emiliania huxleyi* the Bering Sea. *Geochimica et Cosmochimica Acta* **67**, 1507-1519.
- Harris, P. G., Zhao, M., Rosell-Melé, A., Tiedemann, R., Sarnthein, M., and Maxwell, J. R. (1996). Chlorin accumulation rate as a proxy for Quaternary marine primary productivity. *Nature* **383**, 63-65.
- Harwood, J. L., and Russell, N. J. (1984). "Lipids in Plants and Microbes." Allen and Unwin, London.
- Hatcher, P. G., Simoneit, B. R. T., MacKenzie, F. T., Neumann, A. C., Thorstenson, D. C., and Gerchakov, S. M. (1982). Organic geochemistry and pore water chemistry of sediments from Mangrove Lake, Bermuda. *Organic Geochemistry* **4**, 93-112.
- Hedges, J. I., and Oades, J. M. (1997). Comparative organic geochemistries of soils and marine sediments. *Organic Geochemistry* **27**, 319-361.
- Hedges, J. L., Cowie, G. L., Ertel, J. R., Barbour, R. J., and Hatcher, P. L. (1985). Degradation of carbohydrates and lignins in buried woods. *Geochimica et Cosmochimica Acta* **49**, 701-711.
- Henrichs, S. M. (1992). The early diagenesis of organic matter in marine sediments: Progress and perplexity. *Marine Chemistry* **39**, 119-149.
- Henrichs, S. M. (1993). Early diagenesis of organic matter: the dynamics (rates) or cycling of organic compounds. In "Organic Geochemistry: Principles and Applications." (M. H. Engel, and S. A. Macko, Eds.), pp. 101-117. Plenum Press, New York.
- Herbert, T. D. (2001). Review of alkenone calibrations (culture, water column, and sediments). *Geochemistry, Geophysics, Geosystems* **2**, Paper number 2000GC000055.
- Higginson, M. (1999). "Chlorin Pigment Stratigraphy as a New and Rapid Palaeoceanographic proxy in the Quaternary." University of Bristol.

Chapter 1: Introduction

- Ho, E. S., and Meyers, P. A. (1994). Variability of Early Diagenesis in Lake-Sediments - Evidence from the Sedimentary Geolipid Record in an Isolated Tarn. *Chemical Geology* **112**, 309-324.
- Huang, Y. S., Dupont, L., Sarnthein, M., Hayes, J. M., and Eglinton, G. (2000). Mapping of C-4 plant input from North West Africa into North East Atlantic sediments. *Geochimica Et Cosmochimica Acta* **64**, 3505-3513.
- Huc, A. Y. (1988a). Aspects of depositional processes of organic matter in sedimentary basins. In "Advances in Organic Geochemistry." (L. Mattavelli, and L. Novelli, Eds.). Pergamon, Oxford. *Organic Geochemistry*, **13**, 263-272.
- Huc, A. Y. (1988b). Sedimentology of organic matter. In "Humic Substances and Their Role in the Environment." (F. H. Frimmel, and R. F. Christman, Eds.), pp. 215-243. Wiley, Chichester.
- Hunt, J. M. (1979). "Petroleum Geochemistry and Geology." W.H.Freeman and Company, San Francisco.
- Ikehara, M., Kawamura, K., Ohkouchi, N., Murayama, M., Nakamura, T., and Taira, A. (2000). Variations of terrestrial input and marine productivity in the Southern Ocean (48°S) during the last two deglaciations. *Paleoceanography* **15**, 170-180.
- Ishiwatari, R., Houtatsu, M., and Okada, H. (2001). Alkenone-sea surface temperatures in the Japan Sea over the past 36 kyr: Warm temperatures at the last glacial maximum. *Organic Geochemistry* **32**, 57-67.
- Jackson, L. L., and Blomquist, G. J. (1976). Insect waxes. In "Chemistry and Biochemistry of Natural Waxes." (P. E. Kolattukudy, Ed.), pp. 201-233. Elsevier, Amsterdam.
- Jeffrey, S. W., and Vesk, M. (1995). Introduction to marine phytoplankton and their pigment signatures. In "Phytoplankton pigments in oceanography." (S. W. Jeffrey, R. F. C. Mantoura, and S. W. Wright, Eds.), pp. 37-85. UNESCO, Paris.
- Kawamura, K. (1995). Land-derived lipid class compounds in the deep-sea sediments and marine aerosols from North Pacific. In "Biogeochemical Processes and Ocean Flux in the Western Pacific." (H. Sakai, and Y. Nozaki, Eds.), pp. 31-51. TERRAPUB, Tokyo.
- Kawamura, K., and Ishiwatari, R. (1985). Distribution of lipid-class compounds in bottom sediments of fresh-water lakes with different tropic status, in Japan. *Chemical Geology* **51**, 123-133.
- Kawamura, K., Ishiwatari, R., and Ogura, K. (1987). Early diagenesis of organic matter in the water column and sediments: Microbial degradation and resynthesis of lipids in Lake Haruna. *Organic Geochemistry* **11**, 251-264.
- Keely, B. J., Harris, P. G., Popp, B. N., Hayes, J. M., Meischner, D., and Maxwell, J. R. (1994). Porphyrin and chlorin distributions in a Late Pliocene lacustrine sediment. *Geochimica et Cosmochimica Acta* **58**, 3691-3701.
- Keely, B. J., and Maxwell, J. R. (1991). Structural characterization of the major chlorins in a recent sediment. *Organic Geochemistry* **17**, 663-669.
- Keil, R. G., Montluçon, D. B., Prah, F. G., and Hedges, J. I. (1994). Sorptive preservation of labile organic matter in marine sediments. *Nature* **370**, 549-552.
- Kennicutt II, M. C., and Comet, P. A. (1992). Resolution of sediment hydrocarbon sources: multiparameter approaches. In "Organic Matter: Productivity, Accumulation and Preservation in Recent and Ancient Sediments." (J. K. Whelan, and J. W. Farrington, Eds.), pp. 308-339. Columbia University Press, New York.
- Kjemperud, A. (1986). Late Weichselian and Holocene shoreline displacement in the Trondheimsfjord area, central Norway. *Boreas* **15**, 61-82.

- Li, J., Philip, R. P., Pu, F., and Allen, J. (1996). Long-chain alkenones in Quinghai Lake sediments. *Geochimica et Cosmochimica Acta* **60**, 235-241.
- Louda, J. W., Palmer, S. E., and Baker, E. W. (1980). Early Products of Chlorophyll Diagenesis in Japan Trench Sediments of Deep Sea Drilling Project. Sites 434,435 and 436. *Initial Reports of the Deep Sea Drilling Project* **56,57(2)**, 1391-1396.
- Louda, W. J., Liu, L., and Baker, E. W. (2002). Senescence- and death-related alteration of chlorophylls and carotenoids in marine phytoplankton. *Organic Geochemistry* **33**, 1635-1653.
- Lowe, J. J., and Walker, M. J. C. (1997). "Reconstructing Quaternary Environments (2nd edition)." Longman, Hong Kong.
- Madureira, L. A. S., Conte, M. H., and Eglinton, G. (1995). Early diagenesis of lipid biomarker compounds in North Atlantic sediments. *Paleoceanography* **10**, 627-642.
- Madureira, L. A. S., van Kreveld, S. A., Eglinton, G., Conte, M. H., Ganssen, G., van Hinte, J. E., and Ottens, J. J. (1997). Late Quaternary high-resolution biomarker and other sedimentary climate proxies in a northeast Atlantic core. *Paleoceanography* **12**, 255-269.
- Marlowe, I. (1984). "Lipids as palaeoclimatic indicators." Unpublished Thesis thesis, University of Bristol.
- Marlowe, I. T., Brassell, S. C., Eglinton, G., and Green, J. C. (1990). Long-chain alkenones and alkyl alkenoates and the fossil coccolith record of marine sediments. *Chemical Geology* **88**, 349-375.
- Marlowe, I. T., Green, J. C., Neal, A. C., Brassell, S. C., Eglinton, G., and Course, P. A. (1984). Long chain (n -C₃₇-C₃₉) Alkenones in the Prymensiophyceae. Distribution of Alkenones and lipids and their Taxonomic significance. *British Phycology Journal* **19**, 203-216.
- Meyers, P. A. (1990). Impacts of of regional Late Quaternary climate changes on the deposition of sedimentary organic matter in Walker Lake, Nevada. *Palaeogeography Palaeoclimatology Palaeoecology* **78**, 229-240.
- Meyers, P. A. (1997). Organic geochemical proxies of paleoceanographic, paleolimnologic, and paleoclimatic processes. *Organic Geochemistry* **27**, 213-250.
- Meyers, P. A., and Benson, L. V. (1988). Sedimentary biomarker and isotopic indicators of the paleoclimatic history of the Walker Lake basin, western Nevada. *Organic Geochemistry* **13**, 807-813.
- Meyers, P. A., and Ishiwatari, R. (1993a). The early diagenesis of organic matter in lacustrine sediments. In "Organic Geochemistry, Principles and Applications." (M. H. Engel, and S. A. Macko, Eds.). Plenum Press, New York.
- Meyers, P. A., and Ishiwatari, R. (1993b). Lacustrine organic geochemistry- an overview of indicators of organic matter sources and diagenesis in lake sediments. *Organic Geochemistry* **20**, 867-900.
- Meyers, P. A., Leenheer, M. J., Eadie, B. J., and Maule, S. J. (1984). Organic geochemistry of suspended and settling particulate matter in Lake Michigan. *Geochimica et Cosmochimica Acta* **48**, 443-452.
- Miles, J. A. (1994). "Illustrated Glossary of Petroleum Geochemistry." Clarendon Press, Oxford.
- Muller, A., and Mathesius, U. (1999). The palaeoenvironments of coastal lagoons in the southern Baltic Sea, I. The application of sedimentary Corg/N ratios as source indicators of organic matter. *Palaeogeography, Palaeoclimatology, Palaeoecology* **145**, 1-16.
- Muller, P. J., Kirst, G., Ruhland, G., von Storch, I., and Rosell-Mele, A. (1998). Calibration of the alkenone paleotemperature index U-37(K⁺) based on core-tops from the eastern South Atlantic and the global ocean (60 degrees N-60 degrees S). *Geochimica Et Cosmochimica Acta* **62**, 1757-1772.

Chapter 1: Introduction

- Nakai, N., and Koyama, M. (1991). Die Rekonstruktion von Paläoumweltbedingungen unter Berücksichtigung der anorganischen Bestandteile, des C/N- und des Kohlenstoff-Isotopenverhältnisses am Beispiel des 1400-m-Bohrkerns aus dem Biwa-See. In "Die Geschichte des Biwa-Sees in Japan." (S. Horie, Ed.), pp. 149-160. Universitätsverlag Wagner, Innesbruck.
- Ohkouchi, N., Kawamura, K., Kawahata, H., and Taira, A. (1997). Latitudinal distributions of terrestrial biomarkers in the sediments from the Central Pacific. *Geochimica et Cosmochimica Acta* **61**, 1911-1918.
- Pelejero, C., and Calvo, E. (2003). The upper end of the $U^{K_{37}}$ temperature calibration revisited. *Geochemistry Geophysics Geosystems* **4**, art. no.-1014.
- Philp, R. P. (1985). Biological markers in fossil fuel production. *Mass Spectrometry Reviews* **4**, 1-54.
- Poynter, J. G., and Eglinton, G. (1991). The biomarker concept - strength and weaknesses. *Fresenius Journal of Analytical Chemistry* **339**, 725-731.
- Prahl, F., Herbert, T., Ohkouchi, N., Pagani, M., Repeta, D., Rosell-Melé, A., and Sikes, E. (2000). Status of alkenone paleothermometer calibration: Report from Working Group 3. *Geochemistry Geophysics Geosystems* **1**, Paper number 2000GC000058.
- Prahl, F. G., Bennett, J. T., and Carpenter, R. (1980). The early diagenesis of aliphatic hydrocarbons from Dabob Bay, Washington. *Geochimica et Cosmochimica Acta* **44**, 1967-1976.
- Prahl, F. G., Collier, R. B., Dymond, J., Lyle, M., and Sparrow, M. A. (1993). A Biomarker Perspective on Prymnesiophyte Productivity in the Northeast Pacific-Ocean. *Deep-Sea Research Part I-Oceanographic Research Papers* **40**, 2061-2076.
- Prahl, F. G., and Muehlhausen, L. A. (1989). An organic geochemical assessment of oceanographic conditions at Manop site C over the past 26, 000 years. *Paleoceanography* **4**, 495-510.
- Prahl, F. G., Muehlhausen, L. A., and Zahnle, D. L. (1988). Further Evaluation of Long-Chain Alkenones as Indicators of Paleoceanographic Conditions. *Geochimica Et Cosmochimica Acta* **52**, 2303-2310.
- Prahl, F. G., and Wakeham, S. G. (1987). Calibration of Unsaturation Patterns in Long-Chain Ketone Compositions for Paleotemperature Assessment. *Nature* **330**, 367-369.
- Qiu, L., Williams, D. F., Gvordzov, A., Karabanov, E., and Shimaraeva, M. (1993). Biogenic silica accumulation and paleoproductivity in the northern basin of Lake Baikal during the Holocene. *Geology* **21**, 25-28.
- Rashid, M. A. (1985). "Geochemistry of Marine Humic Compounds." Springer-Verlag, New York.
- Repeta, D. J., McCaffrey, M. A., and Farrington, J. W. (1992). Organic geochemistry as a tool to study upwelling systems: recent results from the Peru and Namibian shelves. In "Upwelling Systems: evolution since the Early Miocene." (C. P. Summerhayes, W. L. Prell, and K. C. Emeis, Eds.), pp. 257-272. Geological Society Special Publication.
- Rosell-Melé, A. (1994). "Long-chain alkenones, Alkyl Alkenoates and Total Pigment Abundances as Climatic Proxy-Indicators in the Northeastern Atlantic." Unpublished Ph.D. thesis, University of Bristol.
- Rosell-Melé, A. (1998). Interhemispheric appraisal of the value of alkenone indices as temperature and salinity proxies in high-latitude locations. *Paleoceanography* **13**, 694-703.
- Rosell-Melé, A. (in press). Biomarkers and proxies of climate change. In "Global changes in the Holocene." (A. Mac Kay, R. W. Battarbee, H. J. B. Birks, and F. Oldfield, Eds.). Edward Arnold, London.

- Rosell-Melé, A., Bard, E., Grimalt, J., Harrison, I., Bouloubassi, I., Comes, P., Emeis, K.-C., Epstein, B., Fahl, K., Farrimond, P., Fluegge, A., Freeman, K., Goñi, M., Güntner, U., Hartz, D., Hellebust, S., Herbert, T., Ikehara, M., Ishiwatari, R., Kawamura, K., Kenig, F., Leeuw, J. d., Lehman, S., Müller, P., Ohkouchi, N., Pancost, R. D., Prahl, F., Quinn, J., Rontani, J.-F., Rostek, F., Rullkotter, J., Sachs, J., Sanders, D., Sawada, K., Schneider, R., Schulz-Bull, D., Sikes, E., Ternois, Y., Versteegh, G., Volkman, J., and Wakeham, S. (2001). Precision of the current methods to measure alkenone relative (UK37) and absolute abundance in sediments: results of an inter-laboratory comparison study. *Geochemistry, Geophysics, Geosystems* **2**, Paper number 2000GC000141.
- Rosell-Melé, A., Carter, J., and Eglinton, G. (1993). Distributions of long-chain alkenones and alkyl alkenoates in marine surface sediments from the North East Atlantic. *22* **3-5**, 501-509.
- Rosell-Melé, A., Carter, J., Parry, A., and Eglinton, G. (1995a). Determination of the UK37 index in geological samples. *Analytical Chemistry* **67**, 1283-1289.
- Rosell-Melé, A., Eglinton, G., Pflaumann, U., and Sarnthein, M. (1995b). Atlantic core-top calibration of the UK37 index as a sea-surface palaeotemperature indicator. *Geochimica et Cosmochimica Acta* **59**, 3099-3107.
- Rosell-Melé, A., Jansen, E., and Weinelt, M. (2002). Appraisal of a molecular approach to infer variations in surface ocean freshwater inputs into the North Atlantic during the last glacial. *Global and Planetary Change* **34**, 143-152.
- Rosell-Melé, A., and Koç, N. (1997). Palaeoclimatic Significance of the Stratigraphic Occurrence of Photosynthetic Biomarker Pigments in the Nordic Seas. *Geology* **25**, 49-52.
- Rosell-Melé, A., Maslin, M. A., Maxwell, J. R., and Schaeffer, P. (1997). Biomarker evidence for "Heinrich" events. *Geochimica et Cosmochimica Acta* **61**, 1671-1678.
- Rosell-Melé, A., Weinelt, M., Sarnthein, M., Koç, N., and Jansen, E. (1998). Variability of the Arctic front during the last climatic cycle: application of a novel molecular proxy. *Terra Nova* **10**, 86-89.
- Sawada, K., Handa, N., Shiraiwa, Y., Danbara, A., and Montani, S. (1996). Long-chain alkenones and alkyl alkenoates in the coastal and pelagic sediments of the northwest North Pacific, with special reference to the reconstruction of *Emiliania huxleyi* and *Gephyrocapsa oceanica* ratios. *Organic Geochemistry* **24**, 751-764.
- Schöner, A., Menzel, D., Schulz, H. M., and Emeis, K. C. (1998). Long-chain alkenones in Holocene sediments of the Baltic Sea - A status report. *Meereswissenschaftliche Berichte, Inst. f. Ostseeforschung* **34**, 122-124.
- Schulz, H. M., Schöner, A., and Emeis, K. C. (2000). Long-chain alkenone patterns in the Baltic Sea - an ocean- freshwater transition. *Geochimica Et Cosmochimica Acta* **64**, 469-477.
- Schulz, H. M., Schöner, A., Emeis, K. C., and Rosell-Melé, A. (1997). Long-chain alkenones in Holocene Sediments of the Baltic Sea. In "18th Intern. Meeting on Organic Geochemistry." pp. 279-280.
- Sheng, G., Cai, K., Yang, X., Lu, J., Jia, G., Peng, P., and Fu, J. (1999). Long-chain alkenones in Hotong Qagan Nur Lake sediments and it's paleoclimatic implications. *Chinese Science Bulletin* **44**, 259-263.
- Sicre, M.-A., Bard, E., Ezat, U., and Rostek, F. (2002). Alkenone distributions in the North Atlantic and Nordic sea surface waters. *Geochemistry, Geophysics, Geosystems* **3**, 10.1029/2001GC000159.
- Sikes, E., and Sicre, M.-A. (2001). The relationship of the tetra-unsaturated C₃₇ alkenone to salinity and temperature: implications for paleo studies. *Geochemistry Geophysics Geosystems* **Submitted**.
- Sikes, E. L., and Sicre, M. A. (2002). Relationship of the tetra-unsaturated C-37 alkenone to salinity and temperature: Implications for paleoproxy applications. *Geochemistry Geophysics Geosystems* **3**, art. no.-1063.

Chapter 1: Introduction

- Sikes, E. L., and Volkman, J. K. (1993). Calibration of alkenone unsaturation ratios (uk37) for paleotemperature estimation in cold polar waters. *Geochimica et Cosmochimica Acta* **57**, 1883-1889.
- Sikes, E. L., Volkman, J. K., Robertson, L. G., and Pichon, J. J. (1997). Alkenones and alkenes in surface waters and sediments of the Southern Ocean: Implications for paleotemperature estimation in polar regions. *Geochimica Et Cosmochimica Acta* **61**, 1495-1505.
- Simoneit, B. R. T. (2002). Biomass burning - a review of organic tracers for smoke from incomplete combustion. *Applied Geochemistry* **17**, 129-162.
- Sonzogni, C., Bard, E., Rostek, F., Lafont, A., Rosell-Mel, A., and Eglinton, G. (1997). Core-top calibration of the alkenone index versus sea surface temperature in the Indian Ocean. *Deep-Sea Research* **44**, 1445-1460.
- Spooner, N., Getliff, J. M., Teece, M. A., Parkes, R. J., Leftley, J. W., Harris, P. G., and Maxwell, J. R. (1995). Formation of mesopyropheophorbide a during anaerobic bacterial degradation of the marine prymnesiophyte *Emiliana huxleyi*. *Organic Geochemistry* **22**, 225-229.
- Spooner, N., Harvey, R., Pearce, G. E. S., Eckardt, C. B., and Maxwell, J. R. (1994). Biological defunctionalisation of chlorophyll in the aquatic environment II: action of endogenous alga enzymes and aerobic bacteria. *Organic Geochemistry* **22**, 773-780.
- Summerhayes, C. P., Kroon, D., Rosell-Melé, A., Jordan, R. W., Schrader, H. J., Hearn, R., Villanueva, J., Grimalt, J. O., and Eglinton, G. (1995). Variability in the Benguela Current upwelling system over the past 70,000 years. *Progress in Oceanography* **35**, 207-251.
- Summons, R. E. (1993). Biogeochemical cycles: a review of fundamental aspects of organic matter formation, preservation and composition. In "Organic Geochemistry: Principles and Applications." (M. H. Engel, and S. A. Macko, Eds.). Plenum Press, New York.
- Sun, M.-Y., Lee, C., and Aller, R. C. (1993). Laboratory studies of oxic and anoxic degradation of chlorophyll-a in Long Island Sound sediments. *Geochimica et Cosmochimica Acta* **57**, 147-157.
- Talbot, M. R., and Johannessen, T. (1992). A high resolution palaeoclimatic record for the last 27,500 years in tropical West Africa from the carbon and nitrogen isotopic composition of lacustrine organic matter. *Earth and Planetary Science Letters* **110**, 23-37.
- Teece, M. A., Getliff, J. M., Leftley, J. W., Parkes, R. J., and Maxwell, J. R. (1998). Microbial degradation of the marine prymnesiophyte *Emiliana huxleyi* under oxic and anoxic conditions as a model for early diagenesis: long chain alkadienes, alkenones and alkyl alkenoates. *Organic Geochemistry* **29**, 863-880.
- Ternois, Y., Sicre, M. A., Boireau, A., Beaufort, L., Miquel, J. C., and Jeandel, C. (1998). Hydrocarbons, sterols and alkenones in sinking particles in the Indian Ocean sector of the Southern Ocean. *Organic Geochemistry* **28**, 489-501.
- Ternois, Y., Sicre, M. A., Boireau, A., Conte, M. H., and Eglinton, G. (1997). Evaluation of long-chain alkenones as paleo-temperature indicators in the Mediterranean Sea. *Deep-Sea Research I* **44**, 271-286.
- Thiel, V., Jenisch, A., Landmann, G., Reimer, A., and Michaelis, W. (1997). Unusual distributions of long-chain alkenones and tetrahymanol from the highly alkaline Lake Van, Turkey. *Geochimica et Cosmochimica Acta* **61**, 2053-2064.
- Thierstein, H. R., Geitzenauer, K., Molino, B., and Shackleton, N. J. (1977). Global synchronicity of late Quaternary coccolith datum levels: validation by oxygen isotopes. *Geology* **5**, 400-404.
- Thompson, S., and Eglinton, G. (1978). The fractionation of a recent sediment for organic geochemical analysis. *Geochimica et Cosmochimica Acta* **42**, 199-207.

- Tissot, B. P., and Welte, D. H. (1978). "Petroleum Formation and Occurrence." Springer-Verlag, Berlin.
- Tromp, T. K., Van Cappellen, P., and Key, R. M. (1995). A global model for the early diagenesis of organic carbon and organic phosphorus in marine sediments. *Geochimica et Cosmochimica Acta* **59**, 1259-1284.
- Tyson, R. V. (1995). "Sedimentary Organic Matter: Organic Facies and Palynofacies." Chapman & Hall, London.
- Volkman, J. K. (2000). Ecological and environmental factors affecting alkenone distributions in seawater and sediments. *Geochemistry, Geophysics, Geosystems* **1**, Paper number 2000GC000061.
- Volkman, J. K., Barrett, S. M., Blackburn, S. I., Mansour, M. P., Sikes, E. L., and Gelin, F. (1998). Microalgal biomarkers: A review of recent research developments. *Organic Geochemistry* **29**, 1163-1179.
- Volkman, J. K., Barrett, S. M., Blackburn, S. I., and Sikes, E. L. (1995). Alkenones in *Gephyrocapsa oceanica*: Implications for studies of paleoclimate. *Geochimica et Cosmochimica Acta* **59**, 513-520.
- Volkman, J. K., Burton, H. R., Everitt, D. A., and Allen, D. I. (1988). Pigment and lipid compositions of algal and bacterial communities in Ace Lake, Vestfold Hills, Antarctica. *Hydrobiologia* **165**, 41-57.
- Volkman, J. K., Eglinton, G., Corner, E. D. S., and Forsberg, T. E. V. (1980a). Long-chain alkenes and alkenones in the marine coccolithophorid *Emiliana huxleyi*. *Phytochemistry* **19**, 2619-2622.
- Volkman, J. K., Eglinton, G., Corner, E. D. S., and Sargent, J. R. (1980b). Novel unsaturated straight-chain C37-C39 methyl and ethyl ketones in marine sediments and coccolithophore *Emiliana huxleyi*. In "Advances in Organic Geochemistry 1979." (A. G. Douglas, and J. R. Maxwell, Eds.), pp. 219-227. Pergamon, Oxford.
- Wakeham, S. G., and Lee, C. (1993). Production, transport, and alteration of particulate organic matter in the marine water column. In "Organic Geochemistry, Principles and Applications." (M. H. Engel, and S. A. Macko, Eds.), pp. 145-169. Plenum Press, New York.
- Williams, M., Dunckerley, D., de Decker, P., Kershaw, P., and Chappell, J. (1998). "Quaternary Environments (2nd edition)." Arnold, London.
- Yen, T. F. (1975). Genesis and degradation of petroleum hydrocarbons in marine environments. In "Marine Chemistry in the Coastal Environment." (T. M. Church, Ed.), pp. 237. ACS Symposium Series 18, Washington D.C.
- Youngblood, W. H., and Blumer, M. (1973). Alkanes and alkenes in marine benthic algae. *Marine Biology* **21**, 163.
- Youngblood, W. H., Blumer, M., Guillard, R. R. L., and Fiore, F. (1971). Saturated and unsaturated hydrocarbons in marine benthic algae. *Marine Biology* **8**, 190.
- Zhao, M., Dupont, L., Eglinton, G., and Teece, M. (2003). n-Alkane and pollen reconstruction of terrestrial climate and vegetation for N.W. Africa over the last 160 kyr. *Organic Geochemistry* **34**, 131-143.
- Zink, K.-G., Leythaeuser, D., Melkonian, M., and Schwark, L. (2001). Temperature dependency of long-chain alkenone distributions in Recent to fossil limic sediments and in lake waters. *Geochimica et Cosmochimica Acta* **65**, 253-265.

2. Experimental Methodology



Cover image is a Varian 3400 gas chromatograph. It was directly coupled to a Finnigan MAT TSQ 700 triple stage quadrupole mass spectrometer and used for the analysis of alkenone and alkyl alkenoate within class distributions.

Contents

2.1.	Introduction	37
2.2.	Wet Chemistry	38
2.2.1.	Chemicals and preparative equipment	38
2.2.1.1.	Glassware	38
2.2.1.2.	Reagents and Solvents	38
2.2.1.3.	Standards	38
2.2.2.	Special Laboratory Equipment	39
2.2.3.	Sample Work-Up	40
2.2.3.1.	Lipid Extraction of Sediment Samples	40
2.2.3.2.	Clean-Up of Sediment Samples – Compound Class Fractionation.	41
2.2.3.3.	Lipid Extraction of Filter Samples	42
2.2.3.4.	Clean-up of filter samples – saponification	43
2.2.3.5.	Derivatisation (all samples)	43
2.3.	Instrumental Analysis	43
2.3.1.	Elemental analysis (Carbon and Nitrogen)	43
2.3.1.1.	Appraisal of elemental analysis (Carbon and Nitrogen)	44
2.3.2.	Total chlorins	44
2.3.2.1.	Appraisal of total chlorins	45
2.3.3.	Gas Chromatography with FID (GC-FID)	45
2.3.4.	Gas Chromatography Coupled to Mass Spectrometry	46
2.3.5.	Gas Chromatography Coupled to Mass Spectrometry with Ammonia Chemical Ionisation (GC-CI-MS)	46
2.3.6.	Identification and Quantification of Analytes	47
2.3.6.1.	GC- FID	47
2.3.6.2.	Appraisal of GC-FID	48
2.3.6.3.	GC-CI-MS	49
2.3.6.4.	Appraisal of GC-CI-MS	50
2.3.7.	GC-CI-MS compared to GC-FID.	51

Tables

Table 2.1: Notation, and properties of solvents and reagents used in experimental procedures.	38
Table 2.2: Notation, and properties of standards used in experimental procedures.	39

(see volume II for figures).

2.1. Introduction

Many of the experimental procedures performed for this thesis were carried out on a regular basis and were used in most study areas. However, some procedures were specific to an individual chapter. These included:

Chapter 3:

- Measurement of sea surface and water column physical parameters by shipboard instruments and CTD/XBT probes.

Chapter 4:

- Tephra analysis.
- Radiocarbon dating.

Chapters 5:

- Isolation basin hydrographic measurements.

As such the details for these procedures are presented as part of the relevant chapter.

The aim of this chapter is to present the methodology for the following organic geochemical procedures:

1. Pre-cleaning of glass-ware and reagents.
2. Solvent extraction of organic matter (lipids).
3. Lipid class clean up and fractionation.
4. Pigment analysis.
5. Lipid biomarker analysis.
6. %TOC analysis.
7. C_{org}/N analysis.

Sampling strategy, sample retrieval and sample storage for studies from the Nordic seas, Icelandic Shelf and N.W. Scotland are described in chapters 3,4 and 5 respectively. The general scheme applied for all organic geochemical analyses is shown in Figure 2.1. All samples for a particular study area underwent comparable treatment. The differences in the methods used for the sediment and filter samples are indicated in the diagram. Blank analyses were routinely carried out to check for contamination of solvents, utensils or apparatus prior to and during the analysis of samples.

2.2. Wet Chemistry

2.2.1. Chemicals and preparative equipment

2.2.1.1. Glassware

Reusable glassware was cleaned between uses according to the following procedure. After removing residues with tap water and detergent, glassware was immersed for 2hrs in a nitric acid (BDH Chemicals Ltd, Poole, U.K.) solution (1%), then rinsed with tap water, immersed for 12hrs in a solution of tap water and Decon soap (Decon Laboratories Ltd, Hove, UK) at 2%, rinsed with tap water and distilled water, dried in an oven and finally fired in a furnace at 450°C. New glassware (excluding volumetric flasks) was fired at 450°C before usage.

2.2.1.2. Reagents and Solvents

Details of general-purpose solvents and reagents used for lipid extraction, work-up and analysis are listed in Table 2.1. Deionised water was used for preparing reagent solutions. Anhydrous crystalline Na₂SO₄ - used as a drying agent - was pre-extracted (soxhlet) with DCM in batches (100g), dried to remove residual water at 80°C and fired at 450°C for 12hrs. KOH pellets, used to prepare solutions of KOH in MeOH (8% by mass), were pre-cleaned by ultrasonication with DCM for 5 mins three times.

Table 2.1: Notation, and properties of solvents and reagents used in experimental procedures.

<i>Name</i>	<i>Shorthand Notation</i>	<i>Grade</i>
2,2,4-trimethylpentane*	<i>iso</i> -Octane	Specified® 99.84% by GC
Acetone*	---	Certified® 99.99% by GC
Hexane*	---	Distol®
Methanol*	MeOH	Distol®
Methylene chloride*	DCM	Certified® 99.99% by GC
Reagents		
NN-Bis (trimethylsilyl) trifluoroacetamide	BSTFA	98%
Nitric acid†		AnalaR® 69- 70.5%
Potassium hydroxide	KOH	Certified® 87.99%
Sodium Sulfate (anhydrous)*	Na ₂ SO ₄	Certified® 99.50%

Source notes: * Fisher Chemicals Ltd, Loughborough, U.K.; †BDH Chemicals Ltd, Poole, U.K.

2.2.1.3. Standards

Standards were prepared by dissolution in *iso*-Octane in glass volumetric flasks on an *ad hoc* basis. Compounds used as internal and recovery standards are listed in Table 2.2 (page 39). Synthetic alkenone standards (C_{37:2} and C_{37:3}) were provided by Prof. J R

Maxwell (University of Bristol) and were used for method development and for calibration of GC-CI-MS and GC-FID response to mass of alkenones in the GC system. A “sediment standard” was used for measuring procedural and analytical precision. This consisted of a homogenised mixture of oceanic sediments mostly (~80%) from the Nordic Seas. A “sediment blank” was used to monitor for contamination of the procedural and analytical methods. This consisted of a homogenised mixture of oceanic sediments and was prepared by combustion in a furnace at 800°C to combust all organic matter.

Table 2.2: Notation, and properties of standards used in experimental procedures.

<i>Name</i>	<i>Notation</i>	<i>Properties</i>
Dotriacontane	nC ₃₂	97% purity
Hexatriacontane	nC ₃₆	97%
2-Nonadecanone	nC ₁₉ O	97%
Octacosane	nC ₂₈	99%
5 α cholestan-3-one	nC ₂₇ O	97%
Cholestane	nC ₂₇	98%
Colesterol	nC ₂₇ OH	99%
1-Docosanol	nC ₂₂ OH	98%

Source notes: all standards were obtained from Sigma-Aldrich, Gillingham, U.K.

2.2.2. Special Laboratory Equipment

a) A MARS 5 microwave accelerated reaction system equipped with Greenchem pressure vessels with 100ml teflon liners was used for microwave assisted extraction (MAE) of sediment samples. MAE allows processing of up to 14 samples (20g maximum weight) simultaneously at controlled temperatures with magnetic stirring.

b) Labconco Centrivap[®] concentrator was attached to a cold trap unit (Labconco Corporation, Kansas City, Missouri 64132, U.S.) and a KNF Laboport[®] vacuum pump (KNF Neuberger, UK). The system eliminates solvent from a sample by evaporation at low pressure. Heating and a centrifugal force could be applied– to speed the process and to prevent bumping, respectively. Typical conditions were negative pressure of 8-10 bar with heating of 45°C applied after 20 minutes to remove methanol. Up to 12 samples could be processed simultaneously.

c) A customised vacuum chamber was attached to a cold trap unit (Labconco Corporation, Kansas City, Missouri 64132, U.S) and an Edwards RV5 Vacuum pump (Edwards, Crawley, Sussex, U.K.). The system eliminates water from a sample by sublimation at low pressure (lyophilization or “freeze drying”). The system had the advantage that hundreds of samples could be freeze-dried during ~48 hrs, unattended.

d) A Büchi rotary evaporator R-114 and water bath B-480 (Büchi Laborstechnik AG, Postfach, Switzerland) were used for the evaporation of large volumes of solvents from round bottom flasks. This was used for filter samples.

e) A vacuum manifold (Alltech, Carnforth, U.K.) with nitrogen blow-down was attached to a water pump and cold trap. This unit was used for the evaporation of small volumes of solvent in GC vials.

f) A Grant Boekel BBA Block heater (Grant Instruments Ltd, Cambridge, U.K.) was fitted with a custom made manifold for nitrogen blow-down. This unit was used as an alternative to the Labconco Centrivap[®] for the elimination of solvent from up to 24 test tube samples.

g) A Dionex High Pressure Liquid Chromatograph (HPLC) (Dionex Corp. Sunnyvale, California USA) consisting of a P 580 series pump (manufacturer) attached to a photodiode array detector (PDA-)100 and an ISCO Foxy Jr[™] fraction collector (ISCO, Inc. Lincoln, Nebraska, USA). The system was operated in off-column mode, for UV-vis spectrophotometry or attached to a column for compound class fractionation.

2.2.3. Sample Work-Up

2.2.3.1. Lipid Extraction of Sediment Samples

- 1) The freeze-dried sediments were broken up and ground to a fine powder in their glass storage vials with a spatula and glass pestle (both implements were rinsed with DCM and dried between samples).
- 2) Weighed aliquots of the crushed samples (0.2-5g) were transferred to pre-weighed Teflon[™] microwave vessels. A known concentration of internal standard and 9ml of DCM/MeOH (3:1) was added.

- 3) Batches of 12 vessels (10 validation samples, 1 blank and 1 “sediment standard”) were loaded into the MARS 5 microwave and extracted at 70°C for 5 minutes.
- 4) After extraction the solvent/sediment mixture was transferred from the microwave vessels to test-tubes and centrifuged (3000rpm for 5min). The solvent supernatant containing lipid extracts was decanted to a test-tube.
- 5) To increase recovery, an additional 3ml of DCM/MeOH (3:1) was added to the extracted sediment and the mixture was shaken. The solvent/sediment mixture was again centrifuged (3000rpm for 5min) and the 2nd supernatant product was added to the test tube containing the first.
- 6) The combined solvent extract was concentrated to dryness by centrifugal evaporator or with nitrogen blow-down.
- 7) To remove residual water, the dry extract was redissolved in 300 μ l of DCM and eluted through a glass pipette containing extracted cotton wool and anhydrous crystalline sodium sulphate. This operation was repeated three times.
- 8) The dried extracts were placed in a vacuum manifold and the solvent was removed under a gentle stream of nitrogen and a light vacuum, and subsequently stored (sealed) at -20°C until pigment analysis or fractionation by HPLC.
- 9) When all the samples for a study area were ready, the organic extracts were re-dissolved in 500-2000 μ l of acetone. An aliquot of each vial of 20 μ l was injected on the HPLC for pigment analysis, collected and combined with the total sample, taken to dryness with nitrogen and stored (sealed) at -20°C ready for HPLC fractionation.

2.2.3.2. Clean-Up of Sediment Samples – Compound Class Fractionation.

Clean-up is necessary to remove those compounds that may interfere during GC analysis of the sample. The approach followed was to isolate a fraction containing the analytes of interest (alkenones, alkyl alkenoates and *n*-alkanes). This was performed by HPLC using a system with consisted of a Thermo Hypersil[®] column (50 × 4.6mm) packed with Lichospher[®] Si100 5 μ m silica, and a Thermo Hypersil[®] guard column. Fractions were collected using a Foxy Jr automatic collector. The system was flushed with MeOH between analytical sessions. A solvent program was adapted from Schulz *et al* (2000). Modifications included the use of a shorter column for faster elution times.

Samples were redissolved in 110 μ l Hexane, drawn into a syringe and injected into the HPLC. Four fractions were collected in test tubes by eluting at 1ml min⁻¹ with:

- 1) hexane (1.375 ml).....aliphatic and cyclic alkanes (nC₃₆ & nC₂₇)
- 2) hexane/DCM (17:3; 3.5 ml).....aliphatic ketones (nC₁₉O, C_{37.2} & C_{37.3})
- 3) DCM (2.25 ml).....cyclic ketones (nC₂₇O)
- 4) Acetone (2.25 ml).....sterols, alcohols and polars (nC₂₂OH, C₂₇OH)

The fractions were concentrated using a centrivap[®]. Fractions 1 and 2 were combined, dried under nitrogen (vacuum manifold), and stored sealed at -20°C until analysis.

The reproducibility of the procedure to fractionate organic extracts was tested with a mixture of standards (hexatriacontane, cholestane, 2-nonadecanone, C_{37.2} alkenone, C_{37.3} alkenone, 5 α cholestan-3-one, cholesterol, 1-docosanol) at a concentration of ~100ng/ μ l for all standards except for the alkenones, which had a combined concentration of ~20ng/ μ l. Recoveries of the fraction classes were greater than 90-98% for all standards with a precision of \pm 3.3% (at 95% confidence). The U₃₇^{K'} value of the synthetic alkenone standards (~0.2) was not significantly altered by the procedure. The accuracy at 2 σ being 0.008 U₃₇^{K'} units (by GC-FID), or 0.11°C using the Muller *et al* (1998) calibration.

2.2.3.3. Lipid Extraction of Filter Samples

- 1) Following removal from storage (at -20°C), a known quantity of an internal standard was added (nC₃₂) to the Whatman GF/F glass fibre filters containing the particulate material.
- 2) The lipids were extracted by ultrasonication with 20ml of DCM/MeOH (3:1, three times) and the supernatant was decanted and filtered through soxhlet extracted cotton wool into 100ml round bottom flasks.
- 3) The solvent extracts were taken to dryness in a rotary evaporator, adding small quantities of acetone to remove residual water (by the formation of an azeotropic mixture).
- 4) The dry extracts was re-dissolved in 3ml DCM/MeOH (3:1) and transferred (repeated \times 3) to test-tubes which were taken to dryness in a centrivap.

2.2.3.4. *Clean-up of filter samples – saponification*

The dry organic extract was hydrolysed in sealed test-tubes (screw tops were Teflon lined) with a 3-ml solution of KOH/MeOH 8% for 36 hrs. The neutral fraction was recovered with 3ml of hexane (three times). The combined hexane extracts were washed with water (previously distilled and solvent extracted), in a test-tube to remove residual KOH traces. The hexane was transferred to a test-tube, and taken to dryness. The extract was re-dissolved in 300 μ l and filtered through a pasteur pipette containing cotton wool and sodium sulphate, dried under nitrogen and stored sealed, at -20°C, until analysis.

2.2.3.5. *Derivatisation (all samples)*

Prior to analysis, sample extracts were derivatised by adding 40 μ l of BSTFA and 100 μ l DCM. The vial containing the sample was sealed and left overnight at room temperature, or for 1 hour at 80°C. Then the solution was dried (vacuum manifold or Centrivap[®]), and stored or re-dissolved in *iso*-octane (10-500 μ l) and spiked with a recovery/GC standard of a known concentration prior to GC analysis.

2.3. Instrumental Analysis

2.3.1. Elemental analysis (Carbon and Nitrogen)

Work up and analysis was performed at the Autonomous University of Barcelona.. Measurements were done using 4x 3.2 mm silver cups (Cat. #D2000) previously cleaned by soxhlet extraction with acetone/hexane mixture (1:1) for 8 hours, then dried in a fume cupboard and heated at 250°C for 12 hours. Approximately 1 mg of the dry sediment was weighed into each silver cup. The cups were placed on the Teflon plate and left overnight in a desiccator or to remove moisture. To remove inorganic carbon (carbonate), samples were saturated with deionised water (1-2 drops were added to each cup using a syringe) and placed in a 2500 ml desiccator containing ~250 ml concentrated hydrochloric acid overnight in a fridge. The acid in the desiccator was replaced with each new batch of samples (ca. 80 samples in a batch). HCl and water were removed by placing samples in an oven at ~50°C for 1.5 hours. After that, the cups were closed and left overnight in a desiccator. Determination of total organic carbon contents (%TOC) and C_{org}/N was performed on CHN elemental analyser EA1108, (Carlo Erba Instruments).

2.3.1.1. Appraisal of elemental analysis (Carbon and Nitrogen)

Procedural and analytical **reproducibility** was determined for the analyses with a homogeneous “sediment standard” (analysed once for every 10 samples to be validated). The average **reproducibility** was:

- 0.25% (2σ) for %TOC
- 1.42 (C_{org}/N units at 2σ) for C_{org}/N

2.3.2. Total chlorins

For total pigment analysis, the organic extract obtained after microwave extraction and before it was cleaned up, was re-dissolved in 500 μ l of acetone and mechanically stirred (Whirlmix). An aliquot of the solution was analysed by absorbance spectrophotometry, using an HPLC system, consisting of Dionex P 580 series pump attached to a Dionex PDA-100 photodiode array detector. The system was operated in off-column mode, with an isocratic flow of acetone (1ml/min) each sample being injected three times. An absorbance spectrum was generated for a range of visible wavelengths ($\lambda = 380\text{nm} - 800\text{nm}$), the absorbance was measured for the whole range at a 5nm bandwidth, using 770nm as a reference wavelength. Data acquisition and integration were made with Dionex Chromeleon PC based software. Integration of the last two absorbance peaks produced an averaged peak area (the first was to flush the system). The procedure followed aims to quantify the total pigment abundance of the sample, not individual pigments. Provided that chlorophylls, their derivatives, and some carotenoids have similar absorption maxima the absorbance measurement at a fixed wavelength of 410nm and 664nm is approximately representative of such total abundance (Rosell-Melé, 1994). The relative magnitude of an absorbance for a given wavelength (A_λ) per gram dry sediment (M) was expressed as P_λ and calculated by:

$$P_\lambda = \frac{(A_\lambda \times DF)}{M} \quad (2.1)$$

Where DF was the dilution factor

The spectrophotometer light source was allowed to stabilise for one hour prior to analysis. Samples from within a core were generally analysed on the same day to avoid errors from any systematic day-to-day shift in instrumental response. If analysis was

needed on subsequent days then several samples from the first set of analyses were taken as references, and analysed at the beginning of the session to check for significant signal drift (i.e. greater than 1 sigma), which in fact was never observed. The analysis of pigments was non-destructive, and the aliquots put through the HPLC system were recovered and combined with the rest of the sample.

2.3.2.1. *Appraisal of total chlorins*

Procedural and analytical **reproducibility** was determined for the analyses with a homogeneous “sediment standard” (analysed once for every 10 samples to be validated). The overall average **reproducibility** had a CV of 12% (at 2σ).

2.3.3. **Gas Chromatography with FID (GC-FID)**

This was performed using a Fisons 8000 Series gas chromatograph fitted with a flame ionisation detector (FID). Aliquots of $1\mu\text{l}$ were injected either manually or by an AS 800 auto-sampler. The split/splitless injector was held at 300°C . Injections were made in splitless mode (purge valve open with 3 ml m^{-1} flow, split valve closed), using the hot needle technique (needle held in injector for 2 s before injection and 5 s after) the injector liner was purged after 20s (purge valve open with 2 ml m^{-1} flow, split valve open with 20mlm^{-1}). Two column types and temperature programs were used during the thesis to perform separation:

- a) An SGE BP-1 fused silica column ($30\text{m} \times 0.25\text{mm}$ i.d., coated with $0.25\mu\text{m}$ film thickness). The oven temperature program was: 60°C held for 1 min, 60°C to 200°C at a rate of $20^\circ\text{C min}^{-1}$, 200°C to 290°C at a rate of 6°Cmin^{-1} , held at 290°C for 30 min, 290°C .to 310°C at a rate of $20^\circ\text{C min}^{-1}$ and held at 310°C for 2 min.
- b) An SGE BP-1 fused silica column ($60\text{m} \times 0.25\text{mm}$ i.d., coated with $0.25\mu\text{m}$ film thickness). The oven temperature program was: 60°C held for 1 min, 60°C to 200°C at a rate of $20^\circ\text{C min}^{-1}$, 200°C to 305°C at a rate of 20°Cmin^{-1} , held at 305°C for 20 min, 305°C to 320°C at a rate of $15^\circ\text{C min}^{-1}$ and held at 320°C for 35 min.

Hydrogen was used as a carrier gas (18psi head pressure). Data acquisition and integration were made with Dionex Chromeleon PC based software.

2.3.4. Gas Chromatography Coupled to Mass Spectrometry

When quantifying *n*-alkanes by GC-FID, the correct allocation of GC peaks was checked for a number of samples by confirming the chemical structure of the individual compounds by mass spectrometry (MS). GC-MS was performed using HP6890 GC coupled to MS5973 MS (HP/Agilent) at the Autonomous University of Barcelona. Injector temperature was 300°C (splitless mode). Separation was achieved with an HP-5MS capillary column (30 m x 0.25 mm internal diameter, film thickness 0.25 µm). Helium was used as a carrier gas (10.58 psi) and the oven-temperature program was 80°C to 150°C at 15°C min⁻¹, 150°C to 300°C at 6°C min⁻¹ and 300°C for 30 min. The mass spectrometer was operated in electron impact mode (ionising energy 70 eV); ion source temperature 250°C, mass range *m/z* 40-800. Individual compounds were identified by comparing mass spectra with those in the literature.

2.3.5. Gas Chromatography Coupled to Mass Spectrometry with Ammonia Chemical Ionisation (GC-CI-MS)

The instrumental set-up was based upon the methods of (Rosell-Melé, 1994). Analysis was performed by the author or by Dr's J. Carter & I. Bull at the N.E.R.C. Organic Mass Spectrometry Facility (School of Chemistry, University of Bristol) using a Varian 3400 gas chromatograph fitted with a septum equipped programmable injector (SPI) which was directly coupled to a Finnigan MAT TSQ 700 triple stage quadrupole mass spectrometer. Aliquots of 1 µl were injected by a CTC A200S autosampler. The SPI was operated in "high performance" non-vaporizing mode, whereby the injector was held at 80°C during injection then rapidly temperature programmed from 80-300°C at 200°Cmin⁻¹. GC separation of the analytes was achieved using a 50m, 0.32mm i.d. fused silica column, with 0.12 µm CPSIL5-CB film thickness (Chrompack). The oven temperature program was: 200-300°C at 6°Cmin⁻¹ with no initial hold time and a final isothermal period of 10 minutes. Hydrogen was employed as a carrier gas with a head pressure of 8psi.

Operating conditions for the mass spectrometer were optimised for sensitivity with respect to the C₃₇ methyl alkenones. The conditions used were: ion source temperature 160°C, electron energy 70eV, electron current 400 µA, and electron multiplier voltage at 1500V with an electrometer gain of 10⁸. Chemical ionisation was achieved using high

purity ammonia (BOC micrographic grade) introduced to the ion source through the conventional CI gas inlet. The pressure inside the ion source was regulated to *ca.* 0.85 Torr, giving rise to a pressure of 4.5×10^{-6} Torr in the vacuum manifold. Ten ions, corresponding to the $[M+NH_4]^+$ species of the analytes (Table 1.1, chapter 1) were monitored by scanning the third quadrupole with a scan rate of 0.1 sec per Dalton. The overall analysis was governed from the TSQ 700 using an Instrument Control Language (ICL) procedure, which controlled the autosampler, the GC and the MS.

Once acquired the data were processed in Durham by the author using PC based Xcaliber software. Integrated peak areas were written into a Microsoft Excel spreadsheet for further processing.

2.3.6. Identification and Quantification of Analytes

The compounds identified and quantified in this thesis consist of several alkenones and alkyl alkenoates spanning the carbon number range C_{37} – C_{38} and - to a lesser extent - *n*-alkanes in the carbon range C_{15} – C_{35} . The IUPAC nomenclature, notation and other details for the alkenones and alkyl alkenoates are given in Table 1.1 (chapter 1.1). The method for identification and quantification was dependent on the method and analysis:

2.3.6.1. GC-FID

Peak identification was based on chromatographic relative retention times. Identification is based on the elution time of each compound compared to a reference compound – either an internal standard injected with the sample or an alkenone standard injected separately using the same conditions – or to several compounds that form a recognisable pattern, according to their relative retention times and abundances. The alkenones form a recognisable pattern in the GC trace, changing only slightly amongst samples from different oceanic locations. The *n*-alkanes typically form a distinctive pattern of a homologous series, and are often the most abundant compound class in the lipid fraction.

Thus, although the relative proportions of the compounds vary, using a specific GC column the elution order is always the same. As a general rule, the elution order in a GC trace, when using the chromatographic conditions described, is a function of the affinity of the compounds for the column and their boiling points. In the case of the alkenones

and alkyl alkenoates, those that have three double bonds are more polar than the diunsaturated species and hence are less retained, elute first, from an apolar column. However, the selectivity of this procedure is not guaranteed. Coelutions of other compounds with the targeted analytes are difficult to recognise, unless the peak shape is distorted. However, this method of analysis remains the most commonly applied in palaeoceanographic studies. Moreover, the samples were cleaned-up to minimize the likelihood of coelutions with the targeted analytes. Representative traces displaying a typical north Atlantic open-ocean pattern for alkenones and *n*-alkanes, and a brackish coastal NW Scottish sample pattern of alkenones and *n*-alkanes, are illustrated in Figures 2.2 and 2.3, respectively.

Quantification of an analyte per gram dry sediment or gram organic carbon (M_A) was made with reference to the mass of internal standard added before extraction (M_{IS}) according to the following calculation:

$$M_A = \frac{(M_{IS}/R_{IS}) \times R_A}{M} \quad (2.2)$$

Where M is the mass of dry sediment or organic carbon, and R_{IS} and R_A are the GC-FID response of the internal standard and target alkenone, respectively (expressed as the integrated peak area).

The percentage recovery (W) of the sample was quantified with reference to mass and response of the internal standard, and to the mass (M_{RS}) and response (R_{RS}) of the recovery or GC standard – added to a sample just before analysis - using the following calculation:

$$W = \frac{M_{RS} \times R_{IS}}{R_{RS} \times M_{IS}} \quad (2.3)$$

2.3.6.2. Appraisal of GC-FID

The **detection limit** of GC-FID was established at ~ 0.5 ng/ μ l. This was determined by injecting a number of increasingly dilute solutions of alkenone standards until the signal obtained was not statistically different (95% confidence) from the background noise. Below 0.5 ng/ μ l the analyte peaks can be detected but not accurately measured. Errors in the estimation of the U_{37}^K index at alkenone concentrations near the limit of

detection (<10ng alkenones) have been reported in the literature (Grimalt et al., 2001; Rosell-Melé, 1994; Rosell-Melé et al., 1995a). The **linearity** of the $U_{37}^{K'}$ index on the GC-FID system used in this study was tested by injecting ($\times 3$) a dilution series of synthetic alkenones with an expected $U_{37}^{K'}$ value of 0.19 ($C_{37:3}:C_{37:2} = \sim 5:1$) (Figure 2.4). At total alkenone concentrations of above 5ng, mean $U_{37}^{K'}$ values were close to predicted (0.20 ± 0.01) with a high precision (C.V. <2.3%), below 5ng there was increasing scatter in the mean $U_{37}^{K'}$ value (± 0.05) and more variable precision (C.V. 1 - 8%) (Figure 2.4). Therefore, during analysis of alkenones for this thesis, by GC-FID, concentrations were monitored and adjusted, whenever possible, so that were above 5ng.

Procedural and analytical **reproducibility** was determined for the analyses with an homogeneous “sediment standard” (analysed once for every 10 samples to be validated). The overall average **reproducibility** for the following measures was:

- Absolute quantification of alkenones & alkenoates = CV of 5.92% (at 2σ).
- Absolute quantification of *n*-alkanes = CV of 9.3% (at 2σ).
- *n*-alkanes $CPI_{25-33} = 0.33$ (2σ of CPI_{25-33} units).
- $U_{37}^{K'} = 0.011$ (2σ of $U_{37}^{K'}$ units), this gives an error of $0.33^{\circ}C$ using the Prahll (1988) calibration.

2.3.6.3. GC-CI-MS

The identification of alkenones by this technique was first performed by Rechka & Maxwell (1988), who performed probe CI spectra of a synthetic $C_{37:3}Me$ standard. Rosell-Melé (1994) later developed the method for identification and integration of the full suite of alkenones and alkenoates using the GC-CI-MS system at Bristol. GC-CI-MS has an advantage over electron impact ionisation in that it barely fragments the target molecule – providing better information on the molecular ion of the compound. The alkenones and alkenoates form an adduct with the reagent ions to form a pseudomolecular ion $[M+NH_4]^+$ through ionic association. The pseudomolecular ion is the base peak – there are also significant ions at $[(M+NH_4)^++1]$ and $[(M+NH_4)^++2]$. It has been suggested that the former may be given by the isotopic contribution of ^{13}C , and the latter by protonation of pseudomolecular ion by the carrier gas (hydrogen) and the $^{13}C_2$ isomer, although these assignments have not been proven (Rosell-Melé, 1994).

An example mass chromatogram of the total ion current and pseudo-molecular ions of the alkenones and alkyl alkenoates is illustrated in Figure 2.5.

Operating conditions for the analytical system and data system (Finnigan MAT ICISI) were supervised by J Carter following the methods of (Rosell-Melé, 1994). The peaks corresponding to the $[M+NH_4]^+$ species of the analytes were integrated to determine the alkenone within-class-distributions.

2.3.6.4. Appraisal of GC-CI-MS

Rosell-Melé et al. (1995b) previously undertook a wide-ranging evaluation and optimization of the GC-CI-MS system used in this thesis. The instrumental set-up for this study used the previously optimised parameters for source temperature and pressure of ammonia chemical ionisation, established by Rosell-Melé et al. (1995b). The **linearity** of the system was measured at the start of analysis, using a dilution series with an expected U_{37}^K value of 0.19 ($C_{37.3}:C_{37.2} = \sim 5:1$) for comparison with the results obtained by Rosell-Melé et al. (1995b). The method was found to provide similar linear quantitation in a range of peak concentrations between 0.02 – 20 ng/ μ l ($20 - 2 \cdot 10^4$ pg/ μ l) (Figure 2.6). At peak concentrations above ~ 20 ng/ μ l the system was overloaded and the measured peaks were truncated. At total alkenone concentrations between $\sim 1 - 12$ ng, mean U_{37}^K values were close to predicted (0.20 ± 0.01) below ~ 1 ng there was an increase in U_{37}^K value (± 0.035). Therefore, during analysis of alkenones for this thesis, by GC-CI-MS, concentrations were monitored and adjusted, whenever possible, so that they did not fall below ~ 1 ng or did not overload the system.

Procedural and analytical **reproducibility** was determined for the analyses with a homogeneous “sediment standard” (analysed once for every 10 samples to be validated). The overall average **reproducibility** for the following measures was:

- $U_{37}^K = 0.017$ (2σ of U_{37}^K units), this gives an error of 0.51°C using the Prah (1988) calibration.
- $U_{37}^K = 0.02$ (2σ of U_{37}^K units), this gives an error of 0.63°C using the Rosell-Melé (summer) (1995c) calibration.
- $\%C_{37.4} = 0.79$ (2σ of %).

The **selectivity** of the method is ensured by identifying each compound from its retention time and the m/z of its pseudo-molecular ion, the abundance of which is used for quantification. Therefore, erroneous peak identification and quantitation are less likely than if only retention time were used.

2.3.7. GC-CI-MS compared to GC-FID.

Rosell-Melé (1995a) have previously compared values of U_{37}^K measured by GC-CI-MS and GC-FID in the same samples. An experiment using synthetic alkenone standards found no statistical difference between the methods. However, in environmental samples greater scatter existed in the relationship, characterised by more frequent overestimation of the $C_{37:3}$ alkenone by GC-FID at high U_{37}^K values (i.e. relatively low abundance of $C_{37:3}$). It was suggested that this may be due to coelution of the $C_{37:3}$ with other compounds, which results in integration errors at low abundances of $C_{37:3}$.

Many of the study areas in this thesis are concerned with the accurate measurement of the relative abundance of the tetra-unsaturated alkenone ($\%C_{37:4}$). This compound typically occurs in very low abundances in mid and low latitudes in open ocean environments. In samples from such an environment the estimation of $\%C_{37:4}$ by GC-FID may be vulnerable to a bias introduced by coeluting compounds. Moreover, this thesis reports some unusually high values of $\%C_{37:4}$ observed in high-latitude open ocean samples. Therefore, utilizing the selectivity of the GC-CI-MS system was important for improving confidence in such novel results. The sea-surface filter samples (chapter 3) were analysed both by GC-CI-MS and GC-FID. The results for values of U_{37}^K and $\%C_{37:4}$ are compared in Figures 2.7 and 2.8 respectively. The plot of the values for U_{37}^K compares with that previously reported by Rosell-Melé (1995a), with both instruments providing similar results but with a slight relative overestimation by GC-FID. The plot of the values for $\%C_{37:4}$ show a linear relationship, but with GC-FID often overestimating $\%C_{37:4}$ - relative to GC-CI-MS - by $\sim 10\%$. This may be due to coelutions of the $C_{37:4}$ with other compounds in the GC-FID system. Something which has been reported as a problem by other workers (Sicre et al., 2002, & Bard pers. comm.) Hence, Figure 2.8 suggests, firstly, the importance of using the GC-CI-MS method in order to obtain accurate $\%C_{37:4}$ values. Secondly, it demonstrates that care should be taken when comparing values of $\%C_{37:4}$ measured by GC-CI-MS to values measured by GC-FID in the literature.

Chapter 2: Experimental methodology

- Grimalt, J. O., Calvo, E., and Pelejero, C. (2001). Sea surface paleotemperature errors in U-37(K') estimation due to alkenone measurements near the limit of detection. *Paleoceanography* **16**, 226-232.
- Muller, P. J., Kirst, G., Ruhland, G., von Storch, I., and Rosell-Mele, A. (1998). Calibration of the alkenone paleotemperature index U-37(K') based on core-tops from the eastern South Atlantic and the global ocean (60 degrees N-60 degrees S). *Geochimica Et Cosmochimica Acta* **62**, 1757-1772.
- Prahl, F. G., Muehlhausen, L. A., and Zahnle, D. L. (1988). Further Evaluation of Long-Chain Alkenones as Indicators of Paleoceanographic Conditions. *Geochimica Et Cosmochimica Acta* **52**, 2303-2310.
- Rechka, J. A., and Maxwell, J. R. (1988). Characterisation of alkenone temperature indicators in sediments and organisms. *Organic Geochemistry* **13**, 727-734.
- Rosell-Melé, A. (1994). "Long-chain alkenones, Alkyl Alkenoates and Total Pigment Abundances as Climatic Proxy-Indicators in the Northeastern Atlantic." Unpublished Ph.D. thesis, University of Bristol.
- Rosell-Melé, A., Carter, J., Parry, A., and Eglinton, G. (1995a). Determination of the UK37 index in geological samples. *Analytical Chemistry* **67**, 1283-1289.
- Rosell-Melé, A., Carter, J., Parry, A., and Eglinton, G. (1995b). Novel procedure for the determination of the Uk37 in sediment samples. *Analytical Chemistry* **67**, 1283-1289.
- Rosell-Melé, A., Eglinton, G., Pflaumann, U., and Sarnthein, M. (1995c). Atlantic core-top calibration of the UK37 index as a sea-surface palaeotemperature indicator. *Geochimica et Cosmochimica Acta* **59**, 3099-3107.
- Schulz, H. M., Schoner, A., and Emeis, K. C. (2000). Long-chain alkenone patterns in the Baltic Sea - an ocean- freshwater transition. *Geochimica Et Cosmochimica Acta* **64**, 469-477.
- Sicre, M.-A., Bard, E., Ezat, U., and Rostek, F. (2002). Alkenone distributions in the North Atlantic and Nordic sea surface waters. *Geochemistry, Geophysics, Geosystems* **3**, 10.1029/2001GC000159.

3. Distribution of long-chain alkenones in the Nordic Seas



Cover image - The RRS James Clark Ross - steaming through sunshine and "pancake" ice - approaches the ice pack in the East Greenland Current, during cruise JR51 (August 2000). On this campaign samples, with remarkably high %C_{37:2} values, were collected from polar waters.

Contents

3.1.	Introduction _____	56
3.2.	Aim and Objectives _____	58
3.3.	Background _____	59
3.3.1.	The contemporary physical and ecological oceanography of the Nordic Seas_	59
3.3.1.1.	Physical Oceanography _____	59
3.3.1.2.	Ecological Oceanography _____	62
3.4.	Study Specific Experimental _____	64
3.4.1.	Filter samples, retrieval and storage _____	64
3.4.2.	Cores _____	66
3.5.	Results & Discussion _____	70
3.5.1.	Summary of <i>in situ</i> oceanographic conditions _____	70
3.5.2.	Alkenone Distributions in the Nordic Seas _____	72
3.5.2.1.	Absolute abundance _____	72
3.5.2.2.	%C _{37:4} _____	73
3.5.2.3.	U ^K ₃₇ and U ^K ₃₇ ' _____	84
3.5.2.4.	C38 alkenones _____	88
3.5.3.	Alkenone distributions in core PL-96-126 – further appraisal of %C _{37:4} as a palaeo-SSS indicator. _____	89
3.6.	Conclusions _____	91

Tables

Table 3.1:	Typical ranges of physical properties for the main surface water masses of the Nordic Seas. _____	60
Table 3.2:	JR44 filter sample information – collection and analytical data. _____	68
Table 3.3:	JR51 filter sample information – collection and analytical data. _____	70
Table 3.4:	Summary of Nordic Seas alkenone degradation studies. _____	81
Table 3.5:	Results of species counts of coccolithophores and coccospheres for JR51 filters. _____	83

(see volume II for figures)

3.1. Introduction

Over the last decade, the alkenone unsaturation index U_{37}^K has been widely adopted by palaeoceanographers as a proxy to estimate past SSTs. This index measures the relative abundance of the di- and tri-unsaturated C_{37} alkenones ($C_{37:2}$, $C_{37:3}$). The tetra-unsaturated compound ($C_{37:4}$) is not incorporated in U_{37}^K , this is practical because $C_{37:4}$ is rarely found in measurable quantities in temperate to low latitudes. Moreover, a number of studies have demonstrated that while the temperature response of $C_{37:2}$ and $C_{37:3}$ is relatively linear, the environmental controls on the biosynthesis of $C_{37:4}$ are less certain (e.g. Freeman and Wakeham, 1991; Prahl and Muehlhausen, 1989; Prahl and Wakeham, 1987; Rahman, 1995; Rosell-Melé, 1998; Sikes and Sicre, 2002).

In the northern North Atlantic, SSTs reconstructed from alkenone indices are subject to increasing error in regions where present SST falls below $\sim 6^\circ\text{C}$ (annual mean 0-30m) (Levitus, 1982; Rosell-Melé et al., 1993). Coincidentally, in these sub-polar and polar regions the abundance of $C_{37:4}$, relative to the other C_{37} alkenones ($\%C_{37:4}$) increases significantly (Rosell-Melé, 1998). Globally, the main source organism of alkenones is assumed to be *Emiliania huxleyi*, however this species is rare in polar and arctic waters (Baumann et al., 2000) and the dominant polar coccolithophore *Coccolithus pelagicus* is not known to produce alkenones. Alkenone patterns, characterised by high values of $\%C_{37:4}$, are found in lacustrine sediments, where they are produced by an unknown (but non-*E. huxleyi*) biological source (e.g. Cranwell, 1985; Zink et al., 2001). Therefore, it is uncertain whether the biological precursor of the oceanic cold water alkenones (characterised by high $\%C_{37:4}$) is *E. huxleyi* or a currently unknown algae.

Recent studies have suggested that $\%C_{37:4}$ in high northern latitudes may have a relationship to salinity (Harada et al., 2003; Rosell-Melé, 1998; Rosell-Melé et al., 2002; Sicre et al., 2002) and several studies have attempted to apply the $\%C_{37:4}$ measurement

downcore as a proxy for palaeo-salinity (Bard et al., 2000; Rosell-Melé, 1998; Rosell-Melé et al., 2002). The prospect of a proxy that can estimate palaeo-salinity changes or identify meltwater events is highly desirable. This is especially true for the Nordic seas where winter sea surface densification and formation of deep-water masses play a key role in driving the global thermohaline circulation.

Further investigation of alkenone distributions in the Nordic seas surface waters is necessary, as previous North Atlantic water column studies have reported no (Conte and Eglinton, 1993; Thomsen et al., 1998) or very few (Sicre et al., 2002) results from the Arctic and Polar water masses. The advantage of studying water column particulate organic matter (POM) is that alkenone systematics can be directly compared to ocean parameters *in situ*. Moreover, an advantage of filtered seawater samples – compared to sediment traps - is that it enables a relatively large number of samples to be collected and a large geographic area to be covered. However, the approach is limited in that it can only provide a temporal and spatial “snap shot” measurement of environmental conditions, rather than an integrated seasonal and depth signal. Furthermore, in the case of senescent bloom material, potential temporal offsets exist between the time of alkenone synthesis and collection/measurement of temperature.

Each approach has advantages and limitations, therefore it is important to combine and compare data obtained from water column POM, sediment and culture studies, in order to constrain the processes that set alkenone distributions in ocean sediments. In the Nordic Seas, a more comprehensive water column POM survey is needed to compliment the extensive surface sediment studies of alkenone distributions by Rosell-Melé (1998; 1995).

3.2. Aim and Objectives

The overall aim is to clarify, delimit and extend the application of alkenone proxies for palaeoceanographic studies in sub-polar to polar regions, with particular reference to alkenone distributions in sea surface POM. Samples from across the spectrum of property gradients (i.e. covering all the characteristic water masses) of the Nordic seas were obtained during two cruises of the RRS *James Clark Ross* (JCR) in 1999 & 2000. A special advantage of the JCR is the ice strengthened hull (see appendix I, Plate Ia). This facilitates sampling in environments such as the East Greenland Current, under conditions of up to ~80% sea ice (see appendix I, Plates Ib & Ic).

The main objectives were:

- To investigate the relationship between the relative abundance of alkenone distributions (especially %C_{37:4}) in sea surface POM to sea surface variables and coccolithophore biogeography in the Nordic Seas.
- To compare alkenone distribution data from sea surface POM samples with previously reported sedimentary data from the Nordic Seas.
- To place the Nordic Seas sea surface POM data in a global context.
- To compare alkenone distributions with palaeoceanographic reconstructions of SST, SSS and ice-cover derived from dinoflagellate cyst (dinocysts) assemblages in the same core.

3.3. Background

The background for biomarker and organic matter applications is given in chapter 1. The background in this section is a brief outline of the contemporary physical and ecological oceanography of the Nordic Seas, and is relevant to this chapter (3) and chapter 4. The classic work on the Nordic Seas region is *The Norwegian Sea* by Helland-Hansen and Nansen (Helland-Hansen and Nansen, 1909). Several syntheses have been written since, work up to 1945 is summarised by Sverdrup *et al* (1946), from 1945 to 1963 by Lee (1969), from 1972-1985 by Hopkins (1991). Comprehensive reviews of the physical oceanography have been made by Coachman and Aagaard (1974) and by Johannssen (1986) and the hydrography of the water masses was reviewed by Swift (1986). In the last few decades, several reviews have concentrated on the formation of deep-water masses in the Nordic Seas and the exchange of water across the Greenland-Scotland ridge; processes that play a key role in the global thermohaline circulation (e.g. Dickson and Brown, 1994; Hansen, 1985; Hansen and Østerhus, 2000; van Aken and Becker, 1996). Longhurst (1998) recently reviewed the region with special reference to the control of the physical oceanography on pelagic biogeography.

3.3.1. The contemporary physical and ecological oceanography of the Nordic Seas

3.3.1.1. Physical Oceanography

The Nordic Seas are an area of strong east to west hydrographic gradients; characterised by seasonal and spatial variations in the physical properties of the surface waters (SST, SSS), sea ice distribution and deep water formation. The present surface current system is characterised by the interaction of relatively warm (6 -15°C) and saline (>35 psu) Atlantic source waters and cold (<5°C), less saline (<34.4 psu) polar source waters. Table 3.1 (page 60) gives typical properties for the main surface water masses. Figures 3.1 and 3.2 illustrate the surface to near surface circulation and deep water flows respectively. Figure 3.3 illustrates the major oceanic fronts. The bathymetry is also illustrated in Figures 3.1 -3.3. The bottom topography of the Nordic seas region strongly affects the complex circulation and distribution of the water masses.

Comparison of the figures highlights the correlations between topography, circulation and frontal systems. Current and water mass acronyms used in this thesis are summarised in Figures 3.1 - 3.2.

Table 3.1: Typical ranges of physical properties for the main surface water masses of the Nordic Seas.

<i>Acronym</i>	<i>Name</i>	<i>Temperature range (summer)</i>	<i>Salinity range (psu)</i>
NAW	North Atlantic Water	~6°C →	35.30 →
MNAW	Modified North Atlantic Water	7.0 → 8.5°C	35.10 → 35.30
NCW	Norwegian Coastal Water	5 → 17°C	~30.0 → 35.0
AW	Arctic Water	~3 →	34.4 → 35.0
PW	Polar Water	-1.5 → 5°C	< 34.4, in summer as low as 29psu

Sources: (Conkright et al., 1998; Hansen and Østerhus, 2000; Johanessen, 1986; Swift, 1986)

The Atlantic inflow reaches the Nordic seas via the Greenland-Scotland ridge and has several branches (Figure 3.1). The North Atlantic Current (NAC) sends one branch north; part of which passes west of Iceland (the Irminger Current, IC) (Stefánsson, 1962). The IC continues through the east of the Denmark Strait, where some of the water is diverted into a branch turning southwestwards to run parallel to the East Greenland Current, so that only a part ends up in the North Icelandic Current (NIIC) (Dietrich et al., 1975). This current flow is maintained even in winter when the proximity of the East Greenland Polar Front (PF) gives rise to strong property gradients (Johanessen, 1986). On its path further eastwards, the NIIC feeds the North Icelandic shelf area with relatively warm, saline water which, however, rapidly loses its Atlantic character (heat and salt) so that the percentage of Atlantic water reduces to less than 30% by the northeastern corner of Iceland (Stefánsson, 1962).

Another more pronounced branch of Atlantic water flows southeast of Iceland splitting into lesser currents - flowing over the Rockall-Hatton Plateau and east of the Faroes (Hansen and Østerhus, 2000). This is joined in the east by the Continental Coastal Current (CSC), whose waters are slightly warmer and more saline, a result of having

some Mediterranean input and having not been partially mixed with northern waters in the Gulf Stream (Hansen and Østerhus, 2000).

The advection north of Atlantic water has a profound influence on the Northern seas and climate of Western Europe, releasing a large amount of sensible heat ($\sim 5 \times 10^{21}$ cal/yr) to the atmosphere (Broecker and Denton, 1989). The NAC carries Atlantic source water far north, even as far as the Kara Sea (Dickey et al., 1994). To the west, it forms a frontal jet (nomenclature varies; in this case the Arctic Front) and to the east, it is bounded by the salinity dominated Norwegian Coastal Front (NCF) (Johanessen, 1986; Saetre and Mork, 1981) (Figure 3.3). This front is an unstable eddy field formed between the NAC and the Norwegian Coastal Current (NCC). The source of the latter is the return of Atlantic water heavily diluted by the brackish outflow from the Baltic Sea and runoff from the Norwegian fjords and from Western Europe (Johanessen, 1986).

These two components flow north, being modified by eddy mixing at the front as they proceed (Johanessen, 1986). Off North Cape, most water from the combined flow passes eastwards into the southern Barents sea, while some continues north, contributing to the West Spitsbergen Current (WSC) (Hopkins, 1991) (Figure 3.1). The water passing into the southern Barents Sea feeds the gyral circulation, which returns westwards to the south of Spitsbergen (Johanessen and Foster, 1978).

Polar waters enter the upper layers of the region from the Arctic Ocean (Swift, 1986). The East Greenland Current (EGC) carries polar water southward and out through the Denmark Strait (Figure 3.1), while two branches transport small amounts eastward into the interior basins; the Jan Mayen Current (JMC), to the north of the Jan Mayen Fracture Zone, and the East Icelandic Current (EIC), which flows southeast along the continental slope northeast of Iceland (Figure 3.1) (Swift, 1986).

Between the regions dominated by the polar and Atlantic source waters, lies a region where the two source waters mix in two anticlockwise gyres. These regions are characterised by upper layer waters that are relatively cold (0 to 4°C) and saline (34.6 to 34.9 psu) (see Figure 3.1). This is Swift's (1986) Arctic Province (or Arctic Waters AW). Its upper waters are warmer and more saline than the polar water in the East

Greenland Current though still cooler and less saline than the Atlantic water. Moreover, the waters of this region are denser than either of the surface source-water masses ($\sigma_t = 27.5$ to $28+$) (Swift, 1986).

This dense AW contributes greatly to the vertical instability of the region; so that winter cooling and wind mixing cause strong deep convection (Dickson and Brown, 1994). Deep convection occurs most prominently at the locations illustrated in Figure 3.2 (Hansen and Østerhus, 2000). The processes of formation are complex and vary with location and time. It is now recognised that there are two distinct mechanisms for creating deep water. In the Greenland Sea (in winter) surface water may be convected directly to the bottom waters masses by deep convection in the open ocean (e.g. Aagaard et al., 1985). The second formation mechanism involves dense water being formed in the shallow shelf regions surrounding the Arctic Ocean, through brine rejection during the formation of sea-ice (e.g. Aagaard et al., 1985; Midttun, 1985). The deep water and intermediate water masses accumulated in the Norwegian and Greenland basins overflows, intermittently, the submarine ridge. Overflow occurs at various specific locations – through the Denmark Strait, between Iceland and the Faeroe Islands and through the Faeroe-Shetland Channel (Brown et al., 1998; Hansen and Østerhus, 2000).

The complex systems of warm and cold currents in the Nordic Seas are arbitrarily delimited by a number of ocean fronts, which reflect strong quasi-permanent boundaries in the temperature and salinity fields. The fronts are convergence zones of cold, less saline water with warm saline water such that the strong changes in the temperature and salinity compensate each other with regard to density (Johannessen, 1986). Figure 3.3 illustrates the five distinct fronts found in the region as defined (geographically) by Johannessen (1986). It should be noted that a problem with the graphical representation of fronts and of currents - such as those in Figures 3.3 - is that they appear both misleadingly linear and permanent. Considerable water mass exchange of course takes place across fronts through small and mesoscale eddies (e.g. Allen and Smeed, 1996; Allen et al., 1994; Johannessen et al., 1983; NORSEX_Group, 1983).

3.3.1.2. Ecological Oceanography

The water masses and fronts identified in Figures 3.1 and 3.3, broadly coincide with the boundaries of ecological provinces of the region (Longhurst, 1998). These provinces are

distinguished by *inter alia*: data collected for phytoplankton productivity and herbivore and zooplankton ecology, which is controlled by seasonal insolation, mixed layer depths, brackish water stratification and pycnocline- and nutricline -depths.

The ecology of the polar waters is distinctive (from lower latitudes) as phytoplankton growth is primarily controlled by light availability and temperature, rather than by nutrient availability (Longhurst, 1998). Diatoms and haptophytes are the most abundant and important constituents of the nano- and micro-plankton of polar waters (Marchant and Thomsen, 1994). There is a relatively small – compared to warmer regions - contribution from picoplankton ($< 3.0 \mu\text{m}$ diameter) (Trotte, 1985). It is principally the effects of the freeze-thaw cycle that control the pelagic ecology. Thawing sea ice in spring releases fresh water to create strong density gradients, whereas freezing in the autumn results in brine rejection, causing instability and deep mixing. Therefore, in the early spring the water column is mixed, nutrient levels are high and net carbon fixation is not yet established (Smith and Brightman, 1991). In late spring, the thawing and receding ice edge results in strong stability conditions conducive to phytoplankton blooms (increase in standing stock) of extremely high productivity ($15\text{--}700 \text{ mg C/m}^3/\text{day}$) (Longhurst, 1998). The colonial stage of the haptophyte *Phaeocystis pouchetti* commonly dominates the phytoplankton of the ice-marginal zone (Marchant and Thomsen, 1994). *Coccolithus pelagicus* is the most commonly reported coccolithophore in polar waters, occurring at temperatures between $0 - 10^\circ\text{C}$ as far north as 86° (Baumann et al., 2000; Honjo, 1990), while recent work has found a large number of lightly calcified coccolithophore species in polar waters (Marchant and Thomsen, 1994, and refs. therein). The only known regional alkenone producer *E. huxleyi* is reported as rare in regions not influenced by Atlantic surface water (Winter et al., 1994). Copepod species dominate the herbivore and mesozooplankton communities with protists only accounting for 10-20 % of biomass (Longhurst, 1998).

In the Arctic waters, as in the Polar regions, the effect of the seasonal freeze-thaw cycle is important - although the occurrence of spring brackish layers is less pronounced - and is spatially patchy (Longhurst, 1998). The seasonal production patterns also resemble the polar waters in that production tracks the irradiance cycle. However, a major difference is the greater wind stress, inherent pycnocline instability and deep winter mixed layer depth ($\sim 500\text{m}$) of the Arctic waters. This has implications for the seasonal ontogenetic migrations of the major herbivores (copepods), which may be

disturbed by deep water formation and suffer massive sporadic recruitment failures (Richter, 1994). The colonial haptophyte *P. pouchetti* is the dominant spring bloom organism (Smith et al., 1991). The most common coccolithophore is generally *C. pelagicus*, followed by *E. huxleyi* (Andruleit, 1997). Higher abundances ($100-500 \times 10^3$ cells/l) for *E. huxleyi* than *C. pelagicus* ($10-100 \times 10^3$ cell/l) have been reported in the arctic waters around Jan Mayen, but the species is much less common in the Greenland Sea (Baumann et al., 2000).

In the Atlantic type waters of the Nordic seas, wintertime deep mixing is more moderate than in the Arctic waters. Rapid near surface stabilization occurs in April and May and induces phytoplankton blooms ($\sim 3-4$ mg chl/m³), typically diatoms, followed by the colonial form of *P. pouchetti* and *E. huxleyi*, (Longhurst, 1998; Rey, 1981; Sakshaug and Holm-Hansen, 1984). In the mixed layer, chlorophyll values remain relatively high throughout the summer (>2.0 mg chl/m³) (Longhurst, 1998). *E. huxleyi* is the dominant coccolithophorid followed by *Coccolithus pelagicus* and *Algirosphara robusta* may also be common (Andruleit, 1997; Winter et al., 1994). In late summer blooms of coccolithophores are consistently observed in surface colour images south of Iceland (Brown and Yoder, 1994). Copepods (especially genus *Calanus*) dominate the herbivore and mesozooplankton and also perform seasonal depth migration as in the Arctic province (Longhurst, 1998).

3.4. Study Specific Experimental

3.4.1. Filter samples, retrieval and storage

Filters of seawater POM were obtained onboard the RRS *James Clark Ross* during summer cruises in 1999 (25/7/99 – 28/8/99) and 2000 (28/7/00 – 29/8/00). The cruises were funded by NERC under the Arctic Ice and Environmental Variability (ARCICE) thematic programme. Sample details are given in Tables 3.2 and 3.3 (page 68 & 70), the cruise tracks and sample locations for both cruises are illustrated in Figure 3.4 and Figure 3.5. Uncontaminated seawater was continuously pumped to the ship's laboratories from a supply tube beneath the hull. The depth of the tube inlet beneath the sea surface was approximately 6m depending on ship's load. The supply tube was extended by a further 30cm below the hull, except in ice conditions, when it was flush.

The POM was filtered from seawater collected in the laboratory from the uncontaminated supply. Water column data (SST, SSS, fluorescence) was logged throughout the cruise using the ship's oceanlogger system. The oceanlogger system is a PC-based logging system, with the primary purpose of logging measurements from the ship's continuously-run data sources. Accordingly, it draws data from the ship's pumped uncontaminated supply, plus assorted meteorological parameters. Seawater temperature was measured by a probe mounted near the hull close to the inlet. Salinity was measured, from the uncontaminated supply, by a SeaBird SBE45 thermosalinograph located in the prep room. Fluorescence (Chl. *a* ug/l) was measured by a Turners Instruments fluorometer, also located in the prep room. For each sample collected, the ship's position at start and finish was taken from a Trimble 4000DS differential GPS receiver located on the bridge and the time (GMT) noted. The high resolution oceanlogger data (measurements made every 1s) was converted to files of 1 minute averages. The averaged files were then used to derive Ocean Data View cruise tracks and sea surface property maps and to calculate average measurements of SST and SSS for the period (~20mins) when each POM sample was collected.

During JR44, the salinity readings from 2/8/1999 onwards (filter sample no.13) were considered erroneous due to a malfunction of the conductivity sensors (Bacon and Yelland, 1999). Therefore, for the remaining filter samples, the salinity was taken from the CTD profile obtained at the same station. The operator and work-up methods of the POM samples differed between the two cruises, the details are given below:

a) Cruise JR44 (ARCICE 1999)

Samples were obtained between 25/7/99 – 28/8/99. A seawater sample (volume 110-140 l) was collected into carboys. A concentrated particulate suspension of approximately 1 l in volume was obtained from the seawater sample using a Millipore Pellicon tangential flow filtration system, fitted with two Millipore low protein binding "Durapore" microporous filter membrane cassettes in parallel.

The POM was then isolated from suspension by filtration through a Whatman 70 mm GF/F glass fibre filter within a standard evacuated Buchner funnel/flask apparatus. The vacuum required was provided by a Brook Crompton Betts Model 8524 PVH-A12 corrosion resistant pump. The dry particulate laden filters (~2 per station) were then

placed into a clean 50 ml Teflon – capped Pyrex sample bottle using clean forceps. A 40 ml mixture of DCM/MeOH (3:1) was added and the sample was then sealed and stored in the ship's -20°C refrigerator, until transfer to university refrigerators (-20°C) for storage prior to lipid extraction and analysis.

b) Cruise JR51 (ARCICE 2000)

Samples were obtained on this cruise by the author between 28/7/00 – 29/8/00. Using the ship's underway uncontaminated seawater supply system, a seawater sample (volume 60-153 litres) was collected into carboys. The particulate material was then isolated directly from suspension by filtration through a manifold consisting of 5 Buchner funnel/flask apparatus each holding a Whatman 70 mm GF/F glass fibre filter (pre-cleaned by firing at 450°C) attached to a 20litre glass vacuum chamber. The chamber was evacuating by using a KNF Laboport® vacuum pump.

From each station one filter was retained in a petri-dish for later identification of the coccolithophores. The remainder of the filters were prepared for organic geochemical analysis. The particulate laden filters were examined under binocular microscope and any large copepods were removed with a fine pick. The filters for a station were then placed into a clean 50 ml polypropelene capped (aluminium foil lined) glass bottle using clean forceps. A 100 ml mixture of DCM/MeOH (3:1) was added and the sample was then sealed and stored in the ship's -20°C refrigerator, until transfer to university refrigerators (-20°C) for storage prior to lipid extraction and analysis.

3.4.2. Cores

The boxcores analysed in this study were part of a series of cores obtained by successive cruises of the German vessel the *Meteor* between 1987 and 1989. The cores were sub-sampled on board by A. Rosell-Melé, at 1cm intervals - for the top 5cm - and at 5cm intervals below 5cm. The sub-samples were stored frozen or in a cool room until being freeze-dried. The samples used in this study had been freeze-dried and stored sealed at room temperature since ~1993, prior to analysis for this thesis.

Core PL-96-126 was collected by gravity corer from onboard the R/V *Professor Logachev* in 1996. The core was sub-sampled on board at 10cm intervals by Anne deVernal and colleagues. Sub-samples were stored in a cool room and subsequently freeze-dried prior to analysis.

Table 3.2. JR44 filter sample information – collection and analytical data. “Vol. Lipids” is the volume (in litres) of sea surface seawater filtered for lipid extraction, SST, SST, SSS and Fluorescence were measured using the ships data logging systems except where indicated (*table continued overleaf*).

Sample	Coordinates		Date (1999)	GMT	Vol. Lipids (L)	SST (°C)	SSS (PSU)	Fluorescence (units ?)	Σ LCK (ng/L)	U_{37}^K	%C _{37:4}	C _{37:4} Et/Me	Σ C ₃₇ / Σ C ₃₈
	Latitude (N)	Longitude (E)											
1	62°21.36	3°20.60	24/07	14:13	140	13.2	34.73	6.4	54.5	0.43	0	0.96	1.42
2	64°17.57	5°40.33	25/07	08:39	140	12.7	34.72	9.1	43.8	0.35	0	2.39	1.38
3	65°08.46	8°08.64	26/07	10:50	140	11.9	34.21	26.2	16.4	0.28	4.50	1.08	1.13
4	67°00.32	6°74.48	27/07	08:28	140	11.0	35.12	24.9	7.7	0.36	0	2.31	2.07
5	68°20.02	6°37.71	27/07	13:57	140	10.9	35.12	25.8	2.6	0.34	0	1.92	1.76
6	69°57.68	4°55.16	28/07	10:26	140	9.6	35.10	19.5	59.9	0.23	3.22	1.03	1.44
7	70°79.43	2°71.61	29/07	08:48	140	9.3	35.06	24.9	36.5	0.25	0.85	1.16	1.47
8	71°13.66	2°15.05	29/07	13:35	140	9.3	35.17	21.7	0	0.19	2.50	0.99	1.38
9	72°55.85	-0°39.61	30/07	09:47	130	6.6	34.92	5.1	13.4	0.19	0.76	1.65	1.75
10	73°07.34	-1°47.05	30/07	15:38	140	5.4	34.72	4.0	0	-	-	-	-
11	74°13.35	-3°02.23	31/07	12:21	140	5.1	34.71	7.7	0	-	-	-	-
12	75°56.82	-7°75.95	01/08	13:10	140	5.0	34.61	9.4	0	-	-	-	-
13	76°03.46	-9°24.27	02/08	10:05	140	0.3	30.71*	10.1	0	0.12	72.80	2.09	1.98
14	76°37.29	-10°45.94	02/08	15:13	140	2.1	30.69*	7.8	6.9	0.16	76.91	1.33	2.18
15	80°41.69	5°54.62	10/08	13:07	140	4.9	34.41*	69.1	7.9	0.20	10.46	1.77	1.42
16	79°06.56	1°02.52	13/08	13:15	140	2.1	34.28*	10.9	3.0	0.17	40.09	1.39	1.12
17	78°08.35	1°77.0.3	14/08	13:03	140	1.8	33.03*	6.1	5.4	0.15	64.03	1.07	1.57
18	78°08.32	8°72.3.5	15/08	11:01	140	7.1	34.81*	9.3	2.5	0.22	12.51	0.88	1.25
19	78°71.48	9°05.20	15/08	16:23	140	7.0	34.81*	9.5	1.9	0.26	7.24	1.45	1.50

20	77°51.98	7°28.52	16/08	12:10	140	6.7	35.04*	9.5	0	-	-	-	-
21	77°39.36	6°68.68	16/08	17:04	140	6.7	35.03*	9.7	0	-	-	-	-
22	76°34.34	2°66.92	17/08	08:33	140	6.0	34.90*	9.5	0	-	-	-	-
23	76°00.41	1°51.32	17/08	13:40	140	5.7	34.88*	9.5	0	-	-	-	-
24	74°76.20	-2°16.21	18/08	10:36	110	5.3	34.74*	10.4	0	-	-	-	-
25	71°25.01	.9°59.78	20/08	13:01	140	6.4	34.71*	9.5	13.2	0.13	28.20	1.03	1.43
26	69°22.85	-12°66.74	21/08	11:09	140	6.8	34.66*	11.7	3.2	0.19	11.39	1.26	1.41
27	66°86.66	-17°39.28	22/08	15:14	140	8.5	34.41*	13.9	12.4	0.25	3.94	1.24	1.38
28	67°48.49	-21°51.18	23/08	12:15	140	6.1	34.06*	14.5	33.3	0.18	6.31	1.67	1.56
29	68°71.13	-23°01.14	24/08	08:35	140	4.2	29.65*	14.1	0	-	-	-	-
30	69°22.79	-23°70.43	24/08	16:38	140	2.5	30.93*	13.3	0	-	-	-	-
31	68°13.55	-22°28.25	25/08	12:05	140	4.4	33.07*	14.2	0	-	-	-	-
32	66°69.35	-18°36.52	26/08	11:09	140	7.2	33.58*	16.7	30.4	0.21	4.90	1.14	1.46

* Derived from CTD rather than Thermosalinograph

Table 3.3: JR51 filter sample information – collection and analytical data. “Vol. Lipids” is the volume (in litres) of sea surface seawater filtered for lipid extraction, “Vol. Cocco.” is the volume of seawater filtered through a single filter used for coccolithophores counts. SST, SSS and Fluorescence were measured using the ships data logging system.

Sample	Coordinates		Date (2000)	GM T	Vol. Lipids (L)	Vol. Cocco. (L)	SST°C	SSS (PSU)	Fluorescence (ng/L)	ΣLCK (ng/L)	U^{37}	%C _{37:4}	C _{38Et} /Me	$\Sigma_{C_{37}}/\Sigma_{C_{38}}$
	Latitude (N)	Longitude (E)												
1	67°78.83	7°75.10	28/7	07.40	60	4.3	10.6	34.75	39.5	19.1	0.28	0.35	1.72	1.38
2	69°39.56	5°50.00	28/7	21.57	100	10	10.1	35.32	26.1	5.9	0.36	0	1.69	1.38
3	69°94.05	7°09.67	5/8	17.00	96	9.8	10.0	35.42	19.4	82.8	0.30	0	1.46	1.15
4	73°16.66	9°66.82	6/8	03.31	153	13.4	8.0	35.45	23.9	-	-	-	-	-
5	74°66.67	10°49.99	6/8	14.40	85	9.8	7.5	35.40	33.4	3.2	0.30	3.50	1.74	1.46
6	74°49.86	5°36.53	8/8	20.54	78	9.3	7.3	35.39	43.6	-	0.36	0	1.08	2.54
7	74°81.77	-0°06.03	9/8	13.28	153	9.3	5.9	35.15	17.9	-	-	-	-	-
8	76°02.65	-7°64.46	10/8	10.51	120.5	13.6	-0.6	30.72	21.8	2.9	0.20	60.26	1.47	2.01
9	75°29.56	-5°18.79	11/8	19.29	148.5	14.4	5.6	34.70	16.8	-	-	-	-	-
10	73°44.07	-9°43.56	14/8	07.09	119	12.5	3.4	31.96	16.6	-	-	-	-	-
11	73°02.72	-13°43.83	17/8	07.14	151	15	3.5	31.20	18.6	-	-	-	-	-
12	72°42.87	-15°52.58	24/8	22.25	127.5	15.4	1.8	30.87	18.6	5.4	0.18	51.10	1.36	2.35
13	69°81.30	-19°39.40	25/8	18.41	149.5	29.9	0.8	30.12	16.4	-	0.24	52.00	1.4	1.66
14	67°87.74	-21°32.05	26/8	10.21	100.5	8.9	7.0	34.24	24.7	109.5	0.14	12.78	1.55	1.09
15	67°55.15	-17°12.47	26/8	23.35	110	12.3	7.6	34.71	16	39.4	0.20	11.49	1.17	1.37
16	67°52.07	-12°08.94	27/8	16.12	104.5	9.5	9.1	34.87	17.8	13.2	0.20	12.67	1.18	1.17
17	65°09.01	-9°40.69	28/8	07.58	142	14	8.8	34.98	10.5	-	0.14	6.01	1.17	1.04
18	60°66.16	-3°59.03	29/8	06.57	79	8	12.9	35.60	40.5	6.9	0.39	0	2.07	1.78

3.5. Results & Discussion

3.5.1. Summary of *in situ* oceanographic conditions

As described above sea surface property (SST, SSS & chl. *a*) and ship's positional data were recorded continuously by the JCR data logging systems. Additional, depth profile data was collected during both cruises. Temperature and salinity were measured by 151 CTD probes during JR44. A primary mission of the JR44 cruise was to study the vertical circulation of the ocean, therefore a large number of CTD measurements were made. The primary mission of JR51 was the collection of high resolution bathymetry data, XBT probes (which measured only temperature) were used (27 in total) to calibrate the sonar equipment. The sea surface, depth profile and positioning data were combined and used to create Ocean Data View (ODV) files. ODV is a computer program "for the interactive exploration and graphical display of oceanographic...data" (Schlitzer, 2001). Figure 3.6 - Figure 3.9 are ODV output maps which illustrate the *in situ* oceanographic conditions measured during the two cruises. SST and SSS distributions are illustrated along with a selection of depth profiles in Figure 3.6 & Figure 3.7. *In situ* chlorophyll *a* measurements are illustrated, with SeaWiFs remotely sensed chlorophyll *a* for comparison, in Figure 3.8 & Figure 3.9. The position and extent of sea-ice off the east coast of Greenland is also interpreted from the SeaWiFs images. The assignation of certain black areas in the SeaWiFs chlorophyll images as sea-ice (rather than cloud) was confirmed by reference to SeaWiFs true colour images (not shown).

The typical Nordic Seas ranges of SST and SSS listed in Table 3.1 (page 60) were used to delimit the major water masses and to estimate the positions of the PF, AF and NCF. Primarily, the SSS isoline at 34.4psu was used to estimate the position of the PF, likewise the 35psu isoline was used to estimate the position of the AF (in the northwest) and the NCF (in the southeast). Figures 3.4 - 3.9 reveal that there was considerable variation in the position of these fronts between August 1999 and 2000.

In 1999, the PF seems to follow the continental shelf (Figure 3.4), relatively closely especially south of $\sim 74^{\circ}\text{N}$. Also, the dense sea-ice does not seem to extend south beyond a position level with the Hold with Hope Peninsula (Greenland) at 74°N (Figure 3.8). The polar waters are characterised by cold SSTs of $<5^{\circ}\text{C}$ and as illustrated by the SSS profiles (Figure 3.6), a marked freshening of the top 10m (by meltwater). A contrast

is highlighted in Figure 3.6 between the Polar water depth profile furthest from the PF and two profiles obtained closer to the PF. In the later two cases, there is a warmer intermediate water mass occurring at 20m, presumably a result of mixing near the PF and the denser (more saline) waters sinking beneath the Polar water. In 1999, the AF seems to follow, relatively closely, the line of the Mohns ridge, a position often ascribed as typical for the AF in reviews of Nordic Seas oceanography (e.g. Johannessen, 1986) (see Figure 3.3). This results in a fairly large expanse of AW occupying the Greenland Sea between the Polar waters of the EGC in the west and the Atlantic signature waters in the Norwegian Sea to the east. In the northeastern Nordic Seas, the WSC was observed to carry Atlantic signature waters fairly far north to $\sim 78^{\circ}\text{N}$ where there appears to be a sharp gradient to Polar type waters at $\sim 80^{\circ}\text{N}$. In the depth profiles, the Atlantic and Arctic waters are distinguishable from the Polar waters by warmer temperatures and the absence of a shallow halocline. The profile from the NIIC shows Atlantic waters beneath a sharp halocline (and thermocline) at $\sim 10\text{m}$ depth. This NIIC profile may show the freshening influence of meltwater from the Icelandic Vantajokull ice cap (which partially drains to the northern fjords) and/or mixing with the EGC and EIC. This is consistent with studies which show the progressive loss of Atlantic properties of the NIIC on its passage to the east (Stefánsson, 1962). In 1999, the NCF seemed to follow, fairly closely, the Norwegian continental shelf (see Figure 3.4).

The cruise track in 2000 did not extend as far to the northeast, therefore inter-annual comparisons for this region are not possible. However, in the central, southern and western Nordic Seas, there was a degree of overlap and therefore comparisons can be made. In August 2000 there appeared to be some significant differences in the physical oceanography of the Nordic Seas compared to 1999. In the southwest Nordic Seas, in August 2000, the PF seems to extend much further from the continental shelf (Figure 3.5). The sea-ice also appears to extend further south to a position level with the King Oscar's Fjord (Greenland) at 72°N (Figure 3.9). However, there appeared to be a larger opening of the ice-pack further North, compared to August 1999, with a large polynya visible to the northeast of Greenland (Figure 3.9). In 1999 the AF seemed to follow, relatively closely, the line of the Mohns ridge, (see Figure 3.4) with a fairly large expanse of AW occupying the Greenland Sea. This contrasts with the situation in 2000 where the PF and AF are, geographically, much closer in the central Nordic seas, due to the PF occupying a position further east and Atlantic signature waters pushing much

farther west into the Greenland Sea. North of Iceland the SSTs appear to be warmer than those measured in 1999 despite the greater proximity of the PF. In 2000 the NCF seems to have pushed farther west from the Norwegian continental shelf compared to 1999 (see Figures 3.4 & 3.5). Overall, Figures 3.4 and 3.5 illustrate that there was considerable interannual variability between 1999 and 2000 in the positions of the oceanic fronts. However, POM filter samples were successfully collected from all the major water masses of the Nordic Seas in both 1999 and 2000.

3.5.2. Alkenone Distributions in the Nordic Seas

3.5.2.1. Absolute abundance

Alkenones were detected in all of the major water masses of the Nordic seas, across a spectrum of SST values from -0.5 to 13°C and SSS values from 29.6 to 35.6 (psu). The geographic and water mass distributions of alkenone abundances are illustrated in Figure 3.10 and Figure 3.11. Concentrations of C₃₇ + C₃₈ alkenones (Σ LCK) as measured by GC-FID ranged from 1.8 – 109 ng/L of filtered seawater. Alkenones were absent or not detectable in 21 of the 50 samples after analysis by GC-FID (detection limit of ~1ng). Further analysis by GC-CI-MS (detection limit 0.02 ng) measured alkenones in a further five samples, leaving 16 samples barren of alkenones after analysis by both GC-FID and GC-CI-MS. Ten of the barren samples were obtained from the Arctic waters of the Greenland Sea gyre and six from the polar waters of the East Greenland Current (see Figure 3.1 & Figure 3.10). However, alkenones *were* measured in six of the eleven samples obtained from polar waters in conditions of up to 80% sea ice (see appendix I – plates Ib & Ic). The polar waters were distinct from the Arctic and Atlantic water masses by the consistently low concentrations (0- 7.8 ng/L). The highest concentrations (30 – 109 ng/L) were found in regions influenced by Atlantic source waters, specifically the North Icelandic Irminger Current (NIIC), the Shetland Current (SC) and the Norwegian Atlantic Current (NWAC) (see Figures 3.1, 3.10 & 3.11). However, some low concentrations (<1ng) were also found in the regions strongly influenced by Atlantic waters.

Fluorescence was measured continuously during both cruises and converted to Chlorophyll *a* (mg/m³). It can be considered as a crude measure of phytoplankton standing stock. Higher alkenone concentrations were generally measured in samples with a chlorophyll *a* reading near to or the mean (20 mg/m³). However, a linear

regression ($R^2 = 0.001$) confirms there is no significant linear relationship between the concentration of alkenones and the fluorescence measurements. This suggests that non-alkenone producing phytoplankton groups (e.g. diatoms, dinoflagellates, the haptophyte *P. pouchetti*) contributed significantly to the fluorescence signal and that the productivity of such groups was not tightly correlated with the main producer of the alkenones. This is supported by SeaWiFS data of PIC (a proxy for coccolithophore blooms) which suggest that there were no *E. huxleyi* blooms in the Nordic seas during the periods of the two cruises (Brown, 2003).

3.5.2.2. $\%C_{37:4}$

3.5.2.2.1. $\%C_{37:4}$ in sea surface POM during August 1999 & 2000.

Geographical distribution of values of $\%C_{37:4}$ are shown in Figure 3.13 and Figure 3.14. The most prominent aspect of the data, is the conspicuously high values of $\%C_{37:4}$ in samples obtained from the polar waters of the EGC. High values (i.e. $>5\%$, the typical open marine, mid to low latitude maximum) of $\%C_{37:4}$ have been previously observed in a diverse range of lacustrine environments (Cranwell, 1985; Li et al., 1996; Thiel et al., 1997; Volkman et al., 1988; Zink et al., 2001), in coastal/brackish sediments (Ficken and Farrimond, 1995; Schöner et al., 1998; Schulz et al., 2000) and in the open ocean in high latitudes, (Harada et al., 2003; Rosell-Melé, 1998; Sicre et al., 2002; Sikes et al., 1997) (see Table 1.3, chapter 1). The highest previously reported value for $\%C_{37:4}$ - in the open ocean water column - is 41% obtained from the sub-polar waters of the Bering Sea by (Harada et al., 2003). The highest value for the Nordic Seas is 35%; recorded in a Greenland Sea, POM filter sample by Sicre *et al* (2002) (see Table 1.3, chapter 1). This thesis reports $\%C_{37:4}$ values of $>40\%$ from the six Polar water samples that yielded alkenones, with a maximum $\%C_{37:4}$ of 77% in sample JR44-14 (Table 3.2, page 68). This contrasts with the previous investigation by Sicre *et al* (2002); which did not detect alkenones in the truly polar waters of the Nordic Seas (salinity of <34.4). In fact, the two samples collected on 2nd August 1999 from the EGC yielded the highest $\%C_{37:4}$ values (72 & 77%) observed in any environment: marine, brackish or lacustrine (see Table 1.3, chapter 1).

Examples of the GC-traces of alkenones from different regions of the Nordic seas (and covering a spectrum of alkenone patterns) are illustrated in Figure 3.13. Figure 3.14 highlights the clustering of high $\%C_{37:4}$ values (40 – 77%) within the Polar waters, with

low values (0 – 3%) in Atlantic waters. Low to intermediate values (0 – 28%) were obtained from water masses that are not classified as truly Polar or Atlantic. Further inspection of the samples from the “intermediate” water masses reveal:

- Low %C_{37:4} values of 0 – 4% in the Shetland current. The Shetland Current is an Atlantic source current which has lowered salinities as a result of mixing with the Norwegian Coastal Current (as opposed to low salinity Polar waters).
- Low to intermediate %C_{37:4} values of 4 – 13% in the Icelandic Sea, North Icelandic Irminger and East Icelandic Currents. These are water masses which result from varied mixing of Polar and Atlantic sources.
- A relatively high %C_{37:4} value of 28% from the Jan Mayern Current, a current with a strong source in the East Greenland Current.
- Intermediate %C_{37:4} values of 10 – 12% from the region in the far north in which the West Spitsbergen Current (Atlantic source) mixes with the East Greenland Current.

Examination of the %C_{37:4} values plotted against SST and SSS (Figure 3.15); reveals that %C_{37:4} is linearly correlated to SST (equation 3.1). While, a correlation of slightly higher significance (higher R² and lower relative error of the coefficients) is achieved with SSS (equation 3.2):

$$\%C_{37:4} = -5.5 (\pm 5.5) \times SST + 56.5 (\pm 4.5), R^2 = 0.76 (n = 34) \quad (3.1)$$

$$\%C_{37:4} = -13.4 (\pm 1.2) \times SSS + 472.6 (\pm 42), R^2 = 0.79 (n = 34) \quad (3.2)$$

Using a multiple regression of %C_{37:4} vs SST and SSS, the following equation is obtained:

$$\%C_{37:4} = 311 (\pm 54.1) - 8 \times SSS (\pm 1.7) - 2.8 \times SST (\pm 0.7), R^2 = 0.86 (n = 34) \quad (3.3)$$

Again the relative error is larger for SST than for SSS. Previous work - in the Nordic seas and northern North Atlantic surface sediments (Rosell-Melé et al., 2002) and sea surface POM (Sicre, 2002) - has found a stronger relationship of %C_{37:4} to SSS, than to SST. A similar observation was made by Harada (2003) for a small number of sea surface POM samples from the Bering Sea. Results from this study, however, find little difference in the significance of the correlations of %C_{37:4} to SST and SSS. Moreover, the distribution of %C_{37:4} plotted against SSS (Figure 3.15) displays considerable scatter - especially in polar waters - and %C_{37:4} appears (visually) unconvincing as a linear predictor of SSS.

One problem of attempting to assess the relative influence of SST and SSS on alkenone distributions in the Nordic Seas is the fact that there is a degree of the correlation between the two parameters. However, as illustrated by the scatter of SST versus SSS measurements in 3.14a this relationship is far from linear. In the Nordic Seas both SST and SSS decrease with movement from Atlantic type waters to polar waters, however, SST initially decreases more rapidly than SSS, whereas in the colder waters SSS decreases more rapidly compared to SST. A linear regression suggests that each of the independent variables can only predict about 50% of the variance in the other (see Figure 3.14a). Therefore, if only one independent variable (SST or SSS) controlled $\%C_{37:4}$, and the other had no relationship to $\%C_{37:4}$ it should be possible identify which one was dominant.

3.5.2.2.2. Comparison of $\%C_{37:4}$ distributions with previously reported water column and surface sediment data

Greater insight into the oceanographic significance of the $\%C_{37:4}$ values reported in this thesis may be obtained by comparing the data with previous water column and sediment data obtained from the Nordic Seas and North Atlantic. Figure 3.16 compares the geographic distribution of water column and sediment surface samples collected for this thesis, with surface sediments collected by Rosell-Melé (1998) and POM samples collected Sicre *et al* (2002). In the Nordic Seas region there is considerable overlap of sediment and water column samples; which facilitates a comparison. Figure 3.17 illustrates plots of the water column and surface sediment samples vs SST (a) SSS (b) and by water mass (c).

- *Water column data*

Values of $\%C_{37:4}$ measured in sea surface POM in this study are similar, for a range of SST and SSS considered, to those from suspended POM measured in the fluorescence maximum in Atlantic and Arctic water masses between June and September 1999 (Sicre *et al* 2002). However, no alkenones were detected in polar waters by Sicre *et al* (2002) whereas in this study several samples contained them. At present we do not have an explanation for this discrepancy. It is unlikely that the sensitivity of the technique used is a significant issue. The concentrations of alkenones measured in some of the polar water samples in this study were very low (<7ng/L) and beyond the sensitivity of the FID used. Hence, samples were analyzed by GC-CI-MS, a much more sensitive

technique (see chapter 2). Sicre *et al* (2002) reported values as low as 0.8 ng/L, which suggest their methods should have been sensitive enough to detect alkenones in four of the samples from polar waters analyzed in this study. It might be significant, however that the volume of water filtered by Sicre *et al* (2002) was lower (40 – 60l) than in this study (mean volume filtrated of 125L). Perhaps more significant is that Sicre *et al* (2002) - presuming a correlation between chlorophyll pigments and alkenones - took samples at the depth of the *in situ* fluorescence maximum, which varied across the Nordic Seas. The sampling depth for this study was fixed at 7m. It has been shown in this study that there is not necessarily a correlation between fluorescence and alkenone abundance (see Figure 3.12). Therefore it is possible that the Sicre *et al* (2002) sampling strategy did not guarantee the highest recoveries of alkenones from the water column, in the Polar waters.

If the filtered POM data from the present study and that from Sicre *et al* (2002) are combined and used for regressions of %C_{37:4} against SSS & SST, the linear correlation for %C_{37:4} vs SST (equation 3.4) becomes weaker, compared to a regression based on just the data from this thesis (equation 3.1, R² = 0.78):

$$\%C_{37:4} = -2.7 (\pm 0.3) \times SST + 37.6 (\pm 3.6), R^2 = 0.5 (n = 69) \quad (3.4)$$

The weaker correlation appears to be due to greater scatter in the Sicre *et al* (2002) data for %C_{37:4} vs SST. Combining the data sets also results in a slightly weaker linear correlation for %C_{37:4} vs SSS, when compared to a regression based on just the data from this thesis (R² = 0.79):

$$\%C_{37:4} = -12.7 (\pm 0.9) \times SSS + 450.1 (\pm 33.1), R^2 = 0.72 (n = 69) \quad (3.5)$$

Overall, the combined data set – despite giving a stronger correlation for %C_{37:4} with SSS than with SST – does not present %C_{37:4} as a convincing linear predictor of SSS: due to scatter in the polar water cluster and the inconsistency in the slope of the relationship.

Recently Sikes & Sicre (2003) assessed the global relationship of SST and SSS to %C_{37:4}; the authors reported no discernable relationship of %C_{37:4} in the water column to SST or SSS on a global scale. Two new datasets are now available to add to the global database, since the publication of the Sikes & Sicre (2003) work: this study (Nordic Seas) and Harada *et al* (2003) (Bering Sea). Both new studies report high values of %C_{37:4}

in the surface waters of high northern latitudes. Figure 3.18 illustrates the global distribution of water column $\%C_{37:4}$ versus SSS and SST, with the new data incorporated. The approach of Sikes & Sicre (2003) is adopted, in that samples which do not record $\%C_{37:4}$ are not included. As this would add a large number of zero points at temperatures greater than $\sim 15^{\circ}\text{C}$, confounding the statistics. Values of $\%C_{37:4}$ showed no significant correlation to SST using the new global data-set:

$$\%C_{37:4} = -1.4 (\pm 0.3) \times \text{SST} + 21.2 (\pm 2.6), R^2 = 0.17 \quad (n = 122) \quad (3.6)$$

This is partly due to the data from the Southern Ocean, which clearly contrasts with that from the northern hemisphere in the relationship of $\%C_{37:4}$ to SST. The global correlation of $\%C_{37:4}$ to SSS was stronger, however, SSS only explains about half of the variation in $\%C_{37:4}$ on a global scale:

$$\%C_{37:4} = -9.1 (\pm 0.8) \times \text{SSS} + 321.3 (\pm 27.2), R^2 = 0.52 \quad (n = 122) \quad (3.7)$$

Figure 3.18b clearly highlights a difference in the relationship of $\%C_{37:4}$ versus SSS between the Nordic Seas and Bering Sea basins. Data from both basins feature high values of $\%C_{37:4}$, however, $\%C_{37:4}$ values are higher for the Nordic Seas (50-77%) than for the Bering Sea (18-44%), in polar waters with a similar salinity range (30 – 32 psu). This may suggest that other parameters not measured – such as nutrients – may have an additional influence. Another explanation is that this may reflect regional (i.e. genetic) differences in the physiological response of the of alkenone producers to a given environmental variable. This contrasts with the relationship of $\%C_{37:4}$ to SST, data from the two basins are grouped together when $\%C_{37:4}$ is plotted against SST (see Figure 3.18a). In order to explore further the contradictions in the relationship of $\%C_{37:4}$ to SSS & SST in the northern hemisphere basins, regressions were made using the northern hemisphere data only. The equations show stronger relationships for both SST and SSS with $\%C_{37:4}$ for the northern hemisphere data-set (over the global data-set):

$$\%C_{37:4} = -2.9 (\pm 0.3) \times \text{SST} + 39.9 (\pm 3.4), R^2 = 0.51 \quad (n = 77) \quad (3.8)$$

$$\%C_{37:4} = -9.8 (\pm 0.8) \times \text{SSS} + 348.1 (\pm 27.6), R^2 = 0.66 \quad (n = 77) \quad (3.9)$$

However, the relationship to SSS for the northern hemisphere is weaker than when the Nordic Seas ($R^2 = 0.72$) and the Bering Sea ($R^2 = 0.76$, Harada, 2003) are considered separately. This contrasts with the relationship to SST, which is similar in the Nordic

Seas ($R^2 = .0.51$) to the northern hemisphere as a whole (0.5), but is insignificant in the Bering Sea data-set ($R^2 = 0.17$).

Overall there is no strong global or even hemispherical relationship of $\%C_{37:4}$ to SSS or SST. However, $\%C_{37:4}$ clearly shows some correlation with both parameters in individual basins, the relationship with SSS being generally stronger in the northern hemisphere. Rather than a linear relationship with an individual parameter the data is clustered. In the Nordic Seas this takes the form of a cluster of high $\%C_{37:4}$ values associated with polar waters and a low value cluster with Atlantic waters, with mixing between these two groups in the intermediate water masses (e.g. Arctic waters). The fact that *E. huxleyi* is rare in polar waters suggests that there may be two alkenone producing groups, one associated with polar waters (unknown) and one with Atlantic waters (*E. huxleyi*).

- Surface sediment data

In the Nordic Seas higher values of $\%C_{37:4}$ are generally found in POM samples than in geographically proximal sediments (Figure 3.17). This is especially apparent in the polar water samples (<34.4 psu), where sediment values do not exceed 20% but water column values are 40 – 77%. Reasons for this discrepancy may include:

- Greater relative diagenetic alteration of the $C_{37:4}$ compound than the $C_{37:2}$ and $C_{37:3}$ alkenones.
- The high $\%C_{37:4}$ signal produced in polar surface water is diluted in the underlying sea surface sediments by resuspension and mixing with advected allochthonous matter containing relatively higher abundances of $C_{37:3}$ and $C_{37:2}$ alkenones.

-%C_{37:4} in boxcores and assessment of diagenetic bias

Alkenones – like all lipid compounds – degrade in the water column and in sediments following sequestration. It is sometimes argued that alkenone ratios may be biased through preferential degradation or incorporation - into macromolecular organic matter - of the components with more double bonds ($C_{37:4} > C_{37:3} > C_{37:2}$) (Flügge, 1997; Freeman and Wakeham, 1991; Gong and Hollander, 1999; Hoefs et al., 1998). However, studies that report significant biases (e.g. $>0.5^\circ\text{C}$ in the U_{37}^K index) are outnumbered by papers reporting no or minor biases as a consequence of C_{37} alkenone degradation in the water column or sediments (Grimalt et al., 2000, and references therein). To investigate

whether $C_{37:4}$ is preferentially degraded - which may account for the discrepancy between sea surface POM and surface sediments described above - three box cores from the Nordic Seas were analysed. If the most recently deposited sediments can be retrieved intact, then early diagenesis of the C_{37} alkenones may be investigated. However, if the preferential degradation of the $C_{37:4}$ alkenone is severe, then a consistent trend of decreasing values of $\%C_{37:4}$ should “overprint” any climatic signal in the top most sediments. Boxcores were preferred for this investigation as they usually preserve the top sediments without disturbance – unlike piston corers. The location of the boxcores collected is illustrated in Figure 3.16, results of analysis are given in Figure 3.19 and are summarised in Table 3.4 (page 81) with data from previous work.

Figure 3.19 illustrates for each core the GC-CI-MS response of the C_{37} alkenones in the top sediments (0 to 5 or 10cm) normalized to the top (0cm) sample and the values for $\%C_{37:4}$. The results from boxcores showed that all of the C_{37} isomers experienced an exponential decrease in concentration from the 0cm to 5cm of $\sim 80\%$. This was accompanied by some large changes in the values of $\%C_{37:4}$ e.g. up to 8% between minimum and maximum values in HM71-14. However, $C_{37:4}$ did not consistently degrade faster than the other C_{37} alkenones. Overall, between top (0cm) and bottom measurements (5 or 10cm) $\%C_{37:4}$ was observed to increase by 4.7% in HM94-25 and decrease by 2.2% in HM71-14, while the overall change in HM80-43 of 0.05% was insignificant. The results of the three cores give a mean change in $\%C_{37:4}$ of +0.8 (σ 3.5). These results do not support suggestions that the $C_{37:4}$ compound is especially susceptible to early diagenesis relative to the other C_{37} alkenone compounds – at least once sequestered to sediments.

The only previous work to focus significantly on the relative stability of the $C_{37:4}$ alkenone is an unpublished thesis by Flügge (1997), who studied alkenones in laboratory degradation experiments, sediment traps and boxcores from the Norwegian Sea. The results of the Flügge (1997) study are summarized in Table 3.4 (page 81). Flügge (1997) estimated that $C_{37:3}$ degrades 1.03 times faster than $C_{37:2}$ and $C_{37:4}$ ~ 1.2 times faster, during the early stages of degradation. The mean effect on the $\%C_{37:4}$ value of all the Flügge (1997) experiments is a shift of -2.8%. It should be noted that Flügge used GC-FID for analysis, which may have added uncertainty to the integration of the $C_{37:4}$ alkenone. Results from this thesis (chapter 2) and from Sicre *et al* (2002) have

highlighted problems relating to an unidentified compound that coelutes with the $C_{37:4}$ alkenone. This can be circumvented by using GC-CI-MS (this thesis) or GC-MS Selected Ion Monitoring (Sicre *et al*, 2002). Therefore, the results of Flugge (1997) may record the degradation signal of a coeluting compound as well as that of $C_{37:4}$. Assuming that the Flugge (1997) data has not been biased by a coelutant, the $C_{37:4}$ degradation experiments from this and Flugge's unpublished thesis cover timescales of 2 years (laboratory) to centuries (boxcores) and give a mean reduction of $\%C_{37:4}$ by 2.1%. Clearly, this is not sufficient to account for the huge differences in observed $\%C_{37:4}$ values between the summer water column of the western Nordic Seas and the regional surface sediments.

Therefore, an alternative explanation suggested previously must be invoked, that: alkenones with high $\%C_{37:4}$ values are produced in low abundances in polar waters (see Figure 3.11) and - due to the low abundances - the signal is vulnerable to dilution in the underlying sea surface sediments by resuspension and mixing with advected allochthonous matter containing relatively higher abundances of $C_{37:3}$ and $C_{37:2}$ alkenones.

Table 3.4: Summary of Nordic Seas alkenone degradation studies.

<i>Study</i>	<i>Location</i>	<i>Coordinates</i>	<i>Time Scale</i>	$\Delta\%C_{37:4}$	$\Delta U^{K_{37}}$	<i>Reference</i>
Laboratory degradation experiments						
Aqueous Solution	Lab		32 days	-2.6%	0.04	Flügge (1997)
Sediment (a)	Lab		248	-1.86%	0.05	"
Sediment (b)	Lab		248	-1.89%	0.03	"
Sediment traps						
NB-7	N Norwegian Sea	70°N/ 0°01'W	1 year	-0.75%	0.02	"
NB-8	N Norwegian Sea	70°N/ 4°E	1 year	0.24%	0.00	"
Boxcores						
ARK X/1 31/54 MUC	Greenland Sea	75°N/ 0°18'E	0 – 1000 yr BP	-5.6	0.01	"
M21/5 #323 MUC	N Norwegian Sea	69°7'N/ 0°46'E	"	-10	0.03	"
M26/2 #478 GKG	N Norwegian Sea	70°N/ 0°01'W	"	-6.6	0.00	"
ARK X/1 31/2 MUC	N Norwegian Sea	69°9'N/ 4°E	"	+0.75	0.08	"
M36/3 #246 FLO	Greenland Sea	70°N/ 4°E	"	-6.77	0.03	"
M21/5 #317 MUC	Central Norwegian Sea	67°6'N/ 5°75'E	"	-1.15	0.04	"
M36/3 #203 MUC	Central Norwegian Sea	67.6°N/ 5°8'E	"	-4.42	0.08	"
M36/3 #201 FLO	SE Norwegian Sea	62°8'N/ 2°4'W	"	+3.8	0.12	"
FIM94-25	N Greenland Sea	75°4'N/ 1°2'E	"	+0.05	-0.20	This Thesis
FIM80-45	S Greenland Sea	72°1'N/ 9°1'W	"	+4.7	0.12	"
FIM71-14	W Icelandic Sea/EGC	69°8'N/ 18°W	"	-2.25	0.05	"
			Mean	-2.15	0.03	

3.5.2.2.3. Comparison of high %C_{37:4} distributions to Coccolithophore biogeography

One filter from each sampling station on cruise JR51 was preserved for species counts, in order to further assess the source of the high %C_{37:4} alkenones in the Nordic Seas polar water. Counts of coccospheres and coccoliths were made by P. Ziveri, using microscopes (LM and SEM), the results are presented in Table 3.5 (page 83). Unfortunately, the counts contain an unknown error estimate; as the filter used (GFF), while typical for POM analysis, is not ideal for coccolithophore work and has an unknown filtration efficiency (P. Ziveri pers. comm.). However, the results will still give presence or absence data and species ratios. The dominant species were *E. huxleyi* and *C. pelagicus* f. *pelagicus* with some minor contributions from *C. pelagicus* f. *hyalinus* (*C. pelagicus* motile phase) and in one sample *S. pulchra*. Previous work has demonstrated that the ratio of *E. huxleyi* to *C. pelagicus* is >1 in Atlantic source waters of the Nordic Seas and <1 in arctic and polar water masses (Baumann et al., 2000). This pattern is generally seen in the coccolith counts from the JR51 filters but not in the whole coccosphere data, in which *C. pelagicus* is the dominant in most samples. This suggests that for the methodology used in this thesis, the primary signal may be best preserved by the coccoliths.

Very high %C_{37:4} values were found in three of polar water samples from JR51, in samples 8, 12 and 13. In all three samples the ratio of *E. huxleyi* to *C. pelagicus* was very low. No *E. huxleyi* coccospheres or coccoliths were found in sample 13, in sample 12 only 74/L *E. huxleyi* coccoliths were observed (no spheres) and in sample 8 83/L and 167/L cocco-spheres and -liths were observed respectively. If the concentrations of ΣLCK were high for these samples then an alternative alkenone source would be logical, given the low representation of *E. huxleyi*. However, the alkenone concentrations were low (<5 ng/l) and some evidence of *E. huxleyi* growth or advection was found in two of the samples. Therefore, there is not a compelling case for a novel source.

This issue of the biological source can be further pursued with reference to published data on the coccolithophore biogeography of the region. Earlier work by Norwegian scientists reported *E. huxleyi* to be *generally* but not completely absent from truly polar waters (dominated by diatoms) of the Nordic Seas (Gran, 1929; Paasche, 1960, as

referenced by Winter et al. 1994; Smayda, 1958). A recent study of 410 plankton samples (collected during 1987 – 1995) found that the large *E. huxleyi* summer blooms are limited to the Norwegian and Barents Seas ($>500 \times 10^3$ cells/l) (Baumann et al., 2000). Relatively high numbers ($100-500 \times 10^3$ cells/l) occurred west of Jan Mayen, but further to the north/northwest in the Greenland Sea and EGC *most* samples were barren of *E. huxleyi* (Baumann et al., 2000).

Table 3.5: Results of species counts of coccolithophores and coccospheres for JR51 filters.

Sample	SST	Σ LCK (ng/l)	$\%C_{37:4}$	Single Coccoliths			Single Coccoliths			Notes from SEM
				Total #/L			Total #/L			
				<i>E.</i> <i>huxleyi</i>	<i>C.</i> <i>pelagicus</i>	Ratio E/C	<i>E.</i> <i>huxleyi</i>	<i>C.</i> <i>pelagicus</i>	Ratio E/C	
1	11	19	0	-	-	-	-	-	-	
2	10	6	0	113	340	0.3	3629	454	8.0	
3	10	83	0	-	-	-	-	116	0.0	
4	8			339	339	1.0	2539	508	5.0	
5	7	3	3	116	463	0.3	347	347	1.0	
6	7	0	0	122	4146	0.0	-	366	0.0	Some corrosion
7	6			-	488	0.0	975	610	1.6	
8	-1	3	60	83	334	0.3	167	500	0.3	
9	6			-	-	-	-	-	-	
10	3			-	-	-	-	-	-	
11	4			-	-	-	-	-	-	
12	2	5	51	-	74	0.0	74	515	0.1	
13	1	0	52	-	-	-	-	76	0.0	
14	7	109	13	510	637	0.8	3950	-	-	
15	8	39	11	-	-	-	92	369	0.3	Major corrosion
16	9	13	13	-	-	-	-	-	-	Some corrosion
17	9	0	6	-	-	-	-	-	-	
18	13	7	0	425	142	3.0	3969	284	14.0	Many <i>S. pulchra</i>

The literature confirms that *E. huxleyi* is relatively rare and often absent in the Arctic and Polar water masses. However, *E. huxleyi* is known to be an extremely euryhaline and eurythermal species – being able to withstand salinities much lower than the 29psu of the EGC (11 and 17-18 psu in the Sea of Azov and the Black Sea respectively) (Bukry, 1974). Moreover, it has the largest natural temperature range (1°C – 30°C) exhibited by any coccolithophore (Okada and McIntyre, 1977). Furthermore, *E. huxleyi*'s tolerance of different nutrient and light conditions is demonstrated by a natural distribution in both

eutrophic (e.g. Norwegian Fjords, Conte et al., 1994) and oligotrophic (e.g. subtropical gyres, Ohkouchi et al., 1999) environments between 0 -200m and by laboratory experiments (Prahl et al., 2003). Therefore, *E. huxleyi* is capable of producing alkenones in an environment as extreme as the EGC. However, in order to satisfactorily determine the source of the high %C_{37,4} alkenones in the polar waters, *E. huxleyi* must be shown to be capable of reproducing such high values in culture experiments, under similar physical conditions.

3.5.2.3. U_{37}^K and $U_{37}'^K$

U_{37}^K and $U_{37}'^K$ in sea surface POM during August 1999 & 2000.

Water mass distributions of U_{37}^K and $U_{37}'^K$ are illustrated in Figure 3.20 & Figure 3.21. Scatter plots of $U_{37}'^K$ and U_{37}^K vs SST are illustrated in Figure 3.22. Within the data from this study $U_{37}'^K$ has a relatively weak linear correlation with SST:

$$U_{37}'^K = 0.014 (\pm 0.003) \times \text{SST} + 0.13 (\pm 0.24), R^2 = 0.44, (n = 33) \quad (3.10)$$

This is due, in part, to a loss of correlation between $U_{37}'^K$ and SST below $\sim 10^\circ\text{C}$, whereby further decreases in temperature are not accompanied by a fall in the $U_{37}'^K$ index (which does not fall below ~ 0.2). A stronger correlation between $U_{37}'^K$ and SST is achieved with a 2nd order polynomial regression:

$$U_{37}'^K = 0.002 \times \text{SST}^2 - 0.011 \times \text{SST} + 0.18, R^2 = 0.6 (n = 33) \quad (3.11)$$

In contrast to $U_{37}'^K$, a much strong linear correlation exists between U_{37}^K and SST:

$$U_{37}^K = 0.808 (\pm 0.007) \times \text{SST} - 0.538 (\pm 0.55), R^2 = 0.81 (n = 33) \quad (3.12)$$

This is due to the linear correlation of the relative abundance of the C_{37,4} compound to SST and the inclusion of this compound in the U_{37}^K index (see Figure 3.15 & equation 3.1, page 74).

3.5.2.3.1. Comparison of U_{37}^K and $U_{37}'^K$ distributions with previously reported water column and surface sediment data

In Figure 3.23 the data from this thesis is compared with global distributions of $U_{37}'^K$ and U_{37}^K , measured on mixed layer POM. The data from this thesis includes the first successful measurements of alkenones on water column POM from below 4°C in the North Atlantic; therefore it expands the global water column data-set. In Figure 3.23(a) the global relationship of water column $U_{37}'^K$ to SST is illustrated. The culture equation of Prahl *et al* (1988) – which is statistically the same as Muller *et al's* (1998) core-top

equation - is included in Figure 3.23(a) for reference. A regression of $U_{37}^{K'}$ on SST was calculated using a 3rd order polynomial function; this best represents the reduction in slope of the relationship, at the two ends of the temperature spectrum:

$$U_{37}^{K'} = -3 \times 10^{-5} \times SST^3 + 0.0017 \times SST^2 + 0.007 \times SST + 0.067, R^2 = 0.94 \quad (n = 245) \quad (3.13)$$

At SST > 5 the new Nordic sea data plots within the envelope of previously reported global data (Conte and Eglinton, 1993; Harada et al., 2003; Sicre et al., 2002; Sikes and Sicre, 2002; Sikes and Volkman, 1993; Ternois et al., 1998; Ternois et al., 1997). This reinforces the trend of a systematic difference in slope of the $U_{37}^{K'}$ - temperature relationship, between that derived from water column POM and that derived from culture by Prah *et al* (1988) and from core-tops by Muller (1998), whereby, the POM data generally lie in a field that gives warmer-than-predicted growth temperatures at a given $U_{37}^{K'}$, particularly between ~5-15°C.

The form of the global water column regression compares with results from culture experiments with a number of *E. huxleyi* and *G. oceanica* strains from different ocean basins (Conte et al., 1998). The Conte *et al* (1998) study reported a reduction of slope in the calibration of $U_{37}^{K'}$ to temperatures <12°C and >21°C (for some strains) and suggested that due to such inter-strain differences, locally derived SST calibrations may be preferable to applying the Prah *et al* (1998) equation globally. However, such work does not explain the vexing offset between global surficial sediments (which mostly follow the form of the Prah *et al* (1998) equation and water column POM data. This has raised questions about what factors control the export of alkenone material - produced in the euphotic zone - to depth and how these may influence the alkenone signature imparted to sediments (Herbert, 2001).

At temperatures below 5°C, there is a distinct separation in the field of $U_{37}^{K'}$ - temperature data between the new observations from the Nordic Seas data and that from the Southern Ocean. So that for a given growth temperature the $U_{37}^{K'}$ value in the Nordic Seas is ~0.1 units higher than the $U_{37}^{K'}$ value for the Southern Ocean. This deviation is emphasised by regressions - illustrated in Figure 3.23a - derived using North Atlantic and non-Atlantic data only. A similar divergence in temperature dependence of the $U_{37}^{K'}$ index relationship has also been noted for surficial sediments of the northern North Atlantic and the Southern Ocean (Rosell-Melé, 1998). The new

Nordic Seas water column data suggests that a significant part of the trend observed in the surficial sediments may have a genuine biological component.

If the expanded global water column data-base is used to plot U_{37}^K versus SST then the divergence of values for the Nordic Seas and Southern ocean - compared to $U_{37}'^K$ - is accentuated (Figure 3.23b). This is due to the much higher concentrations of $C_{37:4}$ observed in northern waters. In the surficial sediments of the Nordic Seas there is no significant correlation between $U_{37}'^K$ and SST below 10°C (Rosell-Melé, 1998). This is supported by a regression of $U_{37}'^K$ measured on Nordic Seas water column POM <10°C:

$$U_{37}'^K = 0.008 (\pm 0.0026) \times \text{SST} + 0.16 (\pm 0.018), R^2 = 0.21 (n = 37) \quad (3.14)$$

However, the relationship U_{37}^K to SST measured on Nordic Seas water column POM <10°C is much stronger:

$$U_{37}^K = 0.082 (\pm 0.0093) \times \text{SST} - 0.59 (\pm 0.064), R^2 = 0.69 (n = 37) \quad (3.15)$$

Based on surficial sediments it has been suggested that the U_{37}^K index is used to calculate SSTs in the Nordic Seas region, rather than $U_{37}'^K$ (Rosell-Melé, 1998). The data from this thesis suggest that U_{37}^K does indeed have a stronger relationship to SST than $U_{37}'^K$ at cold temperatures (<10°C) in the Nordic Seas. However, as illustrated by Figure 3.24 there are major differences between distributions of U_{37}^K and $U_{37}'^K$ in the water column POM and surficial sediments of the Nordic Seas for both indices. Therefore any SST calibration based on water column data may have little practical application to SST reconstruction in sediment cores in parts of the region. This contrasts with the Southern Ocean, where the equation for sedimentary $U_{37}'^K$ and summer SSTs agrees with that from surface water POM (Sikes et al., 1997).

3.5.2.3.2. Reassessing the Limits of the $U_{37}'^K$ index

It does not seem that the preferential diagenetic alteration of the $C_{37:3}$ compound (Grimalt et al., 2000, and references therein) or the $C_{37:4}$ compound (this thesis) can be severe enough to account for the differences between water column and core-top values. Alkenone resuspension and reworking is a more likely alternative explanation. There are few studies which have specifically observed modern alkenone reworking in the Nordic Seas. Thompsen *et al* (1998) suggested – on the basis of two sediment traps sites – that in the Norwegian Sea at least, biases may be introduced through

resuspension and lateral advection of alkenone bearing material. However, Flugge (1997) found that alkenone indices (including $\%C_{37:4}$) were not significantly biased in deep sediment traps from the Lofoten basin.

Indirect evidence of potential alkenone bias in the Nordic Seas comes from sediment traps which record coccolithophore assemblages. These show that temporal and regional input of resuspended material to depth is highly variable (Andrulleit, 1997; Samtleben et al., 1995). The most compelling evidence comes from a recent sediment trap study which showed that coccolithophore assemblages in sediment traps 300m above the sea floor in the Greenland and Norwegian Seas were strongly influenced by lateral advection within the nepheloid layer (Andrulleit, 1997). Pertinently, *E. huxleyi* increased from 25 to 51% between 500m and 2300m in the Greenland Sea, but only increased from 58 to 66% between 500m and 2300m in the Norwegian Seas (Andrulleit, 1997). This suggests that a warm bias “overprints” the local signal by advection and that this is more severe in the Greenland Sea than in the Norwegian Sea.

It has been suggested that a $\%C_{37:4}$ value of 5% may be used as a threshold for the limit of the reliable application of the U_{37}^K index in the sediments of the Nordic Seas (Rosell-Melé, 1998). This is based on empirical evidence of alkenone abundances and coccolithophores biogeography, in modern ocean surface sediments the $\%C_{37:4}$ 5% iso-line broadly coincides with the arctic front (see Figure 3.3 and Figure 3.25). This front divides an *E. huxleyi* dominated coccolithophore assemblage (Atlantic source waters) from an assemblage dominated by *C. pelagicus* and which contains fewer *E. huxleyi* numbers (polar and arctic waters) (Baumann et al., 2000).

The evidence outlined above suggests that sediment reworking may be a source of error for the U_{37}^K – SST relationship, in the Nordic Seas region and that this may be most severe in the Greenland Sea. Therefore, the samples that contribute scatter to the U_{37}^K – SST relationship for the region may have a specific geographic distribution – associated with areas of a more active nepheloid layer or sediment mass movements. This may complicate any theoretical biological limit to the U_{37}^K index.

In Figure 3.25 the geographic distribution of the core-top U_{37}^K values - that are responsible for scatter in the U_{37}^K – SST regression – are highlighted. The “scatter”

samples are defined as those that lie above an arbitrary envelope that contains 99% of the data used for the Muller *et al* (1998) core-top equation. The figure shows that the scatter samples are confined to the core-tops from the East Greenland Shelf, the Greenland Basin, Mohns ridge, northern Iceland Plateau and upper Bear Island Fan. Samples from the northern Atlantic, Icelandic Shelf, Norwegian and Lofoten Basins and Barents Seas yield U_{37}^K values that fall within the Muller *et al* (1998) data envelope. This division of samples shows a reasonable agreement with the 5% of $C_{37:4}$ threshold, in that the 5% iso-line divides the Greenland basin from the Norwegian and Lofoten basins. However it does not account for the “scatter” samples from the Bear Island fan. This suggests that several factors must be satisfied to increase confidence in alkenone investigations in the Nordic Seas. Firstly that % $C_{37:4}$ is monitored and used generally as a marker downcore for Arctic water and the limit of the U_{37}^K and U_{37}^K index. Secondly cores from areas which yield modern U_{37}^K values from within the Muller *et al* (1998) data envelope should be preferred e.g. Lofoten plateau, Icelandic shelf.

3.5.2.4. C_{38} alkenones

In addition to large changes in the relative abundances of the C_{37} alkenones, other prominent changes of alkenone within-class-distributions are observed in the new sea surface POM data. The representative GC-traces in Figure 3.13 illustrate increases in the unsaturation of the C_{38} alkenones coeval with the C_{37} alkenones. The general correlation between unsaturation of the C_{37} and C_{38} alkenones is demonstrated quantitatively by comparison of C_{37} and C_{38} alkenone indices and has been reported by a number of previous workers (Marlowe *et al.*, 1984; Rosell-Melé *et al.*, 1993; Yendle, 1989).

Extremely high values of % $C_{37:4}$ (up to 77%) are reported from polar water, in this study. High values of % $C_{37:4}$ have also been previously reported in brackish and lacustrine environments (up to ~60%) (Cranwell, 1985; Ficken and Farrimond, 1995; Schulz *et al.*, 2000; Zink *et al.*, 2001). In sediments from these environments, values of $\Sigma C_{37}/\Sigma C_{38}$ and $C_{38}Et/Me$ have been observed to take values distinctly different from “normal open marine values” (Cranwell, 1985; Schulz *et al.*, 2000). Specifically, in samples with high % $C_{37:4}$ it has been observed that both the above measures often increase in value, due to a drop in relative abundance of the C_{38} alkenones, with the C_{38} Methyls in particular becoming reduced in abundance – often to the point of being

unmeasurable (Schulz *et al*, 2000). In the Baltic Sea, it has been suggested that changes in these indices could help to distinguish marine *E. huxleyi* source alkenones from alkenones produced by an unknown source organism in low salinity (<8psu) waters.

The polar water alkenones in this study may have a novel source, as *E. huxleyi* is relatively rare in polar waters. Moreover, recent work presents evidence that 12 – 41% of DOM in the Arctic Ocean is of terrigenous origin and that fluxes of terrigenous carbon through the upper 200m of the EGC are 2.9-10.3 Tg/yr (Opsahl *et al.*, 1999). Alkenones have been observed in a number of terrestrial lake sediments, including Lake Pichozero in Russia (Zink *et al.*, 2001). It is not known what proportion of the organic matter entering the Arctic Ocean from riverine sources bears lacustrine alkenones (if any) but it is a potential source of bias.

In the data from this study there is no significant correlation between $\Sigma C_{37}/\Sigma C_{38}$ or $C_{38}Et/Me$ and the SST or SSS parameters (see Figure 3.27 & Figure 3.28). Moreover, the polar-water subset is not characterised by a significantly different range of values for these parameters. Plotting the C_{38} ethyl versus C_{38} methyl unsaturation ratios ($U_{38}^K Et$ and $U_{38}^K Me$ respectively, see Table 1.2, chapter 1 for equations) has been suggested as method of using the C_{38} alkenone to confirm *E. huxleyi* as the main alkenone source (Conte *et al.*, 1998). Figure 3.29 shows that the alkenones from this study fall within the data envelope for *E. huxleyi* determined by Conte (1998) on the basis of culture work. Therefore, based on the C_{38} alkenones, there is no evidence for a novel (non- *E. huxleyi*) source for the polar-water alkenones.

3.5.3. Alkenone distributions in core PL-96-126 – further appraisal of % $C_{37:4}$ as a palaeo-SSS indicator.

The objective of this section is to compare alkenone distributions in core PL-96-126 with data from recently developed proxies for palaeo-SSS, SST and sea-ice cover - based on dinoflagellate cyst (dinocysts) assemblages, which are applicable to the polar and sub-polar regions (de Vernal *et al.*, 2001). The aim is to assess the responses of alkenones distributions to environmental changes beyond the limits of currently established applications. The location of the core and general oceanographic features of the region are illustrated in Figure 3.30. Core PL-96-126 is located in a region which has a mean summer SST of 5°C, a SSS of 34.2 psu and which is subject to 3-7 months/year

of >50% sea-ice (Conkright et al., 1998; Voronina et al., 2001). The core-top (10cm) value of $\%C_{37:4}$ is 8%, therefore the region would be considered beyond the threshold for the reliable application of the U_{37}^K or U_{37}^K . However the core-top value of U_{37}^K , using the Rosell-Melé (1995) calibration, gives a reasonable summer SST estimate of 4.7°C.

The results of the analysis are illustrated in Figure 3.31. The alkenones were generally abundant throughout the core, but were not detected in two samples. The downcore $\%C_{37:4}$ record describes four significant phases during which $\%C_{37:4}$ values increase by ~4%. These phases broadly correspond to four events picked out by the dinocysts assemblages, during each event there is a ~3 psu decrease in the SSS proxy and a ~4 month increase in the sea ice cover (month/yr) proxy. However, the timing of the $\%C_{37:4}$ and dinocyst events are not exactly coeval. Two of the events start 1 sample/10cm earlier in the $\%C_{37:4}$ signal at 320cm and 140cm, whereas at 240cm and 30cm the events occur simultaneously in both records. Decoupling of alkenone and microfossil records is possible under certain conditions (Bard, 2001). However, significant differential mixing of the alkenones and dinocysts would not be predicted, as alkenone producers (coccolithophores) - and dinocysts are both members of the nanoplankton. Although dinocysts (~20–100µm) are generally larger than coccolithophores (<20µm) (Lalli and Parsons, 1997).

The $\%C_{37:4}$ values were converted to a reconstruction of palaeo-SSS using the equation of Rosell-Melé *et al.*, (2002). The results differ from the reconstruction of SSS using the dinocysts proxy. The values of SSS derived from $\%C_{37:4}$ being generally higher than the dinocysts at an equivalent depth. Moreover, the $\%C_{37:4}$ reconstruction is characterised by much lower amplitude fluctuations in SSS of – generally - between 34 – 33 psu, whereas the dinocyst method is characterised by fluctuations of between 34 -29 psu. Therefore, while the $\%C_{37:4}$ record is clearly responding to major changes in sea surface salinity (or a correlated variable), the results do not support a direct linear response of $\%C_{37:4}$ to SSS, as modeled previously by the Rosell-Melé (2002) equation. In Figure 3.31, it can be seen that the dinocyst sea-ice cover reconstruction is closely related to SSS. There is a clear association of high $\%C_{37:4}$ values with ice-laden polar and arctic waters, as demonstrated in this thesis. Therefore in order to establish whether $\%C_{37:4}$ may be used to reconstruct sea-ice cover rather than SSS, values of $\%C_{37:4}$ from core-tops in the

Nordic Seas were regressed against average sea ice cover (months/yr) for the core-top locality obtained from the WOD-98 (Conkright et al., 1998). The results, illustrated in Figure 3.32, show that $\%C_{37:4}$ in core-tops has no significant relationship with months/yr with 50% sea ice cover ($R^2 = 0.01$). When the regression is made against months/yr with 20% sea ice cover a more significant correlation occurs, however, this does not explain enough of the variation for $\%C_{37:4}$ to be used as a sea ice proxy ($R^2 = 0.42$).

The results of the SST reconstructions using U_{37}^K and dinocysts methods are also compared in Figure 3.31. The range of summer SSTs reconstructed using the two methods are in reasonable agreement (4 -9°C). However, apart from the bottom 100cm of the core there is little similarity in the records. In this case, the U_{37}^K record must be rejected as $\%C_{37:4}$ is maintained above the threshold of 5% (aside from one data point).

3.6. Conclusions

Alkenones have been measured in POM collected in the mixed layer from across the spectrum of water mass types in the Nordic Seas. Alkenones distributions characterized by low abundances and extremely high $\%C_{37:4}$ values (up to 77%) have been measured for the first time in polar waters (salinity <34.4 psu) under conditions of up to 80% sea-ice cover. Values of $\%C_{37:4}$ across the Nordic Seas show a strong association with water mass type, with clustering of high $\%C_{37:4}$ values (40 – 77%) within the Polar waters, low values (0 – 3%) in Atlantic waters and low to intermediate values (0 – 28%) in other water masses (e.g. Arctic, Norwegian coastal). The new $\%C_{37:4}$ data is linearly correlated to both SST ($R^2 = 0.75$) and SSS ($R^2 = 0.79$). However, the scatter in the relationship does not yet confirm the use of $\%C_{37:4}$ as a palaeo-SSS proxy. When combined with previous sea surface POM data from the Nordic Seas and north Atlantic (Sicre *et al.*, 2001), the data-set shows a stronger correlation to SSS ($R^2 = 0.72$) than to SST ($R^2 = 0.5$). Comparison with a global data set shows that $\%C_{37:4}$ has no consistent global relationship to either SST or SSS.

Comparisons of $\%C_{37:4}$ measured in sea surface POM and surficial sediments of the Nordic Seas, reveal large differences in the slope of the relationship of $\%C_{37:4}$ vs. sea surface parameters. The magnitude of the difference can not be explained by preferential degradation of the $C_{37:4}$ alkenone. Therefore, another explanation must be

invoked – the most obvious being that the %C_{37.4} signal in sea surface POM is vulnerable to dilution in the underlying sea surface sediments by resuspension and mixing with advected allochthonous matter - containing relatively higher abundances of C_{37.3} and C_{37.2} alkenones. This is supported by previous observations of resuspension and biasing of coccolithophore assemblages – particularly in the Greenland Sea.

Comparison of alkenone distributions with coccolithophore assemblage data collected on JR51 and with published coccolithophore data, suggests that *E. huxleyi* cannot be ruled out as the producer of the polar alkenones with the unusually high %C_{37.4} values. An *E. huxleyi* source is supported by the C₃₈ alkenone within-class-distributions.

Values of U^K_{37'} from the new Nordic Seas POM data shows no correlation with SST below 10°C. In contrast to U^K_{37'}, a stronger linear correlation exists between U^K₃₇ and SST (R² = 0.69). This supports previous suggestions that, overall, U^K₃₇ may be a more appropriate index for the Nordic Seas than U^K_{37'} (Rosell-Melé et al., 1995).

Comparison of the new sea surface U^K_{37'} data with a global database reinforces the trend of a systematic difference in slope of the U^K_{37'} versus temperature relationship, between that derived from water column POM and that derived from culture by Prahl *et al* (1988) and from core-tops by Muller (1998). Whereby, the POM data generally lie in a field that gives warmer-than-predicted growth temperatures at a given U^K_{37'}, particularly between ~5-15°C. At temperatures below 5°C there is a distinct separation in the field of U^K_{37'} vs. temperature data, between the new observations from the Nordic Seas and observations from the Southern Ocean.

The new U^K_{37'} and U^K₃₇ data highlights major differences between distributions of U^K₃₇ and U^K_{37'} in the water column POM and surficial sediments of the Nordic Seas for both indices. Therefore, any SST calibration based on water column data may have little practical application to SST reconstruction in sediment cores in the region. A detailed examination of the geographic locations that are responsible for the scatter in the U^K_{37'} versus SST relationship in surficial sediments of the Nordic Seas, was made. The results show a clear geographical division suggesting that East Greenland Shelf, the Greenland Basin, Mohns ridge, northern Iceland Plateau and upper Bear Island Fan are associated with the scatter, while samples from the northern Atlantic, Icelandic Shelf, Norwegian

basin, Lofoten Basin and Barents Seas yield U_{37}^K values that fall within the expected (Muller *et al* 1998) range. This suggests that alkenone data from the latter sites may yield reliable palaeoceanographic reconstructions of SST.

Comparison of alkenone distributions with dinocysts proxies for SSS, SST and sea-ice cover in a late Holocene core from the Barents Sea shows that the $\%C_{37:4}$ record responded to major changes in SSS and/or sea-ice cover. This supports the use of $\%C_{37:4}$ as a general marker for the influence of arctic/polar water in palaeoceanographic reconstructions. However, the use of $\%C_{37:4}$ to derive absolute palaeo-SSS values was not confirmed.

Chapter 3: Distribution of long-chain alkenones in the Nordic Seas

- Aagaard, K., Swift, J. H., and Carmack, E. C. (1985). Thermohaline circulation in the Arctic Mediterranean Seas. *Journal of Geophysical Research* **90**, 4833-4846.
- Allen, J. T., and Smeed, D. A. (1996). Potential vorticity and vertical velocity at the Iceland-Faeroes front. *Journal of Physical Oceanography* **26**, 2611-2634.
- Allen, J. T., Smeed, D. A., and Chadwick, A. L. (1994). Eddies and mixing at the Iceland-Faeroes Front. *Deep-Sea Research I* **41**, 51-79.
- Andrulleit, H. A. (1997). Coccolithophore fluxes in the Norwegian-Greenland Sea: Seasonality and assemblage alterations. *Marine Micropaleontology* **31**, 45-64.
- Bacon, S., and Yelland, M. J. (1999). RRS *James Clark Ross* Cruise 44, Cruise Report No. 33, pp. 140. Southampton Oceanography Centre.
- Bard, E. (2001). Paleooceanographic implications of the difference in deep-sea sediment mixing between large and fine particles. *Paleoceanography* **16**, 235-239.
- Bard, E., Rostek, F., Turon, J.-L., and Gendreau, S. (2000). Hydrological impact of Heinrich events in the subtropical Northeast Atlantic. *Science* **289**, 1321-1324.
- Baumann, K. H., Andrulleit, H. A., and Samtleben, C. (2000). Coccolithophores in the Nordic Seas: comparison of living communities with surface sediment assemblages. *Deep-Sea Research II* **47**, 1743-1772.
- Broecker, W. S., and Denton, G. H. (1989). The role of ocean-atmosphere reorganization in glacial cycles. *Geochimica et Cosmochimica Acta* **53**, 2465-2501.
- Brown, C. W. (2003). Blooms of the coccolithophorid *Emiliania huxleyi* in global and US coastal waters. NOAA-website: <http://orbit-net.nesdis-noaa.gov/orad2/doc/ehux>.
- Brown, C. W., and Yoder, J. A. (1994). Coccolithophorid Blooms in the Global Ocean. *Journal of Geophysical Research-Oceans* **99**, 7467-7482.
- Brown, J., Colling, A., Park, D., Phillips, J., Rothery, D., and Wright, J. (1998). "Ocean Circulation Open University." Butterworth Heinemann, Milton Keynes.
- Bukry, D. (1974). Coccoliths as paleosalinity indicators - evidence from the Black Sea. In "The Black Sea - Geology, Chemistry and Biology." (E. T. Degens, and D. A. Ross, Eds.), pp. 353-633. Amer. Assn. Petrol. Geol. Memoir 20.
- Coachman, L. K., and Aagaard, K. (1974). Physical Oceanography of Arctic and Subarctic Seas. In "Marine Geology and Oceanography of the Arctic Seas." (Y. Herman, Ed.). Springer-Verlag, New York.
- Conkright, M. E., Levitus, S., O'Brien, T., Boyer, T. P., Stephens, C., Johnson, D., Baranova, O., Antonov, J., Gelfeld, R., Rochester, J., and C., F. (1998). "World Ocean Database CD." U.S. Department of Commerce, Washington, D.C.
- Conte, M. H., and Eglinton, G. (1993). Alkenone and alkenoate distributions within the euphotic zone of the eastern North Atlantic: correlation and production temperature. *Deep-Sea Research I* **40**, 1935-1961.
- Conte, M. H., Thompson, A., and Eglinton, G. (1994). Primary production of lipid biomarker compounds by *Emiliania huxleyi*. Results from an experimental mesocosm study in fjords of southwestern Norway. *Sarsia* **79**, 319-331.
- Conte, M. H., Thompson, A., Lesley, D., and Harris, P. G. (1998). Genetic and physiological influences on the alkenone/alkenoate versus growth temperature relationship in *Emiliania huxleyi* and *Gephyrocapsa oceaonia*. *Geochimica et Cosmochimica Acta* **62**, 51-68.

- Cranwell, P. A. (1985). Long-chain unsaturated ketones in recent lacustrine sediments. *Geochimica et Cosmochimica Acta* **49**, 1545-1551.
- de Vernal, A., Henry, M., Matthiessen, J., Mudie, P. J., Rochon, A., Boessenkool, K. P., Eynaud, F., GrØsfeld, K., Guiot, J., Hamel, D., Harland, R., Head, M. J., Kunz-Pirring, M., Levac, E., Loucheur, V., Peyron, O., Pospelova, V., Radi, T., Turon, J.-L., and Voronina, E. (2001). Dinoflagellate cyst assemblages as tracers of sea-surface conditions in the northern North Atlantic, Arctic and sub-Arctic seas: the new n = 677 data base and its application for quantitative palaeoceanographic reconstruction. *Journal of Quaternary Science* **16**, 681-698.
- Dickey, T., Marra, J., Stramska, M., Langdon, C., Granata, T., Plueddemann, A., Weller, R., and Yoder, J. (1994). Biooptical and Physical Variability in the Sub-Arctic North- Atlantic Ocean During the Spring of 1989. *Journal of Geophysical Research-Oceans* **99**, 22541-22556.
- Dickson, R. R., and Brown, J. (1994). The production of North Atlantic Deep Water, sources, rates, and pathways. *Journal of Geophysical Research* **99**, 12319-12341.
- Dietrich, G., Kalle, K., Krauss, W., and Siedler, G. (1975). "Allgemeine Meereskunde." Borntrager, Berlin.
- Ficken, K. J., and Farrimond, P. (1995). Sedimentary lipid geochemistry of Framvaren: impacts of a changing environment. *Marine Chemistry* **51**, 31-43.
- Flügge, A. (1997). "Jahreszeitliche Variabilität von ungesättigten C 37 Methylketonen (Alkenone) in Sinkstoffallenmaterial der Norwegischen See und deren Abbildung in Oberflächensedimenten." Unpublished Ph.D. thesis, Univ. zu Keil.
- Freeman, K. H., and Wakeham, S. G. (1991). Variations in the distributions and isotopic compositions of alkenones in Black Sea particles and sediments. *Advances in Organic Geochemistry* **19**, 277-285.
- Gong, C., and Hollander, D. J. (1999). Evidence for the differential degradation of alkenones under contrasting bottom water oxygen conditions: Implications for paleotemperature reconstruction. *Geochimica et Cosmochimica Acta* **63**, 405-411.
- Gran, H. H. (1929). Quantitative plankton investigations carried out during the expedition with the 'Michael Sars', July-Sept., 1924. *Rapp. Cons. Explor. Mer.*, **LVI**, 1-50.
- Grimalt, J. O., Rullkötter, J., Sicre, M.-A., Summons, R., Farrington, J., Harvey, H. R., Goñi, M., and Sawada, K. (2000). Modifications of the C37 alkenone and alkenoate composition in the water column and sediment: Possible implications for sea surface temperature estimates in paleoceanography. *GEOCHEMISTRY, GEOPHYSICS, GEOSYSTEMS* **1**, Paper number 2000GC000053.
- Hansen, B. (1985). The circulation of the northern part of the Northeast Atlantic. *Rit Fiskideildar* **9**, 110-126.
- Hansen, B., and Østerhus, S. (2000). North Atlantic-Nordic Seas exchanges. *Progress in Oceanography* **45**, 109-208.
- Harada, N., Shin, K. H., Murata, A., Uchida, M., and Nakatani, T. (2003). Characteristics of alkenones synthesized by a bloom of *Emiliania huxleyi* the Bering Sea. *Geochimica et Cosmochimica Acta* **67**, 1507-1519.
- Helland-Hansen, B., and Nansen, F. (1909). The Norwegian Sea, its physical oceanography based upon the Norwegian researches 1900-1904, Report on Norwegian Fishery and Marine Investigations, 2, part 1, No.2., Mallingske, Christiania (Oslo).
- Herbert, T. D. (2001). Review of alkenone calibrations (culture, water column, and sediments). *Geochemistry, Geophysics, Geosystems* **2**, Paper number 2000GC000055.

Chapter 3: Distribution of long-chain alkenones in the Nordic Seas

- Hoefs, M. J. L., Versteegh, G. J. M., Rijpstra, W. I. C., de Leeuw, J. W., and Damste, J. S. S. (1998). Postdepositional oxic degradation of alkenones: Implications for the measurement of palaeo sea surface temperatures. *Paleoceanography* **13**, 42-49.
- Honjo, S. (1990). Particle fluxes and modern sedimentation in the polar oceans. In "Polar Oceanography." (W. O. Smith, Ed.). Academic Press, San Diego.
- Hopkins, T. S. (1991). The GIN Sea a synthesis of its physical oceanography and literature review 1972-1985. *Earth Science Reviews* **30**, 175-318.
- Johanessen, O. M. (1986). Brief overview of the physical oceanography. In "The Nordic Seas." (H. B.G., Ed.), pp. 103-127. Springer-Verlag, New York.
- Johanessen, O. M., and Foster, L. A. (1978). A note on the topographically controlled oceanic polar front in the Barents Sea. *Journal of Geophysical Research* **83**, 45-71.
- Johanessen, O. M., Johanessen, J. A., Morison, J., Farrelly, B. A., and Svendsen, E. A. S. (1983). Oceanographic conditions in the marginal ice zone north of Svalbard in early fall 1979 with emphasis on mesoscale processes. *Journal of Geophysical Research* **88**, 2755-2769.
- Lalli, C. M., and Parsons, T. R. (1997). "Biological Oceanography - An Introduction." Butterworth Heinmann, Oxford.
- Lee, A. J. (1969). The hydrography of the European Arctic and Subarctic seas. *Oceanography and Marine Biology Annual Review* **1**, 47-76.
- Levitus, S. (1982). "Climatological atlas of the worlds oceans: Professional paper No. 13." NOAA., Rockville, Maryland, USA.
- Li, J., Philip, R. P., Pu, F., and Allen, J. (1996). Long-chain alkenones in Quinghai Lake sediments. *Geochimica et Cosmochimica Acta* **60**, 235-241.
- Longhurst, A. L. (1998). "Ecological Geography of the Sea." Academic Press, San Diego.
- Marchant, H. J., and Thomsen, H. A. (1994). Haptophytes in polar waters. In "The Haptophyte Algae." (J. C. Green, and B. S. C. Leadbeater, Eds.), pp. 209-228. A Systematics Association Special Volume, Clarendon Press, Oxford.
- Marlowe, I. T., Green, J. C., Neal, A. C., Brassell, S. C., Eglinton, G., and Course, P. A. (1984). Long chain (*n*-C₃₇-C₃₉) Alkenones in the Prymensiophyceae. Distribution of Alkenones and lipids and their Taxonomic significance. *British Phycology Journal* **19**, 203-216.
- Midttun, L. (1985). Formation of dense bottom water in the Barents Sea. *Deep-Sea Research I* **32**, 1233-1241.
- NORSEX_Group. (1983). Norwegian remote sensing experiment in a marginal ice zone. *Science* **220**, 781-787.
- Ohkouchi, N., Kawamura, K., Kawahata, H., and Okada, H. (1999). Depth ranges of alkenone production in the central pacific ocean. *Global Biogeochemical Cycles* **13**, 695-704.
- Okada, H., and McIntyre, A. (1977). Seasonal distribution of modern coccolithophores in the western North Atlantic Ocean. *Marine Biology* **54**, 319-328.
- Opsahl, S., Benner, R., and Amon, R. M. W. (1999). Major flux of terrigenous dissolved organic matter through the Arctic Ocean. *Limnology and Oceanography* **44**, 2017-2023.
- Paasche, E. (1960). Phytoplankton distribution in the Norwegian Sea in June, 1954, related to hydrography and compared with primary production data. *Fiskeridir. Skr. Havundersøk* **12**, 1-112.

- Prahl, F. G., and Muehlhausen, L. A. (1989). An organic geochemical assessment of oceanographic conditions at Manop site C over the past 26, 000 years. *Paleoceanography* **4**, 495-510.
- Prahl, F. G., Sparrow, M. A., and Wolfe, G. V. (2003). Physiological impacts on alkenone paleothermometry. *Paleoceanography* **18**, 1025, doi:10.1029/2002PA000803.
- Prahl, F. G., and Wakeham, S. G. (1987). Calibration of Unsaturation Patterns in Long-Chain Ketone Compositions for Paleotemperature Assessment. *Nature* **330**, 367-369.
- Rahman, A. (1995). Reworked nannofossils in the North Atlantic Ocean and Subpolar basins: Implications for Heinrich events and ocean circulation. *Geology* **23**, 487-490.
- Rey, F. (1981). The development of the spring phytoplankton out-burst at selected sites off the Norwegian Coast. In "The Norwegian Coastal Current." (R. Sætre, and M. Mork, Eds.), pp. 681-711. Geilo.
- Richter, C. (1994). Regional and seasonal variability in the vertical distribution of mesozooplankton in the Greenland Sea. *Berichte zur Polarforschung* **154**, 1-87.
- Rosell-Melé, A. (1998). Interhemispheric appraisal of the value of alkenone indices as temperature and salinity proxies in high-latitude locations. *Paleoceanography* **13**, 694-703.
- Rosell-Melé, A., Carter, J., and Eglinton, G. (1993). Distributions of long-chain alkenones and alkyl alkenoates in marine surface sediments from the North East Atlantic. *22* **3-5**, 501-509.
- Rosell-Melé, A., Eglinton, G., Pflaumann, U., and Sarnthein, M. (1995). Atlantic core-top calibration of the UK37 index as a sea-surface palaeotemperature indicator. *Geochimica et Cosmochimica Acta* **59**, 3099-3107.
- Rosell-Melé, A., Jansen, E., and Weinelt, M. (2002). Appraisal of a molecular approach to infer variations in surface ocean freshwater inputs into the North Atlantic during the last glacial. *Global and Planetary Change* **34**, 143-152.
- Sætre, R., and Mork, K. A. (1981). The Norwegian Coastal Current, In "Proceedings of the Norwegian Coastal Current Symposium, 9-12 September 1980, GEILO." University of Bergen.
- Sakshaug, E., and Holm-Hansen, O. (1984). Factors governing pelagic production in polar oceans. In "Marine and Phytoplankton Productivity. Lecture Notes on Coastal and Estuarine Studies, Vol. 8." (O. Holm-Hansen, L. Bolis, and R. Gilles, Eds.), pp. 1-18.
- Samtleben, C., Schäfer, P., Andruleit, H., Baumann, A., Baumann, K.-H., Kohly, A., Matthiessen, J., and Schröder-Ritzrau, A. (1995). Plankton in the Norwegian-Greenland Sea: from living communities to sediment assemblages - an actualistic approach. *Geologische Rundschau* **84**, 108-136.
- Schlitzer, R. (2001). Ocean Data View. <http://www.awi-bremerhaven.de/GEO/ODV>.
- Schöner, A., Menzel, D., Schulz, H. M., and Emeis, K. C. (1998). Long-chain alkenones in Holocene sediments of the Baltic Sea - A status report. *Meereswissenschaftliche Berichte, Inst. f. Ostseeforschung* **34**, 122-124.
- Schulz, H. M., Schöner, A., and Emeis, K. C. (2000). Long-chain alkenone patterns in the Baltic Sea - an ocean- freshwater transition. *Geochimica Et Cosmochimica Acta* **64**, 469-477.
- Sicre, M.-A., Bard, E., Ezat, U., and Rostek, F. (2002). Alkenone distributions in the North Atlantic and Nordic sea surface waters. *Geochemistry, Geophysics, Geosystems* **3**, 10.1029/2001GC000159.
- Sikes, E. L., and Sicre, M. A. (2002). Relationship of the tetra-unsaturated C-37 alkenone to salinity and temperature: Implications for paleoproxy applications. *Geochemistry Geophysics Geosystems* **3**, art. no.-1063.

Chapter 3: Distribution of long-chain alkenones in the Nordic Seas

- Sikes, E. L., and Volkman, J. K. (1993). Calibration of alkenone unsaturation ratios (uk37) for paleotemperature estimation in cold polar waters. *Geochimica et Cosmochimica Acta* **57**, 1883-1889.
- Sikes, E. L., Volkman, J. K., Robertson, L. G., and Pichon, J. J. (1997). Alkenones and alkenes in surface waters and sediments of the Southern Ocean: Implications for paleotemperature estimation in polar regions. *Geochimica Et Cosmochimica Acta* **61**, 1495-1505.
- Smayda, T. J. (1958). Phytoplankton studied around Jan Mayan Island March - April. *Nytt. Mag. Bot.* **6**, 75-96.
- Smith, W. O., and Brightman, R. I. (1991). Phytoplankton photosynthetic response during the winter-spring transition in the Fram Strait. *Journal of Geophysical Research* **96**, 4549-4554.
- Smith, W. O., Codispoti, L. A., Nelson, D. M., Manley, T., Buskey, E. J., Niebauer, H. J., and Cota, G. F. (1991). Importance of *Phaeocystis* blooms in the high-latitude ocean carbon cycle. *Nature* **352**, 514-516.
- Stefánsson, U. (1962). North Icelandic waters. *Rit Fiskideildar* **3**, 269.
- Sverdrup, H. U., Johnson, M. W., and Fleming, R. H. (1946). "The Oceans." Prentice-Hall, New York.
- Swift, J. H. (1986). The Arctic waters. In "The Nordic Seas." (B. G. Hurdle, Ed.), pp. 129-153. Springer-Verlag, New York.
- Ternois, Y., Sicre, M. A., Boireau, A., Beaufort, L., Miquel, J. C., and Jeandel, C. (1998). Hydrocarbons, sterols and alkenones in sinking particles in the Indian Ocean sector of the Southern Ocean. *Organic Geochemistry* **28**, 489-501.
- Ternois, Y., Sicre, M. A., Boireau, A., Conte, M. H., and Eglinton, G. (1997). Evaluation of long-chain alkenones as paleo-temperature indicators in the Mediterranean Sea. *Deep-Sea Research I* **44**, 271-286.
- Thiel, V., Jenisch, A., Landmann, G., Reimer, A., and Michaelis, W. (1997). Unusual distributions of long-chain alkenones and tetrahymanol from the highly alkaline Lake Van, Turkey. *Geochimica et Cosmochimica Acta* **61**, 2053-2064.
- Thomsen, C., Schulz-Bull, D. E., Petrick, G., and Duinker, J. C. (1998). Seasonal variability of the long-chain alkenone flux and the effect on the U37k'-index in the Norwegian Sea. *Organic Geochemistry* **28**, 311-323.
- Trotte, J. R. (1985). "Phytoplankton floristic composition and size-specific photosynthesis in the eastern Canadian arctic." Unpublished MSc thesis, Dalhousie University.
- van Aken, H. M., and Becker, G. (1996). Hydrography and through-flow in the north-eastern north Atlantic Ocean: the NANSEN project. *Progress in Oceanography* **38**, 297-346.
- Volkman, J. K., Burton, H. R., Everitt, D. A., and Allen, D. I. (1988). Pigment and lipid compositions of algal and bacterial communities in Ace Lake, Vestfold Hills, Antarctica. *Hydrobiologia* **165**, 41-57.
- Voronina, E., Polyak, L., de Vernal, A., and Peyron, O. (2001). Holocene variations of sea-surface conditions in the southeastern Barents Sea, reconstructed from dinoflagellate cyst assemblages. *Journal of Quaternary Science* **16**, 717-726.
- Winter, A., Jordan, R. W., and Roth, P. H. (1994). Biogeography of living coccolithophores in ocean waters. In "Coccolithophores." (A. Winter, and W. G. Siesser, Eds.), pp. 161-177. Cambridge University Press, Cambridge.
- Yendle, P. W. (1989). "Chemometric Studies of Biochemical and Geochemical Systems." University of Bristol, U.K.

Zink, K.-G., Leythaeuser, D., Melkonian, M., and Schwark, L. (2001). Temperature dependency of long-chain alkenone distributions in Recent to fossil limic sediments and in lake waters. *Geochimica et Cosmochimica Acta* **65**, 253-265.

4. Post-Glacial and Holocene palaeoceanography of the Icelandic shelf



Cover image: Aurora Borealis above Iceland – courtesy of www.iww.is.com



Contents

4.1.	Introduction	103
4.1.1.	Background, aims and objectives	103
4.1.2.	Context – the Icelandic continental shelf	106
4.2.	Study specific experimental	109
4.2.1.	Biomarker analysis	109
4.2.2.	Chronology	110
	Radiocarbon dates	110
	Tephra markers	111
	Age models and stratigraphy	115
4.3.	Results and discussion	117
4.3.1.	Biomarker stratigraphy & correlations	117
	Post-Glacial 11.5 – 15kyr BP	117
	Holocene 0 – 11.6 kyr BP	120
4.4.	Conclusions	129

Tables

Table 4.1:	Collection details and analytical parameters calculated for the cores discussed in the text.	108
Table 4.2:	Radiocarbon dates in cores B997-350PC, B997-325PC, B997-325GC & JR51-GC35 from the North and West Icelandic Shelf.	112
Table 4.3:	Age model regressions for cores linear sedimentation rates.	116

(see volume II for figures)

4.1. Introduction

4.1.1. Background, aims and objectives

Aside from a few historically documented anomalies – e.g. the Little Ice Age and the Medieval Warm Period- the Holocene was regarded, until recently, as a period of climatic stability. Earlier arguments that challenged the stability concept failed to change the status quo (Denton and Karlén, 1973; Pisias et al., 1973). However, palaeoclimatic and palaeoceanographic research over the last decade has suggested that Holocene climate - on a global and regional scale - has experienced higher instabilities than previously thought (Oppo, 1997). Abrupt millennial scale anomalies in proxies for parameters such as temperature, ice rafting, deep water flow strength, aridity and prevailing winds can be recognized in the sediments of the North Atlantic Ocean (e.g. Bianchi and McCave, 1999; Bond et al., 1997; Bond et al., 1999; Calvo et al., 2002; deMenocal et al., 2000; Oppo et al., 2003), ice cores from Greenland (Mayewski et al., 1997; O'Brien et al., 1995), South America (Thompson et al., 1995) and Africa (Thompson et al., 2002) and terrestrial archives as diverse as lakes in Mexico (Hodell et al., 1995) and glacial moraine complexes in Iceland (e.g. Mackintosh et al., 2002; Stötter et al., 1999).

The climatic variability in such records is small ($\sim 2^{\circ}\text{C}$) compared to the dramatic instability and strong cyclicality pervasive in the last glacial period (c.10 – 120 kyr BP). Most famously reflected by the abrupt changes during the period 20 - 80 kyr BP, in which – during some 20 Dansgaard-Oeschger events - temperatures fluctuated over a range of 5 to 8°C (Johnsen et al., 1992). However, understanding the more subtle variability of the Holocene is important for three main reasons:

Firstly, cyclical changes in the ocean-atmosphere system must be constrained if we are to determine possible recent anthropogenic effects on climate. The outcomes of altering the proportions of atmospheric gases can not be accurately modelled, until the underlying natural variability is understood.

Secondly, the amplitudes of natural sub-Milankovitch interglacial variation may - in themselves - be large enough to place a significant strain on future human society and agriculture. During several Holocene climate events sea surface temperatures in the northern North Atlantic changed abruptly (<500 years) by more than 1°C (Calvo et al.,

2002). Furthermore, evidence for variations in monsoonal intensity and markedly more cool/arid conditions in north Africa and southern Asia are coeval with Holocene IRD events in the Atlantic (Bond et al., 1997; Heusser and Sirocko, 1997).

Thirdly, the Holocene period has witnessed the rapid development of human society, from the first Neolithic farmers, through to industrialization. Archaeology has all too often viewed the environment as an essentially passive back-cloth against which human history is acted out (Roberts, 1998). Recent work, such as that by Josenhans *et al.* (1997) has linked sea-level changes to human migration, whilst deMenocal (2001) has correlated records of increased Holocene aridity to discontinuities in human cultures. Such work illustrates that an understanding of Holocene human activity is impossible without records of Holocene environmental change.

The aim of this chapter is to look for evidence of post-Glacial and Holocene climatic changes in high resolution Icelandic shelf marine cores. Accordingly the objectives of this chapter are:

- To investigate north & west Iceland Shelf biomarker records for the post-Glacial and Holocene – especially to see whether it is feasible to derive a meaningful alkenone stratigraphy from this hitherto untackled (for biomarkers) sedimentary environment.
- To place the biomarker records in a regional context by comparison with published palaeoceanographic regional data.
- To compare the SST records from the Icelandic Shelf with terrestrial Icelandic records of glacial advances and environmental change.

Three of the cores studied in this chapter (the B997-cores) were obtained as part of the 1997 IMAGES (International MARine Global change Study) USA/Icelandic project. Hence investigation of these cores forms part of a post cruise analysis that is an international collaboration between workers from the USA, Iceland, Norway, and the EU. The general goals for the IMAGES project are as follows:

- To gain an understanding of the ice sheet/ocean interactions along the northern and western margins of the Iceland Ice Cap and the eastern margin of the Greenland Ice Sheet over the last glacial/deglacial cycle.

- To provide a high-resolution comparison of the Holocene history of the Atlantic water mass off West and North West Iceland in comparison with variations in Polar Water and Arctic Intermediate Water off East Greenland.

Core JR51-GC35 (studied in this chapter) was obtained as part of the ARCICE (ARctic ICE and environmental variability) NERC thematic program. The general aim of the ARCICE project is to enhance our understanding of, and capacity to, predict the fluctuations of Arctic sea-ice and glaciers, which influence climate and sea levels in NW Europe. The investigation of JR51-GC35 forms part of an ARCICE sub-project entitled “Palaeoclimate and dynamics of Arctic continental margins” and contributes to the objective of:

- Geophysical and geological (in this case biogeochemical) investigations, to constrain sedimentation, ice and ocean variability on Arctic continental margins.

4.1.2. Context – the Icelandic continental shelf

The cores studied in this chapter are located on the north and west Icelandic continental shelf. The core locations are shown in Figure 4.1. In Table 4.1 (page 108) pertinent collection and analytical details relating to the cores are summarised. Iceland is located in the southwest of the Nordic Seas (Figure 3.1). A region of strong east west hydrographic gradients, characterised by seasonal and spatial variations in the physical properties of the surface waters (SST, SSS), sea-ice distribution and deep water formation. A general outline of the contemporary physical and ecological oceanography of the Nordic Seas is given in chapter 3 (page 59).

Iceland is located in a position which is sensitive to interactions of the Atlantic source waters, advected by the Irminger (IC) and North Icelandic Irminger Currents (NIIC), and opposing cold Arctic and Polar waters advected by the East Icelandic (EIC) and East Greenland Currents (EGC) (Hansen and Østerhus, 2000; Hopkins, 1991; Malmberg, 1985) (see Figure 3.1). The sites studied in this chapter are today mainly influenced by the warm IC and NIIC. Benthic foraminiferal evidence suggests that the north Icelandic shelf is currently influenced by the NIIC down to a depth of at least 500m (Eiriksson et al., 2000b). Lateral and vertical mixing as a result of the parallel flow of the NIIC and EIC and winter cooling leads to the formation of an intermediate depth water mass (North Icelandic Winter Water, NIWW) in the Iceland sea, which disintegrates by spring or summer (see Figure 3.2) (Swift and Aagaard, 1981). This water mass contributes to the formation of deep waters in the Nordic seas, hence a mechanism exists whereby climatic changes on the Icelandic shelf are linked to the thermohaline circulation.

The north continental shelf of Iceland today is subject to extreme variations in hydrographic conditions which can lead to changes of 5°C averaged through the entire water column (Olafsson, 1999). The variability associated with Iceland's location proximal to the Arctic Front (see Figure 3.1) was demonstrated in the late 1960s by the Great Salinity Anomaly (GSA), triggered by an excursion of freshwater (sea-ice) from the Arctic Ocean (Dickson et al., 1988). This resulted in sharp decreases in both temperature and salinity at hydrographic stations on the north Icelandic shelf, including in Húnaflói trough (see Figure 4.1) (Olafsson, 1999). The Icelandic continental shelf has many troughs characterised by high sedimentation rates of up to 2m/kyr (Andrews

and Giraudeau, 2003). Given these attributes the area has high potential for the identification of millennial scale climatic oscillations that occurred in the Holocene. This has been demonstrated by recent records from the Icelandic shelf of variations in sediment physical properties (Andrews et al., 2003; Andrews et al., 2002b; Andrews et al., 2001b), coccolithophore assemblages and isotopic data (Andrews and Giraudeau, 2003), and benthic foraminiferal assemblages (Eiriksson et al., 2000b). However, no alkenone proxy evidence (i.e. U_{37}^K or U_{37}^K) of palaeo-SST or other biomarker evidence has yet been obtained.

Figure 4.2 illustrates the main environmental controls on the northern shelf. The sites on the north and west shelf are mainly influenced by the IC and NIIC respectively (Figure 3.1). However, on the northern shelf, in particular, this surface flow can be interrupted by incursions of cold and fresh Arctic or Polar water (Olafsson, 1999). Changes in the relative contributions of Atlantic and Polar waters are driven by factors external to the shelf region (Mysak and Power, 1992; Serreze et al., 1992). A third component is glacial, nival and fluvial runoff which transports freshwater and suspended sediments from the adjacent land areas, to the fjords and hence to the shelf. Alkenone biomarkers should be particularly apposite for investigating past changes in the relative influence of the three components. Firstly the U_{37}^K indices may be used to reconstruct palaeo-SST, as long as values of $\%C_{37:4}$ are below the threshold of 5% (Rosell-Melé, 1998). Secondly, prolonged influence by Arctic waters or a significant reduction in shelf SSS's by glacial-runoff waters should be detected by fluctuations in the $\%C_{37:4}$ index to values above 5%.

Table 4.1: Collection details and analytical parameters calculated for the cores discussed in the text. 1: Spacing between successive sub-samples. 2: For Alkenones

Core Name	Cruise (platform)	Coring System	Date obtained	Coordinates	Water depth	Sample thickness	Sampling frequency ¹	Sample dry weight	Biomarkers		Pigments	Quantification technique ²
									U ^k ₃₇	U ^k ₃₇ %C _{37:4}		
B997-350PC	B997 (R/V Bjarni Sæmundsson)	piston	29/7/97	64°16'60 N	238m	2cm	4cm	~2g	✓	✓	✓	CIMS
B997-325GC	B997 (R/V Bjarni Sæmundsson)	gravity	23/7/97	24°01'49 W	348m	2cm	4cm	~2g	✓		✓	FID
B997-325PC	B997 (R/V Bjarni Sæmundsson)	piston	23/7/97	20°59'99 W	348m	2cm	4cm	~1g	✓		✓	FID
JR51-GC35	JR51 (RRS James Clark Ross)	gravity	26/8/00	66°59'96 N	420m	1cm	4cm	~2g	✓	✓	✓	CIMS
				17°57'66 W								

4.2. Study specific experimental

The three B997- cores were obtained as part of the 1997 IMAGES USA/Iceland project. They were opened, described and sub-sampled in the laboratories of the Institute for Arctic and Alpine Research (INSTAAR), Boulder, USA. Core JR51-GC35 was obtained on the 2000 ARCICE cruise and was opened, described and sub-sampled onboard the RRS *James Clark Ross*. All organic geochemical sub-samples were kept either refrigerated or (preferably) frozen at -20°C, between sub-sampling and analytical work-up. Procedures for sampling and analysis for radiocarbon dates and tephra are discussed below in section 4.2.2 (from page 110). Sub-samples for the analysis of sediment physical properties (e.g. MS, particle size, density, TOC) were obtained and analysed either at the INSTAAR sedimentology laboratory (under supervision of J.T. Andrews) or the BOSCOR facility at SOC (by the present author). The sediment physical property data may be published by other workers and is not considered in detail in this thesis.

4.2.1. Biomarker analysis

Details of the analytical procedures for work-up and quantification of alkenones and pigments are given chapter 2. In high latitude environments, alkenone sedimentary concentrations can be very low, and the alkenone signal may be further diluted due to the greater relative inputs of clastic material in continental shelf environments. GC-CI-MS has a greater sensitivity for the analysis of alkenones than GC-FID, and its higher selectivity also allows a greater confidence in measuring alkenone within-class-distributions, particularly %C_{37:4} (see chapter 2). Hence, GC-CI-MS was preferred for the analysis of the sediment cores. However, not all of the samples could be analysed by GC-CI-MS due to unforeseeable operational constraints. Therefore, cores B997-350PC and JR51-GC35, with the highest sedimentation rates (and potentially most diluted alkenone signal), were analysed by this method, and U^K_{37'}, U^K₃₇ and %C_{37:4} are reported. Cores B997-325PC & GC have a lower sedimentation rate were therefore were analysed by GC-FID only. As the accuracy of measuring C_{37:4} by GC-FID is low (see chapter 2) only U^K_{37'} is reported for these cores. All of the cores had some sections where alkenones were undetectable, even after analysis by GC-CI-MS. Additionally, some samples were rejected due the integrated peaks being below the limits of reliable detection identified in chapter 2.

4.2.2. Chronology

AMS ^{14}C dating of either molluscs, planktonic or benthic foraminifera and in one case a tephra horizon, were used to establish the chronologies for cores B997-350PC, B997-325GC/PC and JR51-GC35. Details of the analysis and justification of the adopted age-models are given in the following sections. The lithostratigraphic logs (with dated horizons indicated) and age-depth diagrams for each core are illustrated in Figure 4.3 - Figure 4.5.

Radiocarbon dates

Foraminifera are the most commonly used source of carbon for AMS ^{14}C dating in Atlantic marine cores. Foraminifera were present in most sub-samples in the cores studied for this chapter, however, the total weight retrieved by dry picking often fell below that recommended ($>10\text{mg}$) by the laboratory for a precise AMS ^{14}C date (as recommended by S. Moreton, pers. comm., NERC radiocarbon lab). Therefore, as an alternative to foraminifera, mollusca (bivalves, gastropods, tube worms) were utilised where possible (individually or in combination), to achieve sufficient weight of carbon. Molluscs were identified by Dr H.A. Ten Hove and Dr. R. Moolenbeek at the Zoological museum, University of Amsterdam. Most mollusca were bivalves or scaphopods (gastropods), except for one specimen of *Ditrupa arietina*, an annelid (tube worm). Annelids are not commonly used for radiocarbon dating in palaeoceanography, due to their relatively rarity. However, the sample was considered valid for dating as *Ditrupa arietina* biosynthesises CaCO_3 (i.e. it is not an agglutinate) (H.A. Ten Hove, pers. comm.). Also, AMS ^{14}C radiocarbon dating of annelid tubes for palaeoenvironmental work is not unprecedented (Pickard, 1985; Pickard et al., 1986; Reish and Mason, 2001).

A total of 26 new AMS ^{14}C dates were obtained for this thesis, eight for B997-350PC, eight for B997-325GC/PC and ten for JR51-GC35 (Table 4.2, page 112). Material for dating was picked by the author. At the NERC radiocarbon facility (East Kilbride, UK), the outer 20% by weight of four samples (see Figure 4.2) was removed by etching with dilute HCL. All samples were hydrolysed to CO_2 with 85% with ortho-phosphoric acid at 25°C . The gas was converted to graphite by FE/Zn reduction. Samples were sent to the NSF-University of Arizona AMS facility for analysis. Two basal AMS ^{14}C dates had been obtained previously for B997-350PC (418cm) and B997-325PC (257cm) by J.T. Andrews. Preparation of these dates was at INSTAAR, analysis for B997-350PC

(418cm) was at Arizona and for B997-325PC (257cm) at the Centre for AMS at Lawrence Livermore National Laboratory (CAMS). There is a discrepancy between the dates provided by Prof. Andrews and those obtained during this thesis (Figure 4.3 - Figure 4.5). The reason is unclear. It may be due to a systematic bias between the work-up and analytical methods carried out at the different institutions. Another reason may be that the basal dates, obtained previously, were obtained from foraminifera taken from the core catcher – and that this incorporated some younger material, during passage through the sediments at the head of the core barrel. Inclusion of all the dates would lead to severe dating reversals in the age-depth regressions. Therefore, in order to derive sensible age-models, the previously obtained basal dates are rejected.

We apply the modern reservoir age (ΔR) value of 400 yr (Andersen et al., 1989) as a correction for all AMS ^{14}C dates. Andrews *et al* (2002a) have recently constrained (by AMS ^{14}C dates) the Saksunarvatn (10180 ± 60 cal yr BP) tephra layer in a number of marine cores from the N.W. Icelandic shelf. Comparison of the marine dates with terrestrial ^{14}C dates for this tephra indicates that the modern ocean reservoir correction of 400 yr is applicable to the last 9000 ^{14}C yr BP (Andrews et al., 2002a). Previous workers have applied a 400 yr correction to N. Icelandic shelf, marine core AMS ^{14}C dates as old as 14100 ± 140 ^{14}C yr BP (Eiríksson et al., 2000b). The corrected AMS ^{14}C dates were converted to calendar ages using the CALIB 4.3 program (Stuiver and Reimer, 1993).

Tephra markers

Five tephrochronostratigraphical marker horizons were preliminarily identified in the cores during the production of the lithostratigraphical logs. The horizons were selected visually, on the basis of appearance and apparently higher concentration of basaltic volcanic glass. Detailed petrological analysis was not undertaken. The horizons are indicated in Figure 4.3 - Figure 4.5. The bases of the horizons were measured at:

- B997-350PC at 165 and 172cm
- JRGC-35 at 420 and 430cm
- B997-325PC at 207cm

The horizons in B997-350PC and JR51-GC35 were relatively thin (<0.5 cm). The horizons in JR51-GC35, whilst discrete, occurred as lenses i.e. they did not cut across the full thickness of the core. The horizon in B997-325PC was over 4cm thick, and

Chapter 4: Post-Glacial and Holocene palaeoceanography of the Icelandic shelf

Table 4.2: Radiocarbon dates in cores B997-350PC, B997-325PC, B997-325GC & JR51-GC35 from the North and West Icelandic Shelf. All material was picked by the author, the samples were prepared to graphite at the NERC radiocarbon facility and sent to the university of Arizona NSF-AMS facility for ^{14}C analysis. Except for samples marked with *, which were previously obtained by J.T. Andrews. HCL – outer 20% removed by HCL. † estimated $\delta^{13}\text{C}$ - insufficient material for an independent $\delta^{13}\text{C}$ measurement.

Core	Depth from top (cm)	Laboratory code	Material and weight (mg)	^{14}C age (yr BP $\pm 1\sigma$)	Reservoir corrected age (yr BP $\pm 1\sigma$)	Calibrated age (yr BP $\pm 2\sigma$)	$\delta^{13}\text{C}_{\text{PDB}}\text{‰}$ (± 0.1)
B997-350PC	0-1	AA-46845	Mixed benthic forams (10)	2818 \pm 39	2418 \pm 39	2601 (2704-2424)	-0.3
	5	AA-53120	Sepulid worm tube from <i>Ditrupa arctica</i> (55)	645 \pm 36	245 \pm 36	284 (337-250)	1.9
	42 HCL	AA-53100	Bivalve mollusc <i>Acanthocardia cf. aculeata</i> (juv) (58.7)	9713 \pm 69	9313 \pm 69	10325 (11126-10202)	1.3
	88	AA-53101	Fragments of bivalve mollusc, taxodont, <i>Yonitella</i> (22.6)	10698 \pm 75	10298 \pm 75	11930 (12802 - 11278)	-1.1
	146 – 147	AA-53102	Mixed benthic foraminifera (6.8)	10563 \pm 61	10163 \pm 61	11661 (12273-10870)	-1.3
	196	AA-53103	Gastropod mollusc fragment <i>Opisthobranch. Atyx</i> (22.5)	10916 \pm 64	10516 \pm 63	12585 (12883-11589)	-1.1
	249-250 HCL	AA-53104	Scaphopod mollusc (162.2)	11537 \pm 66	11137 \pm 66	13012 (13755-12676)	0.2
	324 HCL	AA-53105	Bivalve fragment, mussel (106.3)	11966 \pm 87	11566 \pm 87	13445 (13817-13045)	-1.8
	*	418	AA-29211	Benthic forams, <i>N. labradorica</i> (7)	10745 \pm 75	10345 \pm 75	11953 (12805-11416)
B997-325GC	0-1	AA-46846	Mixed benthic forams (10)	1247 \pm 36	847 \pm 36	778 (888-694)	-1.3
	9-10	AA-53121	Mixed benthic forams and bivalve fragments (14.9)	2783 \pm 39	2383 \pm 39	2487 (2685-2350)	-0.5
	31	AA-53106	Gastropod mollusc <i>Lunatia groenlandica</i> (24.5)	4470 \pm 47	4070 \pm 47	4634 (4803-4508)	0.4
B997-325PC	87-88 HCL	AA-53107	Mixed benthic forams (11.2)	6921 \pm 72	6521 \pm 72	7421 (7557-7292)	-1.5
	99-101	AA-53108	Mixed benthic foraminifera and small bivalves <i>Thyasira cf. sarsi</i> (15.6)	7347 \pm 66	6947 \pm 66	7788 (7934-7664)	-1.6
	139-141	AA-53109	Mixed benthic foraminifera and small bivalves <i>Thyasira cf. sarsi</i> (23)	8759 \pm 67	8359 \pm 67	9234 (9756-8988)	-2.0
	171-173	AA-53110	Mixed benthic forams (17.4)	9252 \pm 79	8852 \pm 79	9840 (10288-9551)	-3.0
	211-213	AA-53111	Scaphopod mollusc <i>Dentalium entalis</i> , mixed benthic forams and bivalve fragments (23)	10400 \pm 150	10000 \pm 150	11329 (12250-10847)	-2.6
	*	257	CAM-44869	Benthic foram, <i>N. labradorica</i> (10)	9430 \pm 50	9030 \pm 50	10206 (10559-9815)
JR51-GC35	0-1	AA-46847	Mixed benthic forams (9)	473 \pm 36	73 \pm 36	70 (217-0)	-1.5 †
	54-55	AA-53112	Unknown bivalve mollusc fragments (11.3)	1417 \pm 65	1017 \pm 65	948 (1100-832)	-7.9
	112-113	AA-53113	Gastropod mollusc fragment <i>Buccinid?</i> (and mixed forams (15.2)	2621 \pm 58	2221 \pm 58	2310 (2424-2146)	1.4
	168	AA-53114	Scaphopod mollusc <i>Dentalium entalis</i> (30.2)	3706 \pm 59	3306 \pm 59	3620 (3783-3462)	0.7
	214-215	AA-53115	Mixed benthic forams (9.2)	4612 \pm 70	4212 \pm 70	4826 (4980-4634)	-1.2
	276-277	AA-53116	Bivalve molluscs <i>Thyasira cf. sarsi</i> (11.2)	5541 \pm 44	5141 \pm 44	5910 (5997-5852)	-5.1
	334	AA-53117	Gastropod mollusc <i>Opisthobranch</i> fragments (35.8)	6537 \pm 45	6137 \pm 45	7021 (7172-6918)	-0.9
	384	AA-53118	Scaphopod mollusc <i>Dentalium entalis</i> (35)	8286 \pm 50	7886 \pm 50	8828 (8946-8628)	0.2
	420-421.5	AA-53119	Mixed benthic forams (9.9)	9041 \pm 51	8641 \pm 51	9700 (9842-9156)	-1.8
	449-451	AA-46848	Mixed benthic forams (10)	9403 \pm 58	9003 \pm 58	10128 (10555-9810)	-2.2

consisted of what appeared to be 100% volcanic glass and had a sharp lower boundary. This had already been identified as the Saksunarvatn tephra as part of a survey of the distribution of this tephra layer in the marine sediments north of Iceland (Andrews et al., 2002a). We re-analysed the material from B997-325PC (207cm) at the NERC tephrochronological unit (Dept. of Geosciences, University of Edinburgh) in order to aid identification of the unassigned tephra horizons in cores B997-350PC and JR51-GC35. Analysis of oxides was carried out under the supervision of Dr. P. Hill. Freeze dried samples were sieved at $64\mu\text{m}$ and dried in an oven at 60°C . A portion of the sample was then prepared on a slide. Quantitative analysis was carried out with a Cambridge Instruments Microscan Mk5 using wavelength dispersive spectrometry (WDS) with an accelerating voltage of 20kV, a beam current of 15nA and a beam diameter of $1\mu\text{m}$. For rhyolitic shards a 10s peak count was employed for each element, with two elements measured simultaneously. Due to the relatively high stability of the basaltic shards two peak counts of 10s were undertaken to increase the precision (Hunt and Hill, 1993). Sodium was measured in the first and last counting period, to access the degree of sodium mobilisation. A ZAF procedure (Sweatman and Long, 1969) was applied to correct for atomic number, absorption and fluorescence effects. In addition, counter dead time was also corrected for. Any drift in the readings was monitored by regular analysis of an andradite standard. Calibration was undertaken using a combination of standards of pure, metals silicates and synthetic oxides which contain most of the major elements found in the tephra samples.

The results of the geochemical analysis were compared with tephra data obtained from Iceland by workers at the Edinburgh Geosciences department (Dugmore and Newton, 1997; Wastegard et al., 2001a), as well as data from published sources (e.g. Björck et al., 1992; Boyle, 1999; Eiriksson et al., 2000; Haflidason et al., 2000; Jennings et al., 2002a; Larsen et al., 2001). Tephra data obtained by workers from the Edinburgh Geosciences department were preferred for use as a comparison because the measurements were made using the same equipment and standards, and consequently minimal systematic bias was expected (P. Hill pers. comm.).

The oxide chemistry of the horizons from B997-350PC could not be satisfactorily matched with any of the comparison data. However, the geochemistry of the horizons in JR51-GC35 and B997-325PC showed a good correlation to previously identified

samples of the Saksunarvatn tephra analysed at Edinburgh. Results of these comparisons are illustrated in Figure 4.6 and Figure 4.7. A sample 4 cm below the base of the tephra horizon in core B997-325PC yielded a ^{14}C date of 10000 ± 150 yr BP (reservoir corrected). The closest dated interval in the same core above the tephra horizon at 172cm yields a ^{14}C date of 8852 ± 79 BP (reservoir corrected). Considerable convergence of data shows that the Saksunarvatn tephra was deposited ~ 9040 ^{14}C yr BP (e.g. Birks et al., 1996; Wastegard et al., 2001b; Wastl et al., 1999). Given the average sedimentation rate in the section of the core ($\sim 70\text{cm/kyr}$) the lower bracketing date in B997-325PC is older than would be expected for a level 4cm below the tephra ($10000 \pm 150\text{yr BP}$). However, the correlation of geochemistry to the Saksunarvatn has been confirmed by analysis at two different laboratories and the thickness and depth of the horizon is also consistent with the occurrence of the Saksunarvatn in proximal marine cores (Andrews et al., 2002a). Therefore, we allocated the base of the tephra horizon a calendar age of 10180 ± 60 yr BP (from Andrews et al., 2002a) and use this date as an alternative to the dated mollusc shell at 211 cm in B997-325PC.

Material from immediately beneath the tephra at 420cm in JR51-GC35 yielded a reservoir corrected ^{14}C date of 8641 ± 51 yr. This is 400 yr younger than the expected date for the Saksunarvatn tephra of ~ 9040 yr BP. The basal (450cm) date of the core is 9003 ± 58 yr, therefore, we suggest that the tephra in GC-35 is reworked Saksunarvatn tephra and that genuine *in situ* Saksunarvatn horizon occurs just below the depth to which the core penetrated. The reworking of the Saksunarvatn tephra into younger marine sediments on the N. Icelandic shelf has been previously observed (Andrews et al., 2002a; Andrews and Giraudeau, 2003). This is supported by the physical occurrence of the tephra horizons; as thin discontinuous lenses. Therefore, we do not use the tephra in JR51-GC35 at 420 or 430cm as a chronological marker.

Age models and stratigraphy

The age-depth relationships derived from using the chronological methods outlined above are illustrated in Figure 4.3 - Figure 4.5. The age-model regressions used are listed in Table 4.3 (page 116).

B997-350PC

In B997-350PC there are two distinctive units; between 0-20cm and 20-420cm depth. The transition between these two units is characterised by a change in colour and physical properties such as CaCO_3 and dry bulk density (see Figure 4.3). Radiocarbon dates from the upper section (Table 4.2, page 112) give late Holocene ages but display an age reversal, suggesting reworking of sediments in the upper part of the core or sediment scrambling by the piston coring method. The lower unit between 20 -420cm has consistent colour and physical properties. Based on the equally spaced dates ^{14}C dates obtained during this thesis, there is a linear sedimentation rate of 88cm/kyr through the post-Glacial. The high sedimentation rate is such that we expect no significant attenuation of centennial-millennial scale data by bioturbation (Anderson, 2001; Bard, 2001). Therefore, the lower unit of B997-350PC is used in this thesis to study the early post-Glacial period.

B997-325GC and B997-325PC

A gravity core (B997-325GC) and piston core (B997-325PC) obtained from the same station were spliced on the basis of whole-core MS (see Figure 4.4). This was preferred because piston coring can disturb the top portion of a core, whereas gravity coring is more efficient at preserving the integrity of the top portion. The resulting combined core covers a portion of the Holocene from 2 – 11 kyr and hitherto is referred to as B997-325GC/PC. The age-depth diagram for B997-325GC/PC shows that the linear sedimentation rate has changed down-core. The upper sections experienced lower sedimentation rates, perhaps due to changes in bottom current behaviour/sediment focusing over the Holocene. These possibilities have been invoked to explain the lower sedimentation rates – for some recent Holocene sediments - observed in a number of marine cores obtained from the N. Icelandic shelf (e.g. Eiriksson et al., 2000b). Four age-depth regressions were used to constrain the changes in sedimentation rates (see Table 4.3, page 116). The low sedimentation rates in the shallower part of the core (see Figure 4.4) mean that there may be significant attenuation of centennial-millennial scale

data by bioturbation (Anderson, 2001; Bard, 2001). Therefore, this core is only used in the analysis of general Holocene trends. JR51-GC35 (see below) is preferred for the analysis of Holocene millennial scale variability.

JR51-GC35

JR51-GC35 consisted of one massive unit of consistent colour, occasionally cut by thin horizons of coarser material, probably resulting from small scale mass movements, such as contourites (Dr. Colm Ó Cofaigh, pers. comm) (see Figure 4.5). Physical properties such as wet bulk density, show little deviation down-core (see Figure 4.5). In the top part of the core (0-54cm) the age-depth relationship is characterised by a sedimentation rate of 62 cm/kyr. Below this (54 - 450cm), the sedimentation rate is slightly lower and the age-depth relationship is remarkably linear (Figure 4.5). Thus, we use two linear regressions to derive the age-model (Table 4.3). The core covers a portion of the Holocene from 0 – 10.1 kyr BP. The sedimentation rates are sufficiently high so that we expect no significant attenuation of centennial-millennial scale data by bioturbation (Anderson, 2001; Bard, 2001). This, in addition to the consistent spacing of dated horizons, suggests that JR51-GC35 is suitable for the analysis of centennial-millennial scale variability in the Holocene.

Table 4.3: Age model regressions for cores linear sedimentation rates.

<i>Core, segments</i>	<i>Linear Sedimentation Rate</i>
B997-350PC (one linear segment, top was disturbed)	
Age (>42cm) = (depth + 884.36)/87.07	88cm/kyr
B997-325GC/PC (three linear segments)	
Age (0-9.5cm) = (depth + 3.95)/5.01	6cm/kyr
Age (9.5-31cm) = (depth + 15.4)/10.014	10cm/kyr
Age (31-120cm) = (depth + 79.727)/23.297	23cm/kyr
Age (>120cm) = (depth - 532.15)/72.45	70cm/kyr
JR51-GC35 (two linear segments)	
Age (0-54.5cm) = (depth + 3.8)/0.061	62cm/kyr
Age (>54.5cm) = (depth - 15.71)/0.043	43 cm/kyr

4.3. Results and discussion

4.3.1. Biomarker stratigraphy & correlations

This section describes the major changes in biomarker distributions in the Icelandic shelf cores. The data is compared and correlated – where possible - with published records, to place the results in a wider regional context. In doing so we attempt to gain an insight into the role of the oceanic currents off north Iceland in past climate changes. Intensive changes – particularly in the alkenone indices - are recorded on the west and north Icelandic shelf during the last 15 kyr BP. In Figure 4.8 the results of the analysis of U_{37}^K -SST (B997-350PC & JR51-GC35), $U_{37}^{K'}$ -SST (B997-325GC/PC), total pigments and S/I for the cores are plotted against calendar age. We use the Rosell-Melé et al. (1995) annual SST equation for the cores in which the U_{37}^K index is used (JR51-GC35 and B997-350PC) and the Weaver et al. (1999) equation for B997-325PC (where $U_{37}^{K'}$ rather than U_{37}^K is used). Both calibrations are constructed from NE Atlantic core-top data-sets. The GRIP (ss08cc) ice-core event stratigraphy is included in Figure 4.8 to provide a palaeoclimatic framework for the Post-Glacial. The GRIP (ss08cc) age-model is currently recommended by the INTIMATE¹ group as the type profile for the late-glacial, for the synthesis of marine, terrestrial and ice-core records (Lowe et al., 2001).

Post-Glacial 11.5 – 15kyr BP

Only core B997-350PC from the western Icelandic shelf contained sediments deposited prior to the Holocene. The alkenone record for this period was discontinuous, with certain sections barren of alkenones. In the sections of the core where alkenones are detectable, values of $\%C_{37.4}$ are above the threshold value of 5%. This indicates the presence of arctic or polar waters and/or lowered SSS from terrestrial (glacial) run-off. When $\%C_{37.4}$ is above 5% in sediments, the U_{37}^K -SST estimates have a higher uncertainty. This has been demonstrated in work using modern samples by Rosell-Melé [1998 #409], which first illustrated the increase in scatter of $U_{37}^{K'}$ values in modern surface samples with $>5\% \ \%C_{37.4}$ and by this thesis (chapter 3) which shows that the majority of anomalous $U_{37}^{K'}$ in data from the Nordic Seas surficial sediments occurs above the 5% isoline. Also the association of $>5\% \ \%C_{37.4}$ values with anomalous down-core $U_{37}^{K'}$ data has been observed by Rosell-Melé (1998). Nevertheless, changes in

¹ Integration of Ice-core Marine and Terrestrial Records – a core programme of the International Quaternary Union (INQUA) Palaeoclimate Commission.

$\%C_{37.4}$ and U_{37}^K will indicate the *relative* changes in the influence of cold/low salinity waters versus warmer Atlantic waters. Accordingly, some major changes in the $\%C_{37.4}$ and U_{37}^K values coincide with the major transitions in the GRIP ice-core event stratigraphy (Figure 4.8).

The oldest few samples in the core were deposited between 14.7-15 kyr BP, during the Greenland stadial 2 event (GS-2) and are characterised by low U_{37}^K values of ~ 0.15 . Values of $\%C_{37.4}$ for this period are $\sim 15\%$, well above the 5% threshold that indicates the presence of arctic/polar water and/or lowered salinities. This is followed by an increase in U_{37}^K and a fall in $\%C_{37.4}$ to $\sim 6\%$ indicating a warming trend which reaches a peak at 14.3 kyr BP to coincide with the early part of Greenland interstadial 1 (GS-1) or GS-1e (i.e. the Bølling period). In the Greenland ice cores, GS-1 is punctuated by two distinct episodes of cooling, denoted as GS-1b and GS-1d. In B997-350PC, the start of GS-1d at 14.3 kyr BP is marked by an increase in $\%C_{37.4}$ from $\sim 6\%$ to 15% and associated fall in U_{37}^K indicates an increasing cooling on the western Icelandic shelf.

Subsequently, the alkenones become undetectable, presumably this marks a further strengthening of cold conditions on the western shelf, such that conditions were unfavourable for alkenone producers, but not for phytoplankton in general as chlorin contents remain stable throughout the whole core span. The initiation of the warm GI-1c (Allerød) phase in the GRIP ice core at 13.7 kyr BP, sees alkenones accumulating in a few samples at ~ 13.7 kyr BP. However, these are distinguished by very high values of $\%C_{37.4}$ of $\sim 35\%$. By analogy with modern core-tops (chapter 3) this would indicate polar water conditions. Continuous deposition of alkenones resumes towards the later part of GI-1c at 13.3 kyr BP and continues until 12.8 kyr BP. Over this period the alkenone indices indicate a warming trend continuing up to 13 kyr BP with U_{37}^K increasing and $\%C_{37.4}$ values falling from $\sim 15\%$ to 10%. This warming trend occurs despite and in contrast to a cooling event (GI-1b) in the GRIP ice core between 12.9 – 13.1 kyr BP. This is followed by a slight cooling in the last few samples between 12.8 – 12.9 kyr BP, with an associated increase in $\%C_{37.4}$.

Alkenones become undetectable in B997-350PC at 12.85 kyr BP, coeval with the initiation of the GS-1 (Younger-Dryas) event in the GRIP ice core stratigraphy. No alkenones are detected within the GS-1 interval from 11.5 - 12.8 kyr BP. As with the

GS-1d phase, this presumably marks an abrupt deterioration of conditions on the western shelf, such that conditions were unfavourable for alkenone producers. Alkenones abruptly appear again in the core at 11.5 kyr BP, exactly coeval with the initiation of Holocene (pre-boreal) epoch in the GRIP stratigraphy.

In Figure 4.9, the alkenone data from B997-350PC is compared with a record of ice-front oscillations of Ingólfsson et al. (1997) at Borgarfjörður, S.W. Iceland (see Figure 4.1 for location). There is reasonable agreement between the interpretation of the alkenone record and the ice-front data. Specifically, the major retreats of the ice-front are coeval with “warming” in the alkenone trends (i.e. reduction in %C_{37:4}) and the major re-advances of the ice-fronts are coeval with the periods when the alkenones become undetectable or give extremely high %C_{37:4} values (~30%). We do not attempt further – more detailed - correlations of the B997-350PC Late-Glacial record with the various Late-Glacial time series published from the region (e.g. Eiríksson et al., 2000b). This is due to the incomplete nature of the record, the low concentrations of alkenones and the uncertainties that remain in the interpretation of alkenones patterns with high %C_{37:4} in this region.

In core B997-350PC, values for total chlorin pigments are low and show remarkably little variation from the mean. This is perhaps surprising, as significant perturbations to productivity, especially during GS-1, would be expected and are suggested by the interruptions to the deposition of alkenones. However, observations from this thesis (chapter 3) in the surface waters of the modern Nordic seas, found no correlation between alkenone and chlorophyll abundance. This suggests that the influence of alkenone producers (i.e. *E. huxleyi*) on chlorophyll levels may be insignificant compared to inputs from non-alkenone primary producers (e.g. diatoms, dinoflagellates). The pigments values suggest that low level but significant input of photosynthetic material from non-alkenone producers continued throughout the late-glacial period.

The S/I ratio shows little significant downhole variation, with values ranging between 4 - 6. Thus it seems there is little stratigraphic change in the general composition of the pigments. There is a small increase in values through the GS-1 event, perhaps suggesting a change in production/preservation conditions. However, this deviation is insignificant compared to the excursions in the S/I ratio of up to 150 units reported to occur across

Heinrich layers in the Nordic seas and north Atlantic (Rosell-Melé and Koç, 1997; Rosell-Melé et al., 1997).

Holocene 0 – 11.6 kyr BP

Biomarker records from the Holocene were obtained from B997-350PC (10.6 – 11.5 kyr BP), B997-325GC/PC (1.8 – 10.8 kyr BP) and JR51-GC35 (0 – 10.3 kyr BP). The record from JR51-GC35 covers the longest period at the highest resolution (~60cm/kyr). However, in the early half of the Holocene there are some sections of JR51-GC35, at 8.2 – 8.75, ~7.1 and ~6.2 kyr BP, where alkenones were undetected or were too weak to be integrated accurately. In the case of the 8.2-8.74 kyr BP section, the absence of alkenone may be related to the ~8.2 kyr BP cold event reported in many records including from the N. Icelandic shelf (Andrews and Giraudeau, 2003; Eiríksson et al., 2000b), the North Atlantic (Bond et al., 1997) and in the Greenland Ice cores (O'Brien et al., 1995). Convincing evidence has linked this event to the catastrophic drainage of glacial lakes Agassiz and Ojibwa through the Hudson straight at 8.47 cal. kyr BP (Barber et al., 1999). The other sections of low alkenone abundance in the early half of the Holocene may be related to the abundance of the main alkenone producer *E. huxleyi* on the N. Icelandic shelf. Recently published coccolithophore records from the N. Icelandic shelf show that accumulation rates of *E. huxleyi* fossils were generally much lower in the early Holocene, with - for example - rates ~25 time lower between 6 – 7.8 kyr BP than for the period between 1.2 – 3 kyr BP (Andrews and Giraudeau, 2003).

Aside from a few small sections, the alkenones provide a record which covers most of the Holocene and which highlights a large degree of SST variability on the Icelandic shelf. In addition to the more common $C_{37:2}$ and $C_{37:3}$ compounds, $C_{37:4}$ is also present in cores JR51-GC35 and B997-350PC (we do not report $C_{37:4}$ for B997-325GC/PC). Values of % $C_{37:4}$ are consistently below the 5% threshold, suggesting that - from the very start of the Holocene - there was persistent dominance of Atlantic source waters on the Icelandic shelf. The highest % $C_{37:4}$ values (~4%), in the Holocene, occur early in the epoch between 10.8 – 11.5 kyr BP in core B997-350PC. Later values (0 – 10.3 kyr BP) recorded in JR51-GC35 remain low (> 2%). The early higher values may be related to some freshening of the surface waters on the shelf due to higher run-off in the deglacial period (see Figure 4.1). Although, by analogy with modern core tops in the

Nordic seas, this would only represent a freshening of ~ 0.5 psu (Rosell-Melé et al., 2002).

The Holocene records of total chlorin pigments show some variation over the Holocene in cores JR51-GC35 & B997-325GC/PC. Generally, higher values are seen in the early Holocene in B997-325GC/PC and in the late Holocene in JR51-GC35 and there appear to be a number of fluctuations on a millennial scale. However, the changes are of a relatively small order of magnitude and show no consistent relationship to the U_{37}^K -SST values. This lack of correspondence makes it difficult to link the changes to either productivity or preservation controls.

The S/I ratios again shows little significant downhole variation, with values of ~ 5 . Therefore, there is little stratigraphic change in the general composition of the pigments and it seems that this biomarker proxy is insensitive to Holocene climatic (e.g. IRD) events.

4.3.1.1. General Holocene U_{37}^K -SST trends

The records from the N. Icelandic shelf display a general trend of cooling through the Holocene. This is characterised in B997-325GC/PC by a cooling of 2.5°C (11 to 8.5°C) from 10.8 to 1.8 kyr BP and in JR51-GC35 by a cooling of 2.5°C (10 – 7.5°C) from 10.3 to 0 kyr BP (Figure 4.8).

The data is interesting in the context of recent work which has compared Holocene alkenone-SST trends in a number of cores from sites in the North Atlantic, Mediterranean Sea and northern Red Sea (Rimbu et al., 2003). Based on historical analogies from the period covered by instrumental data and GCM experiments, Rimbu *et al.* (2003) attribute such regional variation in Holocene SST trends to a long-term continuous weakening of a northern hemisphere atmospheric circulation pattern, similar in concept to that of the Arctic/North Atlantic Oscillation. The surface expression is that temperature trends - over the Holocene - in northern Europe and the eastern Mediterranean/Middle East have been negative and positive respectively (Figure 4.10).

This thesis reports the first high-resolution Holocene alkenone-SST data from the Icelandic shelf, a key region with regard to any studies of Holocene changes in NAO

type indices, because the NAO is defined by the surface atmospheric pressure difference between Iceland (Stykkisholmur) and the Azores. In Figure 4.10, the Holocene SST trend lines from B997-325GC/PC and JR51-GC35 are plotted alongside the data from Rimbu *et al.* (2003). The data from this thesis complement previously published data and strongly support the observations of negative Holocene SST trends in the northern Atlantic and thus a negative trend (weakening) in the AO/NAO index. Based on GCM experiments, Rimbu *et al.* (2003) suggest the latitudinal pattern may be attributed to tropical warming during winter, due to increasing solar insolation associated with the earth's precession cycle. The tropical cooling induces a weaker Aleutian Low and a regional shift of the Northern Hemisphere jet. Rimbu *et al.* (2003) suggest that AO/NAO indices may have a role in generating millennial-scale SST trends. This is supported by Dickson *et al.* (Dickson *et al.*, 1996) who suggest that the NAO coordinates the intensity of deep convection at three main Atlantic regions, the Greenland/Iceland Seas, the Labrador Sea and the Sargasso Sea, and thus links to the global thermohaline circulation.

However, Rimbu *et al.* (2003) point out that millennial scale coolings in the northern Atlantic, for example those defined by IRD events and linked to solar forcing (Bond *et al.*, 2001), are discordant with the AO/NAO pattern. Therefore, other processes must be investigated in order to understand the full Holocene SST variability. The records from this thesis are also consistent with recent work by Marchal *et al.* (2002) who investigated Holocene trends of SST in 16 marine cores from the North Atlantic and Mediterranean Sea (36 - 75°N). All of the records showed an apparent long-term cooling through the last 10 kyr of 0.5-3.6°C. The authors attempted to identify consistent trends in the cores, using various statistical methods. They concluded that one factor accounted for 67% of the total variance in SST and there were two possible explanations: a widespread surface cooling (i.e. consistent with many climate proxy records from the N. Atlantic) or a change in the seasonal timing and/or duration of the growth period of alkenone producers (consistent with a divergence between alkenone-SST and microfossil faunal SST observed in two cores).

4.3.1.2. Holocene millennial-scale variability

In this section we concentrate on the millennial scale variability that is superimposed on the mean Holocene cooling trend. For this purpose we use core JR51-GC35 as it has

the longest Holocene record, a linear sedimentation rate and superior dating control compared to B997-325GC/PC. JR51-GC35 has an average sedimentation rate of 43cm (for most of the core) and is sampled every 4cm for U^{K}_{37} -SST. Therefore, there is a data point obtained every ~ 90 yr, enabling the resolution of millennial scale records. The SST oscillations in JR51-GC35 are of a large amplitude; with maximum and minimum U^{K}_{37} -SSTs recorded on the Icelandic shelf as 12°C and 6°C . These oscillations appear to have a degree of cyclicity on a millennial scale, with SST maxima at around 0.5, 1.3, 3.2, 4.2, 5.2, 7.3, and 9.3 kyr BP. The most prominent of these maxima are in the early Holocene between 9 – 10 kyr BP and in the mid-Holocene between 5 – 5.5 kyr BP. Distinguishable in the youngest part of the record is a 3°C cooling. Starting at 300 yr BP this event is coeval with the ‘Little Ice Age’ (LIA). There is abundant historical evidence for social hardship in Iceland during the LIA (Bell and Walker, 1992). It is a story of failed harvests, declining fish catches and an impoverished population retreating from the most severely affected areas in the north of the country (Grove, 1988). A prominent warming in the JR51-GC35 U^{K}_{37} -SST record occurred 1.3 kyr BP, which is broadly coeval with the ‘Medieval Warm Period’ recognised in a number of palaeoclimatic and historical records. For instance, during this period in the decade of the 870s AD (1.2 kyr BP) the Norse first settled in Iceland, where conditions were warm enough to grow barley (Grove, 1988).

A spectral analysis to determine the periodicity of U^{K}_{37} -SST variability could not be performed as the record is incomplete in parts. However, the ‘event pacing’ was estimated by measuring the mean time between the maxima of the main oscillations (defined as exceeding 2°C between peak maxima and trough). The peaks used to estimate the event pacing are labelled in Figure 4.8. This method derives an event pacing of $1450 \text{ yr} \pm 470$ (1σ). Such periodicity compares with the prominent ~ 1500 yr cycles found in a number of palaeoclimatic archives from the northern North Atlantic, including records of drift ice (Bond et al., 2001; Bond et al., 1997) and the speed of Iceland-Scotland overflow water (Bianchi and McCave, 1999).

Jennings *et al* (2002b) recently published Holocene records of palaeohydrology and iceberg rafting from core JM96-1207, on the East Greenland continental shelf (approximately 12° west of JR51-GC35). In Figure 4.9(a&c), we compare the U^{K}_{37} -SST record from JR51-GC35 with the flux of calcium carbonate – a proxy of iceberg-rafting

debris on the East Greenland Shelf – from JM96-1207. The thermal maxima identified in the N. Icelandic shelf show a correlation with the minima in the IRD record from East-Greenland (interpreted as warmings). This is especially true for the most prominent thermal maxima in the record of JR51-GC35, between 9 – 10 kyr BP and 5 – 5.5 kyr BP, which correspond to pronounced minima in the IRD record. Furthermore, the termination of the mid-Holocene optimum in JR51-GC35 at 5 kyr is followed by a trough in SSTs, which is coeval with a pronounced peak in the IRD record of JM96-1207 and the onset of neoglacial conditions (Jennings et al., 2002b). Jennings et al. (2002b) suggest that - because of the rapidity of the changes - the IRD fluxes in JM96-1207 are more likely to be related to the response of tide-water glaciers to sea surface cooling (or enhanced polar water flux), than to glacier oscillations resulting from the internal dynamics of the Greenland ice-sheet. Under conditions of increased polar water flux along East Greenland, icebergs calved in the fjords would retain their debris farther onto the shelf (where it would be recorded in JM96-1207), rather than lose their debris to melting within the fjords, especially if the icebergs were not trapped in permanent sikussaq at the glacier margin (Syvitski et al., 1996). Such a pattern of sensitivity of iceberg melt and debris distribution has been suggested by Dowdeswell et al. (2000) for both Nansen Fjord and Scoresby Sund. The data from JR51-GC35 supports this hypothesis, suggesting that advances of the polar front, associated with weakening of the IC/strengthening of the EGC resulted in increased deposition of calcareous IRD on the East Greenland shelf.

Millennial scale climatic coolings of similar ages to those seen in the U_{37}^K -SST record from JR51-GC35 and the IRD record from JM96-1207 have recently been reported in a number of proxy records from the Northern Iceland shelf (see Figure 4.9d). These include variations in the percentages of *N. pachyderma* and IRD (Eiriksson et al., 2000a), variation in benthic foraminiferal assemblages (Eiriksson et al., 2000b), from coccoliths flux changes - reflecting changes in sea-surface primary productivity (Andrews et al., 2000; Andrews et al., 2001b) – and from integrated IRD proxies (Andrews and Giraudeau, 2003) (Figure 4.9d). The records coincide fairly closely with the record from JR51-GC35. Particular features that are in prominent agreement between records are: the LIA cooling starting at ~500 yr BP, a marked cool episode at ~2.5 kyr BP, and climatic optimum at ~ 5 kyr BP.

Holocene climatic events of similar ages to those defined on the Icelandic and Greenland shelf have also been interpreted from North Atlantic deep-sea cores (Figure 4.9d). In a Sargasso Sea core, Keigwin (1996) found a 1°C cooling during the LIA and during a similar event c. 1500 years ago, and a warming of 1°C during the MWP. Another cool interval associated with increased ice-rafted debris beginning between 4 and 5 kyr BP was recognised, coeval with a trough in U_{37}^K -SSTs in JR51-GC35. Keigwin (1996) suggested that this event marks the beginning of Neoglacial cooling. Bond *et al.* (1997) have documented millennial scale coolings throughout the Holocene in two cores off Ireland (VM 29–191 and VM 23–81) and more recently within a stacked record of cores from East Greenland, from the North Atlantic off Ireland and Nova Scotia (Bond *et al.*, 2001). The Holocene cool intervals are manifested by ice-rafted hematite-coated grains and increased abundances of *N. pachyderma* sinistral at around 1.5, 3.0, 4.5, 5.8, 8.2 and 9.5 kyr BP. They argue that there is a 1470 ± 500 -year cycle to these events that occurs unbroken through the Holocene and beyond and that this can be correlated to variations in solar radiation (Bond *et al.*, 2001).

Giraudeau *et al.* (2000) interpret sea-surface instabilities (EH events denoted by variations in the coccolithophore *E. huxleyi*) correlative to Bond *et al.*'s (1997) events in a core from the Gardar Drift. They attribute the EH events younger than c. 6 ka to closer proximity of the subpolar front in response to decreasing solar insolation. However, they attribute the ~8.2 ka EH event to meltwater from the Laurentide Ice Sheet (Barber *et al.*, 1999).

The sea-surface variability in JR51-GC35 generally corresponds with cooling events in the deep sea, but the closest correlation is achieved with the IRD record in JM96-1207 from the East Greenland shelf (Figure 4.9). It is likely that this is due to their positions relatively close to the polar front and IRD sources and interaction between the IC/NIIC and the EGC; therefore making them sensitive to climate change. Indeed the U_{37}^K -SST fluctuations recorded in JR51-GC35 are of a high amplitude, typically ~2°, but as high as 4°C for the cooling that follows the mid-Holocene optimum at 5 kyr BP.

Correlations with Icelandic glacial record

Such extreme changes in U_{37}^K -SST off N. Iceland should have corresponding events in the Icelandic terrestrial record. Figure 4.9e shows records of Holocene mountain glacier

advances in northern Iceland published by Stötter *et al.* (1999), compared with the U_{37}^K -SST record from JR51-GC35 (see Figure 4.1 for site locations). Evidence of climatic deteriorations coeval with the glacial advances have also been found in records of pollen assemblages and peat accumulation (e.g. Andrews *et al.*, 2001a; Caseldine and Hatton, 1994; Rundgren, 1998). The glacier records show reasonable agreement with the U_{37}^K -SST data, with most advances associated with troughs in U_{37}^K -SST. The major exception being a glacial advance between c.3000-3700 which contrasts with a warm phase in the N. Icelandic shelf U_{37}^K -SSTs and a reduced period of IRD flux in JM96-1207. Possible explanations for this anomaly may be that this expansion – which is from one glacier (Vatnsdalur II) – is caused by internal glacier dynamics, or there may be a dating error. However, the two most prolonged periods of glacier advance, at 10 – 11.5 kyr BP and 5.5 – 6.7 kyr BP are both coeval with cooler U_{37}^K -SSTs in JR51-GC35 (Figure 4.9). Moreover, the termination of the advances are coeval with the two most prominent SST maxima on the N. Icelandic shelf – between 9- 10 kyr BP and 5 – 5.5 kyr BP. Stötter *et al.* (1999) suggest that reductions in SSTs and increases in winter sea-ice north of Iceland reduces the precipitation input to Icelandic glaciers. However, this negative effect on glacier mass balance is more than compensated for by a reduction in equilibrium line altitude (ELA), thus resulting in a net gain in ice mass – and expansion of glaciers. The data from this thesis appears to support this theoretical model for the majority of Holocene glacier expansions in northern Iceland.

Comparison of North Iceland and Norwegian Current

Recent work by Eiríksson *et al.* (2000b) has suggested that during the Late-Glacial period some climatic events in western Europe were coeval with events of an apparently contradictory sign on the North Icelandic shelf. Benthic foraminiferal assemblages suggest a strong (warm) pre-Bølling palaeo-Irminger Current on the N. Icelandic shelf. This contrasts with a particularly cold episode in the North Sea (Rochon *et al.*, 1998) and in the GRIP ice-core (Björk *et al.*, 1998). Furthermore, preliminary oceanic modelling work at the Nansen Environmental and Remote Sensing Centre in Bergen, Norway apparently indicates that increased strength of the Norwegian Current into the Norwegian Sea leads to a cooling of the Iceland Sea north of Iceland, and inversely, that a reduction of the Norwegian Current leads to warming of the Iceland Sea (Helge Drange, pers. comm. As cited by Eiríksson *et al.*, 2000b). However, Eiríksson *et al.* (2000b) found no evidence of such discrepancies between the NIIC and other North

Atlantic or Greenland records during the Holocene. This may have been due to the relative insensitivity of the benthic foraminiferal assemblages studied to lower amplitude Holocene changes. Moreover, the benthic foraminifera studied by Eiriksson *et al.* (2000b) responded to changes in water masses at 300 – 500 meters depth on the shelf, rather than SSTs in the mixed layer.

In Figure 4.11 we compare changes in published Holocene alkenone-SSTs from MD952011, a high resolution core (7m Holocene section) from the Norwegian Sea (Calvo *et al.*, 2002) with the U_{37}^K -SST record from JR51-GC35 on the Icelandic shelf. The comparison shows that there are some general similarities between the records. For example, they both record an overall decrease in mean SSTs during the Holocene, a mid-Holocene Thermal Optimum (TO) and a marked cooling at ~2.5 kyr BP. However, the records show some significant differences in the millennial scale climate events between the NIIC and NC, especially at 3.2, 5, 6.5 and 9 kyr BP. The most prominent example is the timing of the mid-Holocene TO. In MD952011 the mid-Holocene TO is a distinct phase between 6 – 8 kyr BP (with the consistently highest SSTs between 6- -7 kyr BP). Calvo *et al.* (2002) suggest this is supported by data from diatom and foraminifera reconstructions in the eastern Nordic Seas (e.g. Koç and Jansen, 1992; Koç *et al.*, 1993; Sarnthein *et al.*, 1995), by records of mountain glacier retreat in Norway (Nesje and Kvamme, 1991) and European pollen data (Huntley and Prentice, 1988). However, in the records from the eastern Nordic Seas, during the period 6 -7 kyr BP, there is a trough in the U_{37}^K -SSTs on the N. Icelandic Shelf, an increase in IRD events on the East Greenland shelf (Jennings *et al.*, 2002b) and glacier expansion in northern Iceland. The TO in the northern Icelandic and East Greenland records instead occurs at 5- 6 kyr BP, at the same time as the termination of the TO in records from the eastern Nordic Seas and Northern Europe.

A general trend of early-mid Holocene warm conditions, culminating in a mid-Holocene TO and followed by neoglacial cooling is recognised throughout the Arctic areas of the North Atlantic (e.g. Calvo *et al.*, 2002; Jennings *et al.*, 2002b; Koç *et al.*, 1993; Nesje and Dahl, 1993; Williams *et al.*, 1995). An underlying cause of the general cooling trend is the reduction in summer insolation at high latitudes over the last 11 kyr (Berger and Loutre, 1991; Berger, 1978). However, this does not explain the abrupt shift from a thermal maximum to the neoglacial conditions seen in many records. The cause

of this shift is not well constrained (Jennings et al., 2002b). The postglacial isostatic rebound of the Arctic Island Channels has been invoked as a possible explanation (Williams et al., 1995). As these channels rose above the level of the Atlantic layer in the Arctic Ocean, warmer saltier water was excluded from the outflow and dramatically changed the character of the Baffin Current and the Labrador Current (e.g. Jennings, 1993; Osterman and Nelson, 1989). Such a change in the bathymetry of the Arctic Island Channels would affect Baffin Bay, but not the outflow of water from the Arctic Ocean through the Fram Strait, to the Nordic Seas.

Decreased solar insolation beyond a critical threshold, resulting in a change in preferred atmospheric circulation pattern (Andrews et al., 1997; Koç and Jansen, 1994) and NAO (North Atlantic Oscillation) indices (Keigwin and Pickart, 1999) have been presented as possible causes for the neoglacial cooling. The data from this thesis is consistent with neoglacial cooling forced by decreased solar insolation beyond a critical threshold. However, rather than a simplistic advance of the Arctic front as suggested by Koç *et al.* (1993), we suggest that the response of the ocean circulation within the Nordic Seas was more complex than previously suggested; which included differences in the responses of the western (IC & NIIC) and eastern (NC) branches of Atlantic inflow to the Nordic Seas.

The mechanism for a differential response is not proven. However studies of instrumental data collected during the latter half of the 20th century provide some intriguing possibilities. Alekseev et al. (2001) computed water temperature anomalies in the Nordic Seas at 100m for the 1980-1990 period. They found the most positive anomaly (+1) in the northern Norwegian Sea (73°N, 15°E) and the most negative anomaly (-1) in the seas to the north, east and south of Iceland. Blindheim et al. (2000) suggest that the instrumental data from 1950 onwards demonstrates that the oceanographic structure in the Nordic Seas is closely linked with the predominant wind system, which in turn is closely correlated to the NAO mode. This affects the westwards inflow of the Atlantic water in the Nordic seas and the speeds of the currents advecting Atlantic waters (Orvik et al., 2001). Blindheim et al. (2000) suggest that since the 1960s, conditions in the Norwegian Sea and Faeroe-Shetland area have shown little correlation to the conditions in the north Icelandic shelf waters. Circulation of Atlantic

water into the western Nordic Seas has reduced, while there has been a temperature rise in the narrowing Norwegian Atlantic Current (Blindheim et al., 2000).

Most recently Flatau et al. (2003) produced interesting results for the period 1992-1998 using a synthesis of drifter, geostrophic flow (satellite altimetry) and AVHRR-SST² data (1992-1998). They suggest that NAO+ years are associated with intensification of sub-polar westerlies in the Atlantic and northerlies along the Greenland coast; resulting in the intensification of the cyclonic circulation in the Irminger basin. This is associated with negative SST anomalies on the North Icelandic shelf and northwest of Iceland to the East Greenland Shelf (including the region of JM96-1207), but positive SST anomalies further north and to the east.

4.4. Conclusions

Alkenones and chlorin pigments have been measured in three cores collected from the West and North Icelandic Shelf. Major changes in the alkenone distributions are observed in the cores during the post-Glacial and Holocene periods. In the Late-Glacial (when alkenones were detectable) relative changes in %C_{37:4} and U^K₃₇ indicate relative changes in the influence of cold/low salinity waters versus warmer Atlantic waters. Accordingly, major changes in the %C_{37:4} and U^K₃₇ distributions coincide with the major transitions in the GRIP Late-Glacial ice-core event stratigraphy, with alkenone deposition apparently ceasing during the most severe stadials (e.g. GS-1). There is good agreement between the interpretation of the alkenone record from the Late-Glacial and records of ice-front fluctuations from S.W. Iceland.

The records from the N. Icelandic shelf display a general trend of cooling through the Holocene. This is characterised in B997-325GC/PC by a cooling of 2.5°C (11 to 8.5°C) from 10.8 to 1.8 kyr BP and in JR51-GC35 by a cooling of 2.5°C (10 – 7.5°C) from 10.3 to 0 kyr BP. This data supports published reports of negative Holocene SST anomalies in the northern North Atlantic towards the present. Contrasted with records of positive trends in eastern Mediterranean and Middle East, this suggests a negative trend (weakening) in the AO/NAO index during the Holocene (Rimbu *et al.* 2003).

² Advanced Very High Resolution Radiometer

The longest Holocene record, with superior dating control, was obtained from JR51-GC35 from the N. Icelandic shelf. The SST oscillations in JR51-GC35 are of large amplitude; with millennial scale oscillations characterised by deviations of $\sim 2^{\circ}\text{C}$. The oscillations have a distinct cyclicity on a millennial scale, with SST maxima at around 0.5, 1.3, 3.2, 4.2, 5.2, 7.3, and 9.3 kyr BP. The most prominent of these maxima are in the early Holocene between 9 – 10 kyr BP and in the mid-Holocene between 5 – 5.5 kyr BP. Also, distinguishable in the record are events coeval with the Little Ice Age and the Medieval Warm Period.

The U_{37}^K -SST record from JR51-GC35 shows a good correlation with recently published Holocene records of iceberg rafting from on the East Greenland continental shelf. The data from JR51-GC35 suggests that advances of the polar front in the eastern Nordic Seas - associated with weakening of the IC/strengthening of the EGC - resulted in increased deposition of calcareous IRD on the East Greenland shelf.

The millennial scale oscillations in the JR51-GC35 U_{37}^K -SST record also broadly correlate with a number of marine records of Holocene climatic events from the northern Iceland shelf and North Atlantic deep-sea cores. However, the closest correlation is achieved with the IRD record in JM96-1207 from the East Greenland shelf. It is likely that this is due to their positions relatively close to the polar front and IRD sources; therefore making them sensitive to climate change.

The U_{37}^K -SST record from JR51-GC35 also shows close agreement with records of Holocene glacial advances in northern Iceland. Especially, the termination of two major advances which are coeval with the two most prominent SST maxima on the N. Icelandic shelf – between 9- 10 kyr BP and 5 – 5.5 kyr BP.

A comparison of the U_{37}^K -SST records from JR51-GC35 and a core from the eastern Nordic Seas (MD952011) shows that there are some general similarities. However, the records suggest some differences (superimposed on the general trend) of millennial scale climate events between the eastern and western Nordic Seas especially at 3.2, 5, 6.5 and 9 kyr BP. The most prominent example is the timing of the mid Holocene Thermal Optimum (TO). In MD952011, the TO is a distinct phase between 6 – 8 kyr BP, (with the constantly highest SSTs at 6- -7 kyr BP). However, in the records from the eastern

Nordic Seas, during the period 6 -7 kyr BP, there is a trough in the U_{37}^K -SSTs on the N. Icelandic Shelf, an increase in IRD events on the East Greenland shelf (core JM96-1207) and glacier expansion in northern Iceland. Therefore, the data from this thesis suggest that the response of the surface ocean circulation within the Nordic Seas was more complex than previously suggested; possibly characterised by differential responses of the Irminger and Norwegian Currents.

Chapter 4: Post-Glacial and Holocene palaeoceanography of the Icelandic shelf

- Alekseev, G. V., Johannessen, O. M., Korablev, A. A., Ivanov, V. V., and Kovalevsky, D. V. (2001). Interannual variability in water masses in the Greenland Sea and adjacent areas. *Polar Research* **20**, 201-208.
- Andersen, G. J., Hienemeier, J., Nielsen, H. L., Rud, N., Johnsen, S., Svenbjörnsdóttir, Á. E., and Hjartarson, Á. (1989). AMS ¹⁴C dating on the Fossvogur sediments, Iceland. *Radiocarbon* **37**, 53-62.
- Anderson, D. M. (2001). Attenuation of millennial-scale events by bioturbation in marine sediments. *Paleoceanography* **16**, 352-257.
- Andrews, J. T., Caseldine, C., Weiner, N. J., and Hatton, J. (2001a). Late Holocene (ca. 4 ka) marine and terrestrial environmental change in Reykjarfjordur, north Iceland: climate and/or settlement? *Journal of Quaternary Science* **16**, 133-143.
- Andrews, J. T., Geirsdóttir, A., Hardardóttir, J., Principato, S., Gronvold, K., Kristjansdóttir, G. B., Helgadóttir, G., Drexler, J., and Sveinbjörnsdóttir, A. (2002a). Distribution, sediment magnetism and geochemistry of the Saksunarvatn (10,180 +/- 60 cal. yr BP) tephra in marine, lake, and terrestrial sediments, northwest Iceland. *Journal of Quaternary Science* **17**, 731-745.
- Andrews, J. T., and Giraudeau, J. (2003). Multi-proxy records showing significant Holocene environmental variability: the inner N. Icelandic shelf (Húnaflói). *Quaternary Science Reviews* **22**, 175-193.
- Andrews, J. T., Hardadóttir, J., Stoner, J. S., Mann, M. E., Kristjansdóttir, G. B., and Koc, N. (2003). Decadal to millennial-scale periodicities in North Iceland shelf sediments over the last 12000 cal yr: long-term North Atlantic oceanographic variability and solar forcing. *Earth and Planetary Science Letters* **210**, 453-465.
- Andrews, J. T., Hardardóttir, J., Geirsdóttir, A., and Helgadóttir, G. (2002b). Late Quaternary ice extent and glacial history from the Djúpáll trough, off Vestfirðir peninsula, north-west Iceland: a stacked 36 cal. Ky environmental record. *Polar Research* **21**, 211-226.
- Andrews, J. T., Helgadóttir, G., Geirsdóttir, A., Hardardóttir, J., Kristjansdóttir, G., Smith, L. M., Jennings, A. E., and Sveinbjörnsdóttir, A. (2000). The carbonate content of cores on the N Iceland shelf: high-resolution records for the last 5 ka of surface productivity and sea-ice. In *In "CAPE/ICAPP Abstracts: sea ice in the climate system, the record of the North Atlantic Arctic."* 2-6 June 2000, Kirkjubæjarklaustur, Iceland.
- Andrews, J. T., Helgadóttir, G., Geirsdóttir, A., and Jennings, A. E. (2001b). Multicentury-scale records of carbonate (hydrographic ?) variability on the northern Iceland margin over the last 5000 years. *Quaternary Research* **56**, 199-206.
- Andrews, J. T., Smith, L. M., Preston, R., Cooper, T., and Jennings, A. E. (1997). Spatial and temporal patterns of iceberg rafting (IRD) along the East Greenland margin, ca. 68°N, over the last 14 cal.ka. *Journal of Quaternary Science* **12**, 1-13.
- Barber, D. C., Dyke, A., Hillaire-Marcel, C., Jennings, A. E., Andrews, J. T., Kerwin, M. W., Biodeau, G., McNeely, R., Southon, J., Morehead, M. D., and Gagnon, J.-M. (1999). Forcing of the cold event of 8,200 years ago by catastrophic drainage of Laurentide lakes. *Nature* **400**, 344-348.
- Bard, E. (2001). Paleoceanographic implications of the difference in deep-sea sediment mixing between large and fine particles. *Paleoceanography* **16**, 235-239.
- Bell, M., and Walker, M. J. C. (1992). "Late Quaternary Environmental Change: Physical and Human Perspectives." Longman, Harlow.
- Berger, A., and Loutre, M. F. (1991). Insolation values for the climate of the last 10 million years. *Quaternary Science Reviews* **10**, 297-317.

- Berger, A. L. (1978). Long-Term variations of caloric insolation resulting from the earth's orbital elements. *Quaternary Research* **9**, 139-167.
- Bianchi, G. G., and McCave, N. (1999). Holocene periodicity in the North Atlantic climate and deep-ocean flow south of Iceland. *Nature* **397**, 515-517.
- Birks, H. H., Gulliksen, S., Hafliðason, H., Mangerud, J., and Possnert, G. (1996). New radiocarbon dates for the Vedde ash and the Saksunarvatn ash from western Norway. *Quaternary Research* **45**, 119-127.
- Björck, S., Ingólfsson, Ó., Hafliðason, H., Hallsdóttir, M., and Anderson, S. J. (1992). Lake Torfadalsvatn: a high resolution record of the north Atlantic ash zone I and the last glacial-interglacial environmental changes in Iceland. *Boreas* **2**, 115-22.
- Björck, S., Walker, M. J. C., Cwynar, L., Johnsen, S., Knudsen, K. L., Lowe, J. J., Wohlfarth, B., and INTIMATE_group. (1998). An event stratigraphy for the Last Termination in the North Atlantic region based on the Greenland ice-core record: a proposal by the INTIMATE group. *Journal of Quaternary Science* **13**, 283-292.
- Blindheim, J., Borovkov, V., Hansen, B., Malmberg, S. A., Turrell, W. R., and Osterhus, S. (2000). Upper layer cooling and freshening in the Norwegian Sea in relation to atmospheric forcing. *Deep-Sea Research Part I-Oceanographic Research Papers* **47**, 655-680.
- Bond, G., Kromer, B., Beer, J., Muscheler, R., Evans, M. N., Showers, W., Hoffmann, S., Lotti-Bond, R., Hajdas, I., and Bonani, G. (2001). Persistent solar influence on north Atlantic climate during the Holocene. *Science* **294**, 2130-2136.
- Bond, G., Showers, W., Cheseby, M., Lotti, R., Almasi, P., deMenocal, P., Priore, P., Cullen, H., Hajdas, I., and Bonani, G. (1997). A pervasive millennial-scale cycle in North Atlantic Holocene and glacial climates. *Science* **278**, 1257-1266.
- Bond, G., Showers, W., Elliot, M., Evans, M., Lotti, R., Hajdas, I., Bonani, G., and Johnson, S. (1999). The North Atlantic's 1-2kyr climate rhythm: relation to Heinrich events, Dansgaard/Oeschger cycles and the Little Ice Age. In "Mechanisms of Global Climate Change at Millennial Time Scales." (P. U. Clark, R. S. Webb, and L. D. Keigwin, Eds.), pp. 35-58. American Geophysical Union, Washington D.C.
- Boyle, J. (1999). Variability of tephra in lake and catchment sediments, Svinavatn, Iceland. *Global and Planetary Change* **21**, 129-149.
- Calvo, E., Grimalt, J., and Jansen, E. (2002). High resolution U^{K}_{37} sea surface temperature reconstruction in the Norwegian Sea during the Holocene. *Quaternary Science Reviews* **21**, 1385-1394.
- Caseldine, C., and Hatton, J. (1994). Interpretation of Holocene climatic change for the Eyjafjorour area of northern Iceland from pollen-analytical data: comments and preliminary results. In "Environmental change in Iceland. *Munchener Geographische Abhandlungen*." (J. Stötter, and F. Wilhelm, Eds.), pp. 41-62.
- deMenocal, P., Ortiz, J., Guilderson, T., and Sarnthein, M. (2000). Coherent high- and low-latitude climate variability during the holocene warm period. *Science* **288**, 2198-2202.
- deMenocal, P. B. (2001). Cultural responses to climate change during the Late Holocene. *Science* **292**, 667-673.
- Denton, G. H., and Karlén, W. (1973). Holocene climatic variations, their pattern and possible cause. *Quaternary Research* **3**, 155-205.
- Dickson, R., Lazier, J., Meincke, J., Rhines, P., and Swift, J. (1996). Long-term coordinated changes in the convective activity of the North Atlantic. *Progress in Oceanography* **38**, 241-295.

Chapter 4: Post-Glacial and Holocene palaeoceanography of the Icelandic shelf

- Dickson, R. R., Meincke, J., Malmberg, S., and Lee, A. (1988). The "Great Salinity Anomaly" in the Northern North Atlantic 1968–1982. *Progress in Oceanography* **20**, 103-151.
- Dowdeswell, J. A., Whittington, R. J., Jennings, A. E., Andrews, J. T., Mackensen, A., and Marienfeld, P. (2000). An origin for laminated glaci-marine sediments through sea-ice build-up and suppressed iceberg rafting. *Sedimentology* **47**, 557-576.
- Dugmore, A. J., and Newton, A. J. (1997). Holocene Tephra Layers in the Faroe Islands, Frodskaparrit. *The Faroese Journal of Natural and Medical sciences* **4**, 141-154.
- Eiriksson, J., Knudsen, K. L., Hafliðason, H., and Heinemeier, J. (2000). Chronology of late Holocene climatic events in the northern North Atlantic based on AMS C-14 dates and tephra markers from the volcano Hekla, Iceland. *Journal of Quaternary Science* **15**, 573-580.
- Eiriksson, J., Knudsen, K. L., Hafliðason, H., and Heinemeier, J. (2000a). Chronology of late Holocene climatic events in the northern North Atlantic based on AMS C-14 dates and tephra markers from the volcano Hekla, Iceland. *Journal of Quaternary Science* **15**, 573-580.
- Eiriksson, J., Knudsen, K. L., Hafliðason, H., and Henriksen, P. (2000b). Late-glacial and Holocene palaeoceanography of the North Icelandic shelf. *Journal of Quaternary Science* **15**, 23-42.
- Flatau, M. K., Talley, L., and Niiler, P. P. (2003). The North Atlantic Oscillation, surface current velocities, and SST changes in the subpolar North Atlantic. *Journal of Climate* **16**, 2355-2369.
- Grove, J. M. (1988). "The Little Ice Age." Methuen, London.
- Hafliðason, H., Eiriksson, J., and Van Kreveld, S. (2000). The tephrochronology of Iceland and the North Atlantic region during the Middle and Late Quaternary: a review. *Journal of Quaternary Science* **15**, 3-22.
- Hansen, B., and Østerhus, S. (2000). North Atlantic-Nordic Seas exchanges. *Progress in Oceanography* **45**, 109-208.
- Heusser, L. E., and Sirocko, F. (1997). Millennial pulsing of environmental change in southern California from past 24 k.y.: A record of Indo-Pacific ENSO events? *Geology* **25**, 243-246.
- Hodell, D. A., Curtis, J. H., and Brenner, M. (1995). Possible role of climate in the collapse of Classic Maya civilisation. *Nature* **375**.
- Hopkins, T. S. (1991). The GIN Sea a synthesis of its physical oceanography and literature review 1972-1985. *Earth Science Reviews* **30**, 175-318.
- Hunt, J. B., and Hill, P. G. (1993). Tephra geochemistry: a discussion of some persistent analytical problems. *The Holocene* **3.3**, 271-278.
- Huntley, B., and Prentice, C. P. (1988). July temperatures in Europe from pollen data, 6000 years before present. *Science* **241**, 687–690.
- Ingólfsson, Ó., Björk, S., Hafliðason, H., and Rundgren, M. (1997). Glacial and climatic events in Iceland reflecting regional North Atlantic climatic shifts during the Pleistocene-Holocene transition. *Quaternary Science Reviews* **16**, 1135-1144.
- Jennings, A. E. (1993). The Quaternary history of Cumberland Sound, southeastern Baffin Island, Canada: the marine evidence. *Geographie Physique et Quaternaire* **47**, 21-42.
- Jennings, A. E., Gronvold, K., Hilberman, R., Smith, M., and Hald, M. (2002a). High-resolution study of Icelandic tephra in the Kangerlussuaq Trough, southeast Greenland, during the last deglaciation. *Journal of Quaternary Science* **17**, 747-757.

- Jennings, A. E., Knudsen, K. L., Hald, M., Hansen, C. V., and Andrews, J. T. (2002b). A mid-Holocene shift in Arctic sea-ice variability on the East Greenland Shelf. *Holocene* **12**, 49-58.
- Johnsen, S. J., Clausen, H. B., Dansgaard, W., Fuhrer, K., Gundestrup, N., Hammer, C. U., Iversen, P., Jouzel, J., Stauffer, B., and Steffensen, J. P. (1992). Irregular glacial interstadials recorded in a new Greenland ice core. *Nature* **359**, 311-313.
- Josenhans, H., Fedje, D., Pienitz, R., and Southon, J. (1997). Early humans and rapidly changing Holocene sea levels in the Queen Charlotte Islands Hecate Strait, British Columbia, Canada. *Science* **277**, 71-74.
- Keigwin, L. D. (1996). The Little Ice Age and Medieval Warm Period in the Sargasso sea. *Science* **274**, 1504-1508.
- Keigwin, L. D., and Pickart, R. S. (1999). Slope water current over the Laurentian Fan on interannual to millennial time scales. *Science* **286**, 520-523.
- Koç, N., and Jansen, E. (1992). A high resolution diatom record of the last deglaciation from the SE Norwegian Sea: documentation of rapid climatic changes. *Paleoceanography* **7**, 499-520.
- Koç, N., and Jansen, E. (1994). Response of the high-latitude Northern Hemisphere to orbital climate forcing: Evidence from the Nordic Seas. *Geology* **22**, 523.
- Koç, N., Jansen, E., and Hafliðason, H. (1993). Paleoclimatological reconstructions of surface ocean conditions in the Greenland, Iceland and Norwegian Seas through the last 14 ka based on diatoms. *Quaternary Science reviews* **12**, 115-140.
- Larsen, C., Newton, A. J., Dugmore, A. J., and Vilmundardottir, E. G. (2001). Geochemistry, dispersal, volumes and chronology of Holocene from the Katla volcanic silicic tephra layers system, Iceland. *Journal of Quaternary Science* **16**, 119-132.
- Lowe, J. J., Hoek, W. Z., and INTIMATE_group. (2001). Inter-regional correlation of palaeoclimatic records for the Last Glacial-Interglacial Transition: a protocol for improved precision recommended by the INTIMATE project group. *Quaternary Science Reviews* **20**, 1175-1187.
- Mackintosh, A. N., Dugmore, A. J., and Hubbard, A. L. (2002). Holocene climatic changes in Iceland: evidence from modelling glacier length fluctuations at Sólheimajökull. *Quaternary International* **91**, 39-52.
- Malmberg, S.-A. (1985). The water masses between Iceland and Greenland. *Journal of the Marine Research Institute* **9**, 127-140.
- Marchal, O., Cacho, I., Stocker, T. F., Grimalt, J. O., Calvo, E., Martrat, B., Shackleton, N., Vautravers, M., Cortijo, E., and van Kreveld, S. (2002). Apparent long-term cooling of the sea surface in the northeast Atlantic and Mediterranean during the Holocene. *Quaternary Science Reviews* **21**, 455-483.
- Mayewski, P. A., Meeker, L. D., Twickler, M. S., Whitlow, S., Yang, Q., Lyons, W. B., and Prentice, M. (1997). Major features and forcing of high-latitude Northern Hemisphere atmospheric circulation using a 110,000-year-long glaciochemical series. *Journal of Geophysical Research* **102**, 26345-26366.
- Mysak, L. A., and Power, S. B. (1992). Sea-ice anomalies in the western Arctic and Greenland-Iceland-Sea and their relation to an interdecadal climate cycle. *Climatological Bulletin* **26**, 147-176.
- Nesje, A., and Dahl, O. (1993). Lateglacial and Holocene glacier fluctuations and climate variations in western Norway: a review. *Quaternary Science Reviews* **12**, 255-261.
- Nesje, A., and Kvamme, M. (1991). Holocene glacier and climate variations in western Norway: evidence for early Holocene glacier demise and multiple Neoglacial events. *Geology* **19**, 610-612.

Chapter 4: Post-Glacial and Holocene palaeoceanography of the Icelandic shelf

- O'Brien, S. R., Mayewski, P. A., Meeker, L. D., Meese, D. A., Twickler, M. S., and Whitlow, S. I. (1995). Complexity of Holocene climate as reconstructed from a Greenland Ice core. *Science* **270**, 1962-1964.
- Olafsson, J. (1999). Connections between oceanic conditions off N-Iceland, Lake Myvatn temperature, regional wind direction variability and the North Atlantic oscillation. *Rit Fiskideildar* **16**, 41-57.
- Oppo, D. (1997). Millennial climate oscillations. *Science* **278**, 1244-1246.
- Oppo, D., Mcmanus, J. F., and Cullen, J. L. (2003). Palaeo-oceanography: Deepwater variability in the Holocene epoch. *Nature* **422**, 277-278.
- Orvik, K. A., Skagseth, O., and Mork, M. (2001). Atlantic inflow to the Nordic Seas: current structure and volume fluxes from moored current meters, VM-ADCP and SeaSoar- CTD observations, 1995-1999. *Deep-Sea Research Part I-Oceanographic Research Papers* **48**, 937-957.
- Osterman, L. E., and Nelson, A. (1989). Latest Quaternary and Holocene paleoceanography of the eastern Baffin Island continental shelf, Canada: benthic foraminiferal evidence. *Canadian Journal of Earth Sciences* **26**, 2236-2248.
- Pickard, J. (1985). The Holocene fossil marine macrofauna of the Vestfold Hills, Antarctica. *Boreas* **14**, 189-202.
- Pickard, J., Adamson, D. A., and Heath, C. W. (1986). The evolution of Watts Lake, Vestfold Hills, East Antarctica, from marine inlet to freshwater lake. *Palaeogeography, Palaeoclimatology, Palaeoecology* **53**, 271-288.
- Pisias, N. G., Dauphin, J. P., and Sancetta, C. (1973). Spectral analysis of the late Pleistocene-Holocene sediments. *Quaternary Research* **3**, 3-9.
- Reish, D. J., and Mason, A. Z. (2001). Radiocarbon dating and metal analysis of "fossil" and living calcareous tubes of *Protula* (Annelida: Polychaeta). In "Program & Abstracts of the 7th Int. Polychaete Conference." pp. 65, Reykjavik Iceland, 2-6 July.
- Rimbu, N., Lohmann, G., Kim, J. H., Arz, H. W., and Schneider, R. (2003). Arctic/North Atlantic Oscillation signature in Holocene sea surface temperature trends as obtained from alkenone data. *Geophysical Research Letters* **30**, art. no.-1280.
- Roberts, N. (1998). "The Holocene: An Environmental History." Blackwell, Oxford.
- Rochon, A., de Vernal, A., Sejrup, H.-P., and Hafliðason, H. (1998). Palynological evidence of climate and oceanographic changes in the North Sea during the Last Deglaciation. *Quaternary Research* **49**.
- Rosell-Melé, A. (1998). Interhemispheric appraisal of the value of alkenone indices as temperature and salinity proxies in high-latitude locations. *Paleoceanography* **13**, 694-703.
- Rosell-Melé, A., Eglinton, G., Pflaumann, U., and Samthein, M. (1995). Atlantic core-top calibration of the UK37 index as a sea-surface palaeotemperature indicator. *Geochimica et Cosmochimica Acta* **59**, 3099-3107.
- Rosell-Melé, A., Jansen, E., and Weinelt, M. (2002). Appraisal of a molecular approach to infer variations in surface ocean freshwater inputs into the North Atlantic during the last glacial. *Global and Planetary Change* **34**, 143-152.
- Rosell-Melé, A., and Koç, N. (1997). Palaeoclimatic Significance of the Stratigraphic Occurrence of Photosynthetic Biomarker Pigments in the Nordic Seas. *Geology* **25**, 49-52.
- Rosell-Melé, A., Maslin, M. A., Maxwell, J. R., and Schaeffer, P. (1997). Biomarker evidence for "Heinrich" events. *Geochimica et Cosmochimica Acta* **61**, 1671-1678.

- Rundgren, M. (1998). Early-Holocene vegetation of northern Iceland: pollen and plant macrofossil evidence from the Skagi peninsula. *Holocene* **8**, 553-564.
- Sarnthein, M., Jansen, E., Weinelt, M., Arnold, M., Duplessy, J. C., Erlenkeuser, H., Flato, A., Johannessen, G., Johannessen, T., Jung, S., Koc, N., Labeyrie, L., Maslin, M., Pflaumann, U., and Schulz, H. (1995). Variations in Atlantic Surface Ocean Paleooceanography, 50- Degrees-80- Degrees-N - a Time-Slice Record of the Last 30,000 Years. *Paleoceanography* **10**, 1063-1094.
- Serreze, M. C., Maslanik, J. A., Barry, R. G., and Demaria, T. L. (1992). Winter atmospheric circulation in the Arctic Basin and possible relationships to the Great Salinity Anomaly in the Northern North Atlantic. *Geophysical Research Letters* **19**, 293–296.
- Stötter, J., Wastl, M., Caseldine, C., and Häberle, T. (1999). Holocene palaeoclimatic reconstruction in northern Iceland: approaches and results. *Quaternary Science Reviews* **18**, 457-474.
- Stuiver, M., and Reimer, P. J. (1993). Extended ¹⁴C database and revised CALIB radiocarbon calibration program. *Radiocarbon* **35**, 215-230.
- Sweatman, T. R., and Long, J. V. P. (1969). Quantitative electron-probe microanalysis of rock forming minerals. *Journal of Petrology* **10**, 332-379.
- Swift, J. H., and Aagaard, K. (1981). Seasonal transitions and water mass formation in the Iceland and Greenland seas. *Deep Sea Research Part I: Oceanographic Research Papers* **28A**, 1107-1129.
- Syvitski, J. P. M., Andrews, J. T., and Dowdeswell, J. A. (1996). Sediment deposition in an iceberg-dominated glacial marine environment, East Greenland: basin fill implications. *Global and Planetary Change* **12**, 251–70.
- Thompson, L. G., Mosley-Thompson, E., Davis, M. E., Henderson, K. A., Brecher, H. H., Zagorodnov, V. S., Mashiotta, T. A., Lin, P.-N., Mikhalevko, V. N., Hardy, D. R., and Beer, J. (2002). Kilimanjaro ice core records: evidence of Holocene climate change in tropical Africa. *Science* **298**, 589-593.
- Thompson, L. G., Mosley-Thompson, E., Davis, M. E., Lin, P. N., Henderson, K. A., Coledai, J., Bolzan, J. F., and Liu, K. B. (1995). Late-Glacial stage and Holocene tropical ice core records from Huascarán, Peru. *Science* **269**, 46-50.
- Wastegard, S., Björck, S., Grauert, M., and Hannon, G. E. (2001a). The Mjauvotn tephra and other Holocene tephra horizons from the Faroe Islands: a link between the Icelandic source region, the Nordic Seas, and the European continent. *Holocene* **11**, 101-109.
- Wastegard, S., Björck, S., Grauert, M., and Hannon, G. E. (2001b). The Mjauvotn tephra and other Holocene tephra horizons from the Faroe Islands: a link between the Icelandic source region, the Nordic Seas, and the European continent. *The Holocene* **11**, 101-109.
- Wastl, M., Stötter, J., and Caseldine, C. (1999). Tephrochronology - a tool for correlating records of Holocene environmental and climatic change in the North Atlantic region. *Geological Society of America, Abstract Volume* **31**, A315.
- Weaver, P. P. E., Chapman, M. R., Eglinton, G., Zhao, M., Rutledge, D., and Read, G. (1999). Combined coccolith, foraminiferal, and biomarker reconstruction of paleoceanographic conditions over the past 120 kyr in the northern North Atlantic (59°N, 23°W). *Paleoceanography* **14**, 336-349.
- Williams, K. M., Andrews, J. T., Weiner, N. J., and Mudie, P. J. (1995). Late Quaternary paleoceanography of the mid- to outer continental shelf, East Greenland. *Arctic and Alpine Research* **27**, 352-363.

5. Biomarkers and organic matter in coastal environments of N.W. Scotland: assessment of potential application to sea-level studies



Cover image: Sun setting on Rumach "tidal pond" during field work August 2002. Image was taken at mid cycle during a spring-tide.

Contents

<u>5.1.</u>	<u>Introduction</u>	<u>142</u>
<u>5.2.</u>	<u>Aims and objectives</u>	<u>143</u>
<u>5.3.</u>	<u>Background</u>	<u>143</u>
5.3.1.	Isolation basins and their application to sea-level studies	143
5.3.1.1.	Contemporary processes in modern isolation basins	143
5.3.1.2.	Relative Sea-Level	144
5.3.1.3.	Fossil isolation basins and the interpretation of former sea-levels	145
5.3.1.4.	Established sea-level indicators	148
5.3.1.5.	Sea-level index points	149
5.3.1.6.	Indicative Meaning	150
5.3.1.7.	Application of Data from Sea-Level Reconstructions	150
5.3.1.8.	Level of Accuracy	151
<u>5.4.</u>	<u>Approach</u>	<u>152</u>
5.4.1.	Sampling rationale	152
5.4.2.	Study specific experimental	153
5.4.2.1.	Modern basins	153
5.4.2.2.	Fossil basins	153
5.4.2.3.	Analysis for lipid biomarkers and bulk organic properties.	154
<u>5.5.</u>	<u>Site descriptions and results of hydrographic measurements</u>	<u>155</u>
5.5.1.	North-west Scotland	155
5.5.2.	Modern Basins	156
5.5.2.1.	Arisaig	156
5.5.2.2.	Knapdale	158
5.5.2.3.	Kintail	161
5.5.3.	Fossil Basins	162
5.5.3.1.	Arisaig	162
5.5.3.2.	Coigach	163
<u>5.6.</u>	<u>Results and Discussion</u>	<u>166</u>
5.6.1.	Modern Basins	166
5.6.1.1.	Particle size distributions	166
5.6.1.2.	Bulk organic geochemistry	166
5.6.1.3.	Lipid Biomarkers	167
5.6.1.4.	Within Basin Variability – Rumach Tidal Pond.	174
5.6.2.	Fossil Basins	175
5.6.2.1.	Arisaig	175
5.6.2.2.	Dubh Lochan (Coigach)	180
<u>5.7.</u>	<u>Logit Regression Analysis</u>	<u>182</u>
<u>5.8.</u>	<u>Synthesis and Conclusion</u>	<u>186</u>

Tables

Table 5.1: Key stages of the tidal cycle and acronyms used in this thesis	144
Table 5.2: Summary data for modern basins	164
Table 5.3: Summary data for fossil basins	165
Table 5.4: Results of Logit Regression Analysis for Marine/Brackish - Isolated/Lacustrine binomial categorisation by explanatory variables.	185

(see volume II for figures)

5.1. Introduction

Isolation basins are natural coastal rock depressions previously isolated from or connected to the sea by changes in relative sea-level (RSL). Their utility in investigations of RSL change is demonstrated by research in Scandinavia, Greenland and Scotland. They have proved particularly useful in the north and west coasts of Scotland where a comparative dearth of morphological, stratigraphical and biogenic material impeded previous research (Gray, 1983; Shennan, 1989; Shennan, 1992). In this region, isolation basin based studies have provided a rich record of Late Devensian and Holocene RSL changes from 13 kyr ^{14}C to the present (Shennan et al., 2000c). The data obtained from isolation basin based studies tests hypotheses derived from morphological work and various isostatic models (Shennan et al. 1996a; 1994; 1993; 1995; 2000c; 1996b). Previous work employs a combination of lithostratigraphic and biostratigraphic (i.e. microfossil) sea-level indicators to reconstruct sea-level changes within such basins.

Novel proxies for reconstructing sea-level change are desirable because:

Firstly, established microfossil proxies – such as foraminifera - are sometimes partially or entirely absent from isolation basin sediments. Organic carbon compounds are ubiquitous, often abundant, and sometimes overlooked components of oceans, lakes and sedimentary rocks. If specific organic compound classes can be validated as reliable sea-level indicators, then the number of isolation basin sites suitable for investigation increases to include sites that yield an incomplete or inadequate microfossil record.

Secondly, individual proxy methods each have intrinsic uncertainties and errors such as in the allocation of a correct indicative meaning (i.e. the vertical relationship between the local environment in which a sea-level indicator accumulated and a contemporaneous reference tide level). Therefore, multiproxy studies provide a more complete and subtle record of RSL change, leading to greater confidence in conclusions.

5.2. Aims and objectives

The overall aim is to assess the potential application of certain sedimentary components of organic matter (i.e. lipid compounds such as alkenones, *n*-alkanes and chlorophyll derivatives), and bulk organic parameters to RSL change in isolation basin in north-west Scotland.

The objectives of this chapter are:

1. To describe the modern distributions of the lipid compounds and bulk parameters of interest in a range of modern coastal basins, selected for their varying degrees of isolation from the sea.
2. To describe the distributions of the lipid compounds and bulk parameters of interest in a number of down-core samples and to compare them with records of established sea-level indicators derived from the same cores.
3. To determine the potential of alkenones to calculate an indicative meaning of a sea-level point and assess their potential for use in further studies.

5.3. Background

Background for the biomarker and organic matter applications is given in chapter 1, the following background section is specific to this chapter.

5.3.1. Isolation basins and their application to sea-level studies

5.3.1.1. *Contemporary processes in modern isolation basins*

Modern isolation basins (i.e. those with an intertidal sill) may also be termed saline lagoons and further classified as silled, isolated, sluiced, or inlet types, depending on the degree of isolation from the open sea (Joint Nature Conservation Committee, 1996).

Any modern isolation basin has a number of inputs and outputs (hydrological, chemical, biological etc), which vary on a diurnal, seasonal and annual basis. The marine input is controlled by the elevation of the sill, the orientation of the basin relative to the coast and the morphology of the conduit (Davies and Haslett, 2000). The balance of all inputs and outputs together with issues such as basin morphology and the prevailing climate will determine the environmental conditions within the basin.

Figure 5.1- Figure 5.4 describe in a graphical form the conceptual model of the changes in a basin through time during an isolation process caused by a fall in RSL. Figure 5.1 represents a basin at five isolation stages (IS) during a fall in RSL. It illustrates the influence of the sill height and the tidal regime on the salinity of the basin during the transition from fully marine to freshwater conditions. Figure 5.2 illustrates the typical changes in the *in situ* biological assemblage groups through the five stages and the common sediment types which accompany these changes. Figure 5.3 illustrates the three major changes in the hydrographic and depositional conditions in an isolation basin during a fall in RSL and Figure 5.4 illustrates the changes in the organic matter cycle associated with the physical changes highlighted in Figure 5.3

5.3.1.2. *Relative Sea-Level*

Mean sea-level (MSL) for the UK is taken from the Newlyn tide gauge (1915 – 1921). The altitude of any tidal measurement for the UK can be calculated using the Newlyn tide gauge (1915 - 1921) as a reference. Mean tide level (MTL) is the mid-point of the tidal range at a given location. However, most tides are asymmetrical, with the corollary that MSL is often offset above or below MTL. The various key stages of the tidal cycle, together with the relevant acronyms used throughout this chapter, are given in Table 5.1.

Table 5.1: Key stages of the tidal cycle and acronyms used in this thesis

<i>Stage of Tide</i>	<i>Acronym</i>	<i>Tidal Zone</i>
		SUPRATIDAL ZONE
Highest Astronomical Tide	HAT	↑
Mean High Water Spring-Tides	MHWST	
Mean High Water Neap-Tides	MHWNT	
Mean Sea-Level*	MSL	INTERTIDAL ZONE
Mean Tide Level	MTL	
Mean Low Water Neap-Tides	MLWNT	↓
Mean Low Water Spring-Tides	MLWST	
Lowest Astronomical Tides	LAT	
		SUBTIDAL ZONE

*MSL may be above or below MTL.

Changes in RSL at a regional scale are produced through the interaction of eustatic and isostatic factors. The regional signal, however, may be confused at the local scale (Shennan et al., 2000b). The change in RSL ($\Delta\xi_{rsl}$) for a site, at time τ , and location φ , can be expressed schematically as:

$$\Delta\xi_{rsl}(\tau, \varphi) = \Delta\xi_{eus}(\tau) + \Delta\xi_{iso}(\tau, \varphi) + \Delta\xi_{local}(\tau, \varphi) \quad (5.1)$$

where $\Delta\xi_{eus}(\tau)$ is the time-dependent eustatic factor ; $\Delta\xi_{iso}(\tau, \varphi)$ is the total isostatic effect of glacial rebound, including the contributions from both ice (glacio-isostatic) and water (hydro-isostatic); and $\Delta\xi_{local}(\tau, \varphi)$ is the total effect of local processes. Such local processes can also be expressed schematically as:

$$\Delta\xi_{local}(\tau, \varphi) = \Delta\xi_{tide}(\tau, \varphi) + \Delta\xi_{sed}(\tau, \varphi) \quad (5.2)$$

Where $\Delta\xi_{tide}(\tau, \varphi)$ is the total effect of changes in the tidal regime, and the elevation of the sediment with reference to tide levels at the time of deposition, and $\Delta\xi_{sed}(\tau, \varphi)$ is the total effect of sediment consolidation since the time of deposition (Shennan et al., 2000b).

5.3.1.3. Fossil isolation basins and the interpretation of former sea-levels

Pioneering geomorphological work in Scotland in the mid-nineteenth century resulted in the identification of raised beaches and terraces (Chambers, 1848) and led Jamieson (Jamieson, 1865) to propose the glacio-isostasy theory. However, it was not until the 1960's that rigorous and consistent testing of this theory was pursued by Sissons and co-workers (Cullingford and Smith, 1966; Sissons, 1962; Sissons, 1963; Smith et al., 1969), whose approach was based on geomorphological mapping and accurate levelling of all identifiable terraces. This work was limited by the fact that palaeo-shorelines are subject to local variations in uplift resulting from the complex interplay of rheology and ice mass distribution. The record is further complicated and fragmented as relict features are often covered or obliterated by till, aeolian sands and glacio-fluvial deposits etc (Sissons, 1962; 1963).

Such problems are more apparent in Scotland than in Scandinavia, Greenland or North America, where the Weichselian ice sheets were considerably thicker - resulting in faster and greater isostatic rebound, which produced larger sequences of well-defined morphological evidence. In comparison, Scottish morphological evidence of former

RSL change is disjointed, which makes inferences of age, based upon correlation of features from one area to another, particularly conjectural (Lambeck, 1993b). In contrast, studies over the last few decades, based on isolation basins have not relied on inferred dating but have utilised detailed lithostratigraphic and biostratigraphic procedures, and absolute dating (i.e. radiocarbon) techniques. Work on isolation basins has been carried out in Scandinavia (Bondevik et al., 1997a; Bondevik et al., 1997b; Bondevik et al., 1998; Corner and Haugane, 1993; Eronen et al., 2001; Kjemperud, 1981a; Kjemperud, 1981b; Kjemperud, 1986; Svendsen and Mangerud, 1987), Canada (Retelle et al., 1989), Russia (Corner et al., 1999; Snyder et al., 1997), Greenland (Bennike, 1995; Long et al., 1999) and Scotland (Lloyd, 2000; Shennan et al., 1996a; 1994; 1993; 1995; 2000c; 1996b).

Typically, the isolation history of basins can be divided into three basic phases: marine, brackish and fresh as represented by sedimentological and biological evidence (Hafsten, 1983). The hydrological, depositional and organic geochemical changes during these phases are illustrated schematically in Figure 5.3 and Figure 5.4. The time-horizon of most interest to workers wishing to reconstruct former RSL change is the final isolation of the basin from the sea (Kjemperud, 1986), i.e. the transition from brackish to fresh or from IS 4 to IS 5 in Figures 5.1 – 5.4. This may be represented in the sediments by a horizon referred to as the *isolation contact* (see Figure 5.3).

The identification and accurate dating of this horizon in sediment cores recovered from fossil isolation basins, is the prime challenge for palaeo sea-level workers. In theory, the definition of the isolation contact as representing the point at which the basin was finally isolated from the sea should be represented by the point in time when the HAT falls below the height of the sill. Specifically, this is the *hydrological isolation contact*, which describes the total cessation of marine incursions into the basin.

However, Kjemperud (1986) has described how in reality an isolation contact identified in sediments may or may not be coincident with the hydrological isolation event. Kjemperud identifies up to four contacts in sediments resulting from differential processes during isolation and therefore have different implications for RSL reconstructions:

- The *sedimentological isolation contact* is the change from a minerogenic “mostly allochthonous” sediment to a higher TOC “more autochthonous” sediment. This often occurs below the hydrological isolation contact as the main decrease in sediments transported in from the sea typically occurs relatively early in the isolation process.
- The *diatomological isolation contact* (*more generally: the phytological i.c.*). Diatom assemblages are most frequently used as markers for environmental change in isolation basin studies. Therefore, in the literature, isolation contact is often used synonymously with the diatomological isolation contact. It may be considered as “a horizon that was the sediment-water interface at the time when the water in the photic zone of the basin became fresh” (Kjemperud, 1986).
- The *hydrological isolation contact*. As mentioned above, this term describes the total cessation of marine incursions to the basin (Ingmar, 1975). In some studies this is argued to be coincident with the diatomological contact (e.g. Kjemperud, 1986). However, in some basins it is possible for denser sea water to ventilate a basin at higher tides and circulate beneath a relatively fresh photic zone. In this situation the diatomological contact may occur up to 250 years earlier in the isolation process than the genuine hydrological contact (e.g. Faafeng, 1976 as cited by Laidler, 2002).
- The *sediment/freshwater contact*. This is related to the conditions prevailing at the sediment/water interface after hydrological isolation. It can be defined as representing “the time when all trapped sea water is replaced by fresh water” (Kjemperud, 1986). This is especially relevant to large and deep basins (i.e. deep enough so that the basins can not be fully mixed by wind), and can be a source of confusion when inorganic geochemical methods such as stable isotopes are used (Kjemperud, 1986).

The relationship between the isolation contacts of Kjemperud (1986) and the basin hydrology at different stages of isolation are illustrated in Figure 5.5. Much of the isolation theory outlined above has been developed from empirical work in Scandinavia. Isolation basins from that region and from Greenland may record RSL changes of 50-

100m or more and experience a spring tidal range of 1-2m or less (Laidler, 2002). In contrast, Scotland has experienced RSL change of a maximum of 50-40m near the centre of the ice (and considerably less further from the centre), since the last interstadial, with the present mean spring tidal range being c.4m around much of the western coast (Shennan et al., 1994). These factors combine to produce a longer transitional phase, typically of 500-1000 years or more (Long et al., 1999; Zong, 1997) to the more extreme 6500 cal years taken for the isolation of Loch nan Corr (Lloyd, 2000).

Therefore, compared to Scandinavia and Greenland, Scottish basins may provide a higher resolution record of the isolation process and may resolve more subtle changes in RSL over several millennia (Laidler, 2002). However, a disadvantage is that variations in tidal range are often significant when compared to actual differences in RSL change between sites in NW Scotland (Shennan et al., 1994). Therefore, without accurate estimation of indicative meaning (see 5.3.1.6 page 150) and levelling of the basin sill, inter-site differences in the reference tide level may form an appreciable component of what appears to be variation in RSL between locations (Shennan et al., 1994).

Unlike the sea-level research in, for example Scandinavia, there had been only limited focus on “staircases” of isolation basins in Scotland until the series of papers produced by Shennan *et al* from the mid-1990s. These studies concentrate exclusively on the west coast of the country, where sheltered depositional environments are severely restricted, which in part explains the lack of previous research in the area (Shennan et al., 1994; 1993; 1995). Isolation basins were investigated by Shennan and co-workers as one of three sets of depositional environments (raised tidal flats, isolation basins and dune/beach systems). Isolation basins and tidal marshes were determined as the providers of the most reliable, precise sea-level data, using a combination of the lithostratigraphical and biostratigraphical record (Shennan et al., 1994; 2000c).

5.3.1.4. Established sea-level indicators

The following lithostratigraphical and biostratigraphical techniques are commonly employed as sea-level indicators:

- *Pollen analysis*. Palynology was used in the earliest works on isolation basins in Scandinavia (Fægri, 1940) and has been widely used in the Scottish isolation basin studies of Shennan *et al* (1996a; 1994; 1993; 1995; 1996b) in the

determination of sea-level tendencies and reference water levels. As RSL changes, transitions between saltmarsh and terrestrial environments will be recorded in the pollen record.

- *Diatom analysis.* Diatoms are widespread microscopic unicellular alga of the class Bacillariophyceae, which colonise many wet environments exposed to sunlight. The species composition of diatom populations is controlled by particular ecological sensitivities, with the primary focus in most cases being salinity, nutrient supply, competition and sometimes pH (Palmer and Abbott, 1986; Shennan et al., 1993). The resulting diatom assemblage can be used to reconstruct the environmental history of the fossil isolation basins.
- *Foraminiferal analysis.* Foraminifera are protozoa of the class Rhizoflagellates. In saltmarsh environments foraminiferal assemblages often occur in well-defined tidal zones (Scott and Medioli, 1978) and have been applied to sea-level research (e.g. Horton et al., 1999). In isolation basins, however, the elevation is standardised by the sill, therefore other environmental factors, such as salinity have been deemed to control assemblages. However, a recent study by Laidler (Laidler, 2002) did not find a clear relationship of foraminiferal assemblages to salinity.
- *Stratigraphical analysis.* Kjemperud (1986) lists the sediment transition as one of the four isolation contacts because it typically characterises the visible change from clastic marine horizon to a transitional lacustrine clay gyttja, before a freshwater gyttja is deposited following isolation (e.g. Retelle et al., 1989). During a fall in RSL this contact is usually the first to occur as the tidal energy reduces, lowering the rate of deposition of coarser sediments. It provides a useful indicator in the field - as it is usually visible - and can allow preliminary comparison between sites, prior to detailed laboratory analysis.

5.3.1.5. Sea-level index points

A sea-level index point is a datum which can be employed to show vertical movements of RSL, once information about the geographical position, environment, indicative

meaning, altitude and age of a sample are established (Shennan, 1982). Each index point should consist of:

- a geographical position;
- an indicative meaning;
- an age;
- a tendency of sea-level movement.

Through the correlation of numerous sea-level index points in a region, the regional oscillations of RSL during particular time periods can be established (Shennan et al., 1983).

5.3.1.6. Indicative Meaning

To compare samples for age/altitude analysis, a sea-level index point must have an indicative meaning (Shennan, 1982). The indicative meaning of a sample describes the vertical relationship between the local environment, in which a sea-level indicator accumulated and a contemporaneous reference tide level (e.g. HAT or MHWST etc) (Horton et al., 1999; Shennan, 1982; Shennan, 1986; van de Plasshe, 1986). This assessment for each sample is especially important in macrotidal areas (Shennan, 1986).

Each sample is firstly related to its reference tide level, such as mean high water spring-tide (MHWST), before also being defined in terms of its indicative range, or modern vertical range (an estimate of how accurately the tide level can be estimated from the available evidence; (Horton et al., 1999; Shennan et al., 1995). In the case of isolation basins, the indicative meaning is not based on the sample itself, but rather on the elevation of the sill, thus standardising the indicative meaning for the whole site at any given point in time. In the north-west Scottish studies by Shennan *et al.*, basins are assigned a reference tide level in the range MLWST to MHWST (Shennan et al., 1996a; 1994; 1993; 1995; 2000c; 1996b) depending upon the freshwater input into the basin (Shennan et al., 1995).

5.3.1.7. Application of Data from Sea-Level Reconstructions

The acquisition of accurate sea-level index points through isolation basin studies – that employ a consistent methodology - has facilitated the examination of:

- the validity and precision of RSL curves (age-altitude empirical)

- isobase models such as those of Sissons (1963; 1966; 1972; 1983)
- ice-sheet extent/isostatic rebound models proposed by Boulton *et al* (1977; 1985) and Lambeck (1991; 1993a; 1993b; 1995) for Great Britain.

5.3.1.8. *Level of Accuracy*

In considering the value of particular samples as indicators of RSL it is important to consider the possible sources of error. The main sources are considered below:

- *Indicative Meaning.* Some RSL indicators, may not have a consistent reference tide level. The most probable source of error in indicative meaning from isolation basin research comes from the amount of freshwater entering a basin, relative to its volume (Laidler, 2002). Uncertainties have been displayed in the indicative meaning ascribed to the diatomological and hydrological isolation contacts of the upper and main basins at Loch nan Eala, “owing to the significant freshwater input into the system” (Shennan et al., 1994; 1995).
- *Tidal Range.* The tidal record for a site is taken from the nearest primary or secondary port and, as such disregards any variation which may be present between the port and the site. The indicative meaning of a site or sample is based upon its reference water level in the tidal cycle. A constant relative tidal regime (i.e. between sites) through time is assumed in the calculation of the indicative meaning. Past tidal regimes are assumed to relate, in absolute terms, to present tidal conditions. Shennan (1980) acknowledged that through making this assumption the value of the indicative meaning is decreased, but it is necessary whenever sea-level index points with different indicative meanings are being considered. A number of studies have suggested there have been significant changes in the Holocene tidal regime of the Bay of Fundy (Scott and Greenburg, 1993), the north-western European continental shelf (Austin, 1991) and the western North Sea (Shennan et al., 2000a). An in depth study will be required for the western coast of the UK, if past tidal regime changes are to be constrained, and this source of uncertainty confronted (Laidler, 2002).

- *Modern Samples.* The use of modern samples as an analogue for former environments involves a number of basic assumptions which include the following:
 - Modern data-sets should be of consistent taxonomic origin.
 - The modern taxa (or their subsequent biomarkers) are related to the environment in which they live.
 - The taxa (or biomarkers) in the modern data-set are the same biological entities as those in the fossil data, and their response(s) to the environmental variables has not changed significantly over time.

There is also an assumption that the sample being collected is actually a modern sample and not the product of a disturbed sequence. Uncertainties regarding reworking can be minimised by avoiding areas of exposed coastline and basins with strong tidal currents.

- *Levelling.* Altitudinal errors may occur, when levelling the altitude of stratigraphic boundaries, and the upper boundary of the bedrock sill. Shennan (1980; 1982; 1986) identified three different main sources of errors:
 - Measurement of depth of a borehole.
 - Levelling of the site to an Ordnance Survey benchmark, or tying the elevation of a site in the OS National Grid system (via GPS).
 - Accuracy of benchmarks to the second Ordnance Datum (OD) at Newlyn.

Additionally, levelling error may also have been introduced for some fossil isolation basins by human modification. Examples of this are Ardtoe (Shennan et al., 1996a) and Loch nan Eala (Shennan et al., 1994; 2000c) where engineering works have led to the partial removal or burial of the basin sill, making the altitude difficult to determine accurately.

5.4. Approach

5.4.1. Sampling rationale

The aim was firstly to investigate the distribution of the lipid biomarkers and bulk organic properties in a number of modern sites from NW Scotland, which could be

considered analogous to the theoretical stages of isolation illustrated in Figures 5.1 – 5.4. Summary details of the modern sites and their isolation stage are listed in Table 5.2 (page 164), justification for the isolation stage allocation is given in section 5.5 (page 155 onwards). The second aim was to compare the records of the bulk organic and biomarker proxies in cores recovered from fossil isolation basins to records derived from established microfossil sea-level indicators. Details for the fossil basin sediment cores and the justification for their selection are given in Table 5.3 (page 165) and section 5.5.3 (page 162) respectively.

5.4.2. Study specific experimental

5.4.2.1. Modern basins

The hydrographic measurements were made by deploying a sonde from a small boat. Two sondes which could record multiple parameters (multiprobes) were employed, an *Idronaut Srl Ocean Seven 301* and a *YSI 556*. Both measured temperature, conductivity/salinity, oxygen and pH, however, only the *Idronaut Srl* could automatically log pressure/depth. Therefore, when the *YSI 556* was used depth was calculated from the length of line deployed during the logging of a profile. The density anomaly σ_t was derived by the author from salinity, temperature and pressure measurements using an UNESCO endorsed algorithm and Lab Assistant PC based software (Fofonoff and Millard, 1983).

Sediment samples were collected by a sediment grab deployed by wire from a boat and triggered remotely by a messenger weight or in the case of Rumach tidal pond collected by hand during low tide.

5.4.2.2. Fossil basins

Details of the analytical procedures used to obtain and radiocarbon date microfossil records and derive the resulting sea-level index points from the fossil isolation basins are described in Shennan *et al* (2000c) and references therein. A brief summary of the methodology is:

For each fossil basin, a series of boreholes were cored to reconstruct a profile of the basin stratigraphy. One core location was then selected to represent the sequence and resampled to provide sediment for further analysis. Core and basin sill altitude were

levelled to OD using an automatic level and staff. Lithostratigraphy, pollen, diatom, foraminiferal and radiocarbon analyses were prepared using standard procedures (Moore and Webb, 1978; Palmer and Abbott, 1986; Scott and Medioli, 1980; Troels-Smith, 1955). Cores were sealed and refrigerated during the interim between the original microfossil and subsequent subsampling for lipid biomarkers.

5.4.2.3. Particle size analysis

Particle size distributions were measured from subsamples using a Coulter LS 230 Particle Size Machine (PSM). The instrument measures particle sizes in the range of 0.375 μm – 2mm by laser diffraction. Approximately 0.5 – 2 grams of wet sediment were placed in a 50ml test tube and 20mls of 20% hydrogen peroxide in distilled water were added. The tubes were placed in a water bath at 80°C until all the organic material had dissolved (more hydrogen peroxide was added if needed). The samples were centrifuged at 4000 rpm for 4 minutes, and most of the supernatant was discarded. Distilled water was added to the sample and the process was repeated several times until the hydrogen peroxide was diluted. A volume of 20 ml of distilled water and 2 ml of sodium hexametaphosphate (dispersant) were added prior to analysis with the Coulter PSM.

5.4.2.4. Analysis for lipid biomarkers and bulk organic properties.

Following collection samples were stored at -20°C. All samples were prepared according to the procedures described in chapter 2. Quantification of alkenones and alkenoates in N.W. Scottish coastal sediments was by a combination of analysis by GC-FID and GC-CI-MS and quantification of alkanes by GC-FID. The concentrations of alkenones in the majority of the samples was extremely low compared to typical samples from deep sea sediments, with concentrations often less than the minimum of 1ng/ μl previously suggested for accurate peak measurement (Rosell-Melé, 1994) and the 10ng/ μl suggested for accurate estimation of within-class-distributions (Grimalt et al., 2001) when using GC-FID. In the case of within-class-distributions, this problem was circumvented by using GC-CI-MS. GC-CI-MS has an overall sensitivity of ~ 10 pg/ μl i.e. it is two orders of magnitude more sensitive than GC-FID. At the time of the analysis for the N.W. Scottish samples the quantification of alkenones was linear between ~ 20 pg/ μl and ~ 20 ng/ μl (above 20ng/ μl there was overloading of the system

characterised by truncation of the analyte peaks). Moreover, GC-CI-MS has superior selectivity which adds to the accuracy of quantification of within-class-distributions. However, GC-CI-MS was not ideal for accurate measurement of the absolute abundances of alkenones (i.e. $\Sigma C_{37:2} + C_{37:3}$ (ng/g C_{org})) as there was no suitable internal standard and the peak response fluctuates with changes in the pressure of the NH_4^+ source. Therefore, both GC-FID & GC-CI-MS were used for the measurement of absolute abundances of $\Sigma C_{37:2} + C_{37:3}$ (ng/g C_{org}) and results are reported together. This way absolute alkenone abundances were measured relatively accurately when present in abundance (by GC-FID) and less accurate “order of magnitude” measurements were reported when alkenones were below the GC-FID detection limit. Moreover, accurate measurements of within-class-distributions were made down to extremely low concentrations using GC-CI-MS.

5.5. Site descriptions and results of hydrographic measurements

This section summarises the relevant information for the four study areas based upon the general environmental setting. Individual basins are described in terms of their characteristic morphology, sediments, vegetation, tidal regimes and freshwater inputs. The location of the different geographical study areas and the individual study sites are illustrated in Figure 5.6. Each site description is accompanied by a site map (Figure 5.7 - Figure 5.11) and site characteristics are summarized in Table 5.2 & Table 5.3 (pages 164 & 165). Results of multiprobe profile measurements of water column properties are also presented – when available – and these provide additional insights into basin hydrography.

5.5.1. North-west Scotland

The coastline of north-west Scotland is characterised by a succession of sea lochs (fjords), with rocky headlands and sandy embayments. The existence of extensive quite-water depositional environments is restricted (Shennan et al., 1993). The isolation basins/saline lagoons around Scotland vary greatly in size and character. In this study the maximum depth range varied between 5.16m and 0.56m over the full tidal cycle for the isolation basins, while the depth of Loch nan Ceall (open sea loch) was measured at 15.95m (mid cycle, of a tidal range of ~6m).

5.5.2. Modern Basins

This section presents relevant site information for the modern basins studied in this chapter. A summary is given in Table 5.2 , page 164.

5.5.2.1. Arisaig

The rocky, glacially eroded landscape of the Arisaig area provides a series of rock-lipped depressions that have accumulated shallow marine, intertidal, lacustrine and terrestrial sediments since the time of the deglaciation (Shennan et al., 2000c). The geology of the area is part of the Moine succession consisting of sequences of metamorphosed arenites and pelates. Impure calcareous rocks make up a very small part of the sequence (Craig, 1983). Figure 5.7 is a map of the Arisaig area.

5.5.2.1.1. Loch nan Ceall

Loch nan Ceall (56°54'N, 5°45'W) is a sea loch, open to and ventilated by waters from the continental shelf. It is -15.5m O.D. at its deepest point, so that much of its surface sediments are well below LAT (-2.84m OD) (U.K.H.O., 2002). Such sediments are analogous (in terms of depth below OD) to the fully marine sequences described in local fossil isolation basins at ~15 kyr BP when mean RSL was c. + 15m OD, relative to the sill of the basin (Shennan et al., 2000c). Its current isolation status corresponds to isolation stage (IS) 1-2 as illustrated by figures 5.1 -5.4. The location of the site is shown in Figure 5.6, a map of the area (including sampling stations) and site details are given in Figure 5.7 and Table 5.2 (page 164) respectively. Fresh water inputs consist of numerous streams debouching from the surrounding land. The vegetation in the surrounding catchment consists of woodland, moorland and marsh communities on higher ground, grading through low marsh to marine macrophytes on the tidal flats. A vegetation transect across a tidal marsh in the north of the loch was carried out by C. Hillier in June 2002, (see Figure 5.7) and details are given in appendix II.

On 6th August 2002, during mid-tide mid-cycle, *Idronaut Srl* multiprobe profiles were taken from sites LNC 2 and 3 (see Figure 5.12). The profiles illustrate that the water column was well mixed (by tidal friction) with a small range in salinities of ~32.8-33psu and temperatures of ~14.8-16 °C through most of the water column. Some slight freshening (30.29psu) is evident in the topmost measurement (22cm) of station 2, possibly indicating the influence of terrestrial run-off, however this was only observed in one data point.

5.5.2.1.2. Rumach Tidal Pond

Rumach Tidal Pond (RTP) is a basin at the head of the Ru peninsula. The pond is bounded by a rock sill to the north-west and a tidal marsh to the south. The altitude of the sill is 0.27m O.D. (Zong, 1997), close to current MTL of 0.28m OD (U.K.H.O., 2002) and the pond is inundated by the sea during all high tides (MHWNT = +1.18m OD) according to the tidal regime at the nearest port of Mallaig, 15 km away (U.K.H.O., 2002). Therefore, it may be considered to correspond to IS 3 as illustrated in Figures 5.1 - 5.4. The location of the site is shown in Figure 5.6 & Figure 5.7, while Figure 5.8 illustrates the basin (and sampling stations) in detail. Site characteristics are given in Table 5.2 (page 164) (see also photographic plates in appendix II).

C. Hiller carried out vegetation surveys of the basin in June 2002, the resulting description is given in appendix II. The tidal pond is exposed to westerly waves and the surface sediment contains pebbles, shingle and coarse sand. The sediment becomes finer towards the marsh in the southern part of the basin (see Figure 5.41) for particle size results. A small stream runs into the pond from the higher Rumach basins, another stream drains into the south of the basin.

In August 2002, E. Mackie took depth profile measurements for temperature, salinity, dissolved oxygen and pH at stations 1-5 (Figure 5.8) using an *Idronaut Srl* multiprobe every hour during a spring-tide (11/8/02, +2.55 m OD at Mallaig), a neap-tide (4/8/02, +1.15m OD at Mallaig) and a mid-cycle tide (7/8/02, +2.05m OD at Mallaig) for half the tidal cycle (i.e. either HT-LT or LT-HT). The results are summarized in Figure 5.13- Figure 5.19. The figures illustrate that the basin is ventilated by marine water during all tidal cycles including the neap-tide. At high tide the properties of the water in the basin closely resemble that of the August conditions of Loch nan Ceall with salinities of ~32-33 psu and temperatures of ~14-15°C.

During all of the low tides measured - including the spring-tide - there was a general freshening in the upper parts of the water column at most stations (at those where there was some remaining water). Salinity was reduced by a few psu at spring-tide but at mid-cycle and neap-tide reductions down to ~20psu and ~15psu were measured. However, the surface water data is patchy as the *Idronaut* multiprobe could not take measurements consistently in water depths of less than ~20cm, therefore a complete picture of the

property changes in the uppermost layer of the water column was not possible. Despite this the profiles clearly demonstrate the consistent influx of marine water at all high tides and the influence of the fresh water stream which is variable but more pronounced at low tides – even during the spring cycle.

Occasional profiles were taken outside the basin in the waters of Loch nan Ceall (station 6, Figure 5.8). These measurements suggested that the freshening influence of the stream extended at least a short way beyond the basin sill, at least during neap and mid-cycle low tides.

5.5.2.1.3. Loch nan Eala

Loch nan Eala is a fresh water loch, fed by the Brunery Burn, at the eastern end of Loch nan Ceall (see Figure 5.7 & Table 5.2, page 164). It is part of a complex of fossil isolation basins that have been studied by Shennan *et al* (1994; 1993). The present Loch nan Eala was reduced in size by the construction of a channel around AD 1850. The only connection to the sea is through the small valley through which the channel runs. The minimum altitude of the rock ridge between the basin and Loch nan Ceall is +15.27m OD. This would have last operated as a connection to the sea during high relative sea-level in the late Devensian (Shennan *et al.*, 1994). Therefore, as a modern fresh water loch that was once connected to the sea it may be considered to correspond to IS 5 as illustrated in Figure 5.1 - 5.4. C. Hiller carried out vegetation surveys of the basin in June 2002, the resulting description is given in appendix II.

5.5.2.2. Knapdale

Most of Knapdale is forested land with a gentle “rolling” relief interspersed with lochs. The geology is predominantly metamorphosed rock, intruded or overlain by igneous rocks in places (Craig, 1983).

5.5.2.2.1. Craiglin lagoon

Craiglin lagoon is located on the margins of Loch Sween, a sea loch open at its southern end to the continental shelf (NR 775 878). The site location is shown in Figure 5.6, a site map (and sampling station locations) is shown in Figure 5.9, site characteristics are given in Table 5.2 (page 164). The lagoon is connected to Loch Sween via a narrow channel on its west side which passes through a culvert under a forestry road (see photographic plates in appendix II). The culvert has a sill height of 1.417m OD

(Laidler, 2002). There is a small freshwater spring in the channel to the east of the culvert. Some fresh water input will enter the basin from the surrounding land but this is likely to be limited by the forestry plantation. Most of the lagoon has a bottom of fine mud, with tasselweed (*Ruppia sp.*) giving way to the seagrass *Zostera marina* at depth. The lagoon is colonised by a number of algal species from the Cyanophycota, Rhodophycota, Chrysophycota, Chromophycota and Chlorophycota. The marine biology of the lagoon was surveyed as part of a conservation review of coastal lagoons in Scotland (Covey et al., 1998), details are given in appendix II.

The tidal regime at the nearest port (5km away) - for which admiralty tide tables are available- Carsaig Bay has a MHWST of +1.29m OD and a HAT of +1.64m OD (U.K.H.O., 2002). When compared to the sill height of Craiglin lagoon (+1.417m OD) this tidal regime suggests that the lagoon is only ventilated by marine water during higher than average spring-tide high tides and some storm tides. This is supported by a previous site survey which determined that Craiglin lagoon had a tidal range of approximately only 10cm (Covey et al., 1998). Therefore, it might be considered as an excellent analog of a late stage of isolation - corresponding to IS 4 in Figures 5.1 – 5.4. To confirm this, a number of observations and water column profile measurements of the basin were made in August, September and October 2005.

During spring-tides on 11/8/02 (+ 1.39 OD at Carsaig Bay) and 7/10/02 (+1.79m OD at Carsaig Bay) hourly depth profile measurements for temperature, salinity, dissolved oxygen and pH were made using an *Idronaut Srl* multiprobe (stations 1-6) and a *YSI 556* multiprobe (stations 1-5,6) respectively (see Figure 5.20 - Figure 5.23). The results indicated that on both occasions the basin was ventilated by marine water at high tide and for several hours preceding high tide, despite the admiralty prediction that for 11/8/02 the high tide should not quite breach the sill. This is clearly indicated by the increase in salinity at station 6 (closest to the channel) from brackish values (~15-25psu) to a value of ~33psu (the Loch Sween waters proximal to the basin gave salinity values of ~33psu). The ingress of the marine waters was also detected at the deepest station (2) although the shift in values of salinity and temperature was considerably more subtle than for station 6 on both occasions.

The profile measurements also elucidated the stratification within the lagoonal waters - clearly expressed in all of the properties. In August (11/8/02 ST-LT) the lagoon had an epilimnion with temperature and salinity measurements of $\sim 20^{\circ}\text{C}$ and $\sim 15\text{psu}$ respectively, grading through a pycnocline between 40-50cm to a hypolimnion with values of $\sim 25^{\circ}\text{C}$ and $\sim 27\text{psu}$ (see Figure 5.20). In October (7/10/02 ST-LT) the stratification was less pronounced - the epilimnion had temperature and salinity values of $\sim 14^{\circ}\text{C}$ and $\sim 25\text{psu}$ respectively, grading through a deeper pycnocline between 60-100cm to a hypolimnion with values of $\sim 17.5^{\circ}\text{C}$ and $\sim 29.5\text{psu}$ (see Figure 5.22). Such a situation - where denser seawater is able to ventilate a basin at higher tides and circulate beneath a brackish photic zone - has implications for the accumulation of sea-level indicators within the basin and may give rise to the non-contemporaneous deposition of a phytological and a hydrological contact (see section 5.3.1.3, page 145).

The degree of the stratification within such a lagoon will be a function of the interplay of a number of factors including: the density and volumes of the marine waters and fresh source waters ingressing the basin, the net radiative heating or cooling at the surface and mixing by wind stress. Stable stratification is unknown in lakes of less than 40m depth at latitudes of $<70^{\circ}\text{N}$ (Killops and Killops, 1993). Whether this rule maintains for saline lagoons is not known. However, it is likely that given Craiginlough lagoon's shallow depth and exposure to strong westerly winds the stratification has some temporal variability with greater mixing and breakdown in the winter months. Therefore, the observed decrease in the epilimnion-hypolimnion density differential between August and October may well have been a function of increasing wind stress.

One interesting feature of the stratification is that the density gradient is clearly dominated by salinity and the temperature gradient is the opposite of what would be necessary in a stratified lake (i.e. in the lagoon there are higher temperatures in the hypolimnion than the epilimnion). This difference is quite considerable in August with temperatures of $\sim 20^{\circ}\text{C}$ and $\sim 25^{\circ}\text{C}$ in the epilimnion and hypolimnion respectively. The cause of this phenomena is not known, however one explanation may be that the heat energy released by the respiration of the organic matter in the lagoon sediments serves to preferentially warm the deeper waters proximal to the sediment water interface. This is supported by the oxygen profiles for the October (station 2), which suggest that in the hypolimnion there is decreasing dissolved oxygen with depth from 10pmm at 20cm

to the point of anoxia at the water-sediment interface at spring tide-low tide, with a slight increase in oxygen levels with ventilation by marine waters at spring tide-high tide (see Figure 5.22).

The situation observed in August was more complicated with a decrease in oxygen with depth from 14ppm at 10cm to 8ppm at 40cm, an increase through the pycnocline to 17ppm at 50cm followed by a decrease to 15ppm at the sediment water interface (see Figure 5.20). Such variation in the oxygen conditions of the lagoon are not surprising considering the highly variable nature of the stratification suggested for the basin and the variable ingress of oxygenated marine waters. However, significant methanogenesis and therefore persistent anoxic respiration within the upper layers of the lagoon sediments was suggested by the strong smell of methane released when obtaining grab samples of the surface sediments in August 2002. Anoxic conditions within the upper layers of the sediment has implications for the early diagenesis and preservation of sedimentary lipids such as alkenones.

On 3/8/02 and 30/9/02, the lagoon was visited during neap-tide tidal cycles and multiprobe measurements were taken for a few hours around high tide. Neap-tide high-tide was +0.29m OD at Carsaig Bay on 3/8/02 and +0.35 on 30/9/02. On both occasions water was observed to be visibly draining *from* the lagoon to Loch Sween at high tide. Moreover, measurements at station 6 revealed only brackish values of ~8psu and ~25psu in August and September respectively. On 9/8/02, the lagoon was visited during a mid-cycle tide (+1.29 OD at Carsaig Bay). On this occasion, the multiprobe equipment was not functioning, however as with the neap-tide high tides, the water was observed to be visibly draining *from* the lagoon to Loch Sween at mid-cycle high tide. These observations support the suggestion that this basin is generally only ventilated by marine waters on certain spring tide-high tides and is therefore a good exemplar of the latter stages of isolation (i.e. IS 4).

5.5.2.3. Kintail

The geology of Kintail is dominated by Lewisian Gneiss, profoundly ancient (2900 Mya) intensely metamorphosed basement rocks cut locally with dykes of acid and basic igneous rocks (Craig, 1983). This produces a thin soil usually lacking in fertility (Laidler, 2002).

5.5.2.3.1. Loch nan Corr

Loch nan Corr is a fresh water loch with a rock sill at +2.70 OD. Tidal predictions for the nearest port at Dornie Bridge suggest this is only 0.08m above present MHWST and 0.54m below HAT at the (U.K.H.O., 2002). According to such measurements the Loch should be brackish, like Craiglin Lagoon. However, the Loch has been recorded as fresh by previous investigators (Lloyd, 2000), a categorisation confirmed by multiprobe measurement in August 2001 (E.Mackie pers. comm.). Such a discrepancy must be due either to errors in the levelling of the sill height (see 5.3.1.8 page 151) or to differences in local tidal regime in the 10km between Dornie Bridge (the nearest port, see 5.3.1.8 page 151) and Loch nan Corr. The site location is shown in Figure 5.6, a site map (and sampling location) is shown in Figure 5.10, site characteristics are given in Table 5.2 (page 164). The basin which contains the loch was previously connected to the sea and has been utilised in previous isolation basin studies (Lloyd, 2000; Shennan et al., 2000c). Therefore, as a modern fresh water loch that was once connected to the sea, it may be considered to correspond to IS 5 as illustrated in Figures 5.1 – 5.4. However, it differs from Loch nan Eala in that it was connected to sea as recently as 554 yr BP (Lloyd, 2000). C. Hiller carried out vegetation surveys of the basin in June 2002, the resulting description is given in appendix II.

5.5.3. Fossil Basins

This section presents relevant site information for the fossil basins studied in this chapter, a summary is given in Table 5.3 (page 165).

5.5.3.1. Arisaig

See section 5.5.2.1 (page 156) for a description of the Arisaig area.

Loch Dubh, Torr a'Bheithe & Cnoc Pheadir

Previous studies have used isolation basins from Arisaig (Shennan, 1999; Shennan et al., 1994; 1993; 1995; 2000c) to securely constrain relative sea-level, the location of the sites is shown in Figure 5.6 and Figure 5.7, site details are given in Table 5.3 (page 165). Microfossil results from Loch Dubh and Torr a'Bheithe basins were presented in a recent study by Shennan *et al* (2000c) and form part of a “staircase” of basins recording a late Devensian – early Holocene fall in RSL. The two sites will provide a comparison between the biomarker methods and established microfossil methods that in Shennan *et al* (2000c) record of a marine – fresh transition. Cnoc Pheadir is a basin from top of the

staircase sequence. A core from the basin shows a transitional lithostratigraphy, superficially similar to the marine – terrestrial sequences identified in the lower basins of the Arisaig stair-case, but the diatom evidence is ambiguous. Therefore, this core will test the biomarker methods to see if they resolve a situation where microfossil data does not sufficiently support a fully marine phase.

5.5.3.2. Coigach

Although much of the coastline of Coigach comprises of low cliffs, there are a number of sheltered embayments with accumulations of unconsolidated sediments such as Dubh Lochan (Shennan *et al.*, 2000c). The geology consists of the ancient (c. 1000 – 800mya) red sandstones and occasional grey shales of the Torridonian and Stoer groups (Craig, 1983). Coigach is the most northern field site used by the Shennan group for isolation basin work. It contrasts with Arisaig in that it was well outside the Younger Dryas Ice limit and there is no evidence of Late Devensian sea levels higher than present day OD.

5.5.3.2.1. Dubh Lochan

The record from Loch Dubh is interpreted by Shennan *et al* (2000c) to record an early Holocene sea level rise followed by a steady regression and brackish phase until isolation in the mid-Holocene. Therefore, it provides a different test for the biomarker methods; contrasting with the marine – fresh sequences from Arisaig. The site location is shown in Figure 5.6, a site map (and sampling location) is shown in Figure 5.11, site characteristics are given in Table 5.3 (page 165).

Table 5.2: Summary data for modern basins

Basin	Site number (figure 5.8)	Position (Latitude, Longitude)	OS Coordinate (NGR8)	Type of environment	Sill Altitude (m OD)	Approximate Area (ha)			MHWST	HLAT	Max depth at high tide (m)	Approximate Water volume (m ³)		Theoretical stage of isolation (Fig 5.1)
						Mean low water	Mean high water	Low tide				High tide		
Arisaig	1	56°90'17N, 5°90'72W	NM6211 8571	Open sea	na	460	841	2.38	2.96	17.4	35 × 10 ⁶	73 × 10 ⁶	1-2	
Loch nan Cail	2	56°90'94N, 5°88'07W	NM6377 8647	loch										
	3	56°90'69N, 5°85'36W	NM6541 8610											
Rumach tidal pond (RTP)	4	56°89'84N, 5°89'56W	NM6280 8530	Saline lagoon/pond	0.27	0.2	1.2	2.38	2.96	1.9	340	41,000	3	
Loch nan Fiala	5	56°90'63N, 5°83'13W	NM6676 8596	Fresh water loch	15.27	5	5	2.38	2.96	4	100000	100000	5	
Knapdale														
Craiglin Lagoon	6	56°03'15N, 5°57'09W	NR7754 8781	Saline lagoon	1.417	6.8	6.9	1.29	1.64	1.60	51000	55,200	4	
Kintail														
Loch nan Corr	7	57°23'39N, 5°40'94W	NG9425 2103	Fresh water loch	2.7	1.7	1.7	2.62	3.24	2	42500	42500	5	

Table 5.3: Summary data for fossil basins

<i>Basin</i>	<i>Site number (figure 5.8)</i>	<i>Position (Latitude, Longitude)</i>	<i>OS Coordinate</i>	<i>Type of environment</i>	<i>Sill Altitude (m OD)</i>	<i>Relative Sea Level History</i>	<i>Reference</i>
Arisaig							
Cnoc Pheadir	8	56°01'57N 5°84'48W	NM6599 8705		42	Late Devensian RSL fall or above marine limit ?	n.a.
Torr a' Bheithe	9	56°88'90N 5°86'34W	NM6470 8415	Isolation basins	35.2	Late Devensian RSL fall	(Shennan et al., 1994; 2000c)
Loch Dubh	10	56°89'68N 5°82'28W	NM6722 8488		20.56	Late Devensian RSL fall	(Shennan et al., 1994; 2000c)
Coigach							
Dubh Lochan	11	58°06'29N 5°35'21W	NC0227 1308	Isolation basin	5.69	Early Holocene RSL rise through Late Holocene RSL fall	(Shennan et al., 2000c)

5.6. Results and Discussion

5.6.1. Modern Basins

5.6.1.1. Particle size distributions

Particle size distributions vary considerably between the sites (Figure 5.24). This emphasises the diversity of the sedimentary regime represented by the various basins, which is a function of *inter alia*: basin orientation, morphology, depth, tidal regime and catchment inputs. Loch nan Ceall station 3 (IS 1-2) and RTP 1 (IS 3) both have < 7% clay + silt and a large content of coarse sand. This may be explained by their exposed positions to the prevalent westerlies (see Figure 5.7). This is in contrast with the Loch nan Ceall station 2 (IS 1-2), which is situated in the deepest part of Loch nan Ceall (~15m) and is partly sheltered from westerly storms by a bank of shallows and small islets. In this case, clay and silt content rises to 38% (see Figure 5.7). In Craiglin lagoon (IS 4) the abundance of clay + silt is the highest of all the sites rising to ~90%. This suggests that although the lagoon is still ventilated by marine waters, the sheltered location - with a narrow conduit to Loch Sween - effectively buffers the site from tidal and storm energy. This obviously has a dramatic impact on the sedimentary regime, with reduced inputs of coarse material and greatly reduced winnowing of fine material. Loch nan Corr and Loch nan Eala (IS 5) have similar particle size distributions with 72% and 77% clay + silt respectively. These sites are fully isolated from the sea yet have a lower proportion of clay and more coarse material than Craiglin. This may be accounted for by differences in sediment inputs from the basin catchments.

5.6.1.2. Bulk organic geochemistry

The modern samples display a very wide range in values of %TOC, from 0.6% at RTP station 1, to 23.5% in Loch nan Corr (Figure 5.25). There is a general increase in %TOC with isolation (Figure 5.39). Thus, the IS 5 sediments contain the highest values of TOC (15.2% in Loch nan Eala; 23.5% in Loch nan Corr) and there is a marked increase in %TOC between the sediments of the exposed RTP (IS 3) and the highly sheltered Craiglin lagoon (IS 4). However, there is a slight decrease in the TOC values between IS 1-2 (the fjordic sea loch sediments) and IS 3 (RTP). The increase in %TOC with the increasing isolation stages will be a function of a complex interplay of factors (see chapter 1). In this case we have observed that water mass circulation, bottom water oxygen concentrations and particle size vary across the basins, and one may expect autochthonous and allochthonous carbon inputs to vary as well, as discussed later.

Relative concentrations of pigment absorbance at $\lambda = 410$ nm displayed a pattern of variation analogous to %TOC (Figure 5.27). In general, there was a slight decrease in values between IS 1-2 and 3 with an increase in values at IS 4 and IS 5 (Figure 5.39). Loch nan Eala was unusual in that it had much higher values than other samples of IS 4 or IS 5. Results discussed below suggest this may be due to higher plant macrophyte abundance in Loch nan Eala.

Values of C_{org}/N from the modern basins display a range of values from 7.5 at RTP-station 1 to 20.1 in Loch nan Eala (Figure 5.26), with values decreasing slightly from IS 1-2 to 3 and increasing with isolation through IS 4 and 5 (Figure 5.39). Muller and Mathesius (1999) used values of C_{org}/N and δC^{13} to reconstruct marine vs lacustrine phases in fossil lagoons from the southern Baltic Sea. Based on previous work (Bordovskiy, 1965; Prahl et al., 1980) they suggested that a $C_{org}/N > 12$ indicated predominantly terrestrial (lacustrine) organic inputs, a C_{org}/N of < 8 indicated predominantly algal (marine) organic inputs with a C_{org}/N of 8 – 12 characterising mixed inputs. Muller and Mathesius (1999) found that aquatic macrophytes in coastal samples had much higher values of C_{org}/N (mean 17.5) than measured in other algal matter (see Table 1.7 page 24). Therefore, by analogy, in the fully isolated basins in NW Scotland the allochthonous inputs of terrestrial detritus from the catchment area and/or aquatic macrophyte production can overprint the signal from the autochthonous phytoplankton production. Moreover, this suggests that a $C_{org}/N > 12$ may be a useful confirmation of an isolated phase in fossil basin cores.

5.6.1.3. Lipid Biomarkers

5.6.1.3.1. n-Alkanes

n-Alkane concentrations

The modern samples display considerable variation in concentrations of *n*-alkanes (Σ *n*-alkane ng/g dry sed). Values ranged from 2.7ng/g at RTP 1 to 1993ng/g at Loch nan Eala (Figure 5.28a). Generally, values decreased slightly from IS 1-2 to 3 and increased with isolation through IS 4 and 5 (Figure 5.39). Normalisation to organic carbon had little effect on the overall trend (Figure 5.39) but increased marginally the relative abundance of the *n*-alkanes in the samples from IS 1-2 & 3. The much higher concentrations of *n*-alkanes in the samples (normalised to dry sed. or organic carbon) from IS stages 4 & 5 must be a function of inputs and/or preservation, however the

relative importance of these factors is difficult to separate. The higher IS stages however, will likely be associated with greater preservational conditions for lipids given the higher observed %TOC, water column stratification and anoxia observed in IS 4 compared to environments exposed to oxygenated marine water and tidal energy (IS 1-2 & 3). There is considerable difference in the values for the two IS 5 sites of Loch nan Core and Loch nan Eala. This may be a function of the different vegetation noted for the catchment areas (appendix II), catchment inputs and possibly preservation.

n-Alkane within-class-distributions

The most abundant *n*-alkane in all of the samples was the C₂₇ – suggesting significant contribution and preservation of higher plant waxes at all the sites (Wakeham, 1976). The modern samples display a considerable range in values of CPI₂₅₋₃₃ from 2.4 at Loch nan Ceall station 3 to 6.82 at Craiglin station 1 (Figure 5.29). There is a general increase in CPI₂₅₋₃₃ with isolation stage from IS 1-2 to IS 4 and a slight decrease between IS 4 – IS 5 (Figure 5.39). The CPI values from Craiglin and Loch nan Corr are similar to those previously reported for lakes in Scotland and northern England by Cranwell (1973) who reported values from 4.1 – 11.4 with an average of 7.3. This supports the results from C_{org}/N analysis in suggesting considerable increases in the proportion of terrestrially derived organic material with isolation. There is one major inconsistency between the values of C_{org}/N and CPI₂₅₋₃₃ - the Loch nan Eala sample records the highest values of C_{org}/N but a relatively lower value of CPI₂₅₋₃₃ (4) than the other samples from isolation stages 4 & 5 (Figure 5.26 and Figure 5.29). On the basis of the C_{org}/N values alone it might be suggested that Loch nan Eala receives the greatest relative input of organic carbon derived from terrestrial higher plant sources. However, it might be suggested from the CPI₂₅₋₃₃ values that Loch nan Eala received relatively less input of terrestrial material than the other isolation stage 4 & 5 samples. The reason for this discrepancy may be due to high aquatic macrophyte inputs at Loch nan Eala which would raise the C_{org}/N values (Muller and Mathesius, 1999) but lower the CPI₂₅₋₃₃ values. This is supported by the observations of the macrophyte *Potamogeton sp.* growing in the loch (appendix II).

n-Alkane long/short chain length ratio range from 1.8 at Craiglin to 5 at RTP 1 (see Figure 5.30). Long carbon chain-length *n*-alkanes inputs are predominantly from higher plants and those with shorter chains from algae (see chapter 1). Therefore, an increase

in the index would be expected with isolation stage, as observed generally for C_{org}/N and CPI, which are also influenced by terrestrial vs algal inputs (see Figure 5.39). However, this is not observed, and instead there is a maximum of 5 at RTP (IS 3) with all other values $\sim 2-3$. The reason for this is unknown but may be explained by the fact that the short *n*-alkanes are much more vulnerable to degradation than the HMW compounds (Cranwell, 1976; Kawamura et al., 1987) and this may have biased the record in the more oxic basins.

5.6.1.3.2. Alkenones & alkenoates

- C_{37} Alkenone concentrations

Alkenone distributions in the modern basins display considerable variation in abundance. Values for $\Sigma C_{37.2} + C_{37.3}$ alkenones (ng/g dry sed.) ranged from undetectable in IS 5 (both freshwater lochs) to 75 ng/g at Craiglin lagoon station 3 (IS 4) (Figure 5.31). Alkenones were detected in all those sites which receive inputs from marine waters. The overall trend describes a decrease in concentrations between IS 1-2 and IS 3, followed by a sharp increase in IS 4 (Craiglin) and a drop to undetectable levels in the fully isolated IS 5 (freshwater lochs) sites (see Figure 5.41).

The strong variations in alkenone concentrations normalised to dry sediment may have a number of causes. If equal preservation/dilution of alkenones for all the sample sites was assumed then the differences would have to be ascribed to variance in local alkenone production and/or import of alkenone bearing material (i.e. *E. huxleyi* cells) by advection. Considerable variation in these parameters would be expected for the sample sites. Firstly, with regard to local production, *E. huxleyi* is known to populate fjordic Sea Lochs (Conte et al., 1994) in Norway and strains have been recovered from continental shelf seas of the UK and New England (Marlowe et al., 1984). But no reports of known alkenone producers exist for shallow, variable salinity coastal basins such as Craiglin. A previous study of surficial sedimentary alkenone distributions across a salinity transect in the Baltic sea - from fully marine Atlantic source waters to brackish water - found decreasing values of C_{37} alkenones towards the more brackish regions. Furthermore, a survey of algal species in Craiglin lagoon found no known alkenone producers and no haptophytes species (Covey et al., 1998) (see appendix II for species list). For the lacustrine sites, alkenone abundances would be difficult to predict. Previous work has found alkenones present in a variety of lakes (see Table 1.3, page 14), some relatively close to N.W. Scotland in the English lake district (Cranwell, 1985). However, in the

Lake District alkenones were reported present in the surface sediments of only half of the lakes sampled with variable concentrations (Cranwell, 1985). No alkenones have been reported previously in Scottish freshwater lochs, and the controls on their lacustrine distributions are not known.

Therefore, if the major control on the sedimentary concentrations of the $\Sigma C_{37.2} + C_{37.3}$ (ng/g dry sed.) alkenones was *in situ* production, we might predict the highest concentrations of alkenones within the fjordic Sea Lochs, with decreasing values in the brackish basins and with unpredictable results for the freshwater lochs. This trend would be reinforced if another significant driver of alkenone sedimentary concentrations was the influx of alkenone yielding material from fully marine Atlantic source areas. Again higher values would be predicted in the openly ventilated fjordic sea lochs, with lower values expected for the sites of restricted marine circulation, especially for Craiglin lagoon which is only ventilated by marine waters during some spring-tide high tides (see 5.5.2.2.1, page 158).

The results from N.W. Scotland are more complex than the simple decrease with isolation stage that might be predicted if the only controls of $\Sigma C_{37.2} + C_{37.3}$ (ng/g dry sed.) were *in situ* production or export production associated with marine source waters. Therefore, the influence of other controlling factors must be considered, such as dilution by sedimentation rate, loss/sorting of organic material (bearing alkenones) by tidal currents and the alkenone preservation potential of the sediments.

The great variation in sediment regime between the sites is illustrated by their contrasting particle size distributions (Figure 5.24). It is likely that concentrations of the $\Sigma C_{37.2} + C_{37.3}$ alkenones (normalised to dry sediment) have been reduced at the more exposed sites relative to the sheltered locations through dilution by higher sedimentation rates/inputs of clastic material and through greater loss (through tidal winnowing) of alkenones associated with POC and fine mineral particles bearing adsorbed alkenones. This may account for the low values at the extremely exposed RTP station 1 (Figure 5.31a).

Normalisation for TOC had a significant effect on the alkenone distributions. Values for $\Sigma C_{37.2} + C_{37.3}$ (ng/g C_{org}) remained undetectable in the freshwater samples and

ranged up to 3845 ng/g at Loch nan Ceall station 3 (see Figure 5.31b). The trend in $\Sigma C_{37.2} + C_{37.3}$ concentrations between the IS 1-2 and IS 3 stations was reversed when normalized to %TOC, so that the highest values were observed in the open sea loch samples. However, values at RTP were still lower than those at Craiglin, so that the overall trend of values for $\Sigma C_{37.2} + C_{37.3}$ (ng/g C_{org}) describes a large decrease from IS 1-2 to IS 3, followed by a small increase to the IS 4 samples followed by a drop to undetectable values in IS 5 sites (Figure 5.40).

Some of the variation in the concentrations of the alkenones in the modern sites may result from differences in preservation due to sedimentary or water column oxygen content. Investigation of the hydrographic regime at Loch nan Ceall (IS 1-2), RTP (IS 3) and Craiglin (IS 4) revealed the water column of the former two is well mixed and oxygenated, whilst at Craiglin there is at least seasonal stratification and sediment/water interface anoxia. Degradation rates for alkenones in sedimentary samples have been shown to be higher in oxic than in anoxic conditions (Gong and Hollander, 1997; Gong and Hollander, 1999; Madureira et al., 1995; Sun and Wakeham, 1994). However, a microbial degradation study by Teece *et al* (1998) has suggested that degradation of alkenones under certain anoxic conditions can be almost as significant - over a relatively short period - as under oxic conditions. Unfortunately, there is no reliable method for assessing - and correcting for - variation in oxygen controlled biomarker degradation rates.

The preservation of alkenones in NW Scottish sediments may have been partially controlled by sorption to mineral surfaces - leading to stereochemical protection. Previous work suggests that higher sedimentary %TOC (Bergamaschi et al., 1997; Keil et al., 1994b; Mayer, 1993; Mayer, 1994; Premuzic et al., 1982; Tanoue and Handa, 1979) and lipid biomarker abundance (Thompson and Eglinton, 1978) is associated with finer average particle size and higher specific surface area (SSA) in a range of marine environments, and that this is partly due to protection by sorption (Keil et al., 1994a). It is not possible to accurately account for the modification of alkenone concentrations due to sorption to fine particles. However, as an exploration, $\Sigma C_{37.2} + C_{37.3}$ (ng/g C_{org}) was normalised to %clay in Figure 5.32. The resulting values for $\Sigma C_{37.2} + C_{37.3}$ alkenones (ng/g $C_{org}/\%clay$) showed a general decrease of alkenone concentration with increasing isolation stage (Figure 5.40), but created a large variance between the values

for the IS 1-2 sites (Loch nan Ceall stations 2 and 3, Figure 5.32). Such a measure can not be recommended until the relationship between preservation of alkenones and particle size distributions is better understood.

- *Alkenone/ alkenoate within-class-distributions*

The alkenone and alkenoate “fingerprints” for the modern NW Scottish surface sediments are illustrated by the GC-CI-MS total ion chromatograms in Figure 5.33. There is a distinct difference in the distribution patterns observed in IS 1-2 (Loch nan Ceall) and IS 3 (RTP) and that observed in IS 4 (Craiglin). This distinction compares interestingly with the two patterns reported by Schulz *et al* (2000) for the Baltic sea. In this study, the alkenone and alkenoate suite in IS 1-3 (Loch nan Ceall and RTP) resembles a “typical” North Atlantic pattern produced by *E.huxleyi* and Schulz *et al*'s (2000) pattern I from the western Baltic. Whilst the alkenones and alkenoate pattern in IS 4 (Craiglin) resembles Schulz *et al*'s (2000), pattern II from the eastern Baltic Sea (SSS <7.7 psu) with distinctly higher $C_{37:4}$ abundance, lowered abundance of $C_{37:2}$ and very low abundance of C_{38} methyl alkenones.

The reason for such a divergence in alkenone patterns over a relatively small area can not be a function of physiological response of *E. Huxleyi* producers to changes in ambient water temperature. Values for U_{37}^K ranged from 0.13 at Craiglin station 1 to 0.48 at Loch nan Ceall station 3 (Figure 5.38). Converted to SST using the calibration of Muller *et al* (1998) this represents a large range of values from 2.7 – 13.2°C. A large range for such a small geographical area. The values for Loch nan Ceall and RTP give SSTs of ~11-13°C, which compare very well with mean annual WOD 98 values for the region (Conkright *et al.*, 1998) whereas the temperatures from Craiglin (2.6-3°C) are not realistic.

The alkenone patterns must be a function of either i) physiological response to other physiological stresses (such as salinity, or nutrient availability) by an *E. huxleyii* strain, ii) a product of different haptophyte populations, iii) post-depositional bias. The later seems unlikely given the bulk of evidence which suggests modifications of the U_{37}^K are rarely significant even when the concentrations of C_{37} alkenones are severely depleted (Grimalt *et al.*, 2000, and references therein). Therefore, one or a combination of the first two explanations seems more likely.

Values for %C_{37:4} ranged from 3.3% for Loch nan Ceall station 2 to 14.6% at Craiglin station 1 (Figure 5.34), with a general trend towards higher values of %C_{37:4} with isolation (Figure 5.40). The samples from IS 1-3 (Loch nan Ceall and RTP) are between 3-5% which is a “normal” value for North Atlantic alkenones produced by *E.buxleyi* in open marine conditions (see Table 1.3, page 14). The highest values of ~14% are from Craiglin lagoon, which has brackish surface waters (average salinity of ~20 psu when measured on several occasions in August and October 2002). None of the %C_{37:4} values exceed 17%, which is the highest value of %C_{37:4} previously suggested to be produced by *E.buxleyi* in a fjord (Conte et al., 1994). None of the %C_{37:4} values approach the high values (~20% - 70%) reported for lakes, polar ocean waters or the <7.7 PSU waters of the Baltic sea (Bendle and Rosell-Mele, 2001; Cranwell, 1985; Li et al., 1996; Schulz et al., 2000; Thiel et al., 1997; Volkman et al., 1988).

As mentioned in chapter 1, the ratio of C₃₈ methyl to C₃₈ ethyl alkenones (C₃₈Et/Me) was noted by Schulz *et al* (2000) to vary noticeably in sediments from a salinity gradient across the Baltic Sea – with the C₃₈ methyl alkenone being undetectable in the samples from the fresher regions. In the modern samples from NW Scotland, values of C₃₈Et/Me are consistently ~2 in the samples from IS 1-2 & 3 but jump to ~11 in the samples from IS 4, representing an approximately five fold decrease in the relative abundance of the C₃₈ methyl to the C₃₈ ethyl alkenones (Figure 5.35). There is also a sudden increase in the ratio of $\Sigma C_{37}/\Sigma C_{38}$ from IS 1-2 & 3 to IS 4 (Figure 5.36) which partially reflects the decrease in the C₃₈ methyls in the IS 4 (Craiglin) samples.

Variability is also observed in the ratio of alkenoates to alkenones with values for %AA ranging from 3.6% at Craiglin station 1 to 10.8% at Loch nan Ceall station 2 (Figure 5.37). In general, values of % Σ AA are significantly higher in IS 1-2 than the other samples, while there is no significant trend in values of % Σ AA between the IS 3 and IS 5 samples. As for the other measures of within-class-distributions the variation across the sites for % Σ AA may be a physiological response to environmental stress (salinity, nutrient availability), or a product of different haptophyte populations. However, the interpretation of % Σ AA is more complex as alkenoates have been shown to be less resistant to degradation than alkenones (Teece et al., 1998).

The observations of U_{37}^K values in the NW Scottish coastal environments does not negate the application of U_{37}^K for reconstructing SST for paleo-studies in near shelf/coastal environments. Rather they support previous evidence that SSTs derived from U_{37}^K measurements in shallow coastal environments should be treated with caution (Conte et al., 1994; Ficken and Farrimond, 1995). Specifically, attention should be paid to the within-class-distributions to assess if the “fingerprint” resembles that normally associated with *E.buxleyi* production in the open ocean. In other words, if the palaeo-environment had open ventilation to a fully marine continental shelf then the resulting SST estimates may be reasonable, but SST estimates from reduced salinity, lagoonal environments are unusable.

5.6.1.4. *Within Basin Variability – Rumach Tidal Pond.*

There is a high degree of variability between coastal basins in parameters such as the elevation of the sill, the orientation of the basin relative to the coast and the morphology of the conduit. Furthermore, the unique morphology of each basin can lead to a high degree of within basin heterogeneity in the accumulation and preservation of organic matter. In some basins such as Craiglin lagoon, the long narrow conduit and late stage of isolation results in a relatively homogenous sediment regime within the basin. In contrast, in Rumach tidal pond, which has an exposed situation and open communication with the ocean, the interaction of high tidal energy and basin morphology had resulted in an obvious within basin heterogeneity expressed in the parameter of mean particle size.

To investigate the impact of such heterogeneity on the organic geochemical parameters employed in this study, three samples were taken from across the particle size gradient within the basin. A map showing the sampling locations, GC traces and results of analysis are illustrated in Figure 5.41. The sample from station 1 is from the deepest part of the basin, which is permanently submerged by the waters of the pond even at low tides. Due to this location, station 1 was selected to represent the basin for the comparison of modern coastal basins at various isolation stages. This is in keeping with the methodology of isolation basin workers in using surface samples or cores from the deepest sub-tidal parts of basins. In contrast, samples 2 and 3 are from the littoral fringe, locations that are exposed subareally during the tidal cycle. The variability of the minerologic sediment regime between the sample sites is demonstrated by the particle

size distribution which revealed %clay + %silt values of 4.5, 12.6 and 19.4% at stations 1, 2 & 3 respectively.

The impact of such heterogeneity on organic matter accumulation is demonstrated in crude terms by the gradient in %TOC which has values of 0.6, 1.65 & 2.65% at stations 1, 2 & 3 respectively. This variability is also reflected in the various bulk organic geochemical and lipid biomarker measures. However there is great variation in the degree to which the individual measures are effected. In appears that in particular concentrations of the alkenone, *n*-alkanes and chlorin pigments are effected. Some of the alkenone within-class-distributions also show considerable variation, especially %C_{37:4} which displays values of between 3.3 – 10%.

These results highlight the impact of the local variability on biomarker records. This reinforces the need to sample from the deepest part of the basin, avoiding the fringe. This is a policy which is already established for fossil isolation basin studies by current workers, whereby, a series of boreholes is cored to reconstruct a profile of the basin stratigraphy, then one core location is selected (from the centre of the basin) to represent the sequence.

5.6.2. Fossil Basins

5.6.2.1. Arisaig

Previous studies have used isolation basins from Arisaig (Shennan, 1999; Shennan et al., 1994; 1993; 1995; 2000c) to securely constrain relative sea-level changes during the Holocene and back to approximately 13 kyr ¹⁴C BP in the Late Devensian. Microfossil results from Loch Dubh and Torr a'Bheithe basins were presented in a recent study by Shennan *et al* (2000c). The region was covered with relatively thick ice (c. 900m) at the Last Glacial Maximum and these sites form part of a “staircase” sequence that records the regression from the LGM marine limit through to an early-Holocene minimum.

5.6.2.1.1. Loch Dubh

The results of the biomarker and bulk organic geochemical analysis are given in Figure 5.42 & Figure 5.43 along with results of previous lithostratigraphic, microfossil and dating work. The previously reported diatom data shows a rapid transition from marine to freshwater conditions between 540 -539 cm depth. Concentrations of $\Sigma C_{37:2} + C_{37:3}$

alkenones (ng/g C_{org}) are between 250 – 650ng through the core, except for a pronounced peak of 1082 ng at 540.7 just below the diatom isolation contact. The alkenones in the core are distinguished by two distinct within-class-distribution patterns, with the bottom two samples (541.7 – 540.7cm) having values of $\%C_{37.4} < 15\%$, and a high $C_{38}Et/Me$ ratio (C_{38} Methyls were undetected at 540.7cm). This pattern is comparable to that observed in modern samples at the brackish Craiglin lagoon (IS 4). In the samples from 539.7cm upwards in the core, the alkenone distribution pattern is distinguished by values of $\%C_{37.4}$ of $>30\%$, a fall in the ratio of $C_{38}Et/Me$ (i.e. Methyl's become relatively more abundant) and an increase in $\Sigma C_{37} / \Sigma C_{38}$. This distribution pattern is comparable to some of the observations made in lacustrine environments in northern Europe (Cranwell, 1985; Zink et al., 2001), especially the high $\%C_{37.4}$. The relative abundance of alkenoates ($\%AA$) is highest in the bottom two samples (541.7 – 540.7cm) at $\sim 6\%$, falling to an intermediate value of 3.7% at 539cm and is lowest in the top three samples (538.7-536.7cm) with values $< 1\%$. This trend compares with the modern samples, in which $\%AA$ was observed to decrease with isolation. Values of U'_{37} show some variation (0.11 - 0.17) up the core. The bottom two samples (marine phase) give cold SSTs of 2.6 & 2.1°C. This seems a reasonable estimate – for waters proximal to an ablating ice-sheet at 15500 Cal yr BP (the late Dimlington stadial). British coleopteran faunas from this period indicate that British terrestrial temperatures reached a minimal, with the mean temperature of the warmest month no more than 9°C (Atkinson et al., 1987). While, the earliest foraminiferal SST estimates from the Barra Fan (located at the continental shelf ~ 100 km west) date from 15 Cal yr BP and are $\sim 4^\circ C (\pm 2)$ (summer SST, SIMMAX method) (Kroon et al., 1997).

The *n*-alkanes show a sharp increase in abundance and CPI_{25-33} at the same depth (540.7 – 541.7cm) that the concentrations of alkenones drop and $\%C_{37.4}$ increases, suggesting an increase in the trapping of terrestrial plant detritus in the basin, over this period. This is also matched by a sharp increase in abundance of chlorin pigments at this time. However, the *n*-alkane Long/Short ratio and *n*-alkane C_{max} gives a more complicated signal. The *n*-alkane long/short ratio is consistently ~ 1.6 except for a higher value of 2.9 in the bottom sample. This suggests highest terrestrial inputs in the lowest sample. C_{max} is quite variable with C_{29} and C_{27} - typical of higher plant waxes - dominant in the bottom two samples, followed by the algal marker C_{17} dominant for middle two samples (549.7-538.7cm), with C_{29} at 537.7cm and C_{23} in the top sample (536.7cm). This shows

that although relative inputs of terrestrial material may have been increasing through the isolation process, the environmental changes in the basin were also conducive to increasing production and/or preservation of algal inputs (C_{17}), especially around the time of the diatom isolation contact (549.7-538.7cm).

The bulk organic geochemistry supports the inferences made by the concentrations of $\Sigma C_{37.2} + C_{37.3}$ alkenones (ng/g C_{org}) and $\%C_{37.4}$. Bulk $\%TOC$ increases steadily throughout the section of core studied. The C_{org}/N ratio increases from 541.7 – 538.7cm suggesting steadily increasing inputs of organic matter of terrestrial source relative to algal inputs over this period. Values of $C_{org}/N > 12$ - considered to be typical of terrestrial values (Bordovskiy, 1965) - coincided with the diatom isolation contact at 539cm.

Interpretation

Overall, most of the significant changes in the organic parameters seem to occur slightly earlier (1cm) in the core than the major transition recorded by the diatoms. This may be a genuine offset or a function of relatively lower sampling resolution for the biomarker samples. However, allowing for a small error in the depth measurements, the results from biomarker and bulk organic property analysis compare well with the established microfossil proxies. In particular there are “sharp” changes in the concentrations of $\Sigma C_{37.2} + C_{37.3}$ alkenones (ng/g C_{org}) and values of $\%C_{37.4}$ which suggest a marine isolation. It must also be noted that the concentrations of $\Sigma C_{37.2} + C_{37.3}$ (ng/g C_{org}) were high compared to measurements on modern samples. The high concentrations may be a result of the alkenones increasing as a proportion of $\%TOC$ over time (~15 kyr) due to their relative stability compared to other more labile lipid compounds.

5.6.2.1.2. Torr a’Breithe

The results of the biomarker and bulk organic geochemical analysis are given in Figure 5.44 and Figure 5.45 along with results of previous lithostratigraphic, microfossil & dating work. The form of the transition from marine to freshwater conditions in Torr a’Breithe as recorded by diatoms contrasts with Loch Dubh, in that there is just a brief “spike” in marine conditions prior to isolation between 779 -777 cm depth. Values for $\Sigma C_{37.2} + C_{37.3}$ (ng/g C_{org}) faithfully recreate the marine transgression and subsequent isolation observed in the diatoms. This is characterised by maximal concentrations of

1284 ng at 779cm with alkenones immeasurable for all the other samples by GC-FID. However, alkenones (and the within-class-distributions) were measurable for the other samples by GC-CI-MS, although at a low response level compared to the sample at 779cm. The alkenones in the core are distinguished by two distinct within class distribution patterns. In the marine spike, the value of %C_{37:4} is 13.4%, C₃₈Et/Me and $\Sigma C_{37} / \Sigma C_{38}$ are high due to the very low relative abundance of the C₃₈ Methyls. This pattern is similar to that observed in the marine section of the Loch Dubh core and the pattern from the brackish Craiglin lagoon in the modern samples. In the rest of the core %C_{37:4} is >18% and values for C₃₈Et/Me and $\Sigma C_{37} / \Sigma C_{38}$ are much lower, this pattern is closer to that observed in the lacustrine phase of Loch Dubh and lacustrine samples from northern Europe (Ficken and Farrimond, 1995; Zink et al., 2001). This supports the contention that the alkenones deposited in the “spike” are of marine/brackish origin and that the dilute alkenone signal in the rest of the core may have an unknown haptophyte source associated with a fully isolated lacustrine environment.

The values of %AA are highest in the marine phase, with a value of ~8% consistent with the modern fully marine observations. Values were generally much lower in the other parts of the core, apart from an increase in the bottom sample which contradicts the inferences from alkenone concentrations and %C_{37:4}. Values of U^K₃₇ show considerable variation (0.12 - 0.4) up the core. The value for the marine “spike” gives a cold SST of 2.1°C. This is similar to the results from Loch Dubh and again is a very cold estimation. However, foraminiferal SST estimates from the Barra Fan during this period at ~13 kyr BP (Intra Allerød Cold Period) also give cold temperatures of 4°C (±2) (summer SST, SIMMAX method) (Kroon et al., 1997).

n-Alkane concentrations show no overall trend but are characterized by a “spike” in concentration at 779cm. There is a steady increase in CPI₂₅₋₃₃ with isolation from 789 - 767cm followed by a sharp increase in the top sample— suggesting an increase in the trapping of terrestrial higher plant detritus over this period, but with a major influx from the catchment coming after the main isolation event. Measurements of the *n*-alkane Long/Short ratio are characterized by a decrease at 779cm suggesting an increase in the relative inputs of algal organic carbon, during the marine transgression, this is supported by the C_{max} which is the algal C₁₇ at 779cm but is dominated by the higher plant C₂₇ below and C₂₉ above the 779cm. Greater algal production and/or preservation

is also suggested for the top sample as *n*-alkane Long/Short drops and C₁₇ is the dominant homolog.

The bulk organic geochemistry supports the inferences made by the concentrations of $\Sigma C_{37.2} + C_{37.3}$ (ng/g C_{org}) and %C_{37.4}. Bulk %TOC increases sharply at 779cm, while the C_{org}/N ratios surpassed the value of 12 - considered to be typical of terrestrial values (Bordovskiy, 1965) - at 779cm coinciding with the isolation contact. Furthermore the abundance of chlorin pigments in the sediments also increases sharply at 779cm.

Interpretation

The results from the measurements of $\Sigma C_{37.2} + C_{37.3}$ (ng/g C_{org}) and alkenone within-class-distributions, especially %C_{37.4}, compares well with the interpretation based on established microfossil proxies of a marine/brackish incursion at 779cm followed by isolation. The *n*-alkane measurements and bulk organic properties generally support the interpretation of a major environmental change at 779cm. However, the exception is *n*-alkane CPI₂₅₋₃₃ which shows no significant change at this time.

5.6.2.1.3. Cnoc Pheadir

Cnoc Pheadir is a basin from top of the Arisaig staircase sequence. A core from the basin shows a transitional lithostratigraphy superficially similar to the marine – terrestrial sequences identified in the lower basins of the Arisaig staircase. If this were genuine it would be evidence of a new local marine limit of 42m OD. However, the core yielded an ambiguous diatom analysis not supportive of a fully marine stage.

The results of the biomarker and bulk organic geochemical analysis are given in Figure 5.46 and Figure 5.47 along with results of previous lithostratigraphic, microfossil & dating work. Alkenones were only measurable by GC-FID in the top sample of the core with a value for the $\Sigma C_{37.2} + C_{37.3}$ (ng/g C_{org}) of 178ng. Measurement by GC-CI-MS detected alkenones in all of the samples except the bottom sample at 686cm. Both the concentration value derived from GC-FID and the responses on the GC-CI-MS were lower relative to the “marine” samples in the other Arisaig cores. Values of %C_{37.4} are high (>27%) throughout the core, substantially higher than the highest values known for *E.huxleyi* production in a sea loch (17% Conte *et al*, 1994). This supports the diatom evidence that there was no fully marine phase in this basin. Values for $\Sigma C_{37} / \Sigma C_{38}$ and

C₃₈Et/Me both displayed fluctuations up core, whilst no alkyl alkenoates were detected in any of the samples. Values of U^K₃₇' vary between 0.1 and 0.17 up the core but can not be not considered marine in origin and therefore can not give a useful palaeotemperature estimate.

The *n*-alkanes showed a steady increase in CPI₂₅₋₃₃, Long/Short ratio and overall concentrations upcore, suggesting increasing inputs of terrestrial carbon. This is supported by the bulk organic geochemistry with %TOC and the C_{org}/N ratios steadily increasing upcore. The dominant *n*-alkane homolog is C₂₇ for all the samples, suggesting a consistent source of organic carbon inputs. It is worth noting that if the C_{org}/N values were relied on for a palaeoenvironmental reconstruction without the alkenone data, then it might be incorrectly suggested that below ~673cm the organic carbon was marine in origin. This is based upon the suggestion of Muller and Mathesius (1999) that C_{org}/N values of <8 are indicative of dominantly marine carbon inputs.

Interpretation

The results from the measurements of $\Sigma C_{37.2} + C_{37.3}$ alkenones (ng/g C_{org}) and %C_{37.4} support the interpretation of Shennan (pers. comm.) that diatom evidence does not suggest a fully marine phase. Rather the combined data suggest that Cnoc Pheadir was a lacustrine basin that experienced increasing accumulation of terrestrial material – possibly due to a vegetation succession – during the period represented by the core.

5.6.2.2. Dubh Lochan (Coigach)

The record from Dubh Lochan is interpreted by Shennan *et al* (2000c) to record an early Holocene sea-level rise followed by a steady regression and brackish phase until isolation in the mid-Holocene. Therefore it provides an alternate test for the biomarker methods, because in contrast to a relatively rapid marine – fresh transition there is sequence that runs: fresh/terrestrial - saline lagoon/near-shore shelf – saltmarsh transition.

The results of the biomarker and bulk organic geochemical analysis are given in Figure 5.48 & Figure 5.49 along with results of previous lithostratigraphic, microfossil & dating work. The values for $\Sigma C_{37.2} + C_{37.3}$ (ng/g C_{org}) were undetectable by GC-FID below 268cm in the section of the core preceding the marine transgression identified by the

microfossil data. Alkenones were detected by GC-CI-MS in this section but the response was weak. At 268cm (~9000 Cal yr BP) - at exactly the depth where marine foraminifera appear in the core, alkenones become detectable to GC-FID with a $\Sigma C_{37.2} + C_{37.3}$ (ng/g C_{org}) value of 225 ng. Above this level, the $\Sigma C_{37.2} + C_{37.3}$ alkenone (ng/g C_{org}) concentrations remain detectable to GC-FID with values of 50 – 254 ng. The alkenones in the core display a number of changes in within-class-distribution patterns. Below 268cm patterns are characterised by a % $C_{37.4}$ of >18% except in the sample immediately below the marine transition at 272cm which has a value of 7%. Values for $\Sigma C_{37}/\Sigma C_{38}$ and $C_{38}Et/Me$ show an increase in the lower unit followed by a sharp fall in values with the marine transgression. Values of %AA drop from ~7% to 0% in the lower unit before increasing sharply to 9% at the marine transgression.

Above 268cm the alkenone distributions resemble those associated with production in the N. Atlantic by *E.buxleyi*, featuring % $C_{37.4}$ values of <5%. This suggests the alkenones deposited in the basin were of a fully marine source. According to the foraminiferal data following a lagoonal phase, a saltmarsh environment colonises - at least some part - of the basin from 245 cm (~6000 Cal yr BP) upwards. There is a decrease in the alkenone abundances associated with the start of this phase but the % $C_{37.4}$ remains low. This suggests that either i) the alkenone production was continuing *in situ* and the water in the basin must have had consistent fully marine qualities i.e. the foraminiferal signal must be influenced by marsh at the fringe of the basin or ii) the alkenones deposited in the basin were imported with marine water across the basin sill whilst a marsh developed throughout the basin. At 176cm there is a marked increase in $\Sigma C_{37} + \Sigma C_{38}$ (ng/Corg) concentrations to the highest values of 254 ng before values fall to 68ng at 130cm. This peak is not matched by an increase in the abundance of fully marine foraminifera. This discrepancy suggests that this alkenone concentration peak is a function of either i) increased local or regional productivity by the precursor (*E. buxleyi*) or ii) greater preservation of alkenones.

Values of U_{37}^K vary from 0.2 – 0.4 down the core. The initial marine incursion value gives a SST estimate of 12°C, which matches present day mean annual SST for the continental shelf off Coigach (Conkright et al., 1998) and seems a reasonable estimate for the mid-Holocene. This is followed by a decrease in SST's to ~8°C which is cooler than would be expected.

The *n*-alkane concentrations, *n*-alkane CPI₂₅₋₃₃, *n*-alkane Long/Short, %TOC, C_{org}/N and chlorin pigments all show a sharp spike before the marine incursion. This supports pollen and freshwater thecomebian data that suggests that prior to the marine incursion, there was a freshwater lake/marsh environment, that underwent a terrestrial vegetation succession. Coincident with the marine transgression there is sharp change in all these parameters. Interestingly C_{org}/N falls to below <8, to levels considered to be typical of marine organic inputs (Prahl et al., 1980). Above the transition to a fully marine/lagoonal phase, there is an increase in all of the parameters, perhaps associated with the development of a saltmarsh in part of the basin. This is marked more sharply by the increase in the chlorin pigments and in the *n*-alkane Long/Short ratio. All of the parameters show general increases throughout the upper part of the core – suggesting increasing inputs of terrestrial organic matter over this time.

Interpretation

The results from the measurements of $\Sigma C_{37.2} + C_{37.3}$ (ng/g C_{org}) and %C_{37.4}, clearly recreate the sudden marine transgression at ~7000 Cal BP. This compares well with the interpretation based on established microfossil proxies. Following the fully marine lagoonal phase the foraminifera suggest the local development of a saltmarsh environment. This continues to see significant deposition of alkenones with low (<5) values of %C_{37.4} with an abundance peak at 176cm. This suggests that the alkenones deposited were either i) imported with marine water across the sill or ii) they were produced *in situ* in a fully marine environment and therefore saltmarsh signal is not representative of the whole basin. *n*-Alkane measurements and bulk organic properties generally support the interpretations previously made using microfossils and the lithographic description.

5.7. Logit Regression Analysis

It is necessary to quantify the efficiency of the organic geochemical variables at discriminating between isolated and marine/brackish phases in all the samples (objects). Due to the number of variables (13) and objects (31), statistical analysis is necessary to reach systematic conclusions. In a previous, comparable, study in which lipid biomarker concentrations were investigated as indicators of environmental change in cores from Norwegian fjords, Principal Component Analysis (PCA) was used (Ficken and Farrimond, 1995). In that case alkenone abundance was extracted from the data-set as

correlating highly with the first principal component (alkenone within-class-distributions were not explored quantitatively).

In this case, PCA was not considered to be the best approach. At best it provides an indirect answer to the question being considered here. Essentially, the aim is to find which explanatory variables (organic geochemical measurements) can predict the response variables (basin isolation status) with the smallest possible error. In this case the response variable is binary – i.e. “not isolated from the sea (marine/brackish)” *or* “fully isolated from the sea (lacustrine)” based on either previous microfossil work or modern observations. This aim for each explanatory variable is formalised by the following mutually exclusive hypotheses:

H_0 : There is no systematic relationship between the depositional environment (marine/brackish or fully isolated/lacustrine) and the explanatory variable.

H_1 : There is a systematic relationship between the depositional environment (marine/brackish or fully isolated/lacustrine) and the explanatory variable.

For this question a model is required for binary response variables and quantitative (interval and ratio scale) explanatory variables. An ideal discrimination by the explanatory variable would take the form of a step function. However, in practice, a single variable never captures all the information and there are always some sampling and measurement errors. Logit regression ($a + bx$) is a more appropriate approach (Jongman et al., 1995). The function will change from near 0 to near 1 and therefore can be fitted for binary response variables. Moreover, unlike a step function, the slope of the output curve indicates how strong the discrimination is (Cox, pers. comm.). Logit regression comes under the category of generalised linear models (GLM), that includes ordinary regression and ANOVA models for continuous response variables as well as models for categorical response variables (Agresti, 1996). The response variable is coded 0 (isolated/lacustrine) or 1 (marine/brackish). Informally, the model can be thought of as quantifying the probability that a sample will either 0 or 1.

A linear model:

$$Y = a + bx \tag{5.3}$$

is not acceptable, if only because it can lead to predictions above 1 or below 0. An alternative is to use:

$$\text{logit } Y = (Y/(1 - Y)) = a + bx$$

which may also be written as:

$$Y = \exp(a + b x) / [1 + \exp(a + bx)].$$

where a and b are coefficients and x is the value for the measured explanatory variable (Jongman et al., 1995). This represents a sigmoid curve which satisfies the requirement that its values are all between 0 and 1. This defines the systematic part of the response model and because the response can only have two values the error distribution is the binomial distribution with total 1. So the variance of Y is $p(1-p)$.

A major advantage of the method is the output of a *median effective level* (EL_{50}), which occurs at the steepest slope of the curve where $Y = 0.5$ and $x = -a/b$. This represents the level at which each outcome has a 50% chance (Agresti, 1996). This has great practical implications for a study such as this, as it means that a convincing fit of a logit regression will yield a suggested threshold value for the explanatory variable.

Using Stata statistical software (StataCorp, 2003) a curve was fitted by logit regression for each of the explanatory variables (e.g. biomarker concentration, within class ratio etc) to assess their value as a predictor for the binary response variable Y . The model results are illustrated in Figure 5.50 - Figure 5.53 and model details are given in Table 5.4 (page 185). The figures clearly highlight the explanatory variables which show the clearest discrimination in values between the two Y categories. From the figures it appears that the only convincing discrimination is by %C_{37.4} and %AA, illustrated in both cases by a clear sigmoid curve fitted by the regression.

The P -value, the correlation between observed and predicted values and EL_{50} , was calculated for each of the logit regressions and the results are given in Table 5.5. The P -value gives the exact significance level associated with each regression i.e. the decision to reject a null hypothesis when $P < 0.01$ is equivalent to a significance test using a significance level of 1%. Also, expressed as a percentage ($P\text{-value} \times 100$), it gives the probability of making a type I error (incorrectly rejecting H_0). The P -value test of significance goes some way to confirming the initial visual assessment of the logit regressions – at a 1% significance level H_0 can be rejected (and H_1 accepted) only for %C_{37.4}, %AA and C_{37.2} + C_{37.3} (ng/g Corg). The correlation between the values observed for the response variable and the fitted or predicted response by each explanatory

Table 5.4: Results of Logit Regression Analysis for Marine/Brackish - Isolated/Lacustrine binomial categorisation by explanatory variables.

Explanatory Variable	Number of observations	Coefficient	P-Value	Reject H_0		Correlation between observed and predicted values (GLM CORR)	Median Effective Level (EL_{50})
				Significance			
				5%	1%		
%C _{37:4}	29	-0.3936	0.0000	Yes	Yes	0.874	15.43
% Σ AA	29	0.6829	0.0000	Yes	Yes	0.754	4.966
Σ C _{37:2} + C _{37:3} (ng/g Corg)	31	0.0036	0.0050	Yes	Yes	0.462	245
Pigments	31	-0.0002	0.0141	Yes	No	0.407	3995
Σ n-alkane (ng/dry sed.)	31	-0.0003	0.0256	Yes	No	0.395	2941
Σ C ₃₇ / Σ C ₃₈	29	-0.7411	0.0368	Yes	No	0.167	1.820
C _{org} /N	31	-0.108	0.1013	No	No	0.293	13.22
C _{38Et} /Me	28	0.0784	0.1136	No	No	0.265	5.879
UK _{37'}	29		0.1426	No	No	0.267	0.245
n-alkane CPI ₂₅₋₃₃	31	-0.2034	0.1534	No	No	0.241	5.040
%TOC	31	-0.0596	0.2119	No	No	0.204	6.305
Cmax	31	0.1314	0.2134	No	No	0.219	26
n-alkane Long/Short	31	0.5416	0.2824	No	No	0.190	7.577

variable was calculated using GLM CORR, a Stata module designed by N.Cox (Cox, 2003). Zeng and Agresti (2003) suggest this correlation as a general measure of predictive power for GLMs. The output is analogous to an R^2 value in that an output close to 1 may be considered as a strong correlation. Only C_{37:4} (0.874) and % Σ AA (0.754) gave “strong” values of greater than 0.5, with C_{37:2} + C_{37:3} (ng/g Corg) giving a correlation value of 0.462. All the other explanatory variables gave correlation values of 0.167 to 0.407. This illustrates that the absolute concentration of alkenones is not a reliable sea-level indicator. However, what the model can not take account of is that in all of the fossil cores and in the modern sediments, a sharp change is seen in the relative concentration values associated with the transition between marine/brackish conditions and full isolation.

Based on a qualitative visual assessment of the logit regressions and the tests of significance detailed above, only %C_{37:4} and %AA appear to have the potential to successfully predict classifications for NW Scottish coastal sediments deposited under either marine/brackish or fully isolated/lacustrine conditions. Furthermore, of these two measures %C_{37:4} is the stronger candidate on several counts. First, it yielded the more compelling modelling results (see Figure 5.50 and Table 5.4). Second, it is stronger on the basis of chemical principles: %C_{37:4} is based on within class variation of C₃₇ alkenones, a lipid group for which the consistency of within-class-distributions - under differing preservational conditions - has been well documented (as reviewed by Grimalt et al., 2000)). %AA is based on the ratio of alkenoates to alkenones, the interpretation of this measure is made more complex by observations that alkenoates are a more labile compound class than alkenones (Teece et al., 1998).

From Figure 5.50 of the logit regression for %C_{37:4} it can be seen that all of the marine samples had %C_{37:4} of <15% and all the lacustrine samples - except one outlier - had %C_{37:4} values of >17%. The outlier point ("non-marine" %C_{37:4} of 7%) was from the Dubh Lochan core, the sample immediately below the marine transition at 272 cm. The logit regression produced a median effective level of 15.53%. Therefore, this value may be used as a threshold to determine the marine/brackish (<15.5%) or lacustrine/isolated (>15.5%) origin of sediments.

On the basis of a combination of a qualitative assessment and the logit regression analysis, the results suggest that measurement of %C_{37:4}, combined with a knowledge of relative changes in alkenone concentrations may be used to reconstruct sea-level change in NW Scottish isolation basins.

5.8. Synthesis and Conclusions

This is the first study to investigate alkenone distributions in such a diverse range of modern shallow coastal environments. Accordingly, no previous study has reported such diversity of alkenone abundance and within-class-distributions within a relatively small geographical area. Alkenones were present in varying concentrations in surface sediments of all the modern coastal basins that had some communication to the sea but were not detected in two freshwater (lacustrine) lochs.

In the modern basins, alkenone concentrations per gram dry sediment increased in the sheltered environment of Craiglin lagoon (IS 4) relative to the more open marine environments of Loch nan Ceall and RTP (IS 1-2 & RTP). This is suggested to be a function of greater preservation potential of lipids in Craiglin lagoon, due to some combination of – i) less tidal winnowing of POC, ii) more fine sediments for lipids to adsorb to (and be stereo chemically protected), iii) anoxic sediments. However, once normalised to %TOC the highest values were observed in Loch nan Ceall (IS 1-2).

Distinct differences were observed in the alkenone patterns in the more open basins of Loch nan Ceall and RTP (IS 1-2 & 3) compared to Craiglin lagoon (IS 4). This is characterised by increased values of %C_{37.4} and lower relative abundances of C_{37.2} and the C₃₈ methyl alkenones in Craiglin. The reason for such a divergence in alkenone patterns over a relatively small area can not be a function of physiological response of *E. Huxleyi* producers to changes in ambient water temperature. The reason must be a function of either i) physiological response to other physiological stresses (such as salinity, or nutrient availability) by an *E. huxleyii* strain ii) a product of different haptophyte populations iii) post-depositional bias increasing isolation stage in modern basins. However, the values of %C_{37.4} in Craiglin remain <15%, therefore within upper limits previously recorded for *E. huxleyi* (17%) and do not approach values observed in lakes. This and the fact a marine biological survey of Craiglin found no haptophytes suggest the most likely explanation is a result of environmental stresses on *E. huxleyi*.

Results from analysis of fossil isolation basin cores suggested that absolute concentrations of alkenones can not be confidently ascribed to marine or freshwater phases. This may be because of diversity between coastal basins in terms of sediment regime/preservation potential of alkenones. However, the results suggested that changes in the relative concentrations of alkenones within an individual basin down-core are associated with marine-lacustrine transitions.

A logit regression analysis of all the sediment samples was employed to find which of the measured response variables could reliably characterise the sediment samples in terms of a marine/brackish or isolated/lacustrine binomial response variable (depositional origin). The results suggested an excellent efficiency for %C_{37.4} at predicting the depositional origin of the sediments, with %AA and alkenone

concentrations also showing a statistical relationship to the response variable. Other measures of biomarkers and organic geochemical parameters are less consistent in their response to sea-level change and therefore have less utility for sea-level studies. However, *n*-alkanes, C_{org}/N and chlorin pigments may provide other useful “background” information for a more complete environmental reconstruction.

These results suggest that alkenones may be used as an indicator of sea-level in fossil isolation basins. The most appropriate approach would be to use $\%C_{37:4}$ to initially predict a marine or non-marine source for the alkenones. The ultimate decision on the depth assignment for an isolation contact would then be based on a comparison of $\%C_{37:4}$ with changes in the relative concentrations of the alkenones down-core. The results of this study suggest the isolation contact can be identified by a sharp change in alkenone concentrations accompanied by a change in $\%C_{37:4}$ through a threshold value of $\sim 17\%$.

More work is necessary before an indicative meaning can be assigned to alkenones. However, in the modern basins abundant alkenone concentrations with a $\%C_{37:4}$ of $<15\%$ were present in Craiglin lagoon. The lagoon has a sill height 13cm above MHWST, and 22cm below HAT (i.e. the lagoon is only ventilated by marine water during higher than average spring-tide high tides and some storm tides). This suggests that the most appropriate indicative range to ascribe to an isolation contact identified by a change in alkenone abundances and associated within-class-distributions, would be between MHWST and HAT.

- Agresti, A. (1996). "An Introduction to Categorical Data Analysis." Wiley-Interscience, New York.
- Atkinson, T. C., Briffa, K. C., and Coope, G. R. (1987). Seasonal temperatures in Britain during the past 22,000 years, reconstructed using beetle remains. *Nature* **325**, 587-592.
- Austin, R. M. (1991). Modelling Holocene tides on the northwest European continental shelf. *Terra Nova* **3**, 276-288.
- Bendle, J. A., and Rosell-Mele, A. (2001). Appraisal of alkenone indices as temperature and salinity proxies in the GIN seas and Holocene millennial-scale sea surface variability on the Icelandic shelf. In "In the 7th International Conference on Paleoceanography, Sep 16-22, 2001." Sapporo, Japan.
- Bennike, O. (1995). Palaeoecology of two lake basins from Disko, West Greenland. *Journal of Quaternary Science* **10**, 149-155.
- Bergamaschi, B. A., Tsamakis, E., Keil, R. G., Eglinton, T. I., Montluçon, D. B., and Hedges, J. I. (1997). The effect of grain size and surface area on organic matter, lignin and carbohydrate concentrations and molecular compositions in Peru Margin sediments. *Geochimica et Cosmochimica Acta* **61**, 1247-1260.
- Bondevik, S., Svendsen, J. I., Johnson, G., Mangerud, J., and P.E., K. (1997a). The Storegga tsunami along the Norwegian coast, its age and runup. *Boreas* **26**, 29-53.
- Bondevik, S., Svendsen, J. I., and Mangerud, J. (1997b). Tsunami sedimentary facies deposited by the Storegga tsunami in shallow marine basins and coastal lakes, western Norway. *Sedimentology* **44**, 1115-1131.
- Bondevik, S., Svendsen, J. I., and Mangerud, J. (1998). Distinction between the Storegga tsunami and the Holocene marine transgression in coastal basin deposits of western Norway. *Journal of Quaternary Science* **13**, 529-537.
- Bordovskiy, O. K. (1965). Accumulation and transformation of organic substances in marine sediments. *Marine Geology* **3**.
- Boulton, G. S., Jones, A. S., Clayton, K. M., and M.J., K. (1977). A British ice-sheet model and patterns of glacial erosion and deposition in Britain. In "British Quaternary Studies: recent advances." (R. W. Shotton, Ed.), pp. 231-246. Clarendon Press, Oxford.
- Boulton, G. S., Smith, G. D., Jones, A. S., and Newsome, J. (1985). Glacial geology and glaciology of the last mid-latitude ice sheets. *Journal of Geological Society of London* **142**, 447-474.
- Chambers, R. (1848). Ancient sea margins: as memorials of change in the relative relief of sea and land, pp. 337. W.S. Orr and co., London.
- Conkright, M. E., Levitus, S., O'Brien, T., Boyer, T. P., Stephens, C., Johnson, D., Baranova, O., Antonov, J., Gelfeld, R., Rochester, J., and C., F. (1998). "World Ocean Database CD." U.S. Department of Commerce, Washington, D.C.
- Conte, M. H., Thompson, A., and Eglinton, G. (1994). Primary production of lipid biomarker compounds by *Emiliania huxleyi*. Results from an experimental mesocosm study in fjords of southwestern Norway. *Sarsia* **79**, 319-331.
- Corner, G. D., and Haugane, E. (1993). Marine-lacustrine stratigraphy of raised coastal basins and postglacial sea-level change at Lyngen and Vanna, Troms, northern Norway. *Norsk Geologisk Tidsskrift* **73**, 175-197.
- Corner, G. D., Yevzerov, V. Y., Kolka, V. V., and Møller, J. J. (1999). Isolation basin stratigraphy and Holocene relative sea-level change at the Norwegian-Russian border north of Nikel, northwest Russia. *Boreas* **28**, 146-166.

Chapter 5: Biomarkers and organic matter in coastal environments of N.W. Scotland

- Covey, R., Fortune, F., Nichols, D. M., and Thorpe, K. (1998). Marine Nature Conservation Review Sectors, 3, 4, 12, 13, & 15. Lagoons in mainland Scotland and the Inner Hebrides: area summaries., pp. 1-139. Joint Nature Conservation Committee., Peterborough.
- Cox, N. (2003). glmcorr: Stata module for correlation measure of predictive power for GLMs. Public domain code downloadable via <http://ideas.repec.org/c/boc/bocode/s428101.html> (accessed 3 June 2003).
- Craig, G. Y. (1983). "Geology of Scotland." Scottish Academic Press, Edinburgh.
- Cranwell, P. A. (1973). Chain-length distribution of *n*-alkanes from lake sediments in relation to post-glacial environmental change. *Freshwater Biology* **3**, 259-265.
- Cranwell, P. A. (1976). Decomposition of aquatic biota and sediment formation: organic compounds in detritus resulting from microbial attack on the alga *Ceratium hirundinella*. *Freshwater Biology* **6**.
- Cranwell, P. A. (1985). Long-chain unsaturated ketones in recent lacustrine sediments. *Geochimica et Cosmochimica Acta* **49**, 1545-1551.
- Cullingford, R. A., and Smith, D. E. (1966). Lateglacial shorelines in eastern Fife. *Transactions of the Institute of British Geographers* **39**, 31-51.
- Davies, P., and Haslett, S. K. (2000). Identifying storm or tsunami events in coastal basin sediments. *Area* **32**, 335-336.
- Eronen, M., Glückert, G., Hatakka, L., van de Plasshe, O., van der Plicht, J., and Rantala, P. (2001). Rates of Holocene isostatic uplift and relative sea-level lowering of the Baltic in SW Finland based on studies of isolation contacts. *Boreas* **30**, 17-30.
- Faafeng, B. (1976). "En limnologisk undersøkelse av innsjøen Pollen i Ås kommune, med hovedvekt på innsjøhistorie og primærproduksjon." Unpublished Unpublished thesis, University of Oslo.
- Fægri, K. (1940). Quatärgeologische Untersuchungen im westlichen Norwegen. II. Zur spätquartären Geschichte Jærens. Bergens Mus. Årb. 1939-1940. *Naturvitensk* **7**, 201.
- Ficken, K. J., and Farrimond, P. (1995). Sedimentary lipid geochemistry of Framvaren: impacts of a changing environment. *Marine Chemistry* **51**, 31-43.
- Fofonoff, N. P., and Millard, R. C. (1983). Algorithms for computation of fundamental properties of seawater. *Unesco technical papers in marine science* **44**, 15-28.
- Gong, C., and Hollander, D. J. (1997). Differential contribution of bacteria to sedimentary organic matter in oxic and anoxic environments, Santa Monica Basin, California. *Organic Geochemistry* **26**, 545-563.
- Gong, C., and Hollander, D. J. (1999). Evidence for the differential degradation of alkenones under contrasting bottom water oxygen conditions: Implications for paleotemperature reconstruction. *Geochimica et Cosmochimica Acta* **63**, 405-411.
- Gray, J. M. (1983). The measurement of relict shoreline altitudes in areas affected by glacio-isostasy, with particular reference to Scotland. *Institute of British Geographers Special Publication*. In "Shorelines and Isostasy. ." (D. E. Smith, and A. G. Dawson, Eds.), pp. 97-127. Academic Press, London.
- Grimalt, J. O., Calvo, E., and Pelejero, C. (2001). Sea surface paleotemperature errors in U-37(K') estimation due to alkenone measurements near the limit of detection. *Paleoceanography* **16**, 226-232.
- Grimalt, J. O., Rullkötter, J., Sicre, M.-A., Summons, R., Farrington, J., Harvey, H. R., Goñi, M., and Sawada, K. (2000). Modifications of the C37 alkenone and alkenoate composition in the water

column and sediment: Possible implications for sea surface temperature estimates in paleoceanography. *GEOCHEMISTRY, GEOPHYSICS, GEOSYSTEMS* **1**, Paper number 2000GC000053.

- Hafsten, U. (1983). Biostratigraphical evidence for Late Weichselian and Holocene sea-level changes in southern Norway. *Institute of British Geographers Special Publication. In "Shorelines and Isostasy."* (D. E. Smith, and A. G. Dawson, Eds.), pp. 161-181. Academic Press, London.
- Horton, B. P., Edwards, R. J., and Lloyd, J. M. (1999). A foraminiferal-based transfer function: implications for sea-level studies. *Journal of Foraminiferal Research* **29**, 117-129.
- Ingmar, T. (1975). Sjöavsnörningar från aktualgeologiska synpunkter. En översikt. *Dep. Quat. Geol. Lund. Rep.* **3**, 90.
- Jamieson, T. F. (1865). On the history of the last geological changes in Scotland. *Quarterly Journal of the Geological Society of London* **21**, 161-203.
- Joint_Nature_Conservation_Committee. (1996). Guidelines for the selection of biological SSSIs: intertidal marine habitats and saline lagoons. Joint Nature Conservation Committee, Peterborough.
- Jongman, R. H. G., Ter Braak, C. J. F., and Tongeren, O. F. R. (1995). "Data Analysis in Community and Landscape Ecology." Cambridge University Press, Cambridge.
- Kawamura, K., Ishiwatari, R., and Ogura, K. (1987). Early diagenesis of organic matter in the water column and sediments: Microbial degradation and resynthesis of lipids in Lake Haruna. *Organic Geochemistry* **11**, 251-264.
- Keil, R. G., Montluçon, D. B., Prahl, F. G., and Hedges, J. I. (1994a). Sorptive preservation of labile organic matter in marine sediments. *Nature* **370**, 549-552.
- Keil, R. G., Tsamakis, E., Fuh, C. B., Giddings, J. C., and Hedges, J. I. (1994b). Mineralogical and textural controls on organic composition of coastal marine sediments: Hydrodynamic separation using SPLIT fractionation. *Geochimica et Cosmochimica Acta* **57**, 879-893.
- Killops, S. D., and Killops, V. J. (1993). "An Introduction to Organic Geochemistry." Longman, New York.
- Kjemperud, A. (1981a). Diatom changes in sediments from basins possessing marine/lacustrine transitions in Frosta, Nord-Trøndelag, Norway. *Boreas* **10**, 27-38.
- Kjemperud, A. (1981b). A shoreline displacement investigation from Frosta in Trondheimsfjorden, Nord-Trøndelag, Norway. *Norsk Geologisk Tidsskrift* **61**, 1-15.
- Kjemperud, A. (1986). Late Weichselian and Holocene shoreline displacement in the Trondheimsfjord area, central Norway. *Boreas* **15**, 61-82.
- Kroon, D., Austin, W. E. N., Chapman, M. R., and Ganssen, G. M. (1997). Deglacial surface circulation changes in the northeastern Atlantic: Temperature and salinity records off NW Scotland on a century scale. *Paleoceanography* **12**, 755-763.
- Laidler, D. (2002). "Foraminiferal ecology of contemporary isolation basins in northwest Scotland." University of Durham.
- Lambeck, K. (1991). Glacial rebound and sea-level change in the British Isles. *Terra Nova* **3**, 379-389.
- Lambeck, K. (1993a). Glacial rebound of the British Isles - I. Preliminary model results. *Geophysical Journal International* **115**, 941-959.
- Lambeck, K. (1993b). Glacial rebound of the British Isles - II. A high-resolution, high-precision model. *Geophysical Journal International* **115**, 960-990.

Chapter 5: Biomarkers and organic matter in coastal environments of N.W. Scotland

- Lambeck, K. (1995). Late-Devensian and Holocene shorelines of the British Isles and North Sea from models of glacio-hydro-isostatic rebound. *Journal of Geological Society of London* **152**, 437-448.
- Li, J., Philip, R. P., Pu, F., and Allen, J. (1996). Long-chain alkenones in Quinghai Lake sediments. *Geochimica et Cosmochimica Acta* **60**, 235-241.
- Lloyd, J. M. (2000). Combined foraminiferal and thecamoebian environmental reconstruction from an isolation basin in NW Scotland: implications for sea-level studies. *Journal of Foraminiferal Research* **30**, 294-305.
- Long, A., Roberts, D. H., and Wright, M. R. (1999). Isolation basin stratigraphy and Holocene relative sea-level change on Arveprinsen Ejland, Disko Bugt, West Greenland. *Journal of Quaternary Science* **14**, 323-345.
- Madureira, L. A. S., Conte, M. H., and Eglinton, G. (1995). Early diagenesis of lipid biomarker compounds in North Atlantic sediments. *Paleoceanography* **10**, 627-642.
- Marlowe, I. T., Green, J. C., Neal, A. C., Brassell, S. C., Eglinton, G., and Course, P. A. (1984). Long chain (*n*-C₃₇-C₃₉) Alkenones in the Prymensiophyceae. Distribution of Alkenones and lipids and their Taxonomic significance. *British Phycology Journal* **19**, 203-216.
- Mayer, L. M. (1993). Organic Matter at the Sediment-Water Interface. In "Organic Geochemistry: Principles and Applications." (M. H. Engel, and S. A. Macko, Eds.). Plenum Press, New York.
- Mayer, L. M. (1994). Surface area control of organic carbon accumulation in continental shelf sediments. *Geochimica et Cosmochimica Acta* **58**, 1271-1284.
- Moore, P. D., and Webb, J. A. (1978). "An illustrated guide to pollen analysis." Hodder and Stoughton, London.
- Muller, A., and Mathesius, U. (1999). The palaeoenvironments of coastal lagoons in the southern Baltic Sea, I. The application of sedimentary Corg/N ratios as source indicators of organic matter. *Palaeogeography, Palaeoclimatology, Palaeoecology* **145**, 1-16.
- Muller, P. J., Kirst, G., Ruhland, G., von Storch, I., and Rosell-Mele, A. (1998). Calibration of the alkenone paleotemperature index U-37(K') based on core-tops from the eastern South Atlantic and the global ocean (60 degrees N-60 degrees S). *Geochimica Et Cosmochimica Acta* **62**, 1757-1772.
- Palmer, A. J. M., and Abbott, W. H. (1986). Diatoms as indicators of sea-level change. In "Sea-Level Research: A Manual for the Collection and Evaluation of Data." (O. van de Plasshe, Ed.), pp. 457-488. Geobooks, Norwich.
- Prahl, F. G., Bennett, J. T., and Carpenter, R. (1980). The early diagenesis of aliphatic hydrocarbons from Dabob Bay, Washington. *Geochimica et Cosmochimica Acta* **44**, 1967-1976.
- Premuzic, E. T., Benkovitz, C. M., Gaffney, J. S., and Walsh, J. J. (1982). The nature and distribution of organic matter in the surface sediments of the worlds oceans and seas. *Organic Geochemistry* **4**, 467-576.
- Retelle, M. J., Bradley, R. S., and Stuckenrath, R. (1989). Relative sea-level chronology determined from raised marine sediments and coastal isolation basins, northern Ellesmere Island, Arctic Canada. *Arctic and Alpine Research* **21**, 113-125.
- Rosell-Melé, A. (1994). "Long-chain alkenones, Alkyl Alkenoates and Total Pigment Abundances as Climatic Proxy-Indicators in the Northeastern Atlantic." Unpublished Ph.D. thesis, University of Bristol.
- Schulz, H. M., Schoner, A., and Emeis, K. C. (2000). Long-chain alkenone patterns in the Baltic Sea - an ocean- freshwater transition. *Geochimica Et Cosmochimica Acta* **64**, 469-477.

- Scott, D. B., and Greenburg, D. A. (1993). Relative sea-level rise and tidal development in the Fundy tidal system. *Canadian Journal of Earth Sciences* **20**, 1554-1564.
- Scott, D. B., and Medioli, F. S. (1978). Vertical zonations of marsh foraminifera as accurate indicators of former sea-levels. *Nature* **272**, 528-531.
- Scott, D. B., and Medioli, F. S. (1980). "Quantitative studies of marsh foraminiferal distributions in Nova Scotia: implications for sea level studies." Cushman Foundation for Foraminiferal Research, Special Publication No. 17, 58pp.
- Shennan, I. (1980). "Flandrian sea-level changes in the Fenland." Unpublished Unpublished thesis, University of Durham.
- Shennan, I. (1982). Interpretation of Flandrian sea-level data from the Fenland, England. *Proceedings of the Geologists' Association* **93**.
- Shennan, I. (1986). Flandrian sea-level changes in the Fenland. II: Tendencies of sea-level movement, altitudinal changes, and local and regional factors. *Journal of Quaternary Science* **1**, 155-179.
- Shennan, I. (1989). Holocene crustal movements and sea-level changes in Great Britain. *Journal of Quaternary Science* **4**, 77-89.
- Shennan, I. (1992). Late Quaternary sea-level changes and crustal movements in eastern England and eastern Scotland: an assessment of models of coastal evolution. *Quaternary International* **15/16**, 161-173.
- Shennan, I. (1999). Global meltwater discharge and the deglacial sea-level record from northwest Scotland. *Journal of Quaternary Science* **14**, 715-719.
- Shennan, I., Green, F., Innes, J., Lloyd, J., Rutherford, M., and Walker, K. (1996a). Evaluation of rapid relative sea-level changes in north-west Scotland during the last glacial-interglacial transition: evidence from Ardtoe and other isolation basins. *Journal of Coastal Research* **12**, 862-874.
- Shennan, I., Innes, J. B., Long, A., and Zong, Y. (1994). Late Devensian and Holocene relative sea-level changes at Loch nan Eala, near Arisaig, northwest Scotland. *Journal of Quaternary Science* **9**, 261-283.
- Shennan, I., Innes, J. B., Long, A. J., and Zong, Y. (1983). Analysis and interpretation of Holocene sea-level data. *Nature* **302**, 404-406.
- Shennan, I., Innes, J. B., Long, A. J., and Zong, Y. (1993). Late Devensian and Holocene relative sea-level changes at Rumach, near Arisaig, northwest Scotland. *Norsk Geologisk Tidsskrift* **73**, 161-174.
- Shennan, I., Innes, J. B., Long, A. J., and Zong, Y. (1995). Late Devensian and Holocene relative sea-level changes in northwestern Scotland: new data to test existing models. *Quaternary International*, **26**, 97-123.
- Shennan, I., Lambeck, K., Flather, R., Horton, B. P., McArthur, J., Innes, J. B., Lloyd, J. M., Rutherford, M. M., and Wingfield, R. (2000a). Modelling western North Sea palaeoceanographies and tidal changes during the Holocene. In "Holocene land-ocean interaction and environmental change around the North Sea. *Geological Society Special Publication*." (I. Shennan, and J. Andrews, Eds.), pp. 299-319, London.
- Shennan, I., Lambeck, K., Horton, B., Innes, J., Lloyd, J., McArthur, J., and Rutherford, M. (2000b). Holocene isostasy and relative sea-level changes on the east coast of England. In "Holocene land-ocean interaction and environmental change around the North Sea." (I. Shennan, and J. Andrews, Eds.), pp. 275-298. Geological Society, London.
- Shennan, I., Lambeck, K., Horton, B. P., Innes, J. B., Lloyd, J. M., McArthur, J. J., Purcell, T., and Rutherford, M. M. (2000c). Late Devensian and Holocene records of relative sea-level changes

Chapter 5: Biomarkers and organic matter in coastal environments of N.W. Scotland

in northwest Scotland and their implications for glacio-hydro-isostatic modelling. *Quaternary Science Reviews*, **19**, 1103-1136.

- Shennan, I., Rutherford, M. M., Innes, J. B., and Walker, K. (1996b). Late glacial sea level and ocean margin environmental changes interpreted from biostratigraphic and lithostratigraphic studies of isolation basins in northwest Scotland. *Geological Society Special Publication*. In "Late Quaternary of the North Atlantic Margins." (J. T. Andrews, W. E. N. Austin, H. Bergsten, and A. E. Jennings, Eds.), pp. 229-244. Blackwell, London.
- Sissons, J. B. (1962). A re-interpretation of the literature on Lateglacial shorelines in Scotland, with particular reference to the Forth area. *Transactions of the Edinburgh Geological Society* **19**, 83-99.
- Sissons, J. B. (1963). Scottish raised shoreline heights with particular reference to the Forth Valley. *Geografiska Annaler* **45**, 180-185.
- Sissons, J. B. (1966). Relative sea-level changes between 10,300 and 8,300 BP in part of the Carse of Stirling. *Transactions of the Institute of British Geographers* **39**, 19-29.
- Sissons, J. B. (1972). Dislocation and non-uniform uplift of raised shorelines in the western part of the Forth Valley. *Transactions of the Institute of British Geographers* **55**, 145-159.
- Sissons, J. B. (1983). Shorelines and isostasy in Scotland. *Institute of British Geographers Special Publication*. In "Shorelines and Isostasy." (D. E. Smith, and A. G. Dawson, Eds.). Academic Press, London.
- Smith, D. E., Sissons, J. B., and Cullingford, R. A. (1969). Isobases for the main Perth shoreline in south-east Scotland as determined by trend-surface analysis. *Transactions of the Institute of British Geographers* **46**, 45-52.
- Snyder, J. A., Forman, S. L., Mode, W. N., and Tarasov, G. A. (1997). Postglacial relative sea-level history: sediment and diatom records of emerged coastal lakes, north-central Kola Peninsula, Russia. *Boreas*, 329-346.
- StataCorp. (2003). Stata Statistical Software: release 8.0. College Station, TX: Stata Corporation.
- Sun, M.-Y., and Wakeham, S. G. (1994). Molecular evidence for degradation and preservation of organic matter in the anoxic Black Sea Basin. *Geochimica et Cosmochimica Acta* **58**, 3395-3406.
- Svendsen, J. I., and Mangerud, J. (1987). Late Weichselian and Holocene sea-level history for a cross-section of western Norway. *Journal of Quaternary Science* **2**, 113-132.
- Tanoue, E., and Handa, N. (1979). Differential sorption of organic matter by various sized particles in recent sediment from the Bering Sea. *Journal of the Oceanographic Society of Japan* **35**, 199-208.
- Teece, M. A., Getlife, J. M., Leftley, J. W., Parkes, R. J., and Maxwell, J. R. (1998). Microbial degradation of the marine prymnesiophyte *Emiliana huxleyi* under oxic and anoxic conditions as a model for early diagenesis: long chain alkadienes, alkenones and alkyl alkenoates. *Organic Geochemistry* **29**, 863-880.
- Thiel, V., Jenisch, A., Landmann, G., Reimer, A., and Michaelis, W. (1997). Unusual distributions of long-chain alkenones and tetrahymanol from the highly alkaline Lake Van, Turkey. *Geochimica et Cosmochimica Acta* **61**, 2053-2064.
- Thompson, S., and Eglinton, G. (1978). The fractionation of a recent sediment for organic geochemical analysis. *Geochimica et Cosmochimica Acta* **42**, 199-207.
- Troels-Smith, J. (1955). Characterisation of unconsolidated sediments. *Danmarks Geologiske Undersogelse Series IV* **3**, 38-73.
- U.K.H.O. (2002). Admiralty Tide Tables: United Kingdom and Ireland, pp. 1-353. United Kingdom Hydrographic Office, London.

- van de Plasshe, O. (1986). Introduction. In "Sea-Level Research: A Manual for the Collection and Evaluation of Data." (O. van de Plasshe, Ed.). Geo Books, Norwich.
- Volkman, J. K., Burton, H. R., Everitt, D. A., and Allen, D. I. (1988). Pigment and lipid compositions of algal and bacterial communities in Ace Lake, Vestfold Hills, Antarctica. *Hydrobiologia* **165**, 41-57.
- Wakeham, S. G. (1976). A comparative survey of petroleum hydrocarbons in lake sediments. *Marine Pollution Bulletin*.
- Zink, K.-G., Leythaeuser, D., Melkonian, M., and Schwark, L. (2001). Temperature dependency of long-chain alkenone distributions in Recent to fossil limic sediments and in lake waters. *Geochimica et Cosmochimica Acta* **65**, 253-265.
- Zong, Y. (1997). Implications of *Paralia sulcata* abundance in Scottish isolation basins. *Diatom Research* **12**, 125-150.

6. Overview and future Work



Cover Image: Iceberg with Icelandic coast in background – courtesy of www.iww.is.com

Contents

Overview	201
General	201
Chapter 3: Distribution of long-chain alkenones in the Nordic Seas	202
Chapter 4: Post-Glacial palaeoceanography of the Icelandic shelf.	204
Chapter 5: Biomarkers and organic matter in coastal environments of N.W. Scotland:	
Assessment of potential application to sea level studies.	205
Future work	206
Chapter 3: Distribution of long-chain alkenones in the Nordic Seas.	206
Chapter 4: Post-Glacial palaeoceanography of the Icelandic shelf.	207
Chapter 5: Biomarkers and organic matter in coastal environments of N.W. Scotland:	
Assessment of potential application to sea-level studies.	207

Overview

General

The main aim of this thesis has been to develop and extend the palaeoenvironmental application of biomarkers (principally long-chain alkenones) and other components of sedimentary organic matter in the N.E. Atlantic region. In pursuing this aim we have focused on two study areas:

- The polar to sub-polar region of the Nordic Seas.
- The coastal environments of N.W. Scotland.

In both study areas the research can be divided into two general goals:

- Firstly, relating the distribution of biomarkers or organic matter parameters in the modern environment to controlling variables.
- Secondly, based on the above relationship, relating the distribution of biomarkers or organic matter parameters in sediments to past environmental changes.

The Nordic Seas region is important in the broad context of understanding past changes in the ocean-climate system and predicting future responses, of that system, to perturbations (especially anthropogenic forcing). As such it has been the focus of intensive palaeoceanographic research over the past three decades. In the last fifteen years some of that research has included papers on the calibration and application of the alkenone indices U_{37}^K and $U_{37}'^K$. This has been part of the process of rigorously testing alkenones, as proxies for reconstructing past absolute SSTs in the global oceans. In chapters 3 and 4 we built on the previous body of biomarker work in the region. In doing so we attempted to clarify and delimit the reliable application of alkenones in the Nordic Seas and to extend the application of alkenone biomarkers to sub-polar, high sedimentation rate sites in the Icelandic Shelf.

Prior to this thesis the utility of N.W. Scottish isolation basins in investigations of RSL change had been demonstrated by investigations which relied on lithostratigraphy and microfossil faunal assemblages to determine the palaeoenvironmental record. The organic components of isolation basin sediments had not been exploited as alternative proxies to constrain past RSL changes. In chapter 5 we explored the distributions of a number of lipid biomarkers and bulk organic parameters in modern and fossil coastal sediments to determine their potential application to RSL change studies. In doing so

we demonstrated the high potential of alkenones (abundance and within-class-distributions) for further use in RSL studies.

A major difference between the two study areas of the Nordic Seas and N.W. Scotland was the volume of previously published biomarker work. In the Nordic Seas there has been a number of studies which have employed biomarkers for palaeoclimatic reconstructions (e.g. Calvo et al., 2002; Flügge, 1997; Higginson, 1999; Rimbu et al., 2003; Rosell-Melé, 1994; Rosell-Melé, 1998a; Rosell-Melé et al., 1993; Rosell-Melé and Comes, 1999; Rosell-Melé et al., 1995; Rosell-Melé et al., 1997; Rosell-Melé et al., 1998; Sicre et al., 2002; Thomsen et al., 1998) and there has been a huge number of papers using alkenones in other parts of the global deep oceans. Whereas, there have been no previous attempts to apply biomarkers to reconstruct RSL change in isolation basins and only a few reports of alkenones in coastal or brackish environments (Conte et al., 1994; Ficken, 1994; Schulz et al., 2000) The unifying theme across all study areas is that we have explored new ground for palaeoenvironmental work in the marginal environments of the N.E. Atlantic. Where “marginal” refers to both the physical margins (coastal, continental shelf) and the climatic margins (low temperature, polar waters).

Chapter 3: Distribution of long-chain alkenones in the Nordic Seas

In chapter 3 the overall aim was to extend the application of alkenone proxies for palaeoceanographic studies in sub-polar to polar regions. We covered new ground by exploring the distribution of alkenones in the surface waters POM of the Nordic Seas with an unprecedented spatial coverage and concentration of samples. This complimented earlier work, which had surveyed alkenone distributions in the surface sediments of the Nordic Seas (Rosell-Melé, 1998a; Rosell-Melé et al., 1993; Rosell-Melé et al., 1995). Samples from across the spectrum of property (SSS, SST) gradients (i.e. covering all the characteristic water masses) of the Nordic seas were obtained. We were particularly interested in assessing the relationship of $\%C_{37:4}$ to sea surface variables, as previous work had suggested that $\%C_{37:4}$ in the Nordic Seas and North Atlantic may have potential as a palaeo-salinity proxy (Rosell-Melé, 1998b; Rosell-Melé et al., 2002).

The most remarkable discovery was alkenone distributions characterized by extremely high $\%C_{37:4}$ values (up to 77%), measured for the first time in polar waters (salinity

<34.4 psu) under conditions of up to 80% sea ice cover. Values of $\%C_{37:4}$ across the Nordic Seas showed a strong association with water mass type. The $\%C_{37:4}$ data was linearly correlated to both SST ($R^2 = 0.75$) and SSS ($R^2 = 0.79$). The data-set showed a stronger correlation to SSS ($R^2 = 0.72$) than to SST ($R^2 = 0.5$), when combined with previous sea surface POM data from the Nordic Seas and North Atlantic (Sicre et al., 2002). However, the scatter in the relationship did not confirm the use of $\%C_{37:4}$ as a palaeo-SSS proxy.

Comparisons of $\%C_{37:4}$ measured in sea surface POM with the data from surficial sediments of the Nordic Seas revealed large differences in the slope of the relationship of $\%C_{37:4}$ versus SST and SSS. The magnitude of the difference could not be explained by preferential degradation of the $C_{37:4}$ alkenone. Therefore we suggested that the $\%C_{37:4}$ signal in sea surface POM is vulnerable to dilution in the underlying sea surface sediments by resuspension and mixing with advected allochthonous matter - containing relatively higher abundances of $C_{37:3}$ and $C_{37:2}$ alkenones. This was supported by previous observations of resuspension and biasing of coccolithophore assemblages – particularly in the Greenland Sea (Baumann et al., 2000).

Comparison of alkenone distributions with coccolithophore assemblage data collected on JR51 and with published coccolithophore data suggested that *E. huxleyi* could not be ruled out as the producer of the polar alkenones (characterised by the unusually high $\%C_{37:4}$ values). An *E. huxleyi* source is supported by the C_{38} alkenone within-class distributions.

Values of U_{37}^K from the new Nordic Seas POM data shows no correlation with SST below 10°C. In contrast to $U_{37}^{K'}$, a stronger linear correlation exists between U_{37}^K and SST ($R^2 = 0.69$). Supporting previous suggestions that, overall, U_{37}^K may be a more appropriate SST index for the Nordic Seas than $U_{37}^{K'}$ (Rosell-Melé et al., 1995). The new $U_{37}^{K'}$ and U_{37}^K data highlights major differences between distributions of U_{37}^K and $U_{37}^{K'}$ in the water-column POM and surficial sediments of the Nordic Seas for both indices. A detailed examination of the geographic locations that are responsible for the scatter in the $U_{37}^{K'}$ versus SST relationship in surficial sediments of the Nordic Seas, was made. The results showed a clear geographical division suggesting that East Greenland Shelf, the Greenland Basin, Mohns ridge, northern Iceland Plateau and upper Bear

Island Fan are associated with the scatter, while samples from the northern Atlantic, Icelandic Shelf, Norwegian basin, Lofoten Basin and Barents Seas yield U_{37}^K values that fall within the expected range, based on a global core top calibration (Muller et al., 1998). This suggests that alkenone data from the latter sites may yield more reliable palaeoceanographic reconstructions of SST.

Comparison of alkenone distributions with dinocyst proxies for SSS, SST and sea ice cover in a late Holocene core from the Barents Sea showed that the $\%C_{37:4}$ record responded to major changes in SSS/sea ice cover. This supported the use of $\%C_{37:4}$ as a general marker for the influence of arctic/polar water in palaeoceanographic reconstructions. However, the use of $\%C_{37:4}$ to derive absolute values for a particular parameter was not confirmed.

Chapter 4: Post-Glacial palaeoceanography of the Icelandic shelf.

In chapter 4 we successfully used alkenone indices to reconstruct palaeoceanographic conditions on the Icelandic shelf for the post-Glacial period (0 -15 kyr BP). No previous work had applied alkenones to the Icelandic shelf, or to comparable sub-polar, high sedimentation rate, continental shelf sites. Major changes in the alkenone distributions were observed in the cores during the post-Glacial and Holocene periods. In the post-Glacial (when alkenones were detectable) relative changes in $\%C_{37:4}$ and U_{37}^K indicated relative changes in the influence of cold/low salinity waters versus warmer Atlantic waters. Accordingly, major changes in the $\%C_{37:4}$ and U_{37}^K distributions coincided with the major transitions in the GRIP Late-Glacial ice-core event stratigraphy. There was good agreement between the interpretation of the alkenone record from the post-Glacial and records of ice-front fluctuations from S.W. Iceland.

The records from the N. Icelandic shelf displayed a general trend of cooling through the Holocene. This data supported published reports of negative Holocene SST trends in the northern North Atlantic (Marchal et al., 2002; Rimbu et al., 2003). This suggests a negative trend (weakening) in the AO/NAO index during the Holocene, when contrasted with records of positive trends in eastern Mediterranean and Middle East, (Rimbu et al., 2003)

Holocene SST oscillations in JR51-GC35 were of large amplitude; with millennial scale oscillations characterised by deviations of $\sim 2^{\circ}\text{C}$. The oscillations had a distinct cyclicity on a millennial scale. The most prominent U_{37}^{K} -SST maxima occurred in the early Holocene between 9 – 10 kyr BP and in the mid-Holocene between 5 – 5.5 kyr BP. Also, distinguishable in the record were events coeval with the Little Ice Age and the Medieval Warm Period.

The millennial scale oscillations in the JR51-GC35 U_{37}^{K} -SST record broadly correlated with a number of marine records of Holocene climatic events from the Northern Iceland shelf and North Atlantic deep-sea cores. However, the closest correlation was achieved with the IRD record in JM96-1207 from the East Greenland shelf. It is likely that this is due to their positions relatively close to the polar front and IRD sources; locations which are sensitive to climate change. The U_{37}^{K} -SST record from JR51-GC35 also showed close agreement with records of Holocene glacial advances in northern Iceland.

A comparison of the U_{37}^{K} -SST records from JR51-GC35 and a core from the eastern Nordic Seas (MD952011) shows that there are some general similarities. However, the records suggest some differences (superimposed on the general trend) of millennial scale climate events between the eastern and western Nordic Seas especially at 3.2, 5, 6.5 and 9 kyr BP. The most prominent example is the timing of the mid-Holocene Thermal Optimum (TO). In MD952011 the mid-Holocene TO is a distinct phase between 6 – 8 kyr BP, (with the constantly highest SSTs at 6 -7 kyr BP). However, in the records from the eastern Nordic Seas, during the period 6 -7 kyr BP, there is a trough in the U_{37}^{K} -SSTs on the N. Icelandic Shelf, an increase in IRD events on the East Greenland shelf (core JM96-1207) and glacier expansion in northern Iceland. Therefore the data from this thesis suggest that the Holocene history of the surface ocean circulation within the Nordic Seas was more complex than previously suggested, possibly characterised by differential responses of the Irminger and Norwegian Currents.

Chapter 5: Biomarkers and organic matter in coastal environments of N.W. Scotland: Assessment of potential application to sea level studies.

In chapter 5 the overall aim was to assess the potential application of certain sedimentary components of organic matter (i.e. lipid compounds such as alkenones, *n*-

alkanes and chlorophyll derivatives), and bulk organic parameters to RSL change studies in isolation basin in N.W. Scotland. This was the first study to investigate alkenone distributions in such a diverse range of modern shallow coastal environments. Accordingly, no previous study has reported such diversity of alkenone abundance and within-class-distributions within a relatively small geographical area.

A logit regression analysis of all the sediment samples was employed to find which of the biomarker or bulk organic measurements could reliably characterise the sediment samples in terms of a marine/brackish or isolated/lacustrine origin. The results suggested an excellent efficiency for the alkenone index $\%C_{37:4}$ at predicting the depositional origin of the sediments, with $\%AA$ and alkenone concentrations also showing a statistical relationship. Other biomarkers and organic geochemical parameters were less consistent in their response to sea-level change and therefore have less utility for sea-level studies.

These results suggested that alkenones may be used as an indicator of sea-level in fossil isolation basins. The isolation contact could be identified by a sharp change in alkenone concentrations accompanied by a change in $\%C_{37:4}$ through a threshold value of $\sim 15\%$. More work is necessary before an indicative meaning can be assigned to alkenones. Observation from the modern basins suggested that the most appropriate indicative range to ascribe to an isolation contact - identified by a change in alkenone abundances and associated within-class-distributions - would be between MHWST and HAT.

Future work

There are several lines of research that follow logically from the results of this thesis:

Chapter 3: Distribution of long-chain alkenones in the Nordic Seas.

The biological precursor of the polar water alkenones, characterized by unusually high $\%C_{37:4}$ values, should be isolated. Data from this thesis shows that *E. huxleyi* can not be ruled out, despite being relatively rare in coccolithophore surveys of polar waters. Culture experiments on N. Atlantic strains of *E. huxleyi* have been conducted in the past, at temperatures of $>5^{\circ}\text{C}$ and with set salinities at $\sim 35^{\circ}\text{C}$. Further studies should be conducted to see if high $\%C_{37:4}$ values can be induced in *E. huxleyi* populations subjected to polar water type conditions ($<5^{\circ}\text{C}$, $<34.4\text{psu}$).

Populations of the lightly calcified coccolithophore species that have recently been reported as occurring in polar waters - need to be cultured and analysed as a potential source for alkenones (Marchant and Thomsen, 1994). In the past little attention has been paid to these species as – unlike the heavily calcified *E. huxleyi* and *C. pelagicus* - they are not well preserved in sediments and are difficult to identify by microscopy. Further POM filter samples, collected from polar waters, should be obtained for alkenone analysis. A portion of the seawater should be retained for a detailed survey of the phytoplankton. This should include naked and lightly calcified haptophytes.

Once the biological source of the polar water alkenones has been determined the dominant variable/s which control $\%C_{37.4}$ (e.g. SST, SSS, nutrients, light) needs to be determined through culture experiments. This will conclusively determine the usefulness of the information contained in $\%C_{37.4}$ values for palaeoenvironmental reconstructions in subpolar to polar sediments.

Chapter 4: Post-Glacial palaeoceanography of the Icelandic shelf.

Some sections of the core JR51-GC35 in the early half of the Holocene, did not yield alkenones at detectable quantities, or the alkenones were too weak for integration. U_{37}^K -SST records for these sections will be completed by extraction and analysis of larger volume samples.

Detailed records of sediment physical parameters in JR51-GC35 (e.g. sediment particle size, MS) will be produced in collaboration with INSTAAR, so that the U_{37}^K -SST record can be compared with a history of IRD events in the same core.

The data from JR51-GC35 compared with records from the eastern Nordic Seas suggest that the Holocene history of the surface ocean circulation within the Nordic Seas was more complex than previously suggested, possibly characterised by differential responses of the Irminger and Norwegian Currents. Future collaboration with physical oceanographers and modellers may clarify the mechanisms for such behaviour.

Chapter 5: Biomarkers and organic matter in coastal environments of N.W. Scotland: Assessment of potential application to sea-level studies.

Chapter 6 demonstrated the potential of alkenones for reconstruction of past sea-level changes in N.W. Scotland. In order for this proxy to be adopted by the palaeo-sea-level community a larger scale study of modern basins is needed. This is necessary before an indicative meaning can be confidently assigned to specific changes in the alkenone distributions.

Also detailed phytoplankton surveys need to be conducted in parallel with collection of samples for alkenone analysis: in order to determine the contribution of alkenones (at different stages of isolation) from *E. huxleyi* or from other haptophytes known to produce alkenones in coastal areas such as *Isochrysis galbana*.

If specific organic compound classes can be validated as reliable sea-level indicators then the way is open for the application of compound-specific radiocarbon analysis in isolation basins, a development which may improve accuracy in the dating of sea-level index points.

- Calvo, E., Grimalt, J., and Jansen, E. (2002). High resolution $U^{K_{37}}$ sea surface temperature reconstruction in the Norwegian Sea during the Holocene. *Quaternary Science Reviews* **21**, 1385-1394.
- Conte, M. H., Thompson, A., and Eglinton, G. (1994). Primary production of lipid biomarker compounds by *Emiliania huxleyi*. Results from an experimental mesocosm study in fjords of southwestern Norway. *Sarsia* **79**, 319-331.
- Ficken, K. J. (1994). "Lipid and sulphur geochemistry of recent sediments from oxic and anoxic environments." University of Newcastle upon Tyne.
- Flügge, A. (1997). "Jahreszeitliche Variabilität von ungesättigten C 37 Methylketonen (Alkenone) in Sinkstoffallenmaterial der Norwegischen See und deren Abbildung in Oberflächensedimenten." Unpublished Ph.D. thesis, Univ. zu Keil.
- Higginson, M. (1999). "Chlorin Pigment Stratigraphy as a New and Rapid Palaeoceanographic proxy in the Quaternary." University of Bristol.
- Marchal, O., Cacho, I., Stocker, T. F., Grimalt, J. O., Calvo, E., Martrat, B., Shackleton, N., Vautravers, M., Cortijo, E., and van Kreveld, S. (2002). Apparent long-term cooling of the sea surface in the northeast Atlantic and Mediterranean during the Holocene. *Quaternary Science Reviews* **21**, 455-483.
- Marchant, H. J., and Thomsen, H. A. (1994). Haptophytes in polar waters. In "The Haptophyte Algae." (J. C. Green, and B. S. C. Leadbeater, Eds.), pp. 209-228. A Systematics Association Special Volume, Clarendon Press, Oxford.
- Muller, P. J., Kirst, G., Ruhland, G., von Storch, I., and Rosell-Mele, A. (1998). Calibration of the alkenone paleotemperature index $U_{37}^{K'}$ based on core-tops from the eastern South Atlantic and the global ocean (60 degrees N-60 degrees S). *Geochimica Et Cosmochimica Acta* **62**, 1757-1772.
- Rimbu, N., Lohmann, G., Kim, J. H., Arz, H. W., and Schneider, R. (2003). Arctic/North Atlantic Oscillation signature in Holocene sea surface temperature trends as obtained from alkenone data. *Geophysical Research Letters* **30**, art. no.-1280.
- Rosell-Melé, A. (1994). "Long-chain alkenones, Alkyl Alkenoates and Total Pigment Abundances as Climatic Proxy-Indicators in the Northeastern Atlantic." Unpublished Ph.D. thesis, University of Bristol.
- Rosell-Melé, A. (1998a). Interhemispheric appraisal of the value of alkenone indices as temperature and salinity proxies in high-latitude locations. *Paleoceanography* **13**, 694-703.
- Rosell-Melé, A. (1998b). Project takes a new look at past sea surface temperatures. *EOS* **79**, 1-2.
- Rosell-Melé, A., Carter, J., and Eglinton, G. (1993). Distributions of long-chain alkenones and alkyl alkenoates in marine surface sediments from the North East Atlantic. *22* **3-5**, 501-509.
- Rosell-Melé, A., and Comes, P. (1999). Evidence for a Warm Last Glacial Maximum in the Nordic Seas of an Example of Shortcomings in $U_{37}^{K'}$ and $U_{37}^{K'}$ to Estimate Low Sea Surface Temperature? *Paleoceanography* **14**, 770-776.
- Rosell-Melé, A., Eglinton, G., Pflaumann, U., and Sarnthein, M. (1995). Atlantic core-top calibration of the $U_{37}^{K'}$ index as a sea-surface palaeotemperature indicator. *Geochimica et Cosmochimica Acta* **59**, 3099-3107.
- Rosell-Melé, A., Jansen, E., and Weinelt, M. (2002). Appraisal of a molecular approach to infer variations in surface ocean freshwater inputs into the North Atlantic during the last glacial. *Global and Planetary Change* **34**, 143-152.
- Rosell-Melé, A., Maslin, M. A., Maxwell, J. R., and Schaeffer, P. (1997). Biomarker evidence for "Heinrich" events. *Geochimica et Cosmochimica Acta* **61**, 1671-1678.

Chapter 6: Overview and Future Work

- Rosell-Melé, A., Weinelt, M., Sarnthein, M., Koç, N., and Jansen, E. (1998). Variability of the Arctic front during the last climatic cycle: application of a novel molecular proxy. *Terra Nova* **10**, 86-89.
- Schulz, H. M., Schoner, A., and Ermeis, K. C. (2000). Long-chain alkenone patterns in the Baltic Sea - an ocean- freshwater transition. *Geochimica Et Cosmochimica Acta* **64**, 469-477.
- Sicre, M.-A., Bard, E., Ezat, U., and Rostek, F. (2002). Alkenone distributions in the North Atlantic and Nordic sea surface waters. *Geochemistry, Geophysics, Geosystems* **3**, 10.1029/2001GC000159.
- Thomsen, C., Schulz-Bull, D. E., Petrick, G., and Duinker, J. C. (1998). Seasonal variability of the long-chain alkenone flux and the effect on the U37k'-index in the Norwegian Sea. *Organic Geochemistry* **28**, 311-323.

Contents

Figures	1-101
Appendix I	
Appendix II	

List of Figures

<u>Figure</u>	<u>Page</u>
Figure 1.1: Structures and shorthand notation of the alkenones and alkyl alkenoates discussed in the text.	1
Figure 1.2: Structures of chlorophyll <i>a</i> and common derivatives (chlorins) with diagenetic pathways.	2
Figure 1.3: Relationship between mean %TOC content and modern sedimentary environments.	3
Figure 2.1: Analytical scheme used in this thesis for the study of lipids, pigments and C_{org}/N in marine and coastal sediment and filter sample.	4
Figure 2.2: Representative GC-FID trace of the eluting region of <i>n</i> -alkanes, alkenones and alkyl alkenoates for a North Atlantic open ocean sediment samples.	5
Figure 2.3: Representative GC-FID trace of the eluting region of <i>n</i> -alkanes, alkenones and alkyl alkenoates for a NW Scottish brackish, coastal sediment sample.	6
Figure 2.4: Changes in the a) $U^{K_{37}}$ values (squares) and b) coefficient of variation (C.V.) (circles) when standards of synthetic alkenones with an expected $U^{K_{37}}$ of 0.19 are injected at different concentrations into the GC-FID.	7
Figure 2.5: Ammonia chemical ionization mass chromatograms of the total ion current and pseudo-molecular ions of the alkenones and alkyl alkenoates quantified in a lipid extract from a sediment core extracted from the Icelandic continental shelf.	8
Figure 2.6: Linearity of the GC-CI-MS method to quantify the $C_{37:3}$ and $C_{37:2}$ alkenones and changes in $U^{K_{37}}$ values.	9
Figure 2.7: The $U^{K_{37}}$ values of marine sea-surface filter extracts, injected into the GC-FID, plotted against the $U^{K_{37}}$ values of the same samples injected in the GC-CI-MS.	10
Figure 2.8: The $\%C_{37:4}$ values of marine sea-surface filter extracts, injected into the GC-FID, plotted against the $\%C_{37:4}$ values of the same samples injected in the GC-CI-MS.	10
Figure 3.1: Main features of the surface to near-surface circulation in the eastern North Atlantic and Nordic Seas.	11
Figure 3.2: Main areas of densification in the Nordic Seas, paths of deep water flow to the Greenland-Scotland Ridge and overflow to the eastern North Atlantic.	12
Figure 3.3: Main frontal systems of the Nordic Seas.	13

Figure 3.4: JR44 Cruise track (a) and location (b) of sampling stations for filter samples.	14
Figure 3.5: JR51 Cruise track (a) and location (b) of sampling stations for filter samples.	15
Figure 3.6: Oceanographic properties measured <i>in situ</i> during cruise JR44.	16
Figure 3.7: Oceanographic properties measured <i>in situ</i> during cruise JR51.	17
Figure 3.8: Chlorophyll <i>a</i> measurements for cruise JR44.	18
Figure 3.9: Chlorophyll <i>a</i> measurements for cruise JR51.	19
Figure 3.10: Geographic distribution of Σ LCK (ng/l) in the surface waters of the Nordic Seas.	20
Figure 3.11: Distributions of Σ LCK (ng/l) in the surface waters of the Nordic Seas by water mass.	21
Figure 3.12: Distributions of Σ LCK (ng/l) vs fluorescence.	22
Figure 3.13: A) Geographic distribution of $\%C_{37:4}$ in the surface waters of the Nordic Seas, B) representative GC traces of alkenone patterns from different water masses.	23
Figure 3.14: Distributions of $\%C_{37:4}$ in the surface waters of the Nordic Seas by water mass.	24
Figure 3.15: Distributions of $\%C_{37:4}$ vs a) SST ($^{\circ}C$) and b) SSS (psu).	25
Figure 3.16: Geographic distribution of $\%C_{37:4}$ samples from the water column and surface sediments of the Nordic Seas and northern north Atlantic.	26
Figure 3.17: Distributions of $\%C_{37:4}$ in the water column and surface sediments of the Nordic Seas and northern north Atlantic.	27
Figure 3.18: Distributions of $\%C_{37:4}$ in the global water column.	28
Figure 3.19: Distributions of alkenones in boxcores from the Nordic Seas.	29
Figure 3.20: Distributions of $U^{K_{37}}$ in the surface waters of the Nordic Seas by water mass.	30
Figure 3.21: Distributions of $U^{K_{37}'}$ in the surface waters of the Nordic Seas by water mass.	31
Figure 3.22: Distributions of A) $U^{K_{37}'}$ and B) $U^{K_{37}}$ vs SST.	32
Figure 3.23: Distributions of A) $U^{K_{37}'}$ and B) $U^{K_{37}}$ measured on mixed layer POM vs water temperature.	33
Figure 3.24: Nordic Seas distributions of A) $U^{K_{37}'}$ and B) $U^{K_{37}}$ measured on mixed layer POM and surface sediments vs water temperature.	34
Figure 3.25: Identification (a) and geographic (b) distribution of core-top Nordic Seas samples that create scatter in the $U^{K_{37}'}$ index – relative to Muller <i>et al's</i> (1998) core-top calibration	35
Figure 3.26: a) The $\%C_{37:4}$ index plotted against $\%C_{38:4}$ b) the $U^{K_{37}}$ index plotted against $U^{K_{38}}$ for Nordic Seas sea surface POM samples from this thesis.	36

Figure 3.27: Distributions of $\Sigma C_{37}/\Sigma C_{38}$ vs a) SST ($^{\circ}C$) and b) SSS (psu).	37
Figure 3.28: Distributions of C_{38Et}/Me vs a) SST ($^{\circ}C$) and b) SSS (psu).	38
Figure 3.29: $U^{K_{38Et}}$ vs $U^{K_{38Me}}$ in filter samples from the Nordic Seas.	39
Figure 3.30: Location of core PL-96-126, major currents systems and sea-ice averages for the Barents Sea.	40
Figure 3.31: Comparison of alkenone indices with reconstruction of sea surface conditions from dinocyst assemblages in Core PL-96-126 against depth in core.	41
Figure 3.32: $\%C_{37:4}$ vs. 50% Sea ice cover (a) and 20% sea ice cover (b).	42
Figure 4.1: Location of core sites and regional bathymetry.	43
Figure 4.2: Schematic description of the environment of the N. Iceland shelf showing the major controlling variations in sediment, isotope and biota on the N. Iceland shelf (adapted from Andrews and Giraudeau, 2003).	44
Figure 4.3: Calibrated radiocarbon dates plotted against depth, lithofacies log and selected physical properties in core B997-350PC.	45
Figure 4.4: Calibrated radiocarbon dates plotted against depth, lithofacies log and selected physical properties in core B997-325GC/PC.	46
Figure 4.5: Calibrated radiocarbon dates plotted against depth, lithofacies log and selected physical properties in core JR51-GC35.	47
Figure 4.6: Bi-plots of major oxide measurements (%) made on basaltic tephra from B9-97-325-PC2 210cm and previously identified samples of Saksunarvatn tephra.	48
Figure 4.7: Bi-plots of major oxide measurements (%) made on basaltic tephra from JR51-GC35 420 cm and previously identified samples of Saksunarvatn tephra.	49
Figure 4.8: Biomarker records plotted versus calendar age for Icelandic shelf cores.	50
Figure 4.9: Comparison of UK37-SSTs from B997-350 & JR51-GC51 with Late-Glacial and Holocene palaeo-environmental records from North Atlantic and Greenland.	51
Figure 4.10: Comparison of alkenone-SST Holocene trend lines from cores B997-325GC/PC and JR51-GC35 (graphs a,b) with data from Rimbu et al. (2003) (graphs c to m).	52
Figure 4.11: Comparison of Holocene UK37-SST records from the north Icelandic Shelf (JR51-GC35) and the Norwegian Sea (MD952011).	53
Figure 5.1: Schematic representation of an isolation basin during a fall in relative sea-level (adapted from Shennan et al., 1996).	54
Figure 5.2: Conceptual model of biological assemblage change during the isolation process.	55
Figure 5.3: Schematic representation of the hydrological and depositional conditions in an isolation basin.	56
Figure 5.4: Schematic representation of the organic matter cycle in an isolation basin.	57

Figure 5.5: Four isolation contacts.	58
Figure 5.6: Location map of the field study region.	59
Figure 5.7: Loch nan Ceall and Rumach site map.	60
Figure 5.8: Rumach Tidal Pond site map.	61
Figure 5.9: Craiglin site map.	62
Figure 5.10: Kintail site map.	63
Figure 5.11: Coigach site map.	63
Figure 5.12: Loch nan Ceall, salinity and temperature profiles.	64
Figure 5.13: Rumach Tidal Pond water column profiles at station 1 during Spring-tide HT & LT (11/8/02).	65
Figure 5.14: Rumach Tidal Pond depth averaged salinities vs time for spring-tide HT-LT (11/8/02).	66
Figure 5.15: Rumach Tidal Pond water column profiles at station 1 during mid-cycle tide tide LT & HT (7/8/02).	67
Figure 5.16: Rumach Tidal Pond depth averaged salinities vs time for mid-cycle tide LT-HT (7/8/02).	68
Figure 5.17: Rumach Tidal Pond water column profiles at station 1 during neap-tide HT & LT (4/8/02).	69
Figure 5.18: Rumach Tidal Pond depth averaged salinities vs time for neap-tide HT-LT (4/8/02).	70
Figure 5.19: Rumach Tidal Pond salinity profiles for station 6 (outside sill) at various stages of the tidal cycle.	71
Figure 5.20: Craiglin Lagoon water column profiles at station 2 during spring-tide LT & HT (11/8/02).	72
Figure 5.21: Craiglin Lagoon depth averaged salinities vs time for spring-tide LT-HT (11/8/02).	73
Figure 5.22: Craiglin Lagoon water column profiles at station 2 during spring-tide LT & HT (7/10/02).	74
Figure 5.23: Craiglin lagoon depth averaged salinities vs time for spring-tide LT-HT (7/10/02).	75
Figure 5.24: Particle size distributions in modern NW Scottish surface sediments.	76
Figure 5.25: Values of %TOC in modern NW Scottish surface sediments.	77
Figure 5.26: Values of C_{org}/N in modern NW Scottish surface sediments.	77

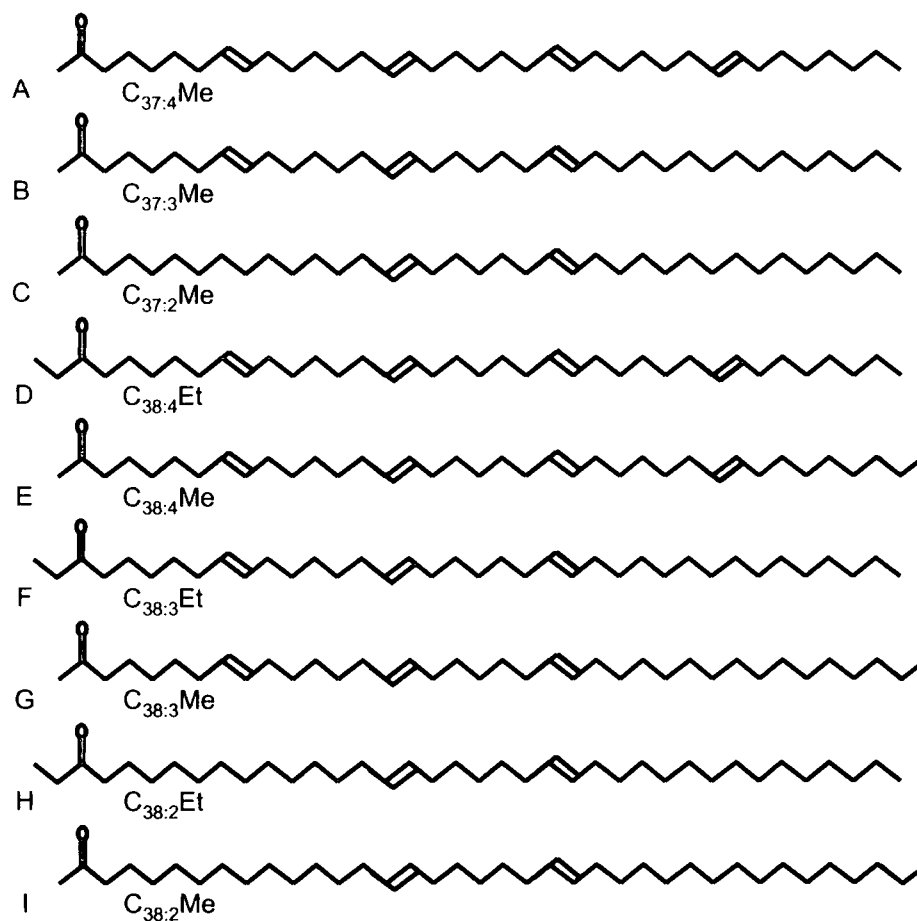
Figure 5.27: Values of absorbance at 410 λ by chlorin pigments in modern NW Scottish surface sediments.	78
Figure 5.28: Concentrations of n-Alkanes in modern NW Scottish surface sediments, normalised to a) grams dry sediments and b) grams organic carbon.	79
Figure 5.29: Values of n-Alkane CPI ₂₅₋₃₃ in modern NW Scottish surface sediments.	80
Figure 5.30: Values of n-Alkane Long/Short ratio in modern NW Scottish surface sediments.	80
Figure 5.31: Concentrations of C _{37:2} + C _{37:3} alkenones in modern NW Scottish surface sediments, normalised to a) grams dry sediments and b) grams organic carbon.	81
Figure 5.32: Concentrations of C _{37:2} + C _{37:3} alkenones in modern NW Scottish surface sediments normalised to grams organic carbon and % clay.	82
Figure 5.33: GC-CI-MS total ion chromatograms for modern NW Scottish surface sediments.	83
Figure 5.34: Values of %C _{37:4} in modern NW Scottish surface sediments.	84
Figure 5.35: Values of C ₃₈ Et/Me in modern NW Scottish surface sediments.	84
Figure 5.36: Values of $\Sigma C_{37}/\Sigma C_{38}$ in modern NW Scottish surface sediments.	85
Figure 5.37: Values of % Σ AA in modern NW Scottish surface sediments.	85
Figure 5.38: Values of U ^K ₃₇ ' and derived SST °C in modern NW Scottish surface sediments.	86
Figure 5.39: Trends in bulk organic properties, n-alkane and pigment distributions in N.W. Scottish surface sediments.	87
Figure 5.40: Trends in alkenone and alkenoate distributions in N.W. Scottish surface sediments.	88
Figure 5.41: Within basin variability – Rumach Tidal Pond.	89
Figure 5.42: Loch Dubh alkenone & microfossil summary.	90
Figure 5.43: Loch Dubh n-alkane, bulk organic geochemistry & microfossil summary.	91
Figure 5.44: Torr a'Bheithe alkenone & microfossil summary.	92
Figure 5.45: Torr a'Bheithe n-alkane, bulk organic geochemistry & microfossil summary.	93
Figure 5.46: Cnoc Pheadir alkenone & microfossil summary.	94
Figure 5.47: Cnoc Pheadir n-alkane, bulk organic geochemistry & microfossil summary.	95
Figure 5.48: Dubh Lochan alkenone & microfossil summary.	96
Figure 5.49: Dubh Lochan n-alkane, bulk organic geochemistry & microfossil summary.	97
Figure 5.50: Logit regressions for marine – non-marine categorisation of modern and fossil NW Scottish coastal sediments by a) %C _{37:4} , b) %SAA, c) C _{37:2} + C _{37:3} (ng/g Corg) and d) P410 [AU/g dry sed].	98

Figure 5.51: Logit regressions for marine – non-marine categorisation of modern and fossil NW Scottish coastal sediments by a) Sn-alkanes (ng/g dry sed.), b) SC37/SC38, c) Corg/N and d) C38Et/Me. _____ 99

Figure 5.52: Logit regressions for marine – non-marine categorisation of modern and fossil NW Scottish coastal sediments by a) UK37', b) CPI25-33, c) %TOC and d) Cmax. _____ 100

Figure 5.53: Logit regressions for marine – non-marine categorisation of modern and fossil NW Scottish coastal sediments by *n*-alkane Long/Short. _____ 101

Alkenones



Alkyl Alkenoates

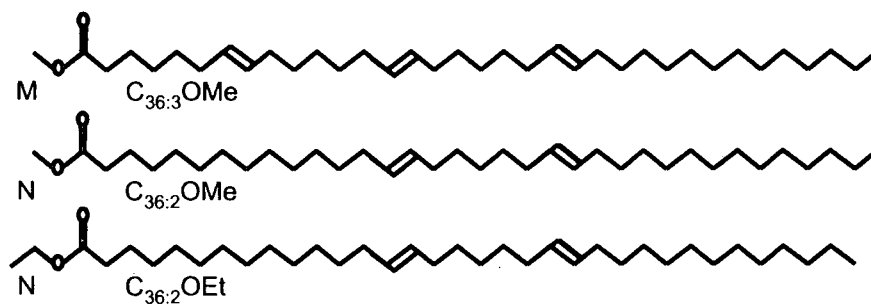


Figure 1.1: Structures and shorthand notation of the alkenones and alkyl alkenoates discussed in the text. The IUPAC names for the compounds are given in Table 1.1.

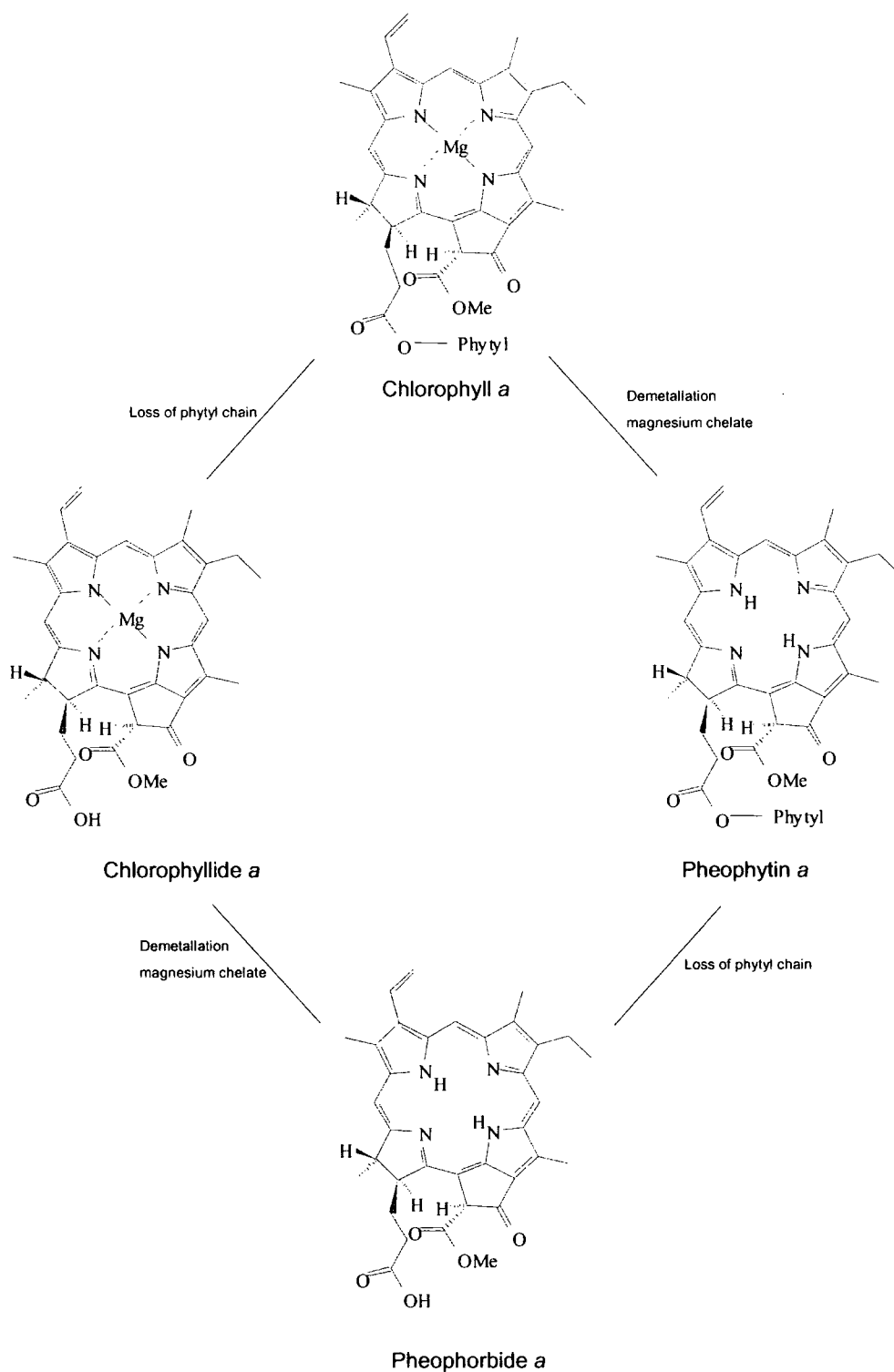


Figure 1.2: Structures of chlorophyll *a* and common derivatives (chlorins) with diagenetic pathways.

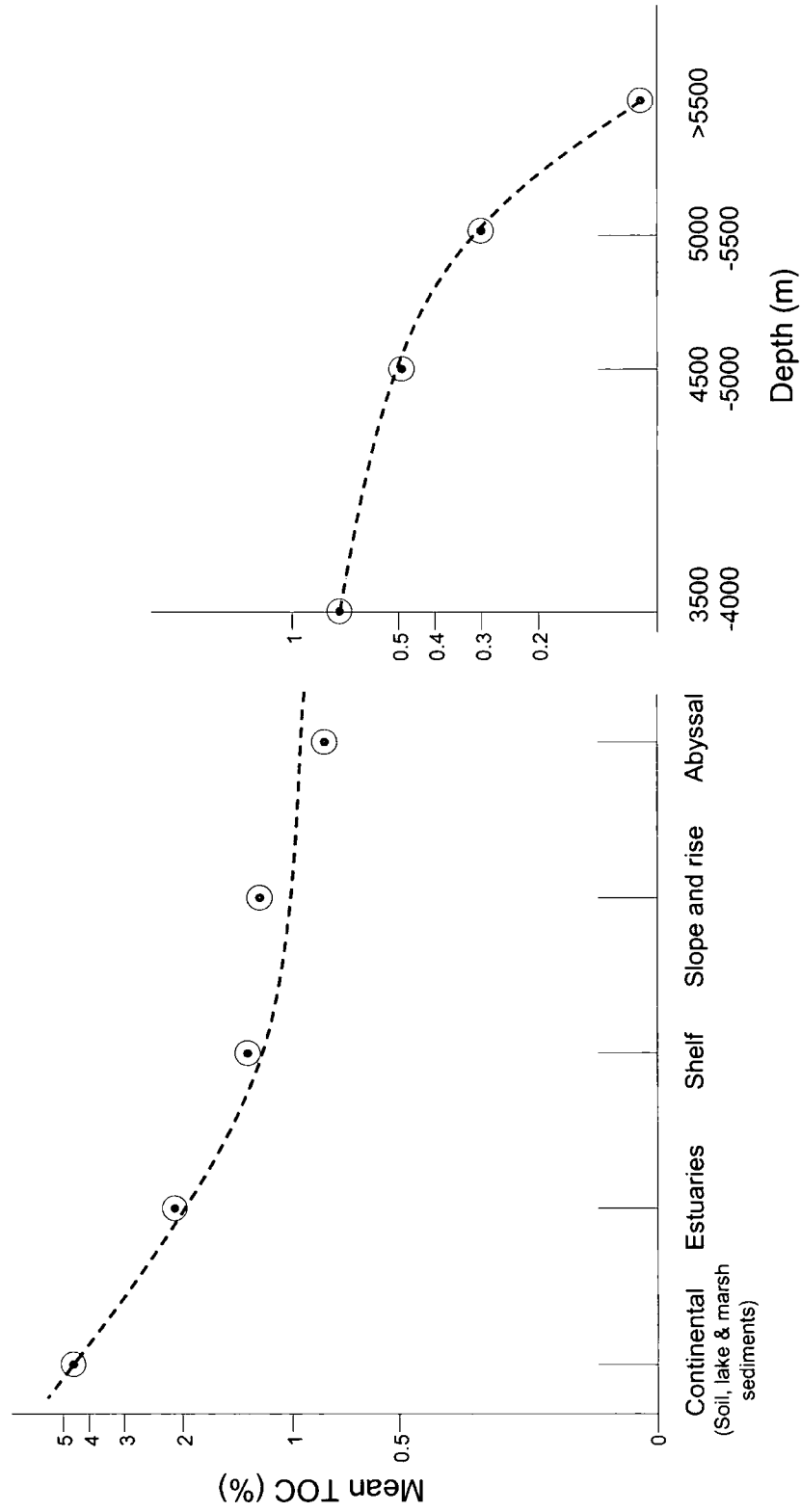


Figure 1.3: Relationship between mean %TOC content and modern sedimentary environments. Data from a composite transect from the continental shelf to the deep sea (after Vigneaux *et al.*, 1980 and Tyson, 1995).

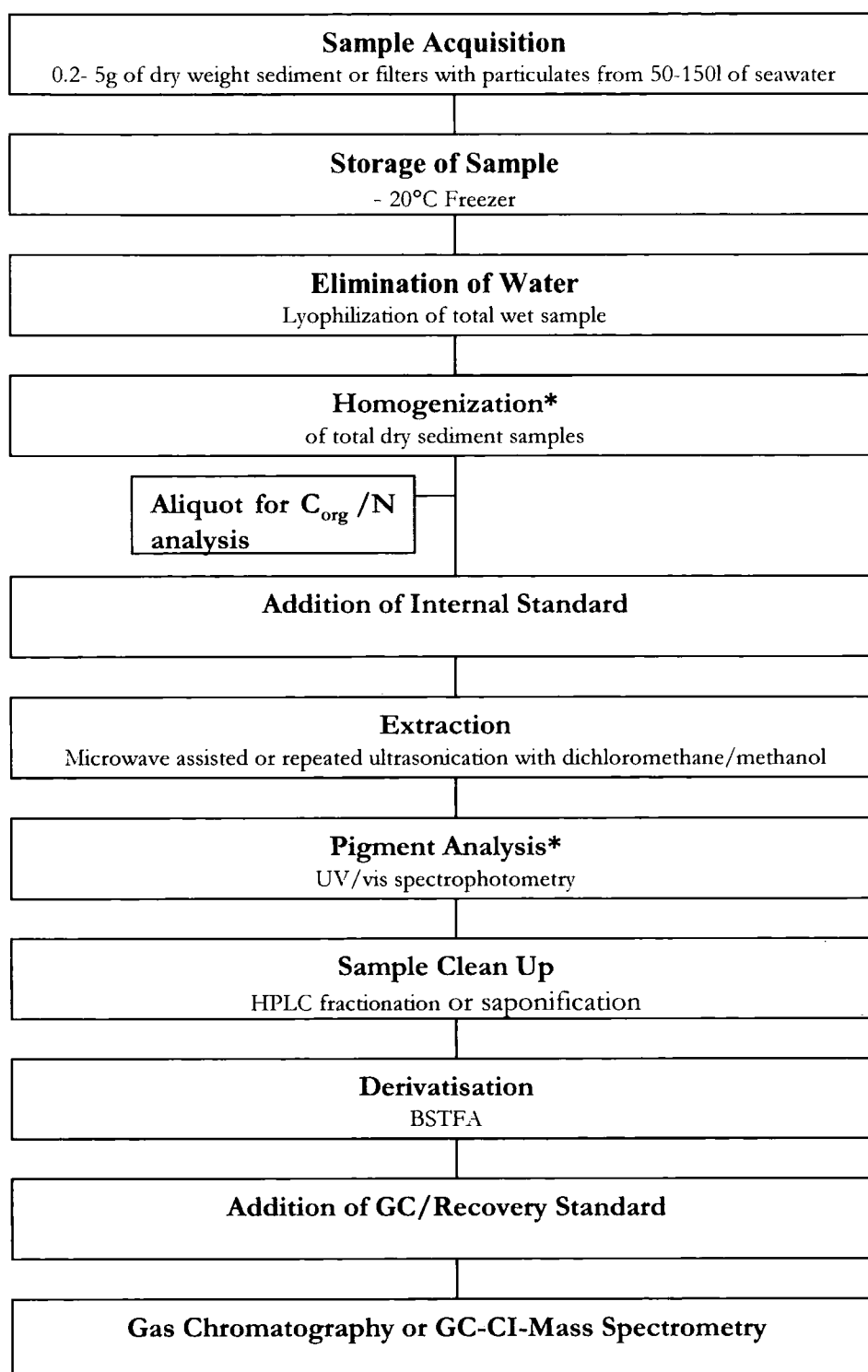


Figure 2.1: Analytical scheme used in this thesis for the study of lipids, pigments and C_{org}/N in marine and coastal sediment and filter samples. * Procedures not employed for filter samples – pigment analysis was not necessary for filters as measurement of sea surface fluorescence was made onboard ship during sample collection.

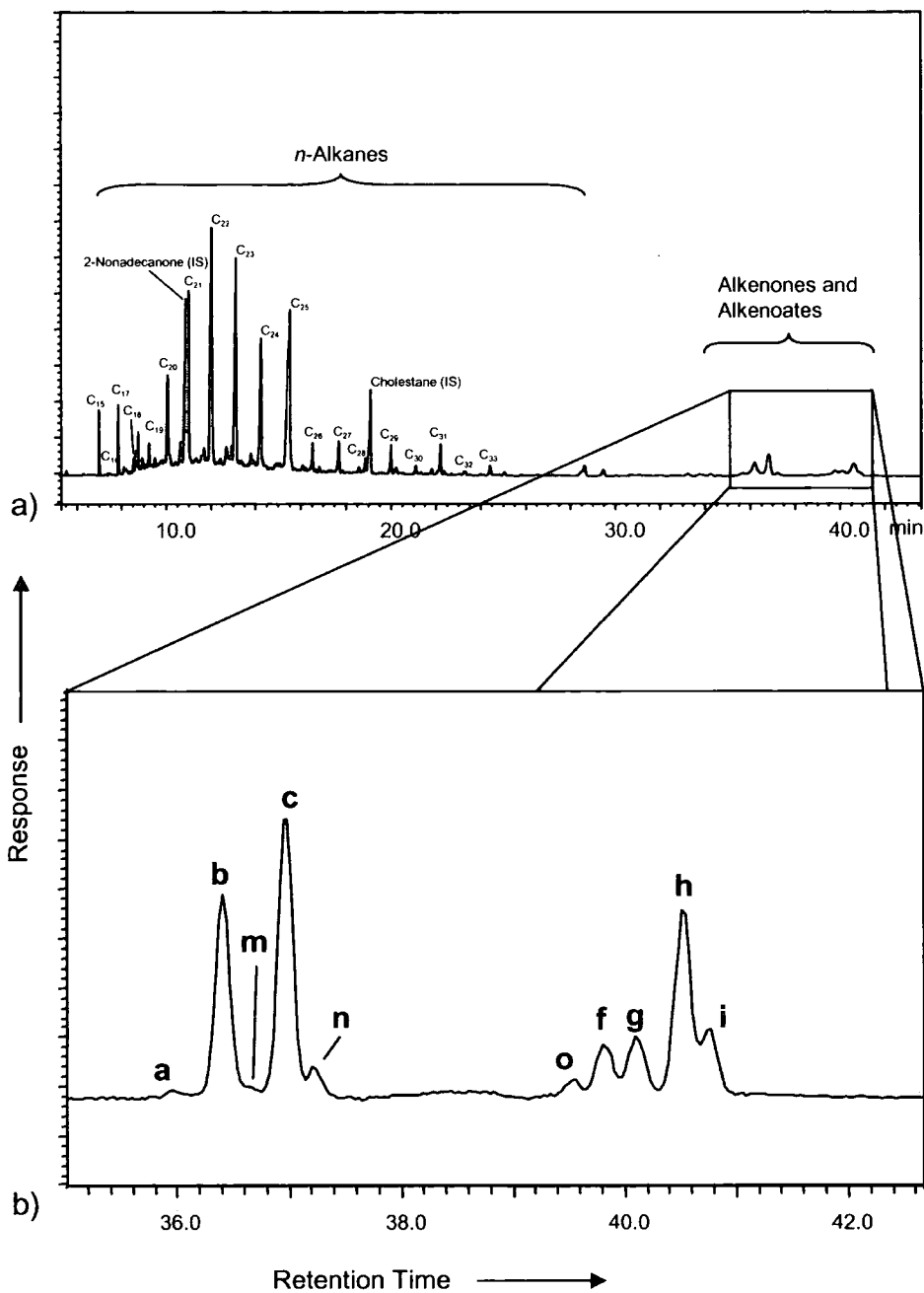


Figure 2.2: Representative GC-FID trace of the eluting region of *n*-alkanes, alkenones and alkyl alkenoates for a north Atlantic open ocean sediment sample. a) Identification of peak designations for *n*-alkanes and internal standards (IS) b) Expanded alkenone and alkyl alkenoate region. Refer to Table 1.1 (chapter 1) for identification of peak designations.

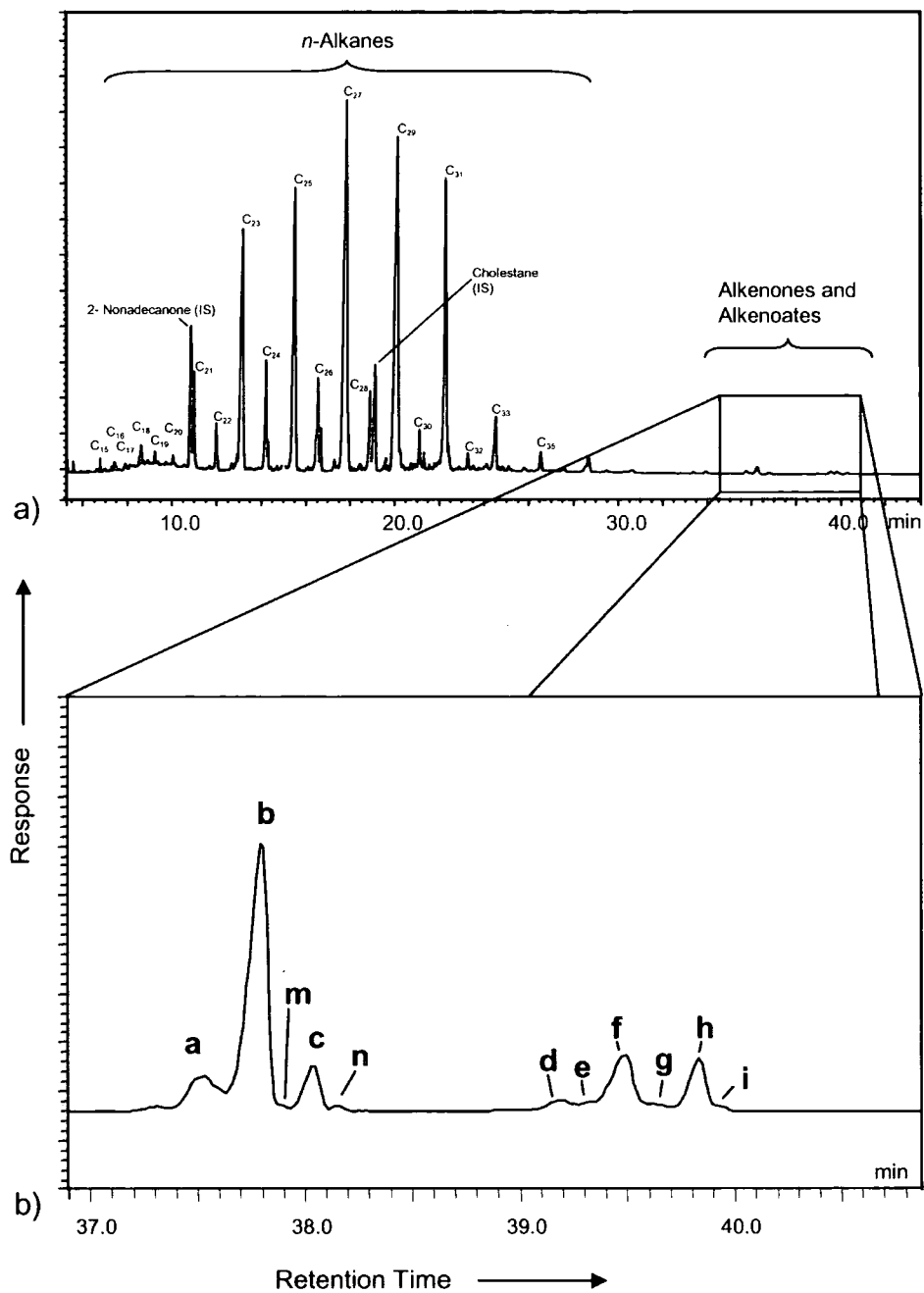


Figure 2.3: Representative GC-FID trace of the eluting region of *n*-alkanes, alkenones and alkyl alkenoates for a NW Scottish brackish, coastal sediment sample. a) Identification of peak designations for *n*-alkanes and internal standards (IS) b) Expanded alkenone and alkyl alkenoate region. Refer to Table 1.1 (chapter 1) for identification of peak designations.

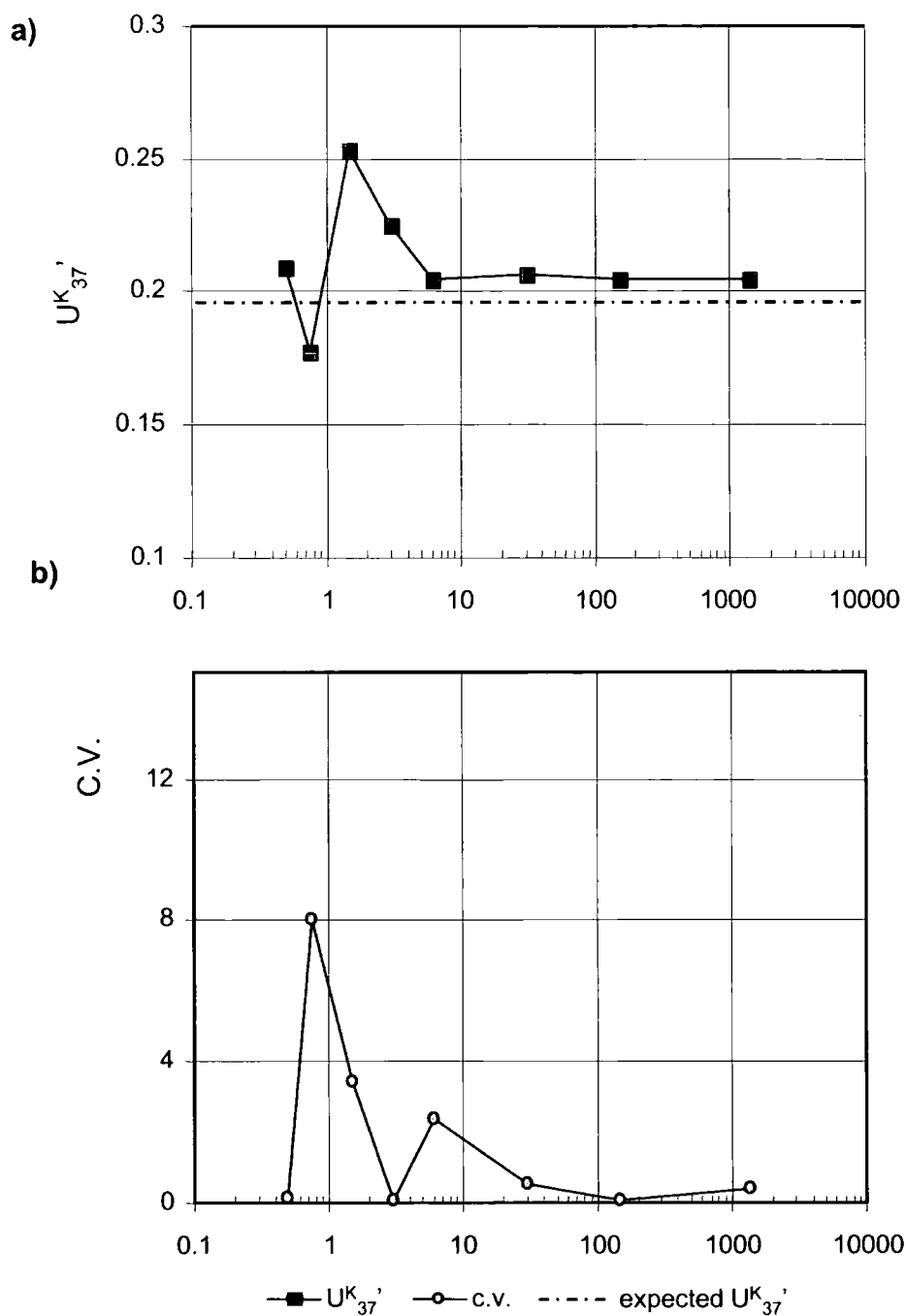


Figure 2.4: Changes in the a) U_{37}^K values (squares) and b) coefficient of variation (C.V.) (circles) when standards of synthetic alkenones with an expected U_{37}^K of 0.19 are injected at different concentrations into the GC-FID. The x-axis in a) is the mean U_{37}^K (of three injections) the x-axis in b) is the C.V.

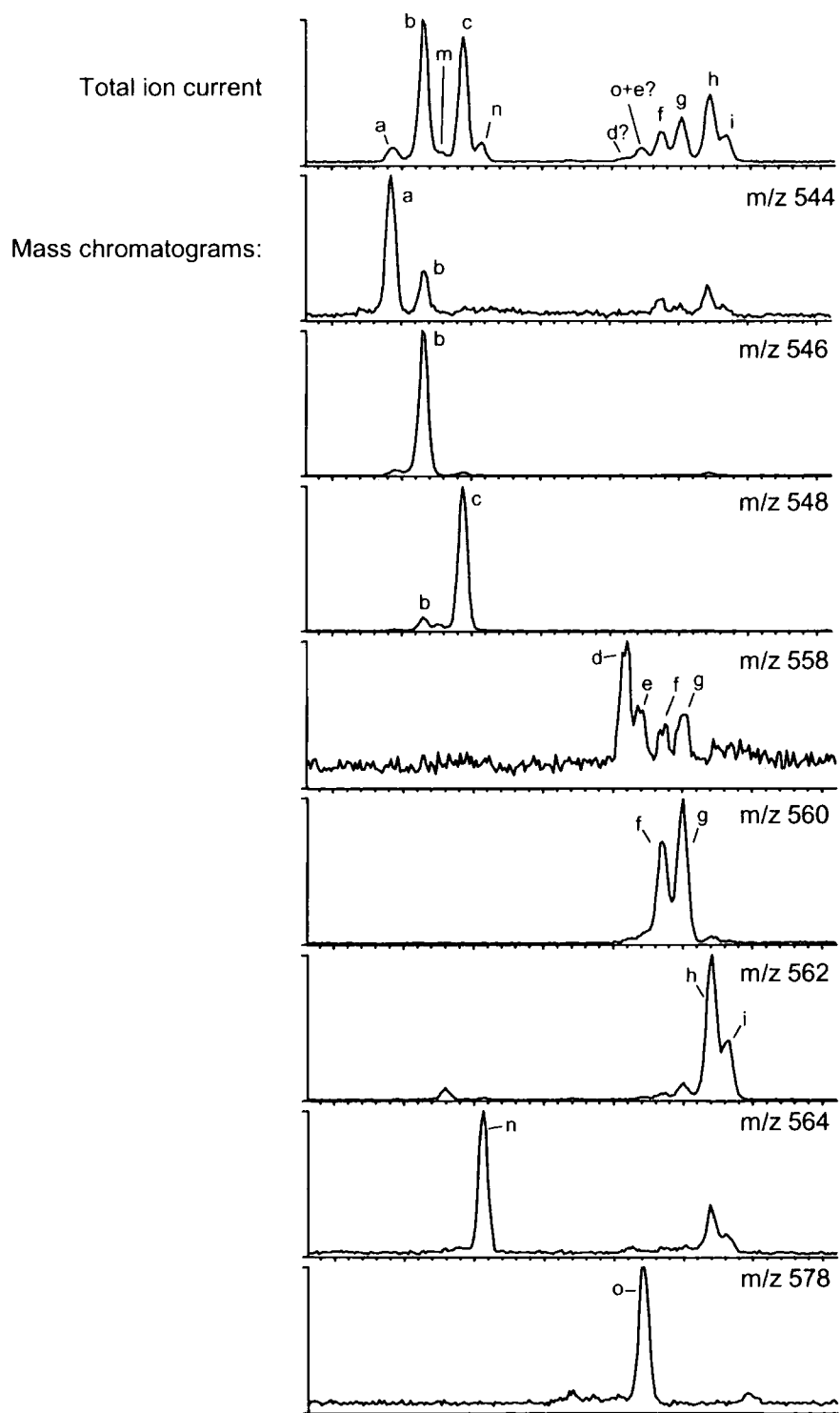


Figure 2.5: Ammonia chemical ionization mass chromatograms of the total ion current and pseudo-molecular ions of the alkenones and alkyl alkenoates quantified in a lipid extract from a sediment core extracted from the Icelandic continental shelf. See Table 1.1 (chapter 1) For compound identities.

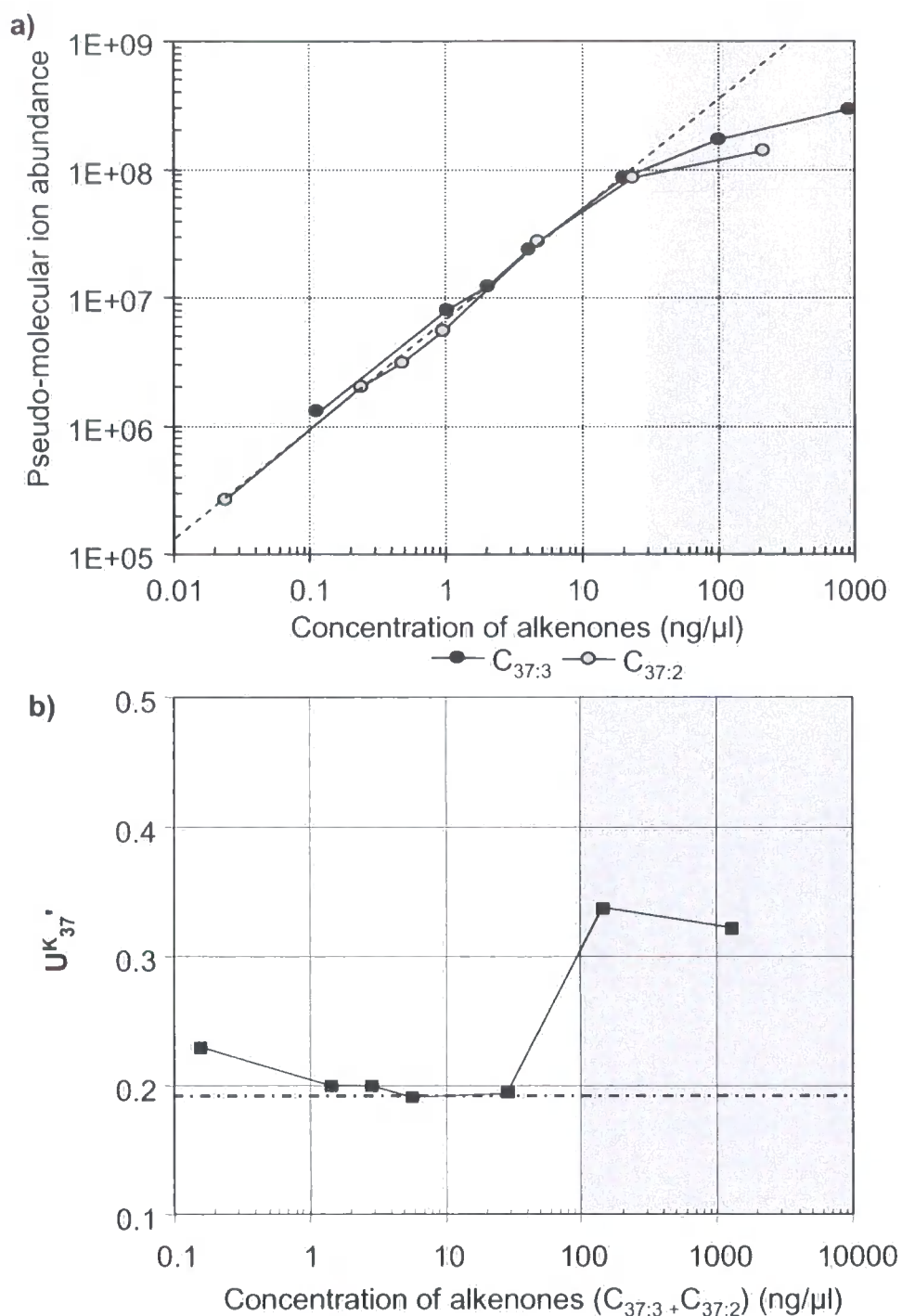


Figure 2.6: Linearity of the GC-CI-MS method to quantify the $C_{37:3}$ and $C_{37:2}$ alkenones and changes in UK_{37}' values. a) The pseudo molecular ion is plotted versus the concentration of $C_{37:3}$ and $C_{37:2}$ in the standard solutions. Both axis have logarithmic scales. The dashed line is a visual aid. B) Changes in the UK_{37}' values (squares) for the standards with an expected UK_{37}' of 0.19. The x-axis is logarithmic. The shaded areas in a) & b) highlight overloading of the system.

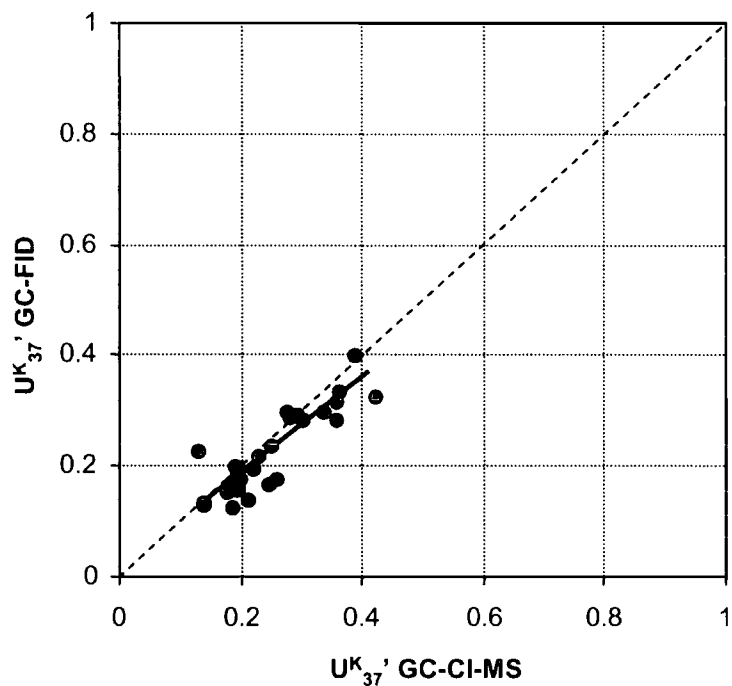


Figure 2.7: The U_{37}^K values of marine sea-surface filter extracts, injected into the GC-FID, plotted against the U_{37}^K values of the same samples injected in the GC-CI-MS. The solid line reflects the linear calibration obtained from both sets of data ($r^2=0.757$), the dashed line is a visual aid.

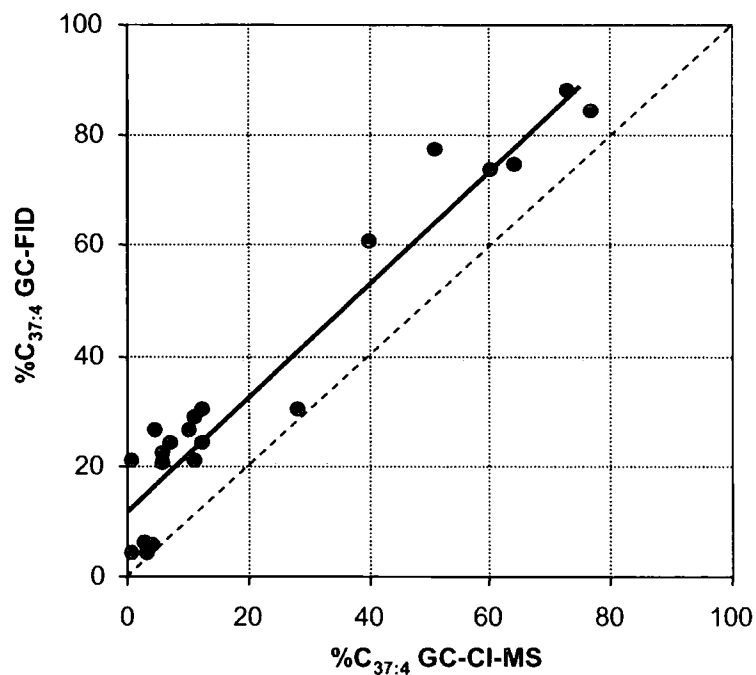
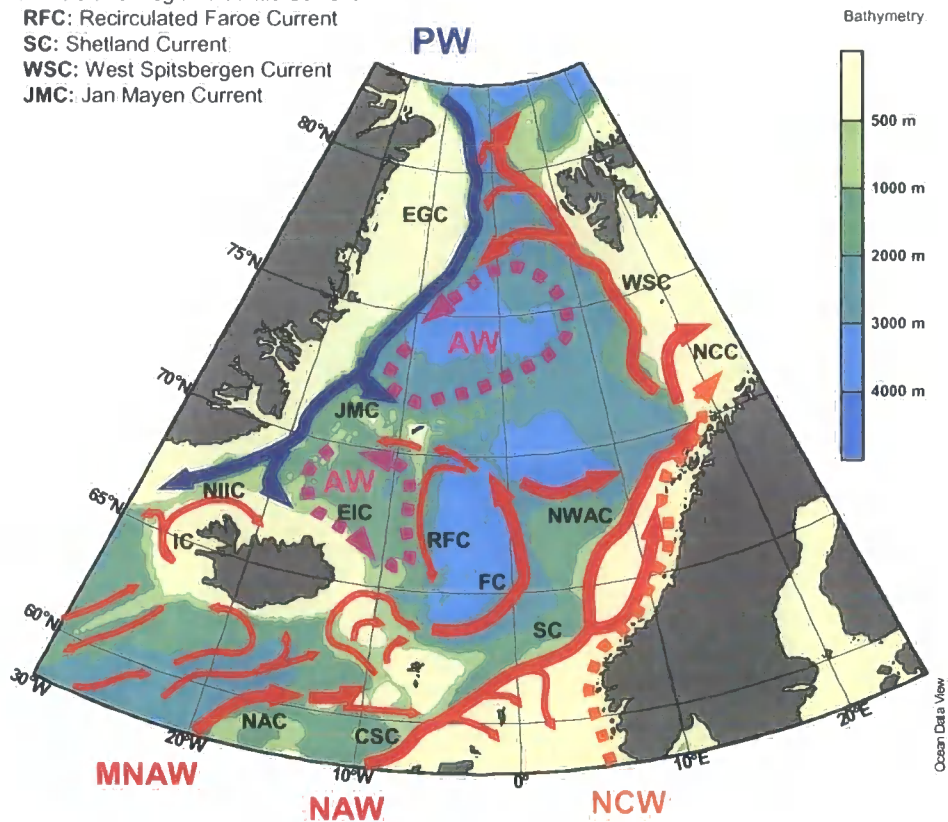


Figure 2.8: The $\%C_{37:4}$ values of marine sea-surface filter extracts, injected into the GC-FID, plotted against the $\%C_{37:4}$ values of the same samples injected in the GC-CI-MS. The solid line reflects the linear calibration obtained from both sets of data ($r^2=0.931$), the dashed line is a visual aid.

Currents:

- CSC:** Continental Slope Current
- EGC:** East Greenland Current
- EIC:** East Icelandic Current
- FC:** Faroe Current
- IC:** Irminger Current
- NAC:** North Atlantic Current
- NCC:** Norwegian Coastal Current
- NIIC:** North Icelandic Irminger Current
- NWAC:** Norwegian Atlantic Current
- RFC:** Recirculated Faroe Current
- SC:** Shelland Current
- WSC:** West Spitsbergen Current
- JMC:** Jan Mayen Current



Water masses:

- MNAW:** Modified North Atlantic Water
- NAW:** North Atlantic Water
- NCW:** Norwegian Coastal Water
- PW:** Polar Water
- AW:** Arctic Water

Figure 3.1: Main features of the surface to near-surface circulation in the eastern North Atlantic and Nordic Seas. Red arrows show Atlantic water flow. Blue, purple and orange arrows indicate flows of Polar, Arctic (mixed) and Norwegian coastal water masses respectively. Water masses transported by the main current branches are indicated. Sources: Hansen & Østerhus (2000); Johannesssen (1986); Swift (1986).

Deep water masses:

- GSDW:** Greenland Sea Deep Water
- AIW:** Arctic Intermediate Water
- NIWW:** North Icelandic Winter Water
- MEIW:** Modified East Icelandic Water
- NSAIW:** Norwegian Sea Arctic Intermediate Water
- NSDW:** Norwegian Sea Deep Water

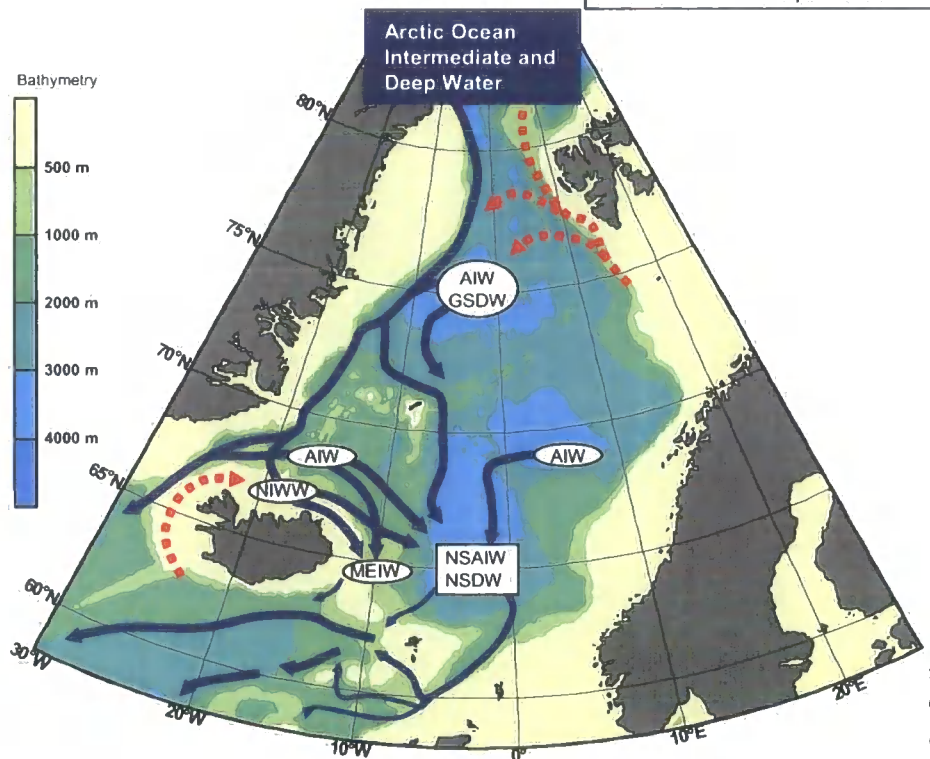
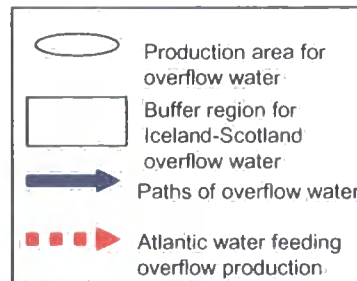


Figure 3.2: Main areas of densification in the Nordic Seas, paths of deep water flow to the Greenland-Scotland Ridge and overflow to the eastern North Atlantic. The thickness of the arrows crossing the ridge indicates magnitude and persistence of flow. Adapted from Hansen & Østerhus (2000).

Oceanic Fronts

PF: Polar Front

AF: Arctic Front

BSPF: Barents Sea Polar Front

NCF: Norwegian Coastal Front

IFF: Iceland-Faeroes Front

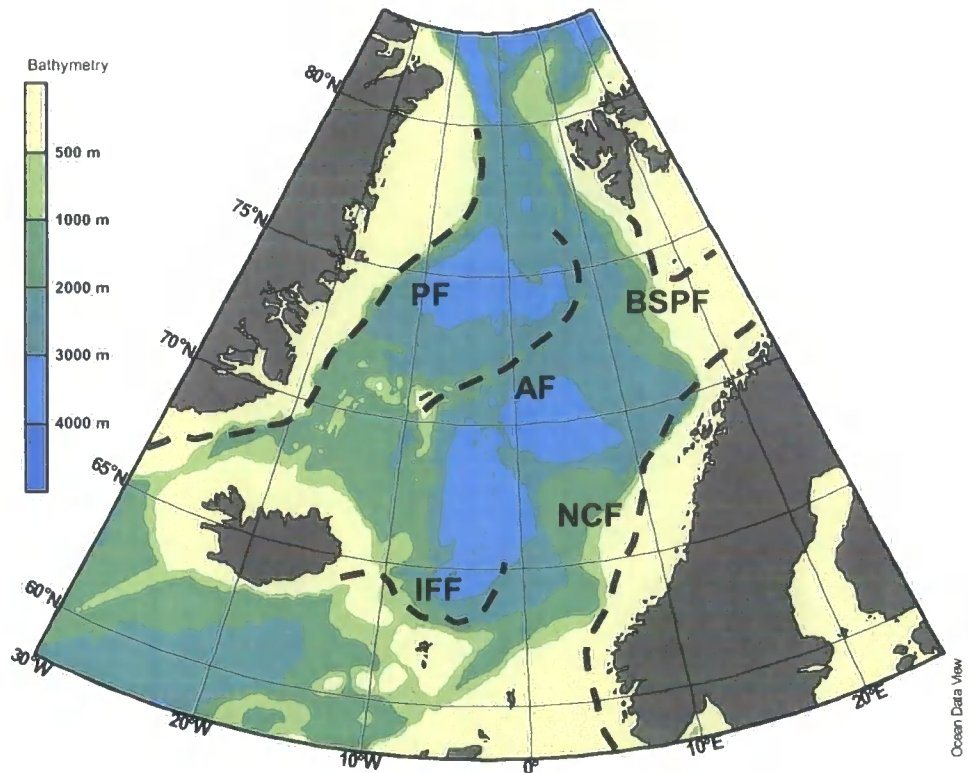


Figure 3.3: Main frontal systems of the Nordic Seas. Fronts are “leaky boundaries” – interfaces of cold and warmer water, with the cold water being less saline so as to have about the same density. Source Johannessen (1986).

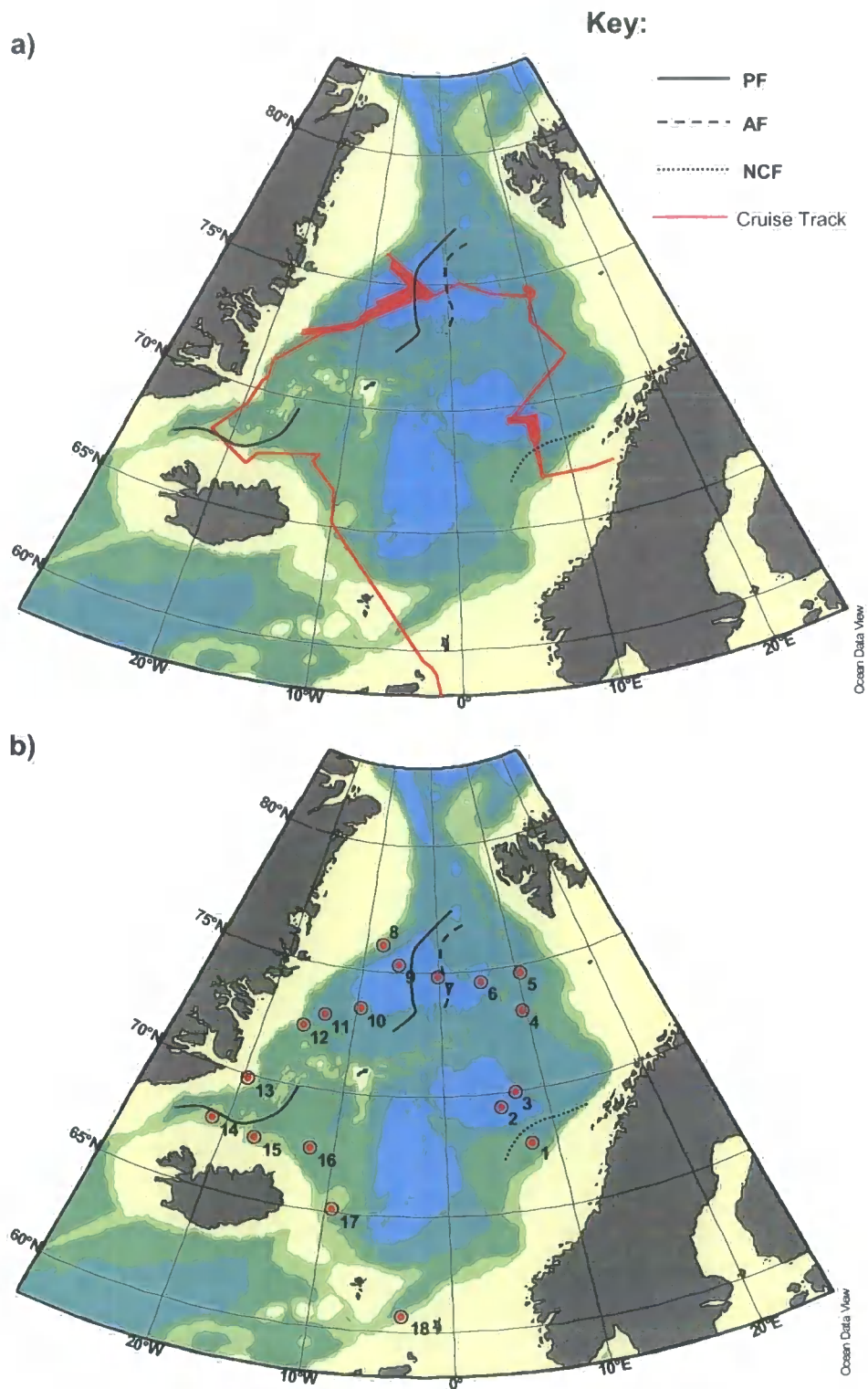


Figure 3.5: JR51 Cruise track (a) and location (b) of sampling stations for filter samples. Positions of ocean fronts derived from *in situ* measurements – see figure 3.7.

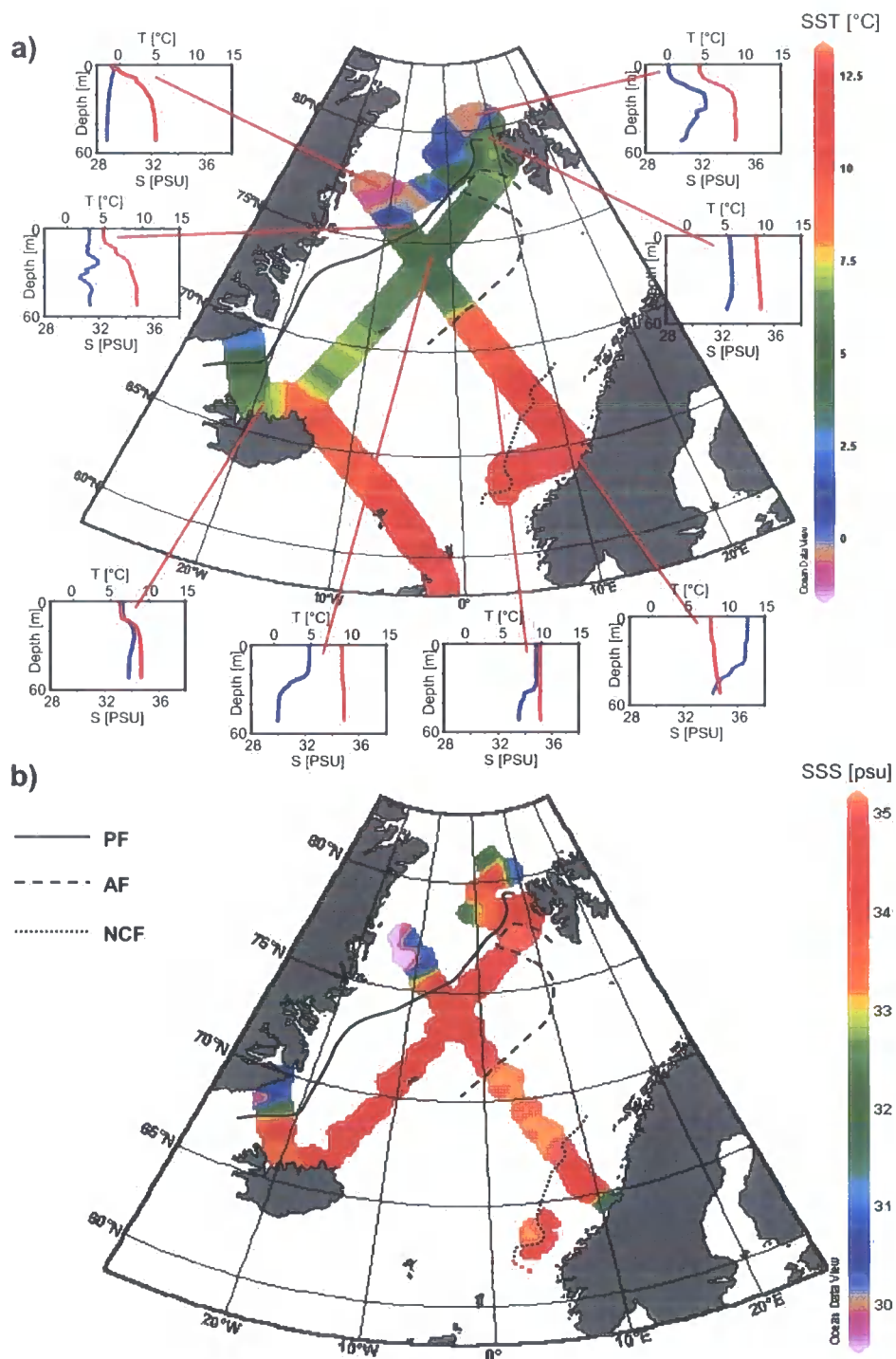


Figure 3.6: Physical oceanographic properties measured *in situ* during cruise JR44. A) Colour gridding shows temperature ($^{\circ}\text{T}$) at 6m depth (from JCR ocean logger). Depth profiles are derived from CTD probes, blue = temperature ($^{\circ}\text{T}$), red = salinity (psu). B) Colour gridding shows salinity (psu) at 0m depth (from CTD's). Isolines show position of Polar and Arctic Fronts based on *in situ* oceanlogger measurements. SST & SSS ranges used to define the water masses delimited by the fronts are given in Table 3.1.

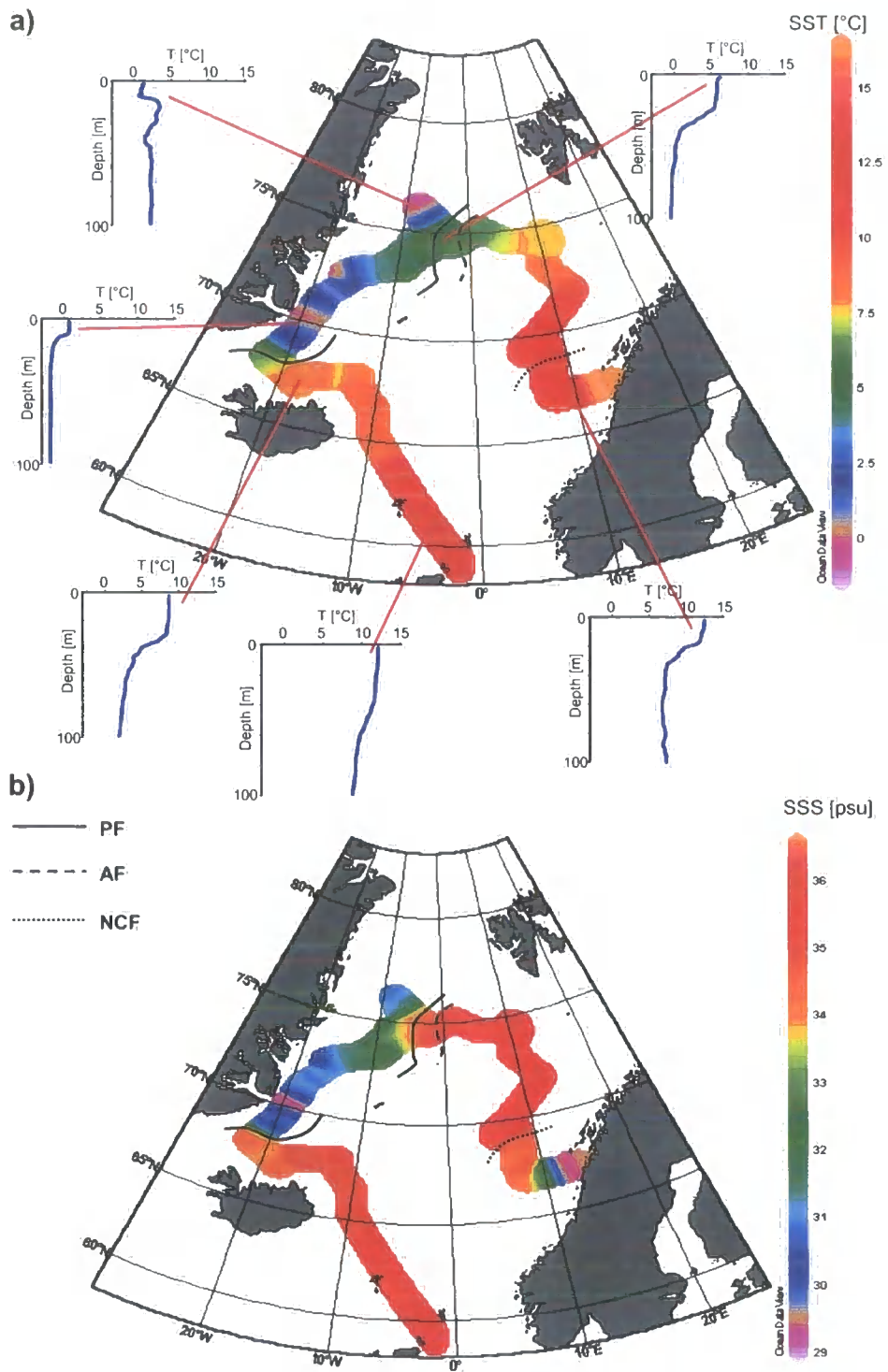
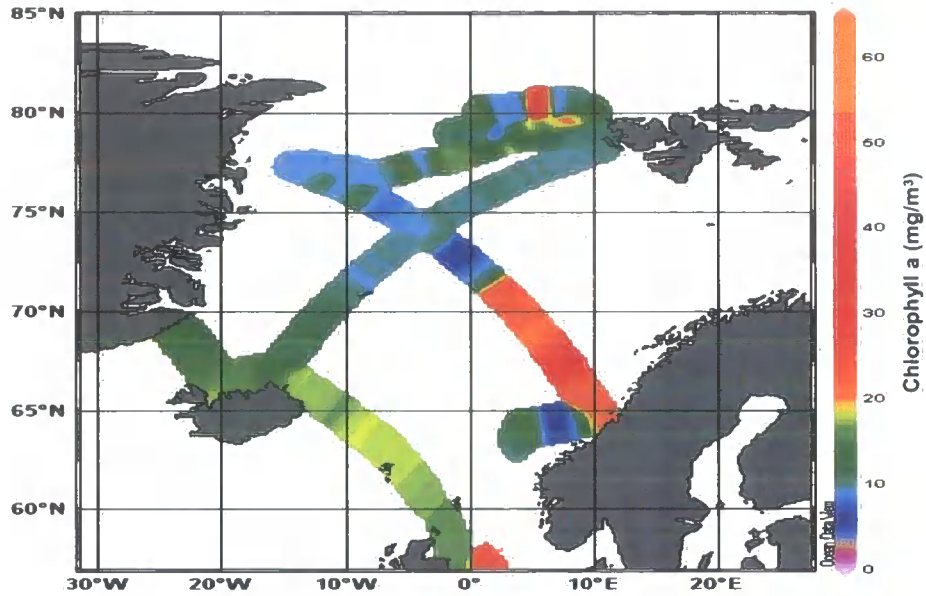


Figure 3.7: Physical oceanographic properties measured *in situ* during cruise JR51. A) Colour gridding shows temperature ($^{\circ}\text{T}$) at 6m depth (from JCR ocean logger). Depth profiles are derived from XTB probes. B) Colour gridding shows salinity (psu) at 6m depth (from JCR ocean logger).

a)



b)

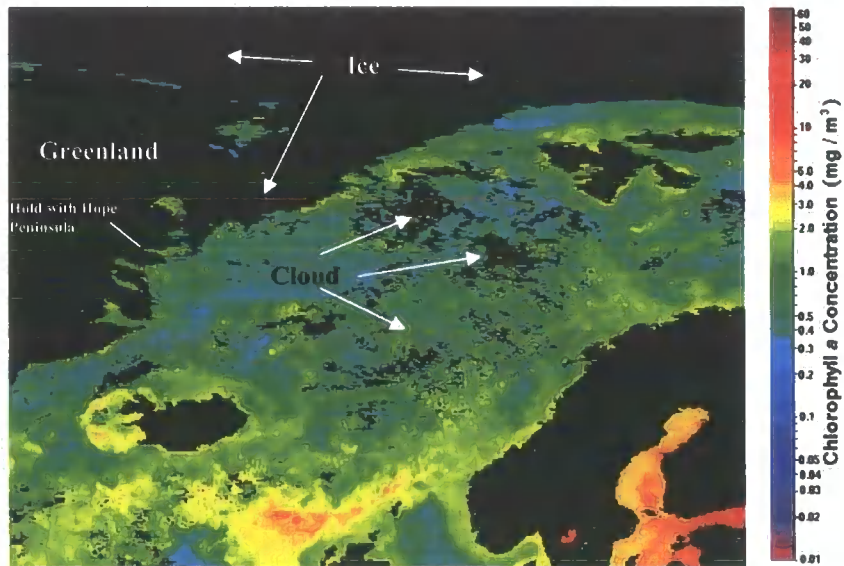
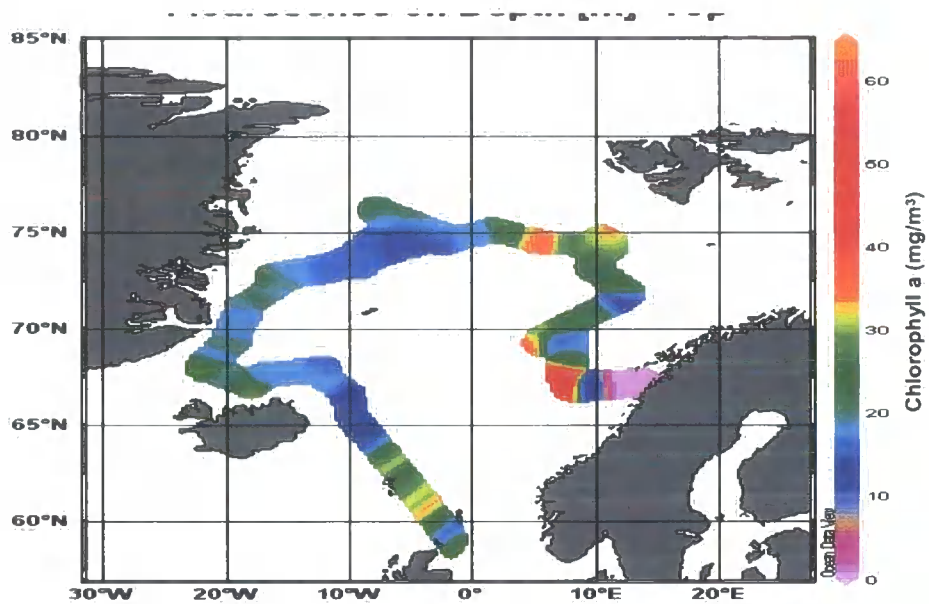


Figure 3.8: Chlorophyll *a* measurements for cruise JR44. A) Colour gridding shows chlorophyll *a* measured *in situ* at 6m depth during JR44 by ship's fluorometer. B) Remotely sensed CZCS Chlorophyll *a* concentrations for August 1999 (Provided by the SeaWiFS Project, NASA/Goddard Space Flight Center and ORBIMAGE).

a)



b)

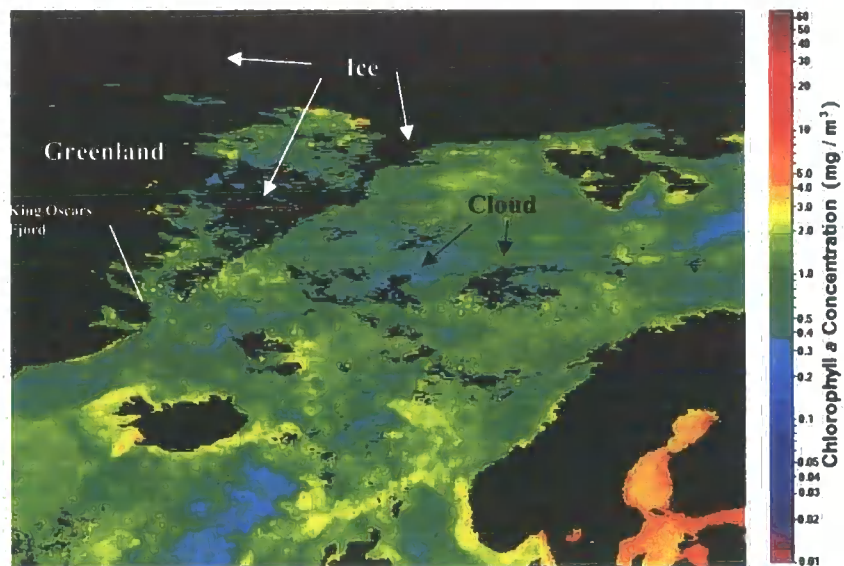


Figure 3.9: Chlorophyll *a* measurements for cruise JR51. A) Colour gridding shows Chlorophyll *a* measured *in situ* at 6m depth during JR51 by ship's fluorometer. B) Remotely sensed CZCS Chlorophyll *a* concentrations for August 2000. Dark areas are ice, land or cloud (Provided by the SeaWiFS Project, NASA/Goddard Space Flight Center and ORBIMAGE).

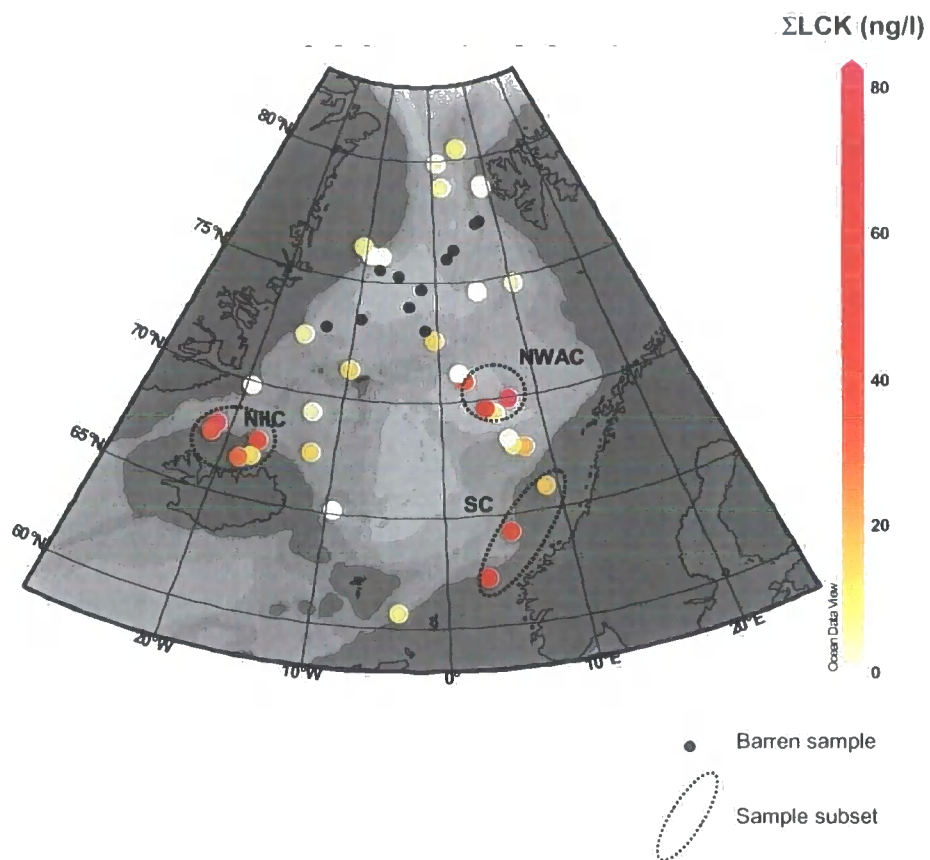


Figure 3.10: Geographic distribution of Σ LCK (ng/l) in the surface waters of the Nordic Seas. Sample subsets obtained from the North Icelandic Irminger Currents (NIIC), Shetland Current (SC) and the Norwegian Atlantic Current (NWAAC) are highlighted (dotted lines). See Figure 3.1 and Table 3.1 for water mass and current details.

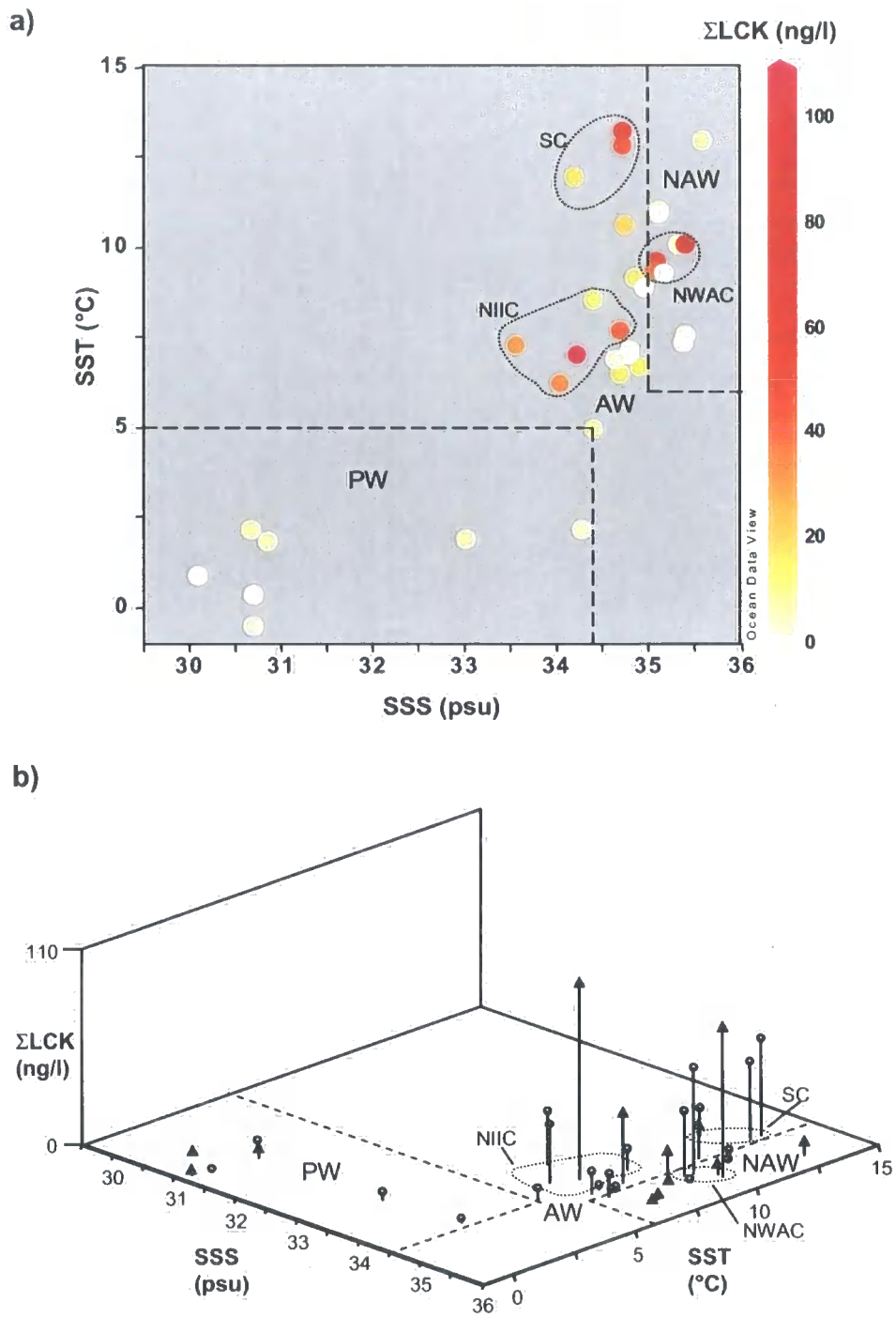


Figure 3.11: Distributions of ΣLCK (ng/l) in the surface waters of the Nordic Seas by water mass. A) ΣLCK (ng/l) vs temperature and salinity with major water masses delimited (dashed lines) and sample subsets influenced by the North Icelandic Irminger Currents (NIIC) and the Norwegian Coastal Current (NCC) highlighted (dotted lines). B) The same data from a 3D perspective, circle symbols = samples from JR44, triangle symbols = samples from JR-51. See Figure 3.1 and Table 3.1 for water mass and current details.

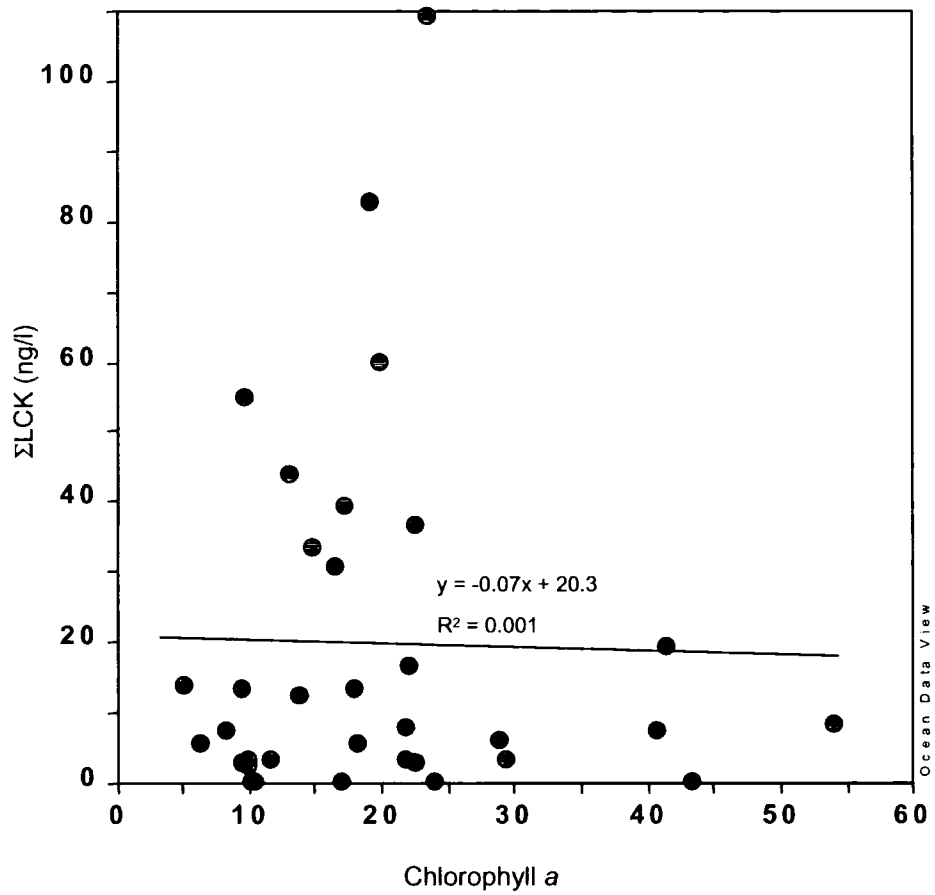
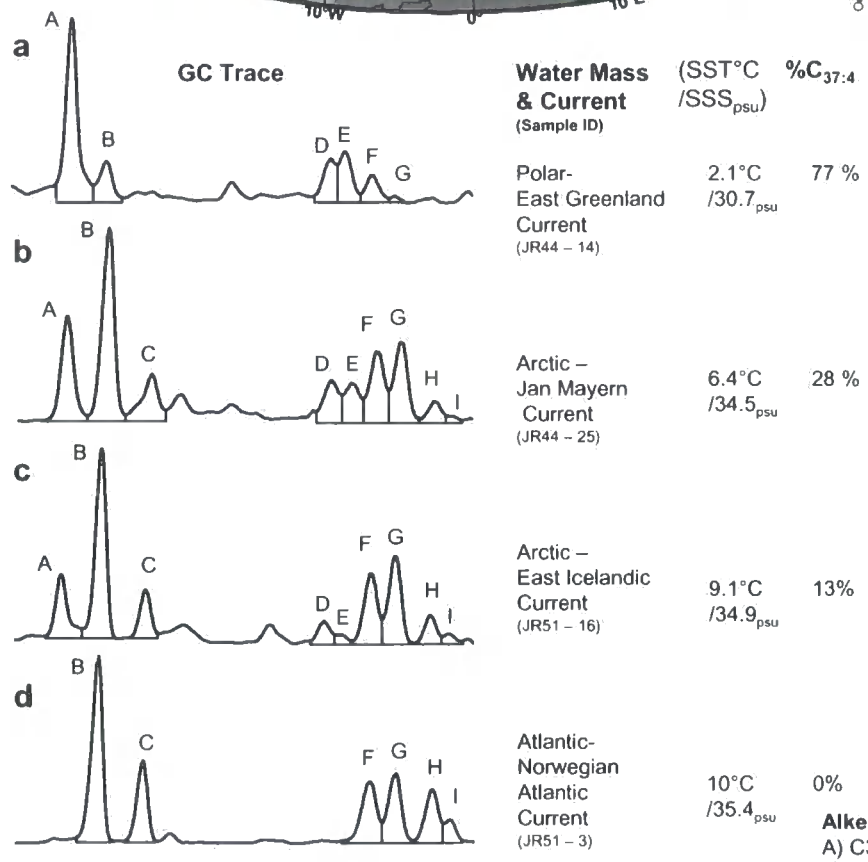
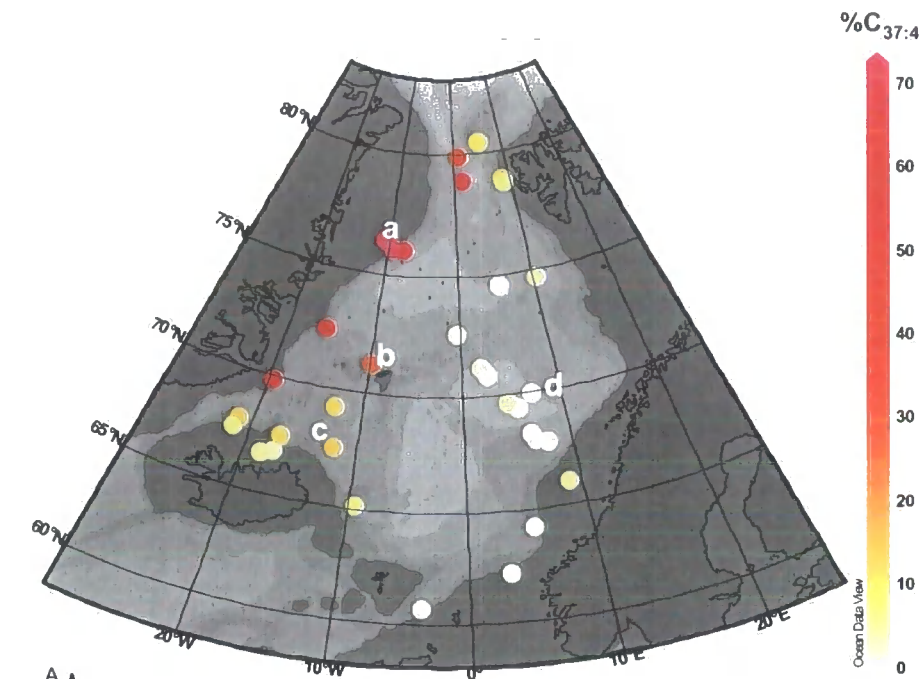


Figure 3.12: Distributions of ΣLCK (ng/l) vs chlorophyll *a*.(from ship's fluorometer).



- Alkenones**
 A) C37:4 Me
 B) C37:3 Me
 C) C37:2 Me
 D) C38:4 Et
 E) C38:4 Me
 F) C38:3 Et
 G) C38:3 Me
 H) C38:2 Et
 I) C38:2 Me

Figure 3.13: Geographic distribution of %C_{37:4} in the surface waters of the Nordic Seas with representative GC-FID traces of alkenone patterns from different water masses. See Figure 3.1 and Table 3.1 for water mass and current details.

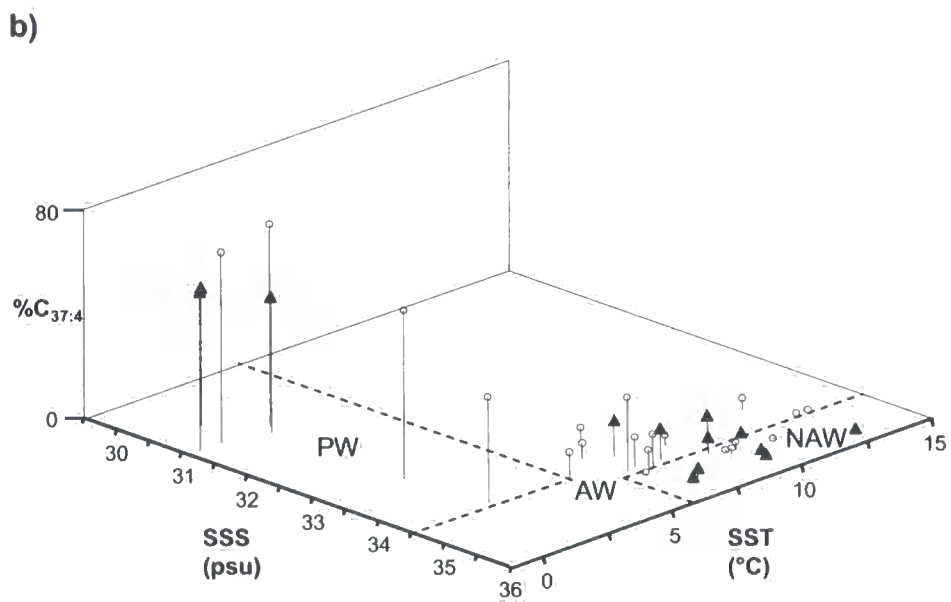
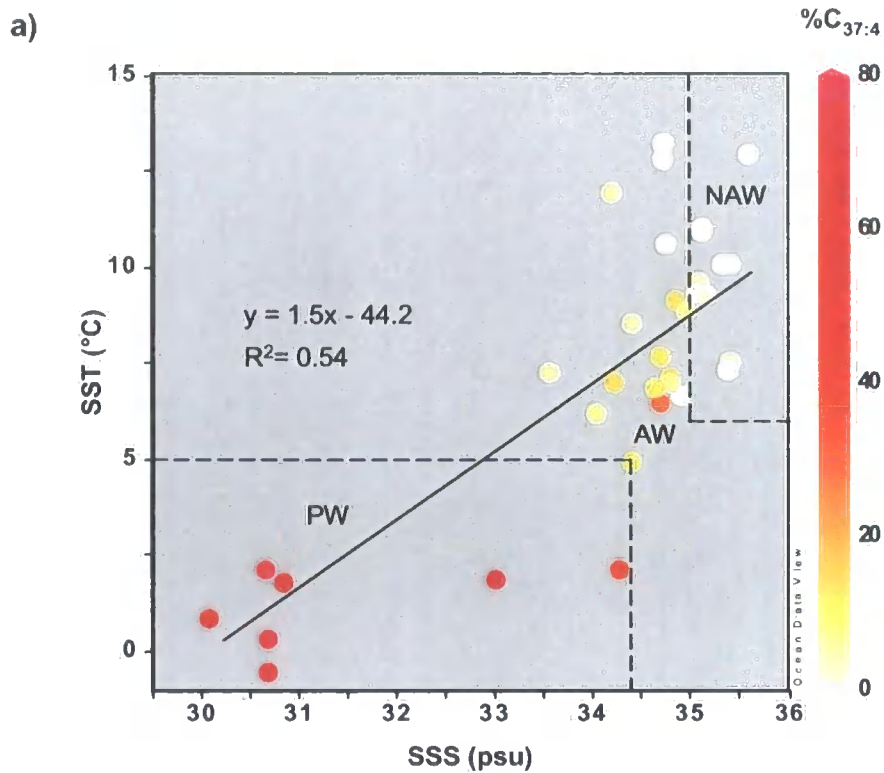


Figure 3.14: Distributions of $\%C_{37:4}$ in the surface waters of the Nordic Seas by water mass. A) $\%C_{37:4}$ vs temperature and salinity with major water masses delimited (dashed lines). B) The same data from a 3D perspective, circle symbols = samples from JR44, triangle symbols = samples from JR-51. See Figure 3.1 and Table 3.1 for water mass and current details.

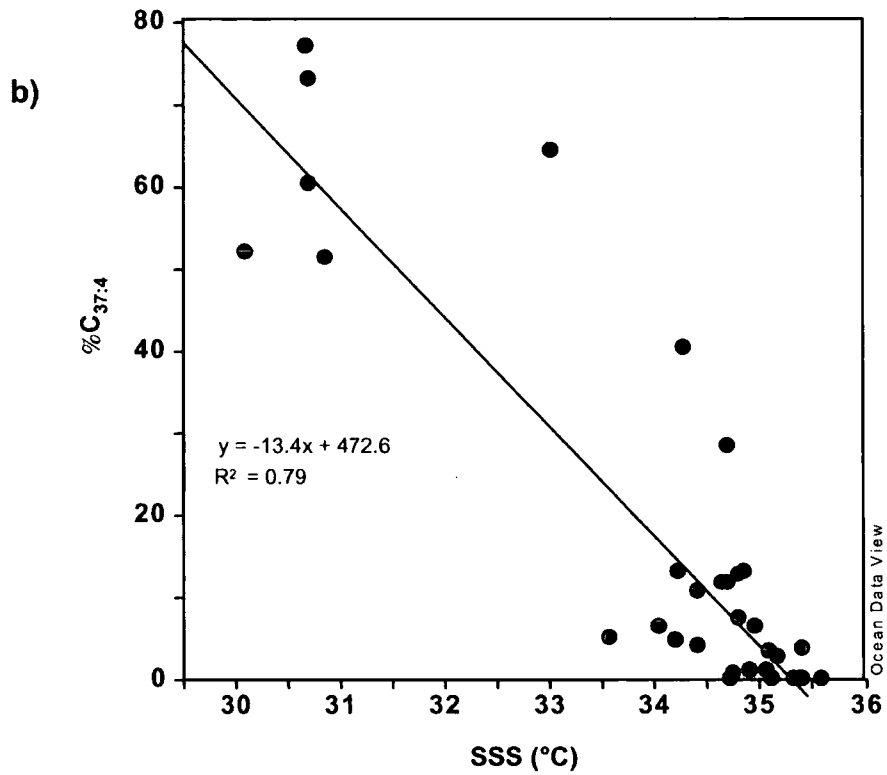
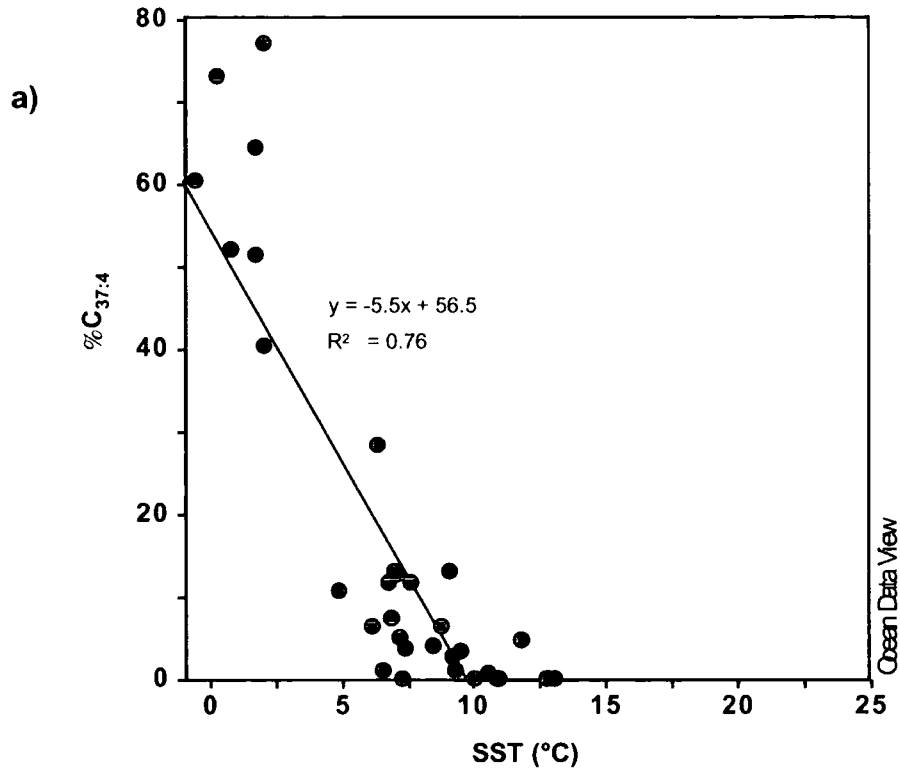


Figure 3.15: Distributions of $\%C_{37:4}$ vs A) SST (°C) and B) SSS (psu) with linear regressions.

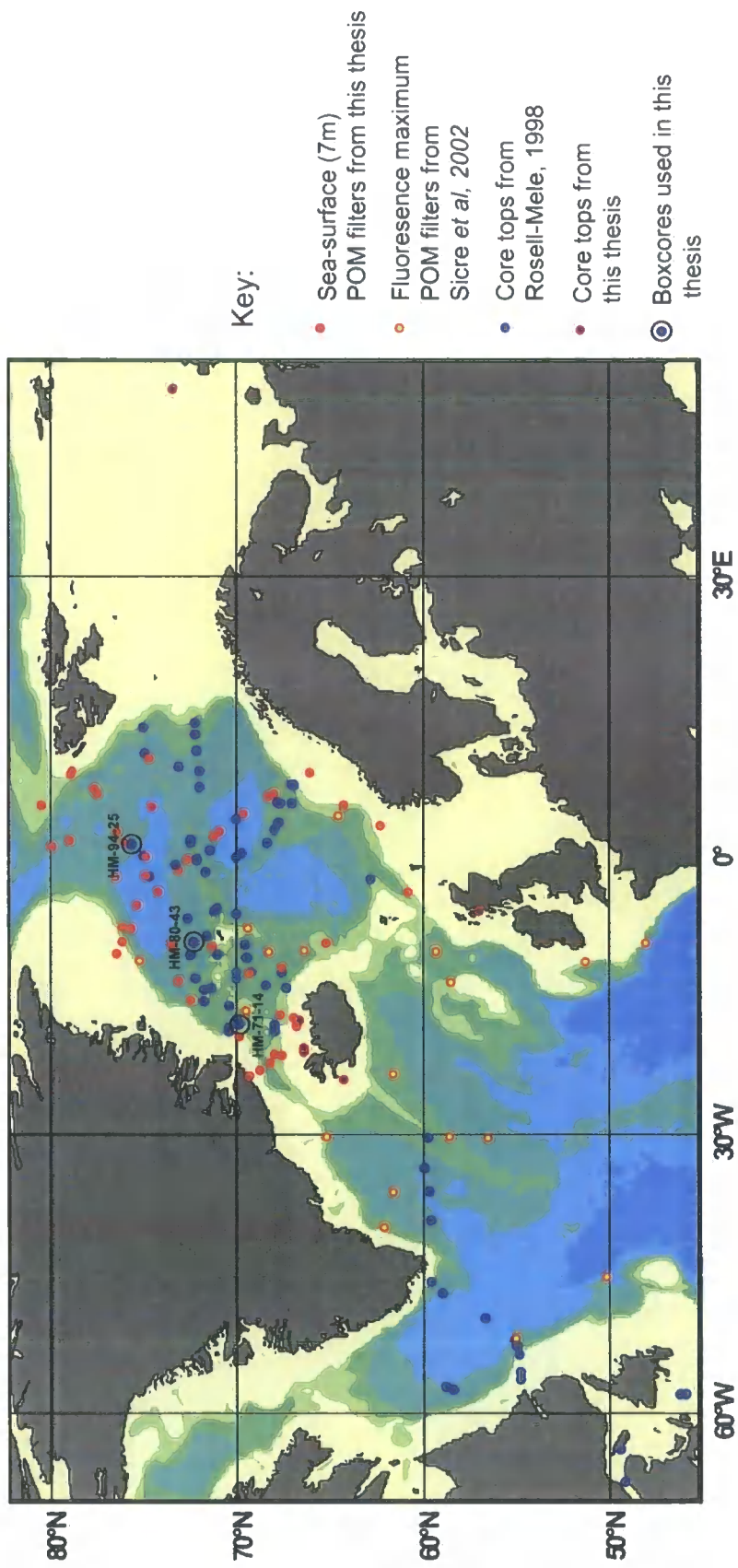


Figure 3.16: Geographic distribution of $\%C_{37:4}$ samples from the water column and surface sediments of the Nordic Seas and northern North Atlantic.

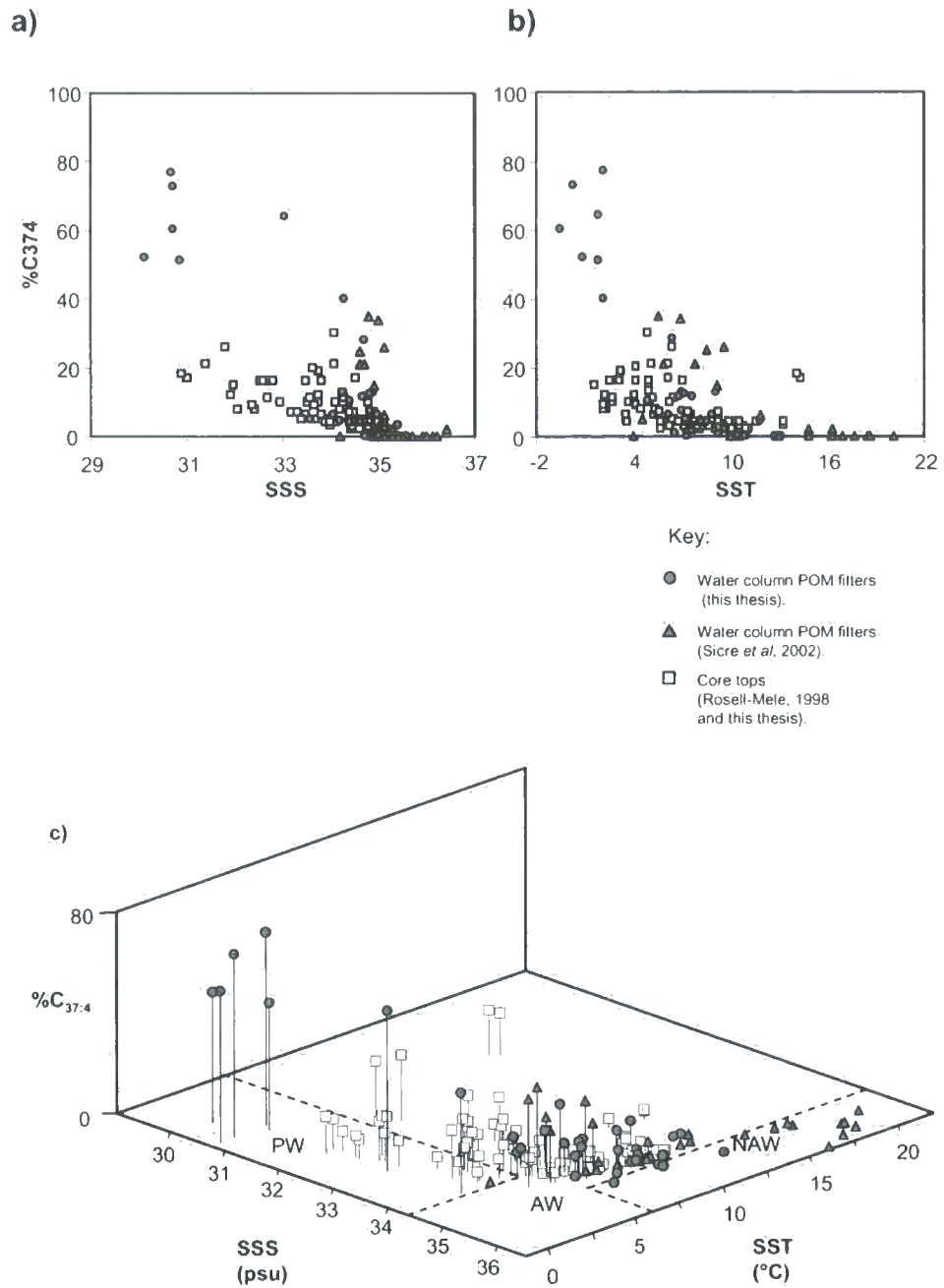


Figure 3.17: Distributions of $\%C_{37.4}$ in the water column and surface sediments of the Nordic Seas and northern north Atlantic. Scatter plots of $\%C_{37.4}$ vs SST (a) and SSS (b) from sample sets illustrated in Fig 3.16 B) 3-D plot of $\%C_{37.4}$ vs SST and SSS with major water masses delimited (dashed lines).

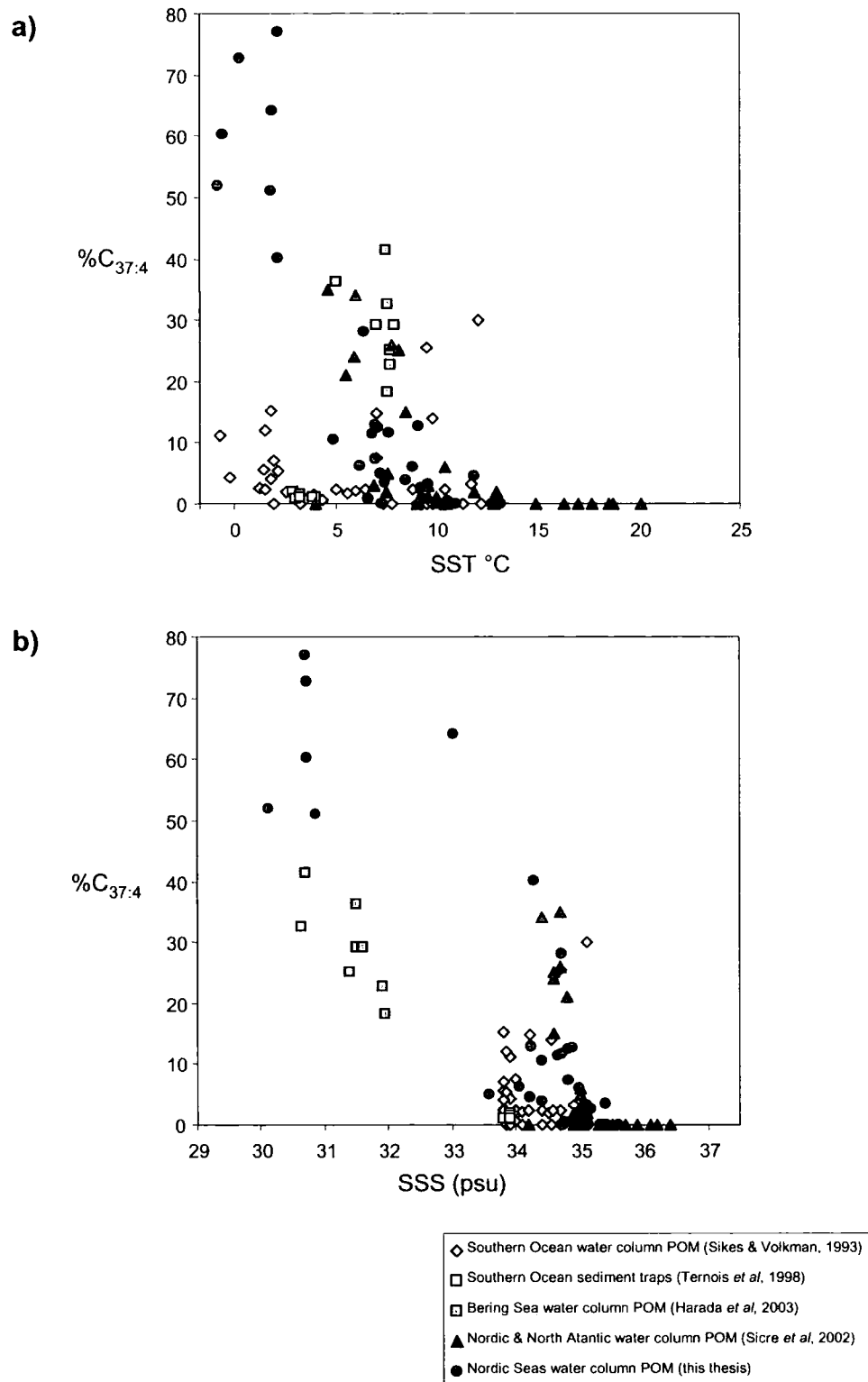


Figure 3.18: Distributions of $\%C_{37:4}$ in the global water column. Scatter plots of $\%C_{37:4}$ vs SST (a) and SSS (b).

C_{37} alkenone response - normalised to top sample (0cm).

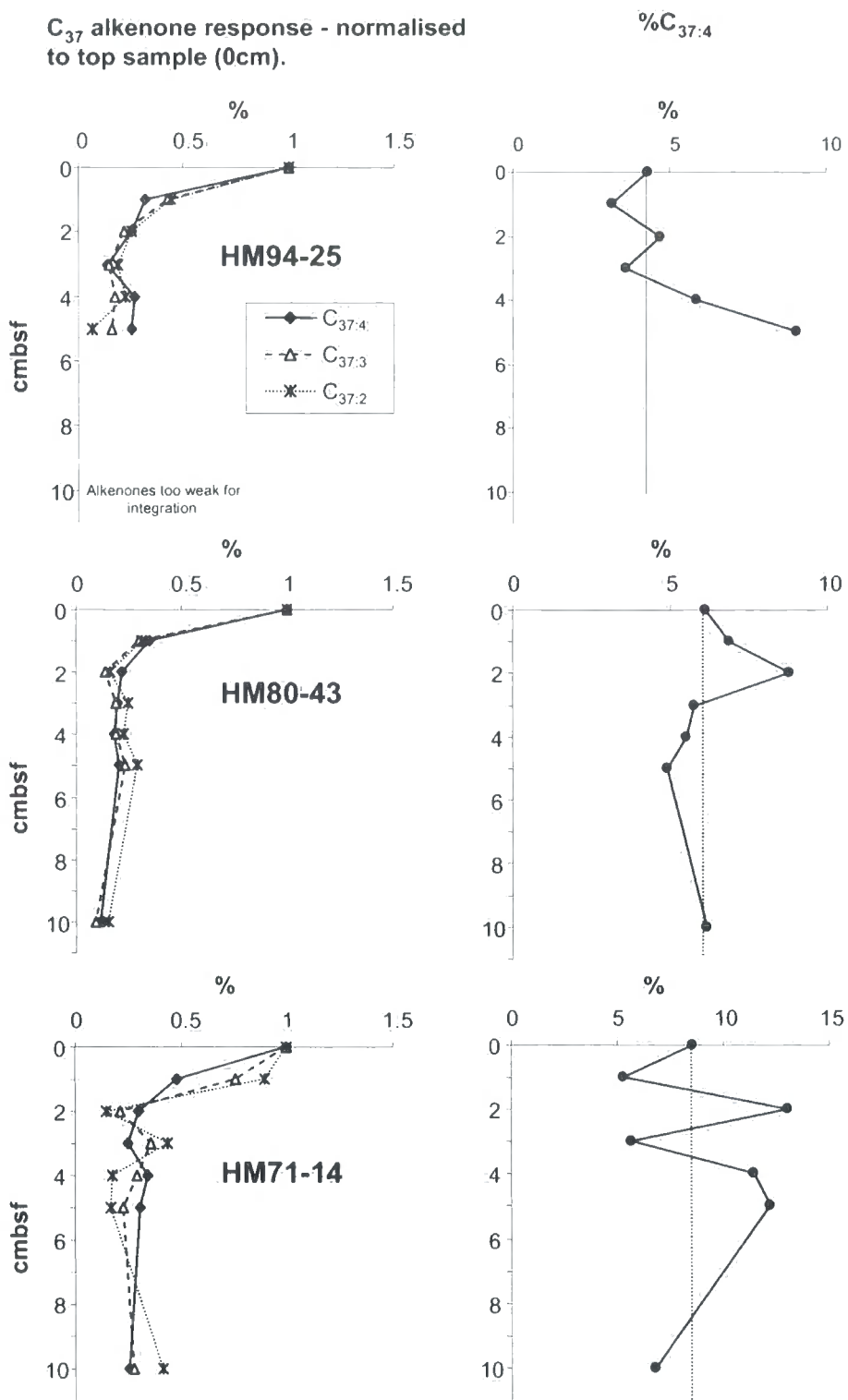


Figure 3.19: Distributions of alkenones in boxcores from the Nordic Seas.

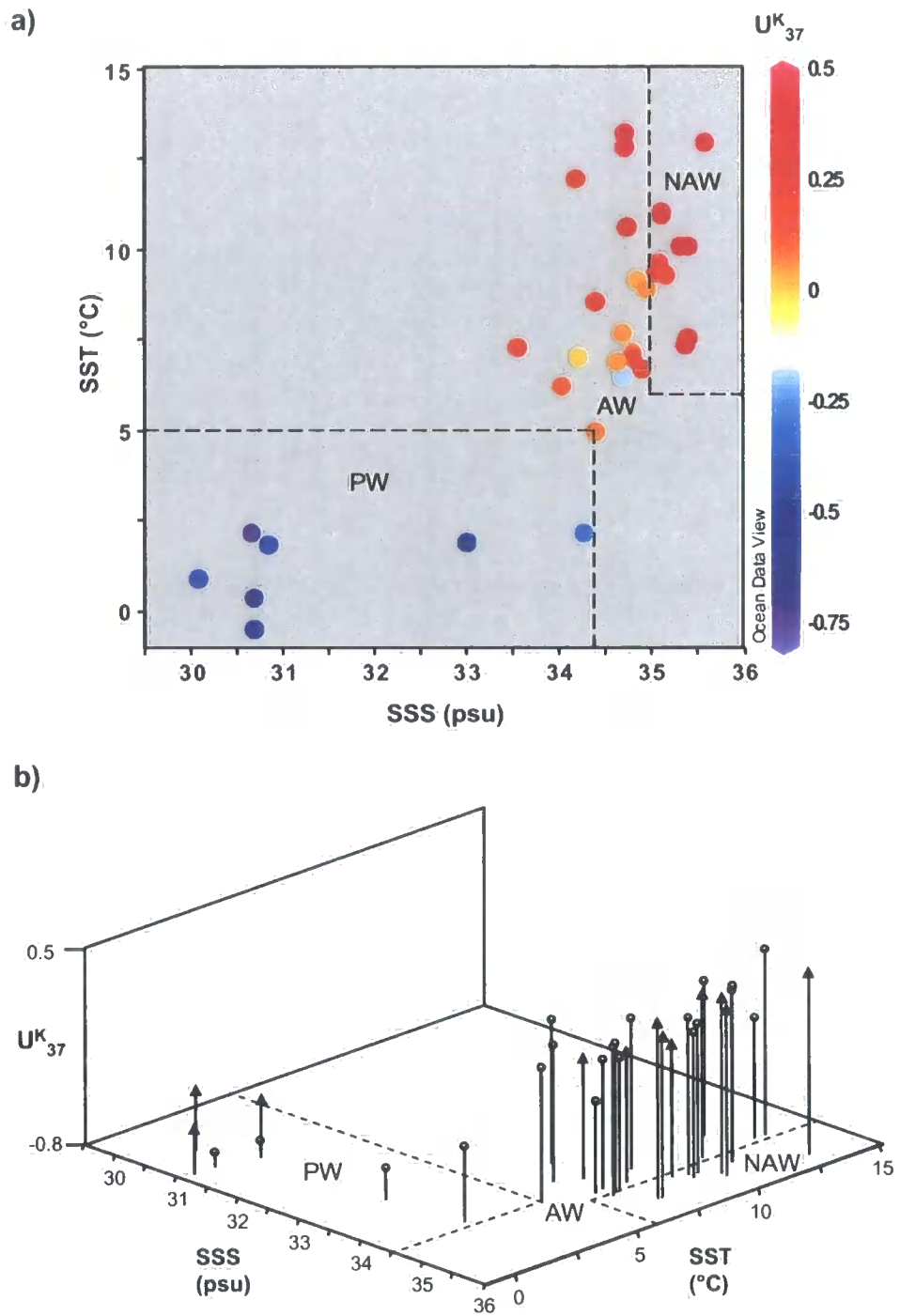


Figure 3.20: Distributions of U_{37}^K in the surface waters of the Nordic Seas by water mass. A) U_{37}^K vs temperature and salinity with major water masses delimited (dashed lines). B) The same data from a 3D perspective, circle symbols = samples from JR44, triangle symbols = samples from JR-51. See Table 3.1 for water mass details.

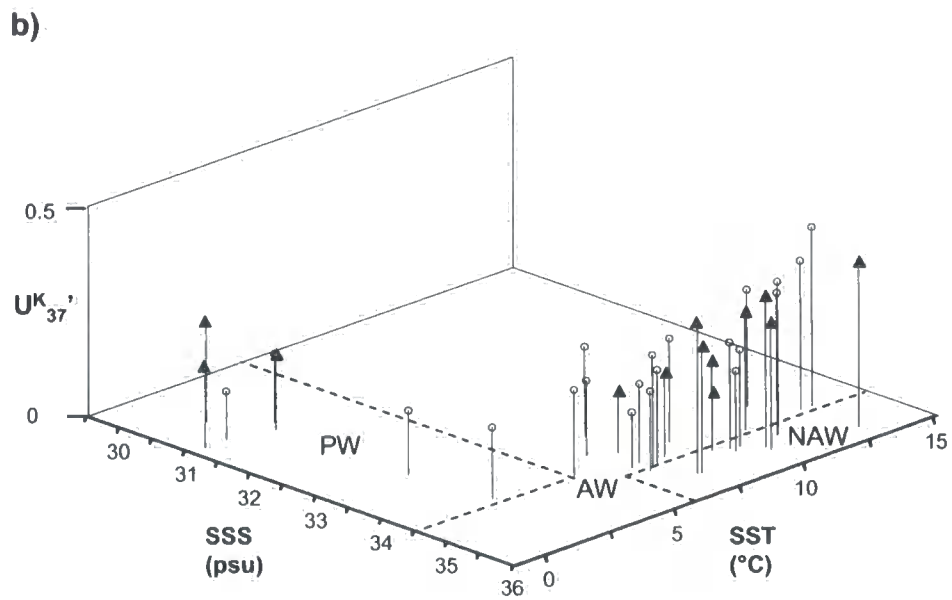
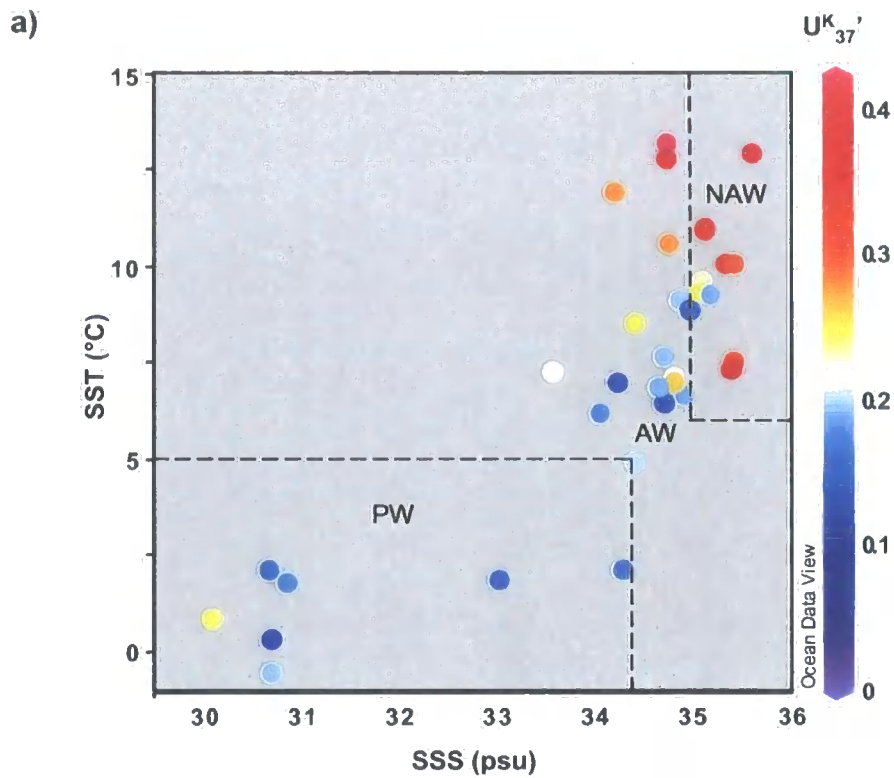


Figure 3.21: Distributions of U_{37}^K in the surface waters of the Nordic Seas by water mass. A) U_{37}^K vs temperature and salinity with major water masses delimited (dashed lines) B) The same data from a 3D perspective, circle symbols = samples from JR44, triangle symbols = samples from JR-51. See Table 3.1 for water mass details.

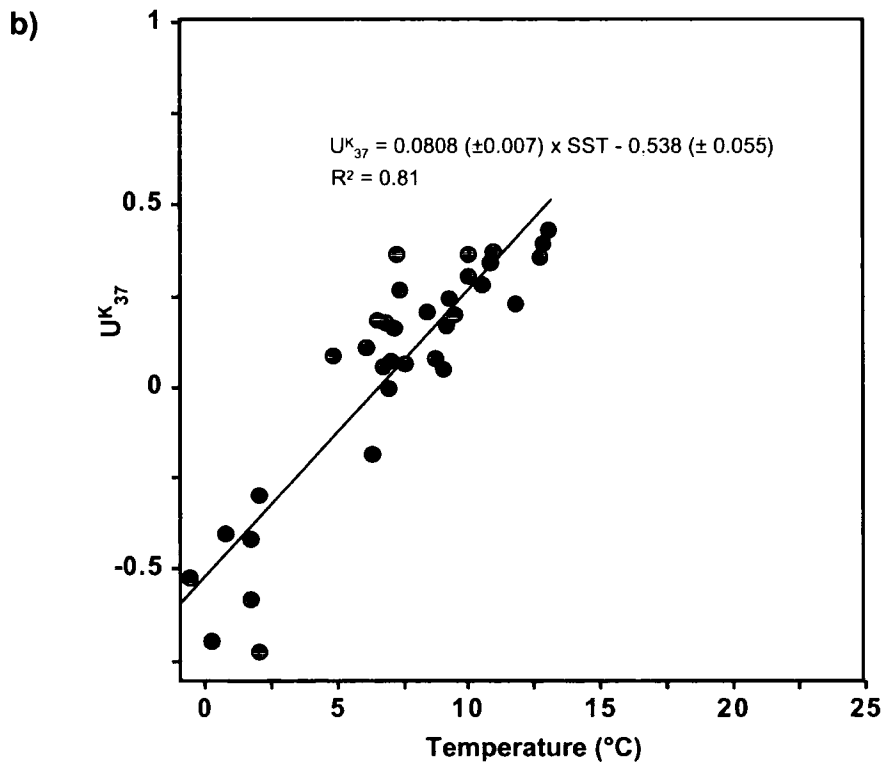
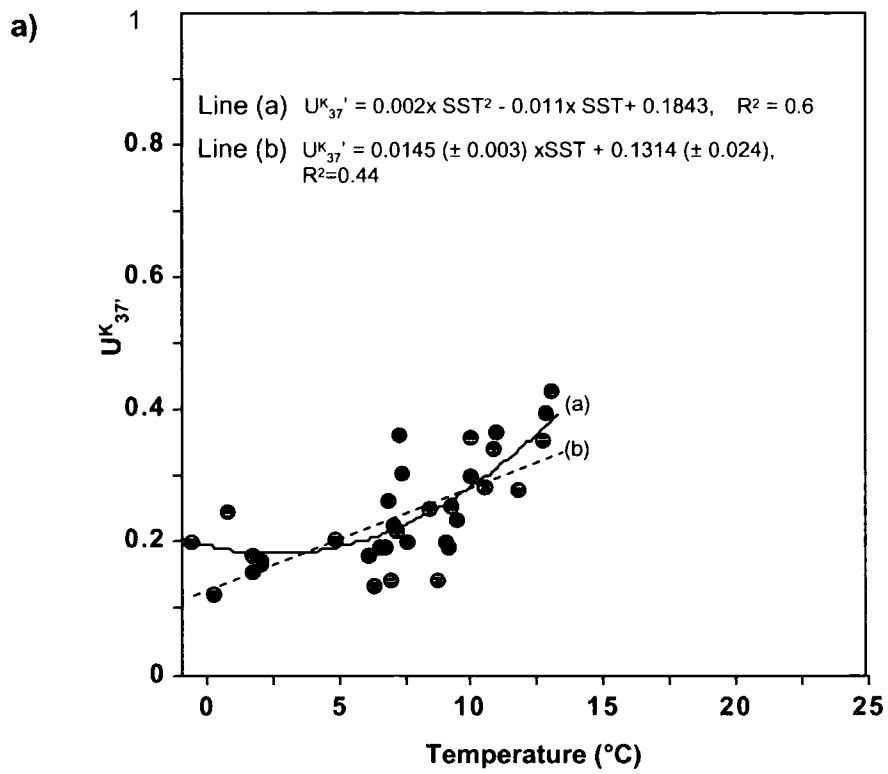
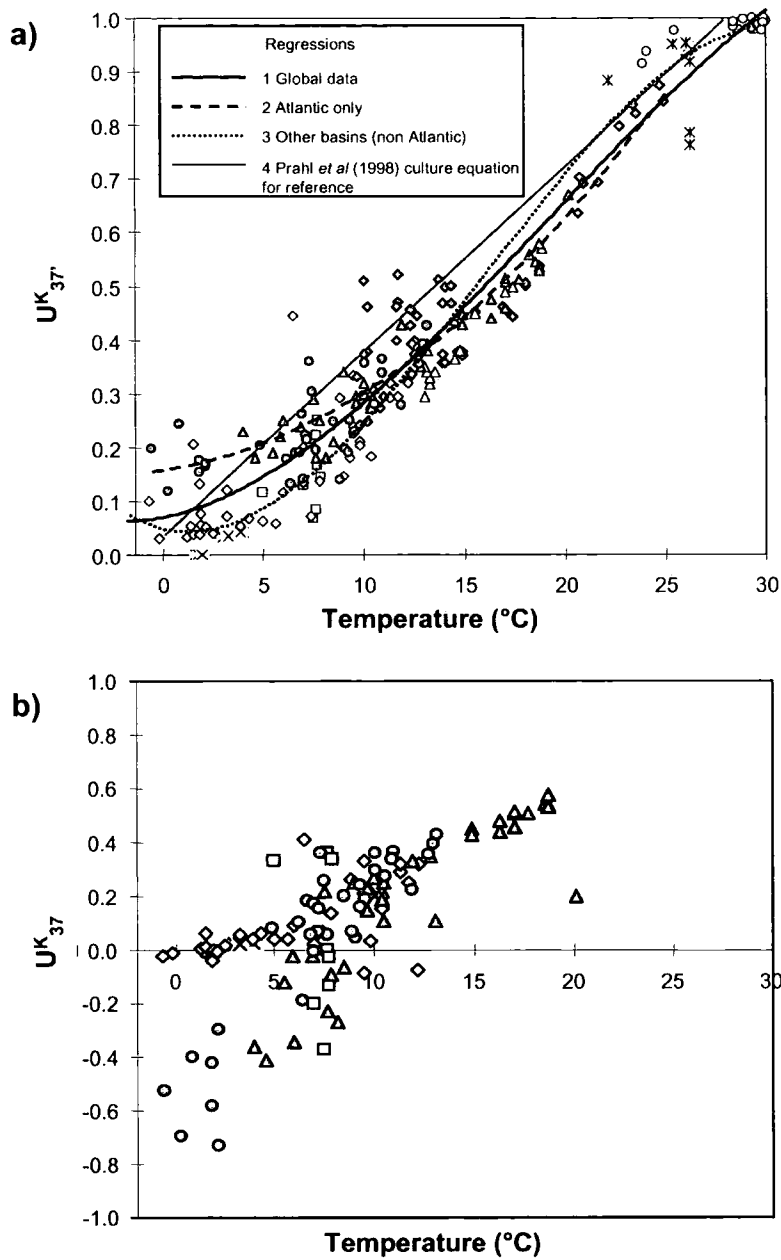


Figure 3.22: Distributions of A) U_{37}^K and B) U_{37}^K vs SST. Solid lines represent linear regressions; dashed line is a second order polynomial regression.



Key:	
Nordic Seas and N. Atlantic	
○	Nordic Seas water column POM (this thesis)
△	Nordic Seas & N. Atlantic water column POM (Sicre <i>et al.</i> , 2002)
◇	N. Atlantic water column POM (Conte and Eglinton, 1993)
Other basins	
×	S. Ocean sed. traps (Ternois <i>et al.</i> 1998)
◇	S. Ocean water column POM (Sikes & Volkman, 1993)
○	Eq.I Pacific water column POM (Sikes and Sicre, 2002)
×	Eq. Atlantic N.W. Africa (Sikes and Sicre, 2002)
□	Bering Sea water column POM (Harada, 2003)
△	Mediterranean Sea water column POM (Ternois <i>et al.</i> , 1997)

Figure 3.23: Distributions of A) U^K_{37}' and B) U^K_{37} measured on mixed layer POM vs water temperature. Data from this thesis and reported in literature. Regressions 1 & 3 are 3rd order polynomial, regression 2 is 2nd order polynomial.

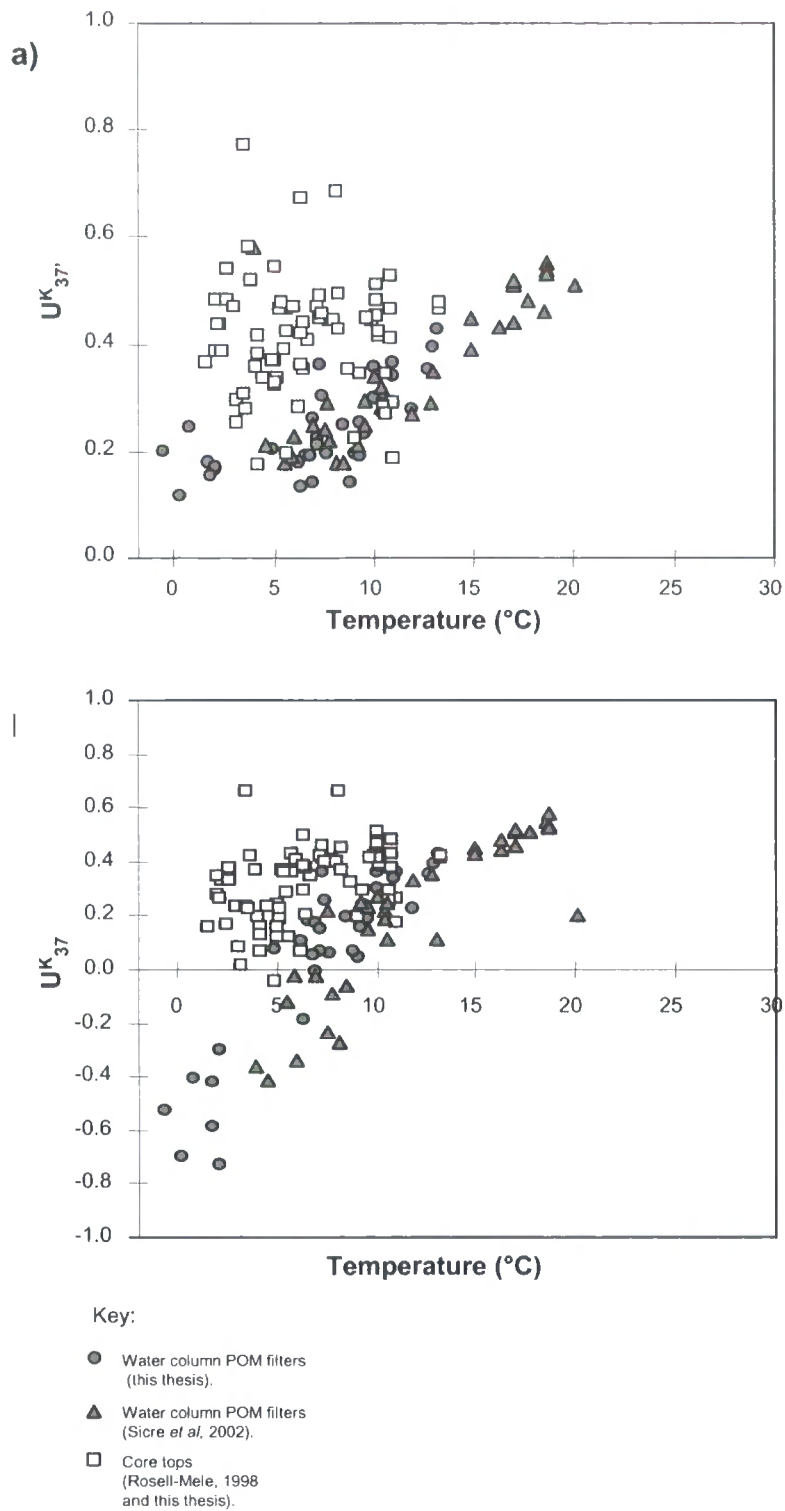


Figure 3.24: Nordic Seas distributions of A) U_{37}^K and B) U_{37}^K measured on mixed layer POM and surface sediments vs water temperature. Data from this thesis and reported in literature.

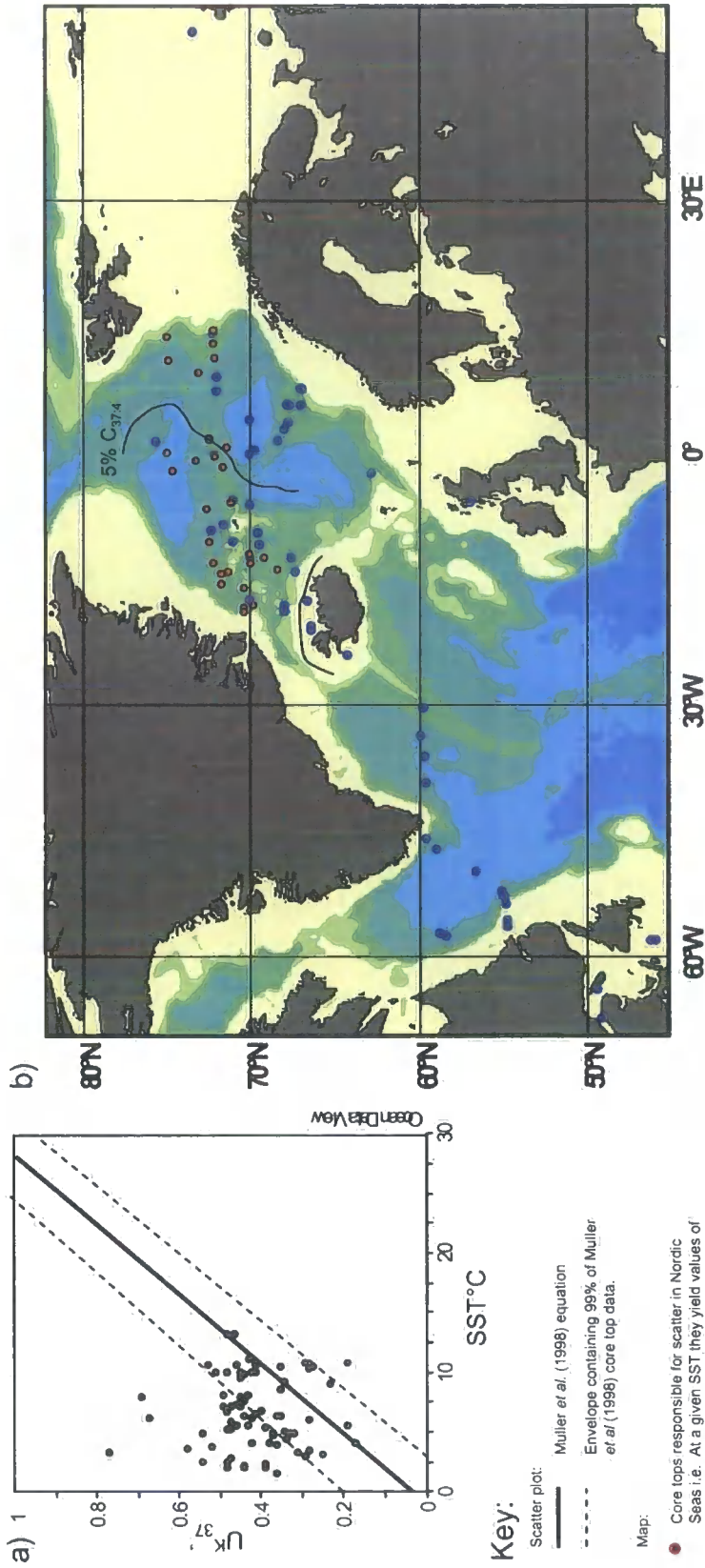


Figure 3.25: Identification (a) and geographic (b) distribution of core-top Nordic Seas samples that create scatter in the U_{37}^K index - relative to Muller et al's (1998) core-top calibration.

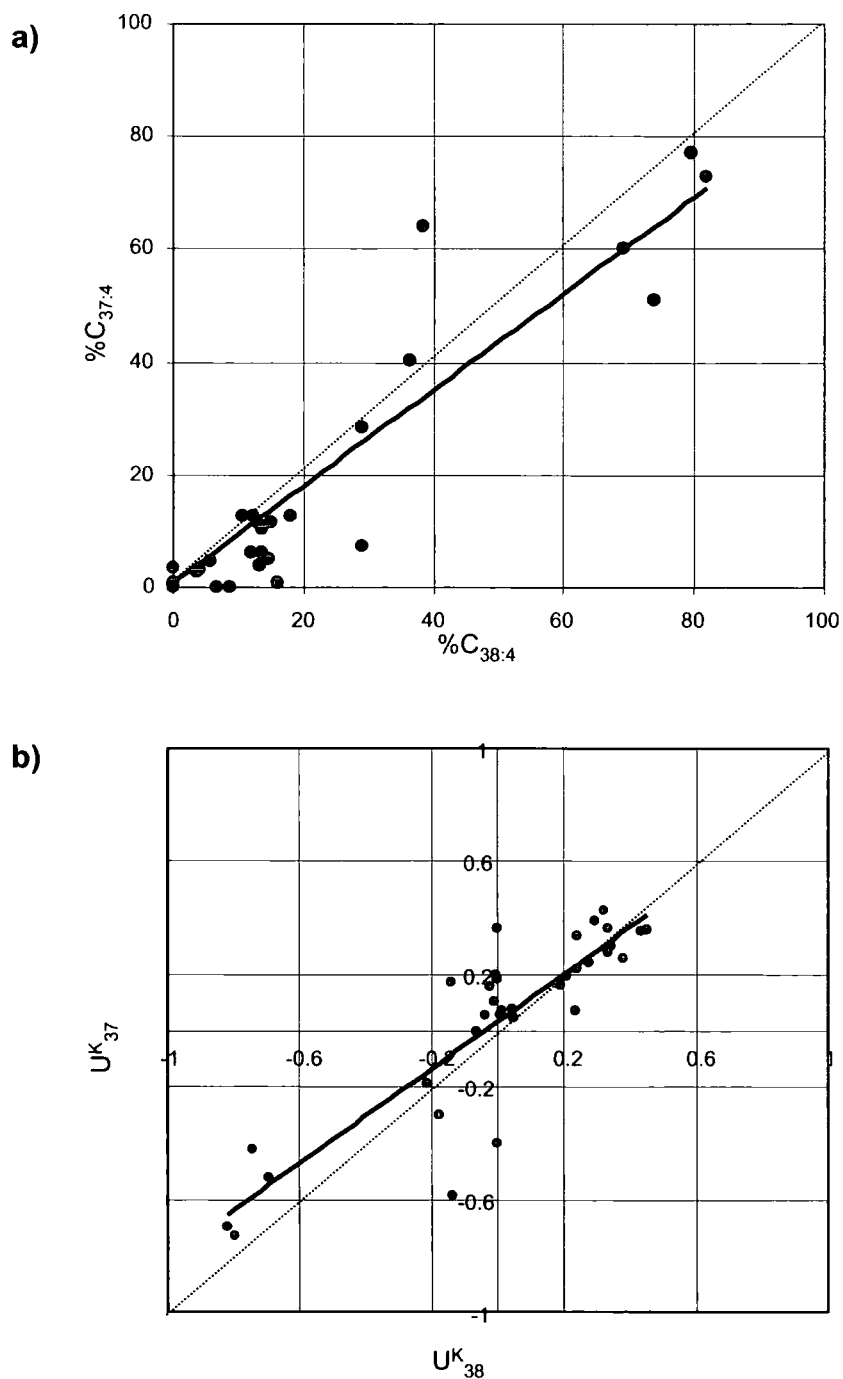


Figure 3.26: a) The $\%C_{37:4}$ index plotted against $\%C_{38:4}$ ¹ b) the U_{37}^K index plotted against U_{38}^K ² for Nordic Seas sea-surface POM samples from this thesis. The solid lines are linear regressions, the dashed lines have been added for illustration purposes.

1) $\%C_{38:4} = (C_{38:4}Et + C_{38:4}Me) / (\Sigma C_{38} \text{ alkenones})$

2) $U_{38}^K = ((C_{38:2}Et + C_{38:2}Me) - (C_{38:4}Et + C_{38:4}Me)) / \Sigma C_{38} \text{ alkenones}$

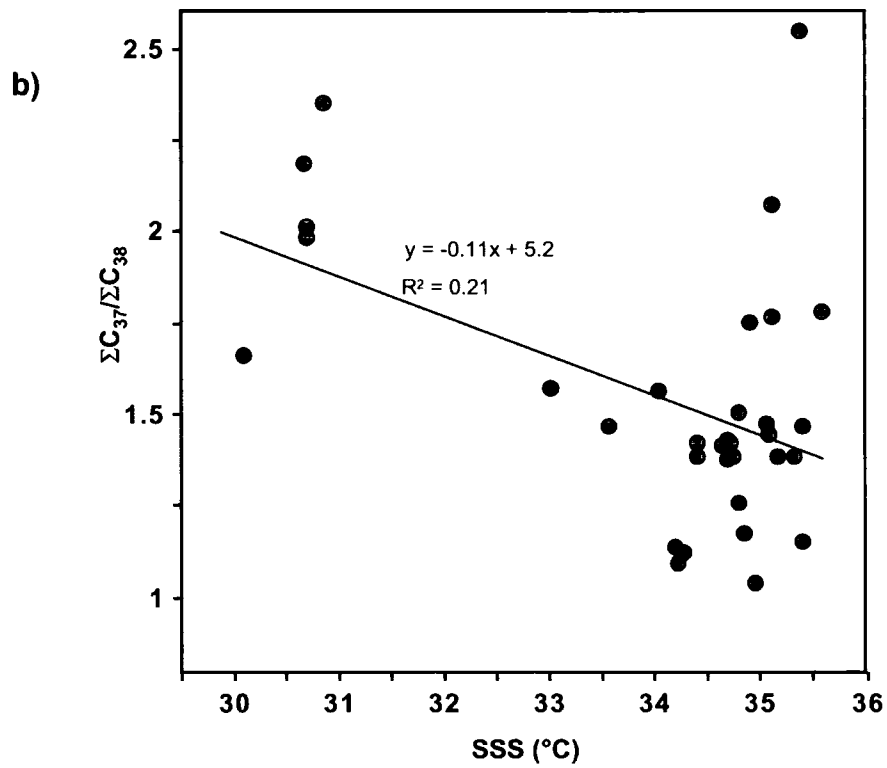
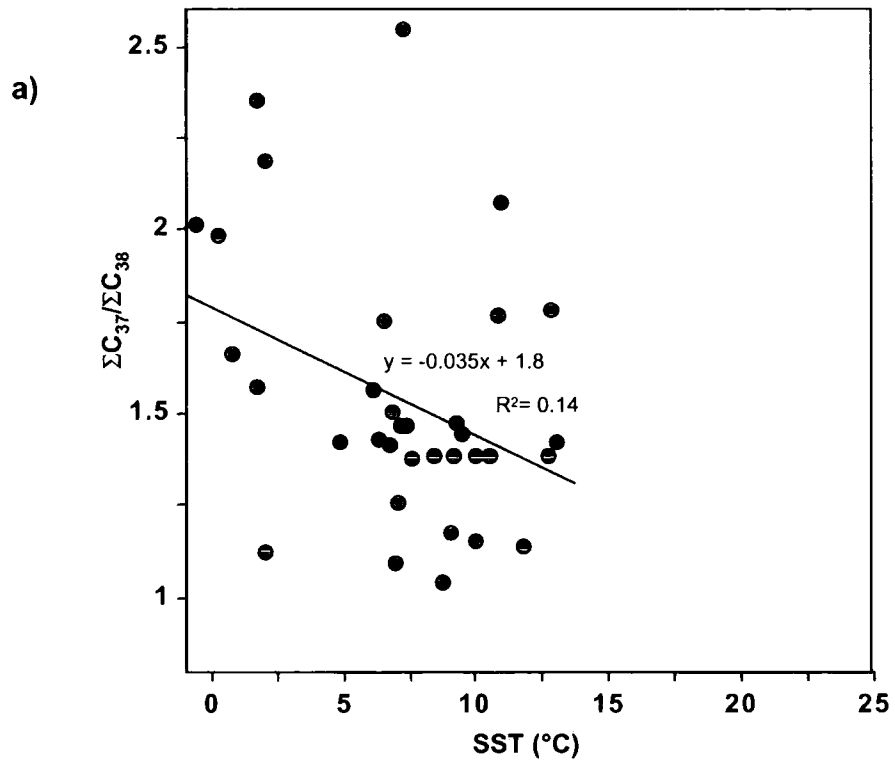


Figure 3.27: Distributions of $\Sigma C_{37}/\Sigma C_{38}$ vs a) SST ($^{\circ}C$) and b) SSS (psu). Lines are liner regressions.

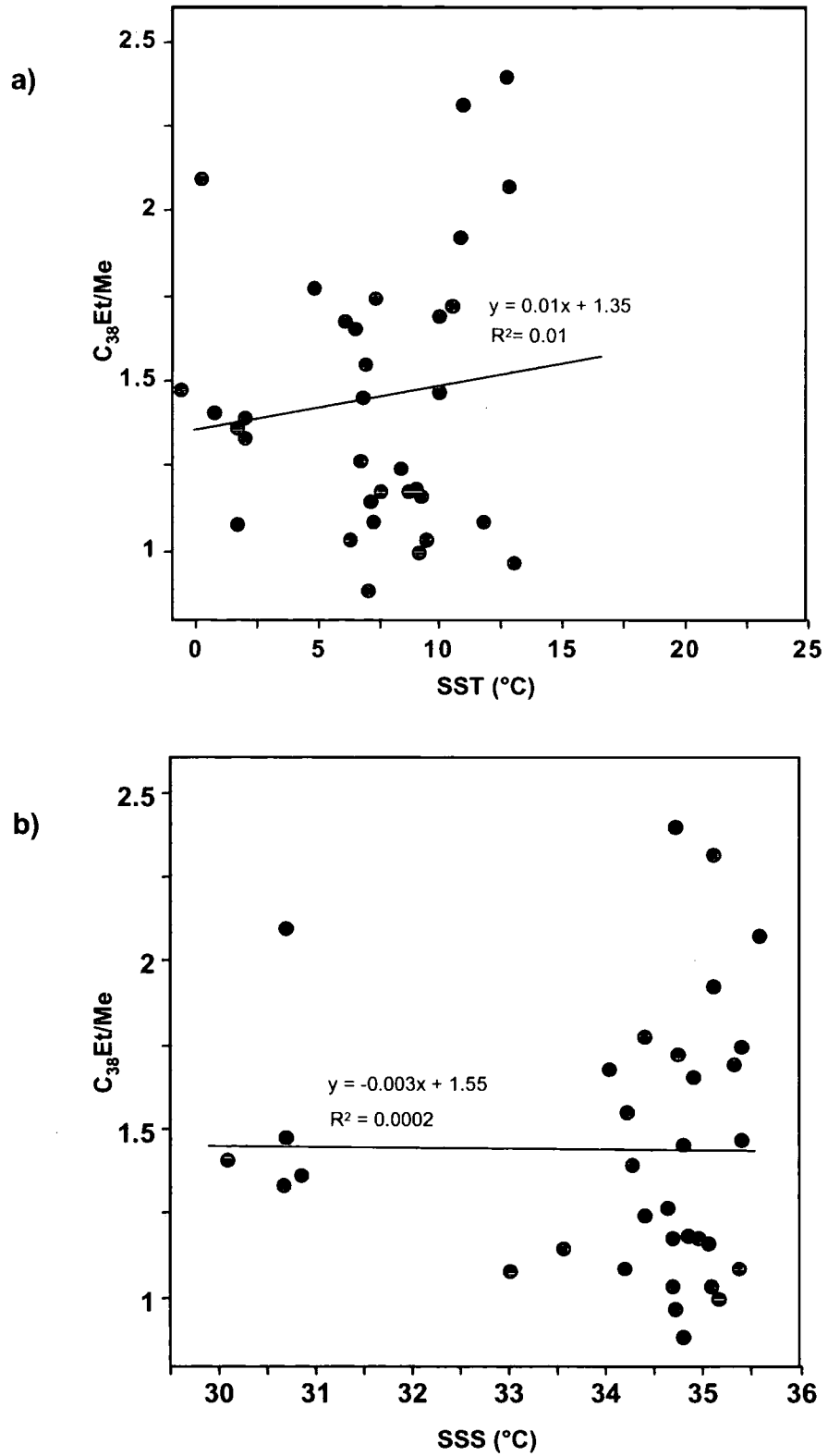


Figure 3.28: Distributions of $C_{38}Et/Me$ vs a) SST (°C) and b) SSS (psu). Lines are linear regressions.

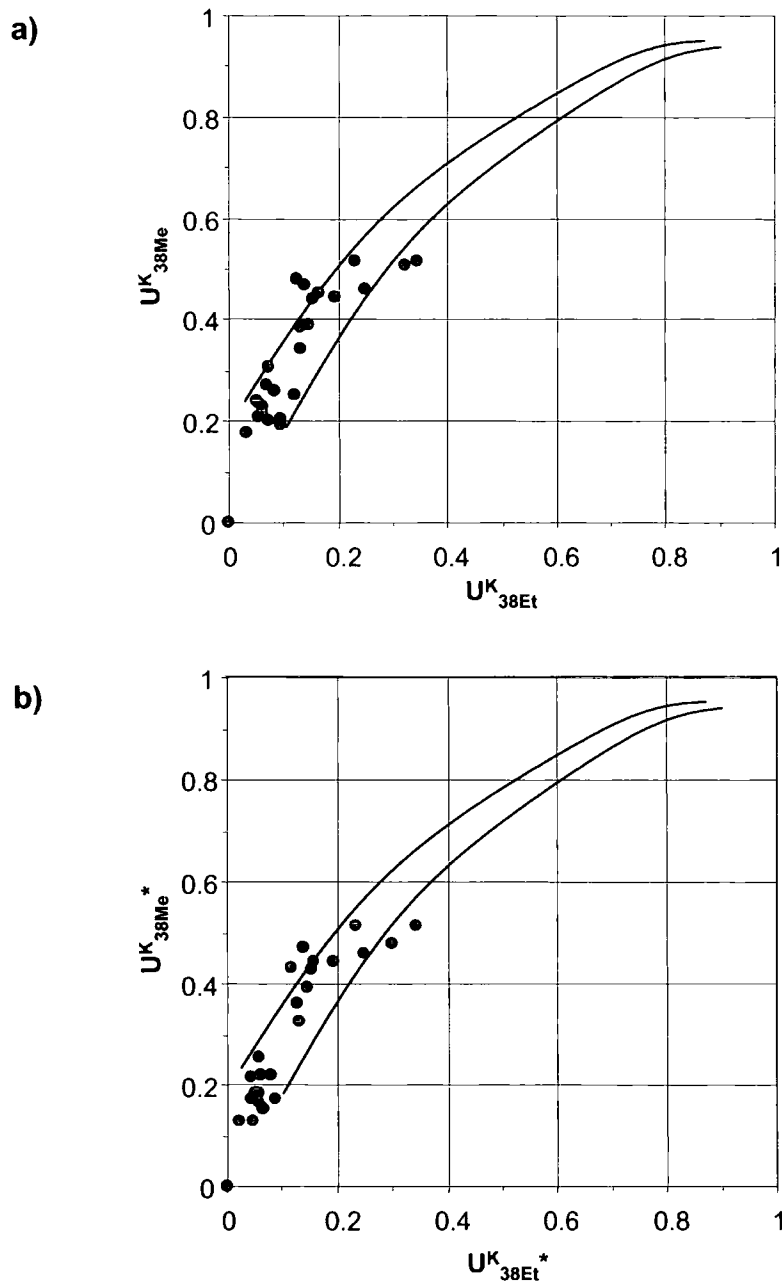
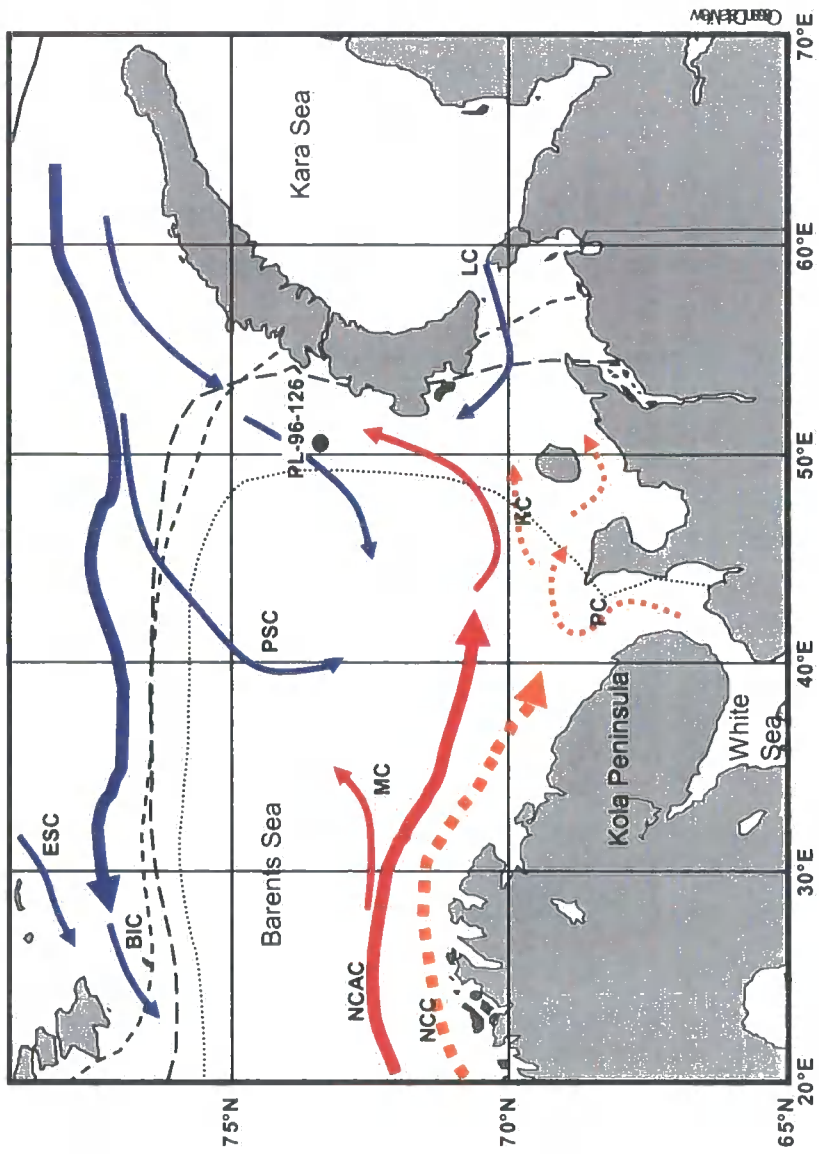


Figure 3.29: Distributions of a) U^K_{38Me} vs U^K_{38Et} b) and $U^K_{38Me}^*$ vs $U^K_{38Et}^*$ (b) for Nordic Seas POM samples. Solid lines are for comparison only and delimit distribution of U^K_{38Me} vs U^K_{38Et} data derived from *E. huxleyi* cultures by Conte *et al* (1998)

Index	Equation
U^K_{38Me}	$= C_{38:2}Me / (C_{38:2}Me + C_{38:3}Me)$
U^K_{38Et}	$= C_{38:2}Et / (C_{38:2}Et + C_{38:3}Et)$
U^K_{38Me}	$= C_{38:2}Me / (C_{38:2}Me + C_{38:3}Me + C_{38:4}Me)$
U^K_{38Et}	$= C_{38:2}Et / (C_{38:2}Et + C_{38:3}Et + C_{38:4}Et)$



Currents:

- ESC: East Spitsbergen current
- BIC: bear Island Current
- NCAC: North Cape Current
- NCC: Norwegian Coastal Current
- PC: Pechora Current
- KC: Kanin Current
- LC: Litke Current
- PSC: Persey Current

- WOD September
Sea Ice 50%+
- - - WOD December
Sea Ice 50%+
- - - - WOD June
Sea Ice 50%+
- WOD March
Sea Ice 50%+

Figure 3.30: Location of core PL-96-126, major currents systems and sea-ice averages for the Barents Sea. Red arrows show Atlantic water flow. Blue & orange arrows indicate flows of polar, coastal water masses respectively. Source: Johannesssen (1986), WOD-CD (1998)

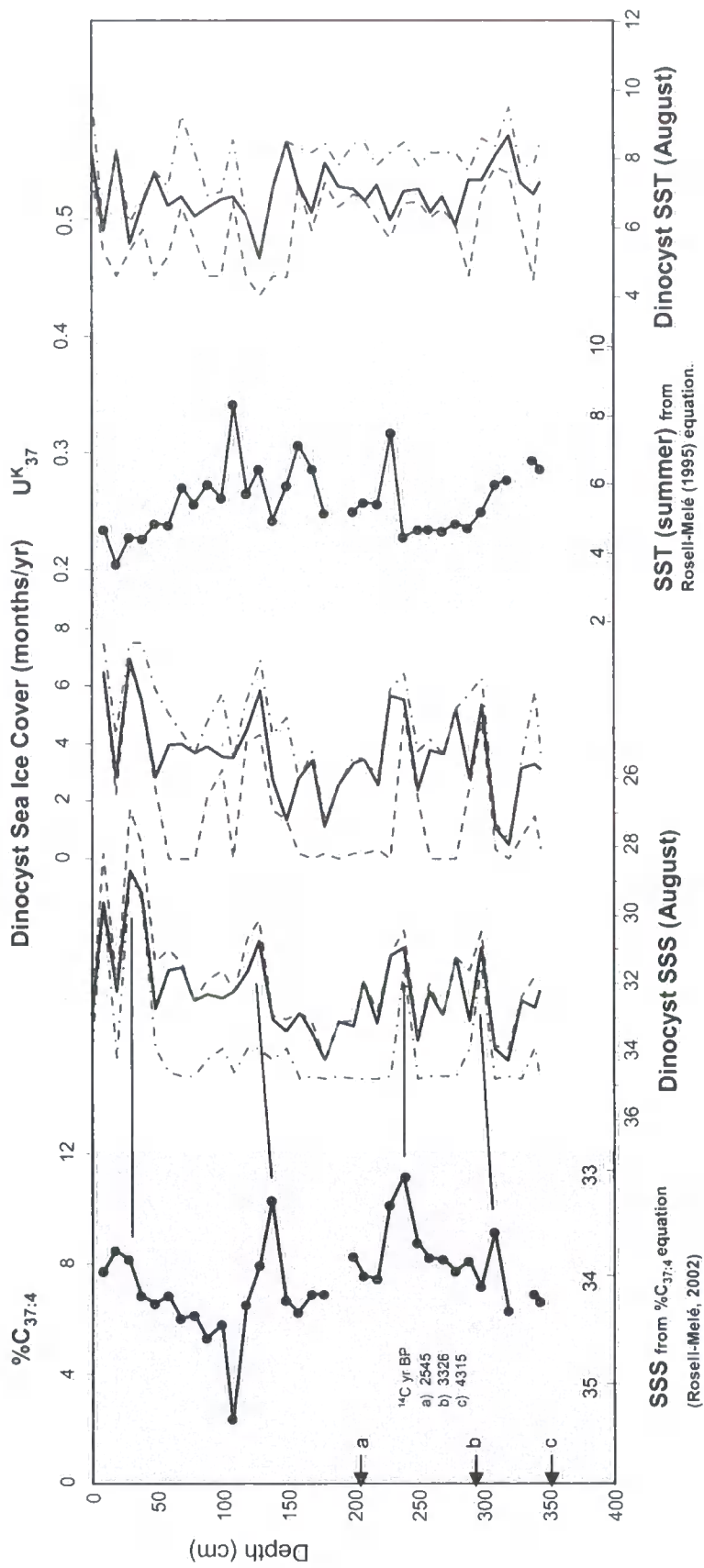


Figure 3.31: Comparison of alkenone indices with reconstruction of sea-surface conditions from dinocyst assemblages in Core PL-96-126 against depth in core. Alkenone data is underlined in grey – dinocyst in white. For dinocyst proxies the solid lines represent the most probable reconstructed values (weighted averages of the 10 best analogues) within a confidence interval delimited by minimum(dashed lines) and maximum (dash-dot lines) values.

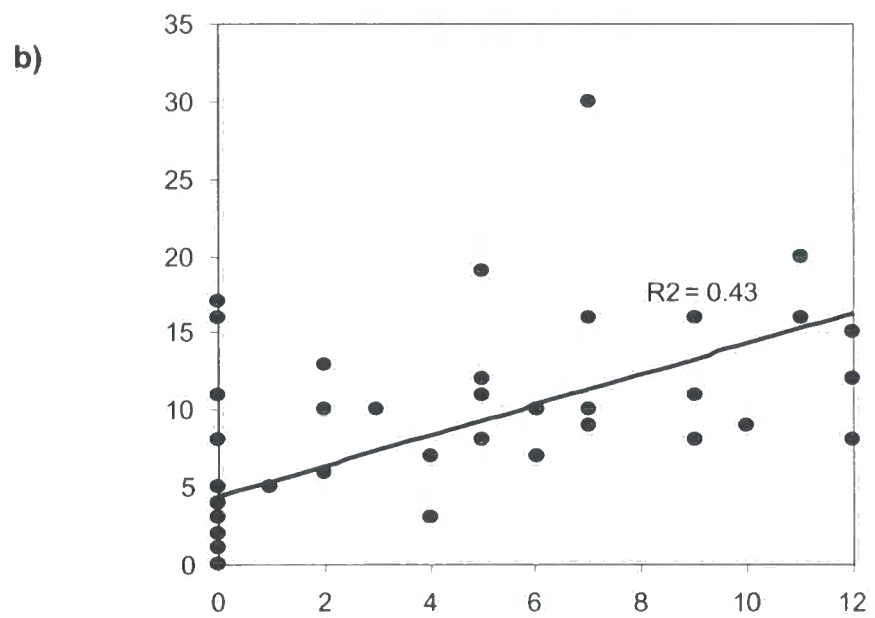
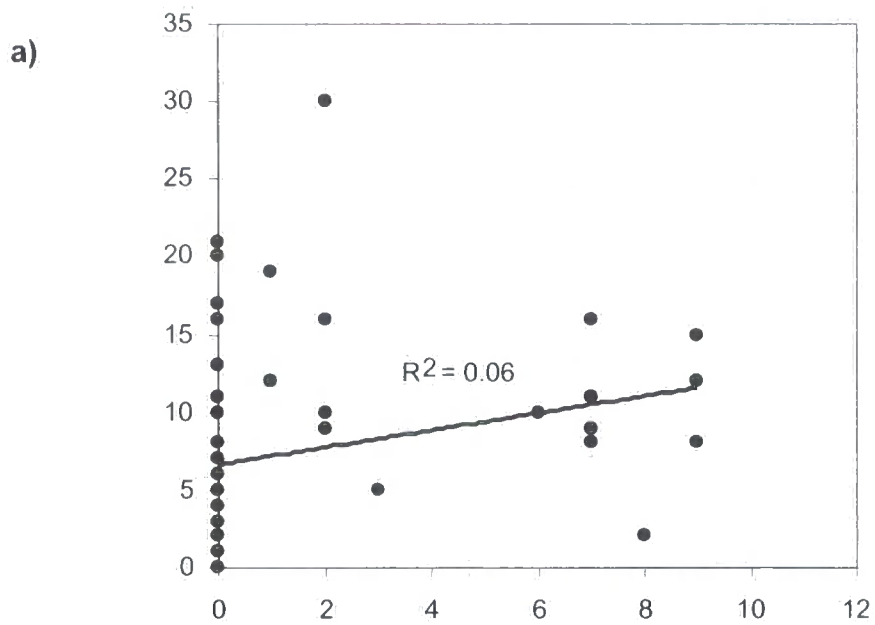


Figure 3.32: Distributions of %C_{37:4} in Nordic Seas core-tops vs 50% sea ice cover (a) and 20% sea ice cover (b). Sea ice cover is months/yr from WOD-98.

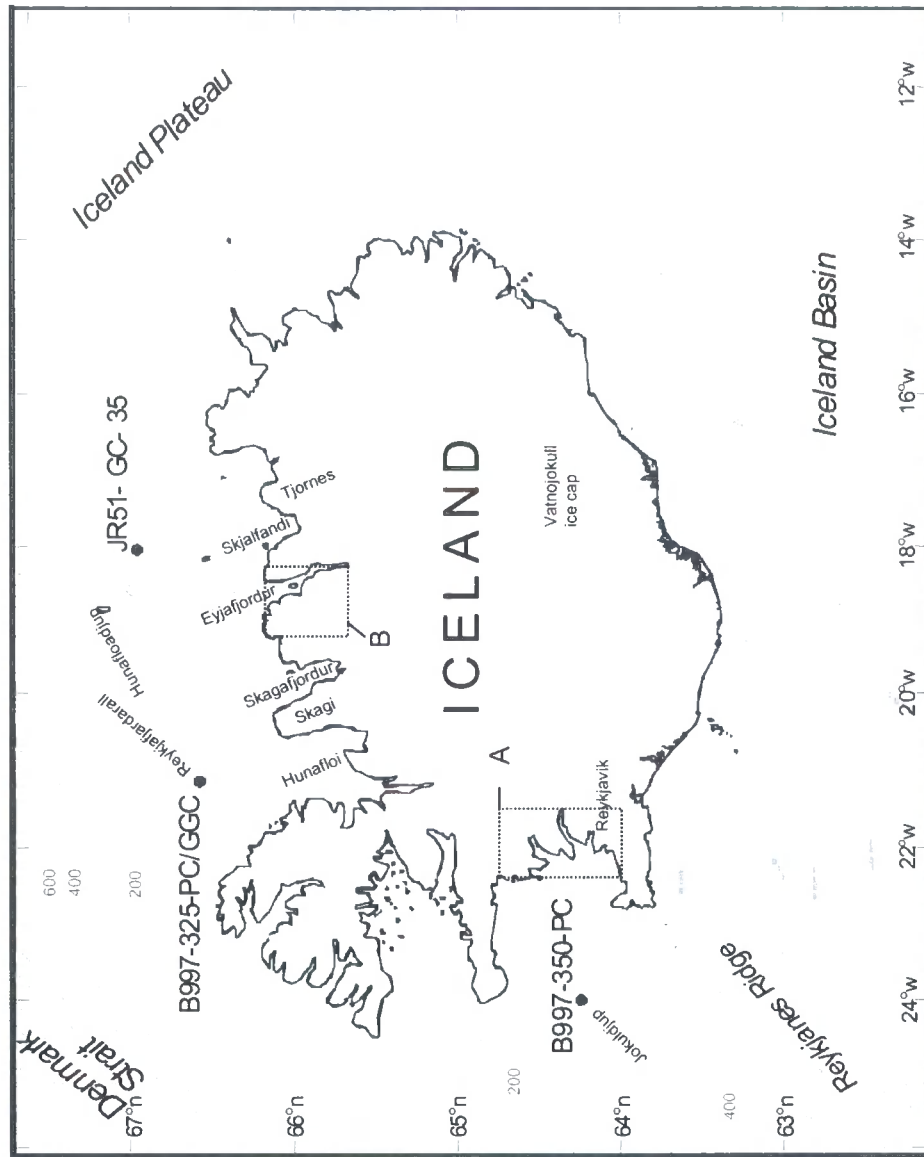


Figure 4.1: Location of Icelandic core sites and regional bathymetry. A) Field region of Ingólfsson et al. (1997) for Late-Glacial – Holocene reconstructions of ice-front oscillations B) Field region of Stötter et al. (1999) for Holocene palaeoclimatic reconstructions based on glacial moraine complexes – referred to in text and Figure 4.9.

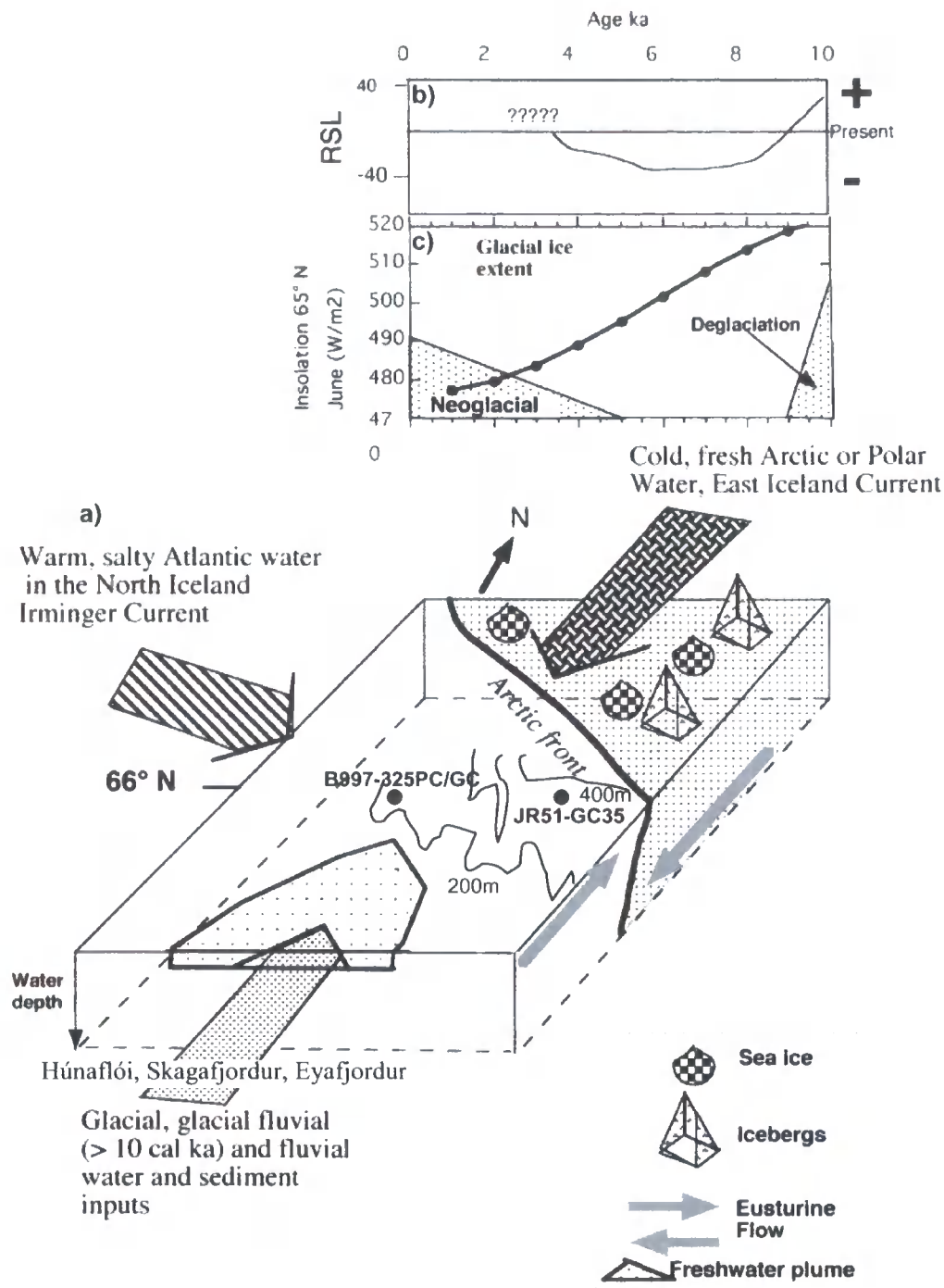


Figure 4.2: Schematic description of the environment of the N. Iceland shelf showing the major controlling variations in sediment, isotope and biota on the N. Iceland shelf (adapted from Andrews and Giraudeau (2003)). The cores are in positions where variations in local run-off, incursions of Polar or Arctic water (with sea ice and icebergs), and changes in the advection of the Atlantic water have varied over the last 10 cal ka (fig 4.2a). Calving glaciers still remained on the Northwest Peninsula until 10 cal kyr BP (fig 4.2c). During the last 10 cal kyr insolation at high northern latitudes decreased with renewed glaciation over the last 5 cal kyr (fig. 4.2b) (Stotter *et al.*, 1999). Relative sea level fell to present sea level by 9-10 cal kyr and then fell another 40m or more (fig. 4.2b).

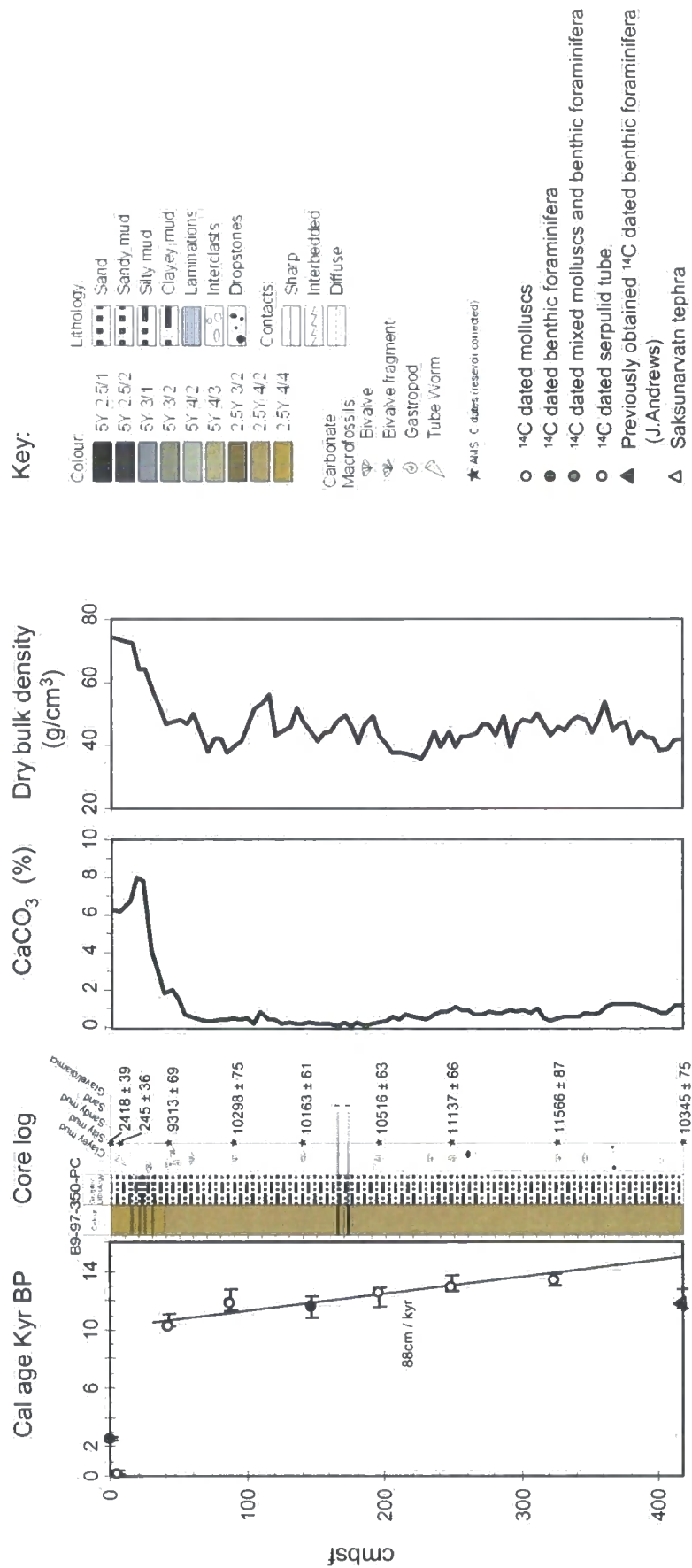


Figure 4.3: Calibrated radiocarbon dates plotted against depth, lithofacies log and selected physical properties in core B997-350-PC. Selected dates are fitted to a linear regression (see text and table 4.2).

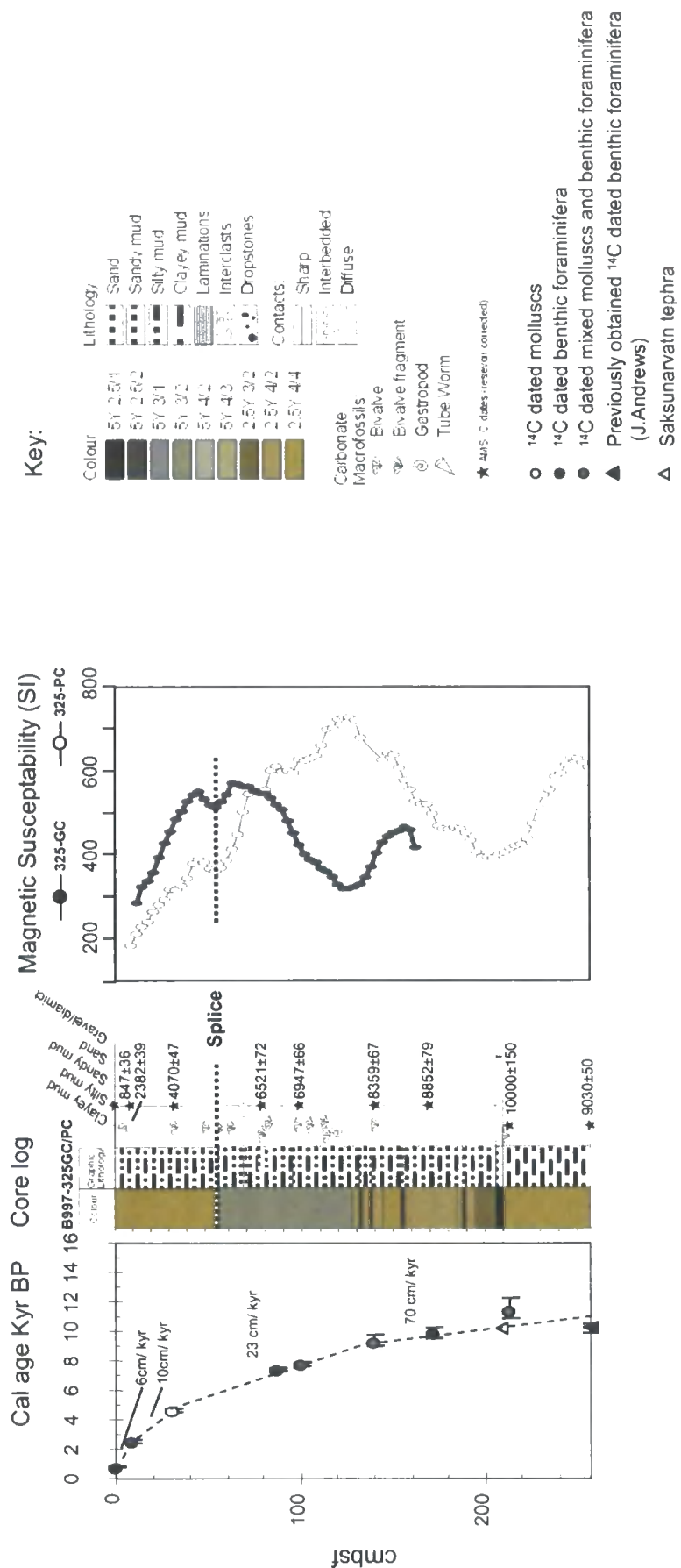


Figure 4.4: Calibrated radiocarbon dates plotted against depth, lithofacies log and selected physical properties in core B997-325GC/PC. Selected dates are fitted to linear regressions (see text and table 4.2).

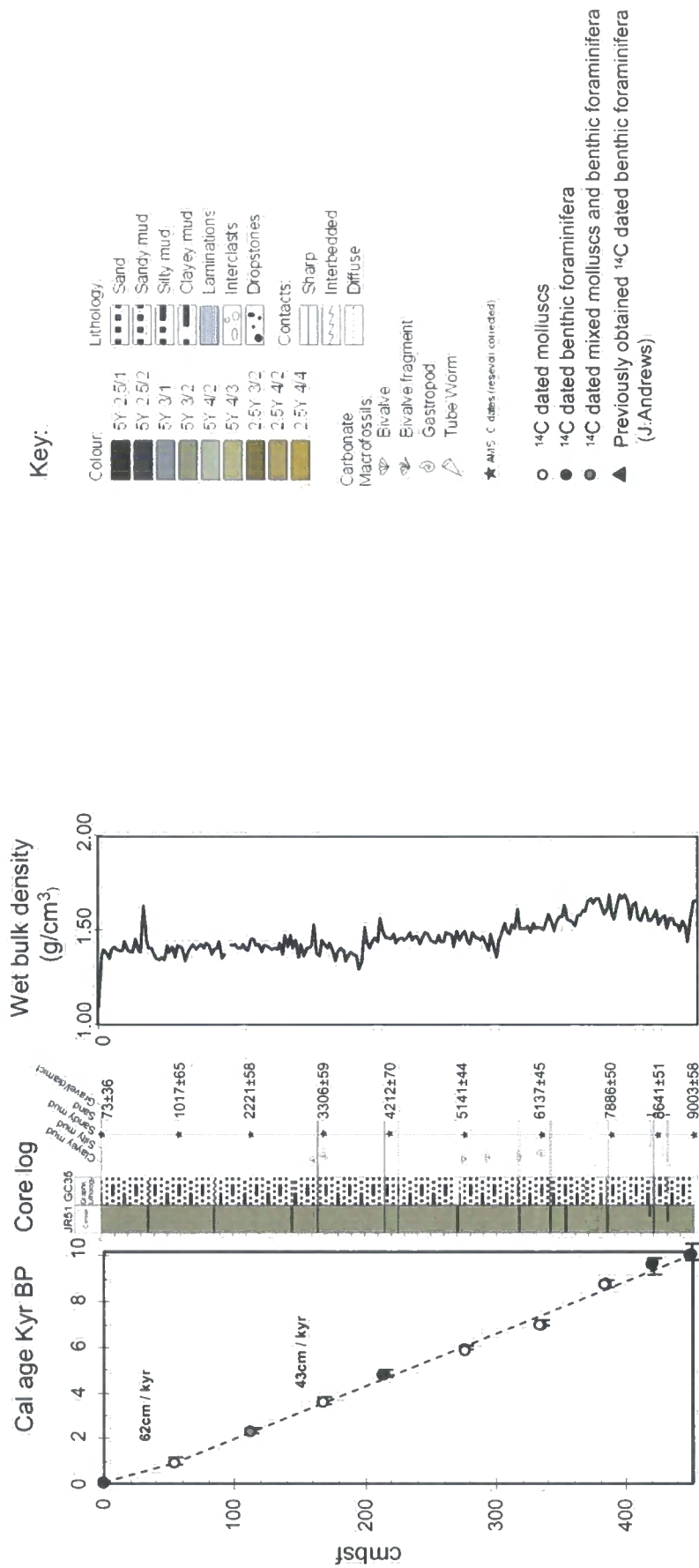


Figure 4.5: Calibrated radiocarbon dates plotted against depth, lithofacies log and selected physical properties in core JR51-GC35. Selected dates are fitted to linear regressions (see text and table 4.2).

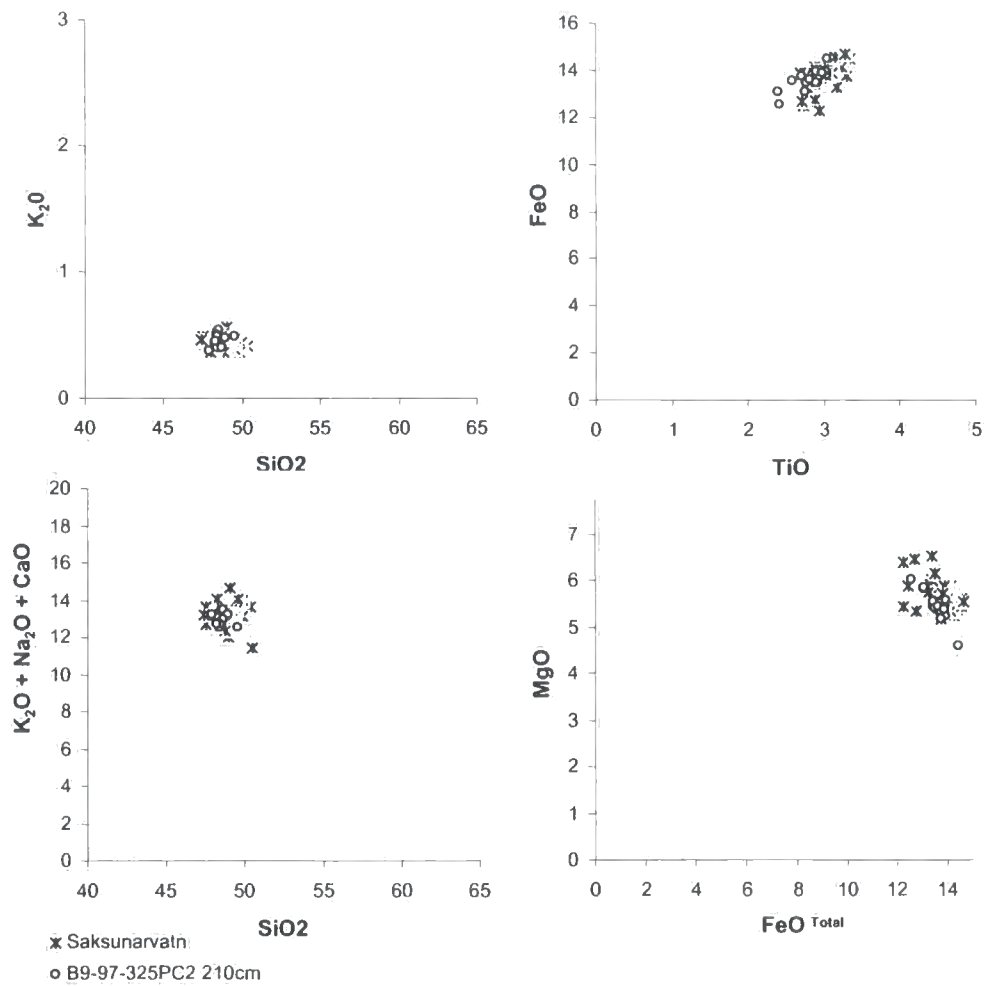


Figure 4.6: Bi-plots of major oxide measurements (%) made on basaltic tephra from B9-97-325-PC2 207cm and previously identified samples of Saksunarvatn tephra. The Saksunarvatn data mark the geochemical distributions from two studies (Dugmore and Newton, 1997; Wastegard *et al*, 2001). These data were preferred for use as a comparison because the measurements were made using the same equipment and standards, thus minimising systematic bias.

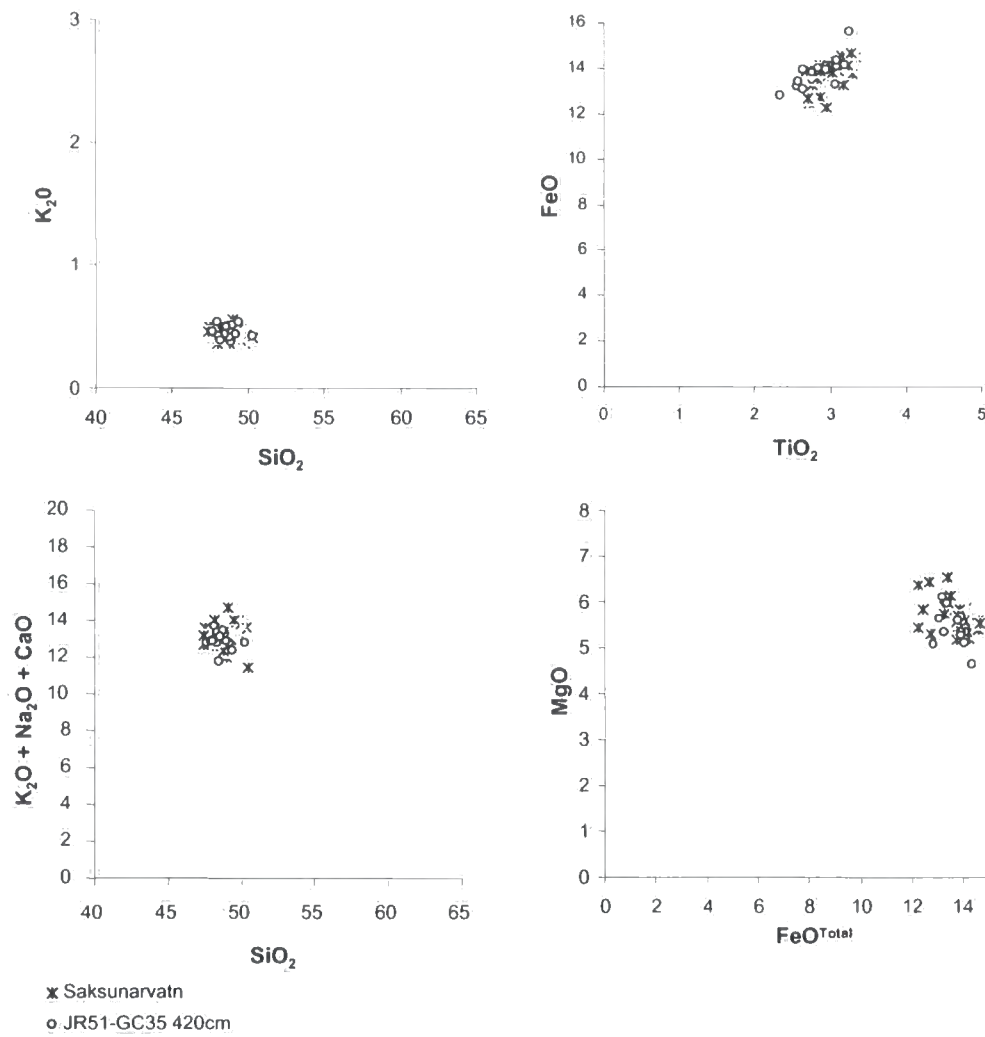


Figure 4.7: Bi-plots of major oxide measurements (%) made on basaltic tephra from JR51-GC35 420cm and previously identified samples of Saksunarvatn tephra (sample from 430cm gave identical results). The Saksunarvatn data mark the geochemical distributions from two studies (Dugmore and Newton, 1997; Wastegard *et al.*, 2001). These data were preferred for use as a comparison because the measurements were made using the same equipment and standards, thus minimising systematic bias.

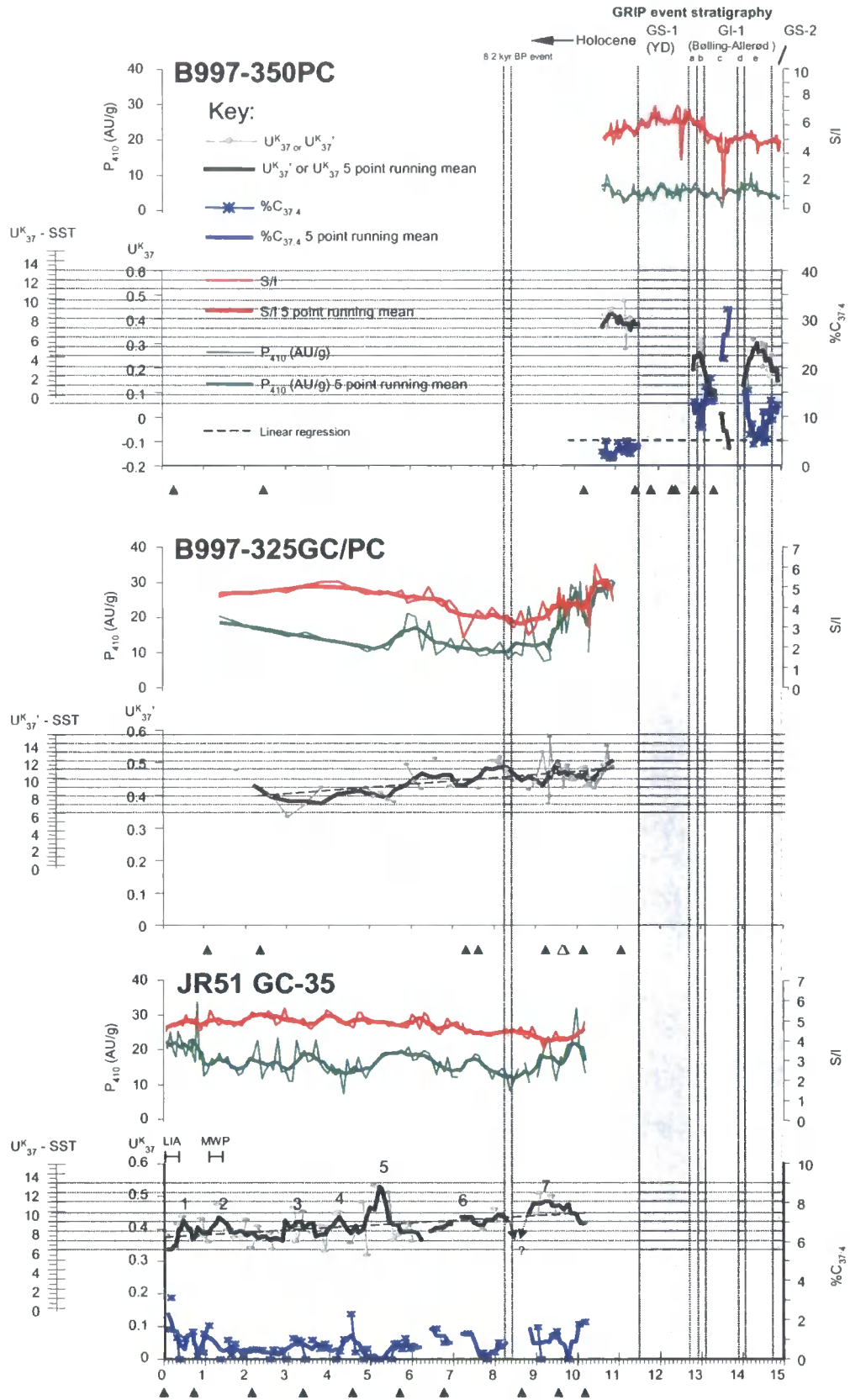


Figure 4.8: Biomarker records plotted versus calendar age for Icelandic shelf cores. \blacktriangle Indicates the AMS ^{14}C dates and Δ shows the age of the Saksunarvatn tephra layer. Grey background indicates cold stadial episodes in GRIP ice-core. Labelled peaks in B997-325-GC/PC and JR51-GC35 were used to estimate event pacing.

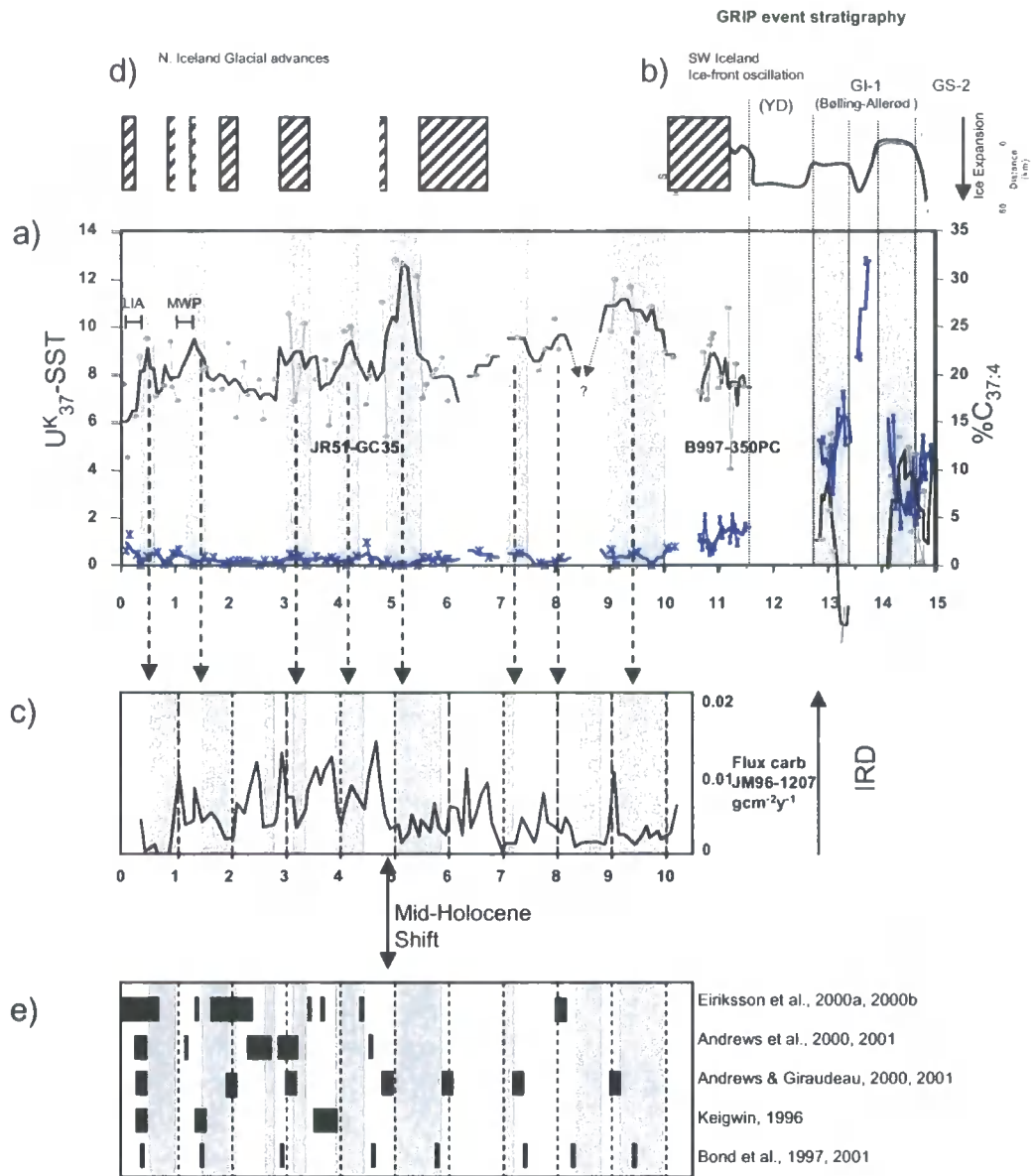


Figure 4.9: Comparison of UK₃₇-SST's from B997-350 & JR51-GC51 with Late-Glacial and Holocene palaeo-environmental records from North Atlantic western Nordic Seas. a) UK₃₇-SST's and %C_{37:4} records from the north and west Icelandic shelf (this thesis), coolings are demarcated as white areas, warmer periods as grey. b) Glacier advances in Northern Iceland, (Stotter *et al.*, 1999). c) Record of IRD intensity from the East Greenland Shelf (Jennings *et al.*, 2002). d) Ice front oscillation in SW Iceland (Ingolfsson *et al.*, 1997). e) Summary of inferred coolings (demarcated in black, superimposed on background derived from Jennings *et al.*, 2002, IRD record) from various marine cores from N. Iceland (Andrews & Giraudeau, 2000, 20001; Andrews *et al.*, 2000, 2001; Eiriksson, *et al.* 2000a, 2000b) off Ireland (Bond *et al.*, 1997) and on the Bermuda rise (Keigwin, 1996). Records are aligned by calendar age BP (not ¹⁴C age).

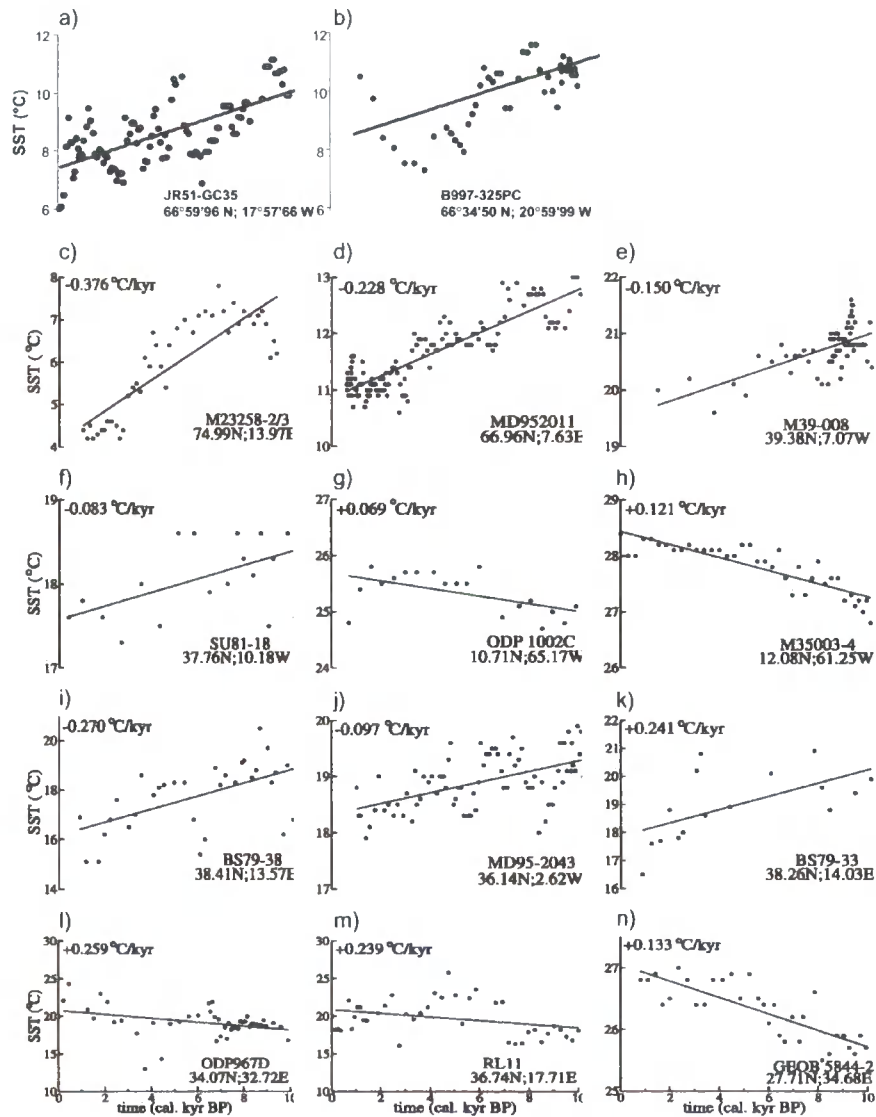
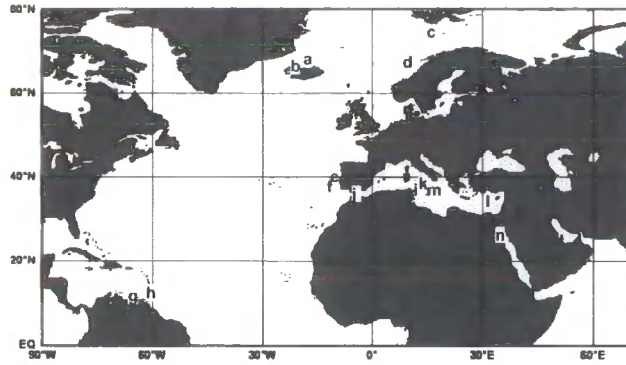


Figure 4.10: Comparison of alkenone-SST Holocene trend lines from cores B997-325GC/PC and JR51-GC35 (graphs a,b) with data from Rimbu et al. (2003) (graphs c to m). Geographic location of SST trend lines are indicated in the map.

Location map illustrating core locations and position of main modern surface circulation currents.

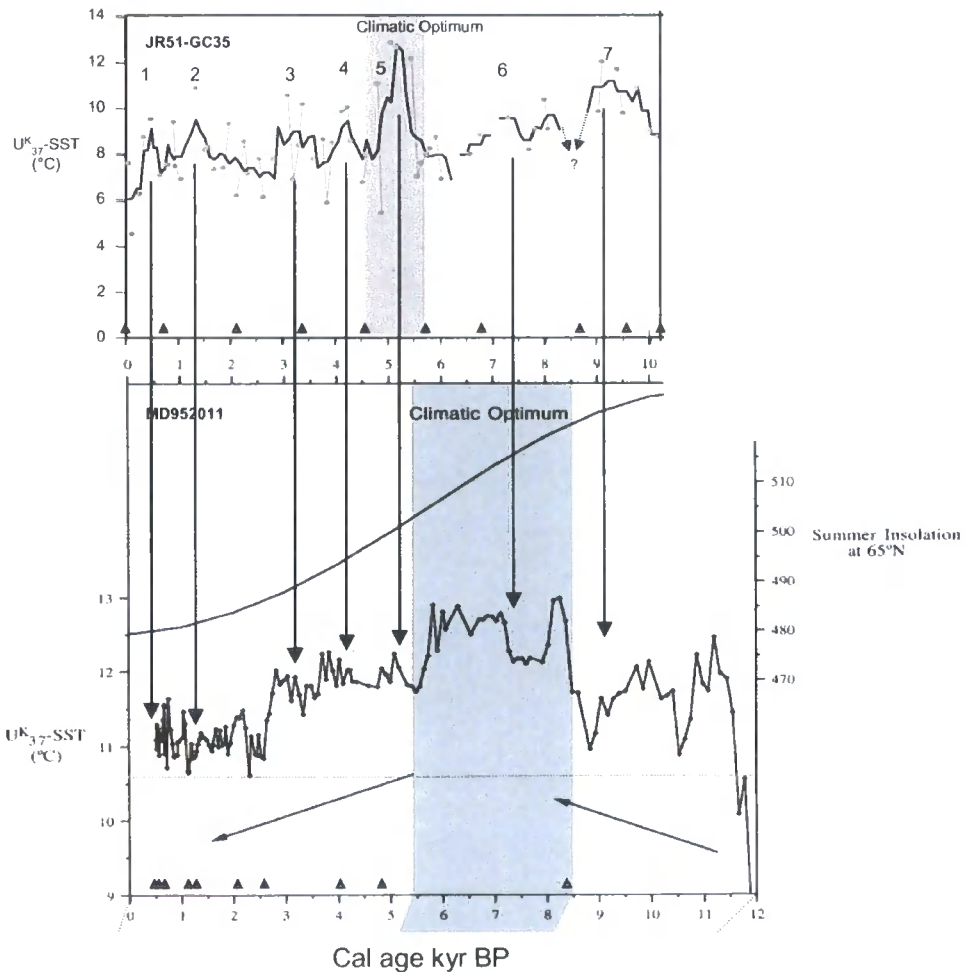
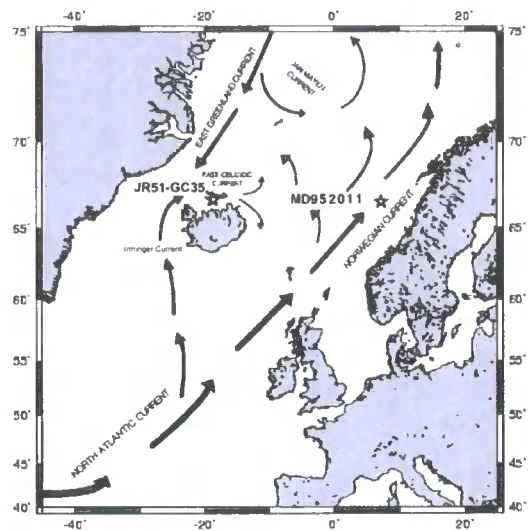


Figure 4.11: Comparison of Holocene UK_{37}^{K} -SST records from the north Icelandic Shelf (JR51-GC35) and the Norwegian Sea (MD952011).

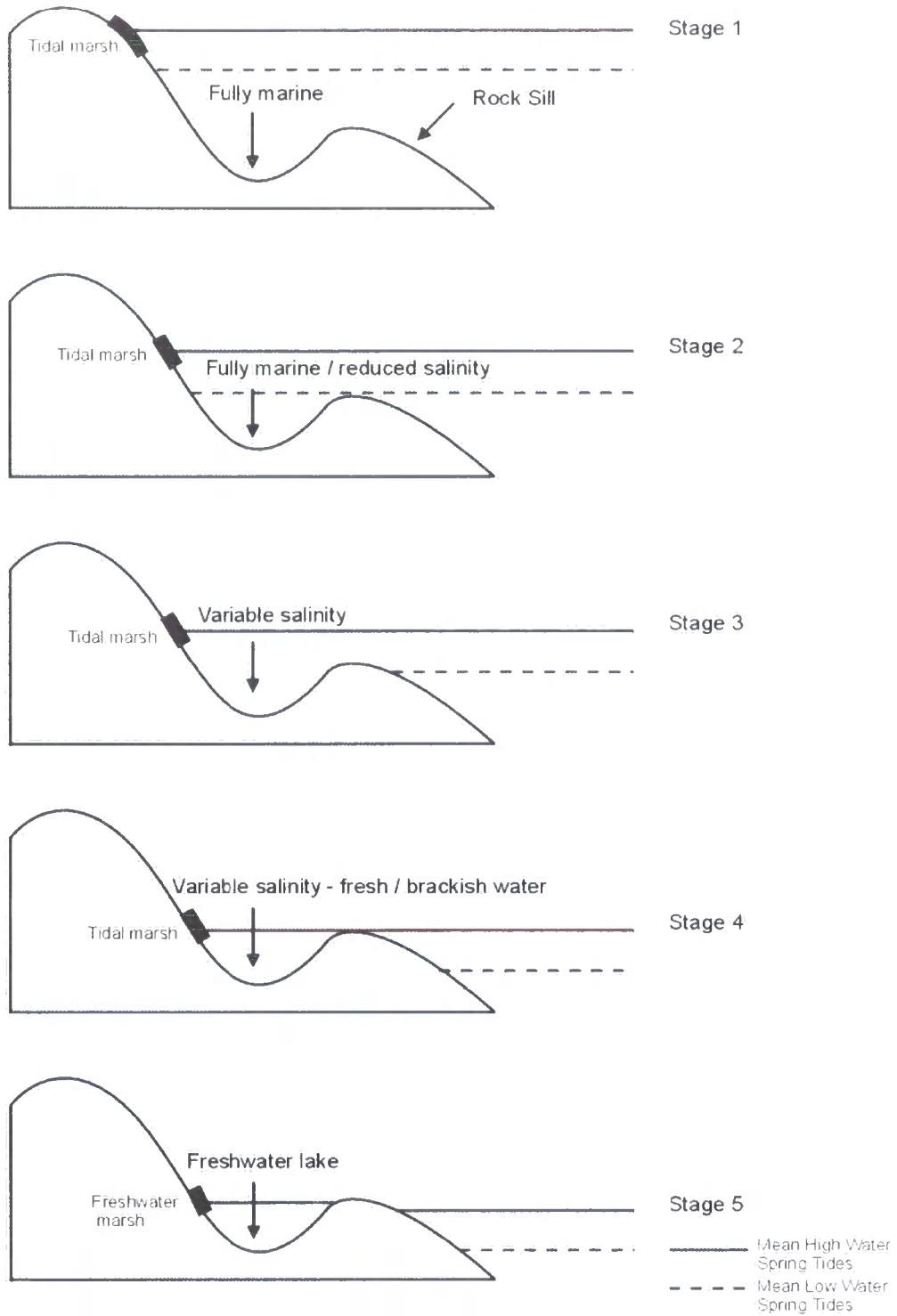


Figure 5.1: Schematic representation of an isolation basin during a fall in relative sea-level (adapted from Shennan et al., 1996). Stages 1-5 correspond with the sequence outlined in Figure 5.2.

Biological Assemblage

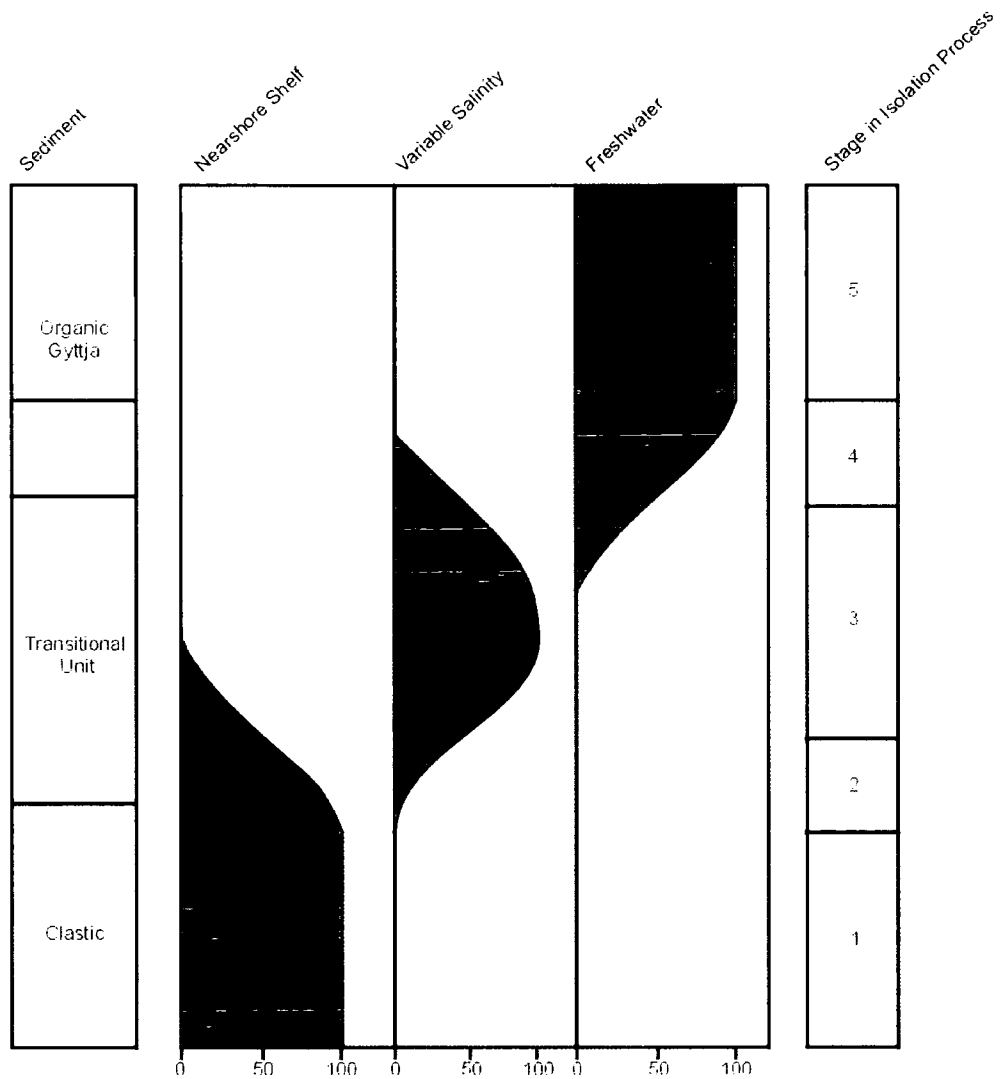


Figure 5.2: Conceptual model of biological assemblage change during the isolation process. The biological assemblage diagram in the centre shows the up-core transition from marine through brackish, to freshwater species. The column on the left indicates the typical sediment types associated with water environment. The column on the right indicates the RSL stage of the basin from as illustrated in Figure 5.1.

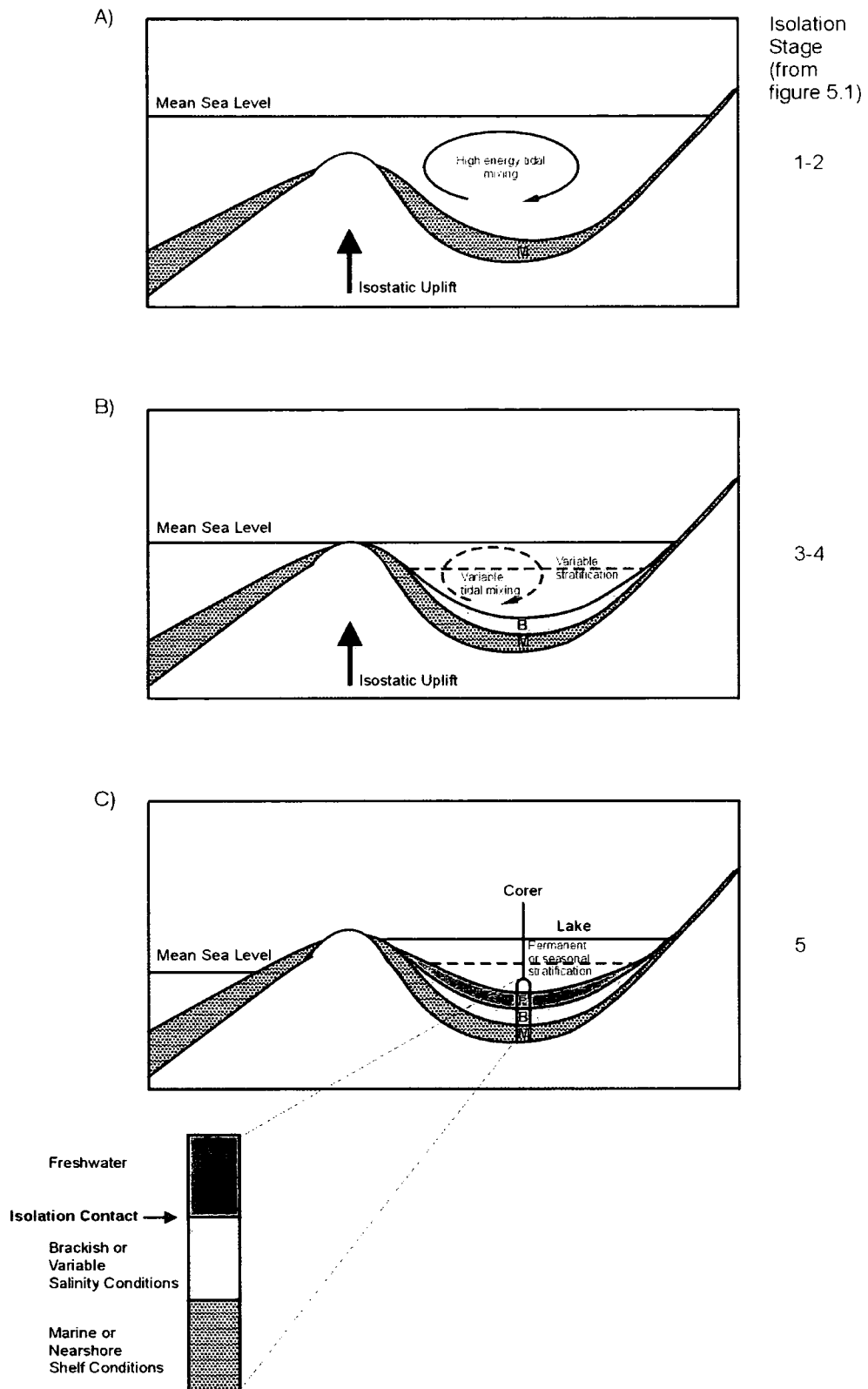


Figure 5.3: Schematic representation of the hydrological and depositional conditions in an isolation basin. Three major depositional stages are illustrated, the corresponding isolation stages from figure 5.1 is also indicated. Adapted from (Kjemperud, 1981).

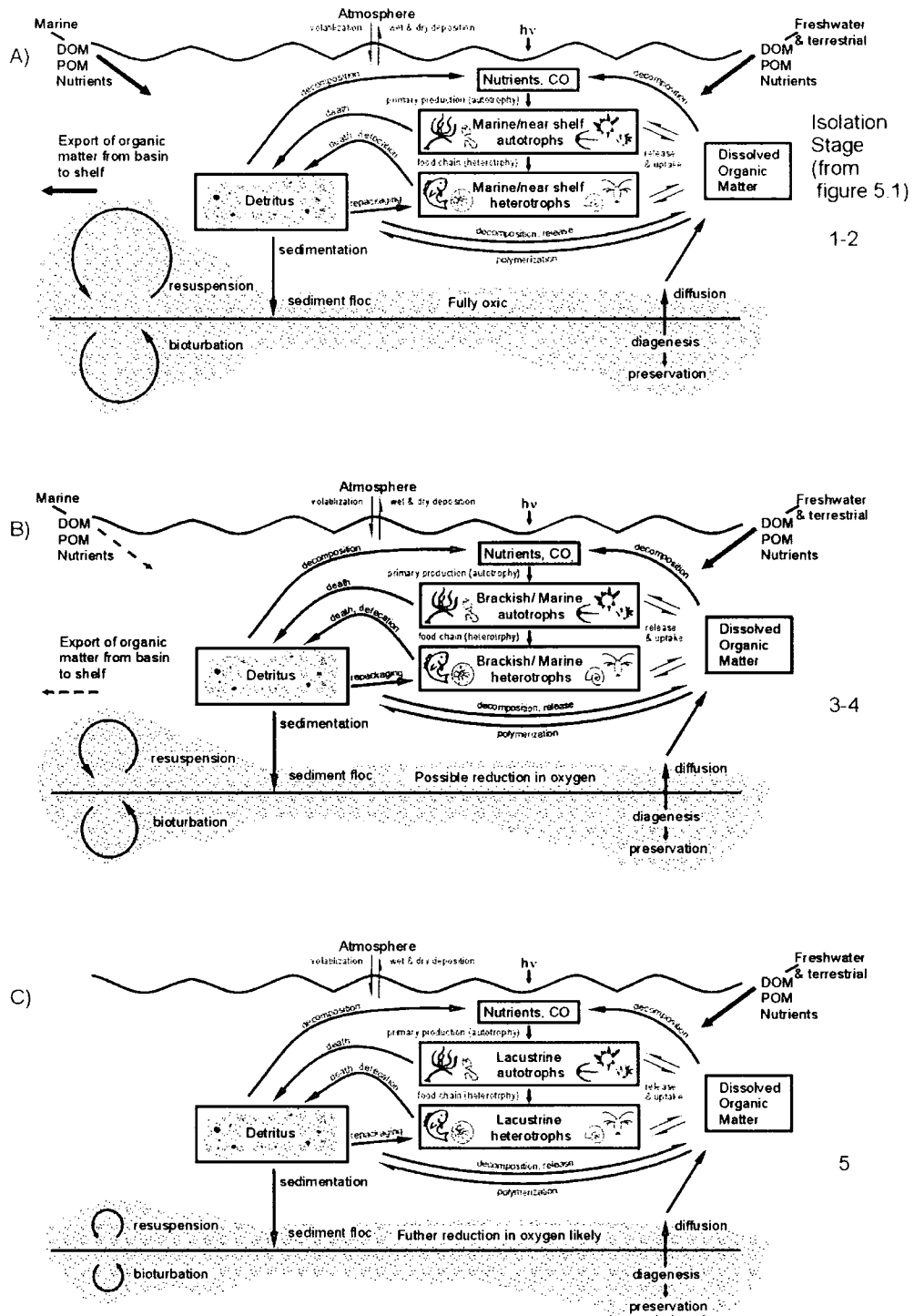


Figure 5.4: Schematic representation of the organic matter cycle in an isolation basin. Three stages are illustrated which correspond to the depositional & hydrological stages (a, b & c) illustrated in figure 5.4. The corresponding isolation stages from figure 5.1 are also indicated. DOM, dissolved organic matter; POM, particulate organic matter.

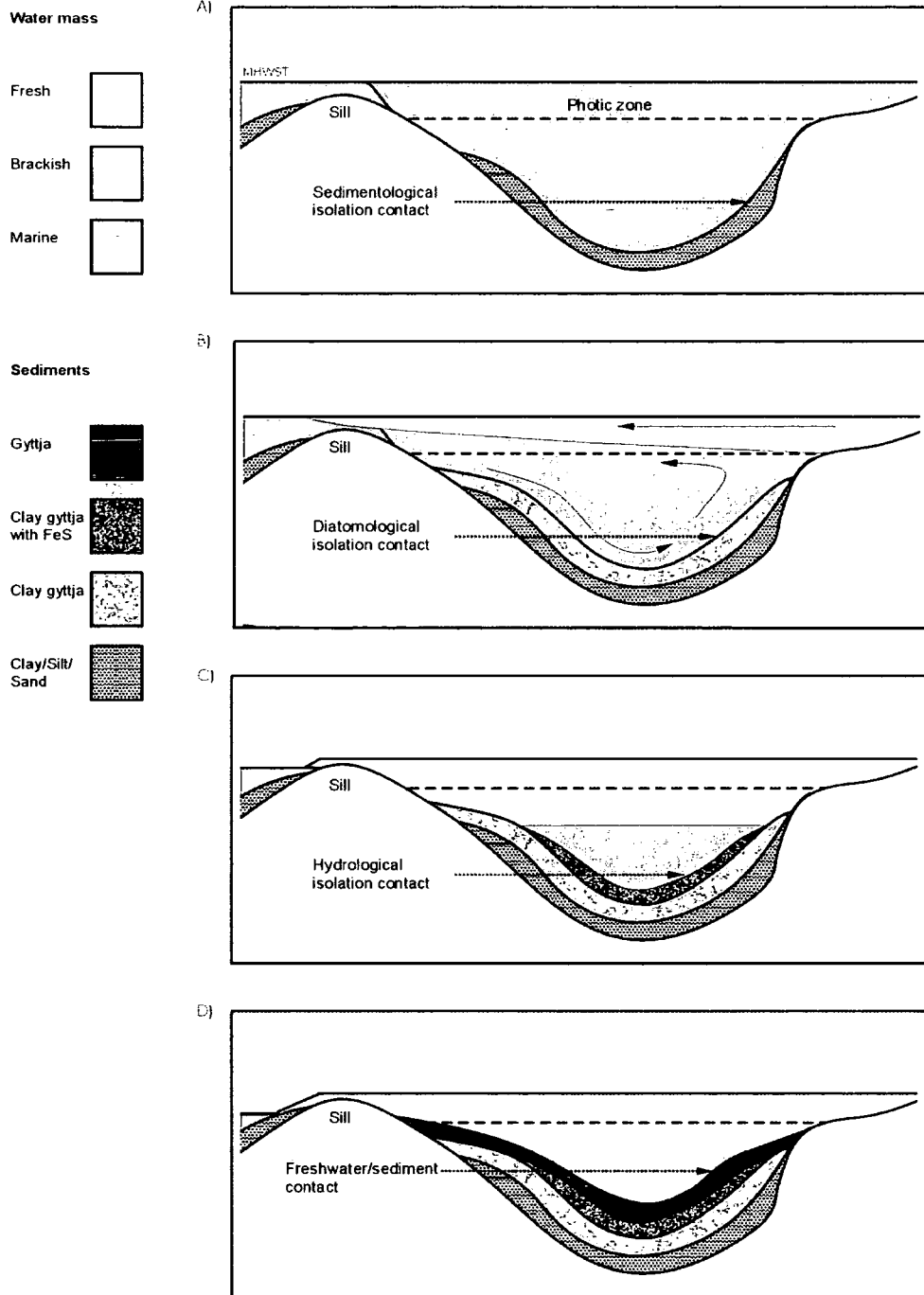


Figure 5.5: Four isolation contacts. A) Sedimentological, B) diatomological/phytological, C) hydrological and D) the freshwater/sediment interface. The latter is rare, other than in deep, well mixed basins. MHWST is Mean High Water Spring Tides (after Kjemperud 1986).

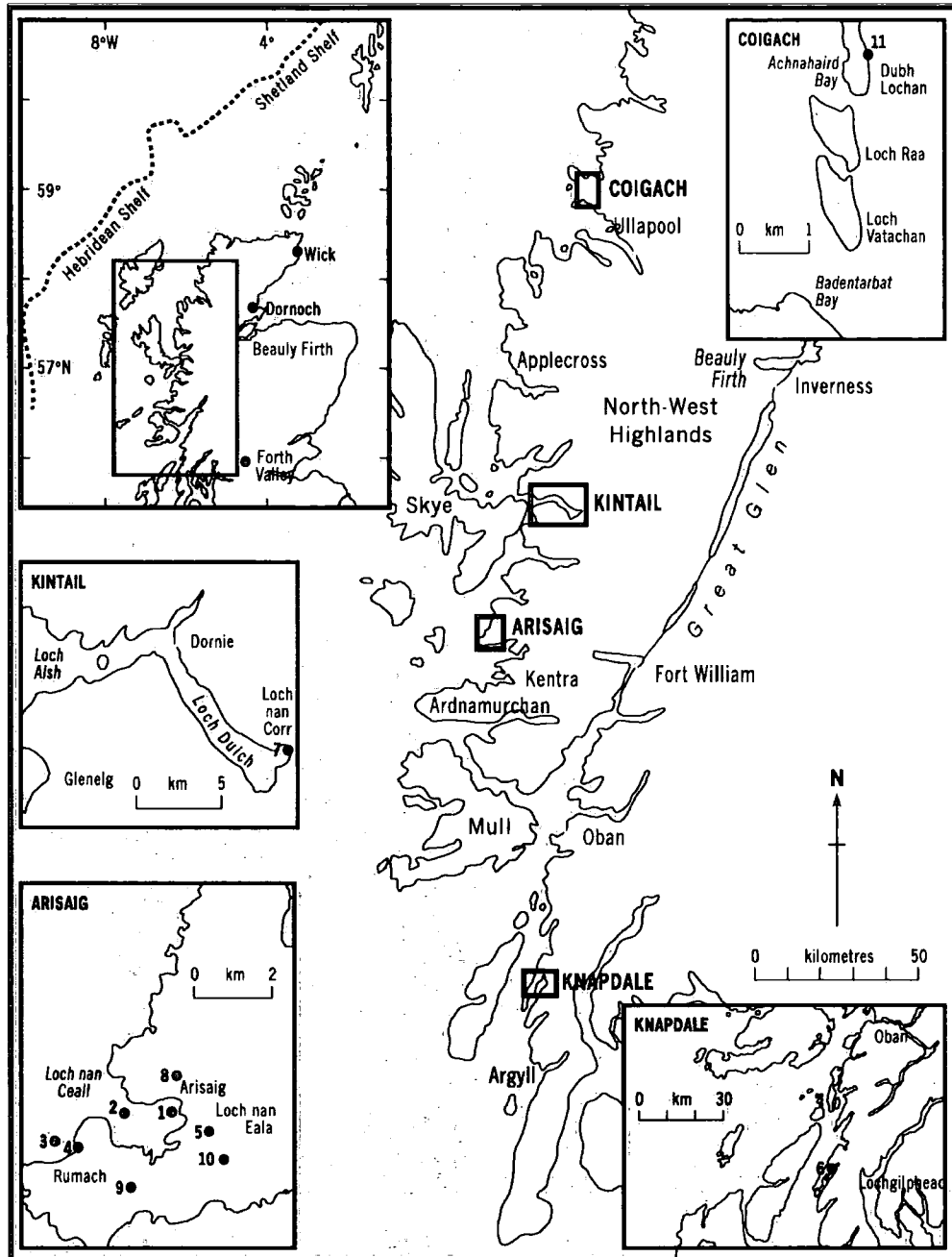


Figure 5.6: Location map of the field study region. Insets show locations of the study areas with the individual sites indicated (see tables 5.2 & 5.3).

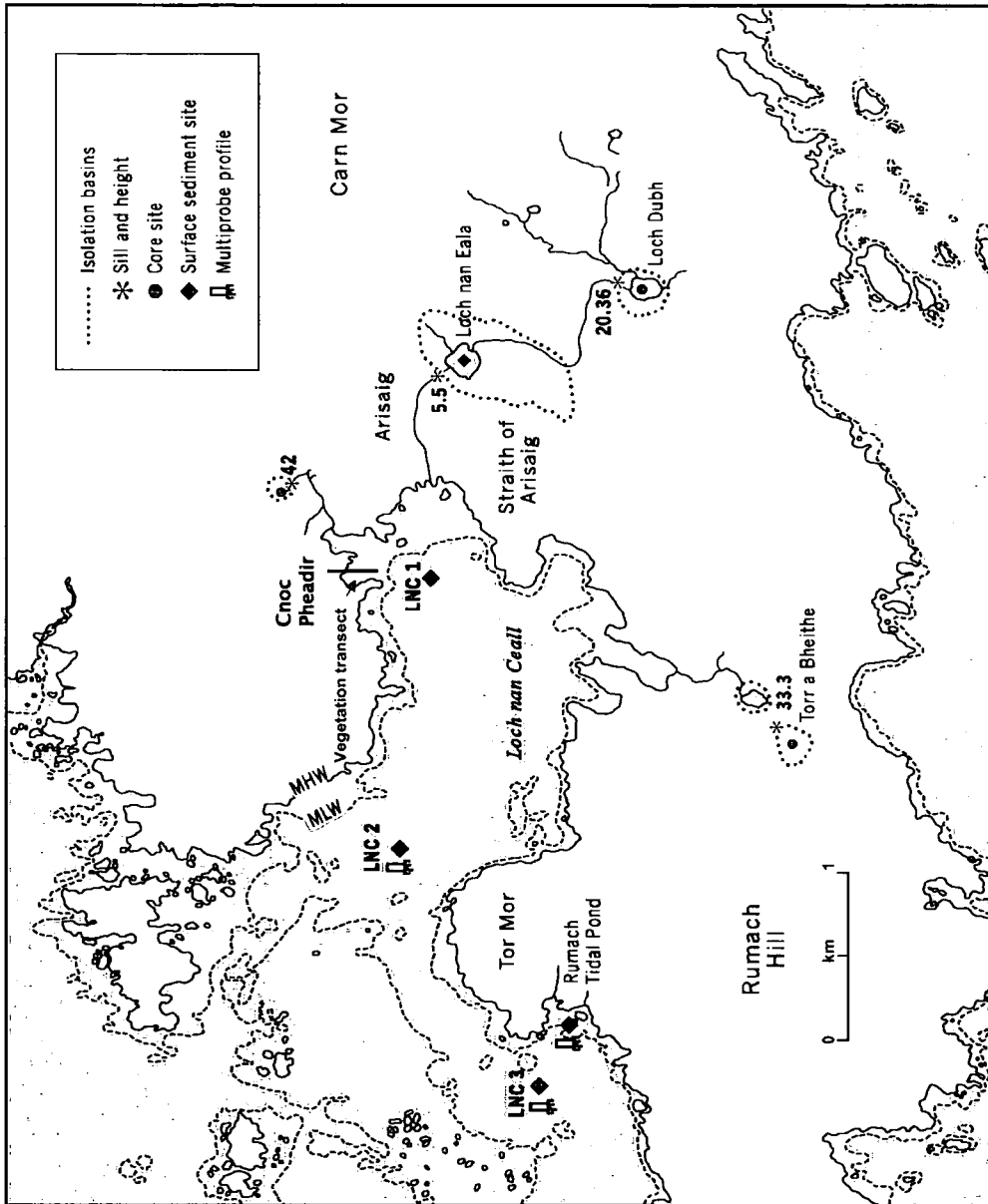


Figure 5.7: Loch nan Ceall and Rumach site map (Arisaig). Insets show locations of the study areas with the individual sites indicated (see tables 5.2 & 5.3).

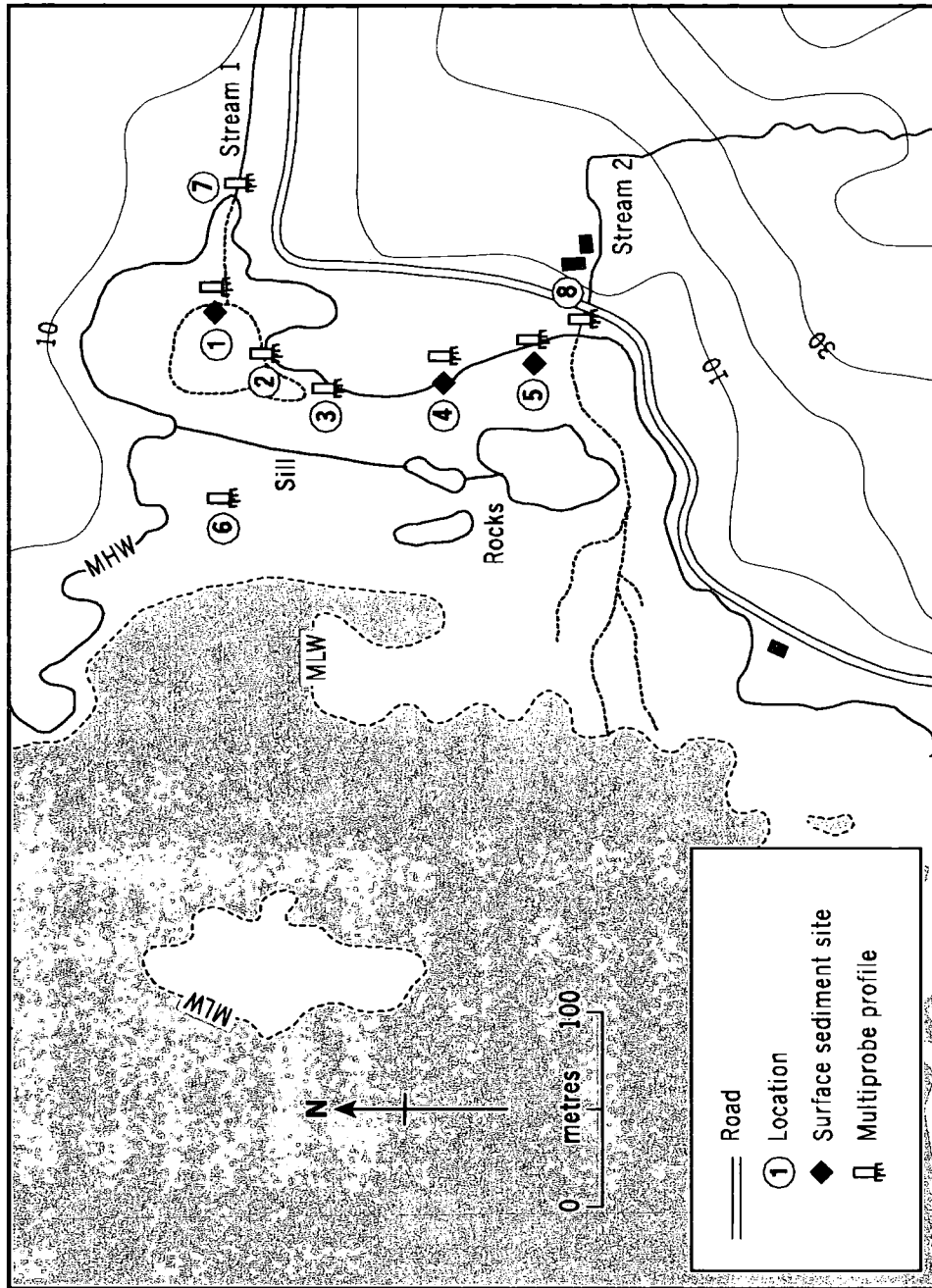


Figure 5.8: Rumach tidal pond site map - showing details for the site. Sampling stations (1-8) and type of sample or data obtained at each station is indicated. The locations of MHW, MLW and the two freshwater stream inputs are also illustrated.

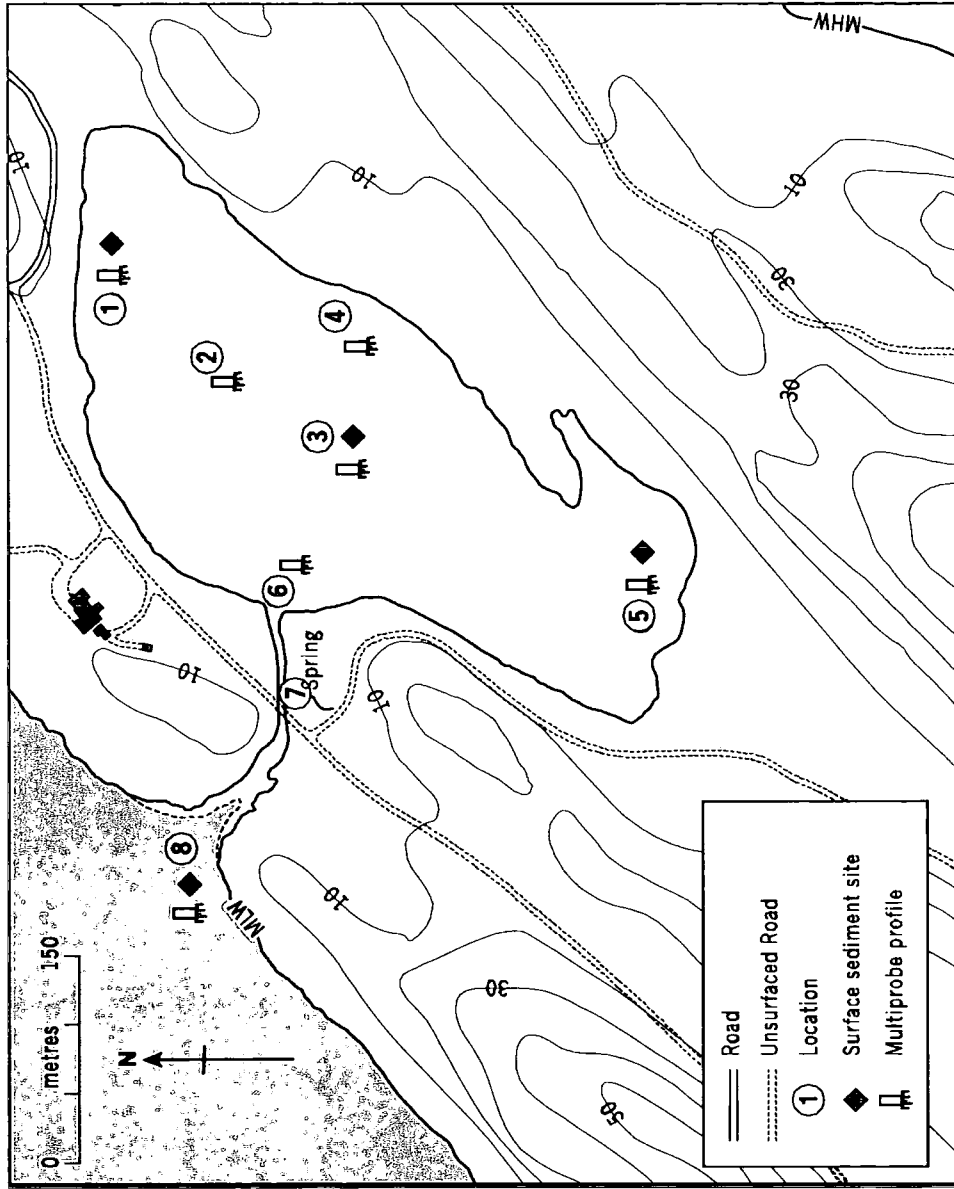


Figure 5.9: Craiglin site map - showing details for the site. Sampling stations (1-8) and type of sample or data obtained at each station is indicated. The locations of MHW, MLW and a freshwater spring input is also illustrated.

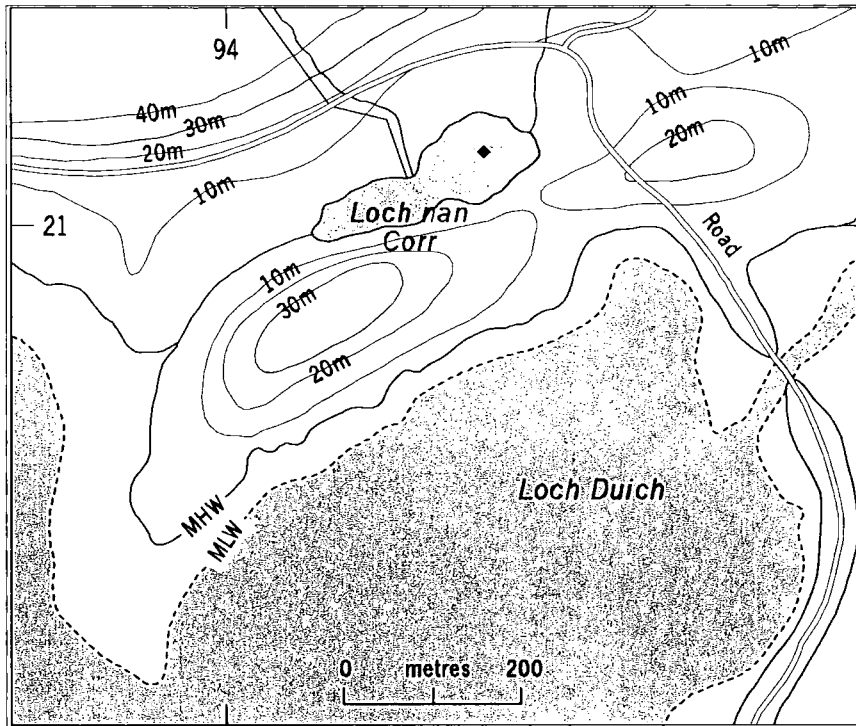


Figure 5.10: Kintail site map - showing details of Loch nan Core site, including surface sediment sampling location (diamond).

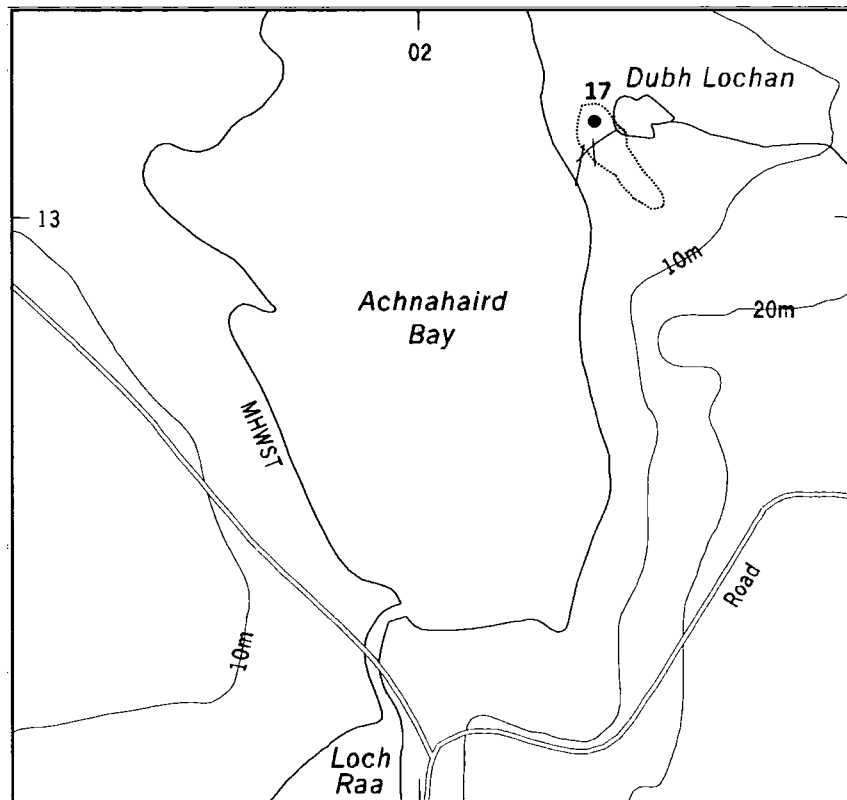


Figure 5.11: Coigach site map - showing details of Dubh Lochan site, including isolation basin and core location (circle).

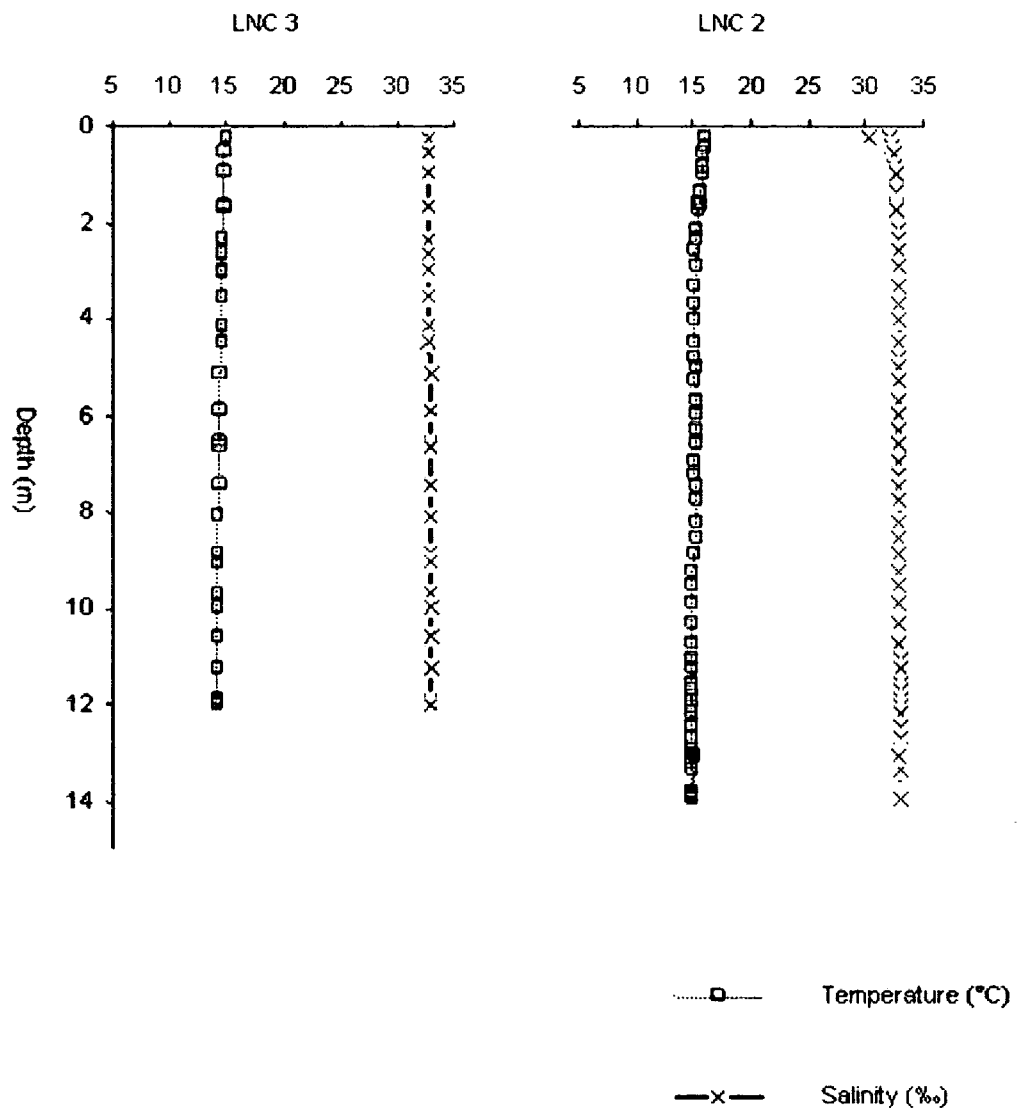


Figure 5.12: Loch nan Ceall, salinity and temperature profiles. Measurements were taken on 6th August 2002, mid-tide, mid-cycle.

Figure 5.13: Rumach Tidal Pond water column profiles at station 1 during Spring-tide HT & LT (11/8/02).

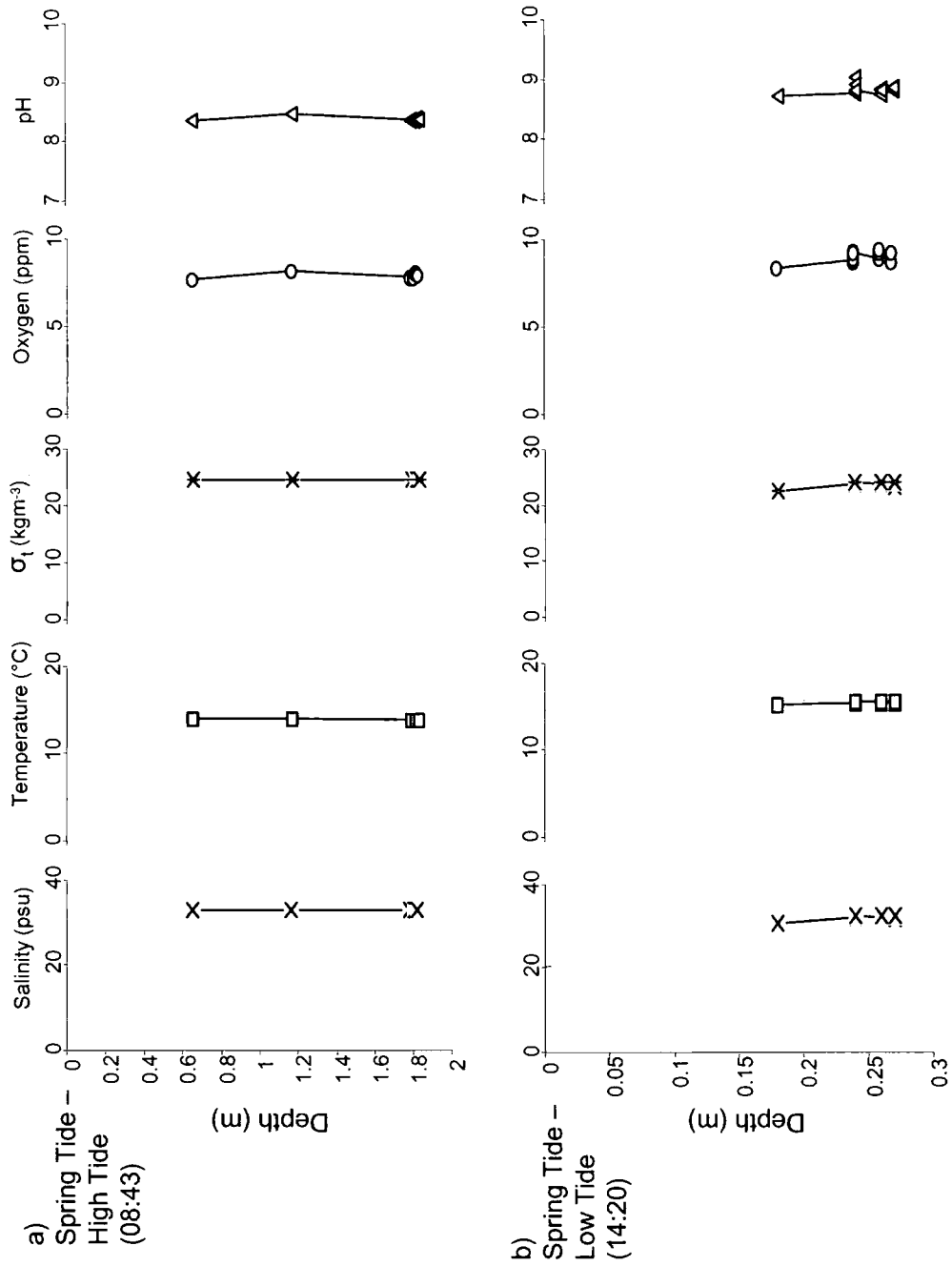
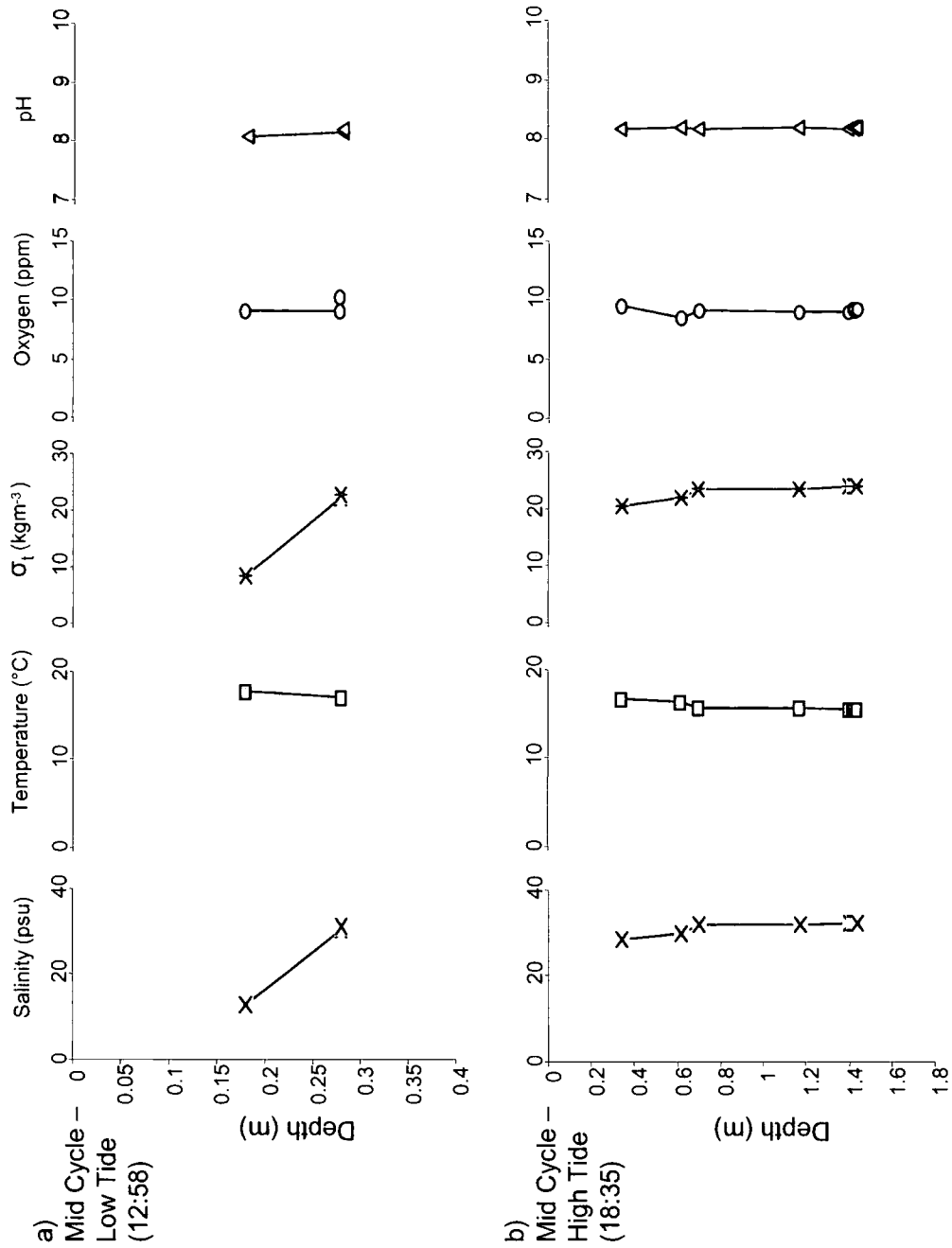


Figure 5.15: Rumach Tidal Pond water column profiles at station 1 during mid-cycle tide
tide LT & HT (7/8/02).



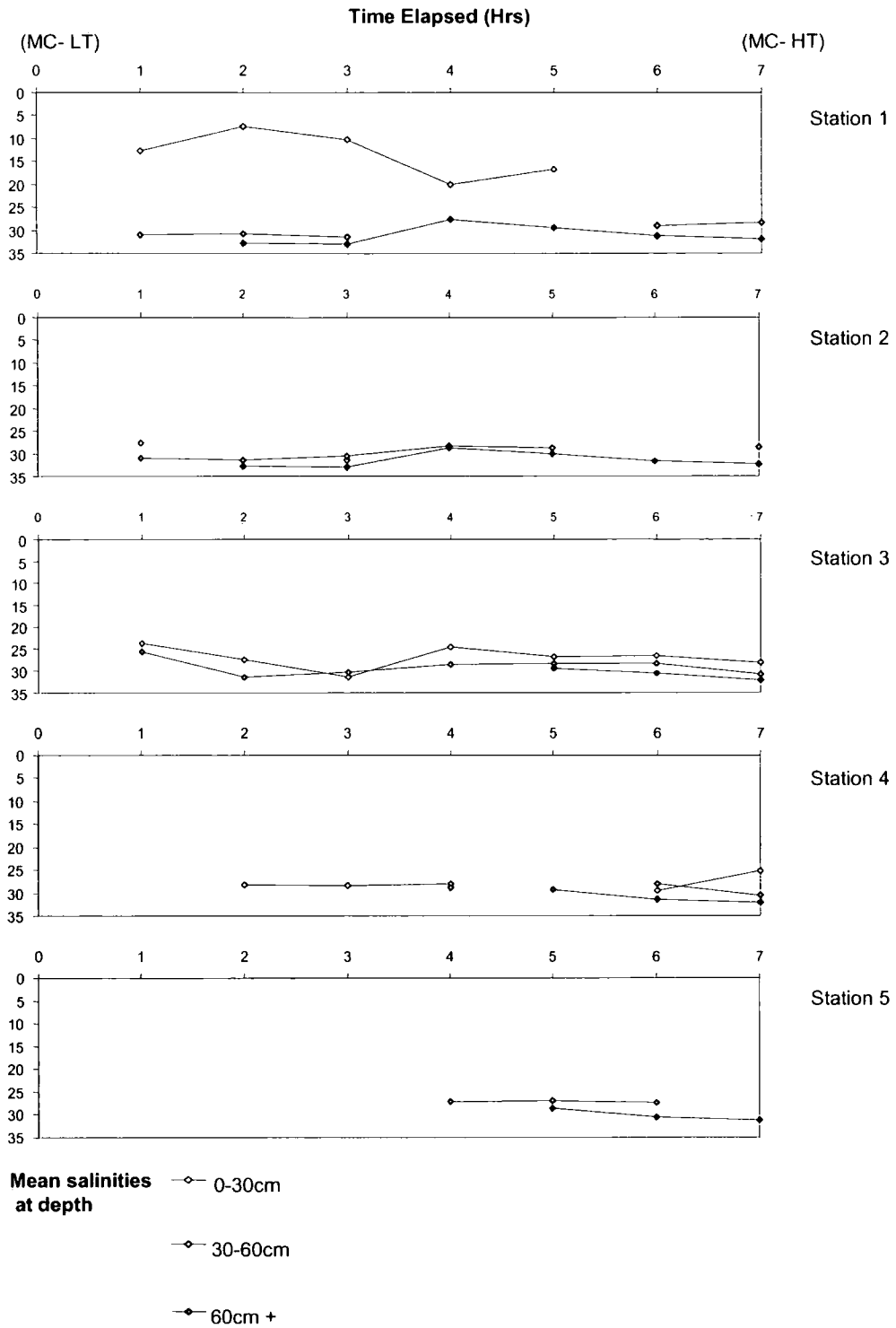
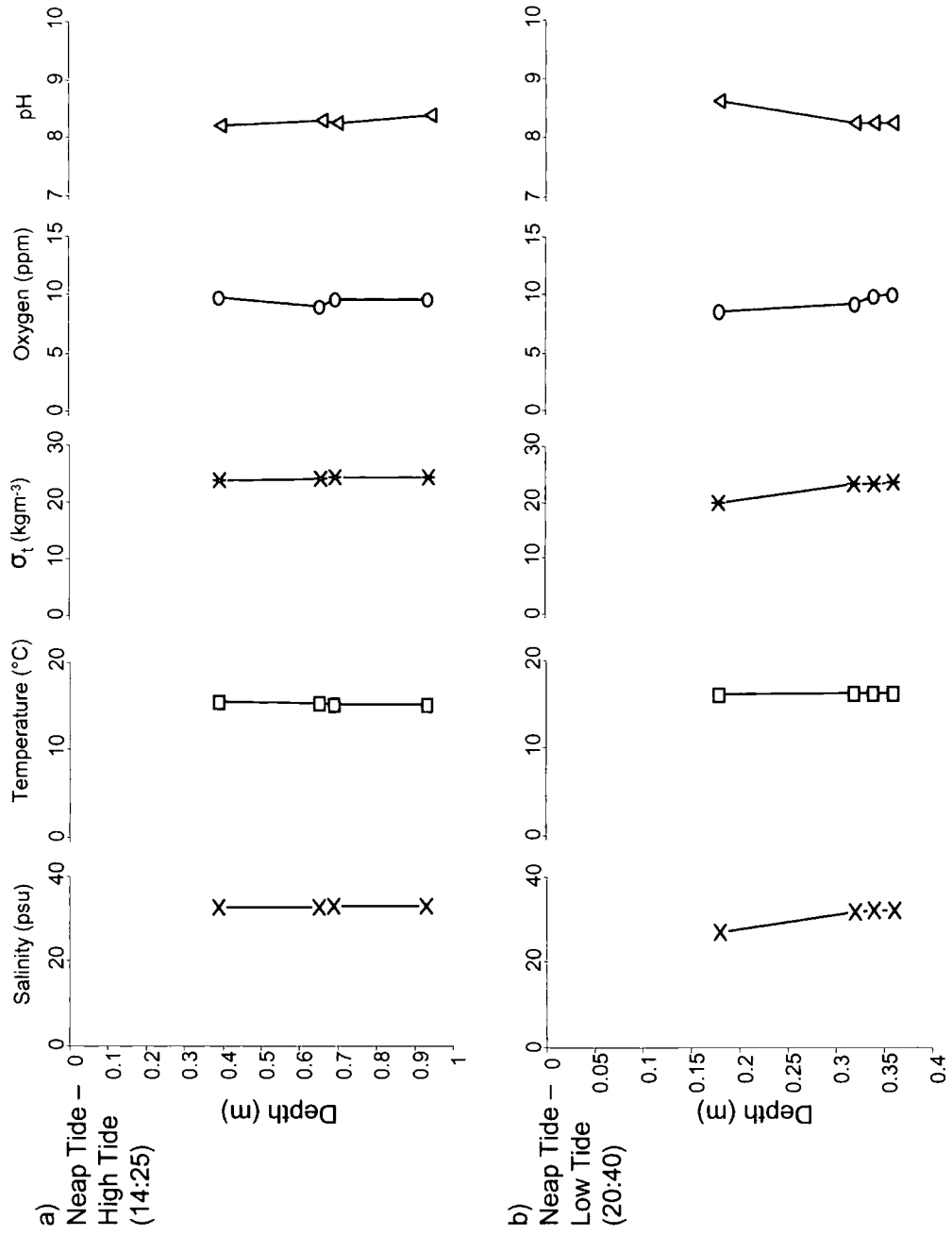


Figure 5.16: Rumach tidal pond depth averaged salinities vs time for mid-cycle tide LT-HT (7/8/02).

Figure 5.17: Rumach Tidal Pond water column profiles at station 1 during neap-tide HT & LT (4/8/02).



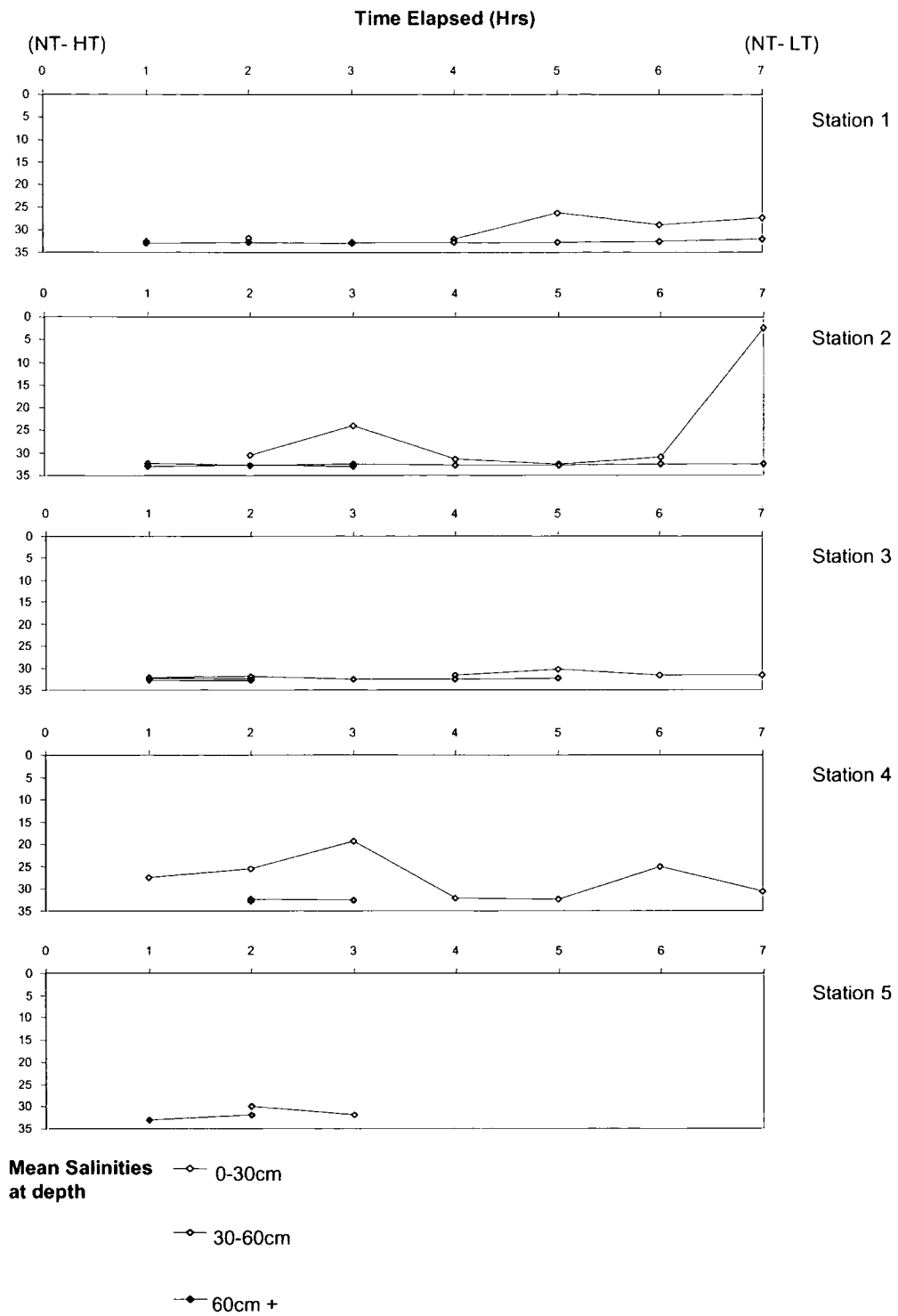


Figure 5.18: Rumach tidal pond depth averaged salinities vs time for neap-tide HT-LT (4/8/02).

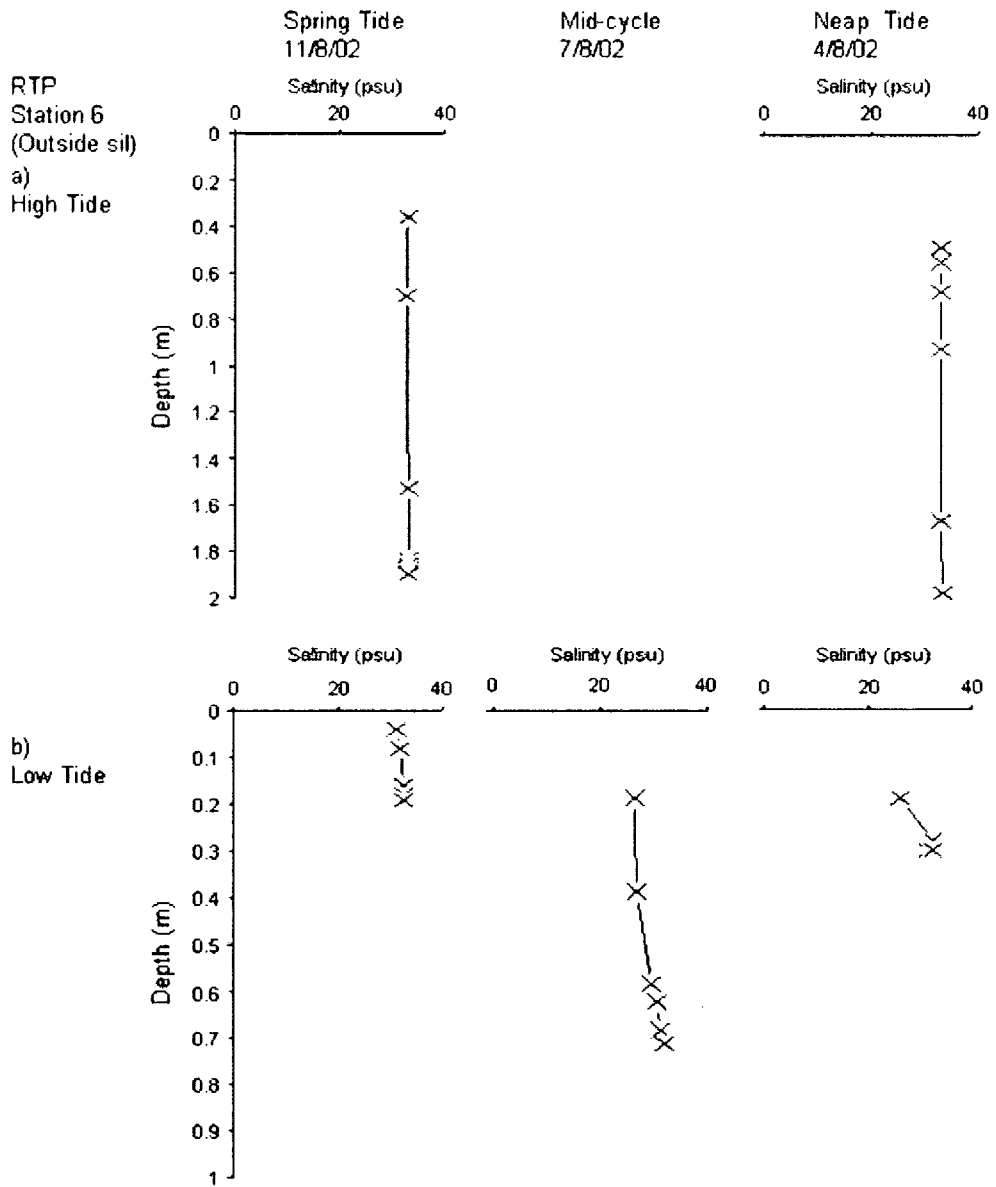


Figure 5.19: Rumach tidal pond salinity profiles for station 6 (outside sill) at various stages of the tidal cycle.

Figure 5.20: Craiglin Lagoon water column profiles at station 2 during spring-tide LT & HT (11/8/02).

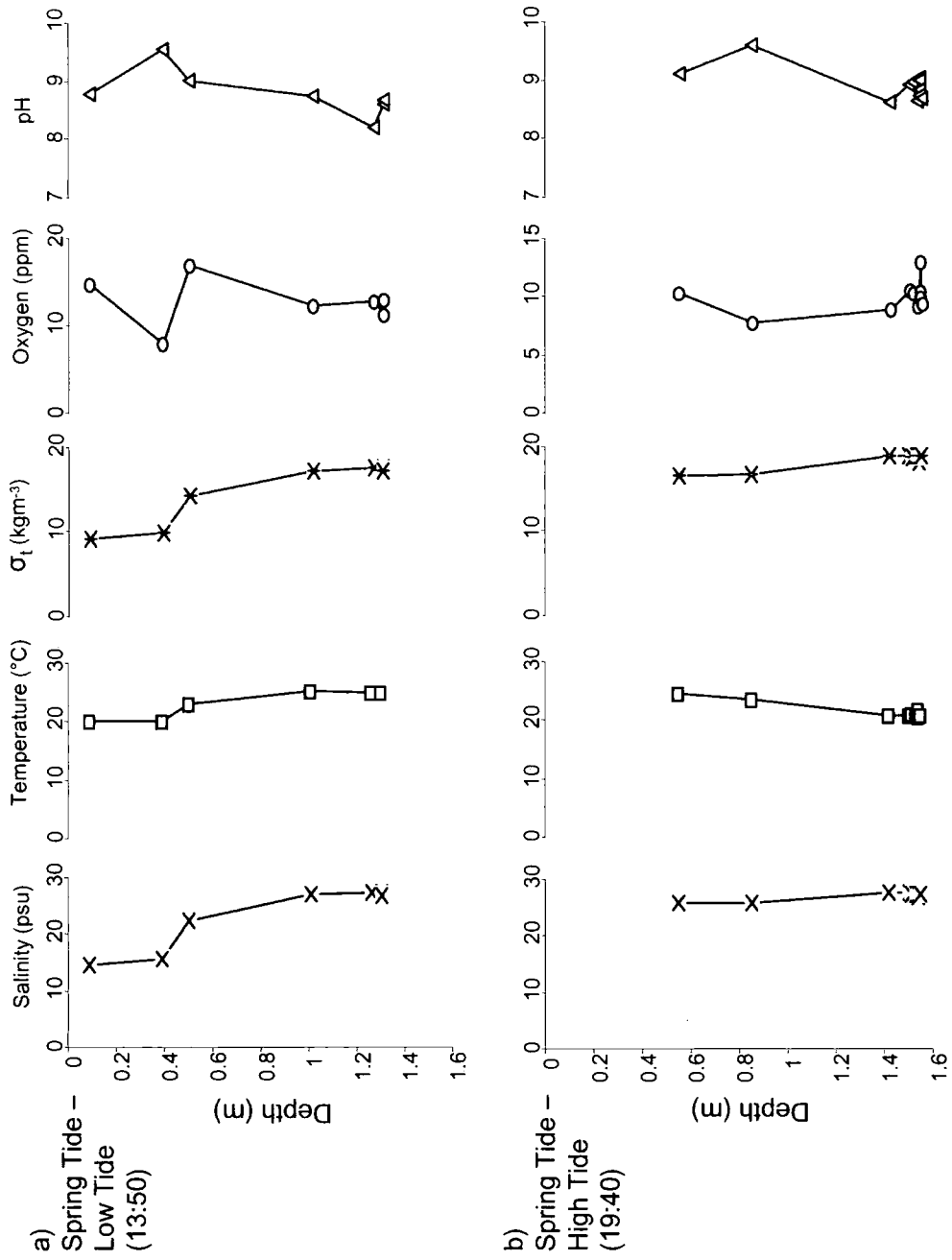
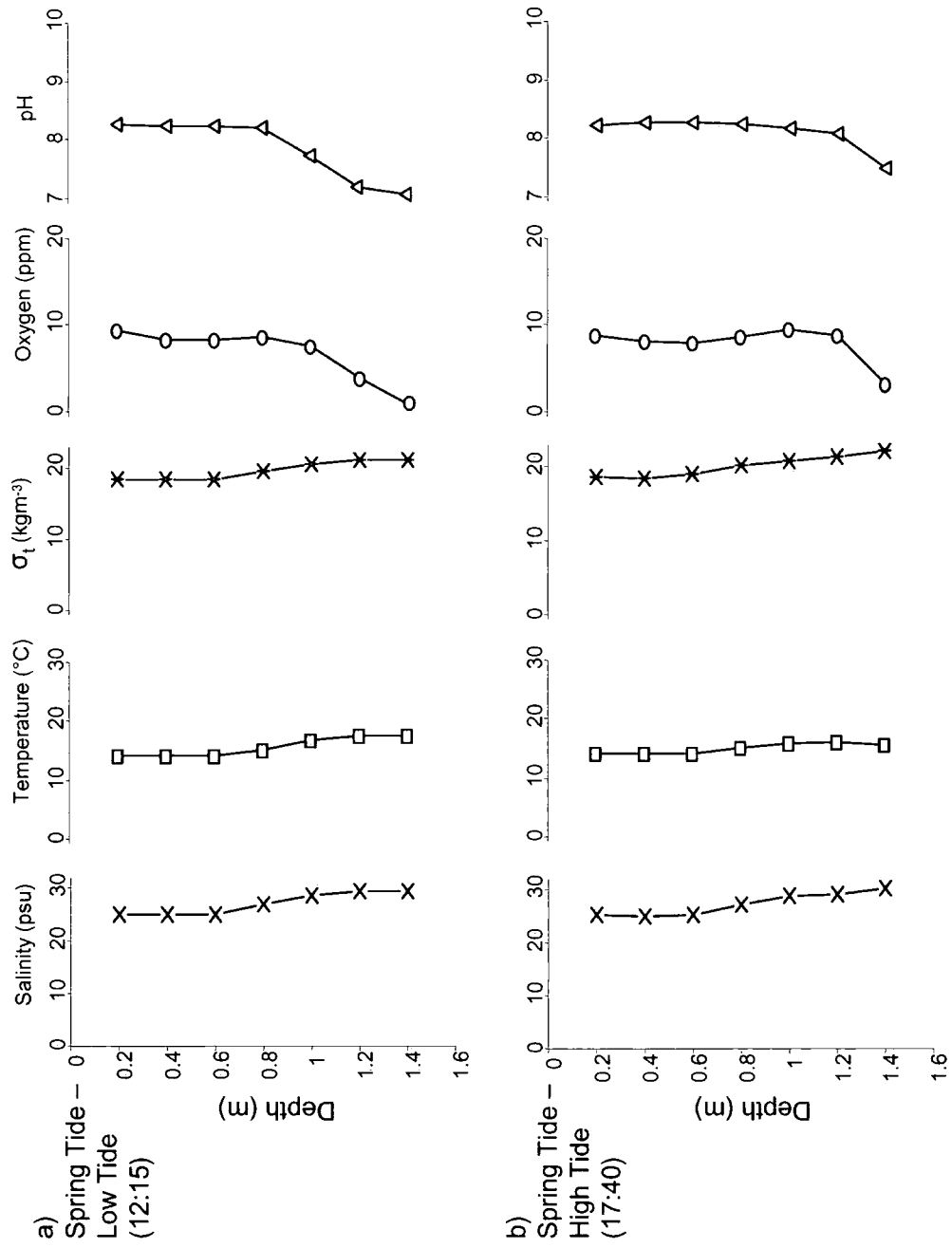


Figure 5.22: Craigin Lagoon water column profiles at station 2 during spring-tide LT & HT (7/10/02).



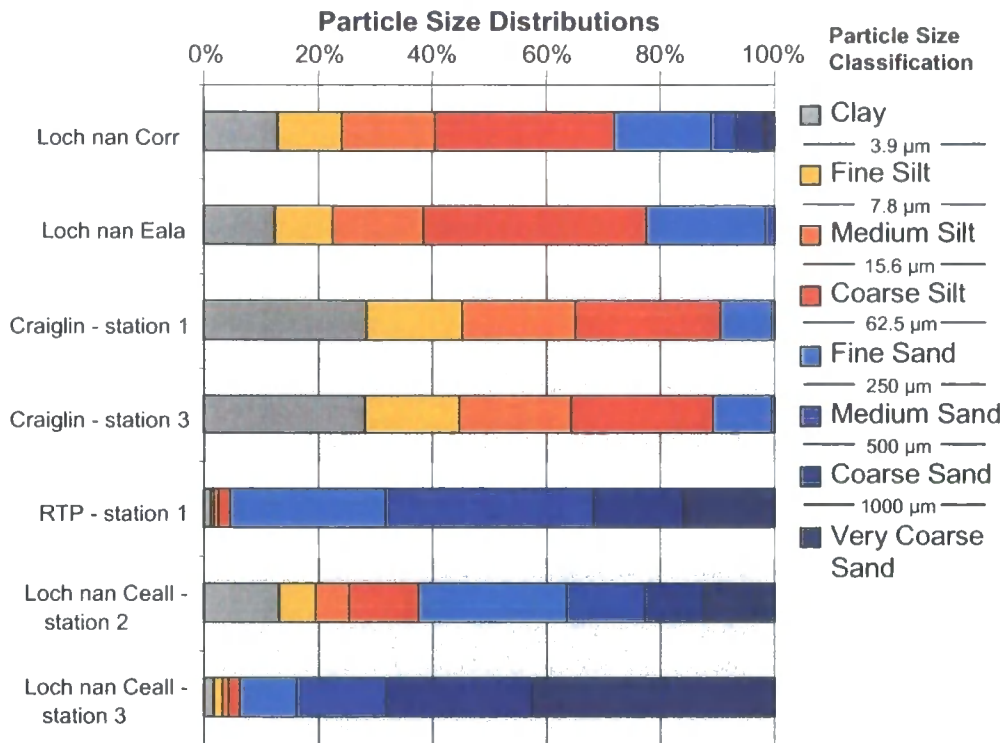


Figure: 5.24: Particle size distributions in modern NW Scottish surface sediments.

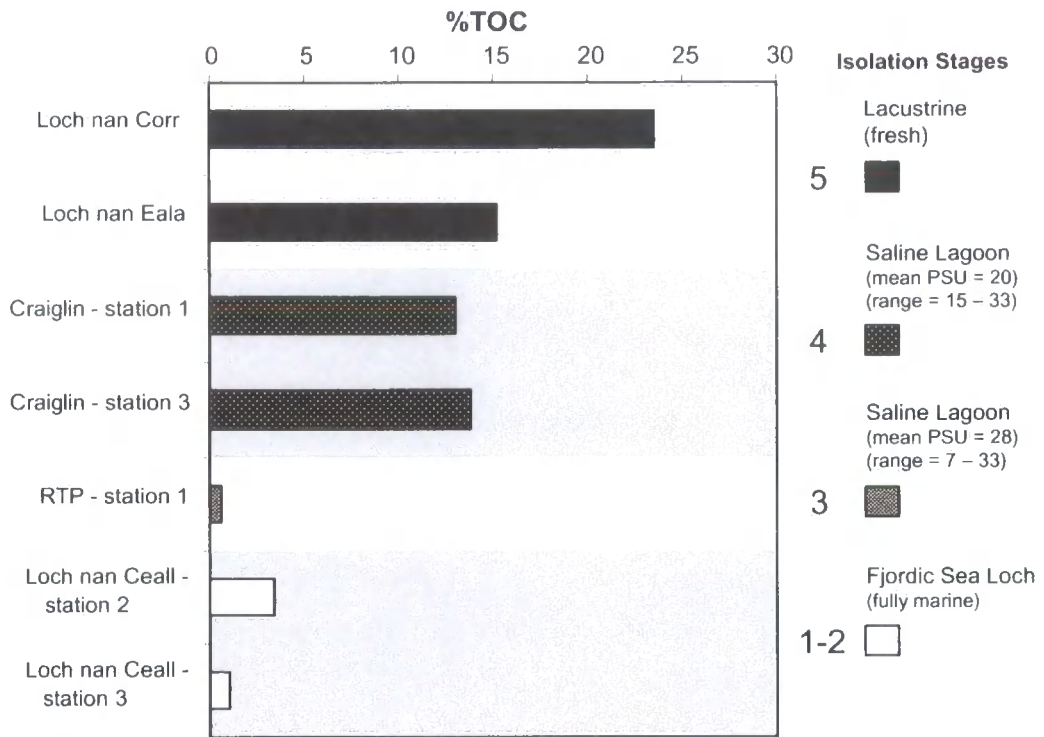


Figure: 5.25: Values of %TOC in modern NW Scottish surface sediments.

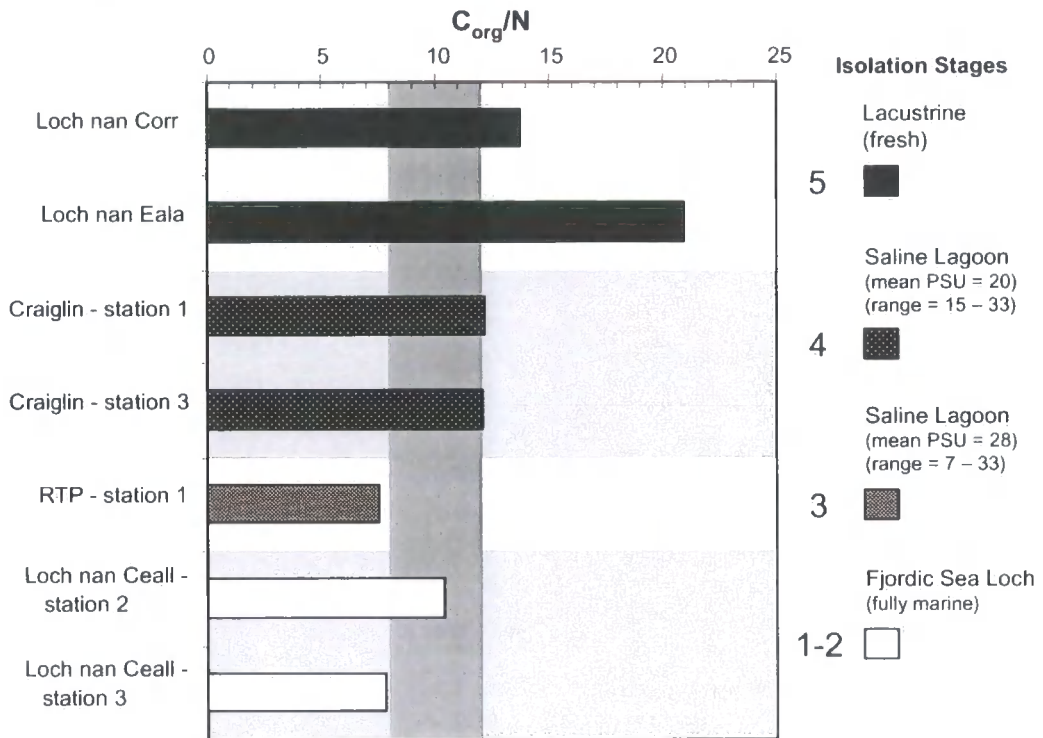


Figure: 5.26: Values of C_{org}/N in modern NW Scottish surface sediments. The shaded area in the plot C_{org}/N plot divides predominantly marine (<8), from predominantly terrestrial (>12) organic inputs according to the typical C/N ratios as described by Bordovskiy (1963) and Prahl et al. (1980) respectively.

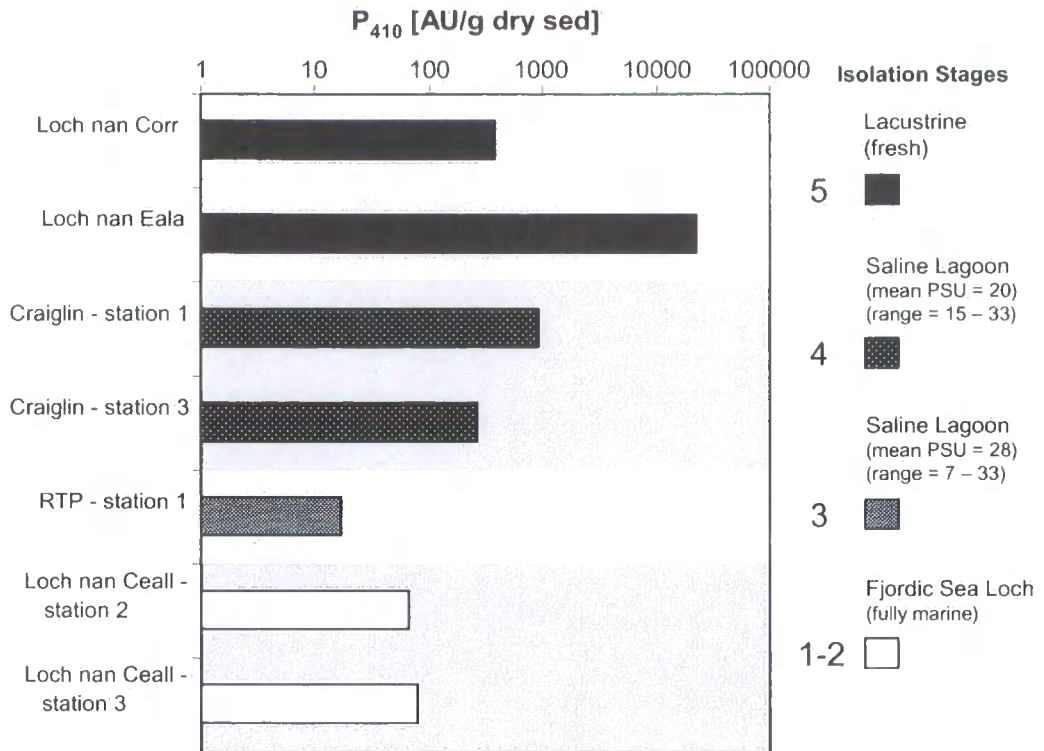


Figure: 5.27: Values of absorbance at 410λ by chlorin pigments in modern NW Scottish surface sediments.

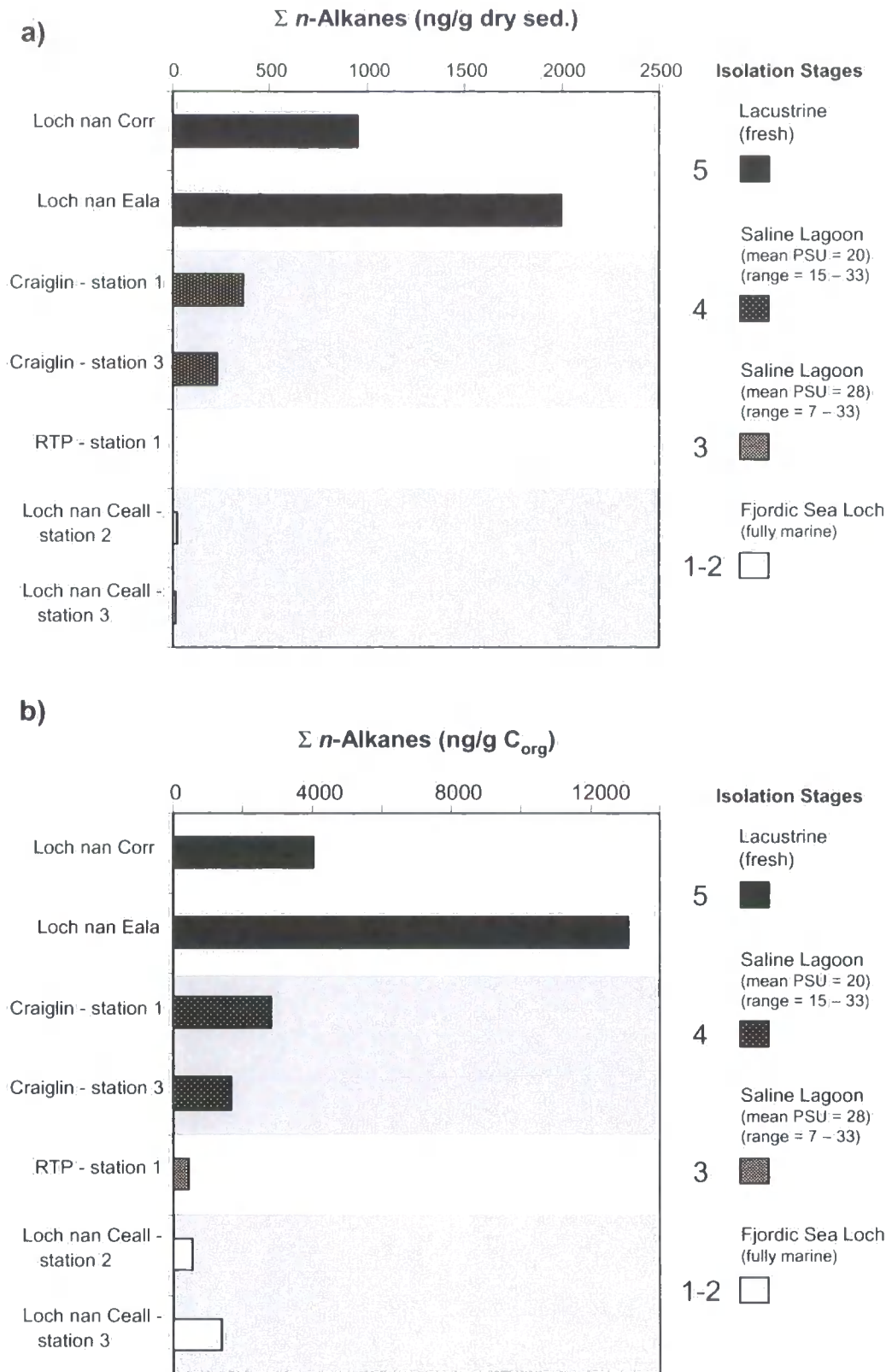


Figure: 5.28: Concentrations of n-Alkanes in modern NW Scottish surface sediments, normalised to a) grams dry sediments and b) grams organic carbon.

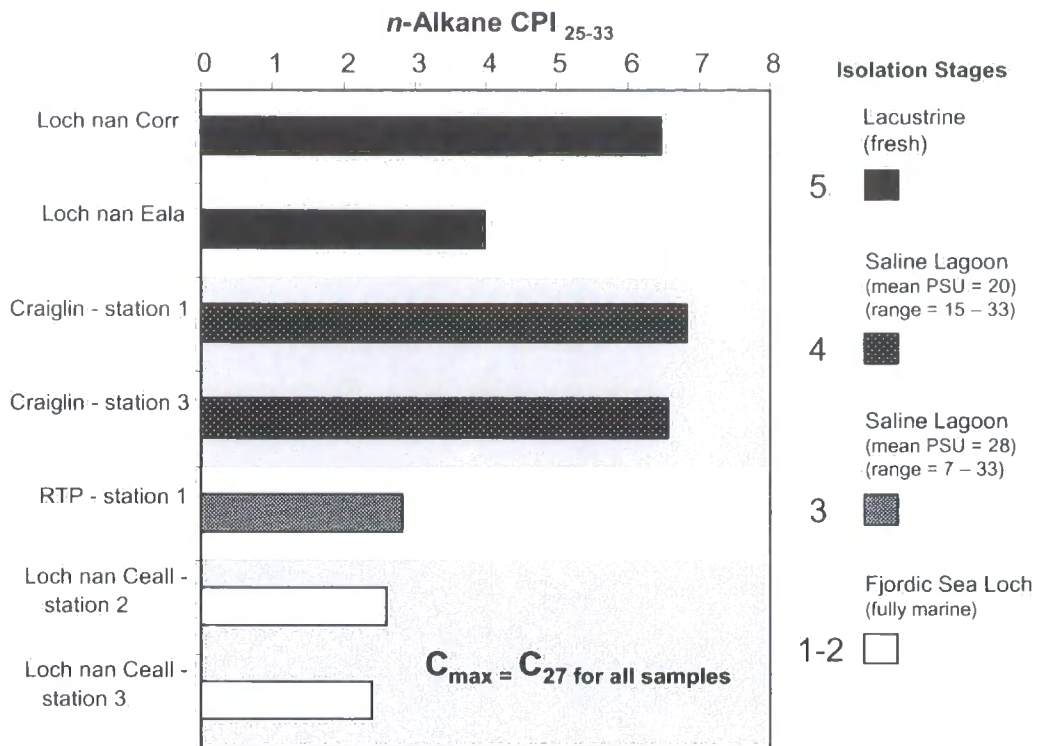


Figure: 5.29: Values of *n*-Alkane CPI₂₅₋₃₃ and dominant C_{max} in modern NW Scottish surface sediments.

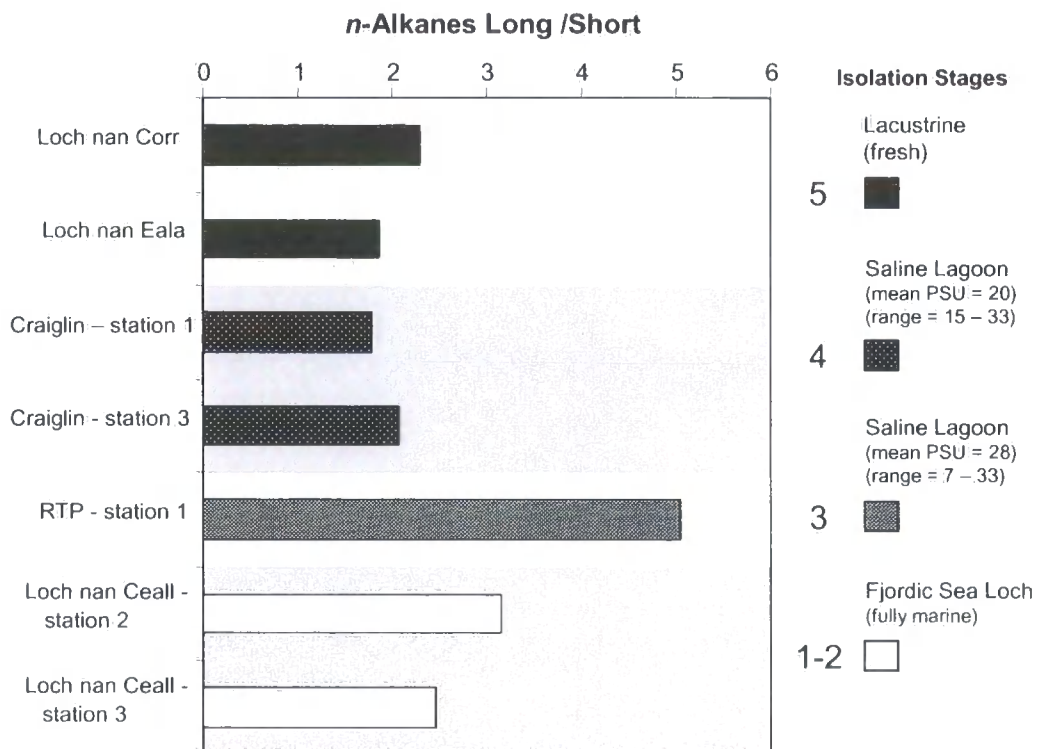


Figure: 5.30: Values of *n*-Alkane Long/Short ratio in modern NW Scottish surface sediments.

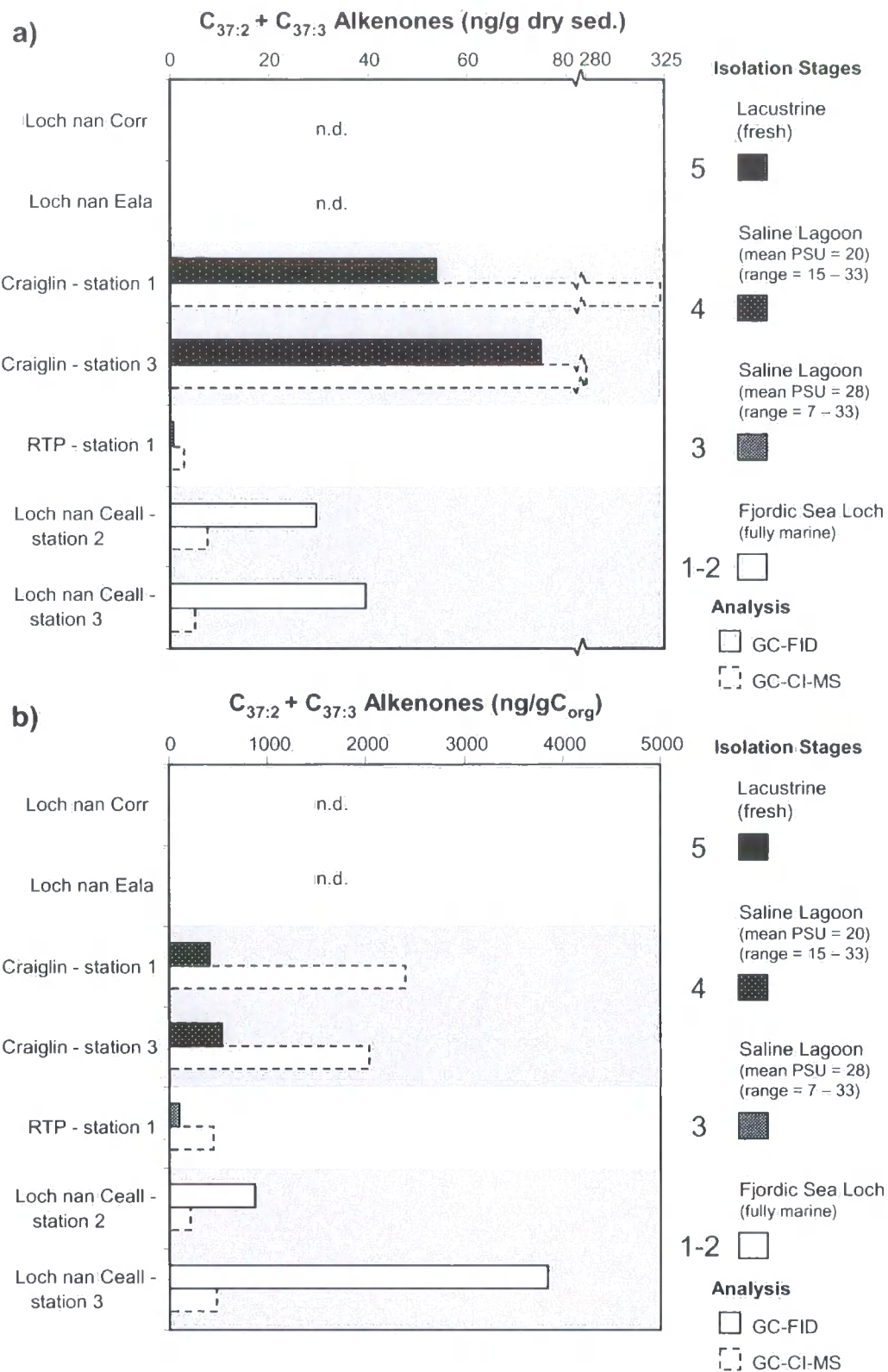


Figure 5.31: Concentrations of $C_{37:2} + C_{37:3}$ alkenones in modern NW Scottish surface sediments, normalised to a) grams dry sediments and b) grams organic carbon.

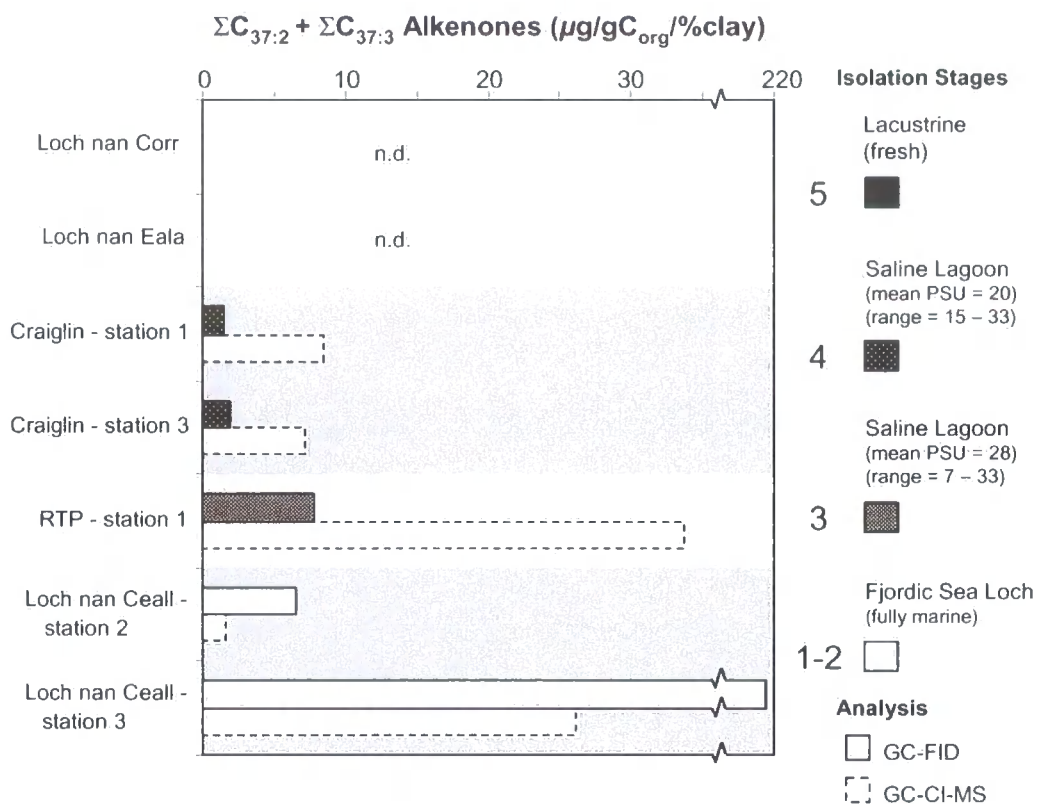


Figure: 5.32: Concentrations of $C_{37:2} + C_{37:3}$ alkenones in modern NW Scottish surface sediments normalised to grams organic carbon and % clay.

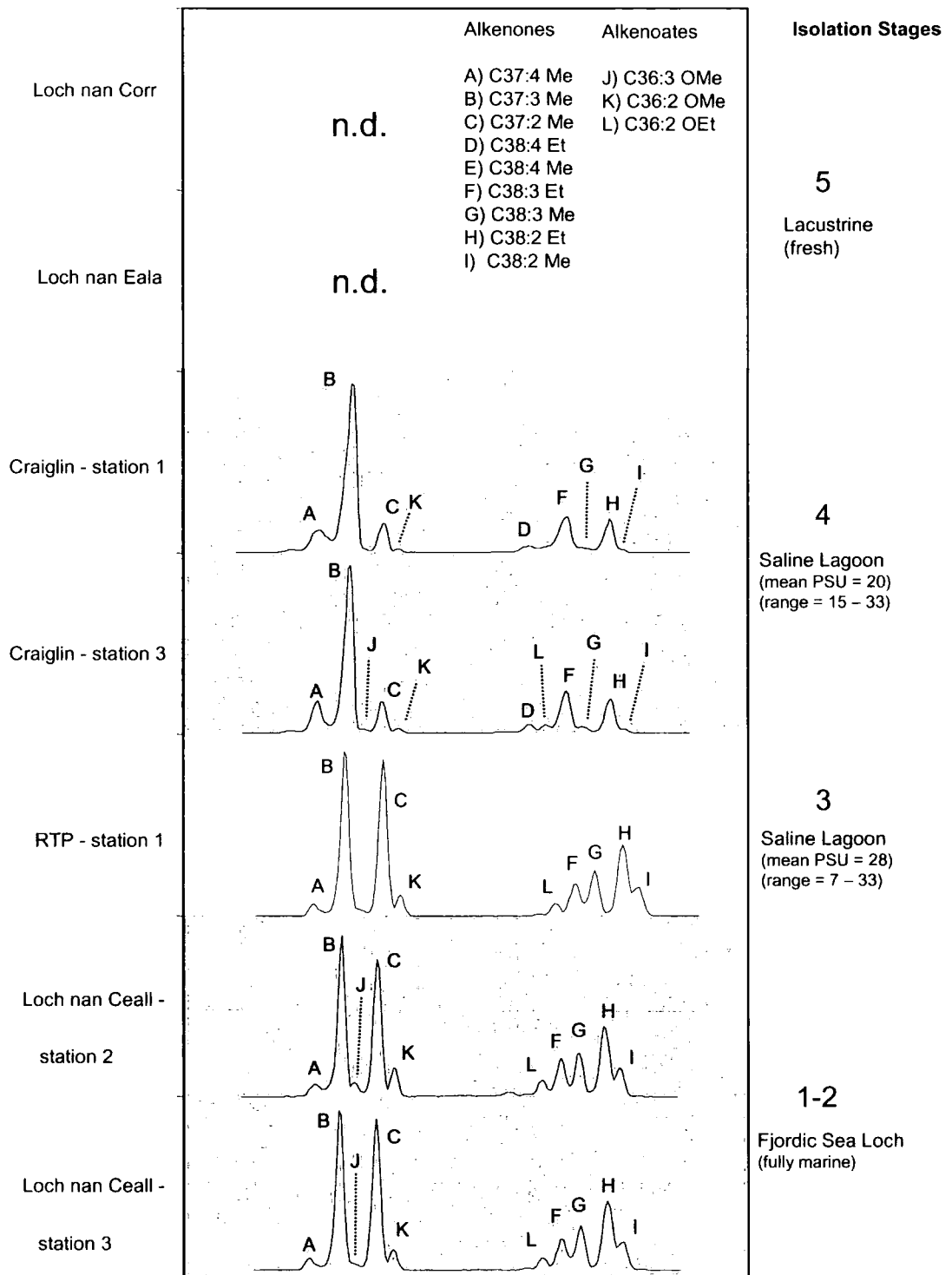


Figure: 5.33: GC-MS total ion chromatograms for modern NW Scottish surface sediments.

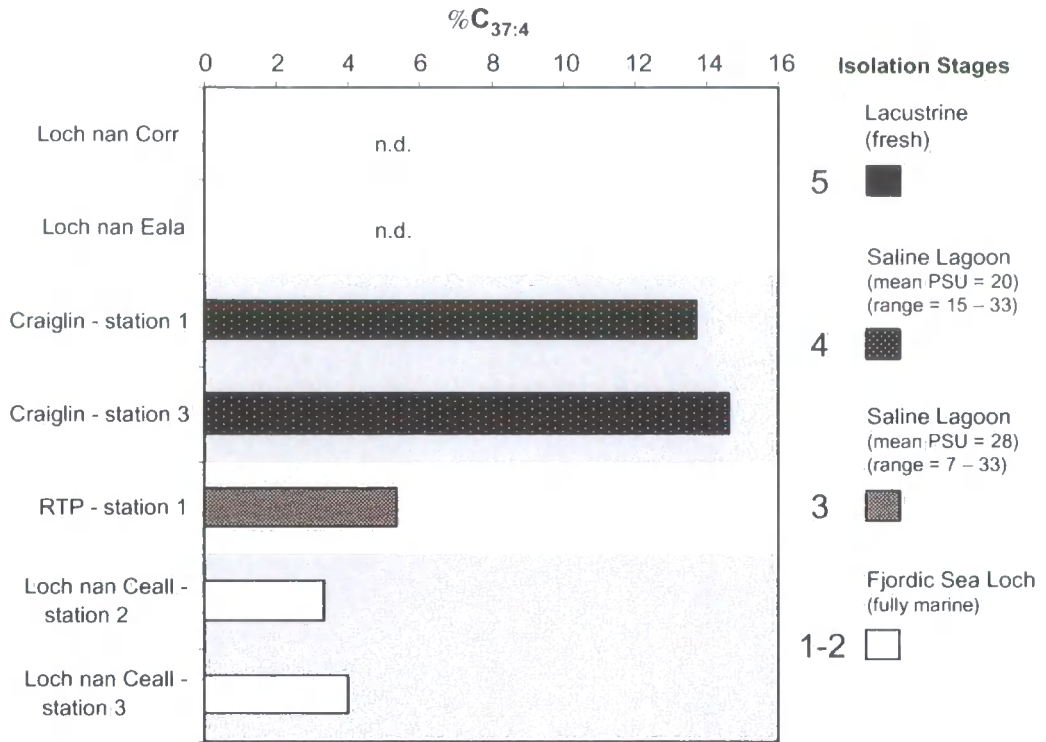


Figure: 5.34: Values of %C_{37:4} in modern NW Scottish surface sediments.

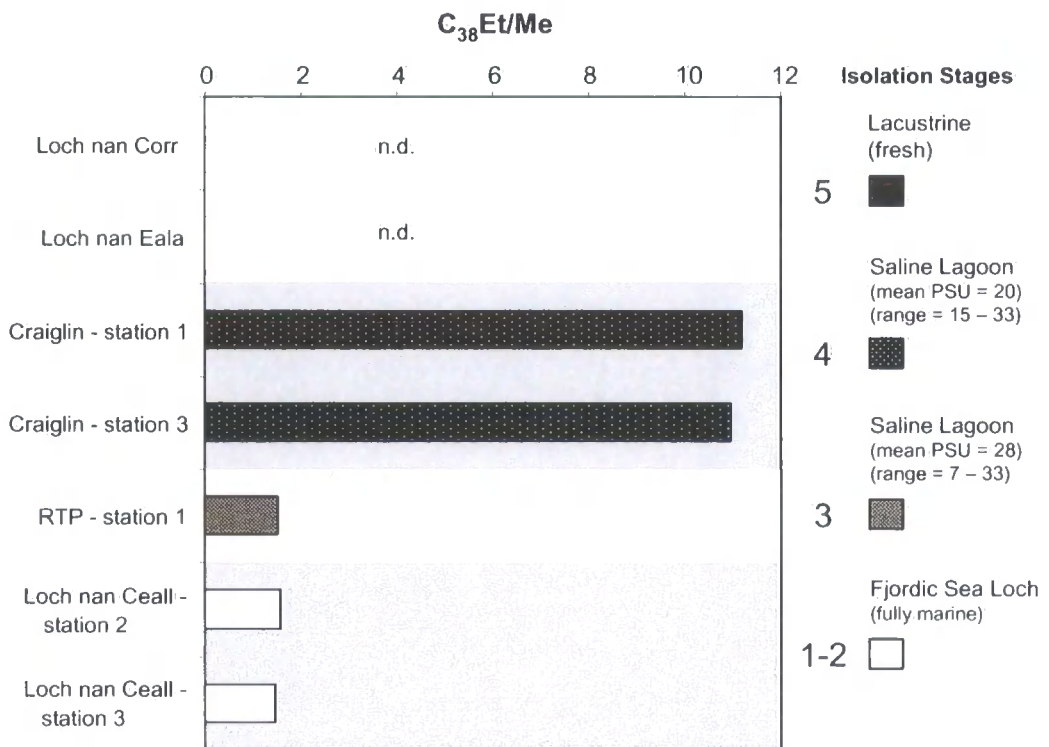


Figure: 5.35: Values of C₃₈Et/Me in modern NW Scottish surface sediments.

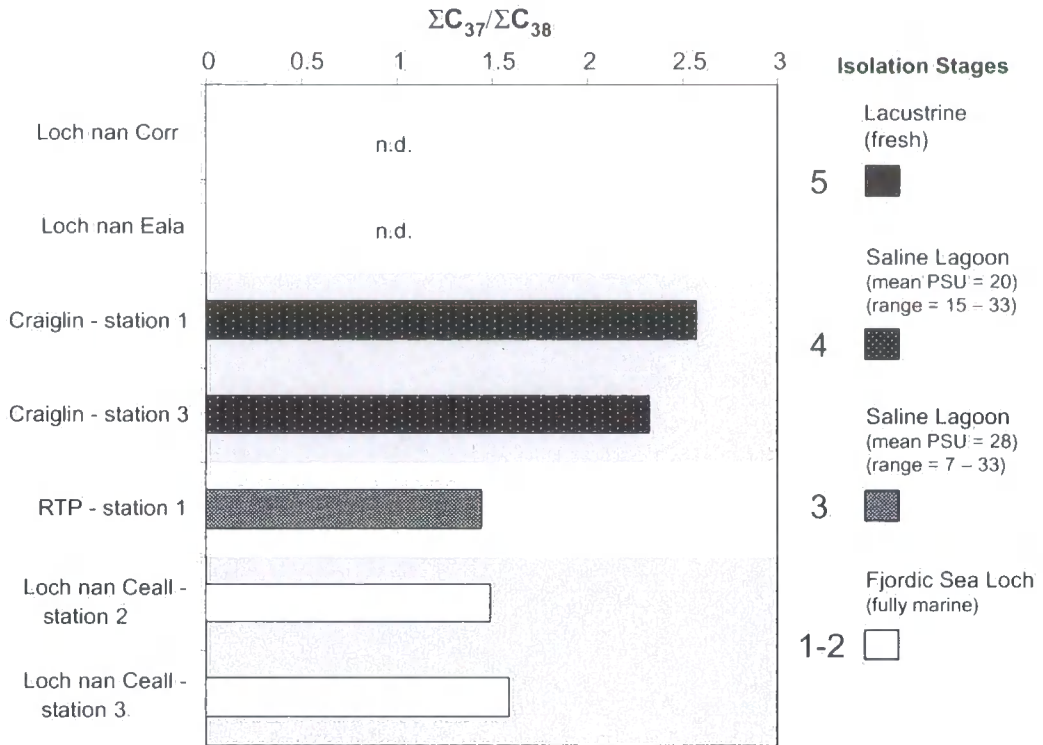


Figure: 5.36: Values of $\Sigma C_{37}/\Sigma C_{38}$ in modern NW Scottish surface sediments.

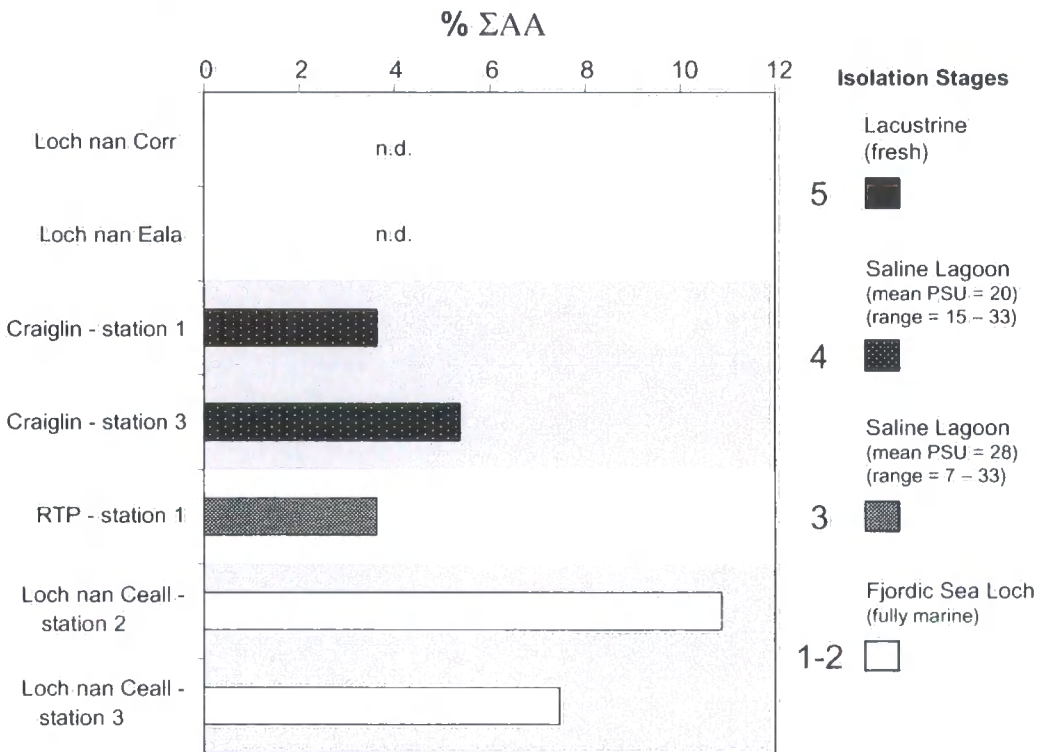


Figure: 5.37: Values of % ΣAA in modern NW Scottish surface sediments.

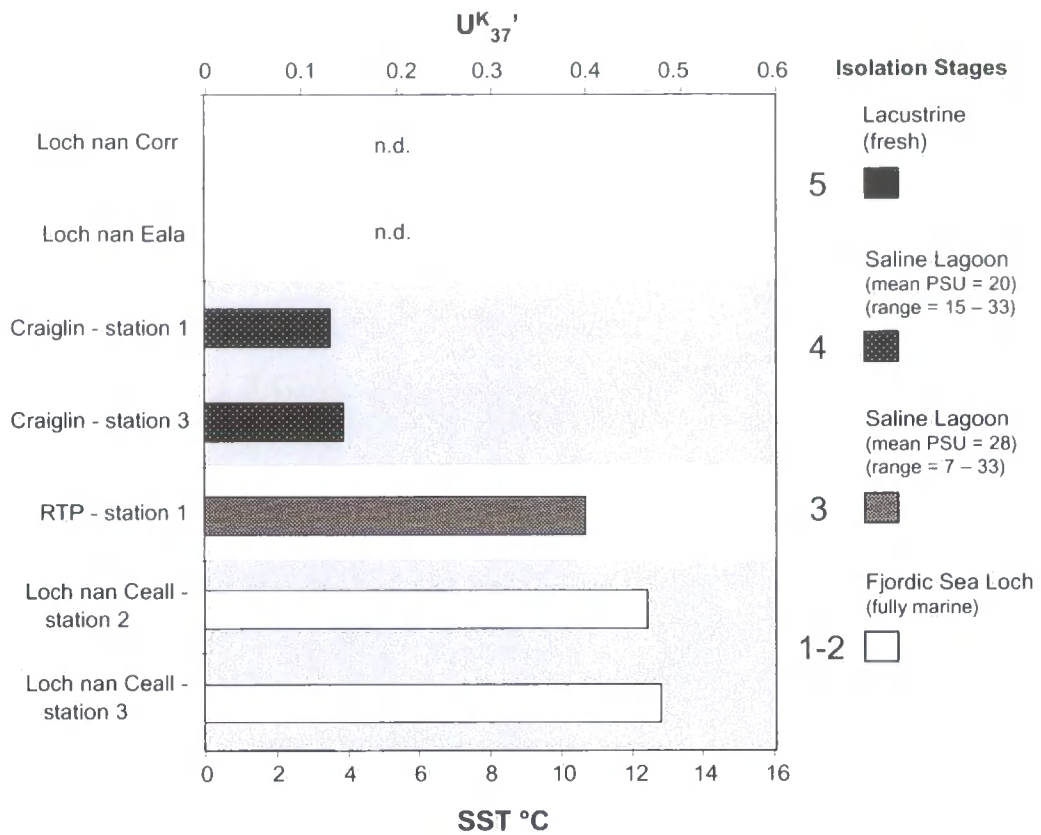


Figure: 5.38: Values of U_{37}^K and derived SST °C in modern NW Scottish surface sediments.

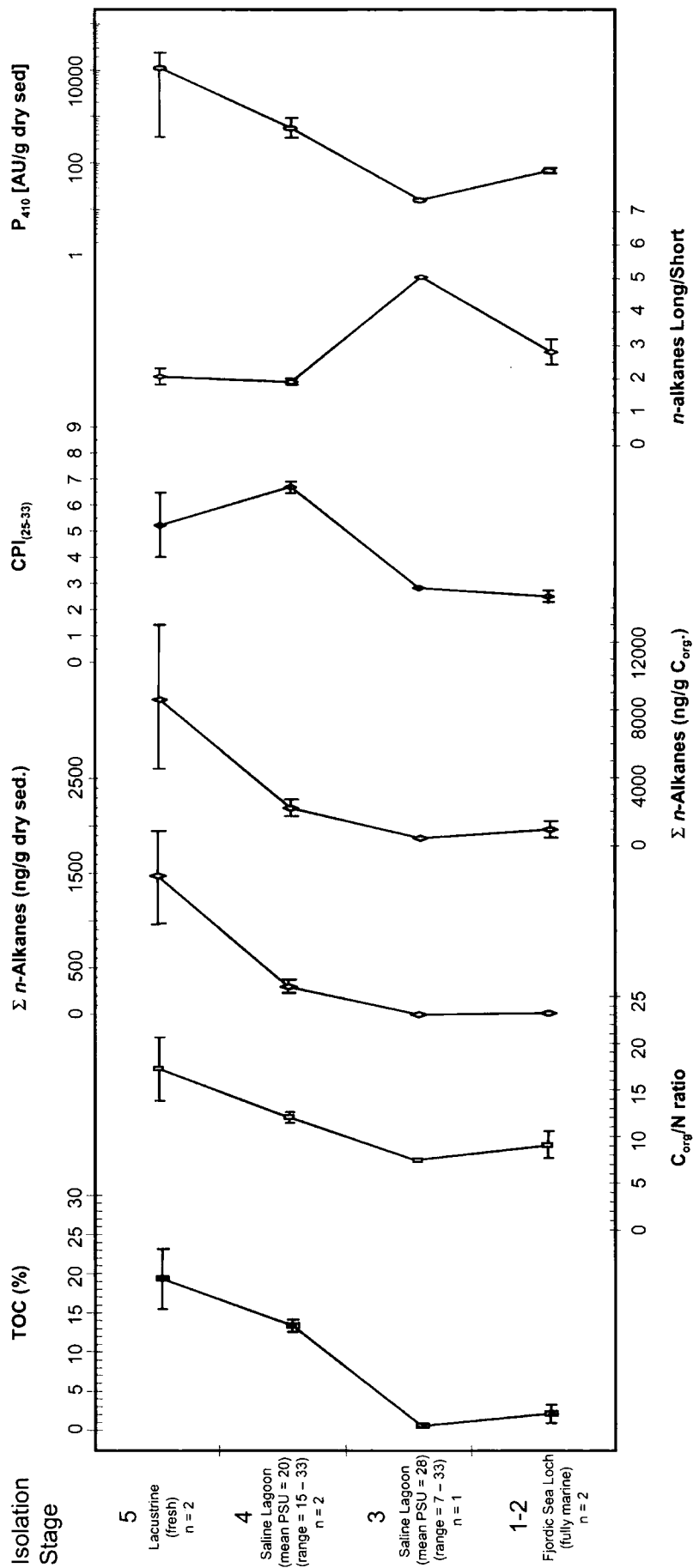


Figure 5.39: Trends in bulk organic properties, n-alkane and pigment distributions in N.W. Scottish surface sediments. Shaded bands indicate theoretical isolation stages. The curves are derived from the data in Figures 5.26- 5.30, the data points are the mean average, the bars indicate minimal and maximal measurements not error.

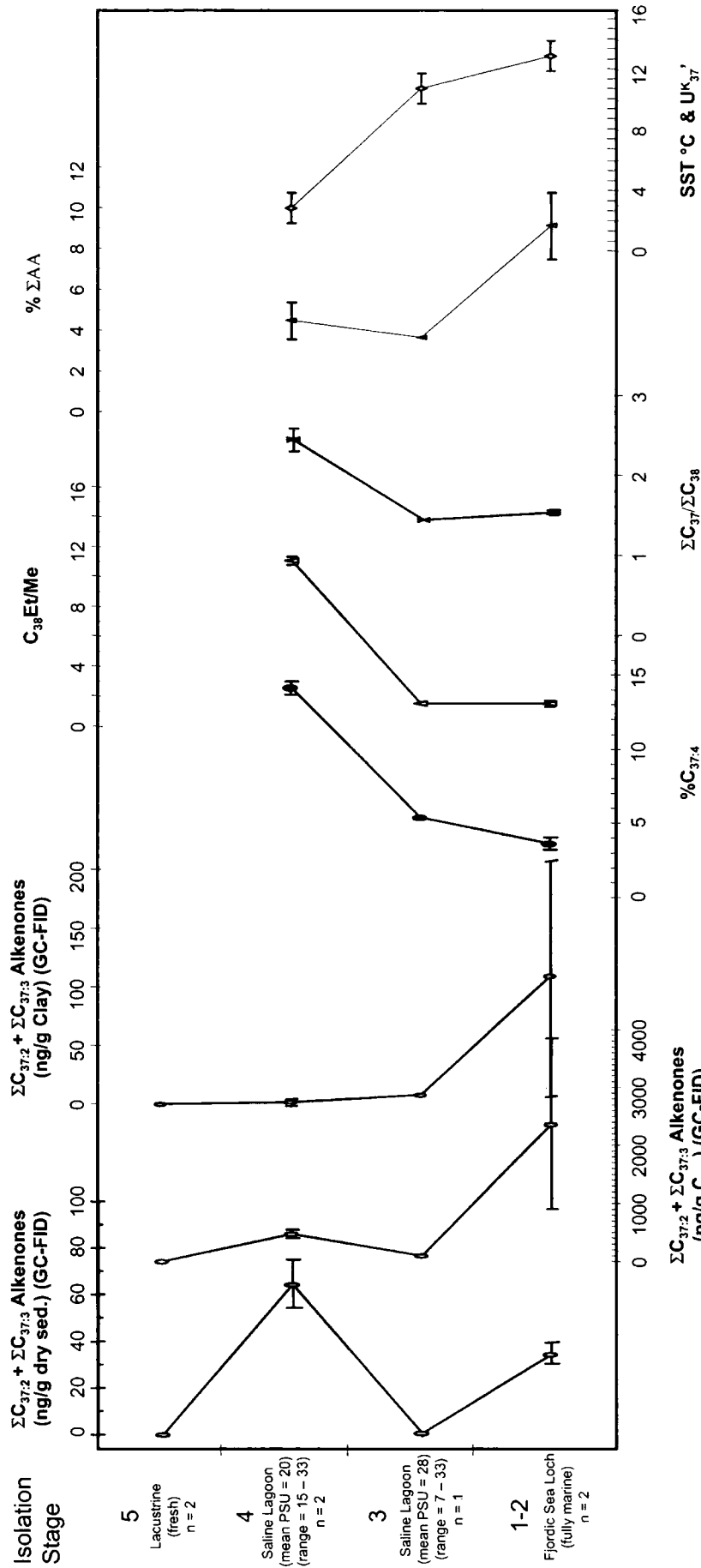


Figure 5.40: Trends in alkenone and alkenoate distributions in N.W. Scottish surface sediments. Shaded bands indicate theoretical isolation stages. The curves are derived from the data in Figures 5.26- 5.3, the data points are the mean average, the bars indicate minimal and maximal measurements not error.

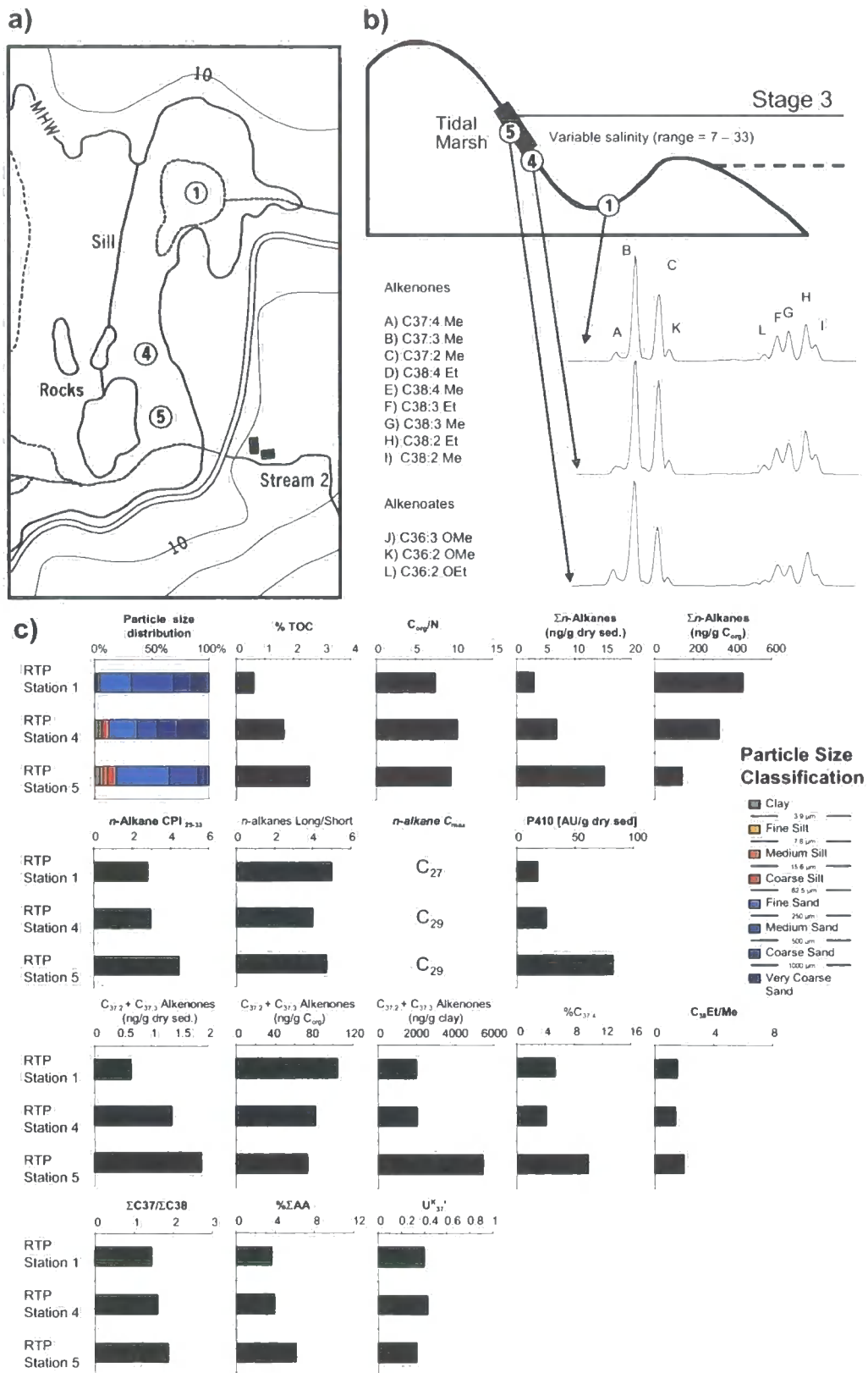


Figure 5.41: Within basin variability – Rumach Tidal Pond. a) Map illustrating locations of sediment samples b) relative positions of RTP samples on isolation stage schematic and sample GC-MS traces c) bar charts of bulk organic and biomarker measurements.

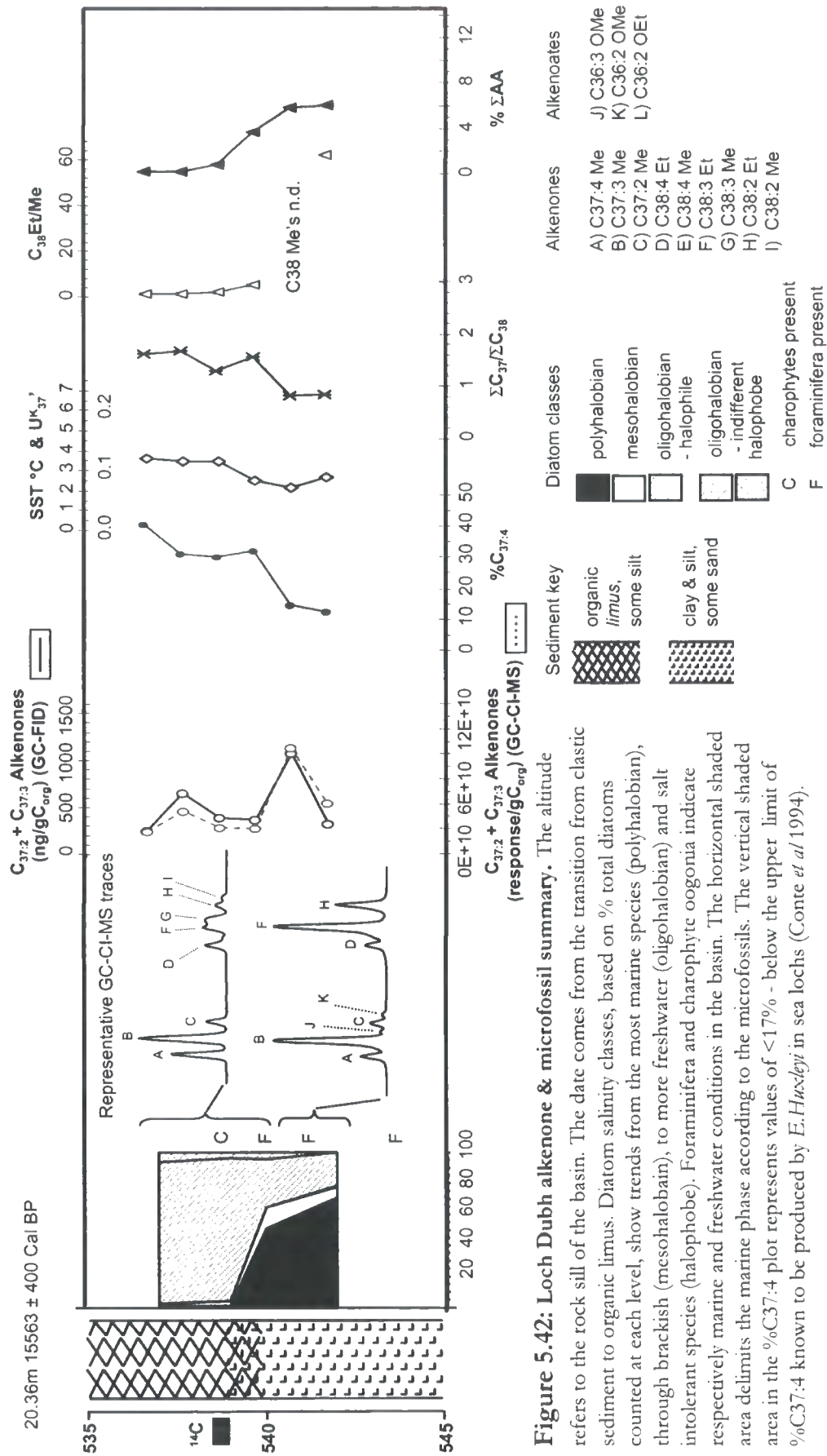


Figure 5.42: Loch Dubh alkenone & microfossil summary. The altitude refers to the rock sill of the basin. The date comes from the transition from clastic sediment to organic limus. Diatom salinity classes, based on % total diatoms counted at each level, show trends from the most marine species (polyhalobian), through brackish (mesohalobian), to more freshwater (oligohalobian) and salt intolerant species (halophobe). Foraminifera and charophyte oogonia indicate respectively marine and freshwater conditions in the basin. The horizontal shaded area delimits the marine phase according to the microfossils. The vertical shaded area in the %C37:4 plot represents values of <17% - below the upper limit of %C37:4 known to be produced by *E. Huxleyi* in sea lochs (Conte *et al* 1994).

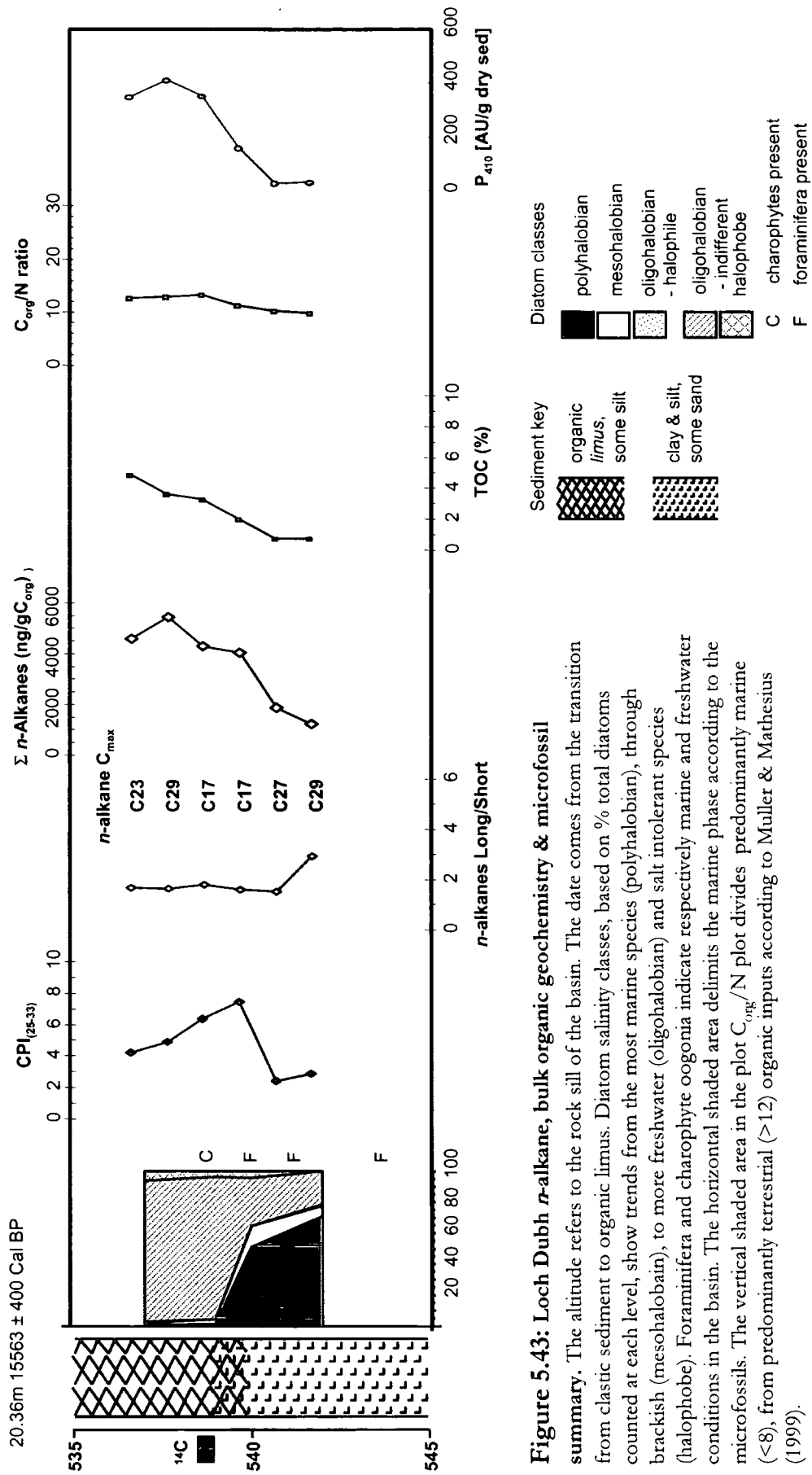


Figure 5.43: Loch Dubh *n*-alkane, bulk organic geochemistry & microfossil summary. The altitude refers to the rock sill of the basin. The date comes from the transition from clastic sediment to organic limus. Diatom salinity classes, based on % total diatoms counted at each level, show trends from the most marine species (polyhalobian), through brackish (mesohalobian), to more freshwater (oligohalobian) and salt intolerant species (halophobe). Foraminifera and charophyte oogonia indicate respectively marine and freshwater conditions in the basin. The horizontal shaded area delimits the marine phase according to the microfossils. The vertical shaded area in the plot C_{org}/N plot divides predominantly marine (<8), from predominantly terrestrial (>12) organic inputs according to Muller & Mathesius (1999).

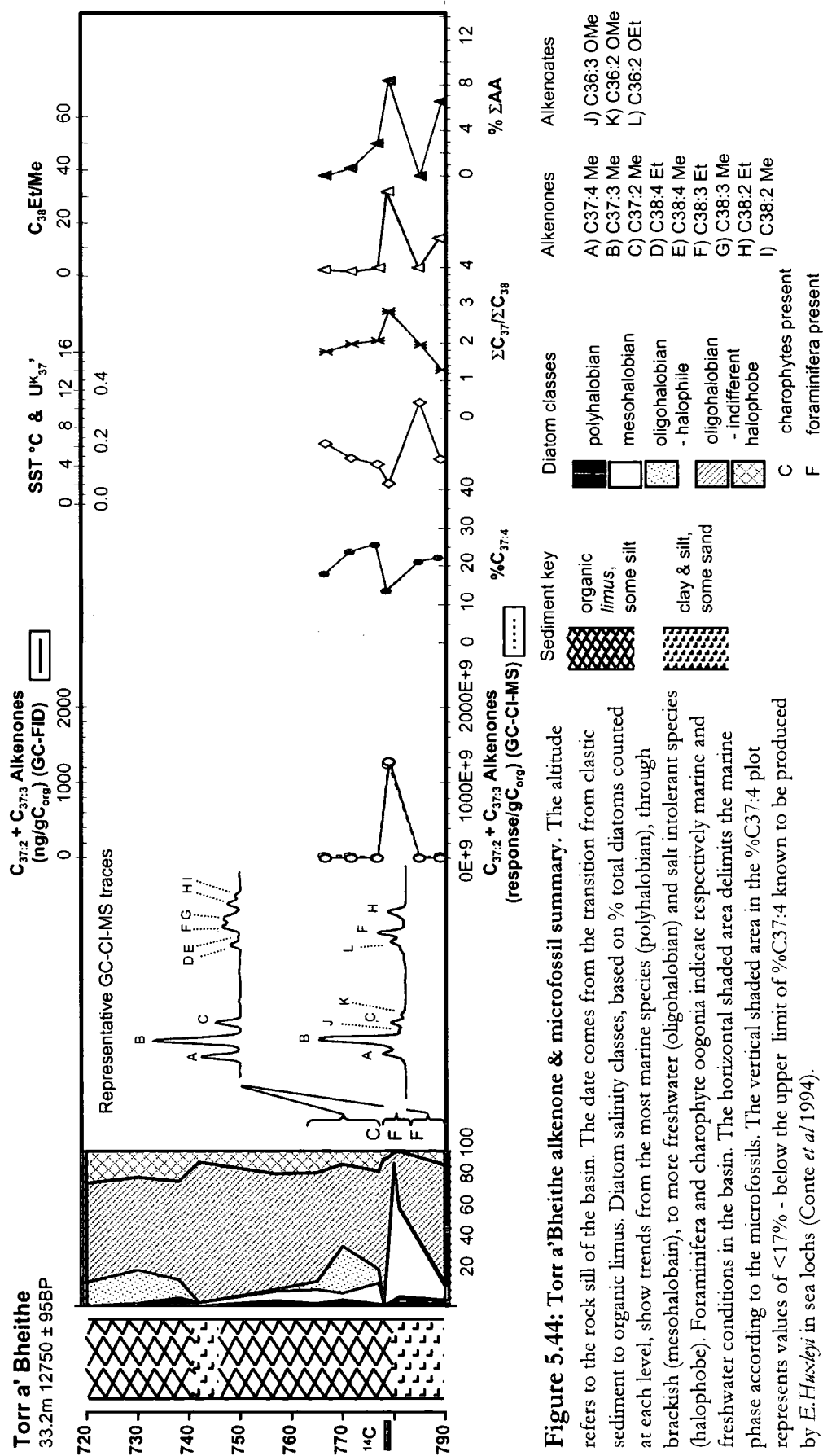


Figure 5.44: Torr a' Bheithe alkenone & microfossil summary. The altitude refers to the rock sill of the basin. The date comes from the transition from clastic sediment to organic limus. Diatom salinity classes, based on % total diatoms counted at each level, show trends from the most marine species (polyhalobian), through brackish (mesohalobian), to more freshwater (oligohalobian) and salt intolerant species (halophobe). Foraminifera and charophyte oogonia indicate respectively marine and freshwater conditions in the basin. The horizontal shaded area delimits the marine phase according to the microfossils. The vertical shaded area in the %C37:4 plot represents values of <17% - below the upper limit of %C37:4 known to be produced by *E. Huxleyi* in sea lochs (Conte *et al* 1994).

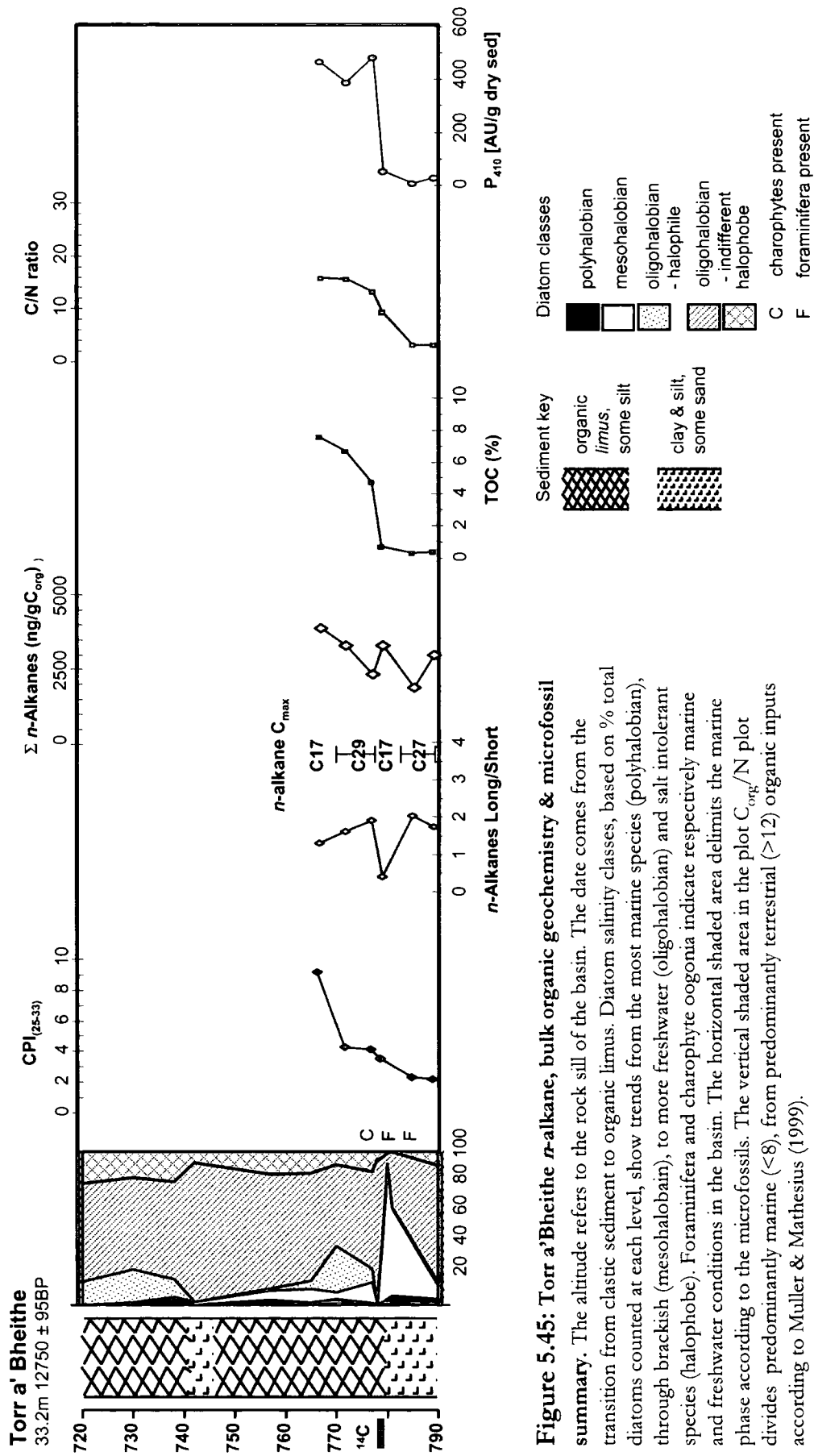


Figure 5.45: Torr a' Bheithe *n*-alkane, bulk organic geochemistry & microfossil summary. The altitude refers to the rock sill of the basin. The date comes from the transition from clastic sediment to organic limus. Diatom salinity classes, based on % total diatoms counted at each level, show trends from the most marine species (polyhalobian), through brackish (mesohalobian), to more freshwater (oligohalobian) and salt intolerant species (halophobe). Foraminifera and charophyte oogonia indicate respectively marine and freshwater conditions in the basin. The horizontal shaded area delimits the marine phase according to the microfossils. The vertical shaded area in the plot C_{org}/N plot divides predominantly marine (<8), from predominantly terrestrial (>12) organic inputs according to Muller & Mathesius (1999).

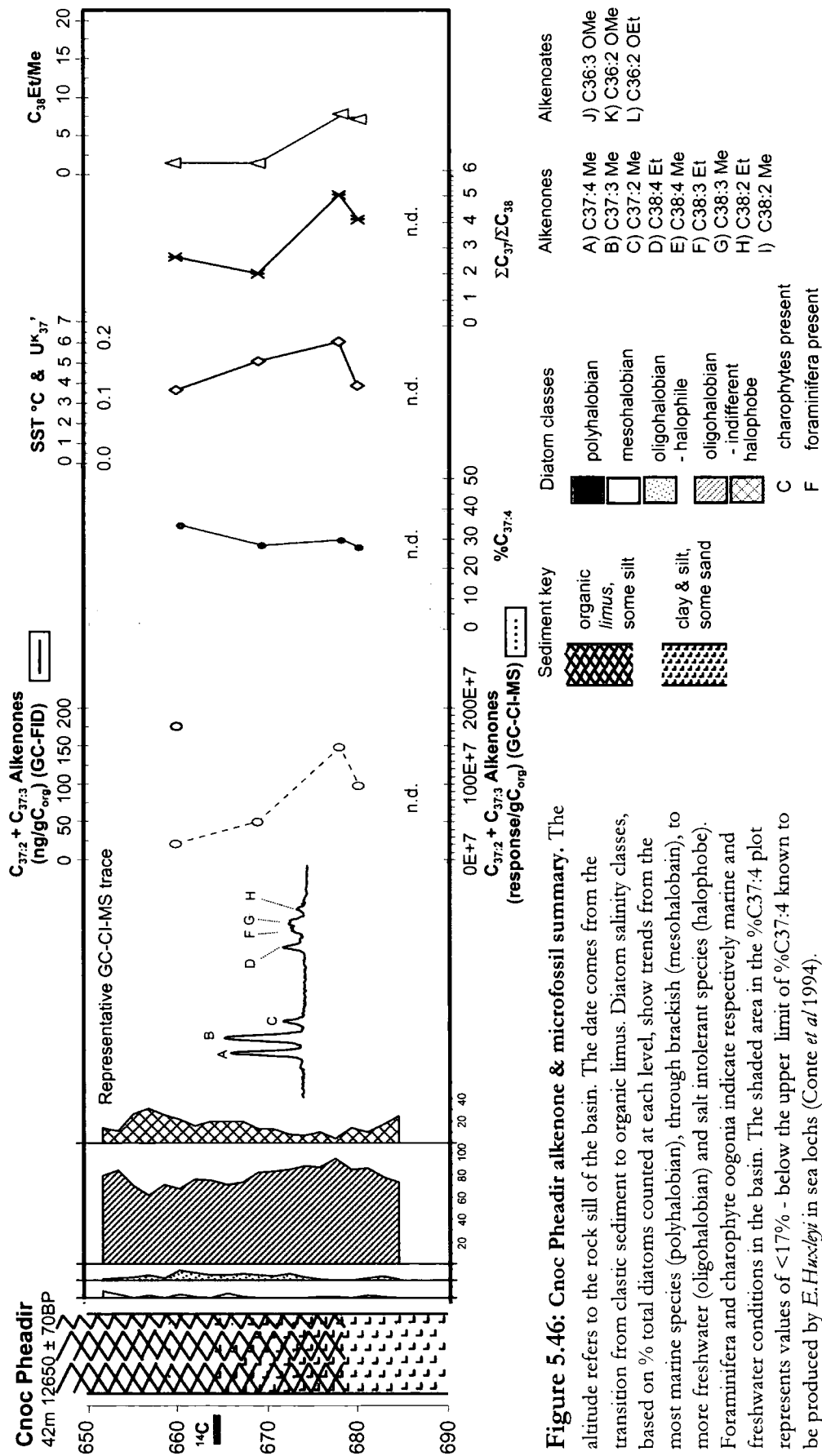


Figure 5.46: Cnoc Pheadir alkenone & microfossil summary. The altitude refers to the rock sill of the basin. The date comes from the transition from clastic sediment to organic limus. Diatom salinity classes, based on % total diatoms counted at each level, show trends from the most marine species (polyhalobian), through brackish (mesohalobian), to more freshwater species (oligohalobian) and salt intolerant species (halophobe). Foraminifera and charophyte oogonia indicate respectively marine and freshwater conditions in the basin. The shaded area in the %C_{37:4} plot represents values of <17% - below the upper limit of %C_{37:4} known to be produced by *E. Huxleyi* in sea lochs (Conte *et al* 1994).

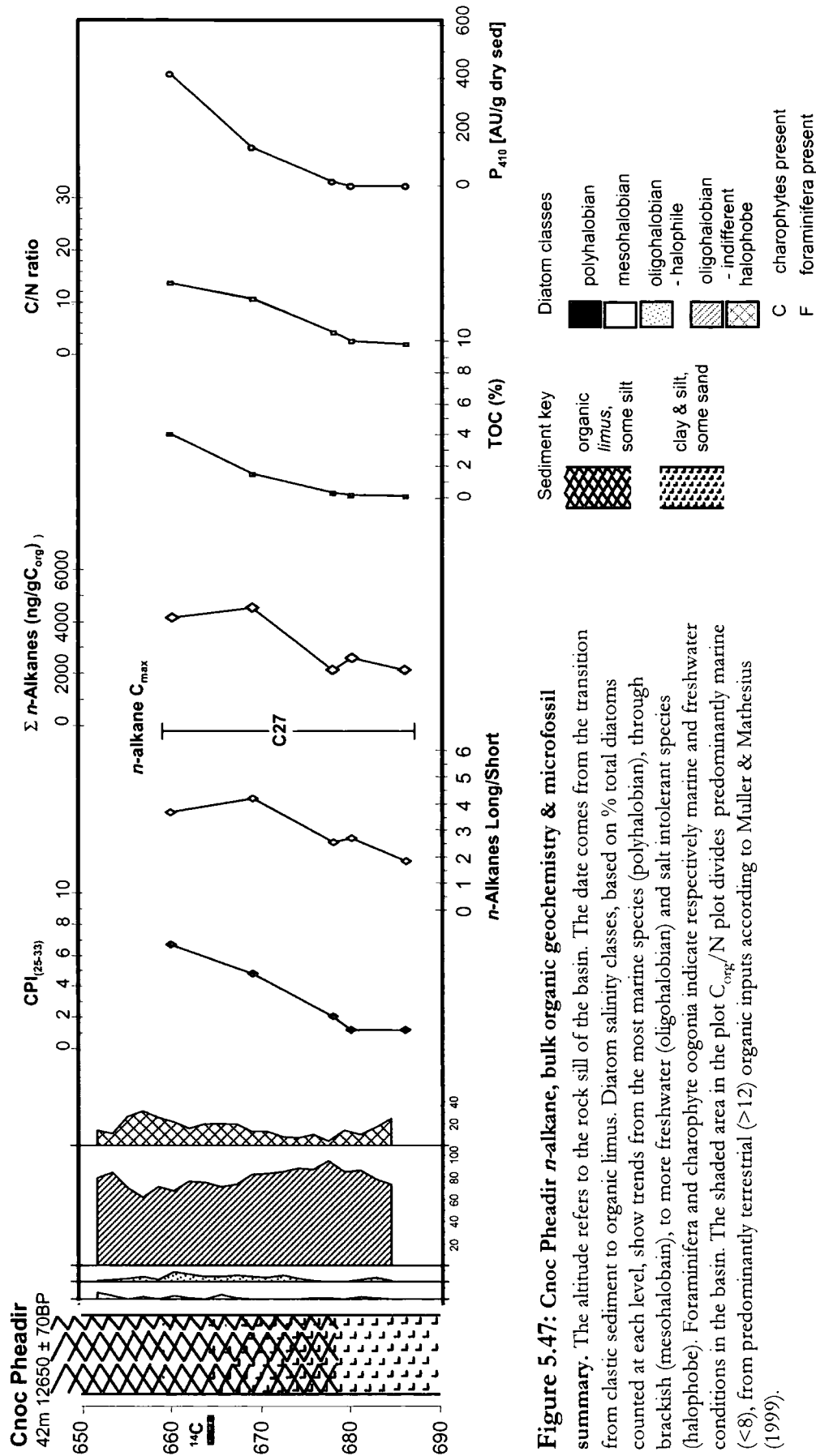


Figure 5.47: Cnoc Pheadir *n*-alkane, bulk organic geochemistry & microfossil summary. The altitude refers to the rock sill of the basin. The date comes from the transition from clastic sediment to organic limus. Diatom salinity classes, based on % total diatoms counted at each level, show trends from the most marine species (polyhalobian), through brackish (mesohalobian), to more freshwater (oligohalobian) and salt intolerant species (halophobe). Foraminifera and charophyte oogonia indicate respectively marine and freshwater conditions in the basin. The shaded area in the plot C_{org}/N plot divides predominantly marine (<8), from predominantly terrestrial (>12) organic inputs according to Muller & Mathesius (1999).

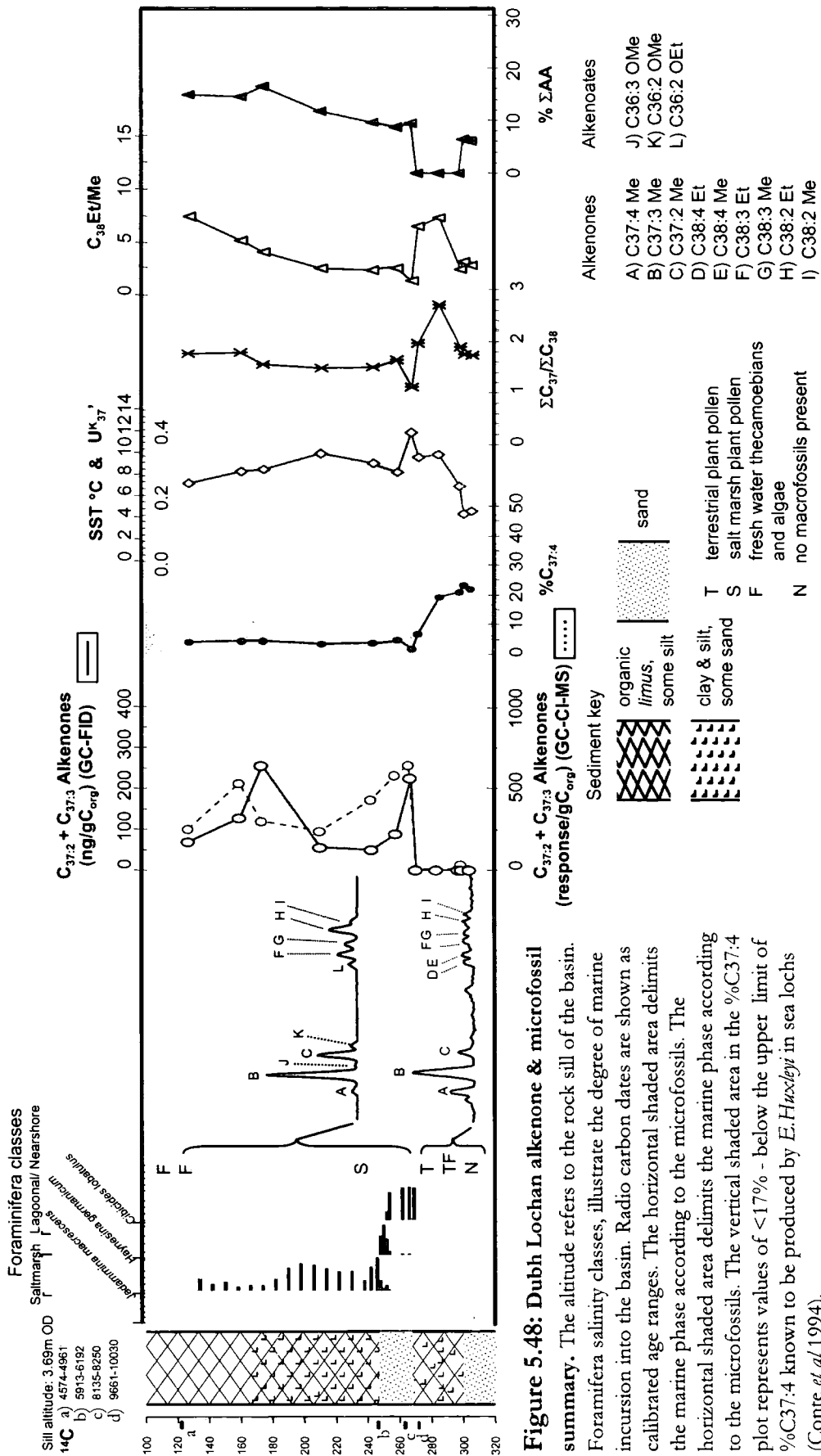


Figure 5.48: Dubh Lochan alkenone & microfossil summary. The altitude refers to the rock sill of the basin. Foraminifera salinity classes, illustrate the degree of marine incursion into the basin. Radio carbon dates are shown as calibrated age ranges. The horizontal shaded area delimits the marine phase according to the microfossils. The horizontal shaded area delimits the marine phase according to the microfossils. The vertical shaded area delimits the marine phase according to the microfossils. The vertical shaded area in the %C_{37.4} plot represents values of <17% - below the upper limit of %C_{37.4} known to be produced by *E. Huxleyi* in sea lochs (Conte *et al* 1994).

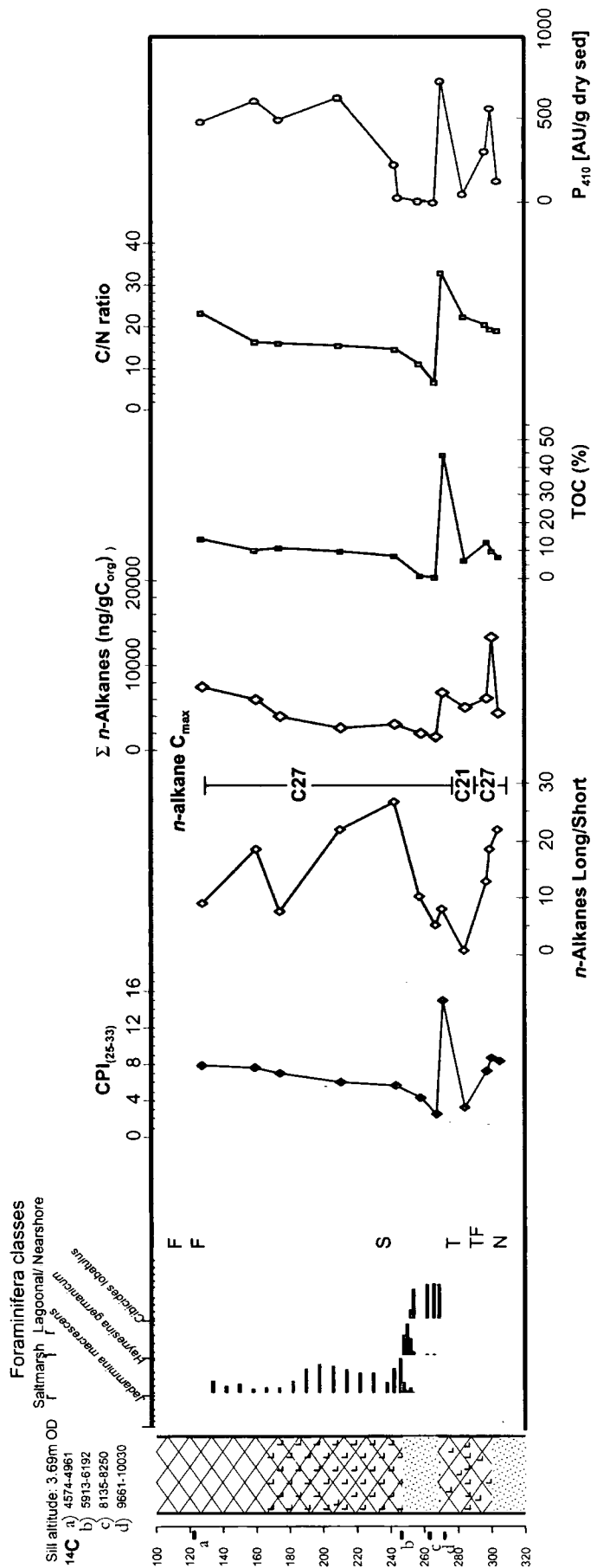
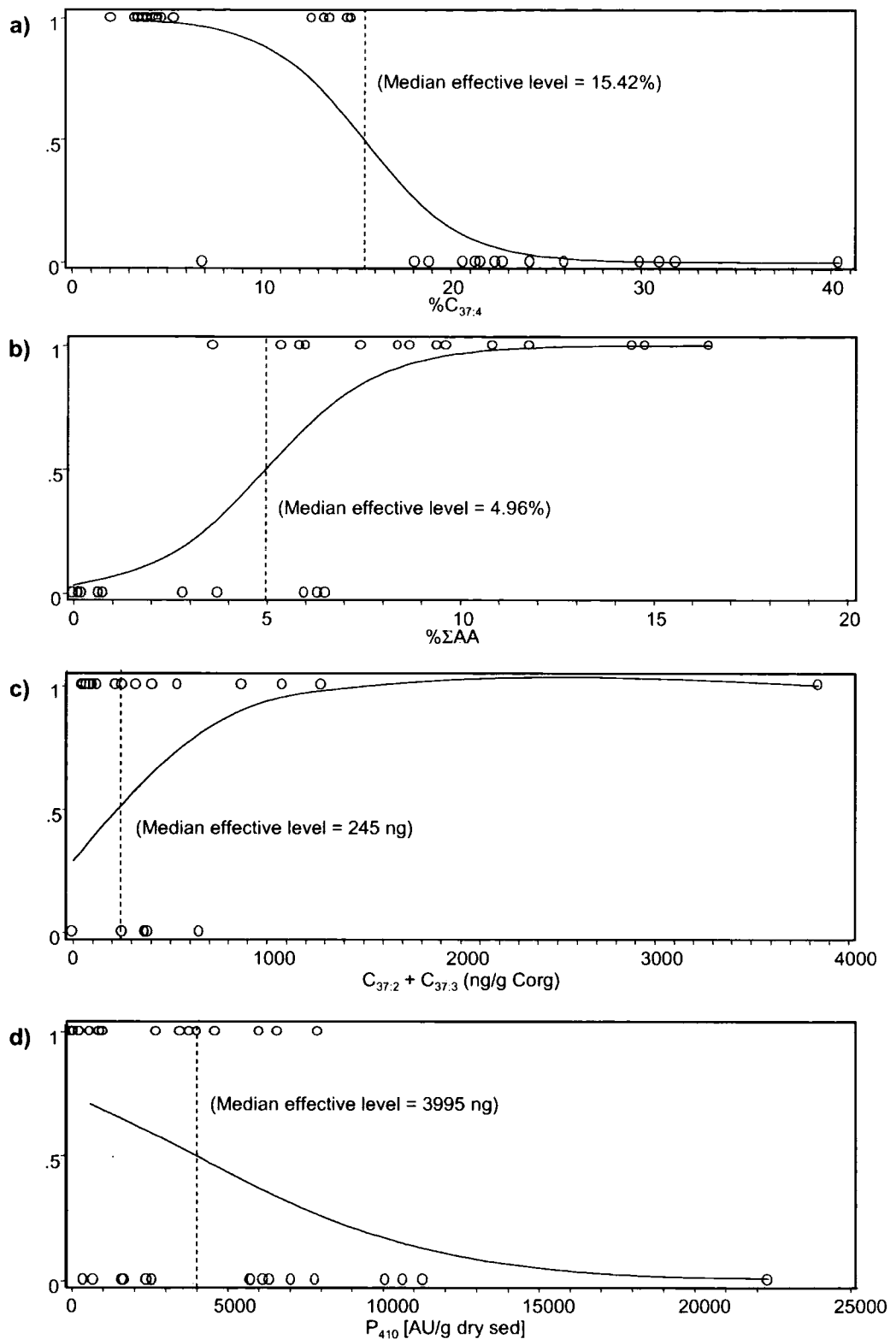
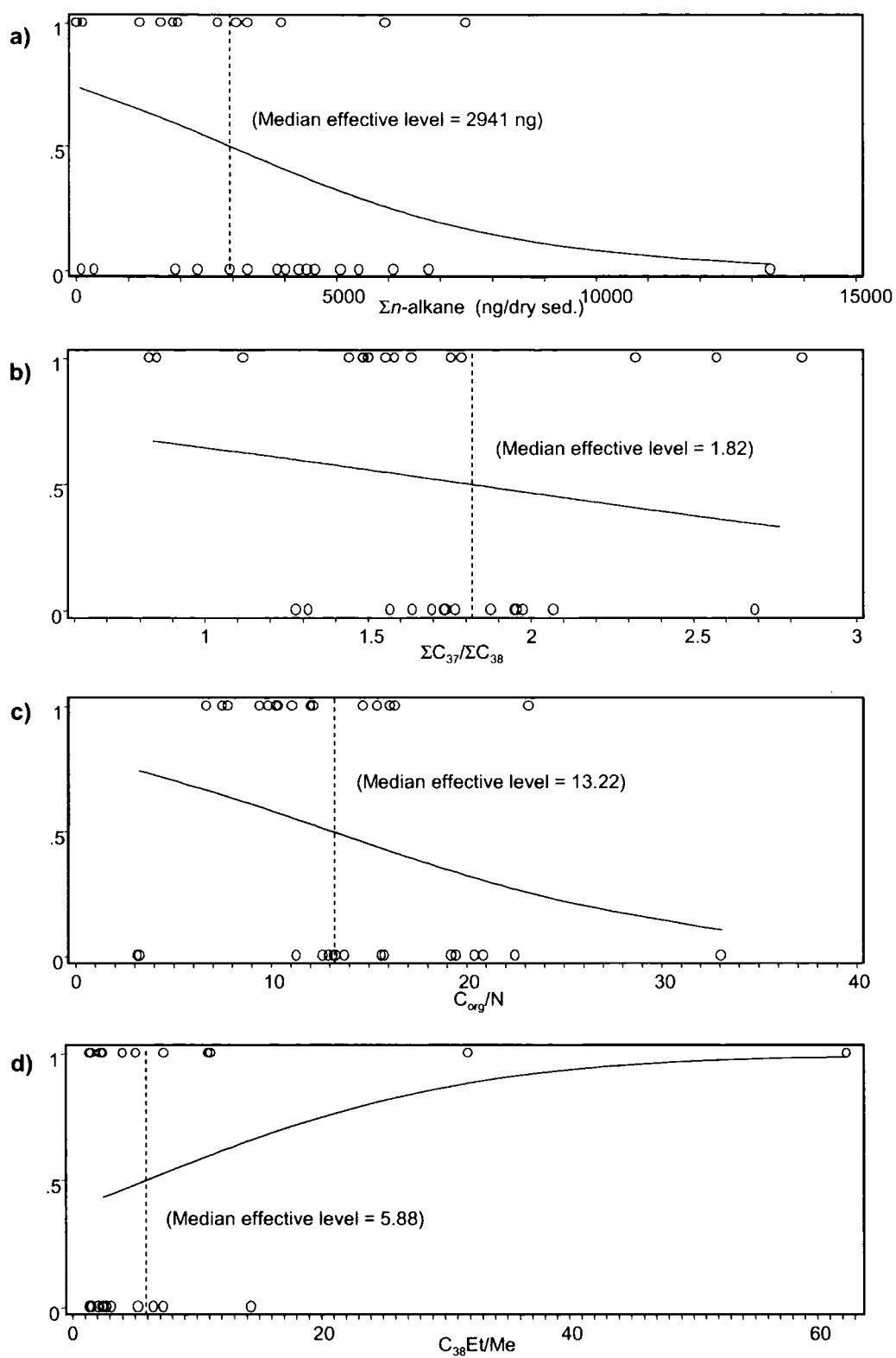


Figure 5.49: Dubh Lochan n-alkane, bulk organic geochemistry & microfossil summary. The altitude refers to the rock sill of the basin. Foraminifera salinity classes, illustrate the degree of marine incursion into the basin. Radio carbon dates are shown as calibrated age ranges. The shaded area in the plot C_{org}/N plot divides predominantly marine (<8), from predominantly terrestrial (>12) organic inputs according to Muller & Mathesius (1999).



Response Variable 1= Marine/Brackish 0= Isolated/Lacustrine

Figure 5.50: Logit regressions for marine – non-marine categorisation of modern and fossil NW Scottish coastal sediments by a) $\%C_{37:4}$, b) $\%\Sigma AA$, c) $C_{37:2} + C_{37:3}$ (ng/g Corg) and d) P_{410} [AU/g dry sed].



Response Variable 1= Marine/Brackish 0= Isolated/Lacustrine

Figure 5.51: Logit regressions for marine – non-marine categorisation of modern and fossil NW Scottish coastal sediments by a) Σn -alkanes (ng/g dry sed.), b) $\Sigma C_{37}/\Sigma C_{38}$, c) C_{org}/N and d) $C_{38}Et/Me$.

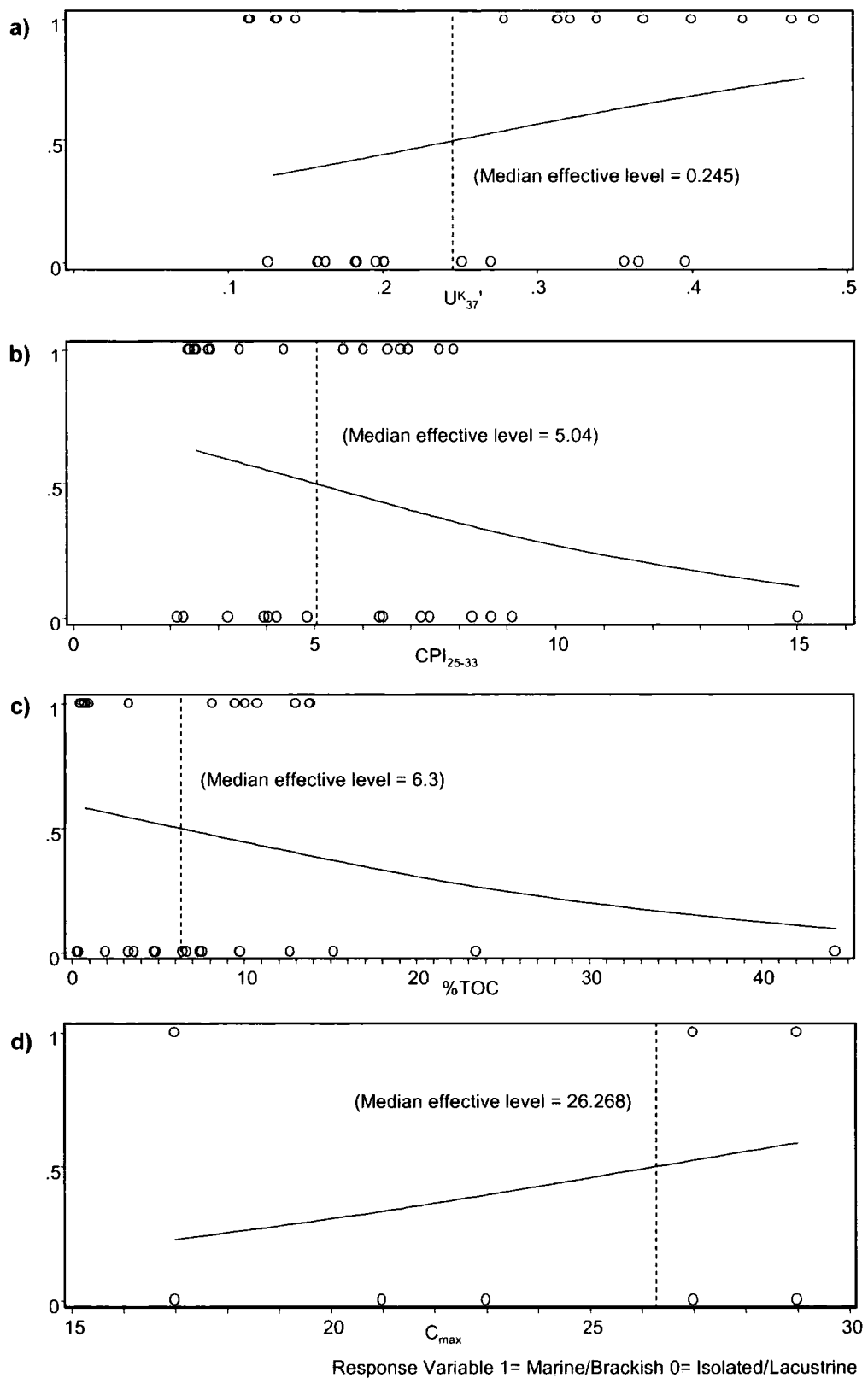


Figure 5.52: Logit regressions for marine – non-marine categorisation of modern and fossil NW Scottish coastal sediments by a) U_{37}^K , b) CPI_{25-33} , c) %TOC and d) C_{max} .

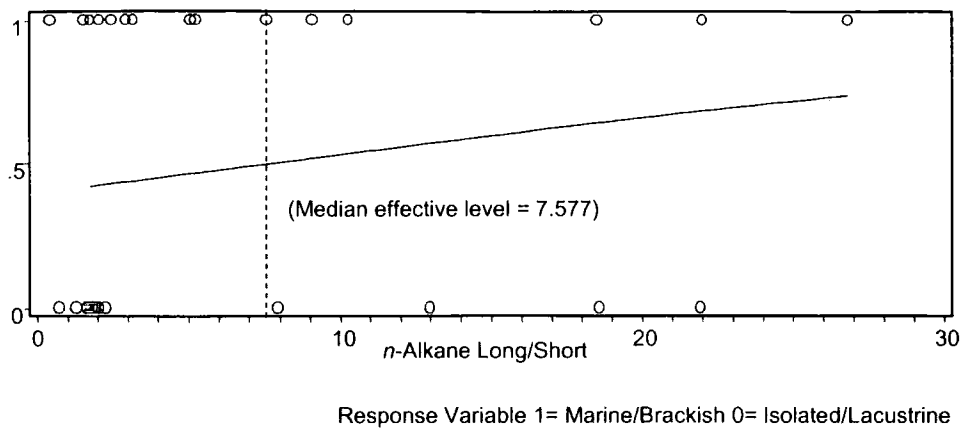


Figure 5.53: Logit regressions for marine – non-marine categorisation of modern and fossil NW Scottish coastal sediments by *n*-alkane Long/Short.

